CRANFIELD UNIVERSITY

PATRÍCIA C. MARMELO

REAL TIME EVALUATION OF WELD QUALITY
IN NARROW GROOVE PIPE WELDING

SCHOOL OF APPLIED SCIENCES

PhD THESIS

Academic year: 2012-13

Supervisor: D. Yapp

October 2012

CRANFIELD UNIVERSITY

SCHOOL OF APPLIED SCIENCES

PhD THESIS

Academic year 2012-2013

PATRÍCIA C. MARMELO

Real Time Evaluation of Weld Quality in Narrow Groove Pipe Welding

Supervisor: David Yapp

October 2012

Aos meus pais, Luis & Angelina Marmelo,
e ao meu grande amigo Anthony.

To my parents, Luis & Angelina Marmelo,
and my dear friend Anthony.

"**If you rest, you rust**", Helen Hayes

ABSTRACT

With the growth in pipeline installations all over the world, there is a great demand for highly productive and robust welding systems. Mechanised pipe welding has been developed over the last 50 years and the present focus is towards development of automated pipeline welding systems. Pipeline welding automation is aimed at reducing costs and improving the installation quality. To attain fully automated pipe welding systems there is a need to rely on sensors and controls systems to mimic human like capabilities, such as visual inspection, in real time. The key aim of this work is to develop and evaluate methods of automatic assessment of weld bead shape and quality during narrow gap GMAW of transmission pipelines. This implies that the measured bead profile will be assessed to determine whether the bead shape will cause defects when the subsequent pass is deposited. Different approaches have been used to conquer the challenge that is emulating human reasoning, all with different objectives in mind. In spite of extensive literature research performed, very little information was found concerning the real time determination and assessment of bead shape quality and none of it was reported to be applied successfully to the pipeline industry. Despite the continuous development of laboratory laser vision systems commercial ones have been on the market for decades, some specifically developed for the welding application. Laser vision sensor systems provide surface profile information, and are the only sensors which can satisfactorily measure bead profile on a narrow groove. In order to be able to use them to automatically assess weld bead shape and quality, a deep understanding of their characteristics and limitations needs to be achieved. Once that knowledge was attained it was then applied to determine the best sensor configuration for this purpose. After that the development of human like judgment algorithms were developed to accomplish the aim that was set. Empirical rules were obtained from an experienced welder regarding the acceptability of bead shapes and were then applied in the developed system with good results. To scientifically evaluate and determine the rules to use in this system, further experiments would be required. The output of the system developed showed very accurate, reliable and consistent results that were true to the external measurements and comparisons performed. The developed system has numerous applications in the pipeline industry and it could easily be implemented on commercial systems.

Keywords:
Pulsed Gas Metal Arc Welding (GMAW-P); Pipeline Welding; Adaptive Control; Bead Shape; Laser Vision Sensor; Weld Quality; Seam Tracking; Multi-pass Welding

ACKNOWLEDGEMENTS

I would like to thank Professor Fernando Ribeiro for the opportunity he created for me to come to Cranfield University and do this PhD.

I would like to thank Allan Ashpole, Brian Brooks, John Savill and Stephen Blackman for their support and expertise in welding. A distinct appreciation and gratefulness goes to my supervisor, David Yapp, for his support, expertise, encouragement and patience throughout the years.

This work would not have been possible without the technical help and support from my friends Agostinho Gil Lopes, Anthony Varughese, Theocharis Liratzis. Never forgetting the help, support and encouragement given by all my friends and family who surrounded me through this journey. I also want to thank Margaret Yapp for all her support and encouragement in the final stage of the writing up.

I would also like to show my gratitude to the people from Servo Robot Inc., Lincoln Electric, Serimax, Meta Vision Systems and Oxford Sensors Technology and Tom Doyle who provided a precious help throughout my PhD. In particular I would like to thank Connie Reichert (EWI), for her help and collaboration in the industrial project.

Thank you.
Obrigada

TABLE OF CONTENTS

TABLE OF FIGURES

TABLE OF TABLES

TABLE OF EQUATIONS

TABLE OF SOFTWARE

SP1 – **Single**
SP2 – **Duo**
SP3 – **Motion**
SP4 – **Laser Profile**
SP5 – **Pipe Girth Welding**
SP6 – **Rig (Single & Dual/Tandem)**
SP7 – **Analysis**

Single is a software package developed to control a single *Lincoln Electric Power Wave F355i* power supply (PS).

Duo is a software package developed to control two *Lincoln Electric Power Wave F355i* power supplies (PSs).

Motion is a software package developed to control the welding head.

Laser Profile is a software package developed to acquire data from the laser sensor, save it to file and .playback the saved data.

Pipe Girth Welding is a software package developed to control one or two *Lincoln Electric Power Wave F355i* power supplies, the Serimax welding head and the Servo Robot laser sensor in pipeline welding conditions.

Rig (Single & Dual/Tandem) is a software package developed to control one or two *Lincoln Electric Power Wave F355i* power supplies, the Serimax welding head and the Servo Robot laser sensor in a rig capable to simulate welding in pipeline conditions.

Analysis is a software package developed to playback and analyse the data acquired with SP5 and SP6. The analysis can be performed both in terms of the welding profile and the weld electrical characteristics.

ABBREVIATIONS

3D	Three Dimensions
AW	Arc Welding
AWS	American Welding Society
BOG	Bead On Groove
BOP	Bead On Plate
BS	British Standards
CCD	Charge Coupled Device
CTWD	Contact Tip to Workpiece Distance
DAQ	Data Acquisition
DLL	Dynamic Link Library
GMAW	Gas Metal Arc Welding
GMAW-P	Pulsed Gas Metal Arc Welding
GTAW	Gas Tungsten Arc Welding
HAZ	Heat Affected Zone
He	Helium
I	Current
MAG	Metal Active Gas Welding
MIG	Metal Inert Gas Welding
NDT	Non-Destructive Testing
NG	Narrow Groove or Narrow Gap
NGW	Narrow Gap Welding
PC	Personal Computer
PS	Power Supply
PSD	Position-Sensing Detector
PSs	Power Supplies
TS	Travel Speed
V	Voltage
WERC	Welding Engineering Research Centre, Cranfield University
WFR	Wire Feed Rate
WFS	Wire Feed Speed

UNITS

A	Ampere
bmp	Beats per minute
Hz	Hertz
m	Meter
s	Second
V	Volt

GLOSSARY

- **Accuracy** – difference between the measured value and the target actual value;
- **Adaptive Control** – type of process control that automatically determines changes in the process conditions and directs the equipment to take appropriate action;
- **Arc Blow** – arc deflection from its normal path caused by magnetic forces;
- **Arc Length** – distance between the tip of the electrode and the weld pool surface, also called *Arc Gap* or *Electrode Gap* (non-standard term);
- **Arc Plasma** – a gas that have been heated by an arc to at least a partially ionized condition, enabling it to conduct an electric current;
- **Arc Strike** – a discontinuity resulting from an arc, consisting of any localized remelted metal, heat-affected metal, or change in the surface profile of any metal object;
- **Arc Voltage** – the voltage across the welding arc;
- **Arc Welding** – a group of welding processes that produces coalescence of workpieces by heating them with an arc. The processes are used with or without the use of pressure and with or without filler metal;
- **Arc Welding Torch** – a device used to transfer current to a fixed welding electrode, position the electrode, and direct the shielding gas;
- **Automatic Welding** – welding with equipment that requires only occasional or no observation of the welding, and no manual adjustment of the equipment controls [1]. Arc welding with equipment that performs the entire welding operation without manual manipulation of the arc or electrode other than guiding or tracking and without a manual welding-skill requirement of the operator;
- **Backing** – a material or device placed against the back side of the joint, or at both sides of a weld in electroslag and electrogas welding, to support and retain molten weld metal. The material may be partially fused or remain unfused during welding and may be either metal or non-metal.
- **Backing Ring** – backing in the form of a ring, generally used in the welding of pipe;
- **Base Metal** – the metal or alloy that is welded, brazed, soldered, or cut. Also called *Base Material or Parent Metal* (non-standard term);
- **Bead** – single run of weld metal deposited in the *Base Material*;
- **Bevel** – an angular edge shape;
- **Bevel Angle** – the angle between the bevel of a joint number and a plane perpendicular to the surface of the member;
- **Burn Through** – non-standard term used for excessive melt-through or a hole through a root bead;
- **Butt Joint** – a joint between two members aligned approximately in the same plane. Also called *Butt Weld* (non-standard term);

- **Cap Run –** non-standard term for the final layer of a groove weld. Can also be called of *Sealing Run*;
- **Concavity** – the maximum distance from the face of a concave fillet weld (or other) perpendicular to a line joining the weld toes;
- **Constant Current Power Source** – an arc welding power source with a volt-ampere relationship yielding a small welding current change from a large arc voltage change;
- **Constant Voltage Power Source** – an arc welding power source with a volt-ampere relationship yielding a large welding current change for a small arc voltage change;
- **Convexity** – the maximum distance from the face of a convex fillet weld (or other) perpendicular to a line joining the weld toes;
- **Crack** – fracture type discontinuity characterized by a sharp tip and high ratio of length and width to opening displacement;
- **Crater** – a depression in the weld face at the termination of a weld bead;
- **Cycle** – the duration of alternating current represented by the current increase from an initial value to a maximum in one direction then to a maximum in the reverse direction and its return to the original value;
- **Defect –** a discontinuity or discontinuities that by nature or accumulated effect render a part or product unable to meet minimum applicable acceptance standards or specifications. The term designates rejectability;
- **Dip Transfer** – non-standard term for *Short Circuit Transfer*;
- **Duty Cycle** – the percentage of time during an arbitrary test period that a power source or its accessories can be operated at rated output without overheating;
- **Dwell Time** – the length of time the electrode is maintained at one of the oscillation extremes;
- **Electrode** – flux coated rod in manual metal arc welding, the tungsten in TIG and plasma welding and the consumable wire in GMAW welding. The welding arc is formed between the parent metal and the tip of the electrode;
- **Field Weld** – a weld made at a location other than a shop or the place of initial construction;
- **Filler Metal** – metal or alloy added in making a welded, brazed, or soldered joint;
- **5G** – a welding test position designation for a circumferential groove weld applied to a joint in a pipe with its axis horizontal, in which the weld is made in the flat, vertical and overhead positions. The pipe remains fixed until the welding of the entire joint is complete;
- **Gap** – non-standard term when used for *Arc Length*, *Joint Clearance*, *Root Opening*;
- **Gas Metal Arc Welding (GMAW)** – an arc welding process that uses an arc between a continuous filler metal electrode and the weld pool. The process is used with shielding from an externally supplied gas and without the application of pressure;
- **Gas Nozzle** – device at the exit end of the torch or gun that directs the shielding gas;
- **Groove** – non-standard term for *Weld Groove*;

- **Groove Angle** – the total included angle of the groove between workpieces;
- **Imperfection** – discontinuity or imperfection detected either by visual inspection or other types of *Non-Destructive Testing*;
- **Included Angle** – non-standard term for *Groove Angle*;
- **Incomplete Fusion** – a weld discontinuity in which fusion did not occur between the weld metal and fusion faces or adjoining weld beads;
- **Inert Gas** – a gas that normally does not combine chemically with materials
- **Joint Penetration** – the distance the weld metal extends from the weld face into a joint, exclusive of weld reinforcement. Also called *Depth of Fusion*;
- **Joint Recognition** – a function of an adaptive control that determines changes in their joint geometry during welding and directs the welding equipment to take appropriate action;
- **Lack of Fusion** – non-standard term for *Incomplete Fusion*;
- **Lack of Penetration** – non-standard term for *Incomplete Penetration*;
- **Mechanized Welding** – welding with equipment that requires manual adjustment of the equipment controls in response to visual observation of the welding. The torch, gun, wire guide assembly, or electrode holder held by a mechanical device;
- **Narrow Gap Welding** – non-standard term for *Narrow Groove Welding*;
- **Narrow Groove Welding** – a variation of a welding process that uses multiple-pass welding with filler metal. The use of small root opening, with either a square groove or a V groove and a small *groove angle*, yields a weld with a high ratio of depth to width;
- **Non-Destructive Examination (NDE)** – the act of determining the suitability of some material or component for its intended purpose using techniques that do not affect its serviceability;
- **Non-Destructive Testing (NDT)** – non-standard term for *Non-Destructive Examination*;
- **Nozzle** – in TIG and MIG/MAG welding is a metal or ceramic tube which directs the shielding gas to the weld area;
- **Parent Metal** – non-standard term for *Base Metal* or *Substrate*. Metal to be joined by welding;
- **Pass or Run** – metal deposited during one traverse of the joint by an arc. In TIG welding without filler, the term melt run may be more correct. Also called *Weld Pass*;
- **Penetration** – non-standard term for *Depth of Fusion*, *Joint Penetration*, or *Root Penetration*;
- **Porosity** – cavity-type discontinuities formed by gas entrapment during solidification;
- **Procedure** – detailed elements of a process or method used to produce a specific result;
- **Profile** – is a calibrated range image obtained from the laser sensor; [2]
- **Pulsed Gas Metal Arc Welding (GMAW-P)** – a gas metal arc welding process variation in which the current is pulsed;

- **Repair** – re-weld on a completed weld to correct a fault detected in the weld by visual or NDT and that is unacceptable by the standards in practice;
- **Resolution** – smallest detectible variation measureable by the sensor;
- **Robotic Welding** – welding performed and controlled by robotic equipment;
- **Sealing Run –** run of weld metal deposited on the reverse side of a butt joint, along the line of the root. May also be called of *Cap Run*;
- **Seam** – non-standard term when used for a welded, brazed, or soldered joint;
- **Semiautomatic Welding** – arc welding system with equipment that controls only the filler feed. The remaining process control is performed manually;
- **Shielding Gas** – protective gas used to prevent or reduce the atmospheric contamination;
- **Sidewall** – non-standard term for *Groove Face*;
- **Spatter** – metal expelled during fusion welding that do not form a part of the weld;
- **Stand-Off** – vertical distance between the sensor and the part to be measured;
- **Tack Weld** – weld made to hold the parts of a weldment in proper alignment until the final welds are made;
- **Undercut** – a groove melted into the base metal adjacent to the weld toe or weld root and left unfilled by weld metal;
- **Weld** – a localized coalescence of metals or nonmetals produced either by heating the materials to the welding temperature, with or without the application of pressure, or by the application of pressure alone and with or without the use of filler material;
- **Weldability** – capacity of material to be welded under the imposed fabrication conditions into a specific, suitably designed structure and to perform satisfactorily in the intended service;
- **Weld Bead** – weld resulting from a pass;
- **Welder** – person who performs manual or semi-automatic welding;
- **Weld Groove** – a channel in the surface of the workpiece or an opening between two joint members that provides space to contain a weld;
- **Welding** – a joining process produces coalescence of materials by heating them to the welding temperature, with or without the application of pressure or by the application of pressure alone, and with or without the use of a filler metal;
- **Welding Arc** – a controlled electrical discharge between the electrode and the workpiece that is formed and sustained by the establishment of a gaseous conductive medium, called *Arc Plasma*;
- **Welding Electrode** – a component of the welding circuit through which current is conducted and terminates at the arc, molten conductive slag, or base metal;
- **Welding Head** – the part of a *Welding Machine* in which a welding gun or torch is incorporated;
- **Welding Machine** – equipment used to perform the *Welding* operation;

- **Welding Operator** – one who operates adaptive control, automatic, mechanized or robotic welding equipment;
- **Welding Position** – the relationship between the weld pool, joint, joint members, and the welding heat source during welding;
- **Welding Power Source** – an apparatus to supply voltage and current suitable for welding;
- **Welding Procedure** – the detailed methods and practices involved in the production of a weldment;
- **Welding Voltage** – see *Arc Voltage*;
- **Weld Joint Mismatch** – misalignment of the joint members;
- **Weldment** – an assembly whose component parts are joined by welding;
- **Weld Metal** – the portion of a fusion weld that has been completely melted during welding;
- **Weld Pass** – a single progression of welding along a joint;
- **Weld Pass Sequence** – the order in which the weld passes are made;
- **Weld Penetration** – a non-standard term for *Joint Penetration* or Root Penetration;
- **Weld Pool** – the localized volume of molten metal in a weld prior to its solidification as weld metal;
- **Weld Recognition** – a function of an adaptive control that determines changes in the shape of the weld pool or the weld metal during welding, and directs the welding machine to take appropriate action.
- **Weld Root** – the points, shown in a cross section, at which the root surface intersects the base metal surface;
- **Weld Seam** – a non-standard name for *Joint*, *Seam Weld*, *Weld*, *Weld Joint*;
- **Weld Toe** – the junction of the weld face and the base metal;
- **Weld Voltage** – see *Arc Voltage*;
- **Wire Feed Speed** – the rate at which wire is consumed in arc cutting, thermal spaying, or welding;
- **Work Angle (pipe)** – the angle less than 90 degrees between a line that is perpendicular to the cylindrical pipe surface at the point of intersection of the weld axis, and a plane determined by the electrode axis and a line tangent to the pipe at the same point. In a T-joint, the line is perpendicular to the non-butting member. This angle can also be used to partially define the position of guns, torches, rods, and beams;
- **Workpiece** – the part that is welded, brazed, soldered, thermal cut, or thermal sprayed.

Other references for this subject: [3]; [4];

1 Introduction

Mechanised pipe welding has been developed over the last 50 years. It all started with the introduction of mechanized welding heads (bugs), moving on to the application of narrow groove bead preparations. After that the torch types started to evolve, the single torch become a dual torch, then a tandem torch and at last the dual tandem torch systems [5, 6]

Although nowadays welding is a mechanised process it is still very reliant on highly skilled welders and on procedure development. The procedure parameters are initially set but the welder typically must control the torch cross seam positioning, oscillation width, and CTWD, as the torch progresses from the 12 o'clock position to the 6 o'clock position. As the torch systems evolved and the welding speeds increased it became very hard for the welder to be able to cope [7]. Adding to the increasing welding speed the welder, for a large diameter pipe, may be standing on top of a ladder for the weld start and laying on his back on the floor at the end of the weld. Welders visually inspect welds before and after welding, and if they detect asymmetric or convex welds, they will grind the affected area to produce a concave shape before they lay the next bead. In the last decade pipeline welding companies have been implementing commercial laser stripe [8] and thru arc [9, 10] systems for seam tracking.

With the growth in pipeline installations all over the world, the need for automation is becoming increasingly important. Pipeline welding automation is aimed at reducing costs and improving the installation quality. It is considered that the oil resources will decrease [11] which might be expected to lead to a reduction in developments in the areas related with pipeline installation. However, this is not occurring. With new sources of natural gas being found, new pipelines are planned for the near future [12]. Since these new sources are located in remote places, long pipelines are required to transport the gas to where its use is required. One of the reasons for the investment in the development of new pipeline installation processes, techniques and materials is the high cost of new pipelines.

There are other reasons that justify the investment into pipeline welding automation, such as higher speeds which lead to higher productivity. Improvement of the weld quality leads to a reduction in the need for repair welds. Repair welds not only are costly in terms of time but also in terms of manpower and consumables. With an automated system, it should be easier to achieve a higher level of consistency, and as a result weld quality will be less dependent on the welders' capabilities. Also, the number of welders available, especially highly skilled ones, is decreasing as manual welding is not perceived as an attractive line of work [13]. Companies around the world are going to great lengths to attract new professionals for this area [14]. Transmission pipelines cannot be welded in a workshop and welds have to be

performed in the field, often in very harsh conditions. Temperatures may either be very high or very low and locations may be remote and ergonomically difficult. Some of the welds performed on transmission pipelines are still performed manually during long shifts. These are some of the reasons why welding is not thought to be an attractive job.

Mechanising welding alone is not very adequate since mechanised systems have difficulty dealing with the variations in part tolerances, hence the need for automation. With the use of sensors to detect those variations and with control systems to compensate for the part tolerances, automation is an attractive route. The skills required from the operators will then be lower than those required for manual or mechanised systems.

With the mechanisation and automation of the welding process there is room for increasing the welding speed. As the welding speed increases so does the demands on the welders. The welders who are able to cope with such speeds are only the very experienced, very skilled ones. Due to the shortage of such skilled welders, and in order to allow for greater speeds to be accomplished, full process automation offers considerable potential for the future [15].

Increasingly higher strength steels such as X80 and X100 are being used for transmission pipelines. These high strength steels have the advantage of allowing the pipe thickness to be reduced and/or gas pressure to be increased. For these types of pipes, narrow joint configurations are used which require less time and material to fill up. The narrow joints bring a series of constrains to the welding conditions. With this type of groove (Figure 1.1) it is more difficult to reach the side of the groove without touching it. As a result, contact tips need to be narrower to allow insertion in the groove and specially to allow oscillation. All the movements need to be very precise as otherwise the contact tip may touch the groove walls creating short circuits or even damaging the equipment.

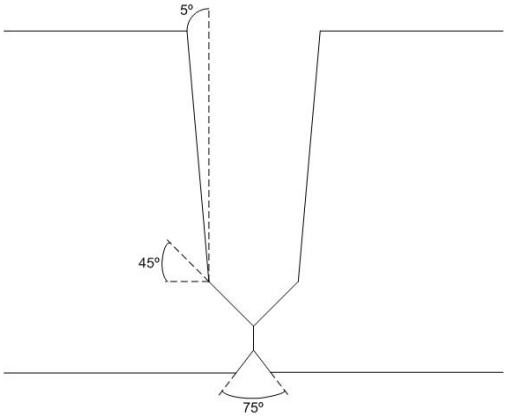

Figure 1.1 – Typical narrow groove configuration.

It is critical that high quality welds are consistently produced. This means the weld reject rate should be typically below 5% is good, and ideally they should be as lower as they can possibly be. This is an important factor as for a 24mm wall thickness, 1m pipe diameter with 8 passes there are 25m of weld. Automated ultrasonic testing systems are now very widely used for weld inspection. These systems can nowadays detect very small defects but they operate mainly when the joint is fully welded. This means that if a defect occurred on one of the first layers it needs to be manually excavated, usually manually welded and re-inspected. For more significant defects the weld must be cut out and rewelded, severely impacting the production. Repairs are a significant issue, and very costly in terms of time and money.

There is hence a strong need for systems that will evaluate the weld quality in real time, without waiting for the post-weld inspection. This way defects can be minimised and problems can be corrected by the mechanized welding bug before they are buried in the weld, and causing subsequently more severe problems and more costly repairs. The development of such systems can be regarded as a key element in the development of fully automatic pipe welding systems, where the weld quality and rejection rate would not depend on the welder skills.

A variety of approaches have been taken for real time evaluation of weld defects. These include:

- Change detection – detection of variations between the acquired values and the ones expected in a good weld, using:
    - Measurement of arc current and voltage;
    - Infra-red light measurement;
    - Acoustics;
    - Spectroscopy;
    - Ultrasonics
- Vision systems
- Many laser vision systems have been developed for laboratory use and there are several commercial laser vision systems available, some of which have been specifically developed for the welding application. Laser vision sensor systems provide surface profile information, typically using either a scanned laser spot or a laser stripe combined with optical triangulation. These sensors are the only ones that can satisfactorily measure bead profile on a narrow groove.
- For the laser spot system both PSD's and linear diode arrays are used to generate the profile data. Laser spot has the advantage of somewhat being less susceptible to reflections from shiny surfaces than the stripe system. A wide range of laser spot sensors is available commercially at a relatively low cost. However, the biggest disadvantage is that the spot must be scanned, either mechanically or by mirrors to generate the profile. One of the first commercially available laser profile systems for the welding industry used mirrors to scan the spot [16].

- Laser stripe systems operate by imaging the projected line of laser light on to a CCD or CMOS array, and interpreting the acquired image. This area of expertise has been subjected to extensive research and development, with great many laboratory systems being developed throughout the years and more than 20 commercial systems available. There are a number of issues related to the use of these systems, including shadowing, and strong reflections from machined surfaces. Nonetheless, in spite of extensive development there is relatively very little information on laser system performance in industrial applications. This type of sensor has extensively and commercially been used for seam tracking, weld volume calculation for adaptive welding, and for post-weld inspection. There has been less work performed concerning the measurement of bead shape for multipass welding during welding, and almost nothing has been reported on automatic determination of bead shape acceptability and quality, which are the key topics of this work.

With the aim of developing automation for the pipeline welding process a study of laser vision sensors was performed. This study involved the exploration of the sensors' capabilities, limitations and its application to the pipeline welding process. The execution of this study required understanding of the welding process of transmission pipelines, its requirements and resources. Once that understanding was obtained, software packages were developed to implement an automated welding system. A monitoring and control software based on the laser sensor and other tools required to perform related tasks were also developed.

2 Literature Review

2.1 Sensors for Narrow Groove Gas Metal Arc Welding

What is a sensor? One of the best definitions of sensor is “A device that measures or detects a real-world condition, such as motion, heat or light and converts the condition into an analogue or digital representation.” [17]

Many types of sensors can be applied to Narrow Groove (NG) GMAW in order to achieve a certain degree of control. The sensors can be divided in two main categories: arc based and external sensors. The arc sensors category embraces a range of sensors which can detect variations in the welding conditions by detecting changes in the welding voltage and/or current. Some of the approaches to arc sensors are: bent wire; two wires in parallel, oscillating tungsten; oscillating arc and rotating arc sensors. External sensors can be sub-divided as: contact; eddy current; electromagnetic; ultrasonic; optical and other. The most commonly used types of sensors for NG GMAW are: arc based sensors (also called through-the-arc or through-arc sensor); contact (tactile); and optical (video and laser stripe or spot) sensors [18-20].

In any control system, and especially adaptive systems, sensors are a critical part as they provide the data for the control algorithms. The acquired data accuracy is very important as incorrect or inaccurate data can cause unexpected outputs from the control algorithms. Below is a description of some of the available sensors for NG GMAW.

2.1.1 Contact Sensors

Contact sensors, also named tactile sensors, were some of the initial sensors to be developed for welding applications. They base their measurement either on an electric current, micro switches, or purely mechanical mechanisms. Purely mechanical mechanisms are used for seam tracking and to detect the weld start and stop locations. Though these systems are inexpensive they are quite inflexible and usually application specific. An extensive review on this type of sensors was done by Holder, et al [21]. A simple example of purely mechanical contact sensor can be found in Figure 2.2 (extracted from [21]). A great disadvantage of this type of sensors is that they wear quite easily due to constant contact between the parts.

If the sensor is micro-switch based it is used to detect the direction of deviation of the weld torch from its position in the groove (Figure 2.1) [20]. The tip of the probe touches the groove centre and as the groove centre changes so does the position of the probe tip. In the opposite end of the probe, inside the sensor, the micro-switches are activated accordingly to the groove variation. This will generate an ON/OFF signal, which is used to decide on the torch positioning adjustments. This type of sensor, according to Ushio and Mao [22], has problems dealing with complex curvy joints and also limits the welding speed. On the other hand if contact sensor is based on an electrical signal that is detected by a probe, the probe can either be the welding wire, welding nozzle or some other part added to the automated equipment. At the beginning of every cycle, typically low voltage (40V) is applied to the probe and the probe is moved towards the part(s) to be welded until it touches it. The movement is slow and involves finding as many points as necessary depending on the specimen complexity and the difficulty of accurately locating them. A simple example of a part location procedure can be seen in Figure 2.3 but it will get more complex as the number of parts to be detected increases. As the complexity increases so does the number of steps for the torch to go from the home to the final position and the time required to perform the sensing process.

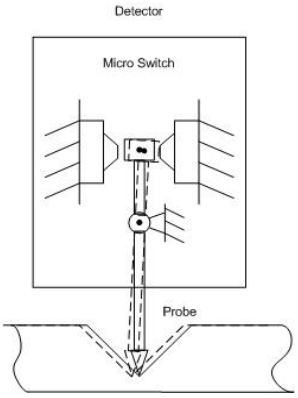

Figure 2.1 – Contact sensor (micro switch).

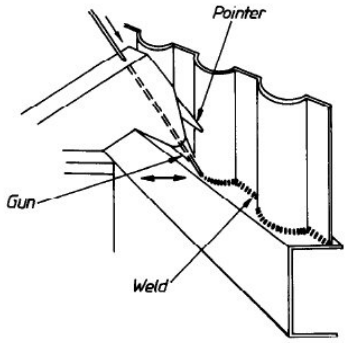

Figure 2.2 – Contact sensor (purely mechanical) [21].

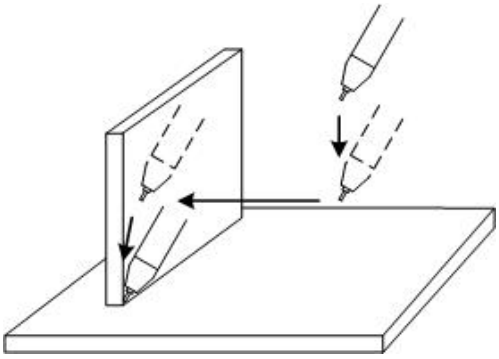

Figure 2.3 – Contact sensor (electrical voltage).

The touch sensor based on an electrical current is not suitable for real time operation and cannot compensate for changes that might occur to the parts during welding as all the sensing is performed prior to weld start. Another limitation of this type of contact sensor is the time it requires to complete the search process, The time increases as the number of parts to be detected increase, thus increasing the system cycle time [23].

The main advantage of this type of sensor is its low cost, simple handing and low maintenance [22]. Though contact sensors are very cheap they are slow and limited in performance and applications [20]. In the specific application of NG GMAW this sensor can be applied but its performance is limited to the physical restrictions caused by the parts configuration, as well as by the other limitations inherent to this type of sensors. The probes may suffer from wear and tear due to the contact with the parts to be welded [24, 25].

Adding to the previous reasons, contact sensors are only capable of extracting limited amount of features and this limits the degree of process automation that can be achieved. Due to these reasons new technologies were evaluated that would allow non-contact sensing and which would also provide more detailed information concerning the welding process.

2.1.2 Non-Contact Sensors

Non-contact sensors category embraces sensors based on several different technologies that do not involve any physical contact between the sensor and the part(s) to be sensed. For welding applications and in particular for NG GMAW several different non-contact sensors can be used. The most common are: through-the-arc; the different vision sensors; and audio. Though the through-the-arc sensor is an arc sensor it falls at the same time into the category of the non-contact sensors. These sensors will be described in more depth below.

2.1.3 Through-the-Arc Sensor

The through-the-arc sensor is an arc based sensor which utilises the welding voltage and/or current to sense what is occurring in the weld in real time. By using the welding arc as data source there is no need to have external sensors attached to the welding torch/gun. The existence of external sensors attached to the welding torch sometimes imposes physical limitations to the system, reducing the torch's manoeuvrability and/or limiting its application depending on the configuration of the parts to be welded.

The data analyses can be performed in real time or not depending on the analysis objective. By analysing the signals in real time it is possible to perform seam tracking and torch height adjustments [20, 26, 27]. Lopes demonstrated the possibility to control the width of oscillation through the use of arc sensors [28]. Post weld data analysis allows the generation of various

weld statistics commonly used to assess weld quality, detect faulty conditions, and predict joint quality [29]. Post weld data analysis can also be used to aid in procedure development [30].

The use of through-arc sensing usually implies electrode oscillation/weaving and is the oscillation movement that causes the differences in the arc voltage, as it can be seen in Figure 2.4. As the electrode approaches the sidewall the arc shortens reducing its voltage. The controller senses the voltages and knows the positions where the readings were made, and then compares the values from positions 2 and 3. If the values are different, correction instructions are sent to the controller in order to adjust to the oscillation centre to match with the actual groove centre.

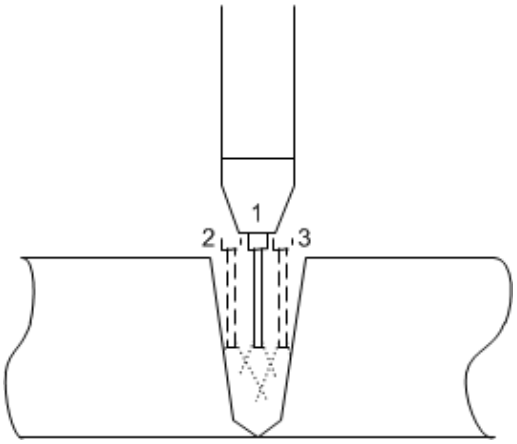

Figure 2.4 – Oscillating torch (linear oscillation).

Using through-arc sensing, unlike with touch sensors, is possible to detect changes to the expected parts location. These differences can occur due to incorrect part production or heat distortion among other reasons, and the arc sensor will still be able to detect then [23]. This sensor when compared with the tactile also has the advantage of decreasing the cycle time as no pre-weld scanning is required. As the sensor is located in the electrode itself there is no gap between the sensed conditions and the welding location leaving no need for a data buffer. At the same time with the inexistence of a sensor attached to the torch, this can more easily manoeuvre and access the weldment [20].

A great disadvantage of arc sensors lies in the noise that is often present in the sensor data due to process characteristics like: arc stability and electromagnetic interference [27]. Another disadvantage that can be pointed out to the use of through-the-arc sensors is the difficulty in applying it to the welding of thin plates. Yu and Na studied vision sensors as a way to overcome this difficulty in seam tracking [31, 32]. Their work focused on the influence of shadowing and lack of field of view on data quality.

The arc instability raises more problems in GMAW when compared to GTAW process. Within GMAW processes, the Dip metal transfer mode has more noise associated with it. When using Spray transfer the arc is more stable but the wire melting may still occur in an unpredictable way introducing noise to the signal. The more stable transfer mode in GMAW is the GMAW-P where typically a droplet is detached per pulse from the wire and very little spatter is generated. However, the rapid changes in voltage and current may make interpretation of the sensor signals difficult. Constant and stable wire feed should be maintained to avoid irregularities in the metal transfer [27]. In depth information on through-the- sensing and its applications has been provided by Lopes [28].

In summary, the arc sensor is quite an attractive choice if all that is required is either seam tracking, contact tip to workpiece distance or oscillation width control. This is an inexpensive solution as it does not need any extra hardware. The measurement is done on the actual weld point so there is no registration and no need for a data buffer. As the measurement is performed on the welding wire there is no susceptibility to sensor damage and if the wire is bent the value read will still reflect the weld condition. This sensor may need to be customized to the power supplies to be used as their specifics in terms of feedback values may not all be the same. Different welding conditions or process variants may also imply that adjustments may be required to the control algorithms. There is very little information that can be extracted from this type of sensor relatively to the bead or preparation width. More importantly no information can be gathered concerning the bead or preparation shape. As the focus of this work is to measure and evaluate bead shape profiles the arc sensor is not applicable and so this option is not going to be pursued.

2.1.4 Vision Sensors

Vision sensors can be traced back as far as 1930's to a company called *Electronic Sorting Machines* in New Jersey, USA. They developed a method to sort out food based on particular filters and photomultipliers [33]. Since then vision sensors have been evolving broadly and with a wide range of applications. This has been possible due to technology developments both in terms of available vision technologies and with the evolution and use of computers in both domestic and industrial applications.

In terms of welding applications, and more particularly arc welding, vision sensors have a great potential but are strongly affected by the welding conditions. The performance of the sensor might be affected by the bright light from the arc, electromagnetic forces, spatter, and reflection from the metal surface, among other conditions. Another drawback from this type of sensor is the complexity of the image analysis required to extract the necessary data and the time required to process it. To overcome these limitations the use of threshold techniques simplifies the image but adds some noise that should be reduced by software algorithms.

In the early stages of the application of vision sensors to arc welding, automation techniques were developed to overcome the problem of arc light. For example synchronising the camera shutter with the GMAW short-circuit frequency [34]; or controlling the wire feed rate in GMAW to acquire the image in the WFR background [35]. Drews and Kings [36] used a strong source of light in order to outshine the arc light, or performed the image acquisition further away from the arc centre, where the arc light is weaker.

A later approach to reduce the complexity of the images was the use of structured light, usually from a laser source. The expression “structured light” refers to a diverse range of light patterns projected into the object to be measured. The light patterns can be generated in different ways through the use of mirrors, light splitters, rotating cylinders or galvanometers among other equipment. The pattern is created by one or a combination of these objects. When a structured light is used, filters are usually added in front of the camera in order to reduce noise. According to Corlet et al [27] the use of structured light reduces the amount of data to be analysed, creates 3D data from a 2D image, and increases the signal-to-noise ratio.

The main application for vision sensors in welding so far is to register and analyse the arc and the weld pool. This can be demonstrated by the volume of work produced in these areas. Corlet et al [27] also demonstrated it may be used to measure the distance between the electrode and the sidewall in order to maintain it constant. Another possible application is to perform adaptive filling as it is possible to extract groove features from the acquired images. Though this is possible, this is highly complex and costly [23]. When using vision sensors, unlike with through-arc sensors, it is necessary to keep in mind that if an arc blow or wire cast occur the arc will no longer be centred with the torch centre line and the measurements will not be reliable [20].

Direct vision is often used as direct control methods, for instance seam tracking by detecting preparation edges. Control actions have also frequently been discerned from weld pool shape measurements.

2.1.5 Laser Vision Sensor

Laser sensors use what is called “structured light”. Structured light, unlike normal lightning which illuminates everything, it illuminates only where the laser light hits the target object. Structured light falls under the direct measurement, triangulation category according to the 3D information classification described by Nitzan et al [37].

The laser technology has also been applied to sensing and is now broadly used. One of the existing laser sensors is the *Laser Vision Sensor*, also known as *Range Sensor* or *3D Laser*

Sensor. This type of sensor was developed in 1986 by Keyence Corporation using a *Diode Laser* [38]. This type of sensor works properly within its field-of-view. Outside its field-of-view it cannot sense the environment correctly and so cannot perform.

Laser vision sensors are non-contact sensors that can be divided in two groups, *Stripe* and *Spot*. Both types of sensors will be explained, giving more focus to the stripe sensors. This type of sensor is applied to the measurement of fragile or distant objects. Its operation can be described as a laser light that is projected into the object to measure while a Charged Coupled Device (CCD) camera captures the reflected image. The obtained information is then processed to determine the object shape and position. With this data, control decisions can be taken.

Laser vision sensors, as they are non-contact sensors, have the advantage over contact sensors of not damaging the objects to be measured and being able to measure cavities where other sensors do not fit or reach. An advantage over a touch sensor is that it is possible to acquire more data points, more accurately, and much faster [39].

As the arc welding environment is broad and intensely illuminated most vision sensors need specific filtering systems and still have difficulty dealing with the acquired data. On the other hand laser vision sensors can overcome this problem by providing a more intense source of light with a specific wave length [40]. The filters used in these systems filter all light except a wavelength range around the laser light wavelength. This allows these sensors to perform well even when the application involves other light sources, even very bright ones as is the case of arc welding. Yu and Na [31], Nakata et.al [41] and Lee [42] researched the influence of arc light on the sensors performance. They accomplished it by varying the geometric arrangement between the sensor internal parts, resolution, materials, positioning among other variables.

An advantage of laser vision sensors in relation to other vision sensors is the possibility to sense the surrounding area of the weld itself [37].

A drawback from this type of sensors can be considered the distance between the welding wire and the place where the laser is scanning at a certain point in time. This distance depends on the geometry of the torch and the laser scanner and it can be as close as 30mm from the weld pool [18] but are usually between 50mm to 100mm ahead of the welding arc [20]. This can be compensated by software, by recording the scanned image associated to a travel position and when the torch reaches that position, that set of data is used. This implies the existence of a buffer to store the groove profiles and also requires the motion to start before the arc strike in order to assure that scanning was performed on the entire groove to be welded. For both these adjustments to be possible, the distance between the arc and the

laser light needs to be previously measured and set into the system so it knows how much to compensate for. This distance is also referred as “sensor registration”.

Another disadvantage of this type of sensors is the joint accessibility. Sometimes the parts to weld are of small dimensions or of constraining geometry which the laser sensor has difficulties reaching. Other times the hardware gets in the way of the torch/sensor head [23].

The high cost of the sensor equipment makes it less attractive than the other seam tracking systems [23]. As the years have been passing and this technology is evolving, it is also becoming cheaper. Adding to this, the fact that this type of sensor can provide more features than just the ones required to perform seam tracking means that they are becoming more attractive and widely implemented.

2.1.5.1 Light Source Types

For laser vision sensors in welding applications, there are two main light source types, spot and stripe. As a spot of light is brighter than a light stripe (considering that the source has the same power characteristics) it has a better signal-to-noise ratio and is less susceptible to suffer influence from the arc light [20].

In a spot type of sensor, also called *Laser Displacement Gauge*, the laser light beam is projected into the object and viewed by the camera located inside the sensor casing.

The stripe sensors are greatly influenced by arc noise and the data requires more time to be processed. Despite this, this type of sensors are more commonly used than the spot ones in welding automation. The spot sensor requires the projected light to be moved in order to generate a profile. This implies that the spot sensor has moving parts inside which the stripe sensor does not require [43]. All this makes stripe sensor more expensive but with a simpler structure when compared to the spot sensor [31].

A variation of the spot sensor is the circular light, although this one has much fewer applications. Examples of this type of sensors are the lasers from Oxford Sensor Technology [44]. This sensor is described later in section 7.1.1.2. Xu el al [45] developed a seam tracking system based on a circular (3D) laser sensor which provided not only with seam finding and tracking capabilities but also surface flatness detection.

2.1.5.2 Principle of operation

The operation principle for both the spot and stripe sensors is based on the triangulation principle. The triangulation principle states that if at the two vertices of a triangle, the side and

two angles are known, subsequently the third vertex can be calculated using straightforward trigonometry. Many authors have described the principles of optical triangulation [13, 46-64].

Curved surfaces tend to have a substantial amount of scattered reflections in different directions and so the acquired image needs to be carefully analysed so it does not generate measurement errors [33]. Another issue to have in consideration is the possibility of shadowing to occur. When shadowing occurs there is a region of the part that is being examined that cannot be seen by the camera. It is important when designing the system to eliminate, if possible, any shadowed areas.

Laser vision sensors are sometimes defined as 3D sensors. Using the consecutive 2D images acquired by the CCD and triangulation methods in conjunction with the position where each individual scan was performed provides the 3rd dimension [40]. The use of 3D sensors allows the acquisition of the object geometry, feature and object location, inspection and navigation. In welding automation it can be used to determine weld features such as volume, thickness, length and height. It can also allow the detection of weld defects such as surface porosity, undercut, misalignment, excess concavity or convexity, under filled grooves [65, 66].

2.1.5.3 CCD versus PSD

PSD stands for *Position-Sensitive Detector* and was first used by Wallmark in 1957 [67]. These detectors were the first to be applied in laser vision sensors. The PSD are analogue detectors in which principle of operation is based on a current that is generated in the detector resistive layer. The detector has two outputs (x1, x2) in opposite sides of the resistive layer and the difference in those two values reflects the light position in the detector (see Figure 2.5). The value of current is influenced by the light intensity that reaches the detector. The PSD will show the centre of the average intensity of the received light. This is often the source of the problem when using this type of detectors as due to secondary reflections the received light is larger than the light beam itself and it will greatly influence the end result of the measurement. PSD's is also very sensitive to surface conditions, so if there is a change of colour or texture in the target, the light spot shape and intensity will change misrepresenting the conditions. Unfortunately, these reasons and some other not referred may cause this type of detector not to perform as expected

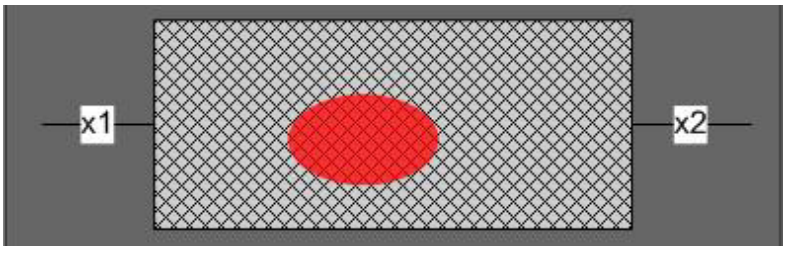

Figure 2.5 – 1D PSD block diagram

In more recent years CCD camera technology was implemented for the laser vision sensors. CCD cameras are made out of grouping tiny individual light gathering elements.

A big advantage of the CCD detectors when compared with the PSD is the fact that they can measure a much greater range of surface types and colours with high accuracy. When using PSDs the sensor alignment with the target was crucial to achieve good results. The use of CCDs reduced the need for careful alignment. Although CCDs are still somewhat susceptible to secondary reflections, this issue was greatly reduced with the introduction of this technology. Unlike PSD that averages light intensity to determine the light centre, CCD bases its detection solely on light intensity regardless of light quantity throughout the sensor. This fact makes out of the two, CCDs the best option when dealing with black or shiny targets. This kind of target still presents problems for the CCD detector but not nearly as much as for the PSD [55]. In the case of this type of detector, the intensity distribution is processed and the pixel with the highest intensity is selected. This way the detector becomes less influenced by stray and secondary reflections. Some CCD based sensors use closed loop control to adjust the laser power in order to compensate for changes to the target surface reflectiveness. With the use of CCD detectors it became possible to reduce the power class of the laser. Most sensors using PSD technology would require a class III laser and with the CCD detectors only a class II laser is required [55].

Both sensors use solid state technology and are packed into standard integrated circuits.

The use of CCD detectors rather than PSD ones greatly increased the performance of triangulation sensors as they overcome most of the performance problems presented with the PSD.

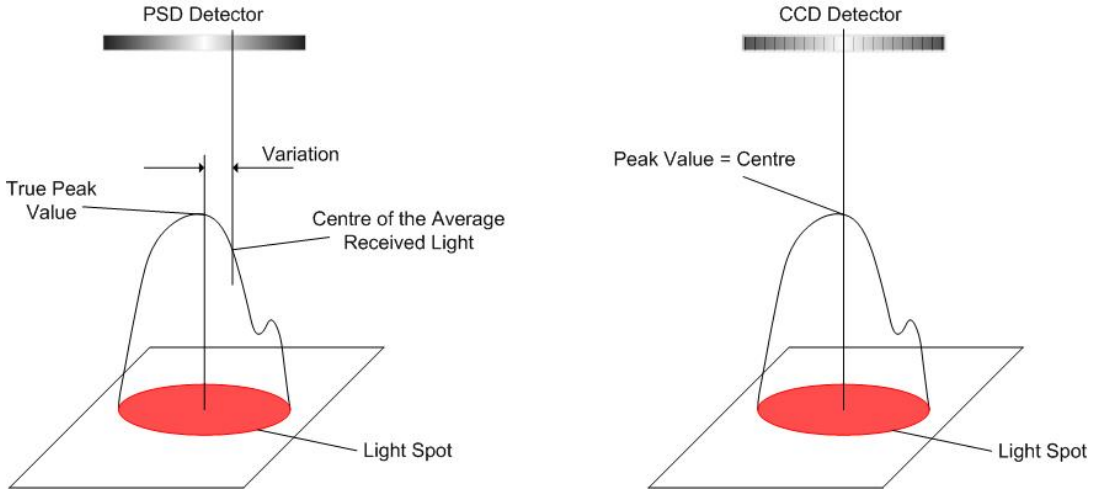

Figure 2.6 – Comparison between PSD and CCD light detection methods.

An in-depth review and comparison of camera technologies can be found in [68].

2.1.5.4 Feature Detection

Feature detection from the scanned image is the fundamental part in the use of laser vision sensors. The features can be detected using various approaches, including template matching and fitted lines. Both have their advantages and disadvantages.

Unexpected or missing features in a weld groove can cause feature detection problems. If an unexpected previous bead or a tack weld are within the field of view they may cause the feature extraction algorithms to have unexpected behaviour and outputs. When this occurs the algorithms may detect a different joint shape or even not detect a weld joint at all. All this makes the recognition algorithms complex and feature extraction more complicated than may be perceived at first.

When extracting data from the intensity images it is necessary to account for the noise contained in the image. The noise can be caused by arc light, spatter, specular reflection, ambient lighting, colour or condition varying surfaces or other sources. Regardless of the source it will invariably interfere with the profile light. The use of filters such as Gaussian, median or other weighted filtering techniques, applied to one or two dimensions can help minimise data noise.

2.1.5.5 3D Laser Scanner (EXAscan™)

The EXAscan™ is a product from Handyscan 3D™ which is a handheld laser scanner. This scanner works in stereo due to two laser stripes being projected onto the object to be measured. The two arrays of light projected onto the object form a cross shaped light. Handyscan 3D™ (Figure 2.7) does not require to be placed at a fixed location from the object nor it has any other positioning limitation. Although it requires that reflective targets are positioned in the object. These targets work as random reference points which allow for the free movement of the scanner without loss in the scanning capability. An example of an object with the targets placed can be seen in Figure 2.8.

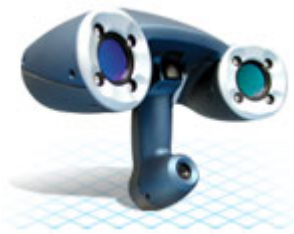

Figure 2.7 – Laser 3D Scanner from Handyscan 3D™ [69].

Figure 2.8 – Handyscan 3D™ Scanner with targets in the object [70].

2.2 Weld Control

An established welding system includes a skilled welder and either manual or semi-automatic welding equipment. Achieving a fully automatic welding system is not as simple as is often thought, since the tasks the welder performs are quite complex and somehow intuitive. In a traditional system the welder performs as the “adaptive control” module in the close-loop control. The welder, besides manipulating the welding equipment, has to observe and listen carefully to the welding so, based on his experience, he can decide on which changes need to be implemented. It might be thought that these functions can simply be replaced by the installation of a camera and a microphone. In fact, due to the harsh welding conditions and the instability and complexity of the welding process, this is not straight forward.

In order to achieve full automatic control of the welding process, the process needs to be broken down in small control tasks. From those smaller tasks a few will be described in depth, as laser vision sensors can be utilised to sense the weld geometry in order to feed the respective control algorithms. Those tasks are: seam tracking; multi-pass welding; adaptive filling; and bead profile assessment. This last both in terms of detecting the surface profile and defect detection.

2.2.1 Seam Tracking

Seam tracking is the ability of following a certain feature, in the case of welding application to follow the weld joint. This is the fastest growing segment of the automated welding market according to Berge [23]. The main reason for that is to allow the automated system to be flexible to deal with the part tolerances and inaccurate placement. A range of sensors can be used to perform seam tracking. Through-the-arc sensing and laser vision sensors are most commonly used to perform this task. Extensive work has been performed in order to develop seam tracking tools. In terms of the use of through-the-arc sensing Lopes compiled the most significant work performed reported in his thesis on“Arc-Based Sensing in Narrow Groove Pipe Welding” [28]. Extensive research has been reported in terms of laser vision sensors applied to seam tracking in [47, 71-80]. For this reason this area of expertise is not going to be described in great detail although some areas will be highlighted.

2.2.2 Adaptive Filling

Adaptive fill control can be easily achieved when using a laser vision sensor as it detects the joint dimensions and this data can be used to select the welding parameters required to fill the joint in the intended manner [23]. It may be possible to extract the groove features from the acquired images, though this is highly complex and costly [23].

2.2.3 Bead Profile Assessment

In multi-pass welding the appearance of insufficient fusion between layers causes the weld to weaken at that point. When it comes to transmission pipelines it means the fault is going to be detected by the post-weld NDT which occurs only when the groove was completely filled. This will imply that corrective measures will have to be taken. This generally means grinding down the finished weld until below the fault position and then rewelding it. This rewelding process will be performed manually. Insufficient fusion is only an example of the defects that may require rewelding if it remains undetected until the NDT testing phase. These corrective measures are time consuming and in many aspects costly. When the defect detected occurred in one of the early layers, the repair work will be major. This shows how important it is to be able to detect defects in real-time. Any measures that can prevent the need for rewelding have clear advantages. A way in which a welder can foresee that an incomplete fusion or other defect may occur is by looking at the previous bead shape. If the bead shape shows strong signs of convexity or other undesirable bead configuration the welder can take corrective actions when welding the next layer. When moving on to a fully automated system where the welder does not exist or has little control over what is happening, the system needs to be able to detect the bead shape and act accordingly.

The lack of reliable sensors able to detect bead geometry in real-time and at the same time capable of working in the harsh welding conditions has so far impaired the development of fully automatic welding systems. As Miller *et al.* points out [81], attempts have been made in the past to achieve this but their success was limited by the sensor limitations. Miller *et al.* used laser ultrasonic technology sensor to determine the weld reinforcement distance. With this information they developed and demonstrated a monitoring and control system for butt welding [81]. This shows that the development of new technologies in sensor technology opens new doors to achieve full automation of the welding processes.

The laser vision sensor cannot detect all types of weld defects. The moment of detection occurs depends on the sensors location in relation to the weld torch. In the case where the sensor is scanning the groove ahead of the torch, the only defects that can be detected are the ones in the previous layer surface. This means that if any defect is identified it can cause one of two actions to be taken. One, in case a minor defect can be corrected by the laying of the next layer with special parameters. Then, the welding parameters are adjusted in order to

compensate for the situation. On the other case, in which the defect is too severe and cannot be corrected by laying the next layer, the weld process can be stopped at that moment and the welder can grind down the defect and reweld it to match the rest of the weld. Alternatively, a flag can be set indicating that at that position a defect occurred and corrective measures can be performed at a more opportune time. This allows for an early stage correction of some if not most of the problems avoiding extensive post-weld repair works.

In spite of extensive research in the change detection systems there is little evidence of industrial application. A few commercial systems have been developed [82, 83] but no published literature has been found on the successful use of these systems in the industry. Most of the reported systems have in fact been tested merely in laboratory by introducing artificial perturbations, such as water or loss of gas flow, and showing the system can detect these perturbations. However, there has been very little published work correlating the industrial production defects and the changes in the measured parameters. In fact, in one of the few studies found, almost no correlation was found between the defects found with inspection and the analysis of changes in the corresponding current and voltage signals [84].

2.2.3.1 Defect detection

Weld defect detection is a difficult task to perform even to an experienced welder. The flexibility of possible shapes, their intensity, working conditions, all this makes it hard to detect defects in the weld. The welders obtain the sensibility necessary to detect the majority of them with time, as they gain experience. Teaching this sensitivity to a machine is an important task when aiming to achieve an automated process.

Nikiforova and Fedotov [85] developed a filtering method to reduce data noise, quantify images and detect their polygonal approximation. They have developed this method to detect weld shape and structure based on digital post-weld X-Ray images. This method cannot prevent defects but it can detect then efficiently post-welding, according to the authors.

2.3 Automated Systems

What is Automation? Automation is a difficult term to define; it can be defined as mechanisation taken to the next level where sensing and decision making capabilities are embedded into the system. Senses can be given to the system through the use of electrical sensors and the intellect can be provided by the control algorithms that run in the computer/microprocessor running the system. The system's intellect is limited to the extent of the control algorithms coverage and that is usually limited to what is initially developed. Unlike the human being, it cannot learn from experience. The expression "… cannot learn from

experience" is not entirely true as that is what artificial intelligence is. In this case the use of artificial intelligence was not explored.

What is the difference between *Automation* and *Mechanisation*? Mechanisation is by definition the use of machines to perform tasks previously performed manually. The same definition can be applied to automation with one difference; mechanised equipment needs to be controlled by a person as it holds no "intelligence". On the other hand an automated system has sensors and "intelligence" which allows the machinery to perform the task by itself. By "intelligence" can be understood the capability of using the sensed working conditions to decide on the action(s) to taken by means of the control algorithms. The aim of mechanisation is to help performing a task while the aim of automation is to use equipment to release the human operator so he can perform other tasks. Both automation and mechanisation are usually utilised either to improve the workers working conditions and/or productivity and the final product.

2.3.1 Automated Welding Systems

What is Automated Welding? According to Berge [23] "… automated welding is any welding process where certain motions of the welding arc are manipulated by a machine, rather than a person." This is a vague definition as it is unclear if is referring to mechanisation or automation. As explained before mechanisation and automation are similar concepts but are not the same and when talking about welding applications these terms are often confused. Another example of confusion in relation to this terms is given by Eichhorn [25] when he states that "fully mechanised welding in which, unlike partial mechanisation, the movement of the heat source, that is to say the welding head, along the joint is carried out and controlled mechanically." and that "automated welding where, in a fully mechanised welding process, the positioning of the parts to be assembled on the welding machine, and their removal when welded, is effected mechanically.". Though this was written in 1985 these concepts are still being used nowadays. In welding applications, as well as in many others, automated welding does not mean only robots. Some automated systems use other types of welding machines. Welding is a unique process that cannot be compared to other processes as the number of variables in the system is abundant and its combinations are endless. This makes the welding process complex to automate.

Why Automate? Besides the usual reason, cost savings, there are other also very important reasons such as: reliability; reduction of human error, fatigue and safety; and repeatability [86-88]. According to Berge [23] the appropriate use of automated systems can increase productivity two to four times compared to the initial values and at the same time improve weld quality and consistency. The productivity is increased by the increase of weld quality, meaning fewer repairs, repeatability, and reduction of the process idle times. All this

increases the competitiveness of a company. Automation reduces the amount of welder/operator intervention in the process reducing the possibility of human error and the need for such experienced and skilful welders. This helps to overcome the growing problem of lack of qualified welders [23, 25, 89], since it will be possible to replace them by welding technician or operators

Automation obviously has drawbacks, automated systems have for example difficulties dealing with inconsistent parts geometry. Nowadays with the increasing capabilities and use of sensors, the systems are becoming more tolerant to inconsistent parts, but the problem increases as the level of automation decreases and the system is less likely to be able to detect the problems. Among the possible problems that may occur, unexpected gaps, joint positioning, and lack of appropriate cleanliness are some of the most common when it comes to welding applications [23].

To perform a weld, a set of steps need to be followed either if it is manual, mechanised or automated welding. The set of steps to be followed depend on the welding process (GMAW, FCAW, GTAW,…) and the degree of automation being used but some basic steps are common to each other. The common basic set of steps is:

1. Start-up;
2. Setup and Adjust;
3. Start Weld;
4. Weld;
5. Stop Weld;
6. Shutdown.

These steps are subdivided into tasks and are mainly those tasks that differ from process to process and with the degree of automation employed.

In the case of the application in question, automated GMAW-P of narrow groove transmission pipelines, the tasks associated with the *Start-up* involve: connecting and powering the hardware; and starting-up the control system. The *Setup and Adjust* step include the selection of the necessary parameter values; readjusting the welding torch to ensure its correct positioning and verifying the welding consumables. On the *Start Weld* phase the start button is pressed and the control system will perform the required tasks in the correct order and timings for the weld process to start. During the *Weld* phase the control system will monitor and control the welding and motion parameters/operations to ensure the weld is performed adequately. When the control system detects the weld should end or the stop button is pressed the *Stop Weld* step starts. In this phase the control system is in charge of stopping the different subsystems. Steps 2 to 5 are repeated for the normal welding operation to be executed. Step 2 might not be necessary and the start step might not need the start button to be pressed depending on the application in question. When the weld process is finished and

the equipment is fully stopped the *Shutdown* phase starts in which the control system and the hardware will be shutdown and powered off. This is a very superficial but elucidative description of the process, as all these steps themselves are comprised of an extensive range of small tasks and procedures.

2.4 Real Time Weld Quality Assessment

Many researchers investigated the possibility of evaluating weld quality in real time based on the voltage and current signals. Most of the work accomplished was performed under laboratory conditions as it can be seen in section 2.4.1.

2.4.1 Assessment Based on Electrical and other Related Parameters

Weld quality can be assessed by the analysis of current, voltage and other signals, as for example acoustic pressure. Among the methods used for the deviation analysis are: statistical process control, analysis of process stability and by comparison with signals acquired from a good weld, sometimes called signature values.

Alfaro [90] reviewed several methods of change detection for quality evaluation. He organised the quality control in three different levels and associated to each of them the parameters which could be evaluated, see Figure 2.9. He indicated that it is possible to detect artificially induced perturbations with examples from several techniques. However, no industrial application data was presented.

Ancona [91] developed and evaluated a system based on plasma emission spectroscopy for defect detection in GTAW. He reported testing the system on an industrial environment to monitor in real-time the root pass of multilayer welded pipe joints with good results. The developed system was able to detect defects such as porosity, hollow caverns, tungsten inclusions, undercut and lack of fusion, with a minimum defect size of 3 mm. He argued that further studies would be required to apply this system to a GMAW process due to the difficulty in steadily collecting the optical emission from the arc plasma.

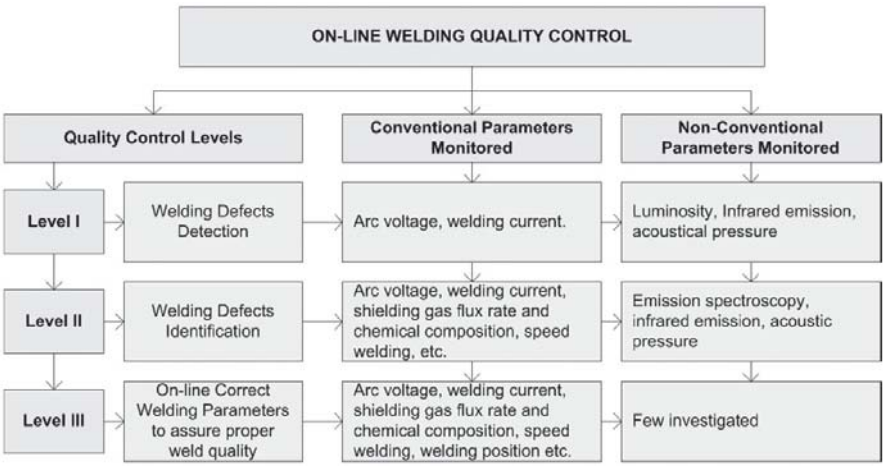

Figure 2.9 – On-line welding quality control levels [90].

Barborak and Conrardy [92] analysed frequency distribution of voltage and current in GMAW lap joints. They concluded that "*Analysis of current and voltage waveforms in mechanized GMAW of steel sheet can be used to provide an indication of waveform disturbances and shows promise for robust detection of gas flow, wire feed, and CTWD disturbances. However, no single waveform attribute can detect all common GMAW process disturbances. Waveforms associated with variations in joint gap and electrode offset are subtler, and may not be reliably detected for many applications using through-arc sensing alone*." They performed statistical and electrical analysis of the acquired signals and related the data to the monitored parameters. They managed to establish a correlation between the monitored parameters analysis, and the different control parameters.

Rehfeldt [82, 93] performed data analysis of GMAW arc voltage and current. In his experimental work he performed one normal/good weld and compared it with 7 other welds produced with artificial disturbances. He considers the results show good reliability in detecting defects due to the artificial disturbances he created, but is not able to detect the seam joint. No industrial trials were reported so it is hard to assess how well the system would actually perform in an industrial environment.

Quinn et al [94] evaluated the response of seven parameters calculated from arc current and voltage to assess response to artificially induced defects. They found a high level of reliability of detecting defects due to artificial process perturbations. They also reported that, in an industrial trial, 5 out of six defective welds were flagged as defective while 514 welds without defects were not flagged. No further information was provided on further industrial applications of this system.

Jones [84] applied statistical process control (SPC) to analyse current and voltage signal data from 41 parts over an eight week period of industrial production of earth moving machinery

parts. He found that "*There were false indications in which subgroups comprised of acceptable welds were indicated as being out of control. Missed indications, where subgroups were comprised of defective welds yet were not identified as out of control, were also frequent.*" He obtained similar uncertain results of the analysis performed to the resistance and power signals. And so he was not able to establish a strong correlation between the input data and defect detection. However, it is quite possible that more sophisticated signal analysis would have been more successful in finding defects.

Simpson and Hughes [83] used "signature images" of stability and compared them to good welds and welds with induced defects, and showed good system capability to detect defects under this circumstances. This system was named "WeldPrint" and sold commercially. Some examples of successful use were given by Simpson and Hughes [83], but there seems to be no published data on the system industrial evaluation, and the system is no longer commercially available.

Verhaege and Meldon [95] used arc voltage and current signals to test the efficiency of simple signal analysis of arc current and voltage systems and commercial ones. The simple voltage and/or current signatures and the Fast Fourier Transform systems developed were not able to detect changes cause by poor shielding under laboratory conditions, but "WeldPrint" was. No industrial experiments to test the same systems were reported.

Koelsch [96] reported on the Fanuc system to monitor welding parameters in real time. It is based on change detection for quality evaluation based on arc length and current. This system has the ability to flag values beyond the desirable value but not likely to produce defects, and to flag situations where defects will be produced. Depending on the situation flagged the system reacts accordingly. Fanuc states this is a reliable system but there were no reported scientific trials to validate their findings.

There is considerable effort in research into real time quality evaluations using electrical and arc related parameters, with demonstrated success in detecting artificially induced defects. However, there have been almost no reported evaluations of such systems in industrial production, and in the one reported evaluation, there was no correlation between signals indicating deviations from the average signals and actual defects.[84]

2.4.2 Assessment Based on Direct Vision Systems

Cook et al [97] developed a real time GTAW and GMAW surface image detection system for quality assessment and compared it with the human quality evaluation for the same weld. They reported having good results on the laboratory trials performed but no industrial experiments were reported.

Schreiber et al [98] presented an online welding quality control system based on a direct vision system mounted on a welding robot. The image behind the torch is grabbed and a stop instruction is sent to the robot controller if a defect is detected. The distinguishing feature of this system when compared to other direct vision systems is the quality learning capability, allowing it to be trained using selected seams every time a new product needs to be inspected. A quality index is obtained from a mathematical model which is used to judge if a seam is acceptable or not. They state the system works robustly under the testing conditions but no indication is made that the system works on an industrial environment.

Kumar [99] used a direct vision to detect image grey scale values and feed them to a neural network capable of discerning a good weld, overfill, underfill or no weld with a 95% accuracy overall. The sensing is performed post-weld and no field trials are yet reported for this system.

Direct vision systems have been applied to weld bead assessment in real time by looking at the weld pool bead shape. This does not give any information on bead surface profile or an assessment on its quality.

2.4.3 Assessment Based on Structured Light Systems

Koelsch [96] reported on a Motoman system to perform post-weld inspection with the Servo Robot laser sensor. The implemented system was capable of analysing the profile for concavity and convexity, toe angle, undercut and leg size over the limits and flag their location for an inspector to perform further inspection.

Reichert [100] reported the development of a pre- and post-weld inspection system using structured light at EWI. The system was designed to scan welds looking at weld quality and discontinuities/defects detection. The difference between a discontinuity and a defect is in the fact that the first will not exceed the specifications in terms of type, size, dispersal and/or location and the second will. With their system they aim at increasing weld inspection repeatability and reduce subjectivity introduced by the inspector's visual assessment perception and base it on codes and specifications objective criteria. They achieved this through the application of different techniques, such as Hough transform, line segmentation, to the bead profile data and the analysis of the reflection profile. Using the 2D profile data they able to attain information regarding leg lengths, weld width, weld toe angles, theoretical throat, concavity/convexity and plate angle. Using the weld profiles together with their x-axis information a 3D model is constructed, which allows the extraction of information regarding surface porosity and cracks, undercut and spatter. There is no indication on the paper indicating that any testing had been performed on narrow groove joints and so some of the conclusions may not be applicable to this type of joint.

White et al [101] developed a structured light vision system capable of detecting the bead shape profile of fillet and butt welds. The system is able to discern plate mismatch, plate angle, toe angles, undercut and leg length. They reported being able to measure welds ranging from 5 to 20mm wide with a 2%, or better, accuracy for the butt welds. Although this is an online system it was developed to look at single layer wide weld preparations and not narrow multipass ones as the ones aimed in the scope of this work. Their system was not designed to look at the actual bead shape or its influence in the production of defect on the subsequent bead.

2.5 State of the Art

Miller [81] stated in 2002 that "*The lack of reliable non-contact, non-destructive, online sensors with the ability to detect defects as they form and with the capacity to operate at high temperatures and in harsh environments is a big obstacle to fully automated robotic welding*". Ten years after, the statement is still valid. Research has been performed but no fully automatic welding system has been developed as no one has yet achieved a subsystem capable of detecting bead shape quality in real time especially not narrow groove welding. Electrical arc characteristics, ultrasonic imagery or weld pool images are incapable of detecting bead shapes. That can only be achieved with structured light sensors and so far no one managed to use them in a control system that is capable of evaluating the bead shape and discern if a subsequent bead can be laid without creating any defect. A clear evidence of it is the lack of published work found in this area despite the extensive research that was performed.

3 Aims and Objectives

3.1 Aims

The key aim of this work is to develop and evaluate a method of automatic assessment of weld bead shape and quality during narrow gap GMAW of transmission pipelines. This implies that the measured bead profile will be assessed to determine whether the bead shape will cause defects when the subsequent pass is deposited.

3.2 Objectives

In order to achieve this aim, the following specific objectives need to be accomplished:

- Development of a pipe welding system with software control of welding parameters and welding torch motion;
- Development and control of experimental rigs to assess the laser stripe system performance;
- Development of software to accurately measured detailed bead shape;
- Assessment of the developed system's performance, and evaluation of performance for a range of different surface conditions. Varying from shinny machined surfaces to graphite painted ones;
- Development of algorithms and software to assess bead shape which include the automatic measurement of bead concavity, convexity and asymmetry;
- Development of rules to determine to determine what bead shape is acceptable for welding over without creating any defects on a subsequent pass;
- System integration in order to produce a friendly user interface displaying the bead quality in real time.

3.3 Programme of Work

The work was devised in order to understand how the laser vision sensor works as well as the data extracted from the laser control unit. After that analysis algorithms were developed to analyse the sensor's data.

Software needs to be purposely built to facilitate the data acquisition and consequent analysis of the parameters that required testing in the scope of this work. Parameters such as depth of field of view and stand-off are initially going to be tested and evaluated. After, the influence of

the sensor position will be tested in terms of sensor rotation and tilt in relation to the weld line. Experiments will also be performed to assess the influence of surface reflectiveness on different surface conditions. Once the sensor's general performance and limitations is tested a final phase of experiments will be performed in order to access its performance when evaluating the weld bead shape and quality. Further tests will be performed to weld end sections to examine its shape and access it's applicability to discern differences between them and the rest of the weld. Different brands and types of laser vision systems will be used on some of the specimens during this work for data and performance comparison.

4 Welding Control System Development

One of the objectives of this work in its initial phase was to integrate pipeline welding motion equipment and arc welding power supplies (PSs). This goal was achieved with the development of two software packages, *Pipe Girth Welding* (SP5) and *Rig* (SP6). The *Pipe Girth Welding* software was developed in order to integrate the welding, motion equipment and a laser sensor system and perform girth welds on actual pipes (Figure 4.1). The *Rig* software was developed for a later phase of the work. This setup involves the same hardware but now the equipment was mount on a purpose built rig (Figure 4.2). This rig is capable of simulating the motion of the welding bug around a pipe.

These software packages needed to be developed in order to integrate on a single system hardware from different vendors. The vendors systems could not be set to work together and would not offer the degree of flexibility required to achieve the intended goals for this work. Before integrating them all together it was necessary to control each of them separately to understand their functioning. The software packages developed for controlling the individual systems were *Single* (SP1) and *Duo* (SP2) for controlling the power supplies, *Motion* (SP3) to control the welding head and *Laser Profile* (SP4) to acquire and playback laser vision sensor data. Once the individual systems were developed their control was then integrated on a single system. *Pipe Girth Welding* (SP5) was developed to perform welds on a band-on-pipe system. *Rig* (SP6) was developed to weld on a rig capable of welding on 360º positions, adept to simulate welding around a transmission pipe. This last software has two versions *Single* and *Dual/Tandem* depending of on the number of power supplies involved. For the final laser vision sensor control algorithms development *Analysis* (SP7) was developed. This software is not only capable of analysing data from the laser vision sensor but also data from a digital oscilloscope and data gathered from the power supplies themselves and relate the data.

4.1 Development of Software Packages

In order to be able to build an integrated system with all the hardware it was first necessary to develop individual software packages to interact with each of the equipment parts. These software packages are: *Single* (SP1); *Duo* (SP2); *Motion* (SP3); and *Laser Profile* (SP4). The first three software packages are described below and the *Laser Profile* software package will be described in section 6.1.2.1.

Figure 4.1 – Welding carrier on a pipeline pipe section.

Legend:

1. Tandem Wire Welding Torch;
2. Laser Vision Sensor;
3. Welding Head;
4. Pipe;
5. Pipe Band.

Figure 4.2 – Rig, with a curved plate setup. For legend see Figure 4.21 on page 52.

4.2 Individual Systems

4.2.1 Hardware

4.2.1.1 Computer

A laptop computer, the Sony PCG-FX109K running Microsoft Windows 2000, was used both for control software development and for program execution. This laptop computer is the centre point of the developed systems.

4.2.1.2 Welding Equipment

The welding equipment includes the mechanised motion system and the arc welding equipment. A description of the equipment used follows.

4.2.1.2.1 Power Supplies

Lincoln Electric Power Wave F355i power supplies (PSs) were used in this work. These are digital robotic PSs which can be used in constant current, constant voltage and pulse welding modes depending on the configurations within the PS [102]. These PSs are part of the robotic range of products from Lincoln Electric. They work in conjunction with the Power Feed 10 Robotic wire feeder using the "ArcLink™" protocol. ArcLink™ is an open, digital communications protocol from Lincoln Electric. ArcLink™ differs from other communications protocols as it was developed by Lincoln Electric™ for the welding industry and can be applied to a range of welding systems from manual metal arc to complex robotic welding systems [103].

The Power Wave F355i PS has a current range of 5 to 425A and a rated output of 350A, 34V at 60% duty cycle. Its physical dimensions are 372 x 530 x 437 mm and weight 45.1kg.

Figure 4.3 – Power Wave F355i power supply [104].

The Power Wave F355i PSs, which were designed for robotic applications, have no control pendant as this task is usually performed by the robot control pendant. In order to control them is possible also to connect them to a computer through an Ethernet cable. This

communication allows the pulse waveform to be tailored to the application needs using *Wave Designer*™. For a better understanding on the software capabilities and functioning the user manual or brochure can be analysed [105]. It also allows control by specially developed software, as in the case of this project. This was possible since Lincoln Electric has made the communication protocol available for this project. The ability to communicate with the PSs was made possible by the use of a DLL package previously developed in agreement with Lincoln Electric for this project [106]. The Power Wave F355i PS(s) can be used in single, dual and tandem applications. In the last two options it can be either in synchronised or unsynchronised mode. In order to use the synchronised mode the use of a phase generator (System Interface) module is required.

4.2.1.2.2 Phase Generator

The System Interface module (K2282-1) will be referred as the phase generator throughout this thesis, as that is the function it serves in the system. See Figure 4.4. The phase generator ensures that in pulsed GMAW using a dual or tandem torch, the PSs waveforms are synchronised. In this case the waveforms are in anti-phase (180º apart).

Figure 4.4 – Lincoln Electric system interface [107].

4.2.1.2.3 Wire Feeder

The wire feeder used is also part of the robotic range of products from Lincoln, the Power Feed 10R (Figure 4.5). This wire feeder communicates digitally with the PS using ArcLink™ communication protocol. The wire feeder has an inbuilt tachometer which provides accurate digital feedback of the wire feed speed [108].

The wire output speed ranges from 1.27 to 20.3 m/min and is able to feed solid wires of diameters between 0.6 to 2.4 mm. Its physical dimensions are 226x261x206 mm and weight 10.2 kg [109].

Figure 4.5 – Lincoln Electric Power Feed 10R [110].

4.2.1.2.4 Consumables

The three main consumables used to perform the experiments were the parent metal, the welding wires and the shielding gas. They will be described below.

4.2.1.2.4.1 Parent Material

The parent material used was a high strength X100 steel. This choice of steel is based on its use in several projects at Cranfield University.

4.2.1.2.4.2 Wires

The GMAW welding wire used throughout the experimental work was the 1.0 mm diameter CARBOFIL NiMo1. This wire was supplied by Air Liquide™.

4.2.1.2.4.3 Shielding Gas

The shielding gas used in the experiments was the standard BOC™ gas "Trimix™". The gas mix proportions are 82.5% Ar, 12.5% CO_2 and 5% He.

4.2.1.3 Motion Equipment

4.2.1.3.1 Welding Head

The welding head's main function is to accurately position the welding torch(es) in order to perform the weld. For this purpose a Serimax Saturmax 5 welding carrier was utilised. The Saturmax 5 is a "bug on band" system. By "bug on band" should be understood a welding carrier performing its motion around the pipe attached to a band that embraces the pipe. The carrier has three motion axes: translation (transverse to the weld); oscillation; and up/down. The welding head also includes as standard an inclinometer which allows angular position measurement around the pipe. The gain from the use of the inclinometer is the possibility to control the welding carrier's position around the pipe. By this it is the possible to place the

welding carrier at any specific location around the pipe or to home it with an accuracy of less than a tenth of a degree. Another advantage is the possibility to adjust the welding parameters according to the bug angular position. Further details concerning the inclinometer can be found in section 4.2.1.3.3.

The standard welding head can be seen in Figure 4.6. Some modifications were necessary in order to be able to accommodate one or two Cranfield tandem torches. It was also necessary to create a bracket to attach the sensor to the welding carrier (Figure 4.7). A description of the bracket and its manoeuvrability is given in section 6.1.1.2 (page 68).

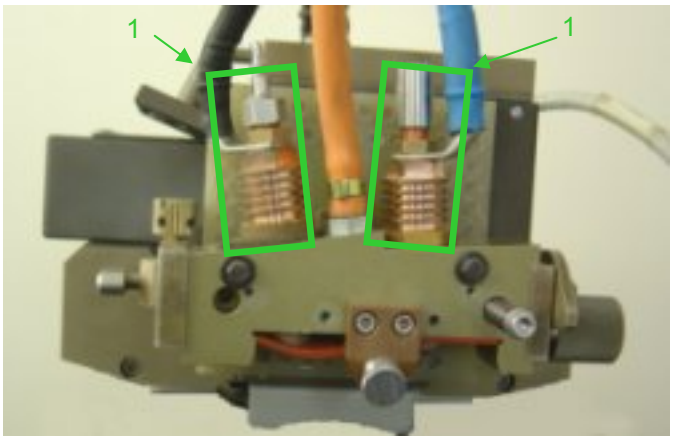

Figure 4.6 – Saturmax 5 (standard torch configuration)

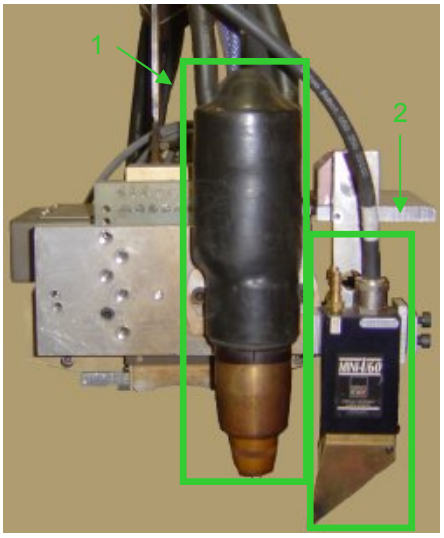

Figure 4.7 – Saturmax 5 (adapted tandem torch and laser sensor)

Legend Figure 4.6

1. Single Wire Torches.

Legend Figure 4.7

1. Tandem Wire Torch;
2. Laser Vision Sensor.

The standard welding head motion controller was specific to the Serimax head control package. In order to ease the portability of the system across different manufacturers a commercial motion controller was acquired and applied to the system. An in depth description of motion controller system is given in 4.2.1.3.4 (page 36).

4.2.1.3.2 Band-On-Pipe System

The band-on-pipe system used to perform the first part of the experimental work was the Serimax system. The system constitutes a pipe band for 38 inch outside diameter pipes and the Saturmax 5 welding head. The welding head is described in section 4.2.1.3.1. The pipe band can be seen in Figure 4.8.

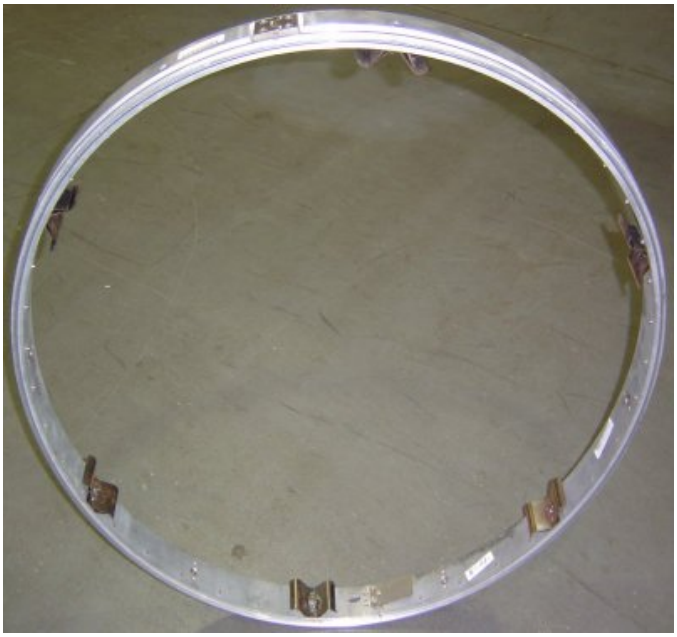

Figure 4.8 – Serimax pipe band.

4.2.1.3.3 Inclinometer

The inclinometer hardware inside the *Saturmax 5* is a SX 42400 Series tilt sensor from Sensorex. This tilt sensor has a working range of two times hundred and forty degrees and cannot retrieve values in the entire circumference. To overcome this limitation two tilt sensors are used. The use of two of these sensors combined and an algorithm to calculate the angle, allows having precise positioning control around the entire pipe.

Connections in the welding head were made to the motion controller analogue inputs so that the values could be transmitted to the computer. In order to develop the algorithm several trials were made to collect data from the sensors. These algorithms are described in 4.2.3.1.1 page 43.

4.2.1.3.4 Motion Controller

The motion controller utilised for this work is a DMC-2280 from Galil Motion Control. This equipment is an eight axes motion controller with two methods of communication to the PC, Ethernet (10/100 Base-T) and Serial Port (RS-232). The connection used during this project was Ethernet.

Figure 4.9 – Galil motion control DMC-2280 [111].

4.2.1.3.5 Amplifiers

Two types of amplifiers were used, the Galil Motion Control ICM/AMP 1900 and the Advanced Motion Controls 12A8K. The Galil amplifier (Figure 4.10) has four on board servo drivers. For the band-on-pipe phase of the experiments one of these drivers was required and two for the second phase. As two of the welding head motors have an inductance outside the amplifier working range two Advanced Motion Control amplifiers (Figure 4.11) were required for the initial phase. For the second phase of the experiments the travel direction is controlled by the sliding table motor. This new motor has a higher inductance than the welding head one, so the new motor was wired to the Galil Motion Control amplifier and one of the Advanced Motion Control amplifiers was no longer required.

Figure 4.10 – Galil motion control ICM/AMP 1900 amplifier [112].

Figure 4.11 – Advanced Motion Controls 12A8K [113].

4.2.1.3.6 Calibration

4.2.1.3.6.1 Welding Carrier Axes

In order to calibrate the three welding head axes, different distances were measured against the encoder steps moved using a measuring tape. This way the accurate length of the encoder step was obtained for each of the three axes.

During the development of the control software it was noticed that there was a physical limitation in the oscillation motion. If the oscillation width was over 5mm there was a limit to the oscillation speed. On further investigation it was observed that there was a compromise between the oscillation speed and width in this equipment. This compromise was converted into a relationship that was embedded in the control software. In order to verify the accuracy of oscillation motion, a linear resistor was attached to the main body of the welding head with the shaft attached to the oscillation arm (Figure 4.12). This resistor was then inserted in a voltage divider circuit (see Figure 4.13) and the voltage at the linear resistor was measured with the digital oscilloscope mentioned in section 7.1.1.3.

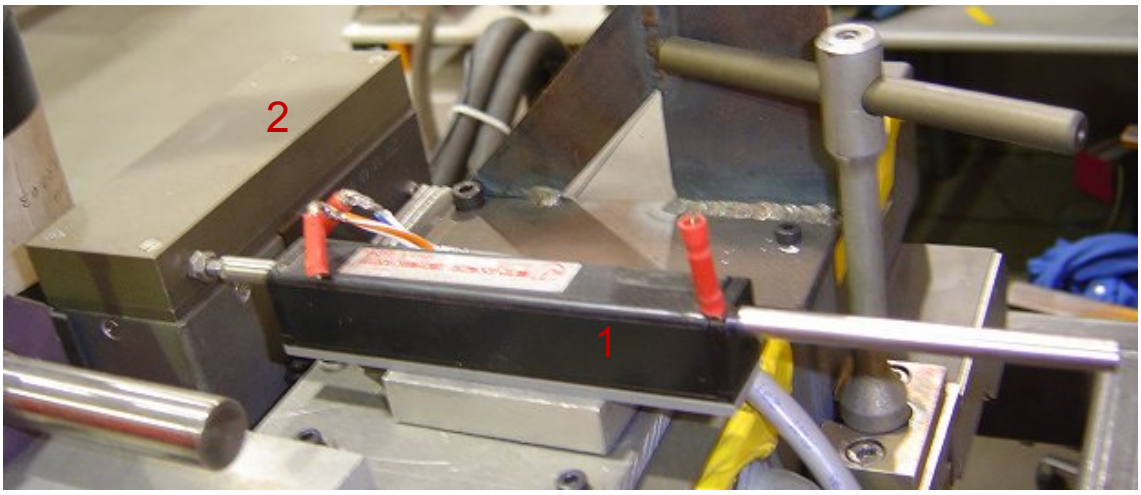

Figure 4.12 – Linear resistor attached to the welding head.

Legend:

1. Resistor;
2. Oscillation Arm

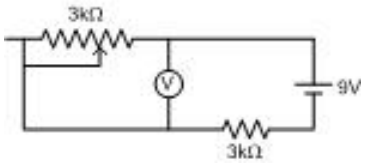

Figure 4.13 – Voltage divider circuit.

4.2.1.3.6.2 Inclinometer

The inclinometer built-in the welding head includes two tilt sensors, SX 42490 from Sensorex. In order to utilise the inclinometer the signals from both tilt sensors had to be connected to the motion controller terminals. This was achieved by a pull-down 470Ω resistor and a 4.7μF capacitor to the GND pin. From there the signals can be accessed by the computer where they are appropriately processed to obtain the welding head angular position. This was developed with the intent of controlling the parameter based on the bug's angular position around the pipe.

Each of the tilt sensors outputs a current between 4 to 20mA that corresponds to the hundred and forty degrees range that they can measure. This current is then converted into a voltage in the motion controller. The obtained voltage ranges from 1.88 to 9.37 V. The combination between the voltage range limits and the values of both sensors will indicate the welding head angular position around the pipe. The algorithm developed to achieve the angular position value will be explained in 4.2.3.1.1 (page 43). As can be seen in Figure 4.14, each of the tilt sensors covers two 140º regions. According to [114] the tilt sensor has an accuracy higher than 1º. The combination of both tilt sensors resulted in the experimentally confirmed resolution of 0.1º. This value was confirmed with a digital inclinometer that has a precision of 0.1º.

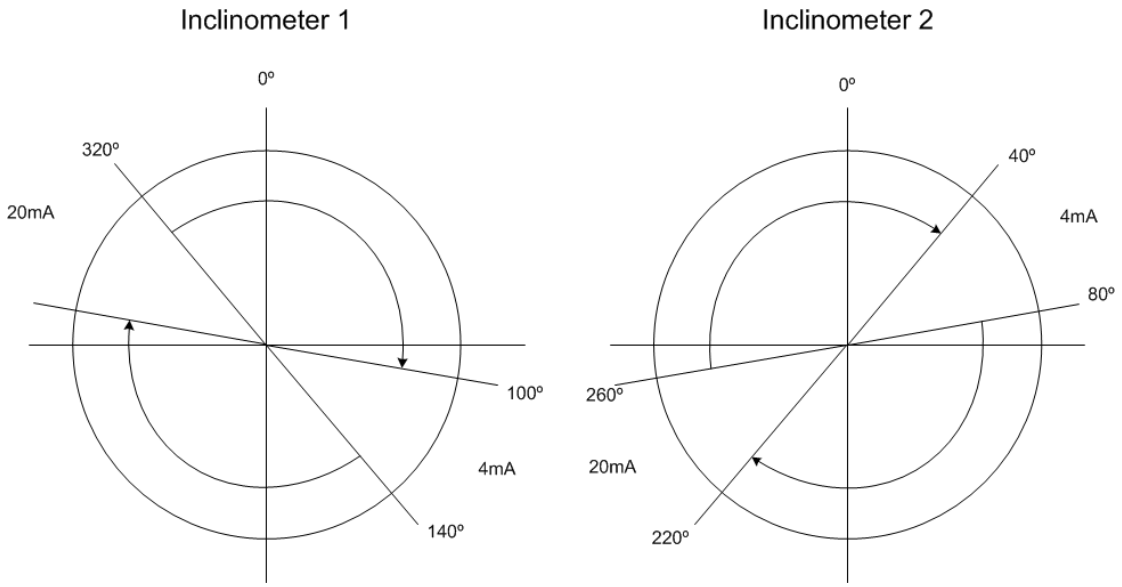

Figure 4.14 – Inclinometer coverage diagram [115].

4.2.2 Software

4.2.2.1 SP1 – Single

The *Single* software was developed during this project with the intent of controlling a single *Lincoln Electric Power Wave F355i* power supply (PS). This PS belongs to the robotic range of PSs from Lincoln Electric, and is normally controlled by the robot interface. In the absence of a robot the only available interfaces are provided by Ethernet and ArcLink™ . As was described in 4.2.1.2.1 ArcLink™ is an industry communication protocol. However, the Ethernet interface was preferred for this project as it is easier to integrate when developing a computer control system. This applies to all software packages developed in the scope of this work that use the Lincoln Electric PSs.

Before running the program, the required configuration files must be in the program directory. These files are: “Single PowerWave.ini” and a “Mode *XXX*.scm” per PS per mode *XXX* defined in the “.ini” file, where *XXX* stands for the mode number. A default file is placed in the program directory when the software is installed. Information on these files can be found in Appendix A containing the program user manual.

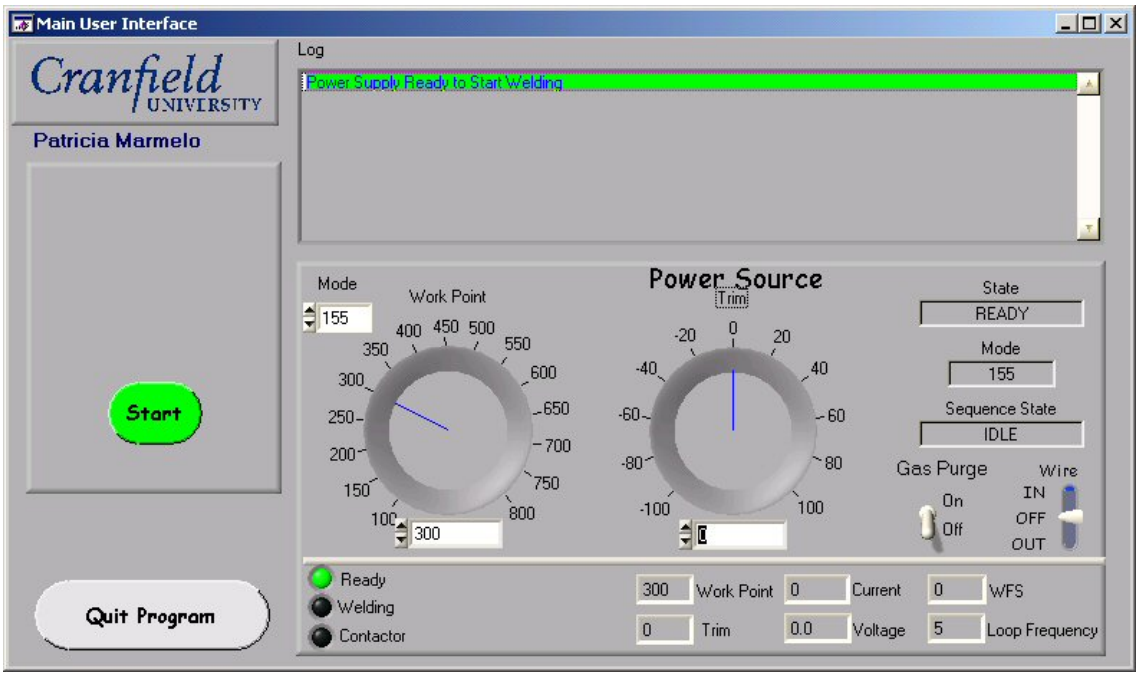

Figure 4.15 – Screenshot of the *Single* software immediately after start-up.

When started, the program will initiate the communications with the Power Supply and will place them in ready state. While in ready state changes to the *Work Point*, *Trim* and *Mode* can be performed. The *Work Point* (WP) is the Wire Feed Speed (WFS) in inches per minute.

By setting the WFS all the other welding parameters are set according to the predefined synergic curve. To better understand the concept of trim and its operation the manufacturer's manuals should be consulted [116]. In this application a representation of the range is displayed in terms of percentage, [-100%; 100%] *Mode* refers to a predefined set *of* rules which are defined to control the performance of the PS for the different stages of the welding process. It can be configured in the "Mode XXX.scm" file. These rules concern among other things the pre and post purge duration and the ability to jog the wire or purge gas. This file configuration is documented in section 3.2 of the software user manual (Appendix A).

In ready state it is possible to purge the gas and jog the wire in or out to prepare for the next weld. It is also possible to change the mode that is going to be used in the PS. Two other operations are possible: start welding and quit the program. To start welding the *Start* button needs to be pressed and the weld sequence will then be started. While welding, gas purge and wire jog functions are disabled as they cannot be performed during welding. When the *Start* button is pressed it is replaced by a *Stop* button that when pressed will halt the weld. When the *Quit Program* button is pressed the PS is shutdown. This implies that the communications are disconnected and the user interface terminated.

This software has two ways of setting the values in the numerical input objects (controls). One that is most intuitive is by sliding the knob objects with the use of the mouse. The other is by double clicking in the control to generate an on-screen numerical keyboard. This allows for a more precise value entry in case the user is having difficulties updating the value with the mouse movement. A description of the program features and functions can be found in Appendix A containing the program user manual.

4.2.2.2 SP2 – Duo

As was explained in section 4.2.1.2.1 the Lincoln Electric PSs have no user interface and one had to be developed in order to operate them. *Duo* software was developed in the course of this project to control a set of two PSs. Unlike the *Single* software, the *Duo* is capable of handling two PSs at the same time. The operation can either be in Dual or Tandem mode according to the process requirements. In the Dual mode there is no synchronism between the PSs and in the Tandem mode their waveforms are synchronized.

Before running the program three or more configuration files must be in the program directory. These files are: "Dual PowerWave.ini" or "Sync PowerWave.ini" depending on the torch type (Dual and Tandem respectively). And a "Mode *XXX*.scm" file per PS per mode defined in the ".ini" file used. Information on these files can be found in Appendix B containing the program user manual. In Appendix B a description of the program features and functions can be found.

The philosophy behind *Duo* is the same. For further information concerning it please refer to section 4.2.2.1.

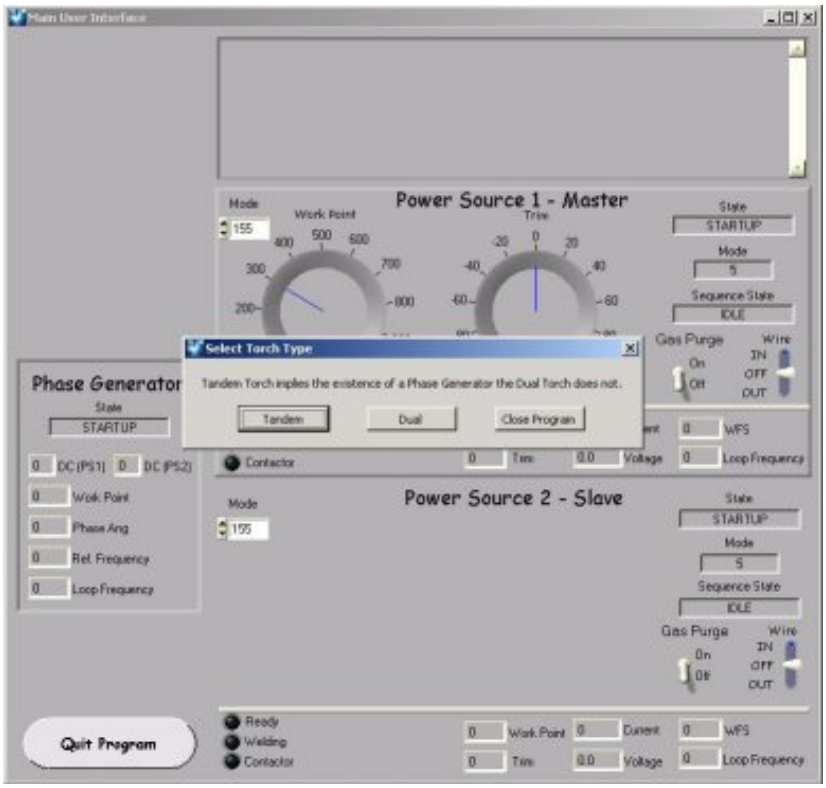

Figure 4.16 – Screenshot of the *Duo* software right after start-up.

4.2.2.3 SP3 – Motion

Motion is a software package developed in this project in order to control the *Serimax Satrumax 5* welding head. The *Motion* software was developed around the *Saturmax 5* welding carrier to work on a band-on-pipe system (Figure 4.1). This welding carrier is supplied with its own motion controller and configuration software. Due to some feature restrictions and also to be able to be vendor independent it was decided to have a commercial motion controller controlling the welding head and other parts of the system. The selected motion controller is the Galil Motion Control DMC-2280. This equipment is described in section 4.2.1.3.4.

In the *Motion* software it is possible to find all the required controls to interface with the welding head. Some of the objects in the screen can be executed while the system is on stand-by and some other can be used either while welding or stand-by. A description of the program features and functions can be found in Appendix C.

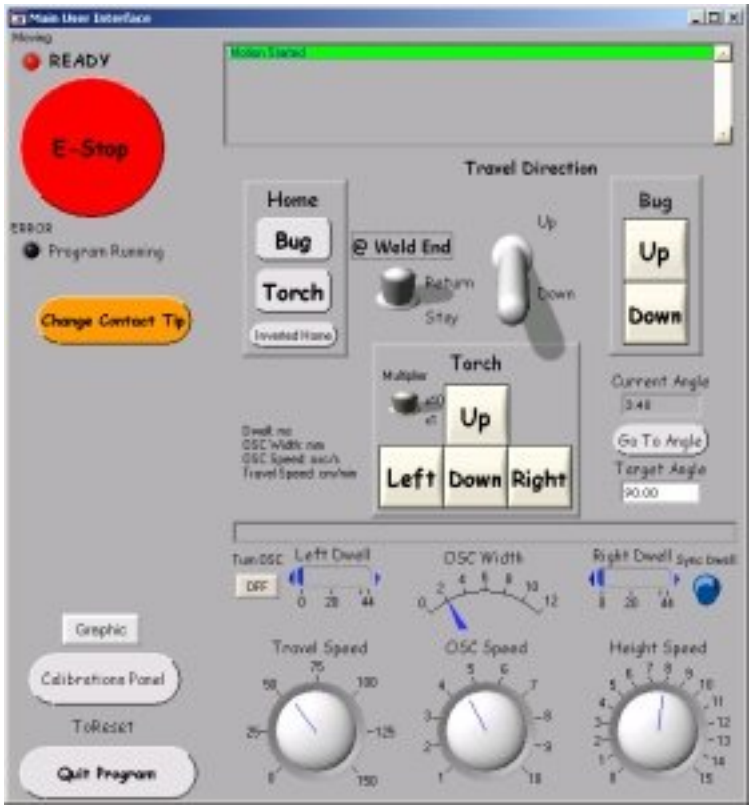

Figure 4.17 – Screenshot of the Motion software at start-up waiting for the weld carrier to reach the home position.

4.2.3 Control Algorithms

4.2.3.1.1 Tilt Sensor

The built-in inclinometer on the welding head is comprised of two tilt sensors. Each of these tilt sensors has two working ranges of hundred and forty degrees each and cannot retrieve values in the entire circumference. To overcome this issue two tilt sensors are used. Each tilt sensor is an analogue sensor which returns a value of current that is converted into a voltage with a resistor at the motion controller analogue inputs. The use of two of these sensors combined with an algorithm to calculate the angular position, allows precise positioning around the entire pipe. In order to develop the algorithm several trials were performed to collect data from the sensors. The *Function Graph* (Figure 4.19) shows some values calculated from the original data retrieved from the sensors. Based on the graphic and other trial tests, an algorithm to calculate angular positioning was developed. The functions will be explained next:

The *F* values are calculated from the lower current range limit of each tilt sensor. The angle value is added or subtracted to the limit value depending on the current growth direction (see

Figure 4.14). The equations required to calculate the inclinometer angles and the *F* values can be seen in Equation 4.1 and Equation 4.2 respectively.

As it can be seen in Figure 4.19 the *F* values do not represent the angular value in all the positions. Depending on the position a specific *F* value has the correct angular position. Which *F* value contains the correct value is determined by a combination of other factors.

Equation 4.1

$$Range1 = MaxV1 - MinV1$$
$$A1 = ((V1 - MinV1)/(Range1/140))$$
$$Range2 = MaxV2 - MinV2$$
$$A2 = ((V2 - MinV2)/(Range2/140))$$

Where :

MaxV1 is the maximum voltage read from the inclinometer 1 at the time of calibration.
MinV1 is the minimum voltage read from the inclinometer 1 at the time of calibration.
MaxV2 is the maximum voltage read from the inclinometer 2 at the time of calibration.
MinV2 is the minimum voltage read from the inclinometer 2 at the time of calibration.
Range 1 and 2 are the amplitude of values given by the inclinometers.
$A1$ is the angle calculated from the voltage of tilt sensor 1.
$A2$ is the angle calculated from the voltage of tilt sensor 2.

Equation 4.2

$$F1 = 100 - A1$$
$$F2 = 140 + A1$$
$$F3 = 40 - A2$$
$$F4 = 80 + A2$$

Hardware calibration is very important for the algorithm accuracy as it is its base. At any time the system can be recalibrated if the results are considered inaccurate. When the inclinometer is calibrated the new voltage values are stored in the welding project file associated to the welding head number and updated in the software. The new values are stored in the *MinV1*, *MaxV1*, *MinV2*, and *MaxV2* to be used in the voltage range calculations.

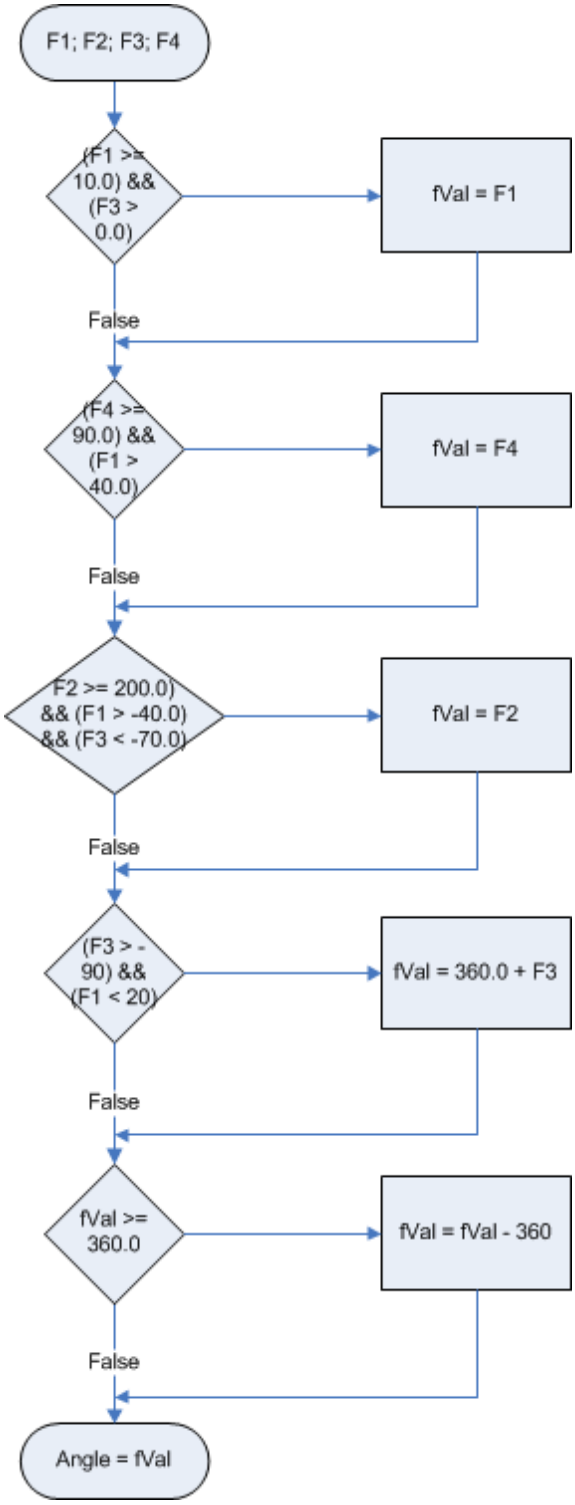

Figure 4.18 – Inclinometer angle determination algorithm.

The inclinometer angle is then calculated based on the algorithm shown in Figure 4.18. With this algorithm a straight line which relates the real angle to be measured with the angle calculated by the algorithm was achieved.

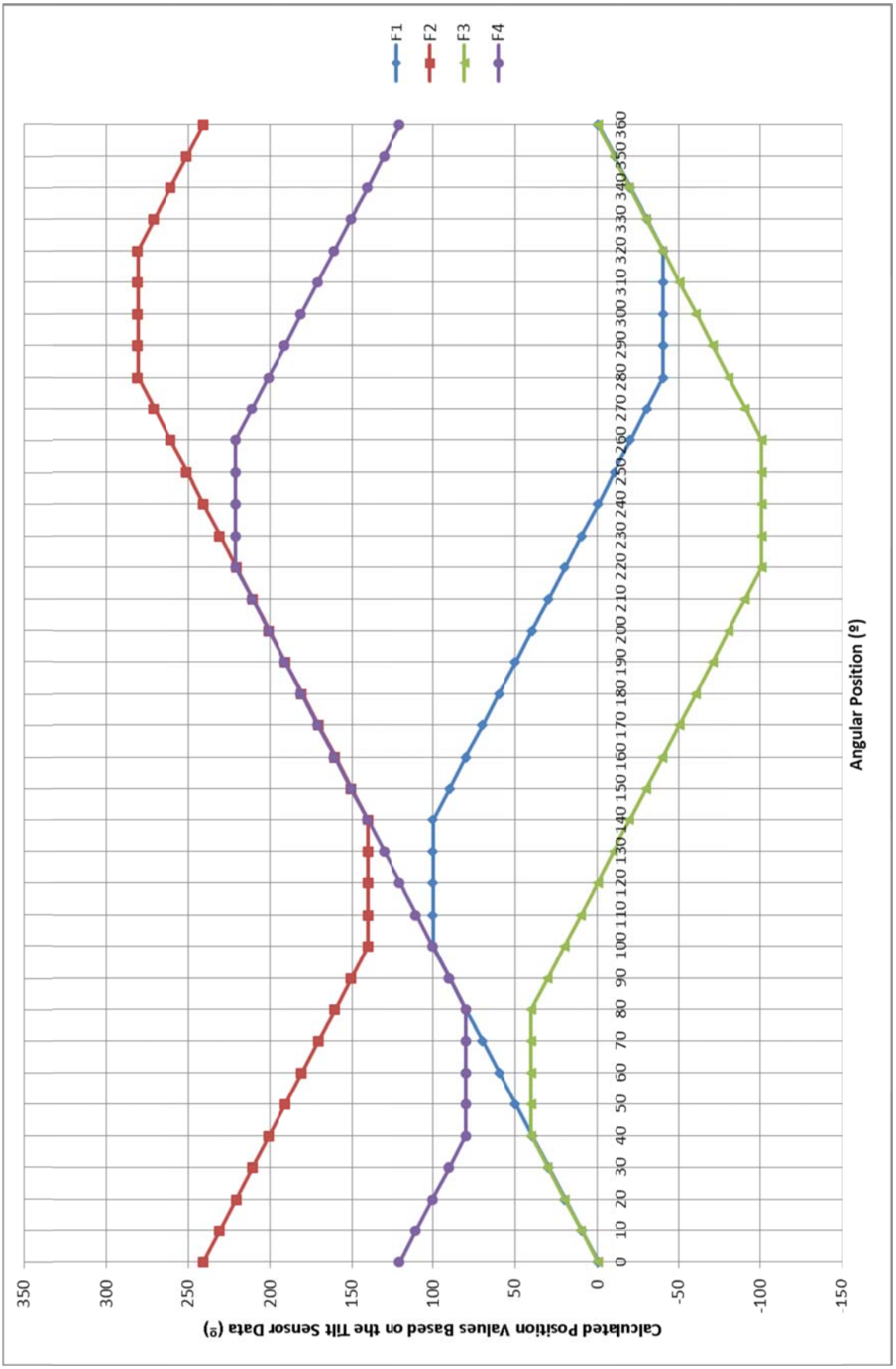

Figure 4.19 – Tilt sensor *F* Values (F1, F2, F3 and F4).

4.2.3.2 Oscillation Dwell

Oscillation dwell is the time spent in the oscillation extremes. The dwell is sometimes used in narrow groove girth welding [117]. The maximum dwell at the end of the oscillation was set at 20% of the total oscillation. This decision was based on previous experience of pipeline welding at Cranfield. With this in mind a control algorithm was developed so that based on a dwell time percentage and the number of oscillations per second the dwell time was automatically determined by the software. The dwell times can be equal (the same value in each side) or independent from each other. To be able to adjust the dwell times in relation to the oscillation speed a series of equations were developed. The referred equations are listed below.

Equation 4.3

$$OscTime = \frac{1}{SpeedOsc} = \frac{1}{nrOsc}$$

Where:

OscTime - Time it takes to complete an oscillation

SpeedOsc - Speed of Oscillation arm

nrOsc - Number of oscillations per second

Equation 4.4

$$OscSpeed = \frac{nrOsc}{\text{sec}\,ond}$$

OscSpeed - Oscilation speed

nrOsc - Number of oscillations

sec*ond* - Unit of time

Equation 4.5

$$1 = nrOsc\left(DwL + DwR + 2 \times MT\right) \Leftrightarrow MT = \frac{1}{2}\left(\frac{1}{nrOsc} - DwL - DwR\right)$$

nrOsc - Number of oscillations per second

*D*wL - Dwell time on the left extreme of the oscillation movement

*D*wR - Dwell time on the right extreme of the oscillation movement

MT - Movement time from one extreme of the oscillation movement to the other

Equation 4.6

$$MSpeed = \frac{MDist}{MT} = \frac{OscWidth}{MT}$$

$MSpeed$ - Speed at which the oscillation arm moves

$MDist$ - Oscillation width

$OscWidth$ - Oscillation width

MT - Movement time from one extreme point of the oscillation to the other

Replacing *Equation 4.4* and *Equation 4.5* in *Equation 4.6*, Equation 4.7 is obtained.

Equation 4.7

$$MSpeed = \frac{OscWidth}{\frac{1}{2}\left(\frac{1}{OscSpeed} - (Dwl + DwR)\right)} = \frac{2 \times OscWidth}{\frac{1}{OscSpeed} - (Dwl + DwR)}$$

$MSpeed$ - Speed at which the oscillation arm moves

$OscWidth$ - Oscillation width

$OscSpeed$ - Oscilation speed

DwL - Dwell time on the left extrem of the oscillation movement

DwR - Dwell time on the right extrem of the oscillation movement

4.3 Pipe Girth Welding

The initial part of the work was developed with the welding head mounted on a band, making it a band-on-pipe system. For this part of the work a group of three software DLLs were created by the partners in the industrial project that this work is related to, as part of the joint project. These DLLs were to be an intermediate layer between the hardware and the control part of the program. They worked as an interface between the motion controller, the power supplies and the laser control box and the control software. They were initially used, however, several practical issues arose, and after numerous attempts at achieving control of the equipment using them, it was decided that the DLL's for the motion controller and the laser control box should not be used. To name a few of the issues that arose, the following can be highlighted: inability to run the motors continuously with the motion DLL, and generation of errors in the motion controller which required the controller to be frequently restarted. It was also restricted in terms of functionalities, one of which that proved to be quite relevant, the angular position detection. On the other hand the laser DLL was slowing down the program execution, and would frequently crash the program while starting up the laser communications. It would not retrieve any data from the laser control unit in case the sensor

was not able to acquire a perfect profile. The DLL used to interface with the power supplies worked with no major issues, and in any case had been provided by the project partners under a confidentiality agreement between that partner and Lincoln Electric. The motion controller communication protocol and requirements are provided with the equipment, and the necessary data from the laser vision sensor was made available under a confidentiality agreement. As a consequence of that only the control algorithms are present in this document and not the code. The initial SP5 – "*Pipe Girth Welding*" software was developed using all three DLLs and a second one was developed using just the power supplies DLL. The initially developed SP5 software will not be described as it was not used to perform any of the experimental work. The SP5 second approach shares numerous features with the SP1, SP2, SP3 and SP6 (Rig) developed in the scope of this work. The shared features will not be described; they will be grouped by software package that contains them. The specific ones to this software will be the only ones to be described.

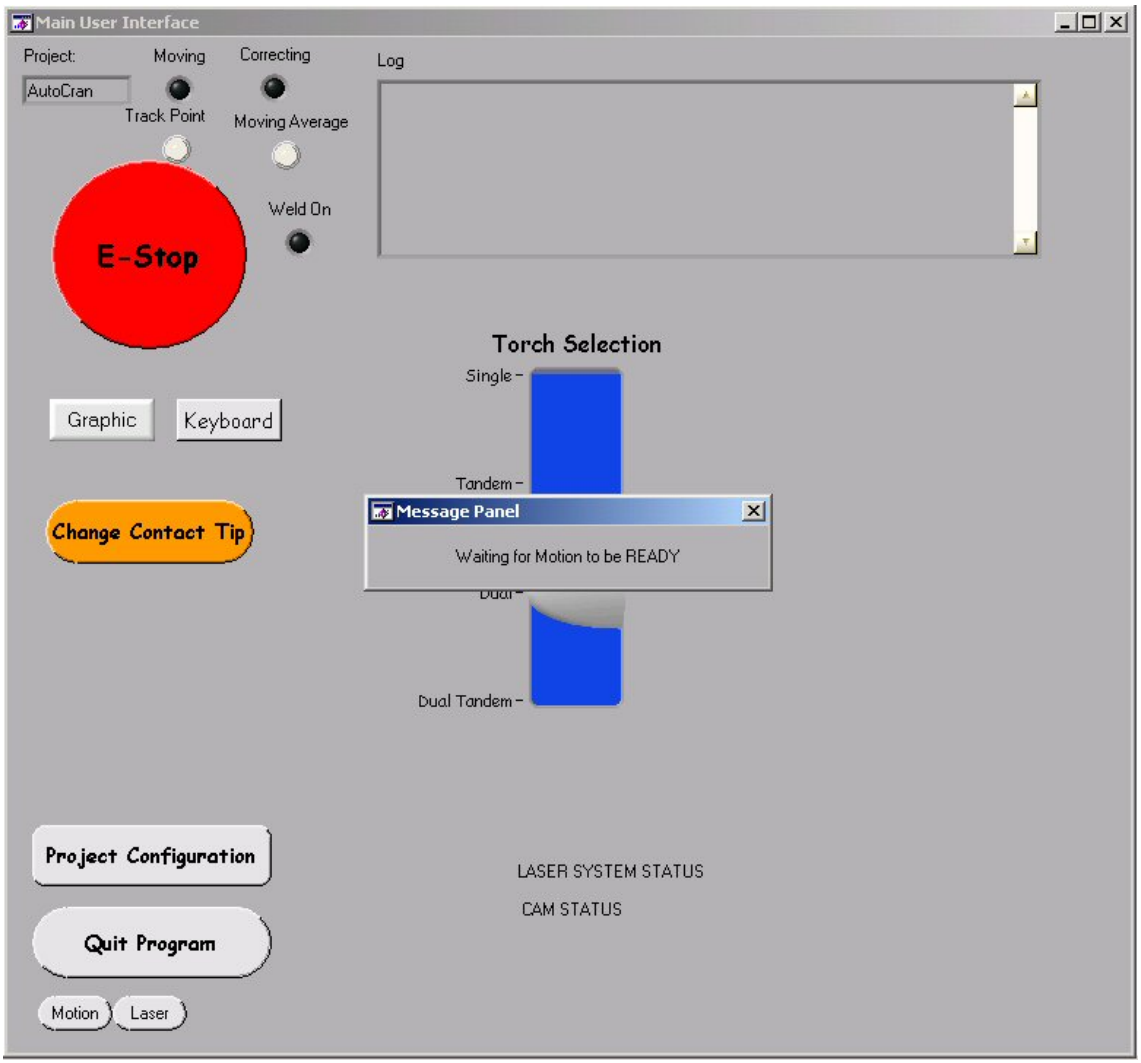

Figure 4.20 – Screenshot of the *Pipe Girth Welding* (SP5) software right after start-up.

The features present in the SP5 are similar to the ones in SP6. The layout is different but the features are very similar. The first difference is the possibility of choosing the torch type when the program starts. This selection determines if one or two power supplies are to be controlled by the software. Another substantial difference is inability of selecting which sub-systems will run when the “Start” button is pressed. In this software all systems are started up as the program starts and they will all run. Emphasis was given to the laser profile visualization so the profile graph takes most of the window space. The settings are not directly accessible in the main window, they need to be visualized on a separate window that can be call by pressing the “Motion”, “Laser” and “PS” buttons in the bottom left corner of the main window. The buttons will open respectively the motion, laser and power supply controls windows. SP5 has the possibility to save project data, it includes: Project Name; Project Location; Project Start and End Dates; Operator Name; among other details. SP5 has a function to change the contact tip which rises the torch bracket to the top creating space to perform the operation and when done it returns to the previous position.

The laser vision sensor is able to scan the joint providing measurement data such as gap, bevel angle or joint surface characteristics while welding. Data coming from the vision sensor was used together with feedback data from the welding power supplies and the motion controller, in the control algorithms. The intent of these control algorithms was to perform online adjustments to the motion and welding parameters so a more stable process with high productivity was achieved. The acquired data provides information regarding the system status and was used in the adaptive control algorithms. The intent of these control algorithms is to perform online adjustments to the motion and welding parameters to compensate for variations in pipe setup. The foundations for this work are accurate monitoring and robust control algorithms. The system approach to pipeline welding includes seam tracking, torch height control and detection of previous seam shape for weld parameter adaption. A test was performed where the weld bead was not parallel to the joint to be welded and the system was able to correct the torch positioning up to the limit of its range. In the developed system the sensor was attached to the torch bracket and it was positioned aligned with the torch. So, when the torch moved, the sensor moved with it. No data was recorded for this test and as mentioned before this test setup was abandoned and the rig setup was used which brought changes in terms of hardware and software that will be described later.

4.4 Rig

The pipe on band system is not practical and quite expensive so the work was moved on to a rig. For the second stage of the work, a new rig (Figure 4.21) was designed and built. This rig was developed to facilitate tests on a wider variety of variables and in a more controllable environment. The welding head that had been used previously was adapted to this rig. The

welding head is now static on this rig and the travel motion is achieved by moving the specimen carrier underneath the welding head. The same PSs and the same vision sensor were integrated in the new system. New software had to be designed as the new rig required a new approach to the situation. The new software, SP6 – "*Rig (Single & Dual/Tandem)*", can monitor and control the PSs, motion and laser equipment similarly to SP5. SP6 has the advantage of allowing only certain elements of the equipment to be used at any given moment. SP6 is described in section 4.4.2.

4.4.1 Hardware

This experimental rig was designed with the intent of performing welds simulating different weld positions around the pipe. The sliding table was implemented in a rotating part of the rig structure which allows the welding head and sliding table to rotate to any given angle between 0 to 180º in both directions (part 2 in Figure 4.21) In order to manipulate the welding torch, the previously used Saturmax 5 welding head was fitted to the rig. As previously indicated, in this setup the laser vision sensor is attached to the welding head main body (Figure 4.22). In this arrangement, the sensor is always roughly aligned with the groove centre and does not move with the torch. The registration between the sensor and the main body is known as well as the torch position in relation to the main body. This allows for the necessary adjustments to be made to the torch positioning in order to centre the torch oscillation with the groove centre.

The motor responsible to drive the sliding table (part 4 Figure 4.21) is a Parvalux PM4C DC (24V, 5.2A, 5.9Nm) attached to a Hewlet Packard HEDS 5540 3 channel optical encoder for position control.

To perform the tests two specimen holders were used. The first holder accommodated curved plates, and the second holder was used for flat specimens. The flat table is shown in Figure 4.21 (part 4).

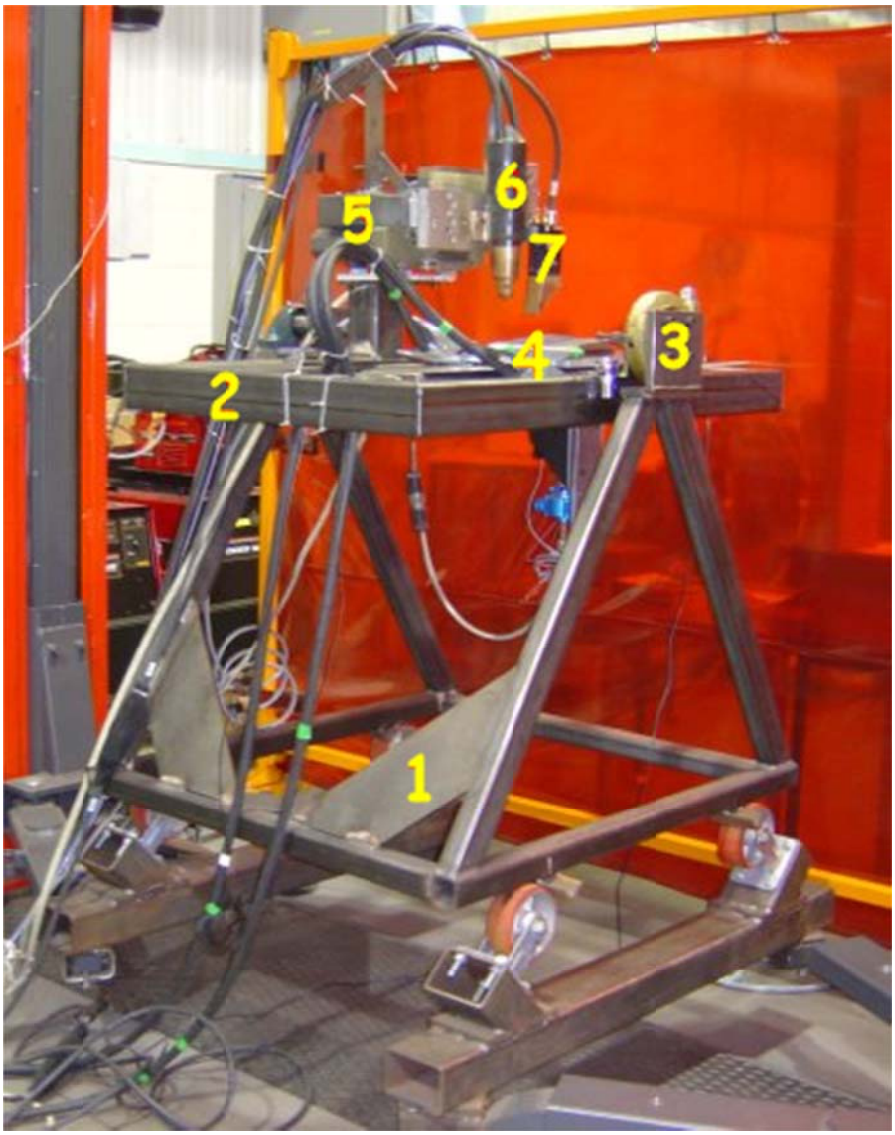

Figure 4.21 – Experimental rig with numbered items.

Legend:

1. Base Structure;
2. Rotating Table;
3. Rotation Pivot;
4. Sliding Table (x direction motion);
5. Welding Head;
6. Welding Torch;
7. Laser Vision Sensor.

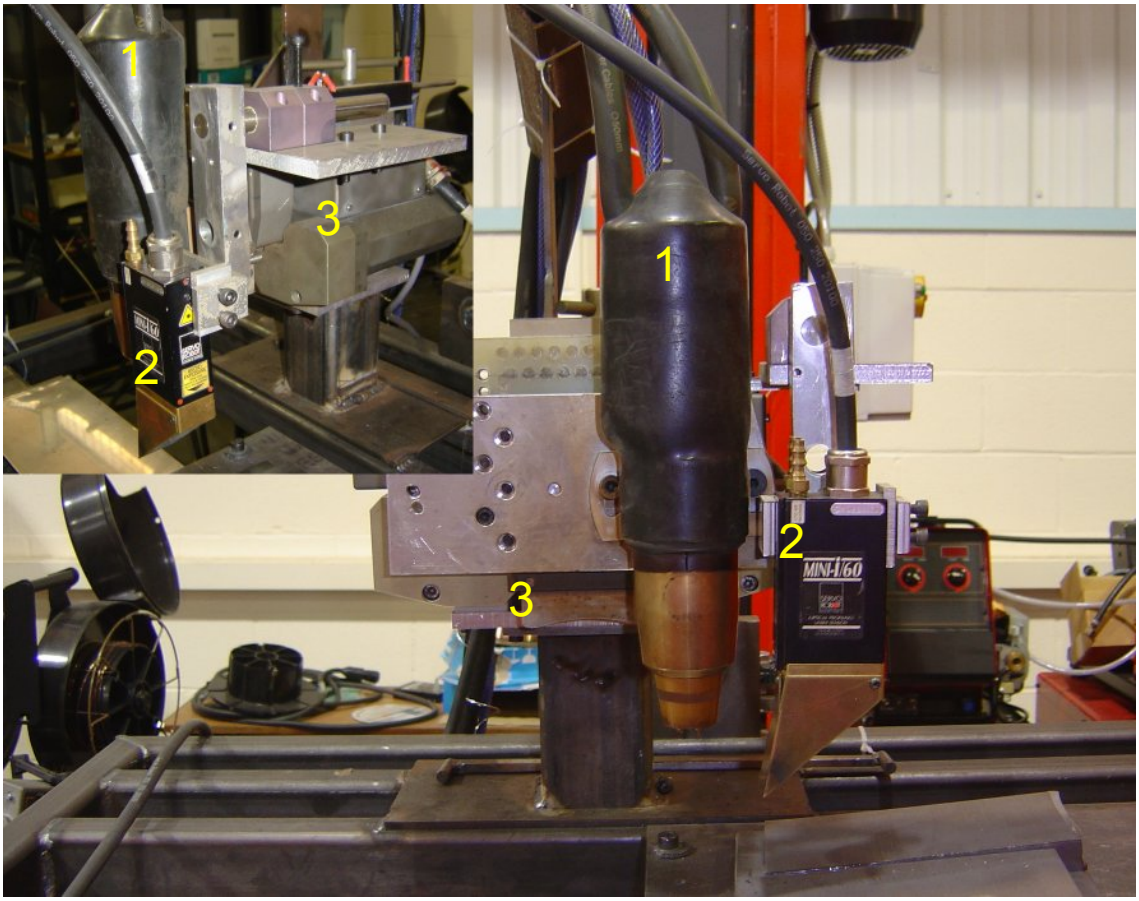

Figure 4.22 – Laser vision sensor attached to the welding head.

Legend:

1. Tandem Wire Welding Torch;
2. Laser Vision Sensor;
3. Welding Head.

4.4.1.1 Calibration

The sliding table required calibration of its travel speed which was performed in a similar way to the welding head axes. The accuracy of the calibration was of 0.5mm confirmed with a measuring tape. The length of the plate used to calibrate the travel speed was 350mm ±0.5mm which reflects 0.14% accuracy. The time required to perform the run of 30 seconds ±0.5 second reflects an accuracy of 1.67%. It can be considered that the sliding table has an accuracy of 2%.

4.4.2 Software

In this case it was easier to develop two versions of this software, one for a single torch configuration and another for a dual/tandem configuration, than having both in the same software. A full description of both versions of the Rig Software (SP6) can be found in Appendix E. A brief description of the software aims and performance is found below.

Although SP6 was fully used to perform some experiments, in the final phase of experiments the SP6 was only used for the motion control and laser scanning. The welds were performed in another rig as part of a different project and were then scanned in this rig using SP6 with the PSs disabled.

4.4.2.1 Single

The aim of this version of SP6 is to control the hardware in such a way that is possible to perform an automated weld using a single torch. A screenshot of the Rig software at startup is shown in Figure 4.23. As part of the startup process the user is asked if it is necessary to lift the torch out of a groove to avoid collisions with the welding plate during the homing process.

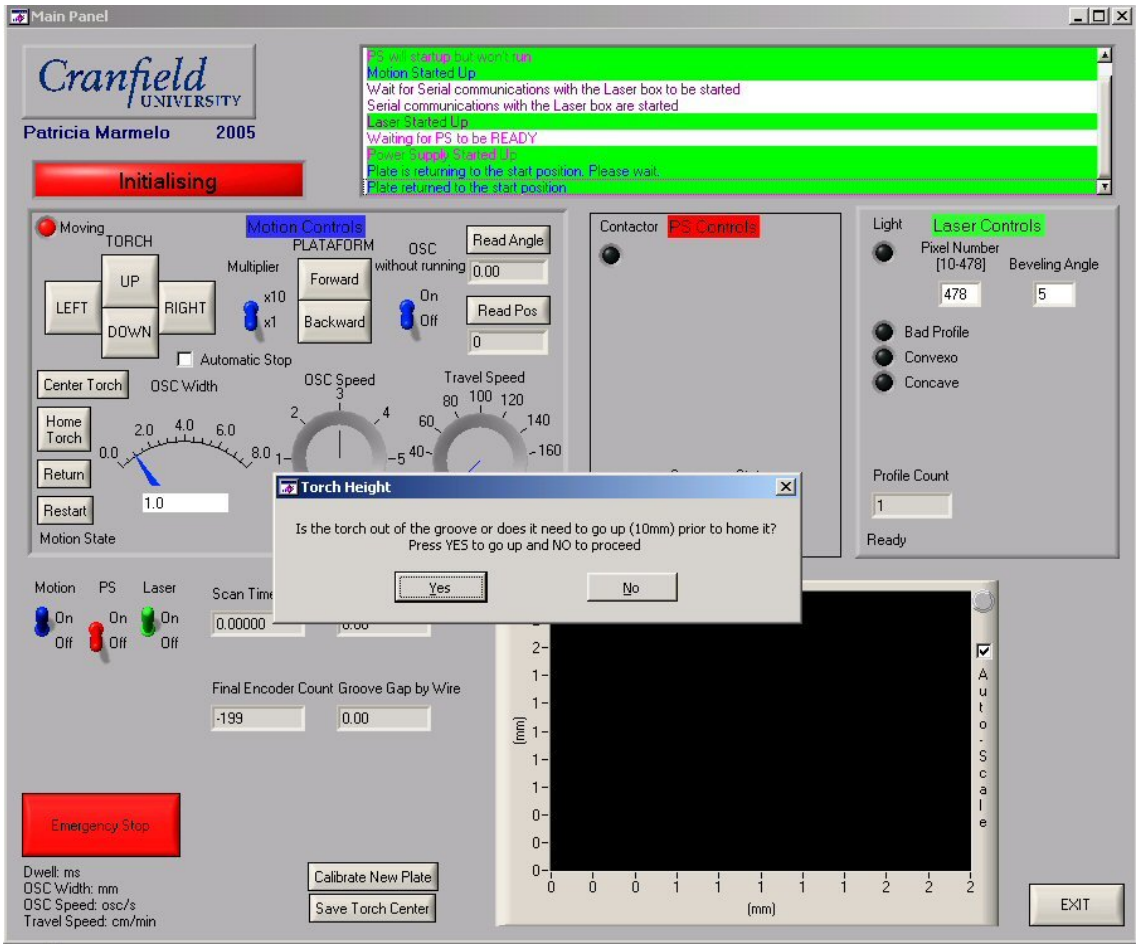

Figure 4.23 – Screenshot of the Rig (Single) software at start-up. Waiting for the user to decide if it is necessary to raise the torch before continuing.

Each of the sub-systems (Motion; PS; and Laser) is associated with a colour. Blue for the Motion objects, red for the PS and green for the Laser. Below the Motion controls area are located three switches, one of each of the referred colours. When either of those switches is

turned OFF the corresponding controls disappear and when the *Start* button is pressed that subsystem will not run. Multiple switches may be OFF at any given time. This is aimed at the need to perform some tasks independently from each other. For example if the need to scan a sample generated in a different place arises, the PS switch can be turned OFF and when the *Start* button is pressed only the motion and laser sub-systems will run allowing for the specimen to be scanned.

4.4.2.2 Dual/Tandem

The dual/tandem version of this program is capable of handling two PSs. In dual mode the power supplies waveforms are not synchronised and in tandem mode they are, by means of a phase generator. The principle and mode of operation is the same as the single version. The differences, both in terms of operation and design reflect the use of a second PS. These differences can be seen when comparing Figure 4.23 and Figure 4.24.

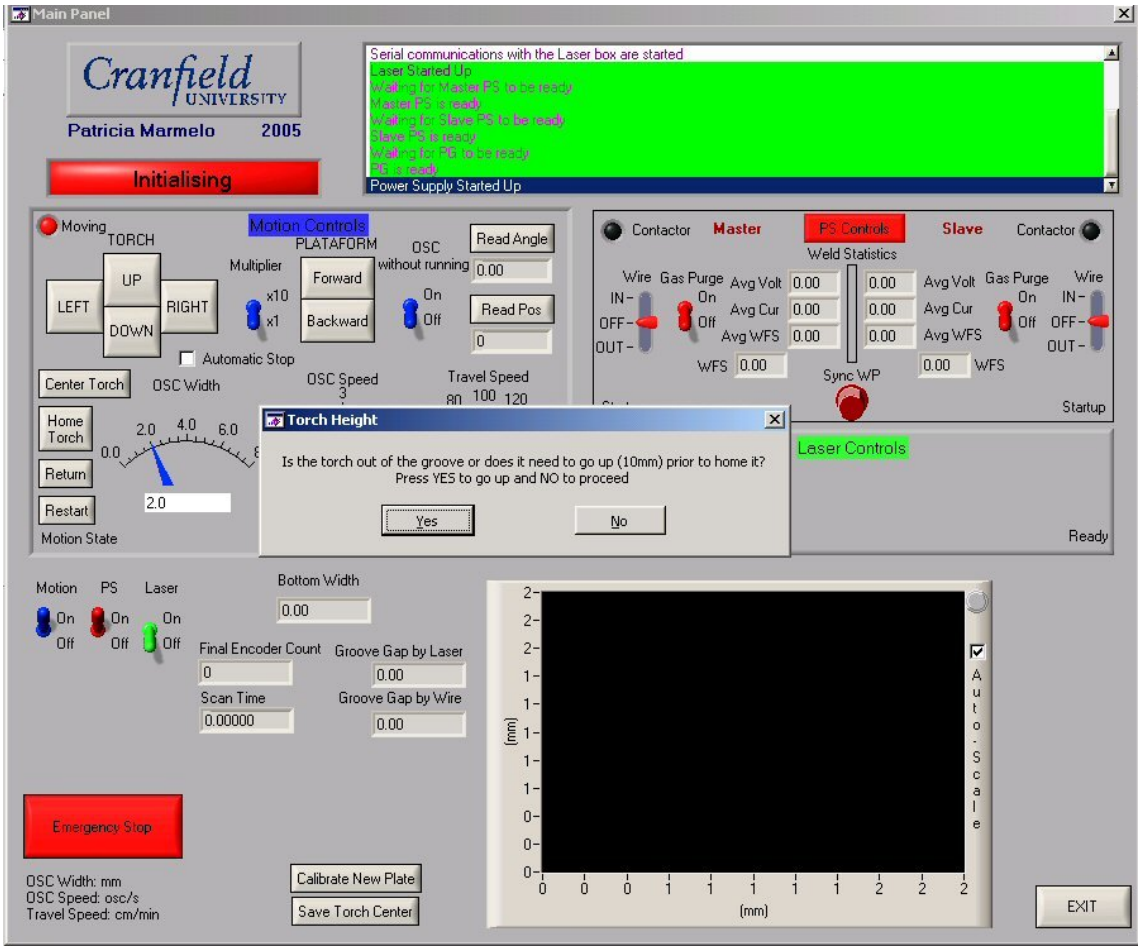

Figure 4.24 – Screenshot of the Rig (Dual/Tandem) software at start-up. Waiting for the user to decide if it is necessary to raise the torch before continuing.

For more information on either of these versions of SP6 look at Appendix E.

5 Seam Tracking and CTWP Control

The aim of the initial phase of this work was to develop a laser sensing adaptive control system for narrow groove mechanized gas metal arc welding of pipelines capable of interfacing with most of the GMAW systems used today. The implementation of this project covers the use of different torch types, adaptive control techniques and copes with parts tolerances (variations in fit-up, pipe bevelling tolerances, pipe eccentricity and wall thickness). This system was developed but no experiments were performed to validate its effectiveness despite the good initial results that were obtained.

5.1 System Development

As described in section 4, in the initial phase of this work a control system was developed to control a band on pipe welding system. This work concerns the development of an adaptive control system for narrow groove pipeline welding. The system in development is a computer based monitoring and adaptive control system, intended to improve current results. It utilises feedback data from the laser vision sensor. The sensor is able to scan the joint providing measurement data such as gap, bevel angle or joint surface features while welding. Data coming from the vision sensor will be used together with feedback data from the welding power supplies and the motion controller, in the control algorithms. The intent of these control algorithms is to perform online adjustments to the motion and welding parameters. This aims for a more stable process with higher productivity.

The system being a computer based monitoring and control system it is capable of achieving current equipment results without depending so much on user intervention. It is able to acquire data from digital power supplies, laser stripe vision sensor and motion controller. This data provides information regarding the system status and is to be used in the adaptive control algorithms. The intent of these control algorithms is to perform online adjustments to the motion and welding parameters to compensate for variations in pipe setup. The foundations for this work are accurate monitoring and robust control algorithms. This novel system approach to pipeline welding will include seam tracking, torch height control and detection of previous seam shape for weld parameter adaption.

5.1.1 Hardware

This system is divided into four major components: welding, motion, vision and computer. Each of these components will be described below. Once fully implemented they will communicate with each other through the control algorithms.

5.1.1.1 Welding

The welding system component contains the Lincoln Electric Power Wave F355i digital power supplies (Figure 5.1), wire feeders (Power Feed 10 Robotic K1780-2) and shielding gas supply (Figure 5.2). For this project these power supplies are controlled by the computer using Ethernet communication and the wire feeders and gas sub-systems are computer controlled through the corresponding power supply. The power supplies and computer exchange data bi-directionally. The computer regularly interrogates the power supplies on their status, and updates to the welding parameters will be sent by the computer to the power supplies. For more specific information about this PSs and the wire feeders check section 4.2.1.2 (page 32).

Figure 5.1 – Digital power supplies.

Figure 5.2 – Wire feed and gas equipment.

5.1.1.2 Motion

The motion system controls all three axes of movement in the welding head in order to place the welding torch(es) in the appropriate position to perform the weld. The three motion axes are responsible for: the travel around the pipe (X); torch oscillation (Y); and torch vertical displacement in relation to the pipe (Z), see Figure 5.4. The motion system is also responsible for retrieving information from two inclinometers inside the welding head. The welding head in

use is a Saturnax 5 with linear oscillation from Serimax. The motion controller used is a DMC-2280 controller together with a ICM/AMP 1900 interconnect module with internal amplifiers and an ICM 2900 interconnect modules with two servo amplifiers (12A8K) from Advanced Motions Controls, see Figure 5.3. The characteristics

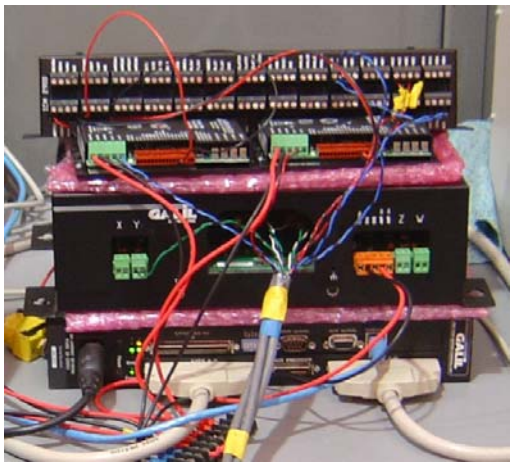

Figure 5.3 – Motion controller equipment.

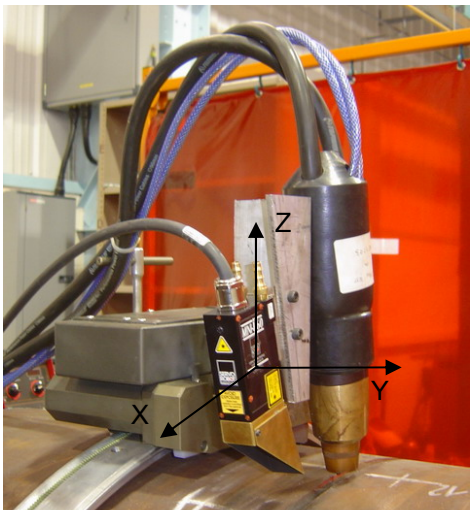

Figure 5.4 – Welding head with tandem torch and laser sensor.

5.1.1.3 Welding Head

The Saturnax 5 commercial welding head from Serimax (Figure 4.6) as stated before had to be modified to be used in this system. The present configuration can be seen in Figure 4.7, the changes were required in order for the welding head to be capable of supporting a variety of welding torches and the laser camera.

5.1.1.4 Laser

The laser system components are a laser camera, control unit and ground fault detector from Servo Robot. The laser camera is a 3D laser vision camera MINI-I 60 based on a laser stripe system. The laser camera's main physical characteristics can be seen in Figure 6.2, the camera uses a 50mW visible diode laser. Transmitted data to the control unit is 14340 points per second with 60 frames of 239 sampling points each. The control unit is pre-programmed with information related to the groove that will be scanned and sends data to the computer through a serial (RS-232) cable. More information concerning the laser sensor hardware can be found in section 6.1.1.1.

5.1.1.5 Computer

A PC acts as central controller. An Intel Pentium III 844MHz processor, 384MB of RAM memory computer running Microsoft Windows XP is being used for development purposes. The computer has the role of receiving information from the remaining parts of the system, processing it on-line with adaptive control algorithms and sending data back to the motion and welding systems with the necessary adjustments.

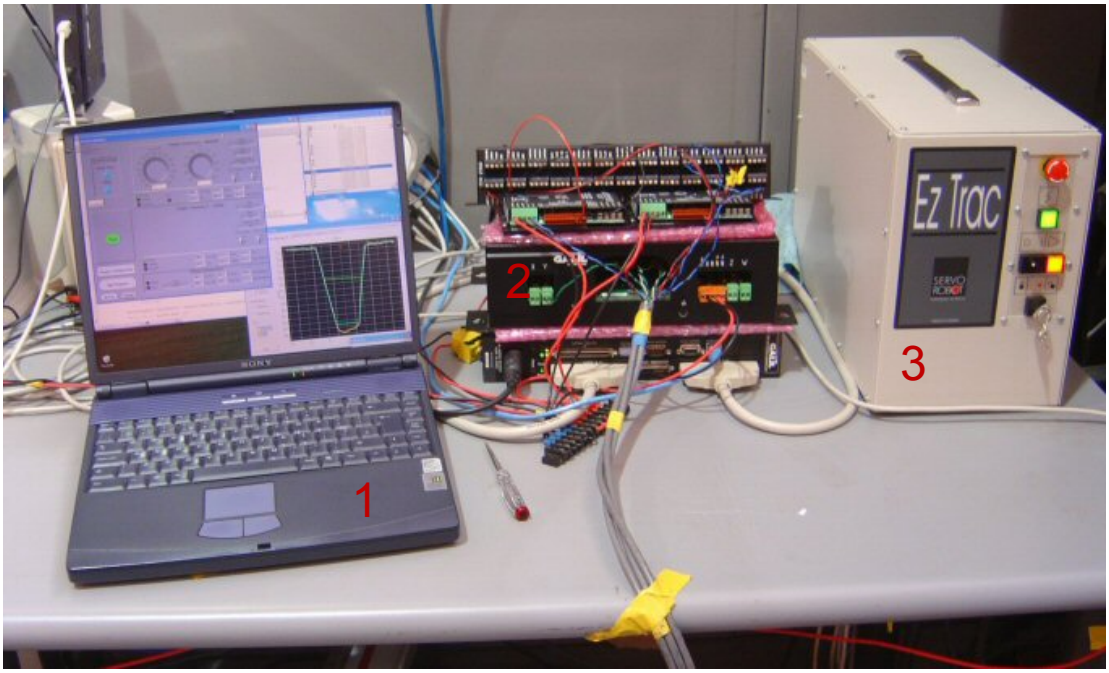

Figure 5.5 – Partial view of the system.

Legend:

1. PC (Personal Computer);
2. Motion Controller;
3. Laser Control Unit

5.1.2 Software

The user interface for this project will ultimately be a push button to initiate the welding. For the moment a User Interface (UI) was developed which is capable of controlling the system in manual and automatic modes. The manual mode was implemented in order to debug and better understand the way the hardware works. The UI in question is capable of controlling the power supplies and the welding head moving on a band.

The UI in question is SP5 – *Pipe Girth Welding Software*. A description of the features and capabilities of SP5 can be found in section 4.3.

5.2 System Performance

5.2.1 Adaptive Control

The adaptive control inputs are data retrieved from the laser control unit, digital power supplies and the motion controller. The main two control algorithms inputs are the laser and inclinometer sensors. This will track the joint and its angular position and help determine the corrective actions to be taken on the welding and/or motion parts of the system. The motion controller provides the control algorithms with accurate positioning of the three axes and the angular positioning around the pipe. The digital power supplies used have data acquisition inbuilt and are able to send that information to the computer for analysis. This information is used for feedback on the power supplies status (startup, idle, welding, error, …) and the welding parameters in order to validate the system operation, as well as for data logging.

The main tasks of the adaptive control algorithms are to perform adaptive fill, real-time seam tracking and previous bead shape recognition. These control algorithms were developed independently from each other.

One of the aims of the systems is to fill the groove with a pre-established number of layers, for that adaptive fill is required. The number of layers required to perform the weld varies with the torch type used. To perform adaptive fill the groove shape is scanned in each pass and then analysed to generate the necessary adjustments to the power supplies and welding head for subsequent passes. The groove pre-scan does not demand a run prior to welding, it occurs due to the offset between the laser head and the torch, see Figure 4.7. The data provided by the laser sensor is used together with other information to determine which weld volume should be deposited to fill the remaining groove in the remaining layers to be performed.

To perform real-time seam tracking the laser sensor is being used. It is used to adjust the oscillation width and centre point according to the groove profile. The system works in a closed loop. The flowchart representing the control loop can be seen in Figure 5.6. This work was developed to accomplish our share of the industrial project but was not applied to the PhD work.

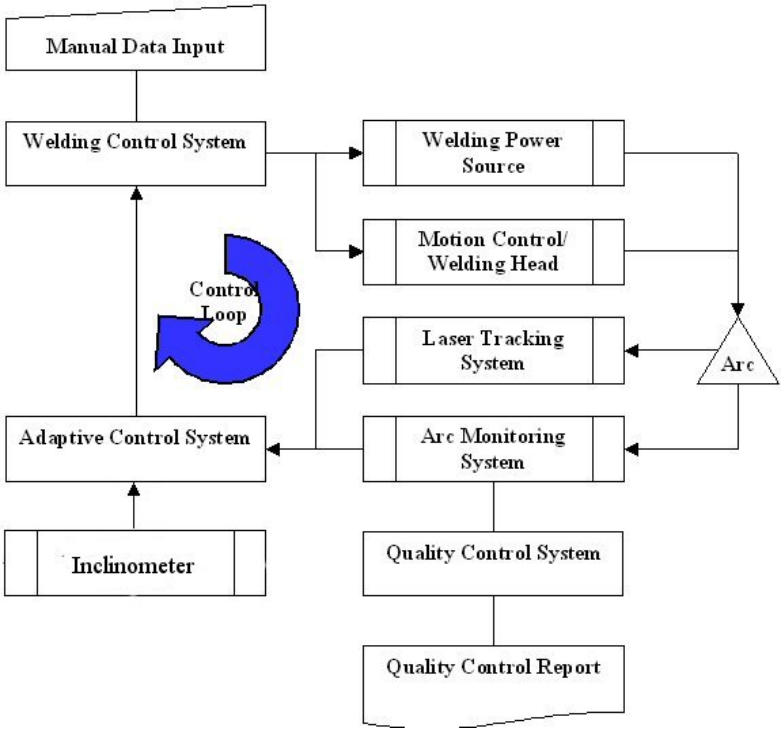

Figure 5.6 – Generic adaptive control loop to be implemented.

6 Laser Vision System Development and Performance

6.1 System Development

In order to gain control and better understand the laser vision sensor a study of the sensors hardware and software components was performed. The result of this study is found below. Once the understanding of how the system performs a simple data acquisition software was developed to interface with the equipment, acquire and playback the sensor data. The software is SP4 – "Laser Profile" which can be seen in Appendix D.

6.1.1 Hardware

Four different sensors were used in this project. The main body of work was performed using the Servo Robot Mini-I60. A Servo Robot Mini-I90, a Meta Vision Systems' MT-10/15, and an Oxford Sensor Technology CSS – Circular Scanning Sensor were also used in the duration of this work. The Mini-I60 and the Mini-I90 were available to use in the project and the choice of using the Mini-I60 was based on its resolution that was greater than the Mini-I90. The MT-10/15 and the CSS sensors were used once each and different specimens were scanned for data and performance comparison.

6.1.1.1 Servo Robot Sensors

The two sensors used from Servo Robot are from the same range of products, 3-D laser-cameras, and have similar specifications. The basic principle of operation for both cameras is an active optical triangulation principle. This principle is briefly described in section 2.1.5.2. The camera contains a 50mW visible laser diode.

Both the Servo Robot sensors (Mini-I60 and Mini-I90) were developed with the harsh welding working conditions in mind. They provide for compressed air circulation to maintain the camera within its working temperature range and clear from welding fumes inside the unit [118]. The cameras have high immunity to arc and laser (YAG and CO_2) welding environments. In both cameras the laser power control is either, automatic or manual, or a combination of both, to better adjust to the changes in the environmental conditions [119].

The sensor physical dimensions are shown in Figure 6.1, Figure 6.2 and Table 6.1.

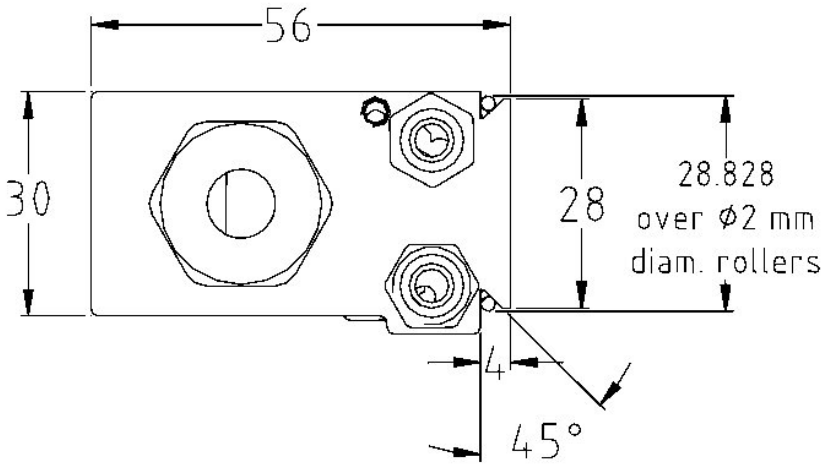

Figure 6.1 – Camera head bracket details [118].

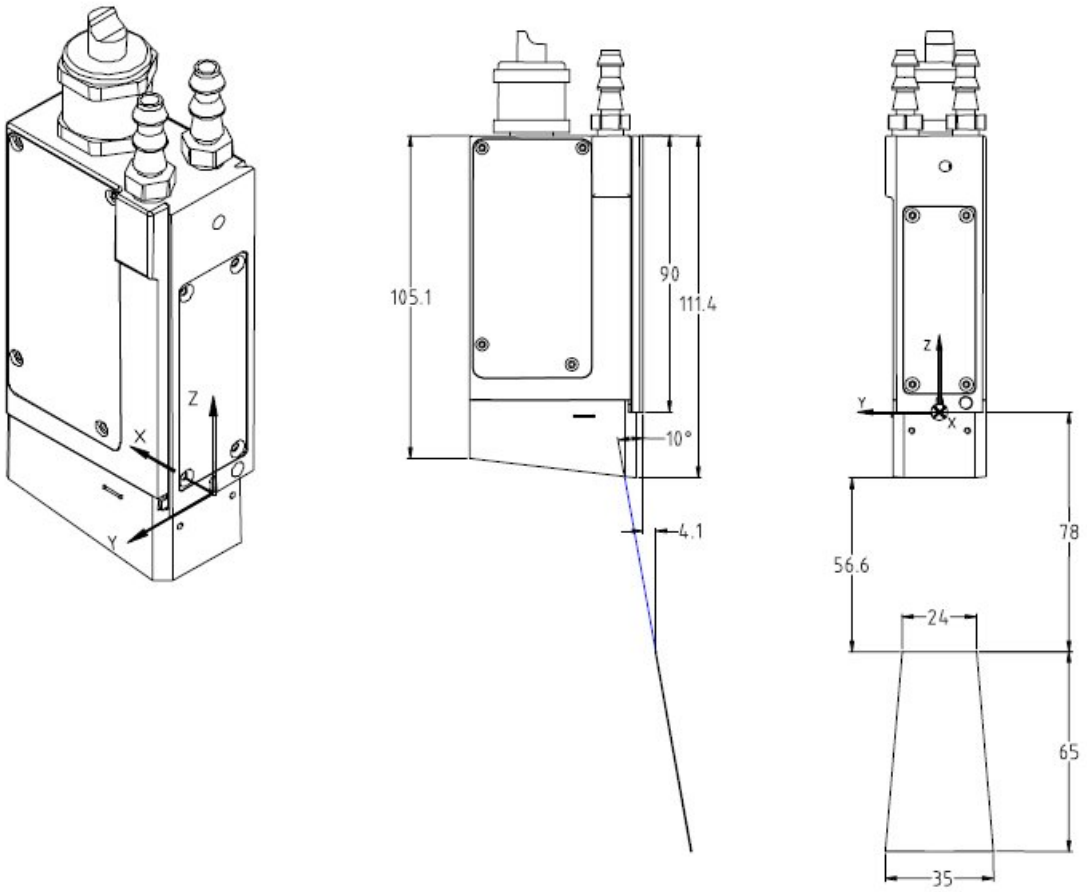

Figure 6.2 – Diagram of the Mini-I60 camera head [118].

Specification		Mini-I 60	Mini-I90
Laser Class		IIIb	IIIa
Stand-Off		56.6 mm	50 mm
Depth of Field		65 mm	90 mm
Width of View	Close Plane	24 mm	38 mm
	Far Plane	35 mm	68 mm
Resolution	Horizontal	0.13 mm	0.24 mm
	Vertical	0.09 mm	0.20mm
Data Rate		14340 points per second	
Points per Profile		239 / 478 points per profile	
Speed		60 / 30 profiles per second	
Weight		500g	
Operating Range Temperature		5º to 45ºC.	

Table 6.1 – Comparison between Servo Robot laser sensor models used.

6.1.1.1.1 EzTrac

EzTrac is the Servo Robot control unit which pre-processes the data gathered by the camera head. It can work in two different interface types: with or without the teach pendant. For this project the sensor was used without the teach pendant (Figure 6.5). All the control was performed through the laptop computer via a serial cable using RS-232c communication interface using specially developed software. To achieve this, Servo Robot made available the set of instructions which allow requesting data from the unit as well as the data format. This was achieved under a confidentiality agreement, and is not described here in detail.

The data points returned by the EzTrac are already in the Cartesian system. The information is computed based on the data extracted from the CCD image and the calibration data. The calibration data is unique to each camera and is loaded into the EzTrac control unit in the factory. A floppy disk containing the configuration data is provided with the system on purchase.

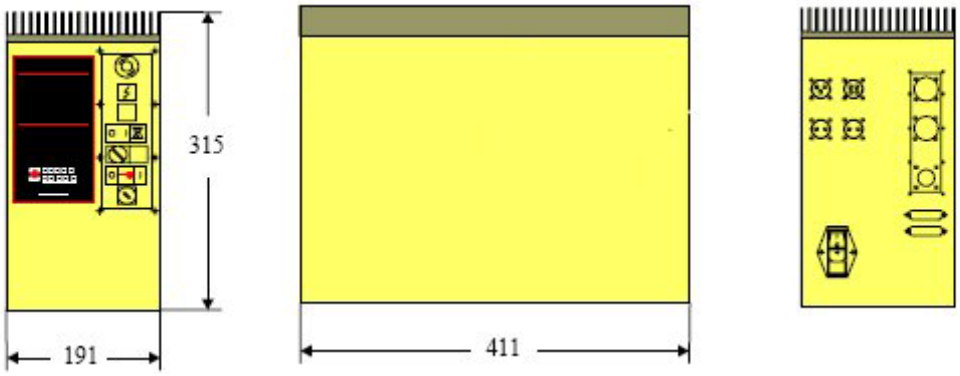

Figure 6.3 – EzTrac control unit standard dimensions and panels [120].

In order to use the control unit for this application some connectors and cables had to be prepared. In the equipment manual each of the connectors has a name/number, the same nomenclature will be observed in this document. The control unit connectors are as follows:

- CN2 – Alarm: this is an Amphenol: 97-3102A14S-2S connector. Pins 'A' and 'B' need to be shunted so an external alarm is not generated. The external alarm output signal can be used to stop other parts of the system in the event of a laser equipment fault.
- CN5 – 'USER' Serial Port: this is a D-SUB connector (DB25P) (female). Between this port and the laptop PC is connected a male (DB25)-female (DB9) cable. This cable allows the control and monitoring of the control unit and camera head from the laptop PC.
- CN6 – Teach: this is a D-SUB connector (DB25P) (male). Here is connected a DB25 (female) connector with pins 1 and 3 shunted to switch the external E-STOP input signal off. When these two pins are not connected to each other an alarm is triggered in the control unit and the laser operation is terminated. This alarm indicates an external alarm was generated by one of the other parts of the system and the laser sensor needs/should be stopped.
- CN8 – Camera: this is an Amphenol: JMS27497E16F42S connector. Here is connected the camera head cable for data transfer between the two parts of the equipment.
- CN9 – Interface: this is an Amphenol: 97-3102A20-29S connector. If pins 'A' and 'B' are not shunted, an external alarm is triggered and the laser operation is terminated. For this application there was no need to connect the external alarm to any other part of the system so the two pins were short-circuited.

The physical dimensions of the EzTrac control unit are shown in Figure 6.3 and the rear panel description is given in Figure 6.4.

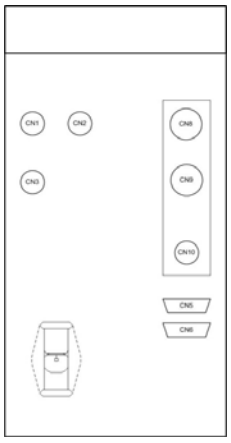

Figure 6.4 – EzTrac control unit rear panel schematic view.

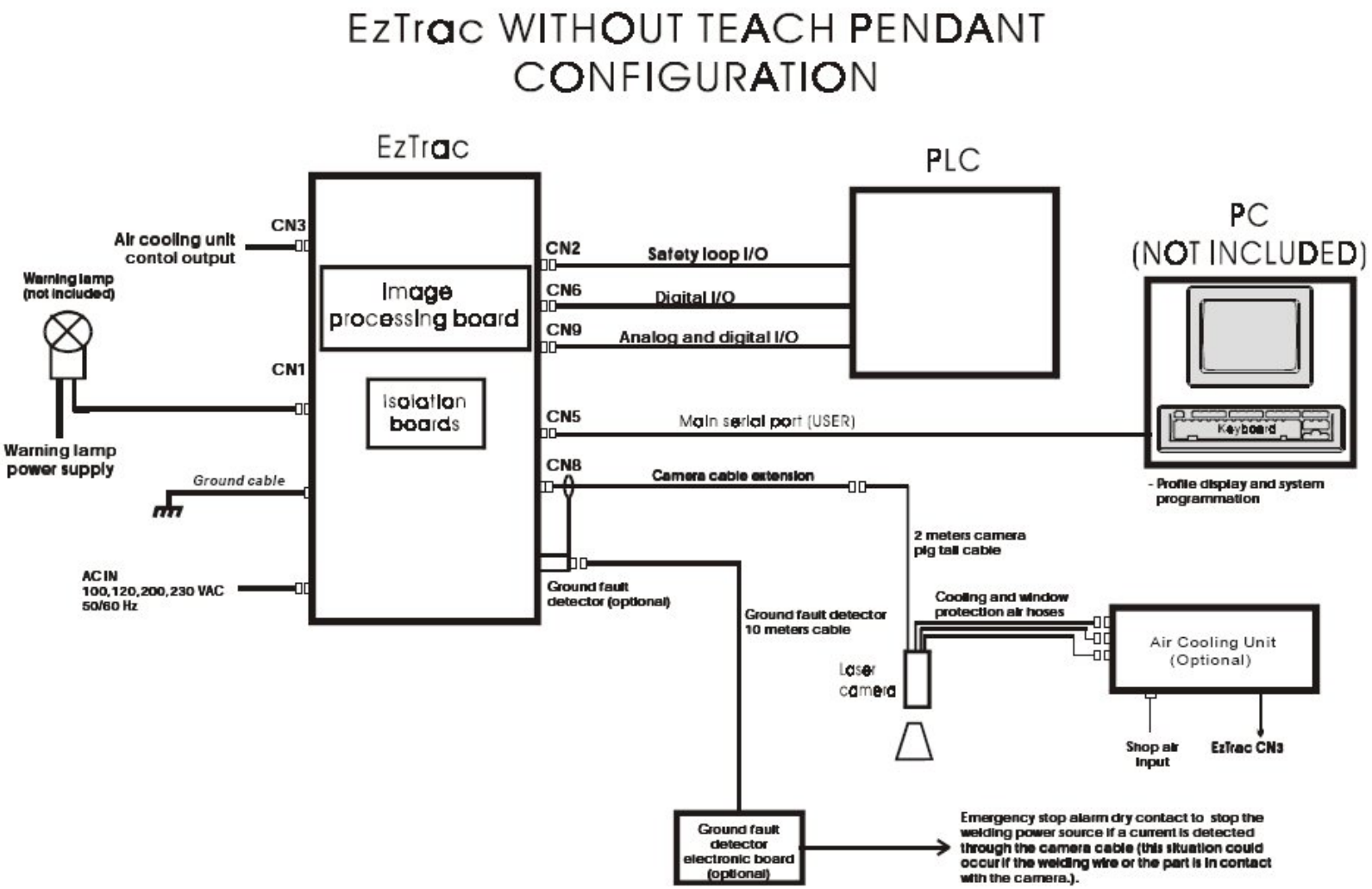

Figure 6.5 – Standard EzTrack without teach pendant configuration [120].

6.1.1.2 Laser Bracket

Two brackets to hold the laser sensor were developed. The first, used during the first phase of the experimental work, hold the laser sensor to the torch support (Figure 6.6). This implied that the sensor would move together with the torch. The second bracket, used in the later stage of the work, was attached to the main body of the welding head (Figure 6.7), maintaining a static position in relation to the welding head.

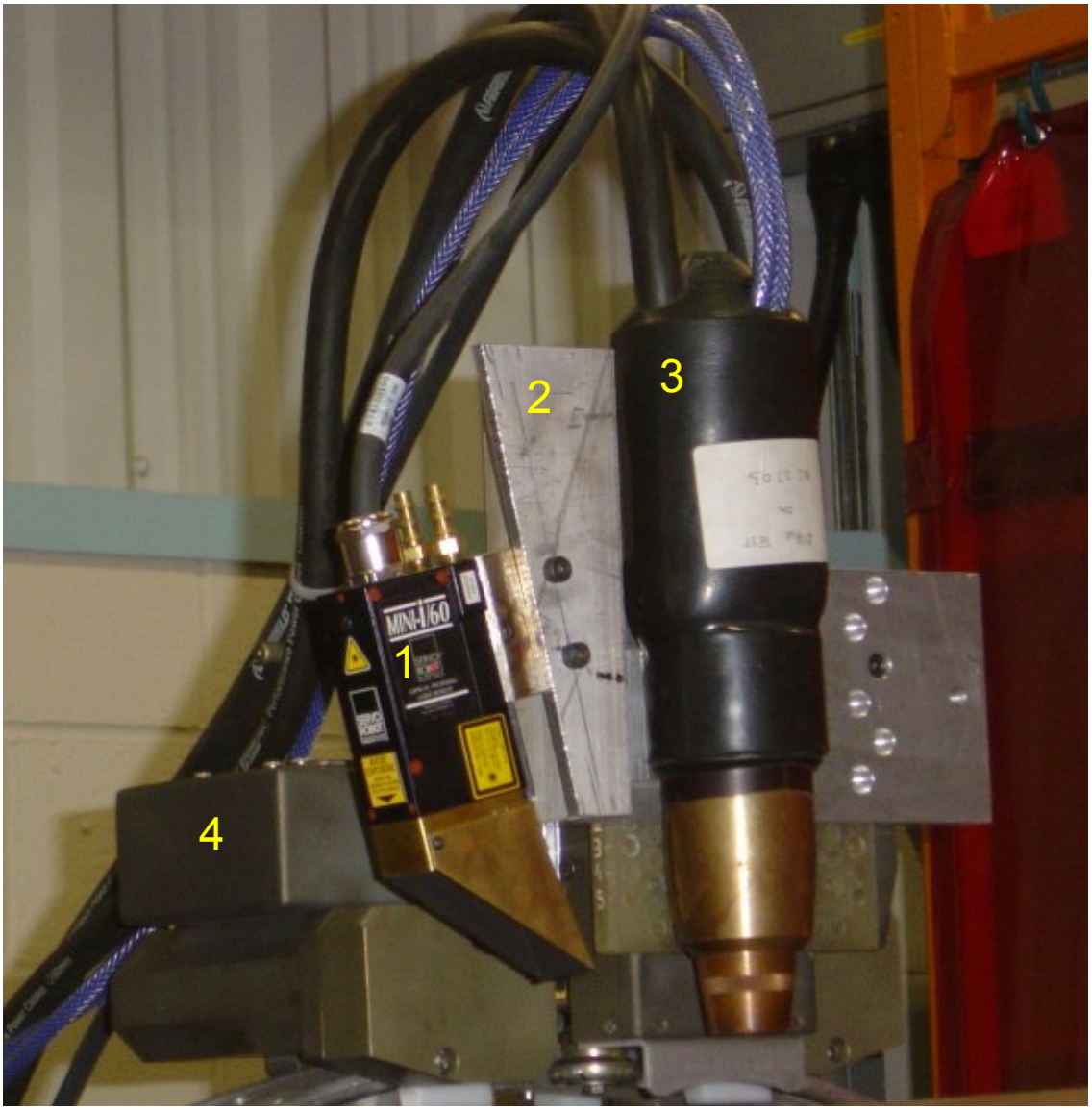

Figure 6.6 – Welding head with laser sensor attached to the torch support.

Laser:

1. Laser Vision Sensor;
2. Laser Bracket;
3. Tandem Welding Torch;
4. Welding Carrier.

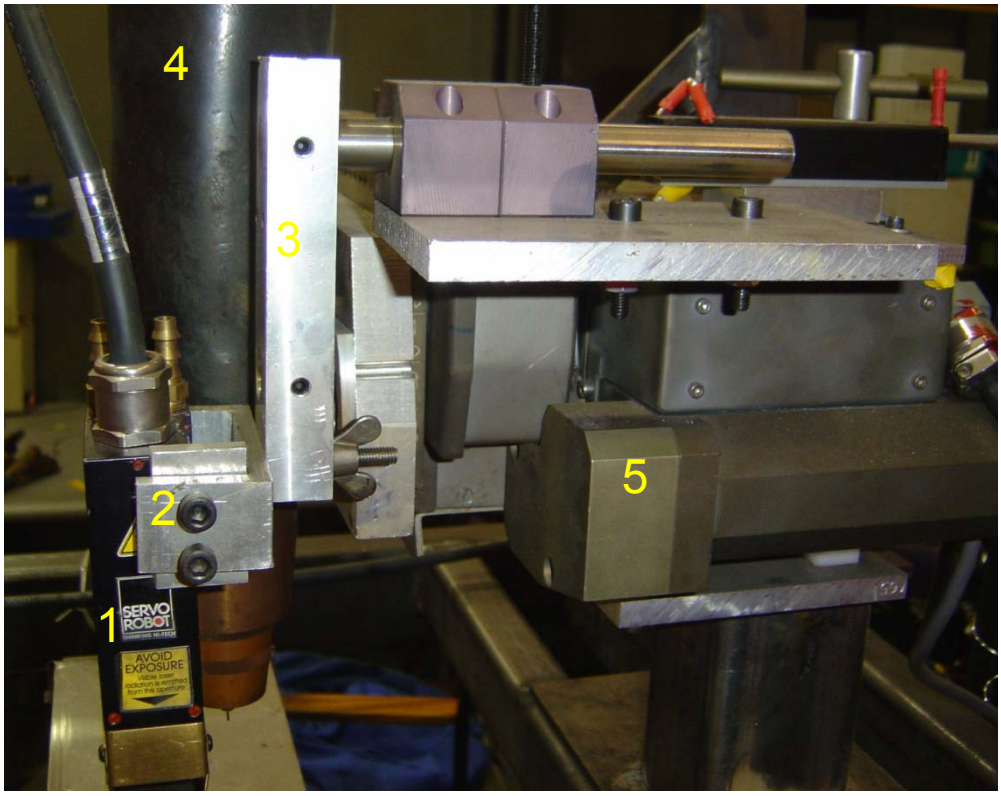

Figure 6.7 – Welding head with laser sensor attached to the main body.

Laser:

1. Laser Vision Sensor;
2. Laser Bracket;
3. Oscillation Arm;
4. Tandem Welding Torch;
5. Welding Carrier.

6.1.1.3 Calibration

Several different calibrations were performed on the laser sensor, including field of view, stand-off, and software filters.

6.1.1.3.1 Field-of-View and Stand-Off

In order to calibrate the field of view a series of experiments were carried out. These experiments involved detecting what area of the projected line is in fact received back by the CCD. This was achieved by placing a small object in the field of view and moved along the X-axis until it disappears from the field of view. The object used was a small metal plate with the following dimensions: 26.2mm x 15.8mm x 2.9mm. The obtained results confirmed the values specified in the manual. These experiments also revealed the shadowing effect on the sensor, which is discussed in section 8.1.

6.1.1.3.2 Software Filters

It was found after a batch of experiments that the measured groove profile was distorted, and that the reported groove wall angles were incorrect. Tests were performed in order to determine the cause of this problem. It was found that the software filters present in the WinUser™ software from Servo Robot were creating the distortion of the groove profile. The filters can be found in the software under the *Visus* menu, *Filters* option.

These filters are intended to smooth the raw data minimising the noise in the detected profile. This has little effect on the reported dimensions and shape of the scanned object if an open vee groove is used. However, for narrow groove pipe welding, the bevel angle is only 5º. In this case, the application of the filters has a significant effect on the reported dimensions. An in depth description of each of the filters and its functionality can be found on pages 16 and 17 of [121]. A number of experiments were performed using both Servo Robot sensors on different specimens in order to determine the influence of the filters. These experiments are described in section 7.3.4.

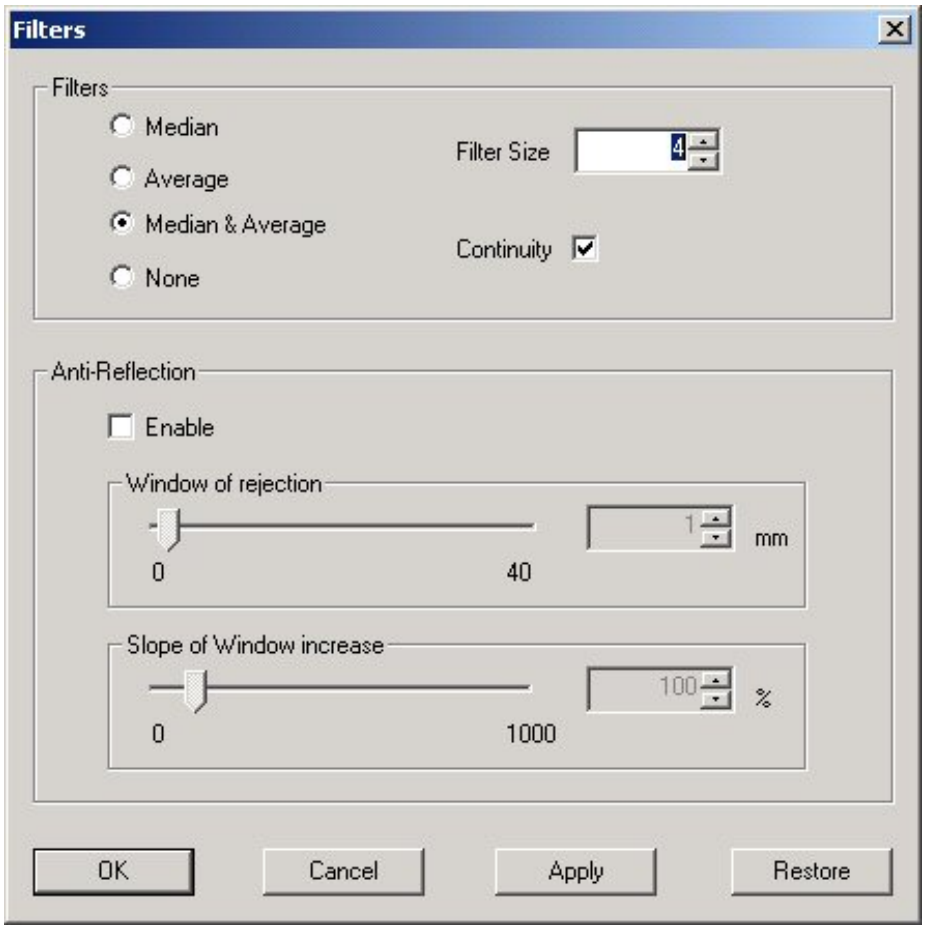

Figure 6.8 – WinUser™ filters selection window.

6.1.2 Software

6.1.2.1 SP4 – Laser Profile

The *Laser Profile* (SP4) software was developed to achieve two main goals. First to create an user interface with the laser control box, with the capability to visualise real time sensor's data and saving it for post-visualisation and processing. The second goal was to be able to load the previously saved data files and playback the data. A detailed description of the software features can be seen in Appendix D.

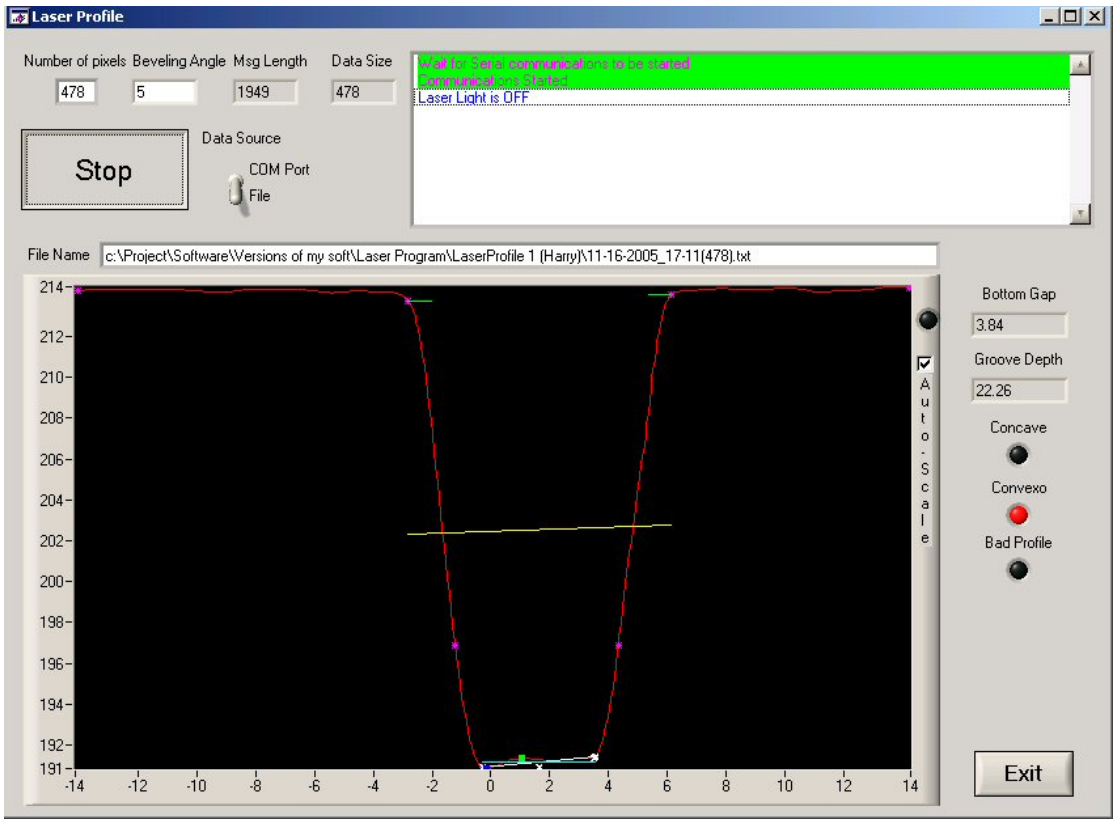

Figure 6.9 – Screenshot of the laser profile software playing back a recorded file.

SP4 is a basic program with only a few data processing capabilities. The algorithms involved on the data processing are described in detail in section 7.1.3. SP4 shares the control algorithms with SP7 – *Analysis Software*. SP7 is a more complex software and has much more data processing capabilities but it includes the features present in SP4.

7 Measurement of Weld Bead Shape

7.1 System Development

This chapter is concerned primarily with the development and testing of a new software package, SP7 – Analysis. SP7 measures and analyse the weld bead shape.

7.1.1 Hardware

For this phase of the work aside from the Servo Robot sensors two new laser vision sensors were introduced. One from Meta Vision Systems™ and another from Oxford Sensor Technology™. In addition, the use of a digital oscilloscope was introduced to visualise and record the arc currents and voltages. These new equipment is described below.

7.1.1.1 Meta Vision Systems Sensor

The Meta Vision Systems (MVS) sensor, the MT-10/15, works on the same principle of operation as the Servo Robot sensors. The laser source is a Class IIIb laser with a maximum output power of 30mW (continuous) and a wavelength between 650-699nm. The sensor head can be cooled down both by the use of air or shielding gas [58].

Specifications:

- Stand-Off: 65mm
- Depth of Field: variable
- Field of View: 15mm
- Maximum gap: 7mm
- Resolution:
    - Horizontal: 0.5mm
    - Vertical: 0.5mm

Figure 7.1 – Meta Vision Systems sensor [122].

7.1.1.2 Oxford Sensor Technology Sensor

The CSS – Circular Scanning Sensor from Oxford Sensor Technology™ differs greatly from in the previously mentioned sensors as this one projects a circular line into the object (Figure 7.2) instead of a straight line [44]. This light shape is achieved by the use of a diode laser light being projected through an off-axis lens (Figure 7.3). This lens is not static as in the other systems. It is attached to a motor whose cyclic motion creates the circular line which is projected into the object. The lens is also used to direct the reflected light back to the CCD camera. The laser source is a Class IIIa laser with a maximum output power of 4.5mW and a wavelength of 670nm. This laser can be connected to a computer either by analogue or a serial link (RS232 or RS485). To maintain the laser within its operating temperature range it has an air cooling system. This cooling system serves a double purpose and aside from managing the sensor temperature it also clears the viewing area from flying particles such as smoke or coolant mist. The sensor has a cylindrical shape with 45mm in diameter and 90mm height.

Figure 7.2 – OST Circular Sensor applied to corner detection [123].

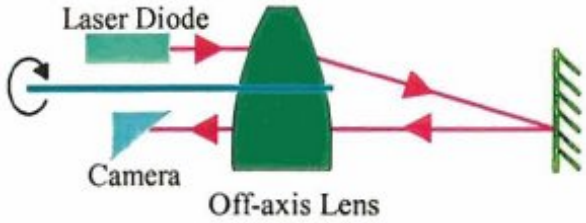

Figure 7.3 – Internal configuration [44].

Specifications:

- Stand-Off: from 30 to 75mm
- Depth of Field: from 20 to 90mm
- Viewing Diameter: from 12 to 76mm
- Scan rate: 7 circular scans per second
- Resolution:
    - Horizontal: from 90 to 350μm
    - Vertical: from 25 to 125μm

7.1.1.3 Oscilloscope

A Yokogawa ScopeCorder DL750 digital oscilloscope (Figure 7.4) was used for different applications in the development of this work. Welding voltage was recorded with the aid of 1:10 ratio voltage probes. To measure currents LEM PR1030 Hall-effect current probes were used. In order to verify the accuracy of the torch oscillation a linear variable resistor was applied to the welding head and the voltage at the resistor was measured. A description of the hardware involved in the measurement is described in section 4.2.1.3.6.1. The ScopeCorder DL750 physical dimensions are 355x250x180 mm and weight is 6.6 kg [124].

Figure 7.4 – Yokogawa ScopeCorder DL750 digital oscilloscope.

7.1.2 Software

7.1.2.1 SP6 – Rig (Single & Dual/Tandem)

In order to perform the experiments the SP6 software was used. A brief description of this software can be found in section 4.4.2 and an in depth description in Appendix E.

7.1.2.2 SP7 – Analysis

The software developed to perform an in depth analysis of the data acquired from the laser vision sensor was SP7, titled *Analysis*. Unlike the previous software developed, the SP7 was not designed to control any equipment. It was developed with the intent of evaluating the data acquired by the digital oscilloscope and either SP4, SP5 or SP6. The data generated by the SP5 and SP6 includes both the laser vision sensor data and the welding voltage, current and WFS retrieved from the PS and the digital oscilloscope.

SP7 was developed over an extensive period of time and was progressively modified as new algorithms were created to provide specific information on weld shape and quality. Only the final version of the software is described in Appendix F.

This software has five windows: *Sensor Selection*, *Data Analysis* (main one), *Feature Selection*, *Weld 3D Model* and *Waveforms*. Each of this windows and the purpose they serve is described in detail in Appendix F.

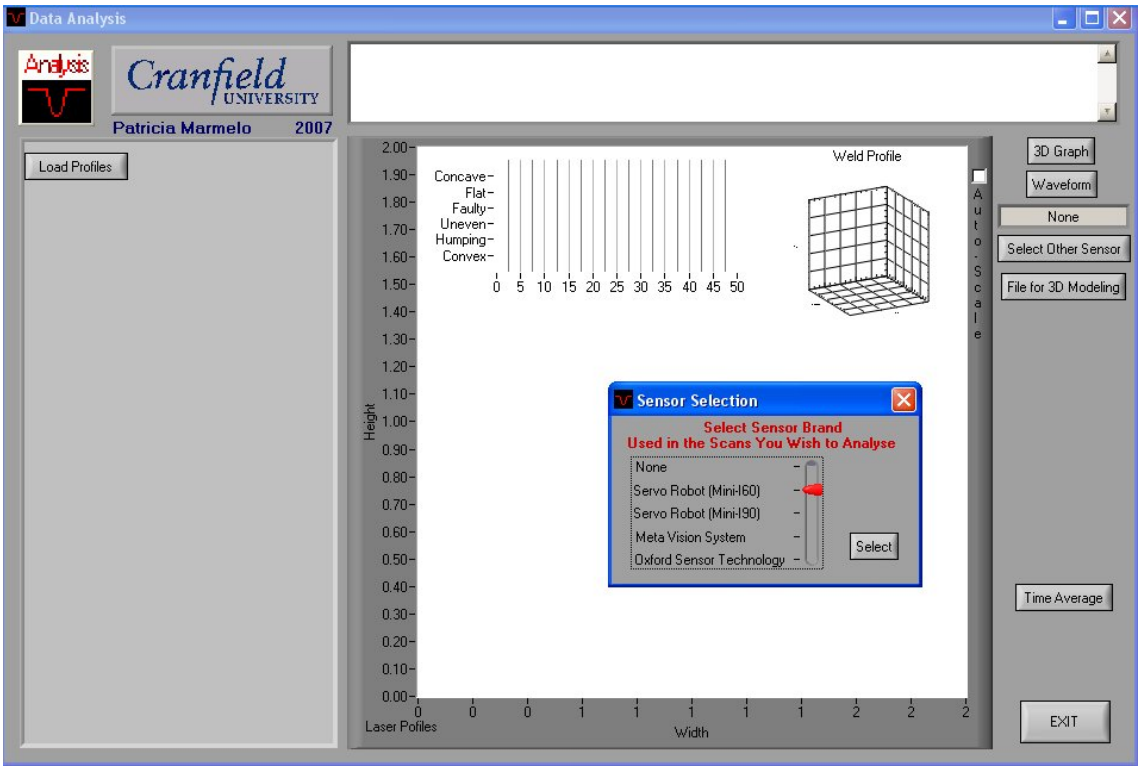

Figure 7.5 – Screenshot of the *Analysis* software immediately after start-up.

This software package is capable of analysing both the electrical data obtained with the SP6 (from the PSs) and the digital oscilloscope, as well as the laser sensor data obtained with the Servo Robot™, or Meta Vision System™ , or Oxford Sensor Technology™ sensors.

SP7 has a vertical and horizontal resolution of 0.01mm. It extracts from the data the following features: bottom and top surface width; groove depth; groove positioning; plate mismatch; breakpoints; and bead profile among others.

7.1.3 Analysis Algorithms

The pivotal point of the work is to develop the algorithms to analyse the data. The main algorithm can be seen in Figure 7.6 and the breakdown of the sub-algorithms involved is described below.

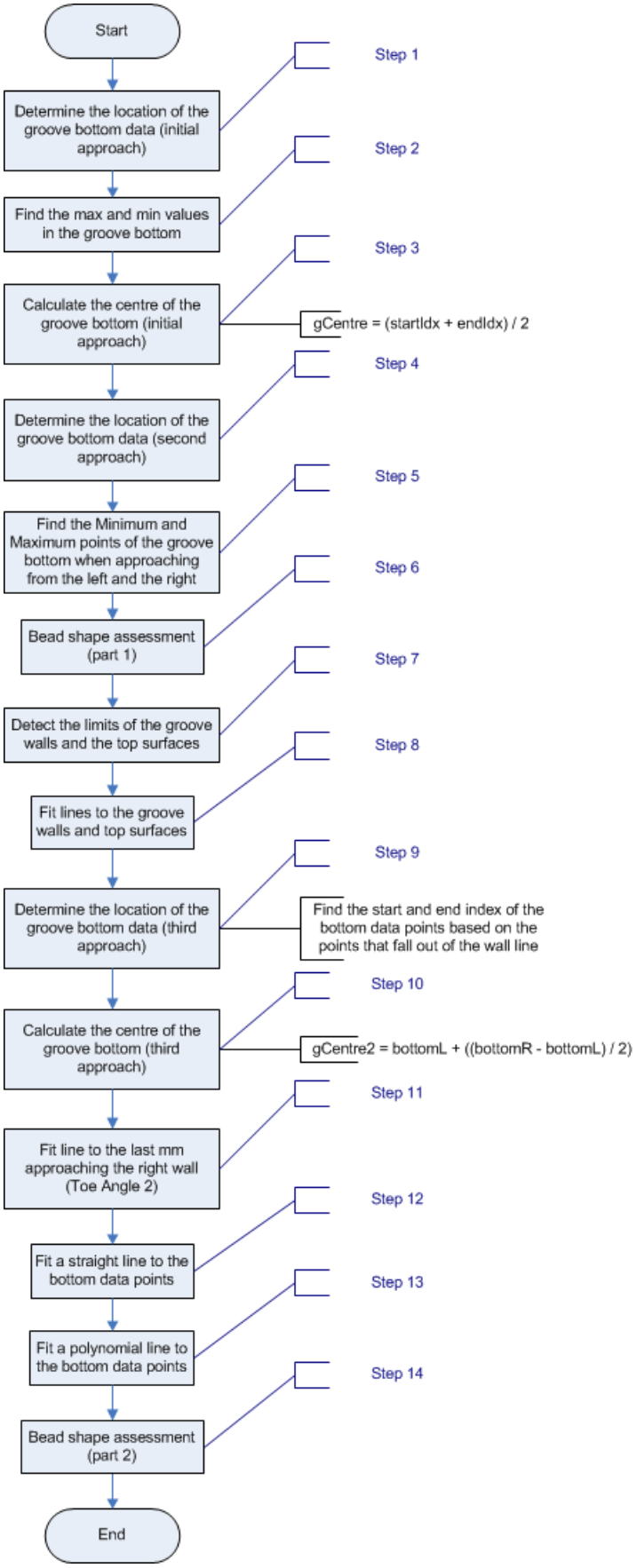

Figure 7.6 – Main Analysis algorithm.

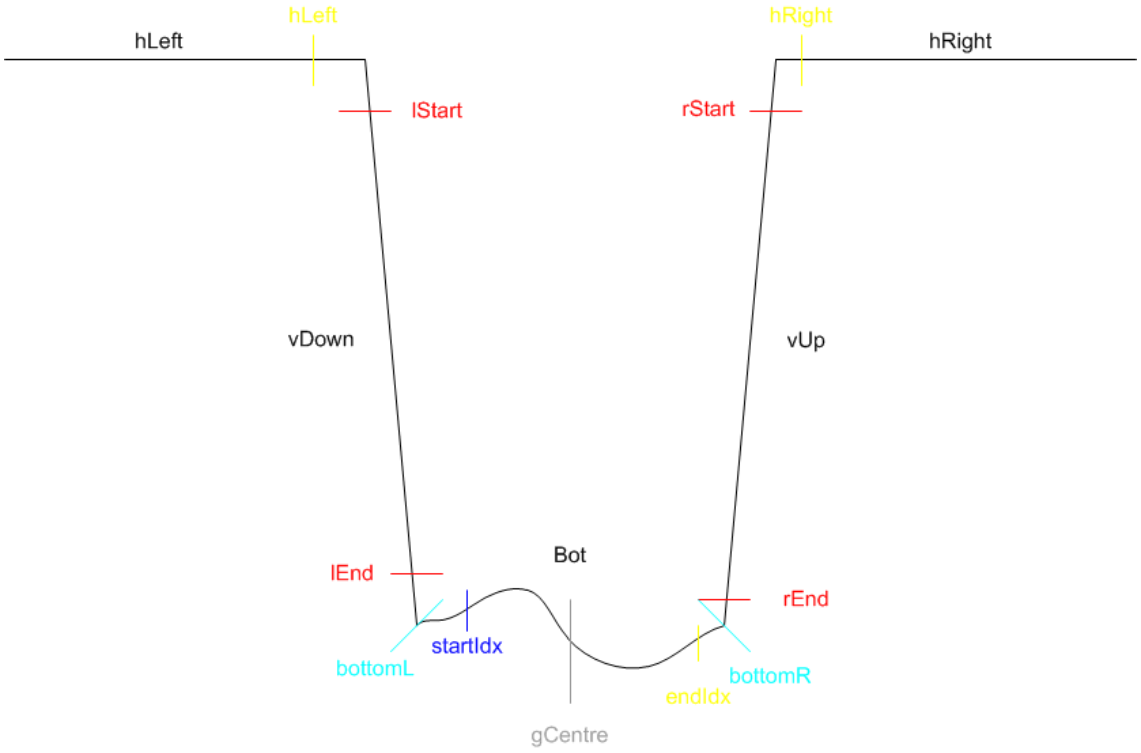

Figure 7.7 – Groove points and lines definition.

Legend:

Lines

- *hLeft* (magenta) - top left horizontal surface
- *hRight* (magenta) - top right horizontal surface
- *vDown* (cyan) - left down sloping wall, the wall between the top left horizontal wall and the groove bottom
- *vUp* (cyan) - right up sloping wall, the wall between the groove bottom and the top right horizontal
- *Bot* (depends on the type of line) - groove bottom

Points

- *hLeft* (yellow) - right limit to the *hLeft* surface
- *hRight* (yellow) - left limit to the *hRight* surface
- *lStart* (red) - top limit of the *vDown* sloping wall
- *lEnd* (red) - bottom limit of the *vDown* sloping wall
- *rStart* (red) - top limit of the *vUp* sloping wall
- *rEnd* (red) - bottom limit of the *vUp* sloping wall
- *bottomL* (cyan) - left limit of the groove bottom
- *bottomR* (cyan) - right limit of the groove bottom
- *statIdx* (blue) - first approach to determine the left end of the groove bottom
- *gCentre* (grey) - Middle point between *startIdx* and *endIdx*
- *endIdx* (yellow) - first approach to determine the right end of the groove bottom

Figure 7.7 shows the definition of the terminology used to define the groove profile points and lines. This is the terminology used in the code of the developed software as well as the one used in the algorithms below.

Groove Bottom Detection (Initial Approach)

The first step to analyse the data is to find the groove bottom location. After attempting several different approaches to breakdown the data and analyse it. It was found that the more assertive way was to start by determine a rough location of the groove bottom and then discern the other features as well as a more accurate location of the groove bottom itself. Previous approaches involved determining first the location of the top surfaces followed by the groove walls and then the groove bottom but this proved inaccurate.

Figure J.1 of Appendix J shows the algorithm involved in determining the initial two indexes that represent the limits of the groove bottom. The algorithm detects and stores the location where the groove slope is the greatest indicating the groove wall locations.

7.1.3.1 Groove Bottom Maximum and Minimum Detection

After determining the start and end of the groove bottom, the profile data in between those points is scanned to find the location of the maximum and minimum points. The algorithm involved in determining those points can be seen in Figure J.2 of Appendix J. Each data point is compared with the current maximum and minimum values. If a more suitable value is found, then the stored value is replaced with the new one and its location is stored in the respective index.

7.1.3.2 Groove Bottom Detection (Second Approach)

After the initial approach to detect the groove walls, the next step is to locate the groove bottom limits. This starts by analysing the data from the groove centre calculated as a result from the first step. The method used to determine an increase in slope of greater than 0.4% (between each measurement point and the third next measurement point. Once this cycle is finished, the new indexes are stored in two new variables in order to maintain both sets of limits. This algorithm can be seen in Figure J.3 of Appendix J.

7.1.3.3 Find the Minimum and Maximum Points of the Groove Bottom

This section of the main algorithm was developed with the intent of scanning the groove bottom to search for two maximum and minimum points. One associated with the left and the other the right side of the groove bottom. The purpose of this is to find significant asymmetries in the bead shape. This scan is performed from the groove bottom outer limits towards its centre. The procedure used to determine the maximum and minimum is similar to the one used in 7.1.3.1. The algorithm can be seen in Figure J.4 of Appendix J.

7.1.3.4 Bead Shape Assessment (part 1)

The algorithm for detecting bead shape irregularities, including asymmetry, is based on the detection of maxima (lmax and rmax) and minima (lmin and rmin) in each half of the groove bottom. This data is then used to determine what types of irregularities are occurring. For example: if either the minima or the maxima overlap (within a tolerance), then the profile must be symmetric (example in Figure 7.8). However, if the tolerance is exceeded, the profile must be asymmetric, as shown in Figure 7.9.

In detail, if an inconsistency is detected, its type is tested by determining if the height difference ('Z' axis) is greater than 1mm or not. Afterwards, which of the points are in fact the groove bottom maximum and the minimum is determined. Based on those values the convexity/concavity amplitude is calculated. If an inconsistency was not found previously the minimum and groove centre height values ('Z' axis) are compared. The comparison helps determine asymmetric profiles (see Figure 7.9). If the height difference is greater than half a millimetre the problem is flagged. Then the concavity/convexity amplitude is calculated the same way. The algorithm can be seen in Figure J.5 of Appendix J and its result in Figure 7.10.

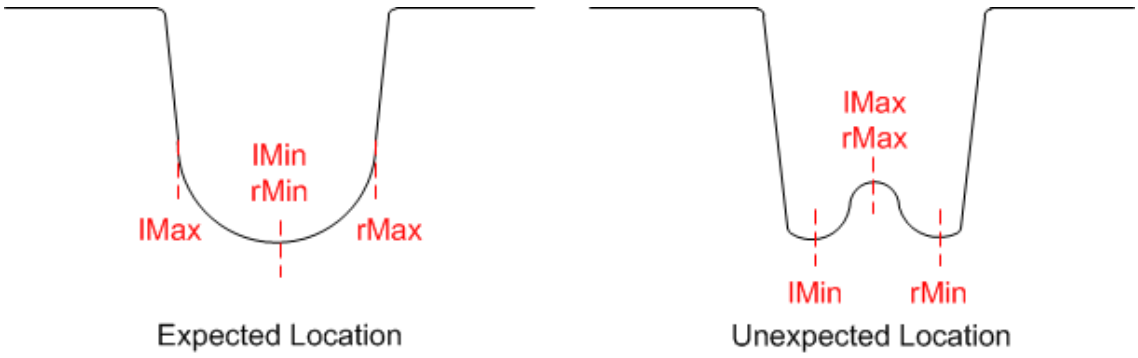

Figure 7.8 – Maxima and minima location.

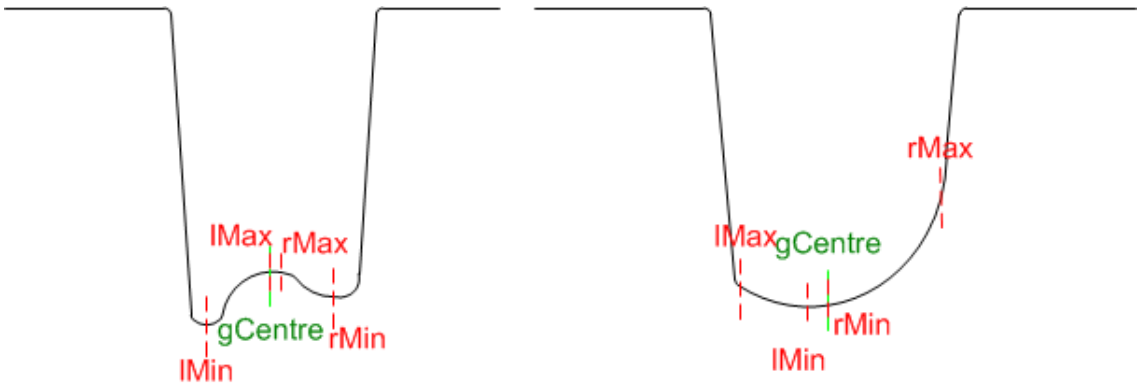

Figure 7.9 – Example of asymmetric groove configurations with the detected points location.

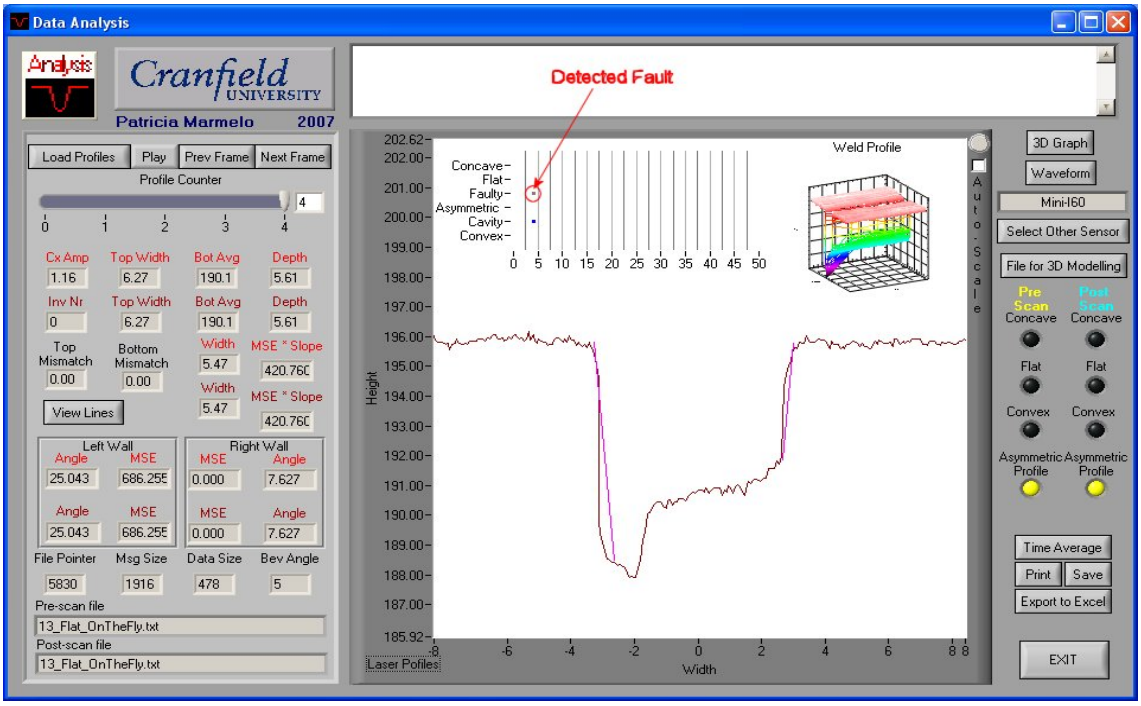

Figure 7.10 – Bead shape sssessment (part 1) slgorithm result.

7.1.3.5 Groove Wall Detection

The groove wall detection algorithm was developed to determine the start and end points of the data sets that compose the groove walls. This algorithm was divided in two identical algorithms, one applicable to the left and another to the right side wall. This was done for easy separation of the procedures. In order to determine the location of the left groove wall limits, the profile data is scanned from the groove bottom left limit towards the beginning of the data. This algorithm looks first for a slope (between data 3 points apart) greater than 0.4%. This defines the start of the grove wall at the bottom. The same comparison procedure is then repeated looking for a slope of less than 0.1%, indicating that the top of the wall has been reached. These steps are repeated in order to find the limits for the right side groove wall. These algorithms can be seen in Figure J.6 and Figure J.7 of Appendix J. The first detects the left side wall limits location and the second the right wall limits.

7.1.3.6 Top Surface Detection

A simple method is used to define the top surface. The first point of the data set is used to define the start of the top surface. A data point at a position equal to 5% of the total data set is then assumed to lie on the top surface. This point and the first point then define a line representing the top surface. This procedure is repeated for the other side of the data set. The algorithm is shown in Figure J.8 of Appendix J.

In practice to detect the top surface or any other straight line all that is required are two data points. Never the less such a small sample can be misleading due to noise in the data. In order to overcome this issue some experiments were carried out to determine how many data points would be enough. Some of the tests involved running the algorithm on profiles that were less than ideal to see how well the algorithm would perform. By less than ideal should be understood a scan in which the groove is very off-centred but in which is still possible to extract both to surfaces. The 5% value was determined after some trial and error experimentation to determine what was the amount of data points that would provide a reliable outcome for this algorithm. To determine this value only scans from the Mini-I60 sensor were used, but the algorithm worked without problems with the other sensors utilised. In the Mini-I60 at the higher resolution 5% of the data points corresponds to 24 data points. And at the lower resolution corresponds to 12 data points. Either of the number of data points was enough to detect the top surfaces.

7.1.3.7 Fit Lines to the Groove Walls and Top Surfaces

After determining the groove walls limits as well as the limits for the top surfaces, straight lines are fitted to those data sets. Before fitting the data, the number of points in each data set is tested as a minimum of two data points per set is required. If the set has less than two data points, the line cannot fitted and the program moves on to fit the next line. To fit the line a LabWindows™ function called “LinFit” is used. The algorithms can be seen in Figure J.9, Figure J.10, Figure J.11 and Figure J.12 of Appendix J.

7.1.3.8 Groove Bottom Detection (Third Approach)

After the groove walls are discerned and the fitted lines are calculated, the groove bottom limits can now be determined more accurately as a deviation from the fitted groove sidewall line. Starting from the lower limit of the groove wall each data point is tested to see if it still fits to the fitted line or not. A tolerance of 1mm is given. If the data point falls into a neighbourhood of 1mm from the fitted line, it is still considered part of the groove wall. If it falls out of that neighbourhood it is considered to be the limit of the groove bottom. This applies to both sides of the groove wall. A new groove centre is calculated based on these new limits. The algorithm performing this approach can be seen in Figure J.13 of Appendix J. This final iteration now determines the final values for the groove bottom limits.

7.1.3.9 Measurement of weld bead toe angle (Toe Angle 2)

The groove bottom area is now scanned starting from the right side limit to collect all data belonging to the last millimetre. The new data set is then fitted a straight line that represents the right side toe angle. This is one of the implemented approaches to calculate the toe angle. This function can be activated in the graph by selecting “Toe Angle 2” in the “Feature

Selection" window. This approach was only implemented to the right side of the groove bottom but the algorithm can easily be extended to cover both sides. The algorithm can be seen in Figure J.14 of Appendix J.

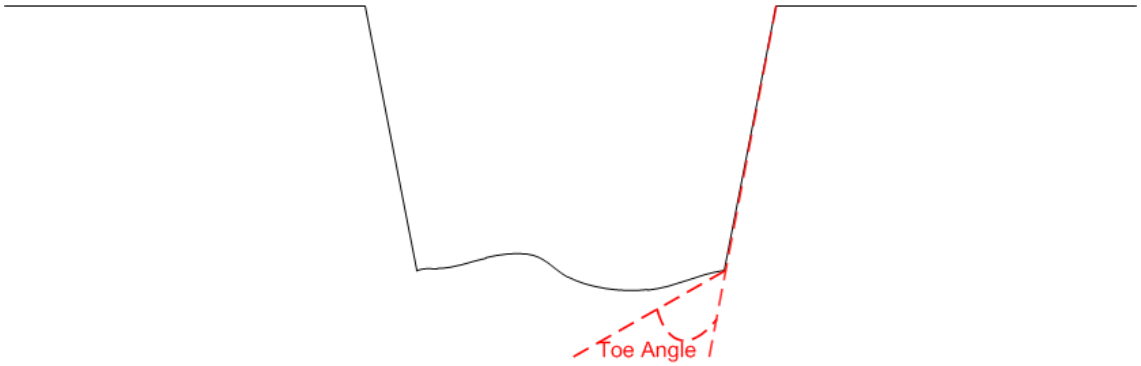

Figure 7.11 – Toe angle.

7.1.3.10 Fit a Straight Line to the Bottom Data Points and Breakpoint Calculation

The first fitting approach to the groove bottom data is a linear fit. A straight line is fitted to the groove bottom data to indicate the slope of the bottom data and to aid in the calculation of the breakpoints. The procedure to fit the line to the groove bottom data is similar to the one used in 7.1.3.5.

The inclination of the bottom surface reveals information concerning the general quality of the groove bottom shape. Based on the obtained line and the previously determined groove walls and top surface walls, the breakpoints are calculated. The algorithm developed to perform these tasks can be seen in Figure J.15 of Appendix J. The breakpoints are calculated based on the intersection of the relevant fitted lines. In the case of the top left breakpoint are the top left surface and the left wall. For the top right breakpoint are the top right surface and the right wall. In the case of the bottom left breakpoint are the bottom surface and the left wall. For the top right breakpoint are the bottom surface and the right wall. For a better understanding of the lines involved and the breakpoints see Figure 7.12. Based on the calculated breakpoints and the average height of the groove bottom and the top surfaces, the groove depth is determined.

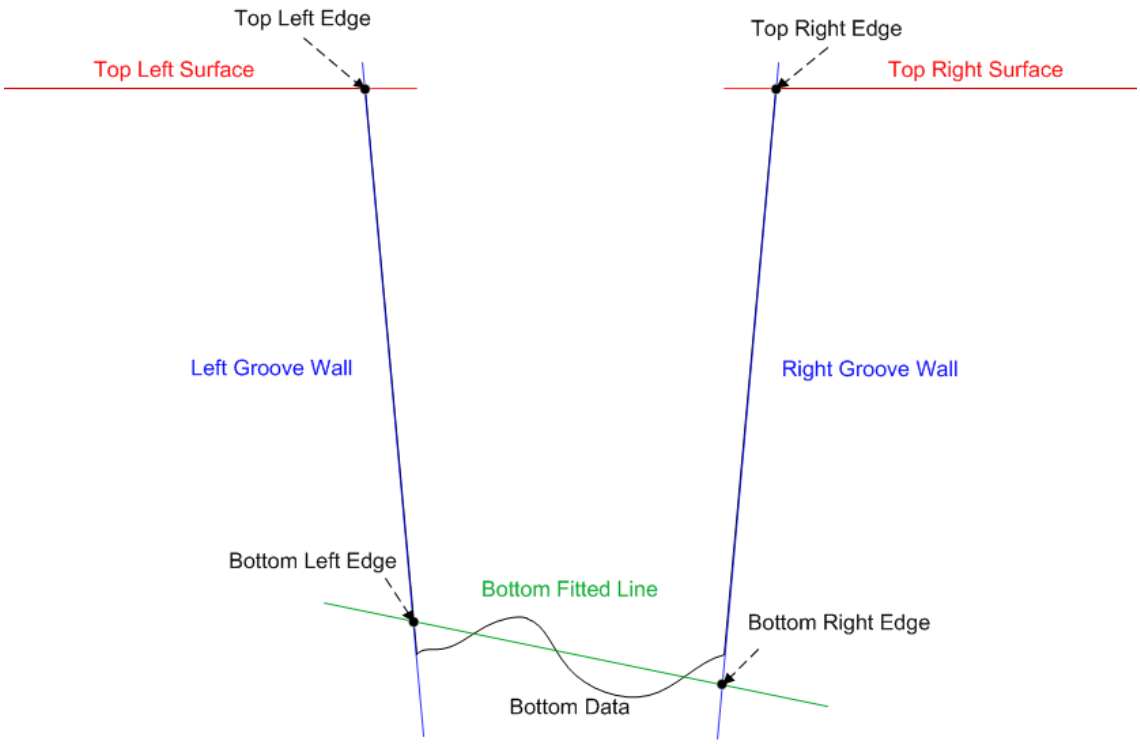

Figure 7.12 – Fitted lines and breakpoints definition.

7.1.3.11 Fit a Polynomial Line to the Bottom Data Points

A polynomial line is fitted to the groove bottom data to give an indication of whether the bead is concave, flat or convex. The polynomial line is not fitted to the entire data set, it is only fitted to three fifths of the data points, in order to avoid misleading data often present near the weld toe edges. This new data set is tested to see if it contains at least two data points so the line can be fitted. For the polynomial line fit the “PolyFit” function of LabWindows™ is used. The result of this algorithm can be visualised in the screen by activating the “Poly Long Bottom 1” feature in the “Feature Selection” window. The algorithm developed to perform these tasks can be seen in Figure J.16 of Appendix J.

This provides information in relation to the flatness of the bead, its inclination and groove depth. A polynomial line of order two is then fitted to the same data set if the user requests it. The user can request it by ticking the appropriate box in the *Feature Selection* window. At this stage the algorithm is ready to decide on the weld bead shape. This is done by accessing the results of the fitted lines MSE (Mean Square Error) and slope values. Using the position of the maximum and minimum value points within the groove bottom is also possible to determine the weld bead convexity/concavity or determine some faulty welds. From the detectable faults, cavities and asymmetric beads can be specifically detected but general faulty beads are consistently detected.

7.1.3.12 Bead Shape Detection

Once the groove sidewalls limits have been detected, is then possible to detect the approximate limits of the weld bead. At this point, it is possible to analyse the groove bottom data. The first step is to determine if the bead is asymmetric or not. Bead asymmetry is determined by the inclination of the straight line fitted to the data points that represent the groove bottom. Afterwards the data is tested for the existence of cavities in the profile, initially for wide cavities and then for narrow ones. Once it is defined that the profile is neither asymmetric nor contains a cavity it is tested for concavity/convexity. To achieve this, the data is first tested to determine if the profile is concave, then flat and in last convex. The algorithm developed to perform these tasks can be seen in Figure J.17 of Appendix J.

7.2 System Evaluation

The system's performance is going to be evaluated in several stages. The initial one includes accessing what influences the sensor control box output. This includes testing the sensor position in relation to the groove, control box parameters, surface conditions and coatings, light reflections and groove types. Afterwards specimens containing a wide range of bead shapes will be analysed in order to develop algorithms capable of not only detecting the different bead shapes (namely flat, concave and convex) but also accessing them for their acceptability and defect detecting.

7.3 System Performance

7.3.1 Initial Trials

Initial trials were performed to test if different stand-off positions within the manufacturer's specification range would alter the value of the measurements. In order to perform the tests a previously welded specimen was used (Figure 7.13). The laser vision sensor Mini-I90™ from Servo Robot™ was used to perform the test. The specimen specification can be seen in Table 7.1. Analysing the same table is possible to discern that the measurements have an accuracy of approximately 0.5mm except for measurement of the machined preparation, where errors occur due to reflections.

The specimen was extracted from a welded pipe in which each layer was stopped before the previous one as can be seen in Figure 7.13. Each layer corresponds to a step in the specimen.

The procedure involved scanning each of the steps with both the digital calliper and the laser vision sensor. Then in each scan the measurement of the top surface was related to the measurement of the bead surface. This way it was possible to determine the depth from the top surface at which each step is located. Each set of scans was repeated at seven different stand-offs: 75.4; 85.4; 95.4; 105.4; 115.4; 125.4; and 135.4mm. The results from this test showed consistency in the results for the tested stand-offs. It also showed the readings from the laser vision sensor were very similar to the measurements performed with the calliper rule (Table 7.1).

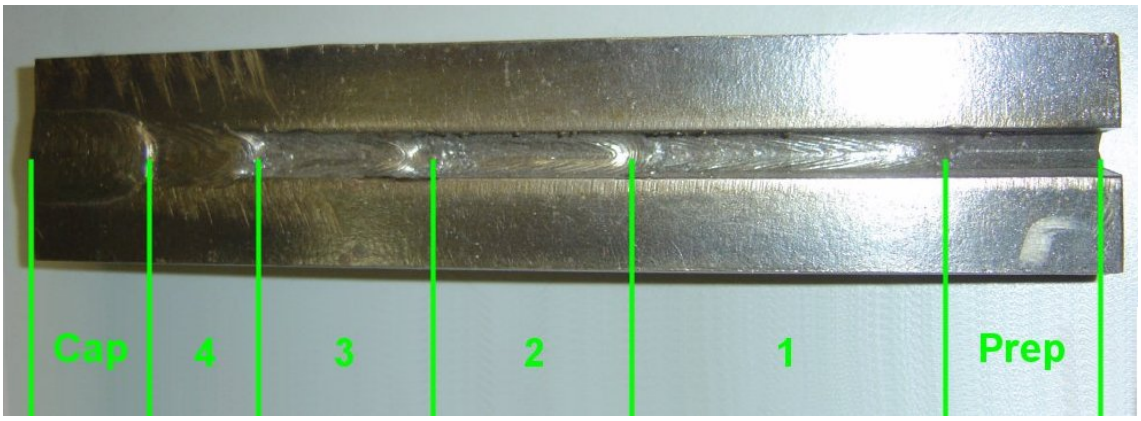

Figure 7.13 – Specimen.

	Specimen		
Sample Width (mm)	33		
Sample Length (mm)	170		
Top Corners Gap (mm)	6.2		
Distance from the Layer to the Top Surface	Digital Calliper Measurement	Laser Sensor Measurement	Measurement Difference
Prep (mm)	12.68	9.91	2.77
1 (mm)	8.63	8.29	0.43
2 (mm)	5.67	5.42	0.25
3 (mm)	3.62	3.88	-0.26
4 (mm)	0.87	1.10	-0.27
Cap (mm)	-1.16	-0.93	0.23

Table 7.1 – Specimen Characteristics.

For the preparation measurement there is a 2.77mm difference between the digital calliper and laser vision sensor measurements that can be attributed to the difficulty to measure with the calliper on that groove shape or to reflections that may occur on the groove bottom that the laser vision sensor may have difficulty dealing with and consequently misdetecting the

groove bottom location. It is more likely that it is the later that is causing the difference measurement.

7.3.2 Influence of Sensor Position

A laser sensor is first and foremost a vision sensor. As any other vision sensor/object, it is influenced by its viewing point. To assess the influence of the viewing point on the sensor performance a groove was scanned repeatedly with the sensor placed in different locations.

Rather than moving the sensor indiscriminately, it was decided after some initial trials that the two factors that would influence the result the most were the sensor "*Tilt*" and "*Rotation*". For these experiments it was decided the sensor would be placed at one single location and its positioning would vary. In this section the experimental procedure will be described and results from the experiments performed to test the influence of sensor tilt and rotation will be shown. Before describing the procedure, some concepts should to be clarified. *Centre* is a vertical line which is perpendicular to the plate surface. *Rotation* is the deviation from this line in the welding direction and *Tilt* is the deviation from this line transverse to the welding direction. This is shown in Figure 7.14. Other concepts also need to be clarified for a better understanding of the data that follows. "*Left Side Length*" is the length of the light projected in the left plate top surface. "*Top Gap*" is the groove width at the top of the groove. "*Right Side Length*" is the length of the light projected in the right plate top surface (see Figure 7.15). "*Light length*" is the sum of "*Left Side Length*", "*Top Gap*" and "*Right Side Length*" values.

This set of experiments was divide in two stages. First, the sensor was rotated having a constant tilt angle of 0 degrees. Secondly, the sensor was tilted and the rotation angle was kept at 10.6 degrees. All scans start with the welding wire at 100mm from the plate's home position. "Home position" is the position zero, the position where the travel axis (X) always returns to when the plate is moved to the beginning of the axis position. This is a repeatable position which is why it was selected as a reference point. The scanned plate has a groove depth of 23mm, 5 degree bevel angles, flat groove bottom and the top gap was measured to be 8.26mm. The plate was previously sprayed with graphite paint. A total of 15 readings were performed per scan with a resolution of 478 points per profile. The initial scan of every experiment was performed 100mm away from the plate edge.

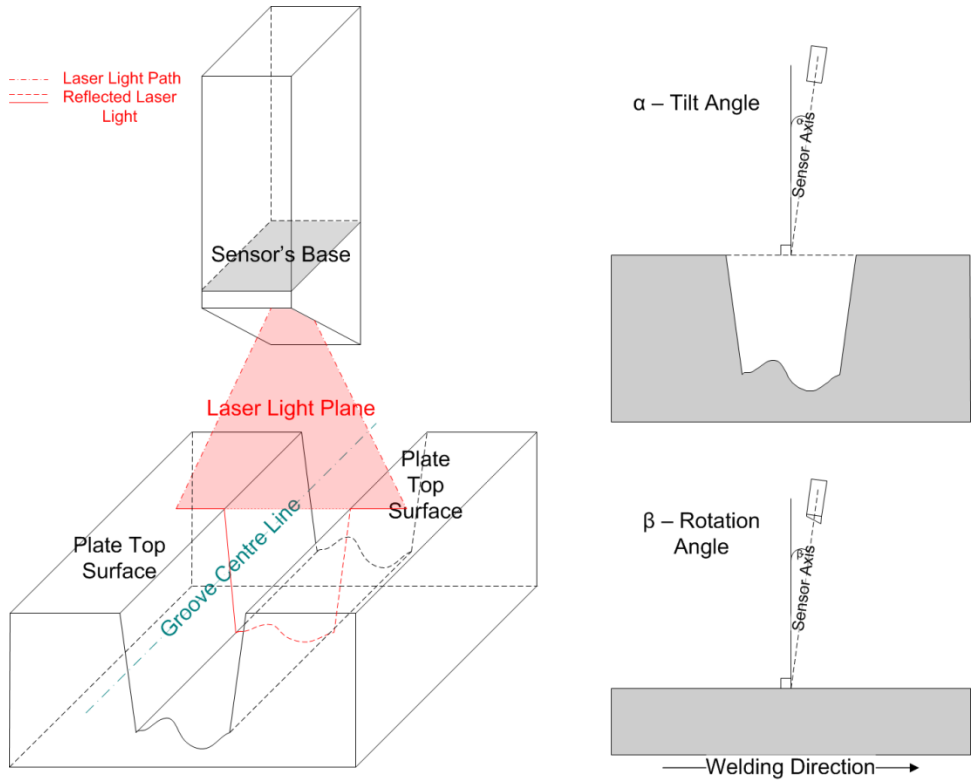

Figure 7.14 – Rotation and tilt description schematic.

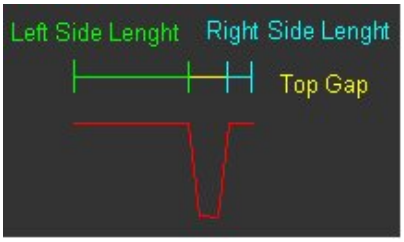

Figure 7.15 – Schematic of profile lengths.

7.3.2.1 Rotation

The sensor rotation produced a horizontal mismatch between the light position in the top surface and the groove bottom. This mismatch was named "*Light mismatch on plate*" and it was measured in every experiment. Two other terms need to be defined. "*Distance from plate home*" which is the measured distance between the plate's home position and the location where the laser light hits the plate on the first scanning position. And "*Distance from the wire*" which is the distance between the point where the wire touches the plate and the projected laser light on the plate. This distance is perpendicular to the laser light projection. A set of seven experiments was designed and performed. The results can be seen in Table 7.2.

The negative value in the "Distance from plate home" and "Light mismatch on the plate" means the light is being projected before what was considered the reference point. An extra

experiment was later performed with a rotation angle of 10.6 degrees. In this experiment, the measured groove depth was 23.21mm.

A sample of the performed scans can be found below from Figure 7.16 to Figure 7.23. As was described previously some support lines were calculated showing the expected location and shape of the groove walls based on the input wall angle. These lines are the pink lines in the graphs. In this case they represent the 5 degrees angle line the walls should have. The small image in the top right corner shows a 3D model of the weld. This model is built using the 2D profiles acquired from the laser vision sensor from the first to the one being currently shown.

Rotation (degrees)	Tilt (degrees)	Distance from plate home (mm)	Distance from the wire (mm)	Light mismatch on plate (mm)	Groove Depth (mm)
0	0	25	32.06	3.45	23.17
3	0	18	42.4	3.43	23.17
6	0	10	47	1.7	23.1
9	0	5	53	1.58	23.2
12	0	-9	63.3	-1.25	23.26
15	0	-21	76	-2.15	23.23
18	0	-31.5	88.8	-3.1	23.24

Table 7.2 – Rotation experiments.

"*Distance from the wire*" is the distance between the plane of laser light and the welding wire, known as the "look ahead" distance, it changes due to the sensor rotation. "*Light mismatch on plate*" is the horizontal distance between the intersection of the plane of the laser light with the plate surface and the groove bottom, for this 23 mm deep groove, and again is affected by sensor rotation.

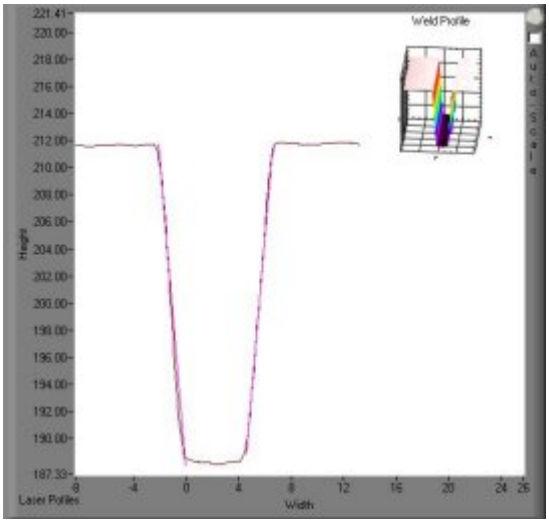

Figure 7.16 – Rotation 0 degrees.

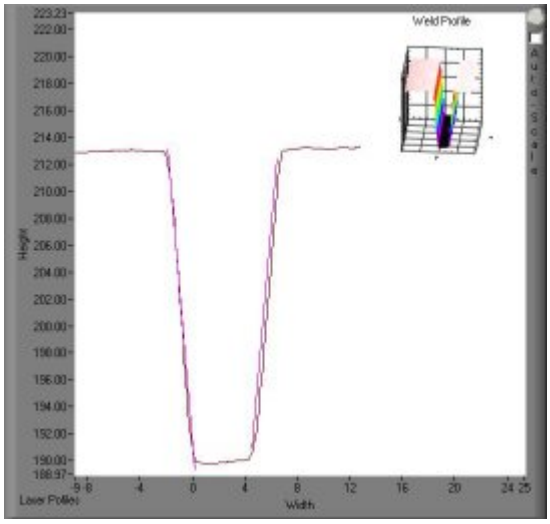

Figure 7.17 – Rotation 3 degrees.

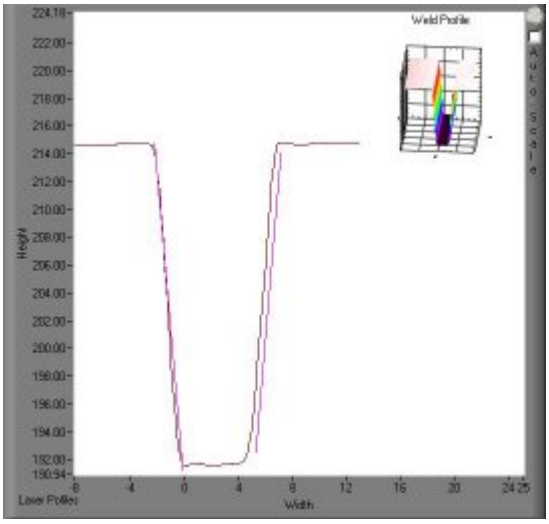

Figure 7.18 – Rotation 6 degrees.

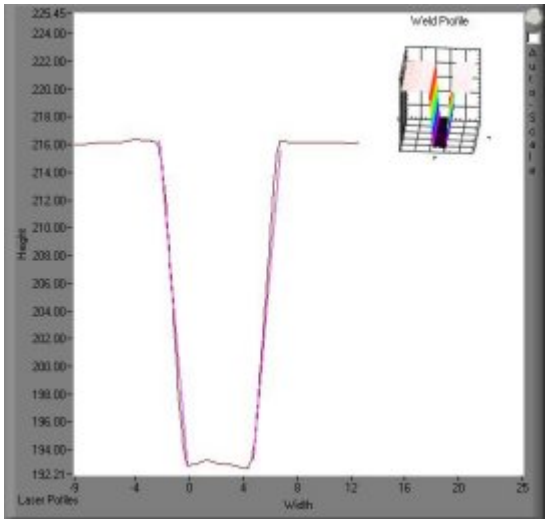

Figure 7.19 – Rotation 9 degrees.

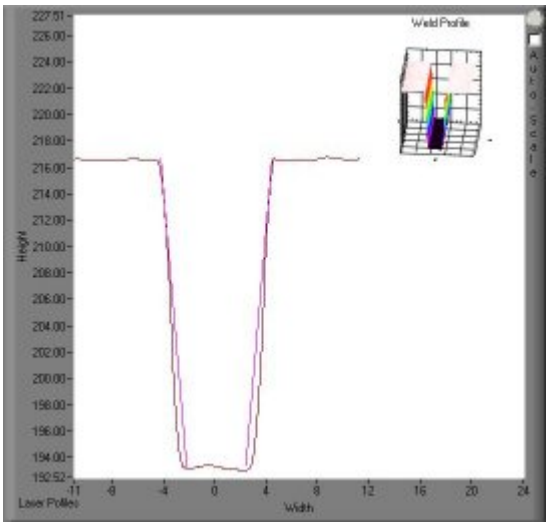

Figure 7.20 – Rotation 10.6 degrees.

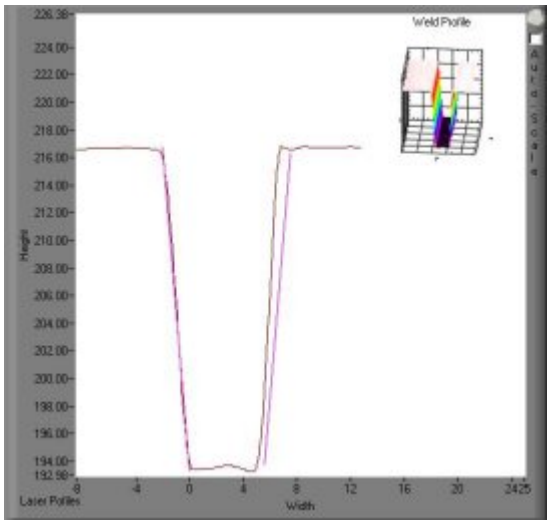

Figure 7.21 – Rotation 12 degrees.

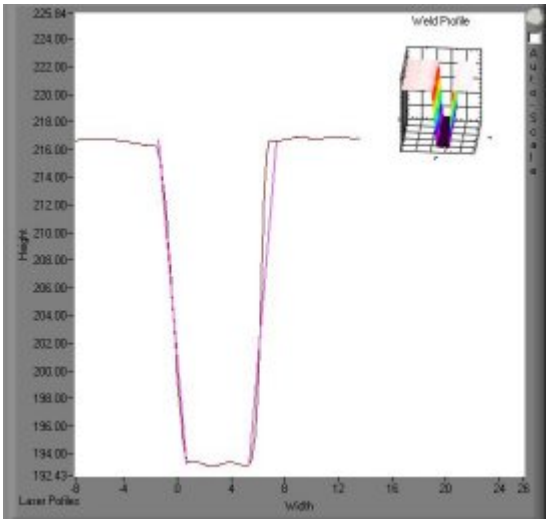

Figure 7.22 – Rotation 15 degrees.

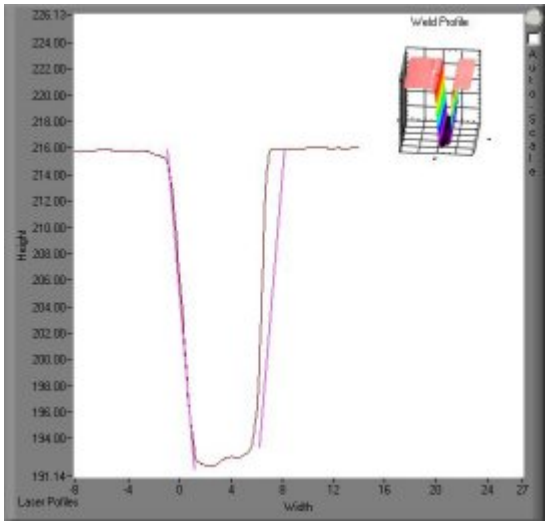

Figure 7.23 – Rotation 18 degrees.

As can be seen in Figure 7.16 to Figure 7.23, there is a good correspondence between the angle of the scanned groove walls and the expected 5 degree walls (pink lines). With exception of the scans performed with a rotation of fifteen (Figure 7.22) and eighteen degrees (Figure 7.23) the groove walls have the same angle as the support (pink) lines. The measurement is clearly relatively insensitive to misalignments in terms of sensor rotation. The sensor should be square with the groove although a low rotation angle will work too. This part of the setup does not require great accuracy.

As can be seen in Figure 7.24 a horizontal light mismatch between the top surface and the groove bottom occurs as the sensor is rotated. On the rotation angles tested, the light mismatch changes linearly and ranges from -3.1mm to 3.45mm. This does not have any influence on the measurement of the groove depth as Figure 7.25 demonstrates. As can also be seen in the same graph, as the rotation angle increases, so does the distance from the light to the welding wire. This means that the higher the rotation angle, on the direction tested, the further ahead the specimen is being examined. This also implies that a higher rotation angle requires a bigger "*Look Ahead Distance*". This entails the scan to commence earlier than with a smaller rotation angle.

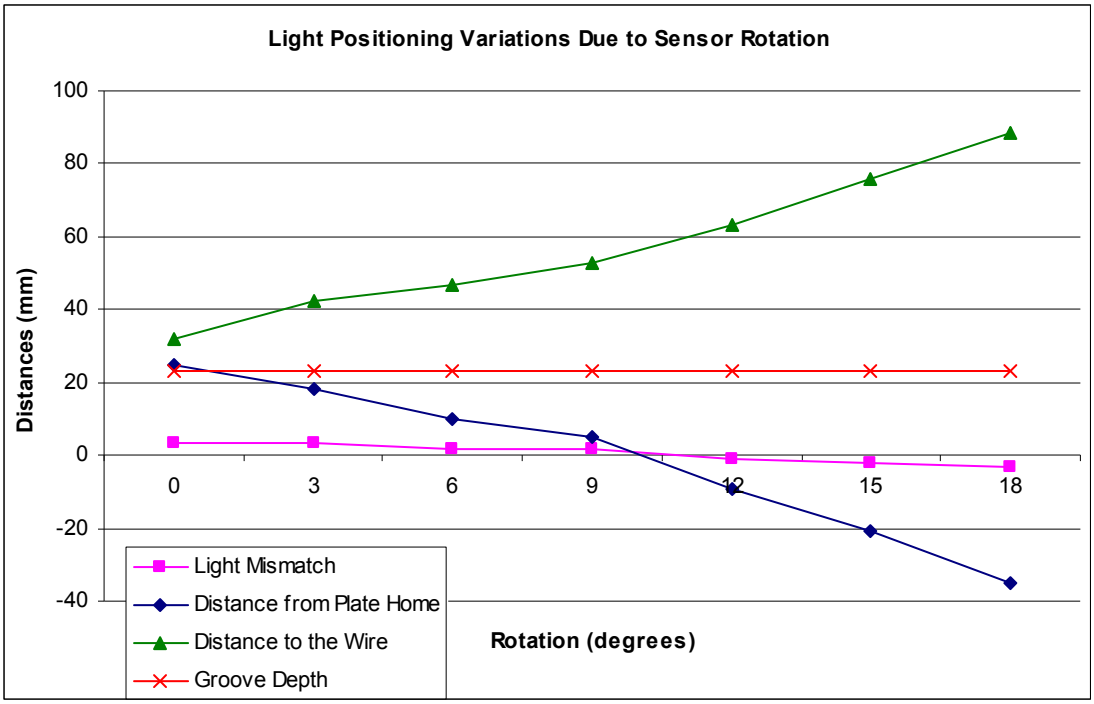

Figure 7.24 – Light positioning variations due to sensor rotation.

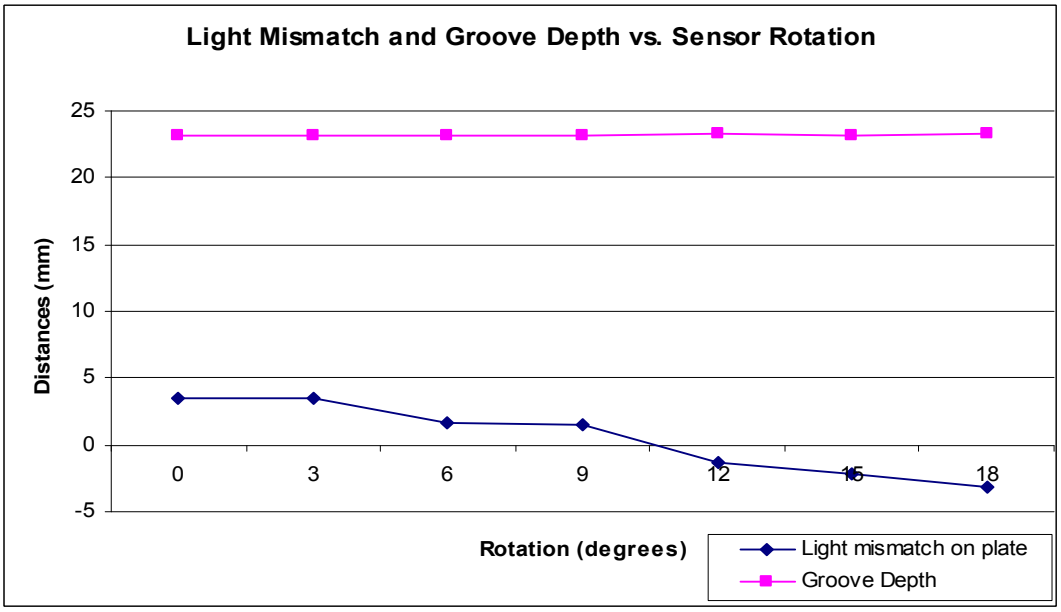

Figure 7.25 – Light mismatch and groove depth vs. sensor rotation.

A straight line was fitted to "*Light Mismatch*" data in order to detect the sensor rotation angle at which the laser light is square with the plate surface. The laser light plane being square with the plate surface is represented in the data by the angle in which the light mismatch is zero. The obtained equation can be seen in Equation 7.1.

Equation 7.1

$$\begin{cases} 1.58 = a \times 9 + b \\ -1.25 = a \times 12 + b \end{cases} \Leftrightarrow \begin{cases} 0 = 9 \times a + b - 1.58 \\ 0 = 12 \times a + b + 1.25 \end{cases}$$

$$\Rightarrow 9 \times a + b - 1.58 = 12 \times a + b + 1.25 \Leftrightarrow 3 \times a = -2.83 \Leftrightarrow a = -0.943$$

$$\Rightarrow b = -9 \times a = 1.58 \Leftrightarrow b = 10.07$$

$$y = a \times x + b$$

$$y = -0.943 \times x + 10.07$$

$$y = 0 \Rightarrow 0 = -0.943 \times x + 10.07 \Rightarrow x = 10.67$$

As was pointed out previously the laser scans (Figure 7.16 to Figure 7.23) do not seem to be greatly influenced by the rotation angles between zero and twelve degrees. In the scans performed on those angles, the groove walls matched with the 5 degrees bevelling angle. Since in practice the rotation angle will be within this range, larger rotation angles were not investigated further.

7.3.2.2 Tilt

The sensor was positioned initially with a rotation of 10.6 degrees and 0 degrees of tilt and it was centred with the groove. It was decided to position the sensor with a rotation of 10.6 degrees as this was the value for which the plane of the laser light is perpendicular to the plate surface, and which therefore produced zero horizontal displacement value. The centre of the laser light was centred on the groove, so that the length of the top right side and top left side was equal. With the sensor positioned in this setup, the distance between the pipe top surface and the laser light source was 113.6mm. Tilting of the sensor caused the “Left Side Length” and “Right Side Length” lengths to have different values. These variations can be seen in Table 7.3. Definitions of “Right Side Length” and “Left Side Length” were given earlier in section 7.3.2 and a schematic can be seen in Figure 7.15. These values were measured in every performed experiment.

The experimentation performed was comprised of nine individual experiments. The setup for this experimentation can be seen in Table 7.3. A sample of the performed scans can be found below from Figure 7.26 to Figure 7.34. The pink lines near to the groove walls represent the 5 degrees angle line the walls should have.

Rotation (degrees)	Tilt (degrees)	Left Side Length (mm)	Right Side Length (mm)	Difference (mm)	Light Length (mm)
10.6	-4	10.05	29.14	19.09	47.35
10.6	-3	13.02	26.57	13.55	47.75
10.6	-2	15.39	24.08	8.69	47.63
10.6	-1	17.28	21.23	3.95	46.67
10.6	0	19.2	19.4	0.2	46.76
10.6	1	22.23	16.76	5.47	47.15
10.6	2	24.41	15.17	9.24	47.74
10.6	3	26.12	13.17	12.95	47.45
10.6	4	28.52	10.97	17.55	47.65

Table 7.3 – Tilt set of experimental data.

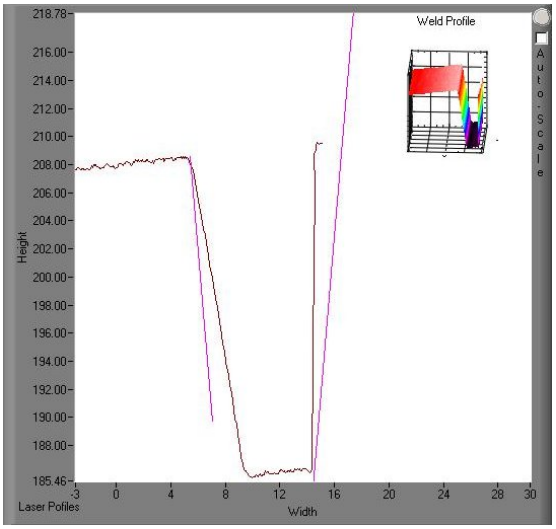

Figure 7.26 – Tilt -4 degrees.

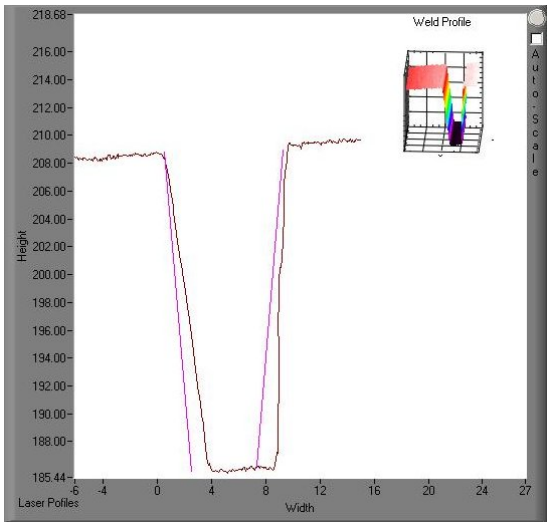

Figure 7.27 – Tilt -3 degrees.

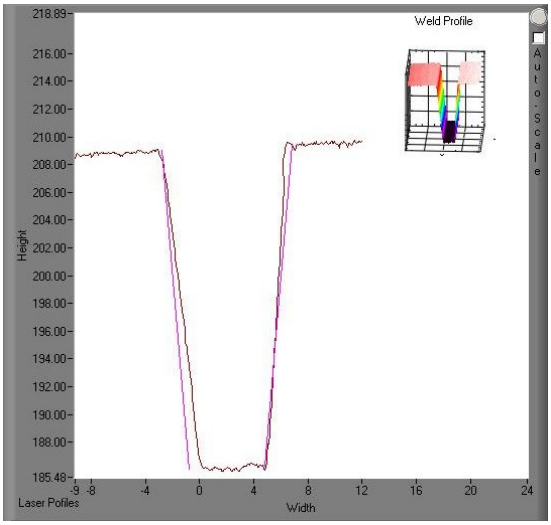

Figure 7.28 – Tilt -2 degrees.

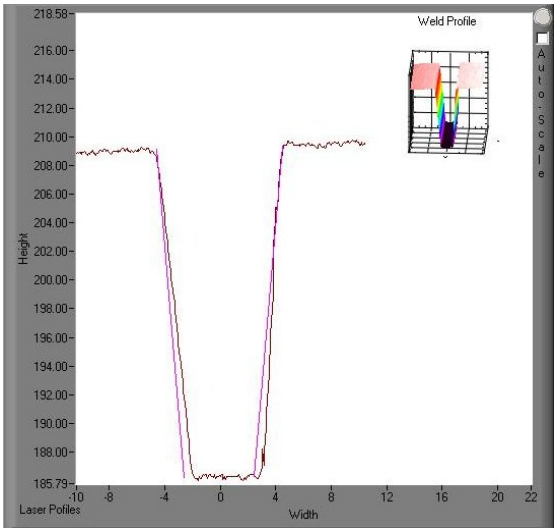

Figure 7.29 – Tilt -1 degree.

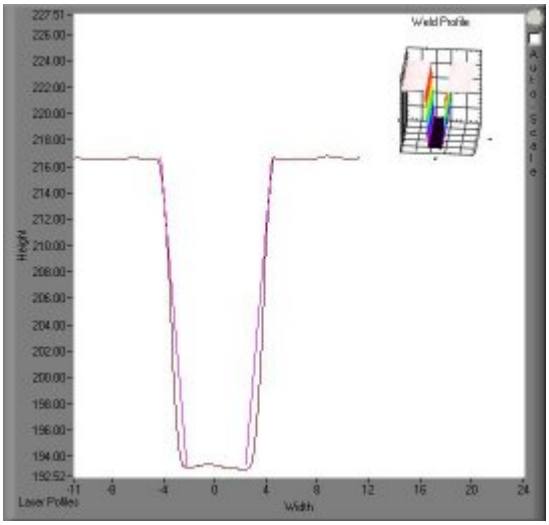

Figure 7.30 – Tilt 0 degrees.

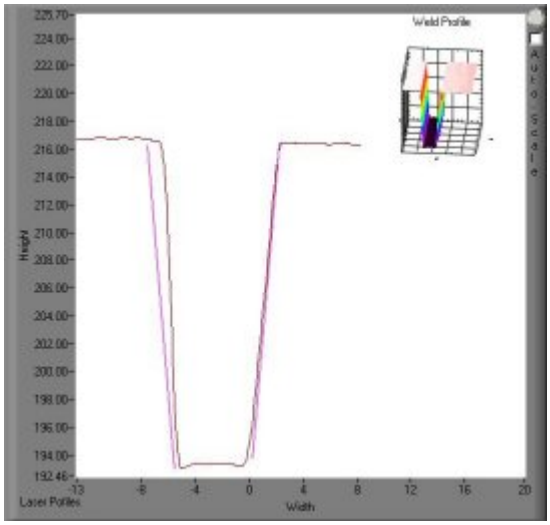

Figure 7.31 – Tilt 1 degree.

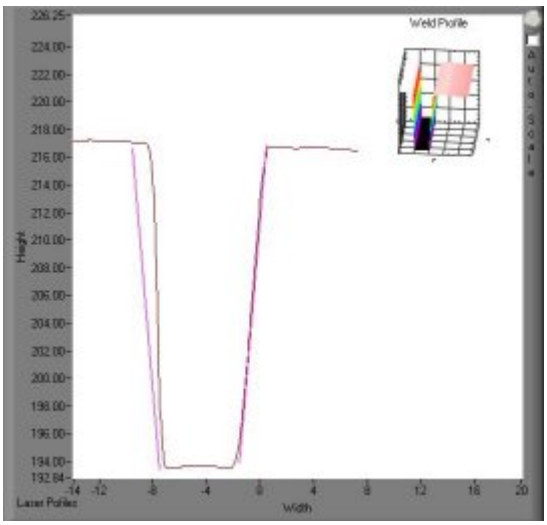

Figure 7.32 – Tilt 2 degrees.

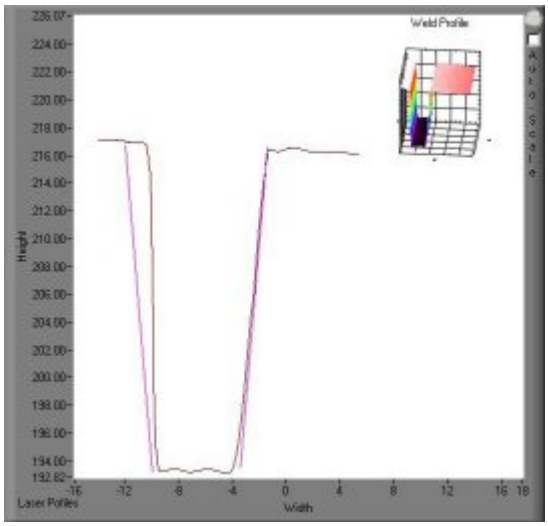

Figure 7.33 – Tilt 3 degrees.

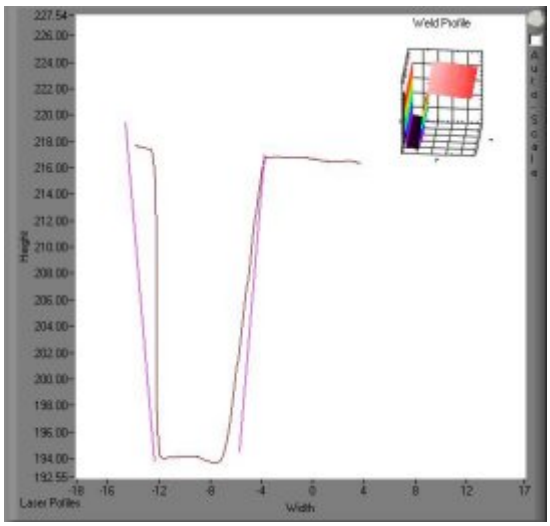

Figure 7.34 – Tilt 4 degrees.

When examining the laser scans from Figure 7.26 to Figure 7.34 is was observed that as the tilt angle was increasing, either positively or negatively, the sidewall opposed to the direction

of the tilt was becoming significantly distorted. This occurs due to the sensor's viewing angle. It gets increasingly difficult to view correctly the referred sidewall. Besides the sidewall distortion, also the groove bottom becomes distorted and appears narrower. These phenomena occur due to the shadowing effect created by the tilting of the sensor. As it is also noticeable in the obtained scans the greater the tilting angle, in eider direction, the more off centre is the groove in the profile.

One of the things that most varied with the sensor's rotation is the left and right side light length on the top surface. This can be seen in Figure 7.35. As the tilt angle increases, the projected laser light starts to reduce its intersection with either the left or right top surface. Although this is not critical in terms of the acquired data quality it can become an issue if the amount of data points representing one of the top surfaces is not 5% or more of the total data points (as described in section 7.1.3.6). This requirement derives from the way the top surfaces detection algorithm works. As the light length decreases in one direction it increases in the opposite side in the same proportion. The total length of the projected light varies slightly around the value 47.3mm (Figure 7.36). Though a variation exists, the width of the range of values is 1.2mm. The variations in the light length may be related with the difficulty in performing the measurements due to the physical restrictions of the equipment. As such they were considered not an actual result of the changes in the sensor's positioning but a result of the measurement conditions.

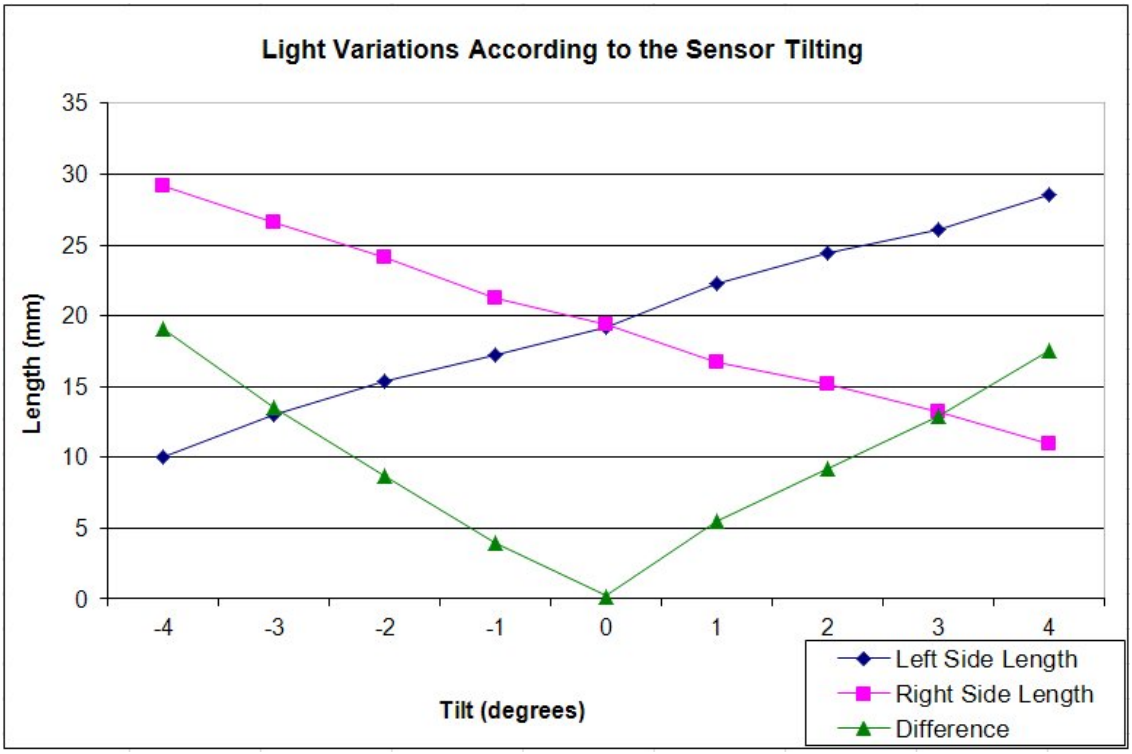

Figure 7.35 – Light variations vccording to the sensor tilting.

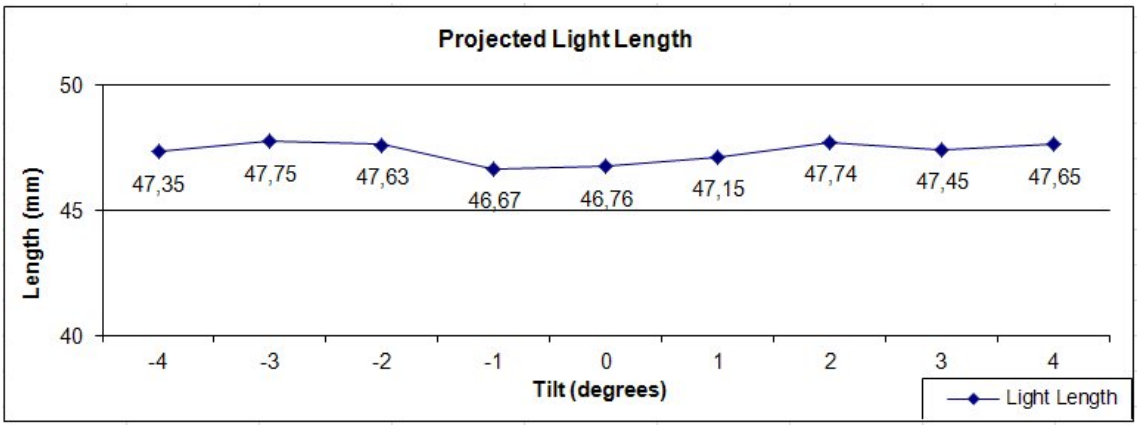

Figure 7.36 – Projected light length.

Based on the obtained results it can be concluded that tilt variations can have a negative significant effect in the acquired profile data. Looking at the results is possible to see that tilting angles of two degrees and greater the groove wall angles start to be distorted. This can be seen when comparing the wall angles with the support (pink) lines. The scans with angles of one, zero and minus one degree the walls and the support lines have the same angles. For the remaining ones the angles are different. From this set of experiments was concluded that the sensor should be quite accurately squared with the groove as this factor is quite determinant to the quality and accuracy of the obtained data.

7.3.3 Influence of Light Reflection

The parent metals used in the transmission pipeline industry are commonly carbon steels of different grades. One of the characteristics of this metal is that when used immediately after machining it is extremely reflective. Initial trials studied the influence of reflectivity on the accuracy and reliability of the scanned profile. The more reflective the object, the more inaccurate the resulting profile is. This becomes ever more significant as the groove walls become steeper. The groove walls in pipe welding application are particularly steep (5º) as can be seen in Figure 7.37. With this in mind, a comparison study was performed on reflective and non-reflective groove walls. The non-reflective configurations were: spray painting the groove walls with white matte paint; spray paint with graphite paint; wet-basting; and the situation where a previous bead was laid and the groove walls are covered in welding fume and are oxidised due to the welding heat. In this last case, the groove bottom shape is not represented by Figure 7.37 but by a groove with this shape where a bead was laid before the scanning was performed.

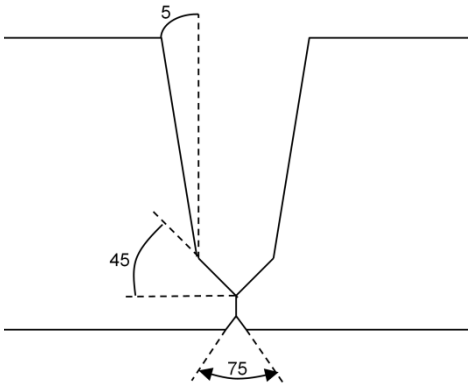

Figure 7.37 – Typical joint configuration for a pipeline application.

7.3.3.1 Reflective Surface

To investigate the effects of a reflective surface on the laser vision sensor performance, scans were performed on a specimen which had just been machined. A machined specimen with highly reflective walls and the geometry of Figure 7.37 can be seen in Figure 7.38. In Figure 7.39 is possible to see the groove resulting scan obtained with the Servo Robot™ Mini-I60. As can be seen in Figure 7.39, the data does not represent the correct groove bottom (see schematic in Figure 7.37 for the accurate shape). The misrepresentation of the groove bottom shape is caused by light reflection in the machined metal. The MT-10/15 sensor from Meta Vision Systems™ (MVS) was also used to scan this plate. It is possible to see in the actual CCD image from the MVS sensor (Figure 7.40) how reflective the surface is and some of the consequences in the acquired image. After processing the image in the sensor's control unit the data set representing the scan is sent to the computer. The received data was plotted using the *Analysis* software. A screenshot of the plotted data can be seen in Figure 7.41

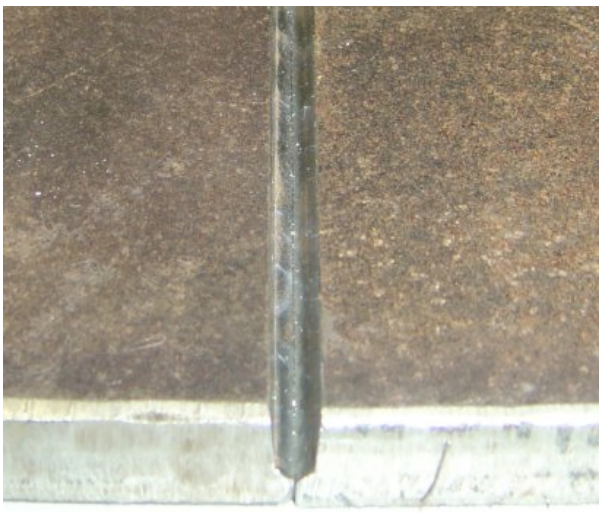

Figure 7.38 – Recently bevelled joint.

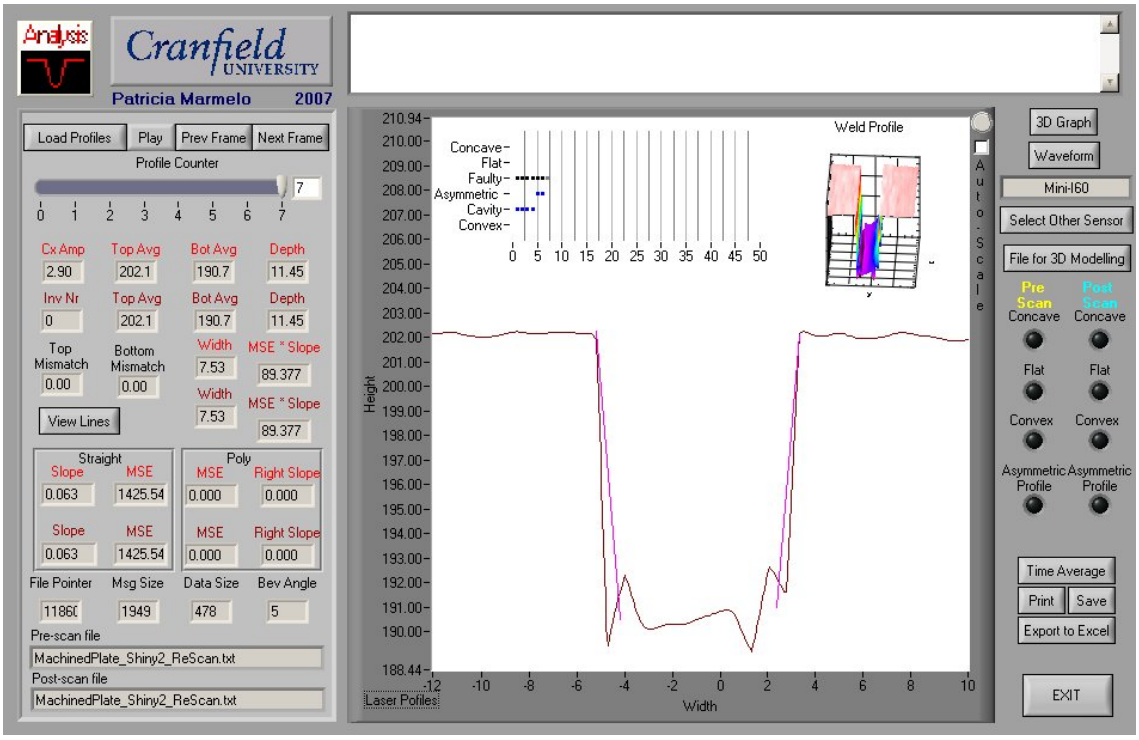

Figure 7.39 – Scan of a reflective groove with the shape described by Figure 7.37 (data from the Mini-I60 sensor).

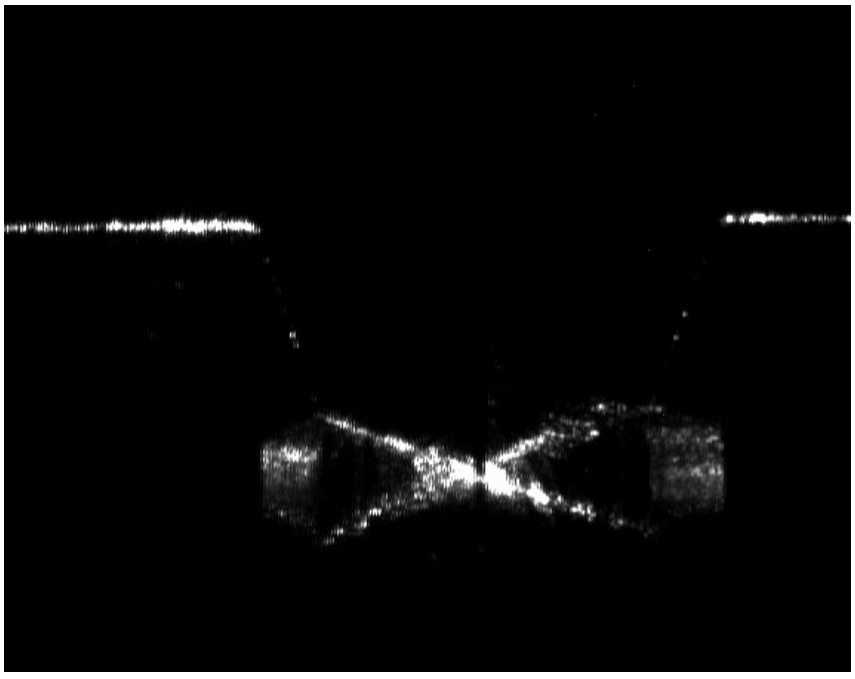

Figure 7.40 – CCD Image from the Meta Vision Systems (MVS) sensor scanning a reflective surface.

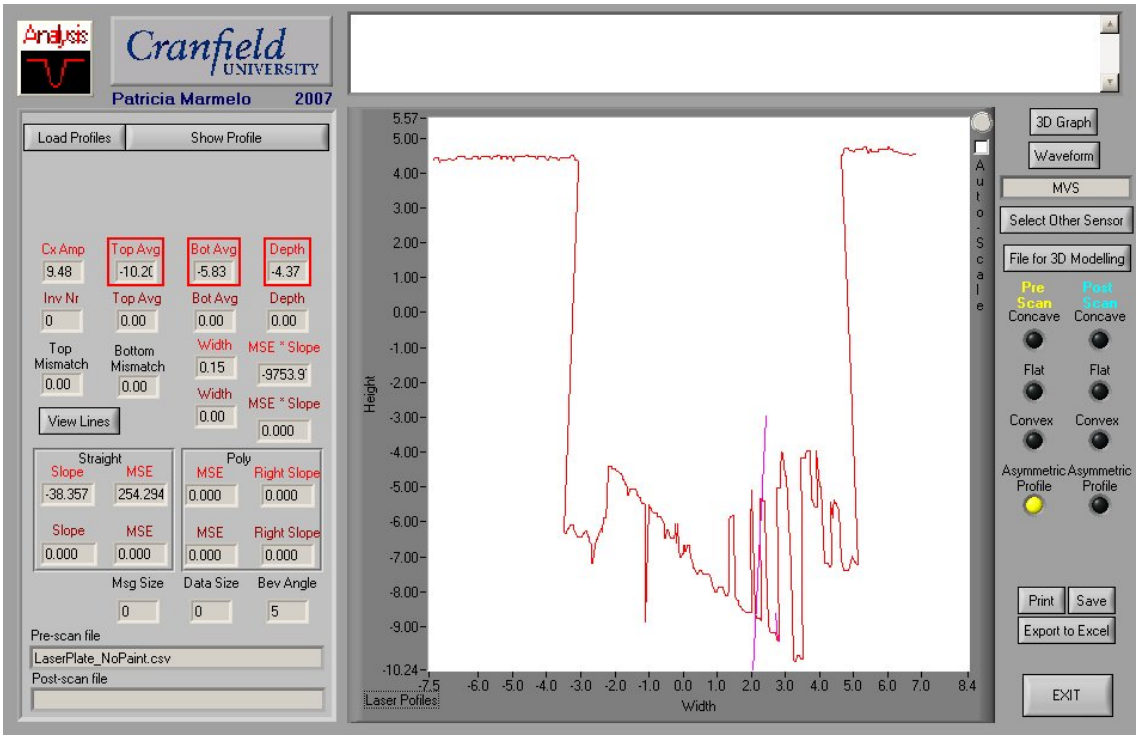

Figure 7.41 – Data from the MVS sensor when the CCD acquired image is as represented in Figure 7.40.

As can be seen in Figure 7.39 and Figure 7.41 both sensors have difficulty scanning machined surfaces with a shape like the one represented in Figure 7.37.

Secondary reflections occur particularly in highly reflective surfaces, such as machined steel, and are a problem when using triangulation vision systems. As noted by Svetkoff and Kilgus in [125], this type of reflection has a strong influence on the triangulation system outcome. To overcome this issue they developed and patented a system to suppress the unwanted secondary reflections. As result of the secondary reflections more parts of the scanned object are illuminated and therefore “viewed” by the receiver when they should not be. This becomes even more significant when using a stripe sensor instead of a spot one as on the spot one only one spot is illuminated the part and at any given time, the light receiver is only looking to that location. While in the stripe sensor, the equivalent to an array of spots is being projected and the sensor is observing a larger area. The sensor is then viewing the intended object area but is also seeing the other parts illuminated by the secondary reflections.

There are two types of reflections: specular and diffuse. Specular reflections are mirror like reflections but diffuse reflections do not form an image. In the case where the recently machined plate is scanned strong specular reflections occur. This is the cause for the groove shape obtained by the CCD inside the MVS sensor (see Figure 7.40). Keeping in mind that the groove shape is the one defined in Figure 7.37, the light that reaches the CCD is a result

of the projected light being reflected in the metal. As it can be observed, the intensity of some light reflections is stronger than the actual light on the object. This way even if the sensor's algorithm rejects data based on intensity it is not capable of rejecting the specular reflections light because it is quite intense.

In Figure 7.41 is the data extracted from the CCD image with the MVS sensor. Observe that the groove walls are outwards. This is due to the incapability of the sensor internal algorithm to deal with this kind of reflections. Another thing to be noticed is the fact that groove bottom does not have a "V" shape, in fact is impossible to discern any shape in that section of the plotted data.

As can be seen in Figure 7.39 and Figure 7.41 both sensors have difficulty scanning machined surfaces with a shape like the one represented in Figure 7.37. On the Servo Robot Mini-I60 it was not possible to access the actual CCD image as it was in the MVS MT-10/15 sensor (Figure 7.40). As such no definitive conclusion can be drawn from comparing Figure 7.39 and Figure 7.41. The difference in the results can simply be related with different lighting conditions in the places where the experiments were performed.

7.3.3.2 White Matte Paint

The use of white matte paint to cover the groove walls was one of the approaches taken to test the sensors reaction to this groove shape. In this particular case, a different groove geometry was used. This new geometry can be seen in Figure 7.42. The painted plate with the projected laser light can be seen in Figure 7.43. With naked eye is possible to see that the amount of reflections in the groove bottom is very small and is just in the bottom corners. As it can be seen in Figure 7.44 the sensor was able to acquire a good representation of the groove geometry. The reflections that with the naked eye can be seen in the bottom corners are not a problem for the sensor as it can be seen in Figure 7.44 profile bottom corners.

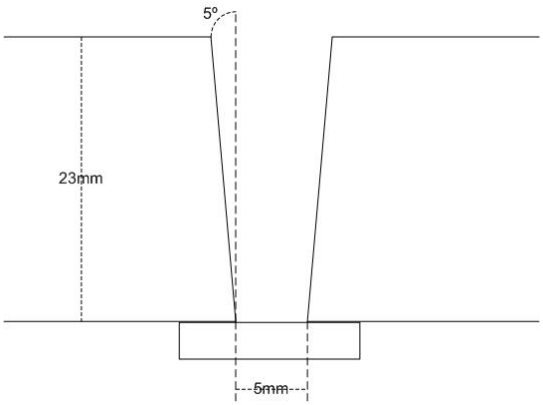

Figure 7.42 – Test plate joint configuration.

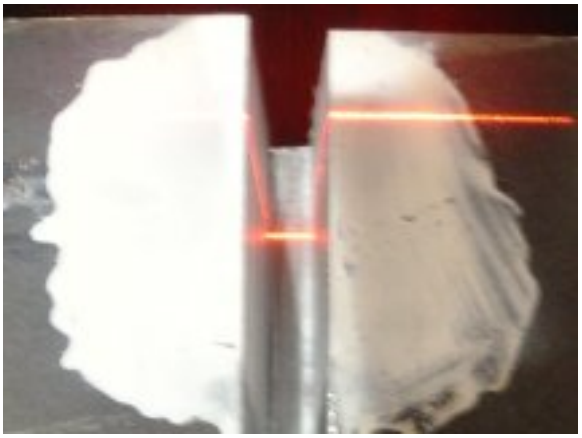

Figure 7.43 – Spay painted with white matte paint.

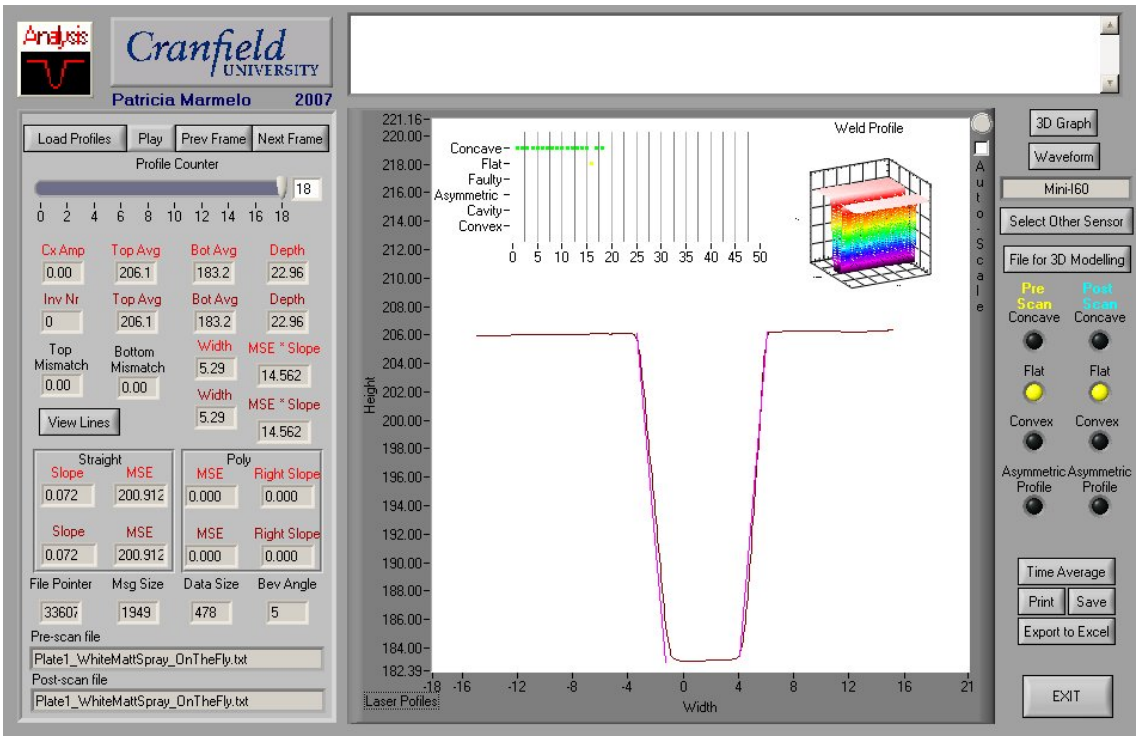

Figure 7.44 – Scan of the spray painted groove with white matte paint seen in Figure 7.43.

A picture of the white matte sprayed test plate can be seen in Figure 7.43. It is possible to see in this picture that the projected laser light reflects in a diffused manner in the groove interior corners. This reflection does not seem to affect the outcome of the laser sensor control unit as can be seen in Figure 7.44. A profile like this was the intended one but this kind of paint cannot be used in practice as this type of paint would alter the chemical properties of the weld. As the paint would boil at the welds' high temperatures it was likely to create air bubbles that would be trapped inside the weld creating porosity. The actual paint residues would also be trapped inside the weld creating inclusions. Either of these situations would result a defective weld that would have to be grinded down and rewelded, most likely manually. This would beat the purpose of using a laser sensor to automate the system because it would require corrective work.

7.3.3.3 Graphite Paint

Another approach taken to overcome the reflections problem was to spray the groove with graphite paint. Once the surface is sprayed, it becomes non-reflective and the measurements can be performed. The graphite paint used was the "Graphit '33' Spray"™. Two test plates were employed, one (*Plate 1*) was the one described in Figure 7.42 and the other (*Plate 2*), described in Figure 7.37.

A picture of *Plate 1* sprayed with the graphite paint can be seen in Figure 7.45. Figure 7.46 shows *Plate 1* scan using the Servo Robot Mini-I60™ sensor. It is possible to see that the scan is accurate, both in terms of sidewall angles and groove dimensions. The expected five degree angle represented in the image by the pink lines match the groove walls from the sensor's data.

The physically measured groove dimensions (see Figure 7.42) are verified by the scan results. See "Depth" and "Width" values in Figure 7.46 for groove depth and bottom width values respectively.

Figure 7.45 – Plate 1 spay painted with "Graphit '33' Spray"™.

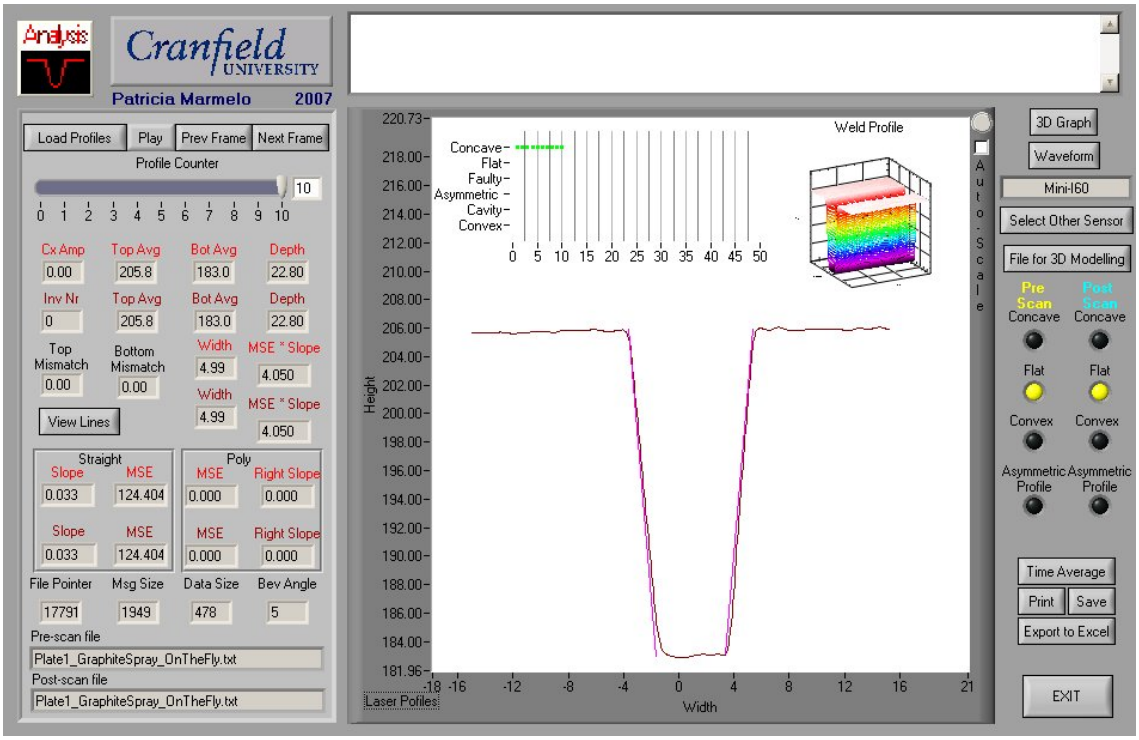

Figure 7.46 –Scan of plate 1 covered with graphite paint (Mini-I60).

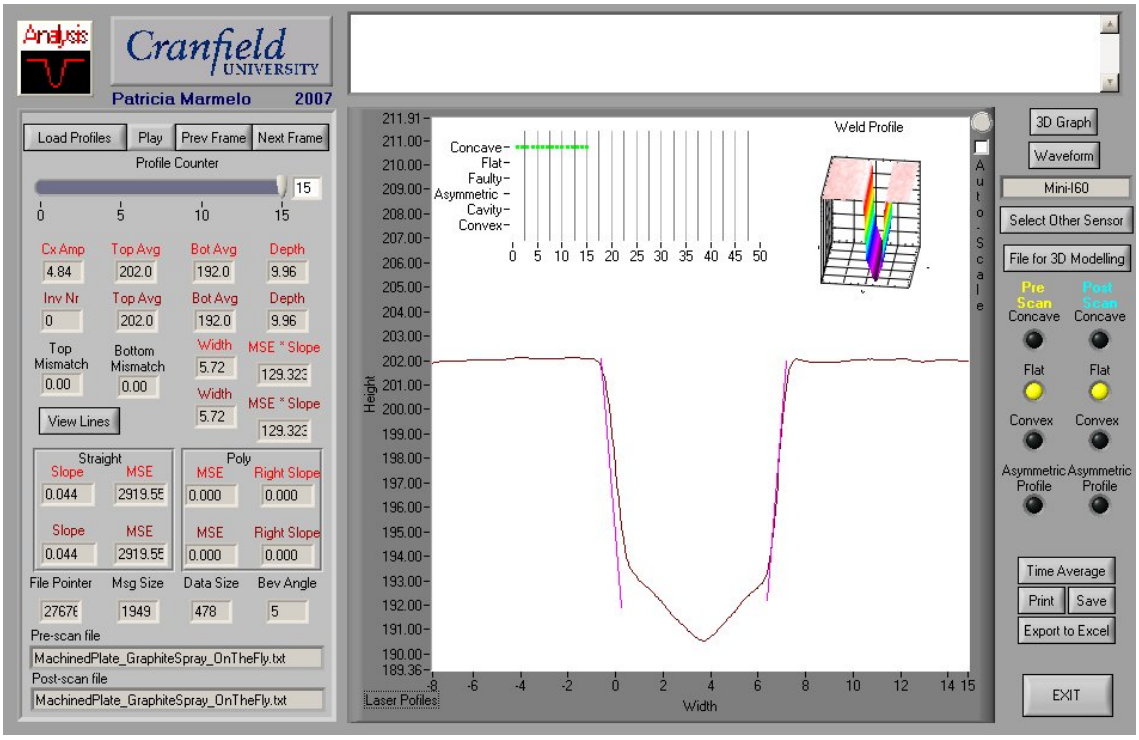

Figure 7.47 – Scan of plate 2 covered with graphite paint (Mini-I60).

After *Plate 2* was covered with graphite paint it also became non-reflective and the resulting scans can be seen in Figure 7.47. It is possible to seen in the 3D “Weld Profile” in the image that throughout the plate the sensor acquires correctly the groove shape, which can be seen in detail in the 2D “Laser Profiles” graph from the same image. When comparing the images from MVS sensor’s CCD (Figure 7.40 and Figure 7.48) is clear that the reflection issues are highly reduced.

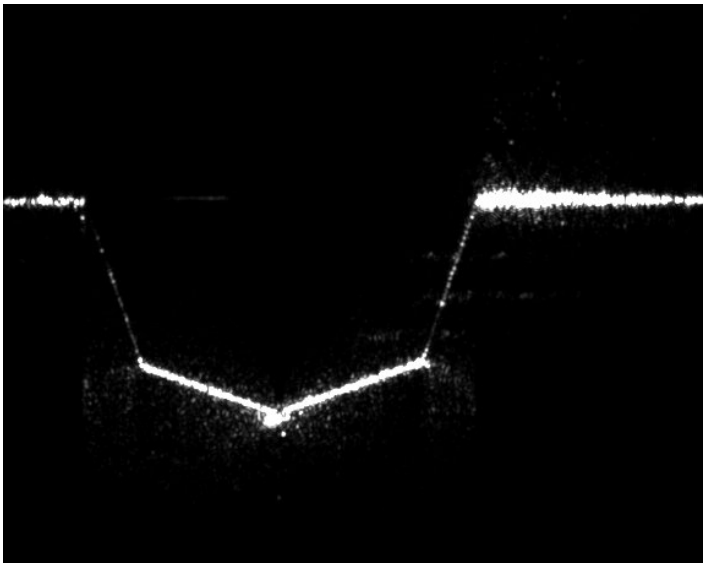

Figure 7.48 – CCD image from the Meta Vision Systems (MVS) sensor scanning plate 2 with graphite coated surface.

The graphite paint was considered an option, as it would not alter the weld properties at the same time it would eliminate the reflectiveness. An image of a plate covered with graphite spray can be seen in Figure 7.45. The obtained results were also accurate as it can be seen in Figure 7.46 and Figure 7.47. Despite this would be a solution to this issue it again was not considered a suitable solution because in terms of field application it would not be a very practical one. In the field, where this work is aimed for implementation, it would be quite time consuming having to hand spray every pipe preparation. In an industrial application that aims to increase its productivity having the production slow down because of such a small part of the production purpose it would be counterproductive.

7.3.3.4 Wet-Blasting

Spraying the groove walls with paint has a number of disadvantages including metallurgical issues with the weld so these approaches are not very viable in field applications. This required the search for a different approach, one that would overcome the reflection issues and still not interfere with the weld quality.

Wet-blasting or sandblasting consists of cleaning or abrading with a strong current of air mixed with sand. As can be seen in Figure 7.49 a wet-blasted surface can become non-reflective. Wet-blasting represents a feasible approach to the issue as it adds nothing to the groove walls and could easily be applied in a pipeline installation site.

The test plate used to perform this test was the one described in Figure 7.42. The resulting scan produced with the Servo Robot Mini-I60™ can be seen in Figure 7.50. The image shows that it is possible to scan effectively a wet-blasted joint to extract its features. As in the case of the use of graphite paint (*Plate 1*) the extracted values from the groove scans match the physically measured values.

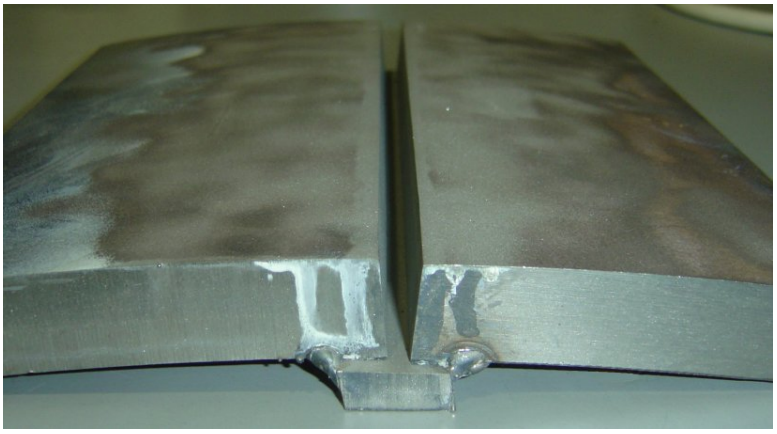

Figure 7.49 – Wet-blasted joint.

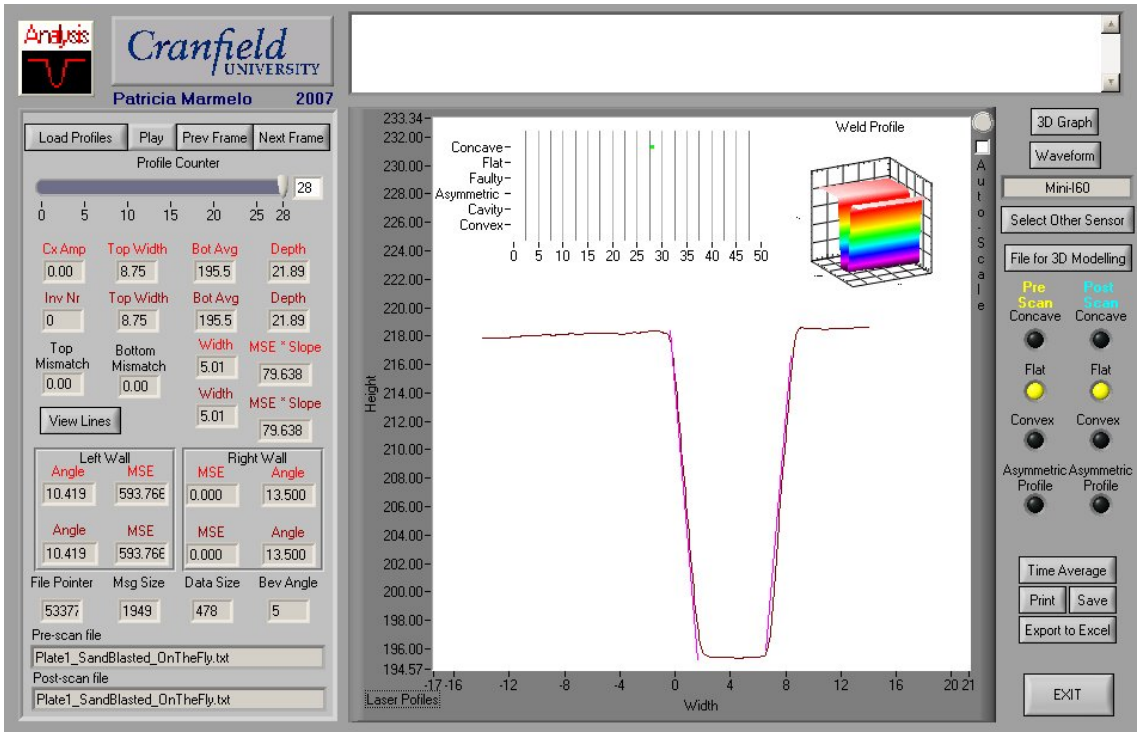

Figure 7.50 – Scan of the wet-blasted plate seen in Figure 7.49.

A reflective prepped material and the same surface after being sprayed with graphite spray can be seen in Figure 7.51. The shiny surface is represented by the red line and the surface sprayed with graphite paint can be seen in a dark shade of red. The pink lines represent the expected location of the real 5 degrees walls. This scans were generated with the software filters ON. As a consequence of the software filters being ON the angle on the walls, even on the graphite painted walls, is distorted. As can be seen in Figure 7.51 for the shiny walls the wall angle is 2 degrees and for the graphite painted walls is 7 degrees. Despite the horizontal displacement between the two scans it can be seen that in the top part of the groove both scans have the same geometry. However, on the groove bottom reflections completely distort the groove shape.

The comparison between the resulting scans from a groove spayed with graphite paint (red colour) and the same groove sandblasted (dark red colour) it can be seen in Figure 7.52. It is possible to see that both situations generate accurate and similar results. The same occurs when comparing the sandblasted groove (red colour) and the same surface previously sprayed with white matte paint (dark red colour). The comparison between the two situations can be seen in Figure 7.53.

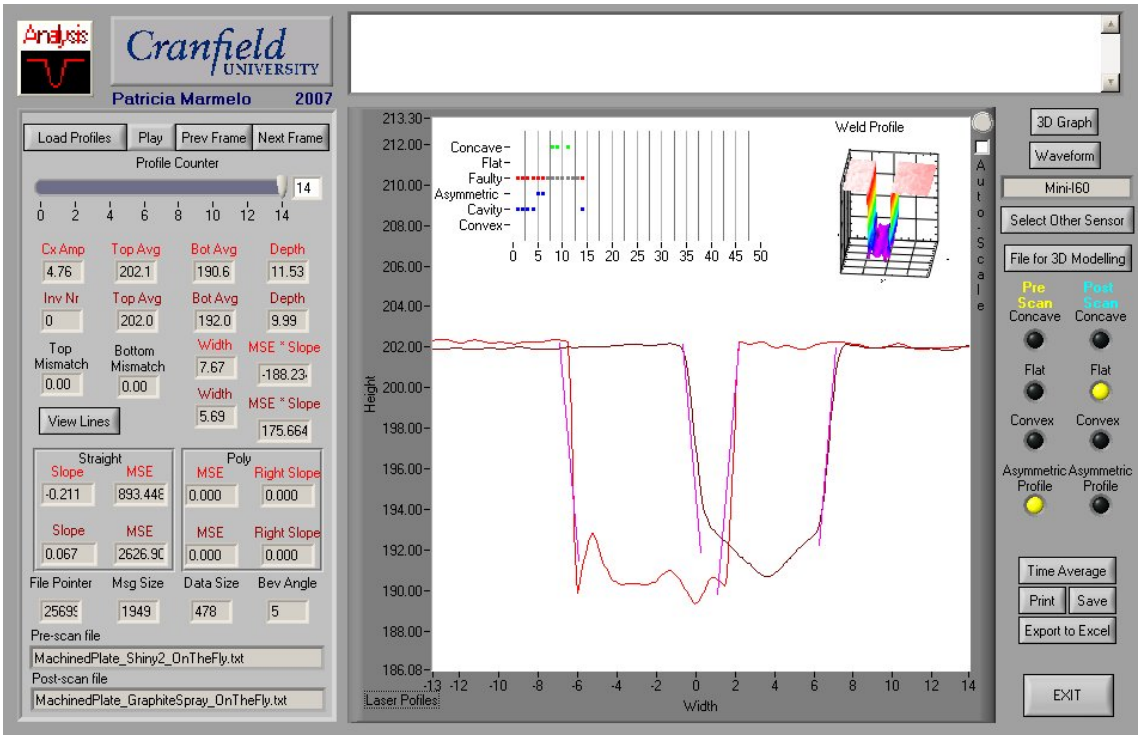

Figure 7.51 – Comparison between the resulting scans of a shiny groove and the same groove after being sprayed with graphite paint.

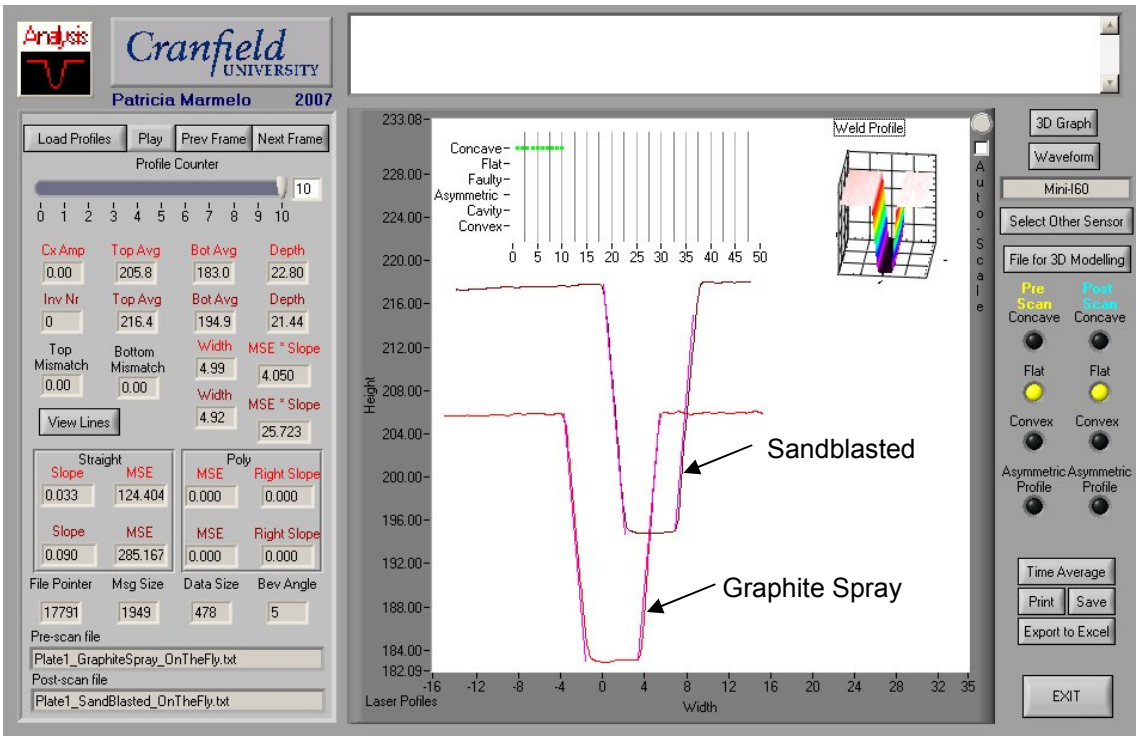

Figure 7.52 – Comparison between the resulting scans of a groove after being sprayed with graphite paint and the same groove after being sandblasted.

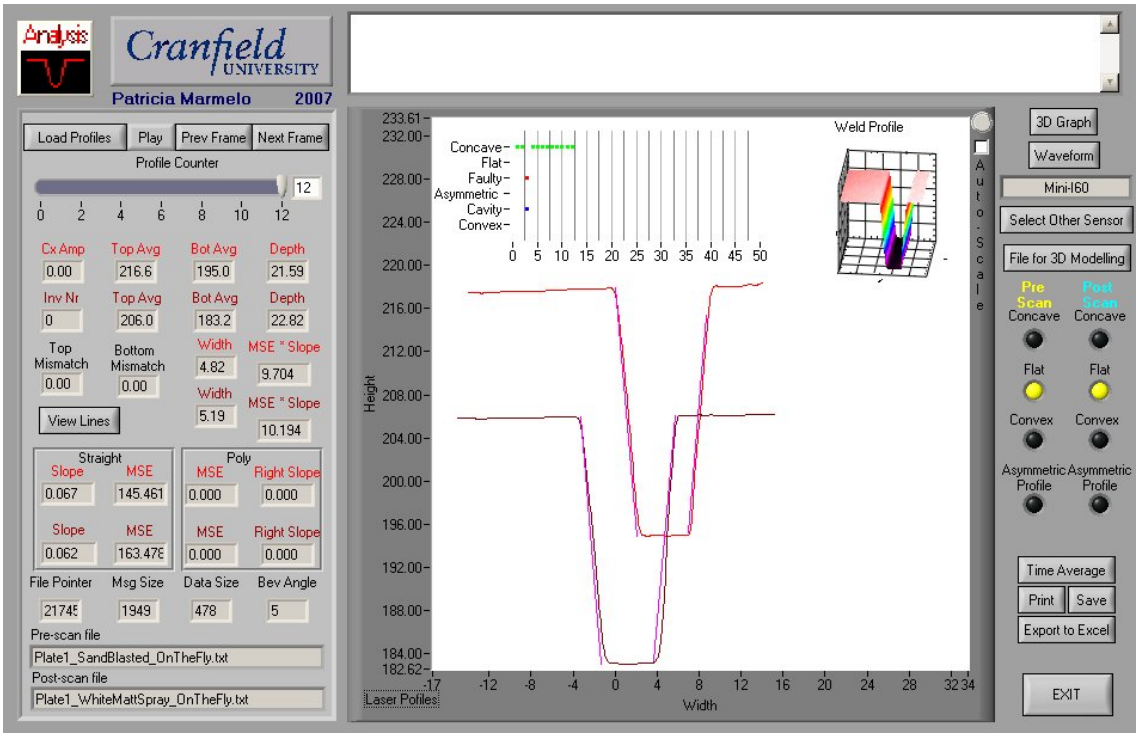

Figure 7.53 – Comparison between the resulting scans of a groove after being sandblasted and the same groove after being sprayed with white matte paint.

7.3.3.5 Walls Covered with Welding Fume Particles

From the initial trials made to assess the issue of light reflection in different setups it was shown that a highly reflective surface such as a just prepped carbon steel pipe joint is very problematic. It was also shown that once the surface is no longer highly reflective the scanning results are accurate. Either when the surface is sprayed with white matte, graphite paint, or when sandblasting is used, the scan results are alike. The same effect occurs when a weld bead has already been laid and the groove walls are oxidised and covered in deposited welding fume. It is not possible to compare any of the previously referred scans with a scan containing at least one bead on the groove as would be comparing two different things. But it is possible to compare a laser scan with a macro of the same weld. This comparison can be seen in Figure 7.54. The data shown represents the laser scan and macro of weld Run 3 performed in the Flat position. This scan was performed with the software filters OFF and so the scan data contains noise that was not smoothed however as can be seen the correspondence between the scan data and the actual groove is very good.

From this point of the work onwards only the Mini-I60 sensor was used.

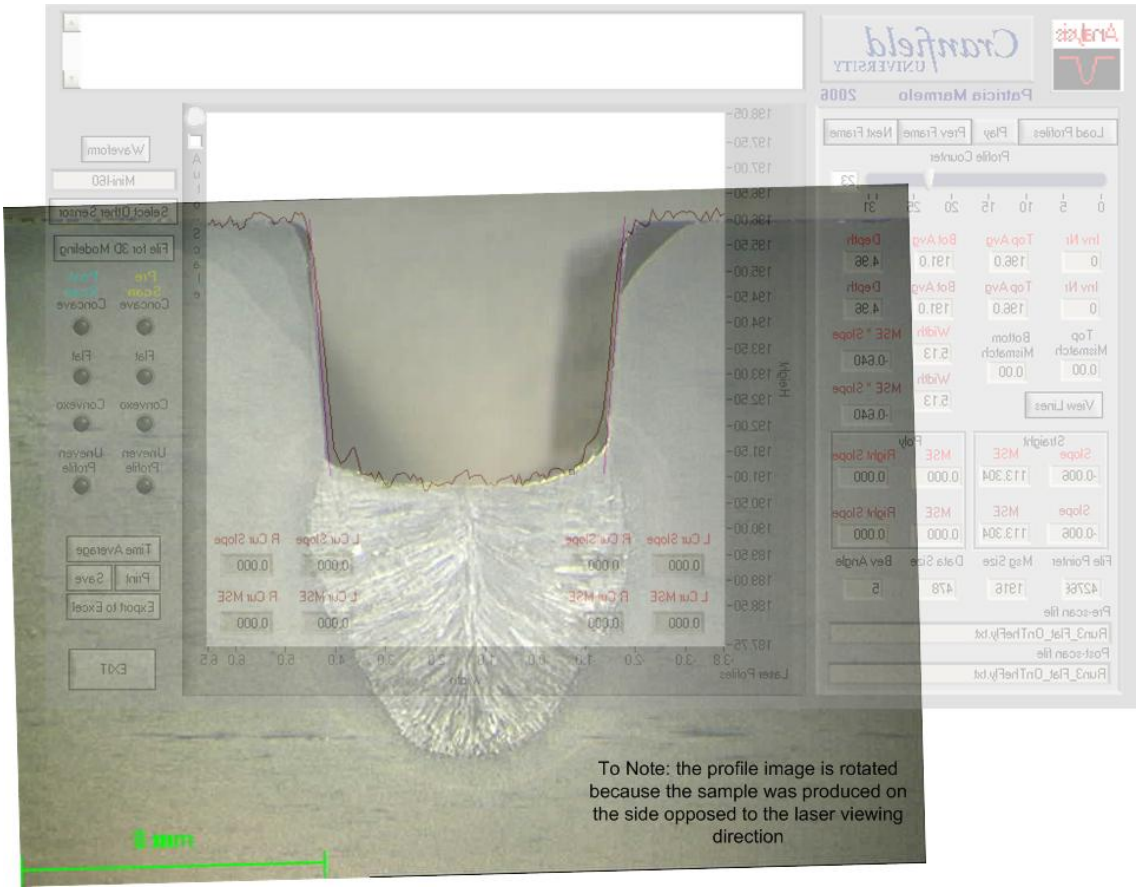

Figure 7.54 – Weld scan superimposed on the macro image of Run 3 in the Flat position.

7.3.4 Influence of the Servo Robot Software Filters

Servo Robot supplies their proprietary software *WinUser™* with their vision systems in order to configure and operate the system from a PC. One of the features in this software is the filters that can be applied to the acquired image (see Figure 6.8). The function of these filters is to smooth the noise in the profile data. For an in depth explanation of the filters view the WinUser™ Software Manual [121]. At the same time that it smoothes the noise in the processed profile it also smoothes some other profile features

In the early stages of the work the results from the laser scans were quite inaccurate when it came to the sidewall angles and the width of the groove bottom. After some tweaking with the data in S4 it became clear that the issue was not related with SP4 but with the data it was using. So a step back was taken and it was decided to evaluate the laser sensor own software, as an attempt to overcome this issue. This proven to be successful after a short while as it became clear with the following set of experiments.

The *Median* filter is applied to remove noise from the profile data and the *Average* one to smooth the acquired profile. *Filter Size* is the term defined by Servo Robot in their software manual [121] and it is not clear what it means although it probably means the number of data points used to perform the filter calculations. *Continuity* is defined in the same manual to be a feature of the VISIUS™ software inside the laser control unit. This feature according to the software manual should be used when the scanned object has a hole or a gap. The software will connect the point before the hole with the one after the hole. This connection is made with a straight line. It was noticed that when scanning reflective pipeline grooves although no holes existed, if *Continuity* was OFF some pixels in the certain locations, corners especially, would have a zero value indicating that a hole was detected in the position. The reason for the zero value found is most likely a consequence of specular reflections. If *Continuity* is kept ON that phenomenon does not occur and no detail in the groove is lost as *Continuity* does not alter the acquired data. As can be seen in Figure 7.55, where the *light red* plot represents the scan with *Continuity* OFF and the *dark red* plot represents the scan with *Continuity* ON, the last data point has a maximum negative value. A maximum negative value represents saturation in the sensor. Saturation occurs when the sensor does not find a value, and the data point automatically assumes the lowest value it can be. This is defined in the code of the control unit program that extracts the data points from the CCD sensor.

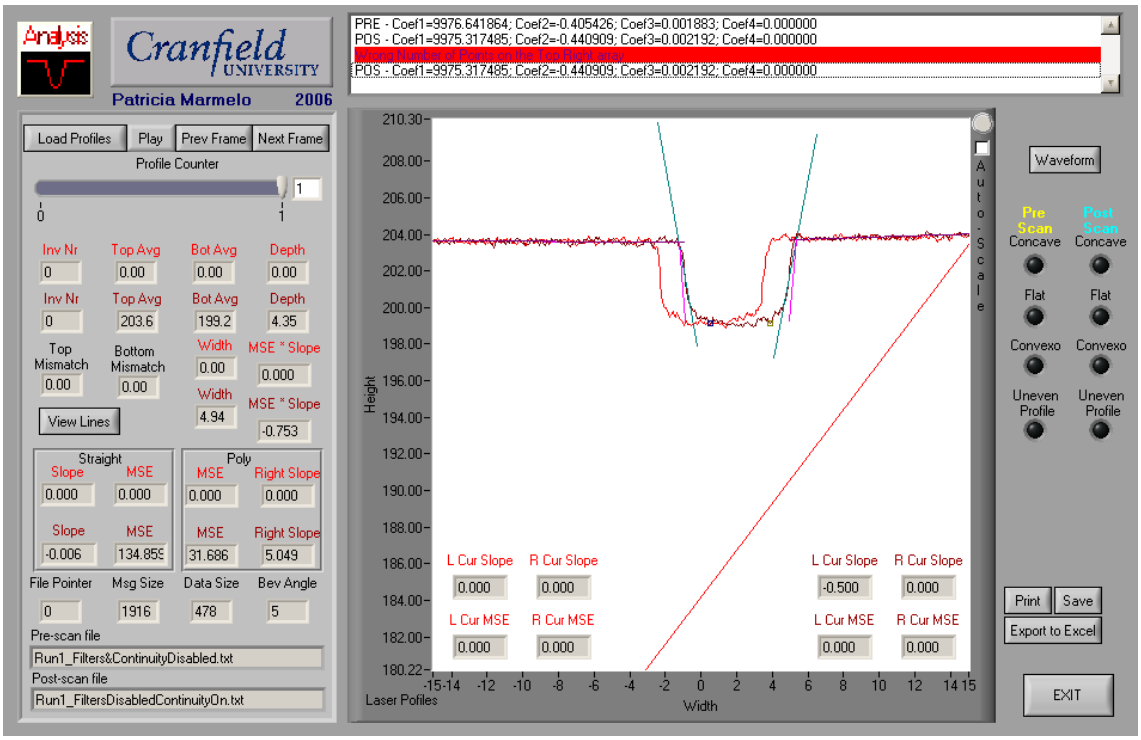

Figure 7.55 – Comparison of Scans Performed with Continuity ON and OFF.

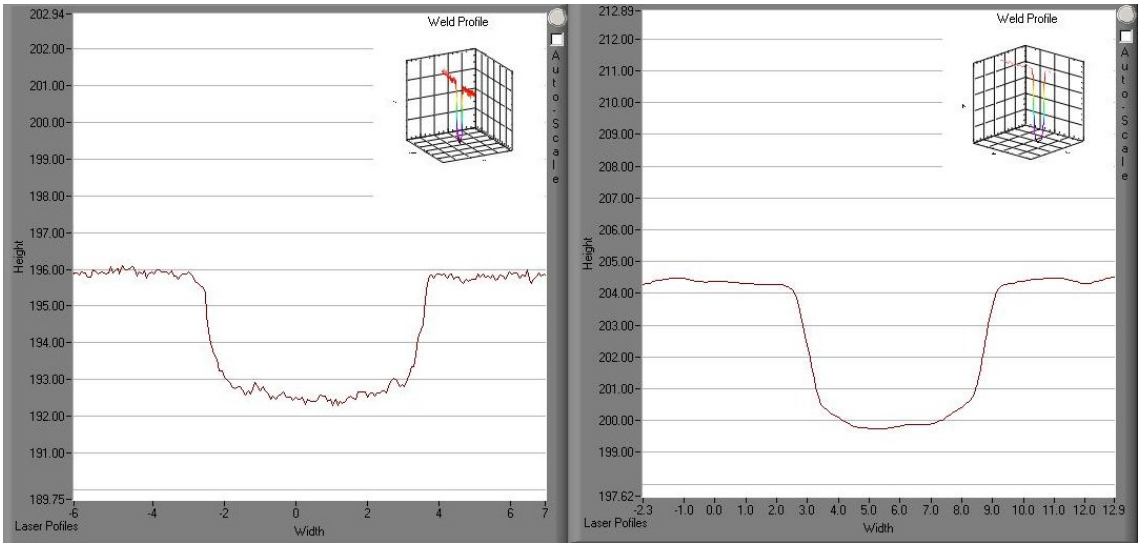

Figure 7.56 – Groove Profile Respectively Without and With WinUser™ Filters Active (*Continuity* ON, *Average* & *Median* ON filter size 10).

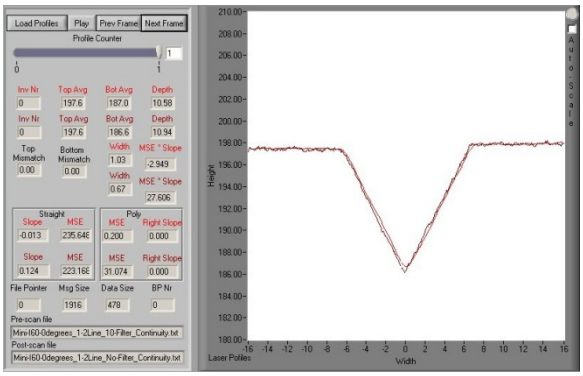

Figure 7.57 – 30 Degrees Bevel Angle Plate (Light Red – Filter Size 10; Dark Red – No Filter; Continuity ON in Both Scans)

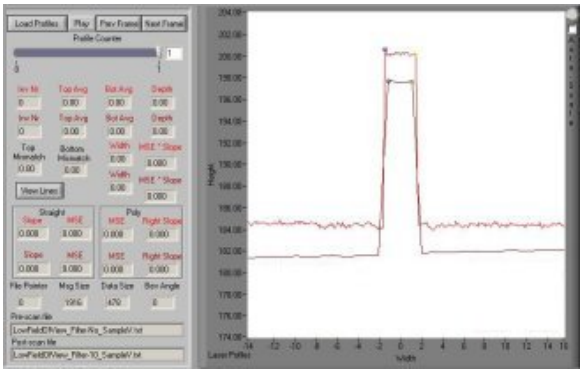

Figure 7.58 – 0 Degrees Walls Metal Block (Light Red – No Filter; Dark Red – Filter Size 10; Continuity ON in Both Scans)

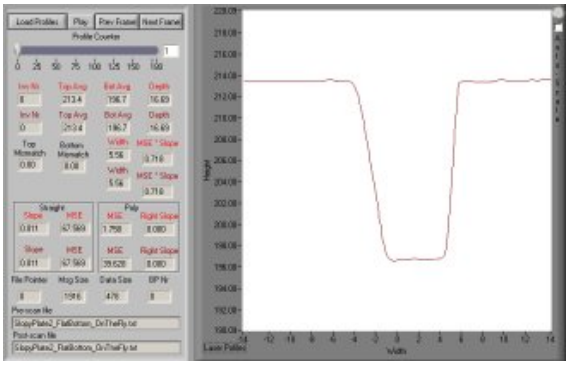

Figure 7.59 – Groove 16.7mm Deep (Filter Size 10; Continuity ON)

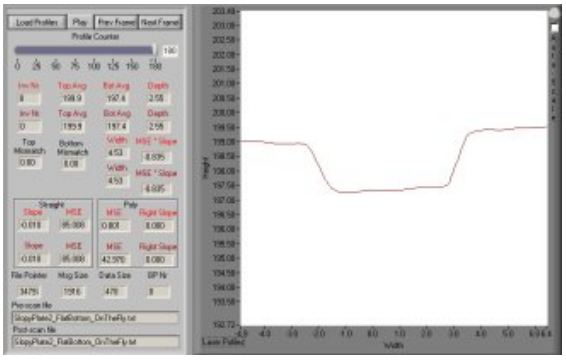

Figure 7.60 – Groove 1.8mm Deep (Filter Size 10; Continuity ON)

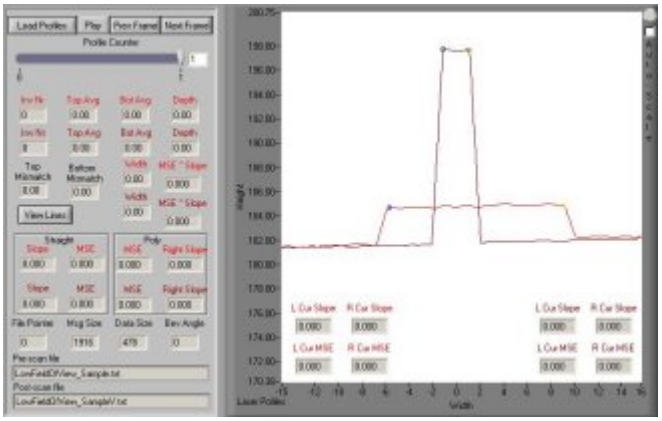

Figure 7.61 – 0 Degrees Walls Metal Block (Light Red – Horizontal Position; Dark Red – Vertical Position; Filter Size 10; Continuity ON in Both Scans)

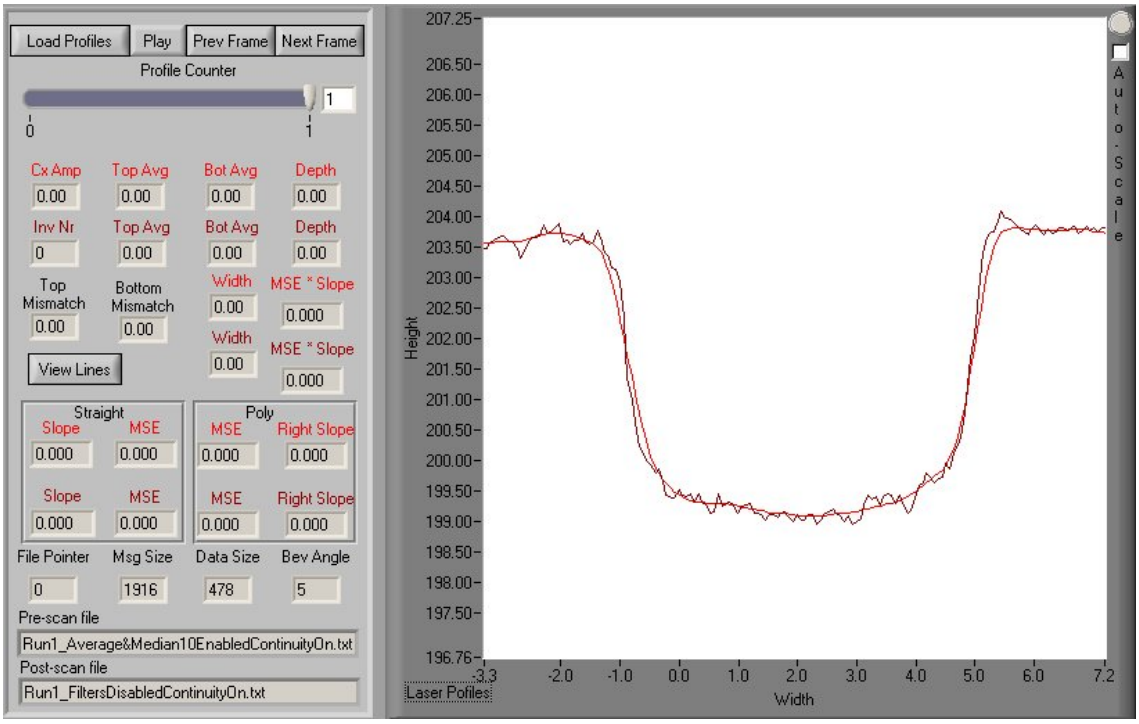

Figure 7.62 – Comparison between a scan with filter size 10 (red) and no filter (dark red); continuity ON; groove 4.3mm deep in terms of data noise.

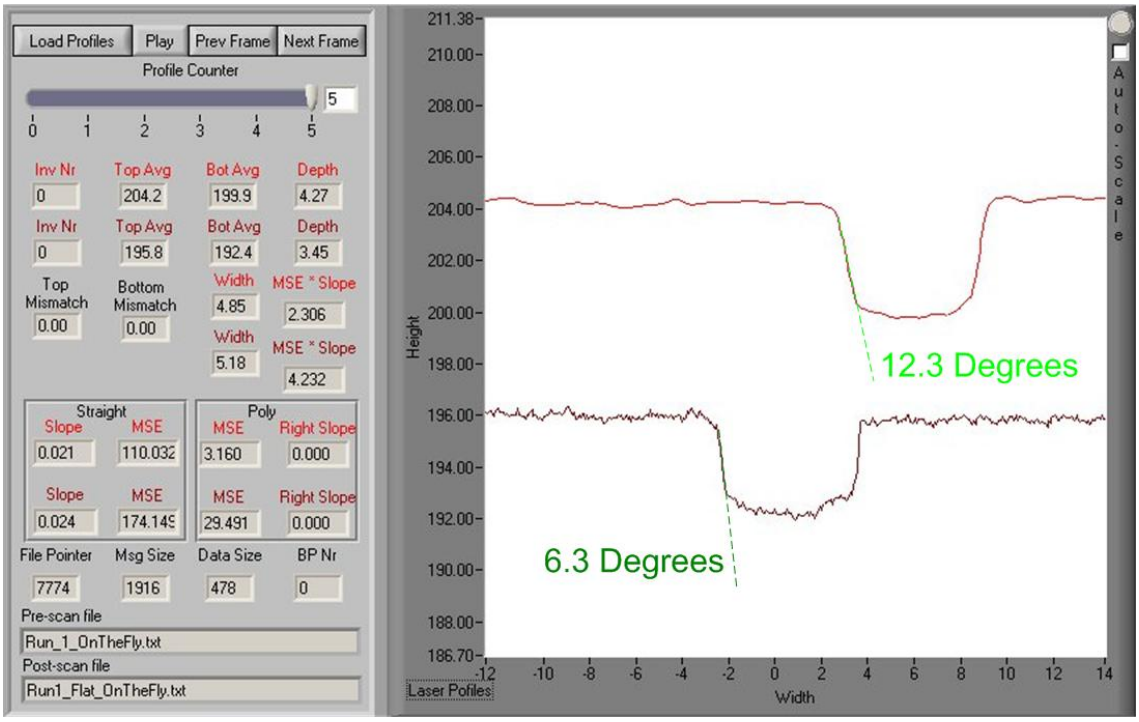

Figure 7.63 – Comparison between a scan with filter size 10 (red) and no filter (dark red); continuity ON; groove 4.3mm deep in terms of groove wall distortion.

The higher the filters size the more steep sidewalls are affected by the filters. Specimens that were prepared with 5 degrees sidewalls when measured with the laser vision system had measured values ranging from 5 degrees (no filter) to 13 degrees (filter 10). The comparison can be seen in Figure 7.62. The shape of the groove bottom did not lose features but they were squeezed into a narrower groove bottom as can be seen in Figure 7.63. In this figure can be seen data acquired with the same filters settings as the ones used in Figure 7.62. In the top profile of Figure 7.63 is possible to see how the use of filters reduces the noise in the profile data. When comparing the top and bottom profiles is possible to see how the use of filters distorts the groove wall angles.

From the obtained results the distortion effects of the different filters are more evident in the groove sidewalls particularly in steep walls (Figure 7.57 and Figure 7.58) and shallow grooves (Figure 7.59, Figure 7.60 and Figure 7.61). On scans represented in Figure 7.58 the scan performed with no filters ON the wall inclination is in fact one degree on both sides and in the scan performed with a filter size of ten the wall inclination measured is 3 degrees on both sides. As the filters use an averaging method to eliminate the noise from the data, used in excess it can distort the data. In steep walls, the top surface last data points influence considerably the wall initial data points. The same way, the last data points from the wall are influenced by the bottom initial data points. What this results in the alteration of the wall angle increasing it. The shallower the groove the less data points the wall is represented by and as a consequence the more the filters tend to alter the groove shape.

Although no experiments were performed to assess a usable filter size for these applications it is clear from the results that the smaller the filter size the better. According to Agapakis [126] the filtering window size has an impact on the quality of the resulting image. He concluded from his experiments that a filter of three to five pixels would give the best results. For the remainder of the work it was decided the scans would be performed with the filters OFF.

7.3.5 Effect of Groove Depth on Software Performance

A test plate was made with an inclined top surface to determine the effect of variation in the groove depth on the acquired data. It was noticed in some of the previous experiments that the shallower the groove, the more distorted was the groove walls data. In order to better understand the causes of this phenomenon and limitations this may cause, a sloping plate was created. This plate besides, having a narrow groove with five and nine degrees sidewalls, also had a sloping top surface. An image of this plate can be seen in Figure 7.66. A schematic of the plate characteristics can be found in Figure 7.64 and Figure 7.65.

For this experiment three scans were preformed, two with the software filters activated and one without. For the first two, one was performed with the groove bottom at a constant distance from the sensor and in the other the top surface was at a constant distance from the sensor. The aim of taking these two approaches was to discern if the positioning had any influence on the sensor performance. A schematic of each layout can be seen in Figure 7.67 and Figure 7.68 respectively. For the one with the filters OFF the scan was performed with the groove bottom at a constant distance from the sensor. Both sets of experiments are described below together with the experimental results.

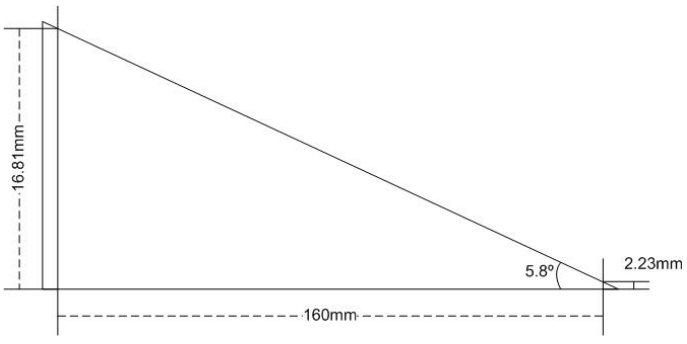

Figure 7.64 – Sloping plate – groove depths.

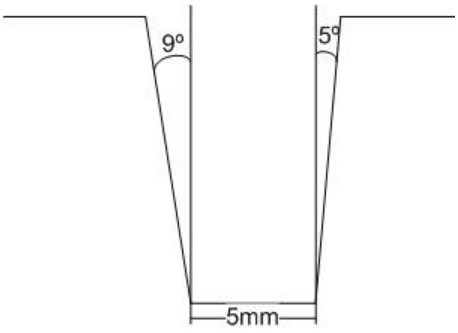

Figure 7.65 – Sloping plate – joint preparation

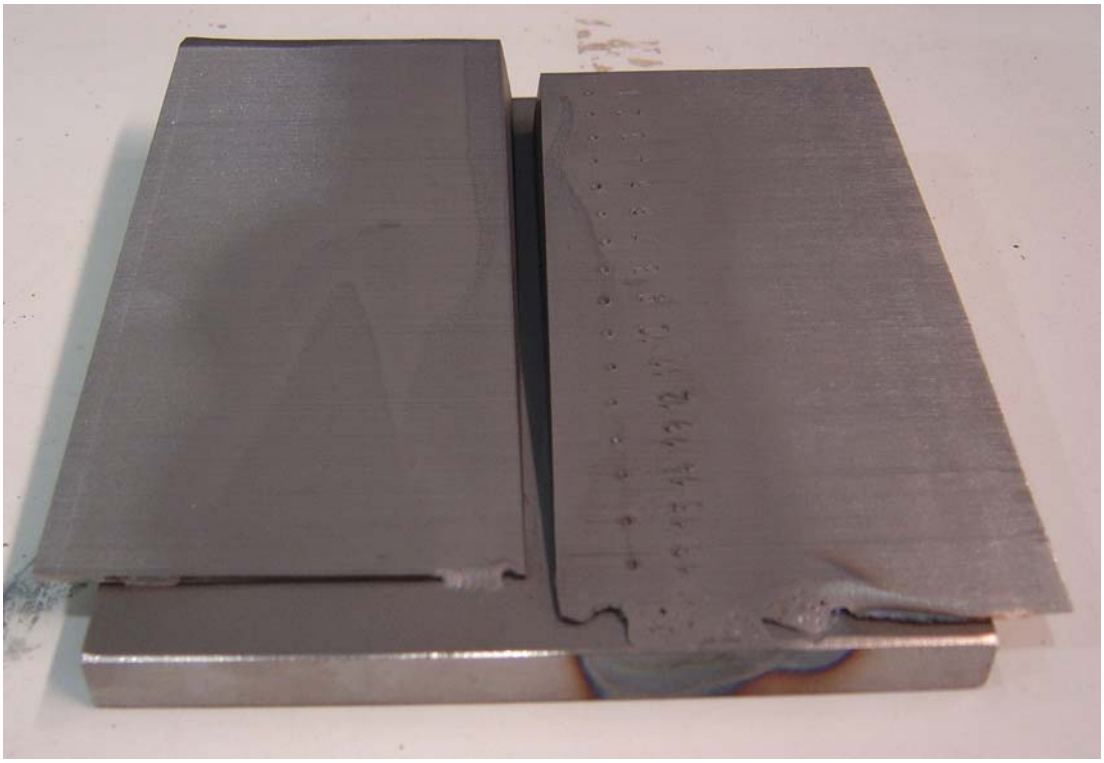

Figure 7.66 – Sloping plate.

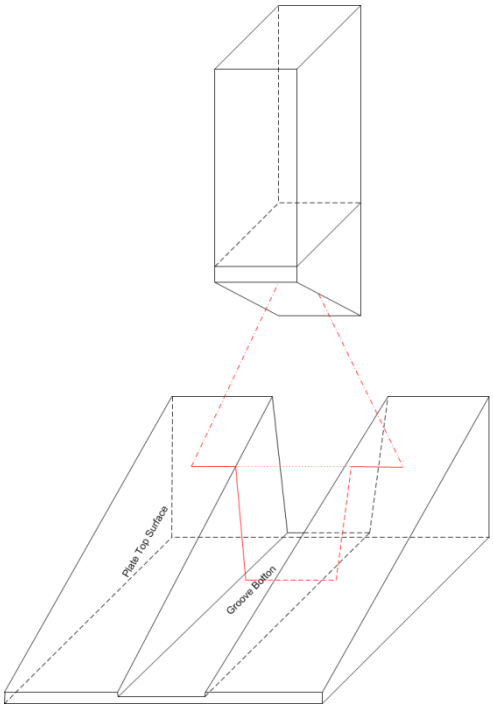

Figure 7.67 – Scan schematic with a constant distance to the groove bottom.

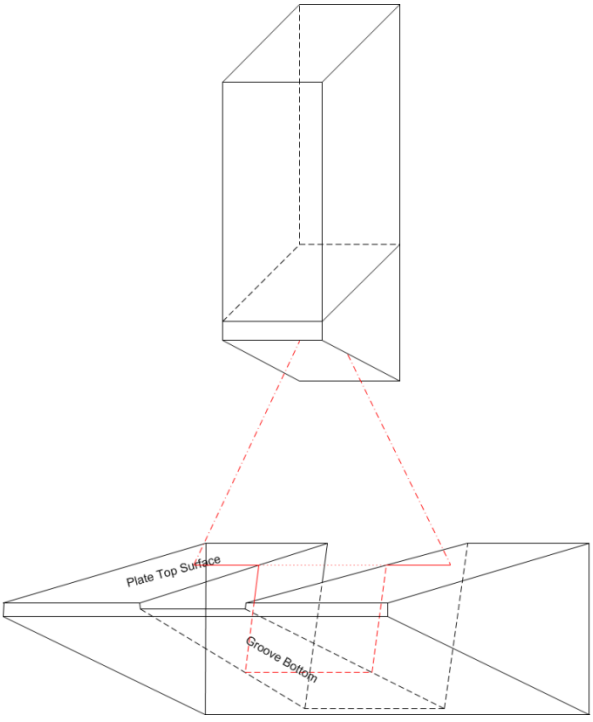

Figure 7.68 – Scan schematic with a constant distance to the top surface.

7.3.5.1 Scan with Filters Activated

The configuration of the WinUser™ software used in this set of experiments can be seen in Appendix H1. The data concerning the experiments performed with the filters activated can be seen in Table 7.4. Screenshots of the *Analysis* software showing the data can be found in Appendix G1 and Appendix G2.

7.3.5.1.1 Flat Groove Bottom

This scan sequence was performed with the test plate laying flat on the specimen holder. A 3D model of the scan results can be seen in Figure 7.69. Note that the Z scale is expanded compared to the X and Y scales. The actual inclination angle of the top surface is 5.8º as can be seen in Figure 7.64.

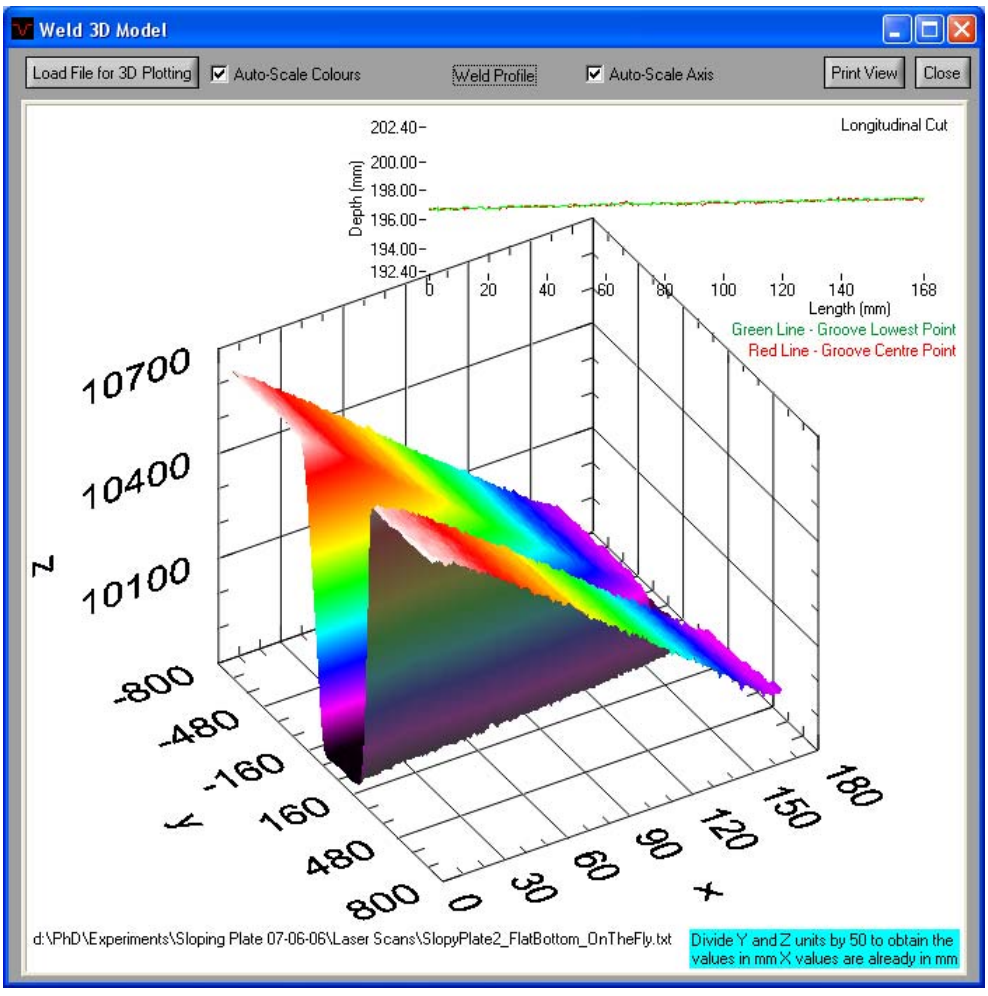

Figure 7.69 – Sloping plate 3D model with the software filters ON and continuity ON – Flat Bottom.

Sample	Profile Nr	Depth (mm)			Top Width (mm)			Bottom Width (mm)			Left Angle(°)			Right Angle(°)		
		Actual	Laser Scan	Difference	Actual	Laser Scan	Difference	Actual	Laser Scan	Difference	Actual	Laser Scan	Difference	Actual	Laser Scan	Difference
SlopingPlate2_FlatBottom_OnTheFly	1	16.7	16.58	0.12	9.35	9.33	0.02	5	5.33	-0.33	9	9	0	5	5	0
SlopingPlate4_FlatTop_OnTheFly	1	16.38	15.4	0.98	9.26	9.5	-0.24	4.93	5.21	-0.28	9	9	0	5	4.5	0.5
SlopingPlate2_FlatBottom_OnTheFly	53	15.09	12.41	2.68	8.95	8.19	0.76	4.5	4.9	-0.4	9	9	0	5	5.5	-0.5
SlopingPlate4_FlatTop_OnTheFly	53	13.98	11.62	2.36	8.26	8.17	0.09	4.5	4.96	-0.46	9	9	0	5	5	0
SlopingPlate2_FlatBottom_OnTheFly	104	7.91	7.85	0.06	6.93	7.41	-0.48	5.2	4.77	0.43	9	9	0	5	6.5	-1.5
SlopingPlate4_FlatTop_OnTheFly	104	6.79	3.48	3.31	6.66			4.7	2.55	2.15	9	9	0	5	5	0
SlopingPlate2_FlatBottom_OnTheFly	155	3.83	3.77	0.06	5.76	6.45	-0.69	4.5	4.59	-0.09	9	13	-4	5	10.5	-5.5
SlopingPlate4_FlatTop_OnTheFly	155	1.87	-1.03	2.9	5.41	6.02	-0.61	4.5	4.46	0.04	9	19.5	-10.5	5	19.4	-14.4
SlopingPlate2_FlatBottom_OnTheFly	1	16.82	16.58	0.24	9.43	9.74	-0.31	5	5.24	-0.24	9	9	0	5	5	0
SlopingPlate2_FlatBottom_OnTheFly	42	13.33	13.44	-0.11	8.29	8.35	-0.06	4.5	4.71	-0.21	9	9	0	5	5	0
SlopingPlate2_FlatBottom_OnTheFly	81	9.92	9.88	0.04	8.22	7.82	0.4	4.5	4.99	-0.49	9	8.5	0.5	5	6	-1
SlopingPlate2_FlatBottom_OnTheFly	125	6.16	6.2	-0.04	6.88	6.91	-0.03	4.7	4.92	-0.22	9	8	1	5	7	-2
SlopingPlate2_FlatBottom_OnTheFly	169	2.99	1.51	1.48	5.5	11	-5.5	4.5	7.65	-3.15	9	15.5	-6.5	5	13.5	-8.5
SlopingPlate4_FlatTop_OnTheFly	1	16.34	15.4	0.94	9.24	9.5	-0.26	4.93	5.21	-0.28	9	8.7	0.3	5	4	1
SlopingPlate4_FlatTop_OnTheFly	39	12.8	13.03	-0.23	8.35	8.17	0.18	4.8	4.78	0.02	9	9	0	5	5	0
SlopingPlate4_FlatTop_OnTheFly	78	9.05	9.66	-0.61	7.81				4.61	-4.61	9	8.5	0.5	5	4	1
SlopingPlate4_FlatTop_OnTheFly	117	5.35	3.03	2.32	6.28	2.02	4.26	4.5	2.24	2.26	9	9	0	5	7	-2
SlopingPlate4_FlatTop_OnTheFly	157	1.77	-1.31	3.08	5.41						9	23	-14	5	22.5	-17.5

Table 7.4 – Sloping plate with activated filters set of experimental data.

It is clear from Table 7.4 that very poor agreement is obtained for groove depths below 6mm. Figure 7.70 shows good agreement between actual and laser scan measurements for groove depths above 6mm.

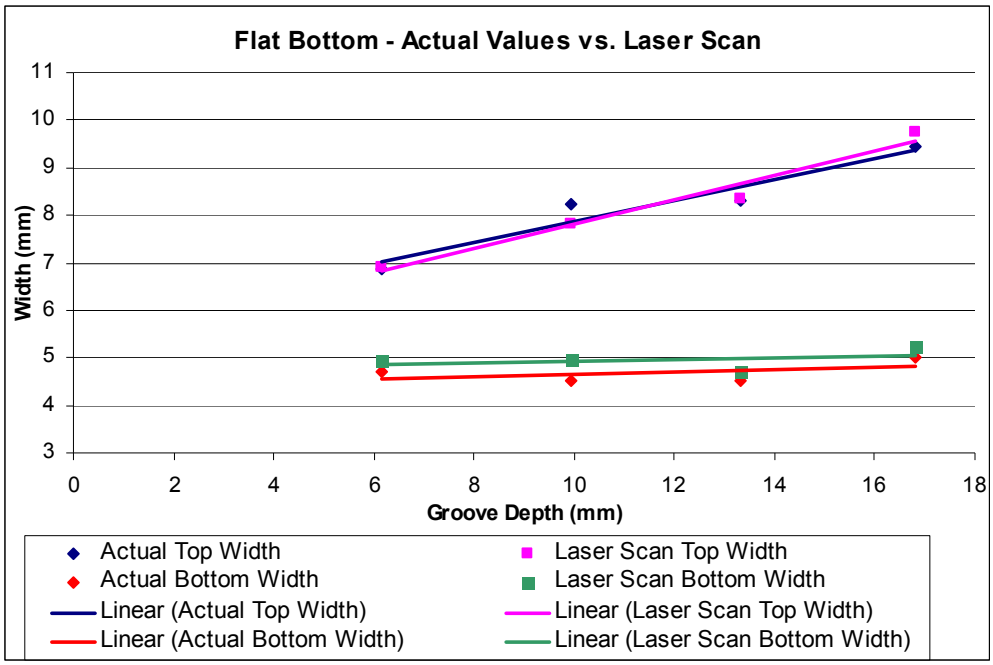

Figure 7.70 – Flat bottom data – measured values vs. software calculated values (partial set, above 6mm groove depth).

7.3.5.1.2 Flat Top Surface

This scan sequence was performed with the test plate base inclined in such way that the top plate surface was horizontal. Figure 7.71 shows the 3D model scan results. In Figure 7.72 it is apparent that above 6mm of groove depth, there is a good agreement between the actual left side wall angle and the readings from the laser sensor with both the flat bottom and flat top configurations. Significant deviations occur below 6mm groove depth. Similar results are obtained for the right side wall below 6mm groove depth, Figure 7.73. Figure 7.74 demonstrates that, once again, for values above 6mm of groove depth there is good agreement between the actual top and bottom widths and the calculated widths based on the sensor data.

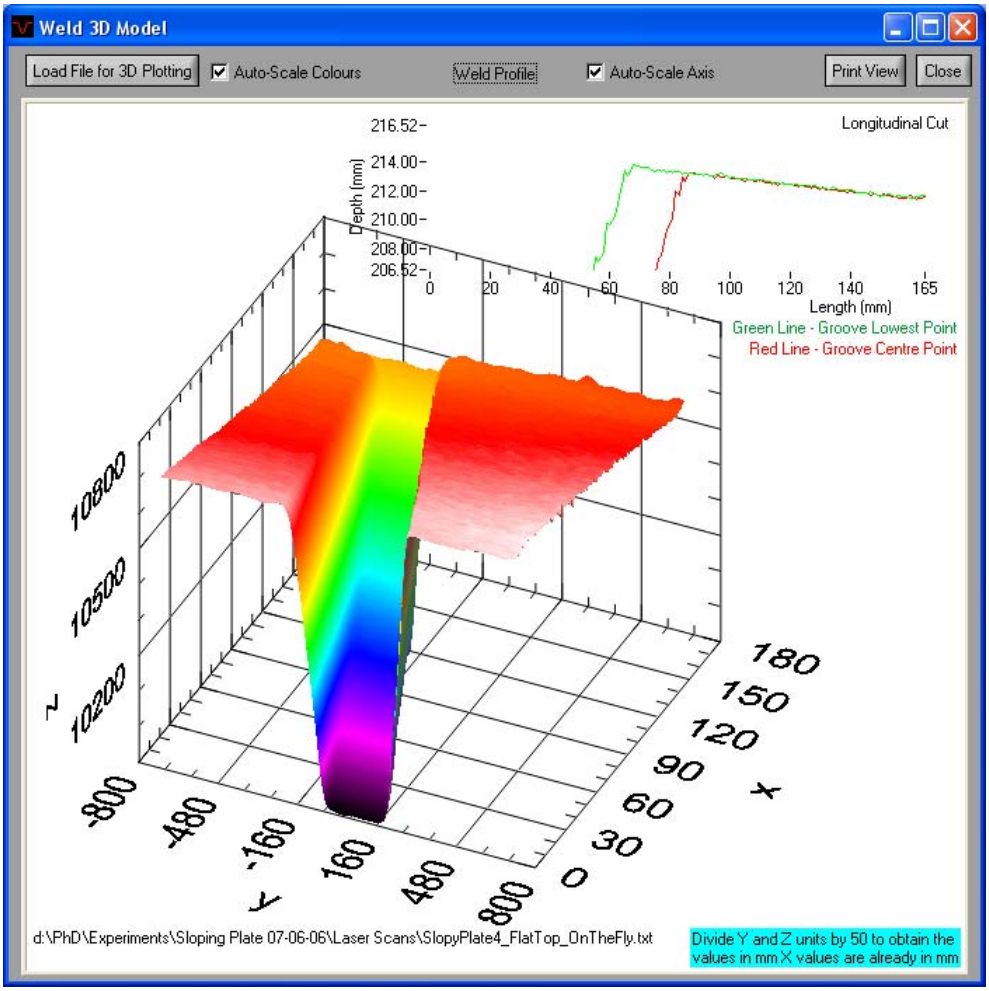

Figure 7.71 – Sloping plate 3D model with the software filters ON and continuity ON – Flat Top.

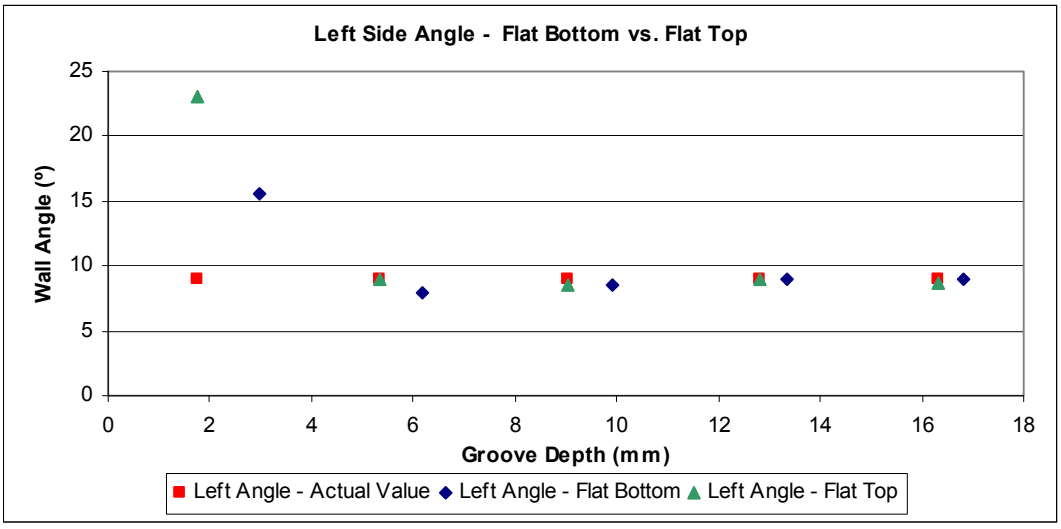

Figure 7.72 – Left side wall angle – comparison between flat bottom and flat top.

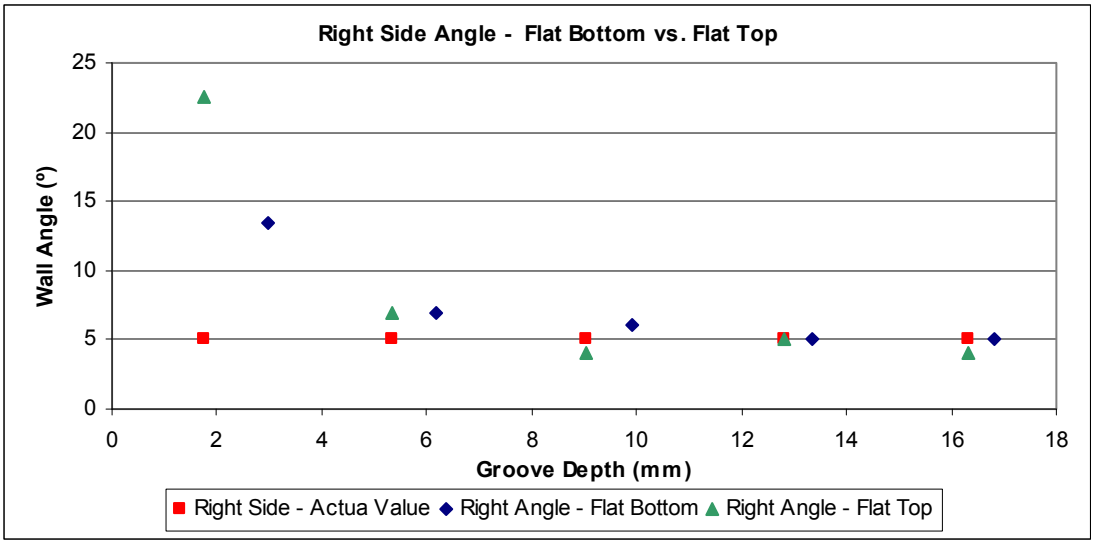

Figure 7.73 – Right side wall angle – comparison between flat bottom and flat top.

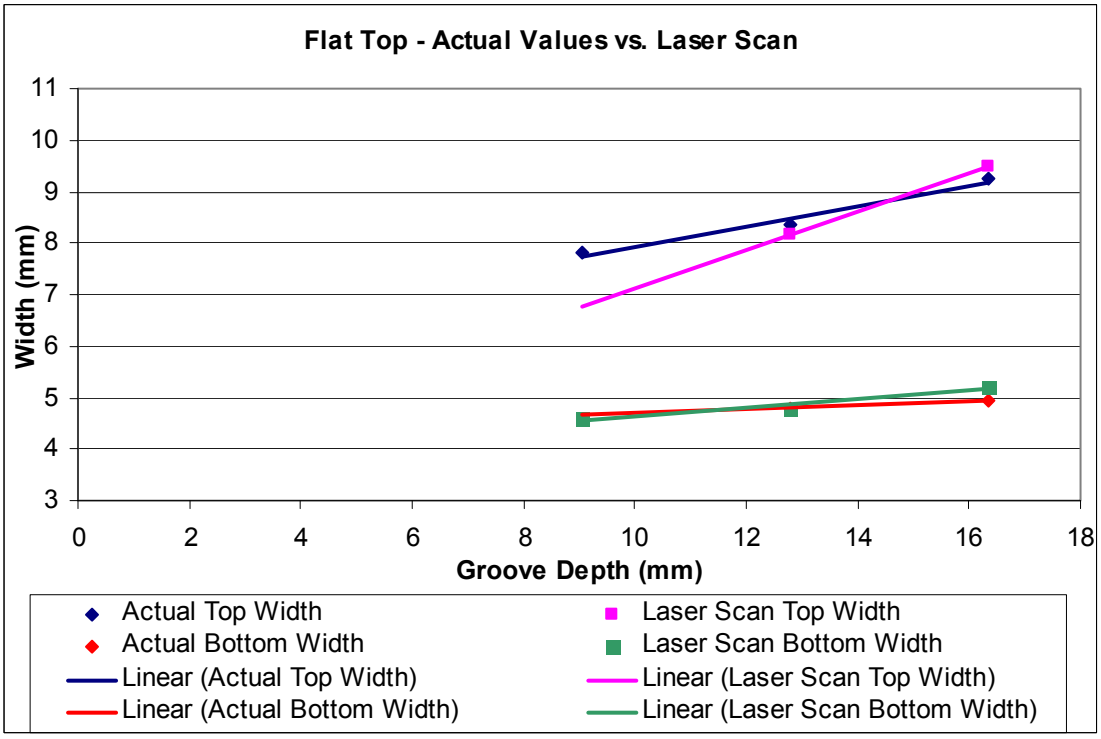

Figure 7.74– Flat bottom data – measured values vs. software calculated values (partial set, above 6mm groove depth).

7.3.5.2 Without the Filters Activated

The configuration of the WinUser™ software used in this set of experiments can be seen in Appendix H2. The data concerning the experiment performed with the filters deactivated can be seen in Table 7.5. Screenshots of the *Analysis* software showing the data can be found in

Appendix G3.The screenshots have the calculated measurements superimposed that can be compared with the values outputted by SP7.

7.3.5.2.1 Flat Groove Bottom

This scan sequence was performed with the test plate laying flat on the specimen holder. This plate bed is part (*4*) of the rig described in section 4.4.1 (page 51). A 3D model of the scan sequence can be seen in Figure 7.75. The actual inclination angle of the top surface is 5.8º as can be seen in Figure 7.64.

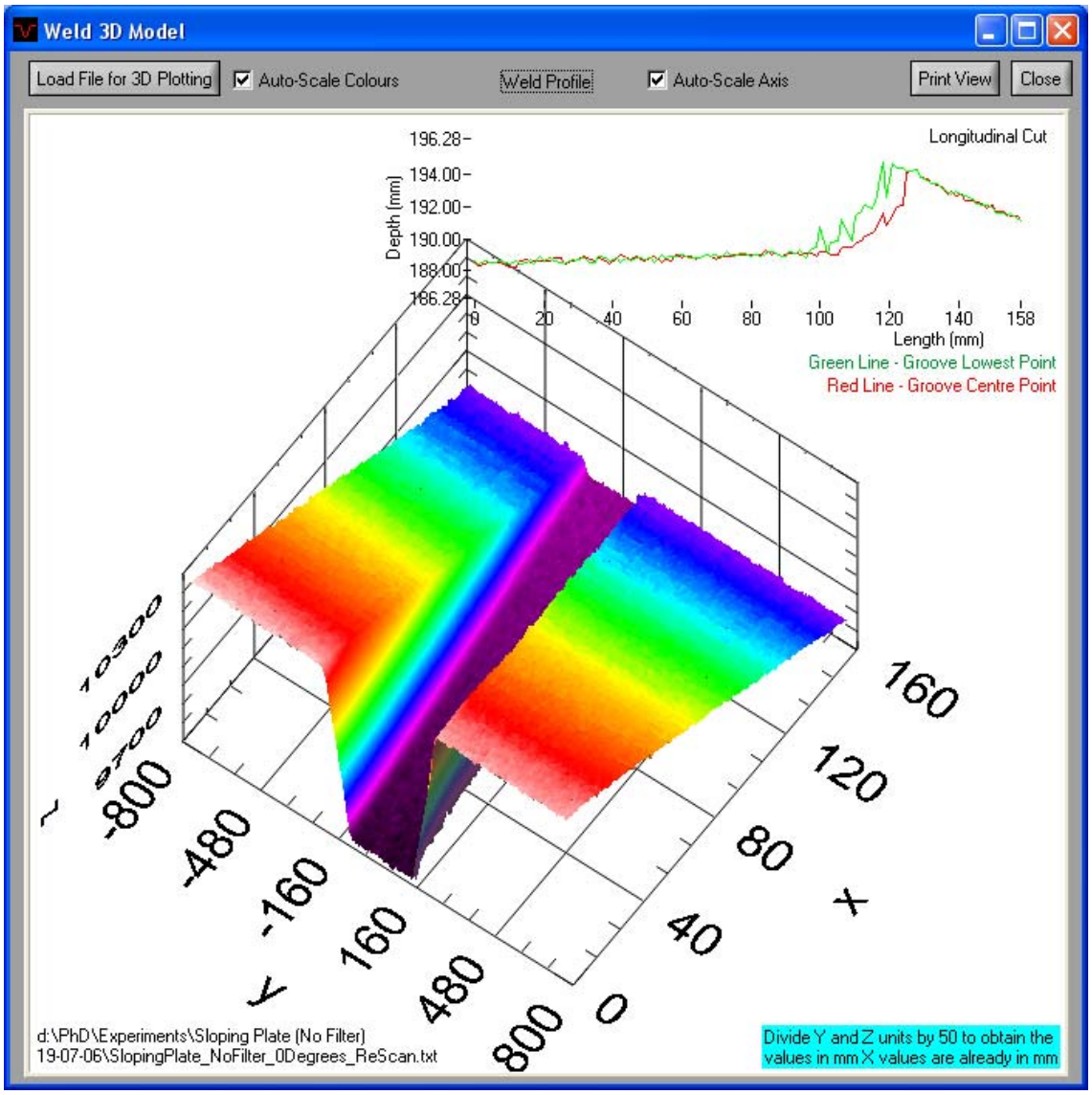

Figure 7.75 – Sloping plate 3D model with the software Filters OFF and Continuity ON – flat bottom.

In Figure 7.76 is shown a comparison between the values manually measured of the profiles printout with the values obtained from the *Analysis* software. Unlike the case of the activated filters, in this case the manually measured data is very similar to the data obtained with the

Sample	Profile Nr	Depth (mm)			Top Width (mm)			Bottom Width (mm)			Left Angle(°)			Right Angle(°)		
		Actual	Laser Scan	Difference	Actual	Laser Scan	Difference	Actual	Laser Scan	Difference	Actual	Laser Scan	Difference	Actual	Laser Scan	Difference
SlopingPlate_NoFilter_0Degrees_ReScan	1	16,83	15,66	1,17	9,56	9,24	0,32	5,21	5,23	-0,02	7,37	7,328	0,042	6,36	8,622	-2,262
SlopingPlate_NoFilter_12Degrees_ReScan	1	17,66	16,72	0,94	9,66	9,4	0,26	6,49	6,18	0,31	7,69	6,8	0,89	2,56	21,645	-19,085
SlopingPlate_NoFilter_0Degrees_ReScan	35	12,83	11,48	1,35	8,17	8,01	0,16	4,98	5,02	-0,04	7,1	7,373	-0,273	6,36	8,179	-1,819
SlopingPlate_NoFilter_12Degrees_ReScan	35	13,38	11,48	1,9	8,31	8,26	0,05	4,86	5,74	-0,88	8,05	6,62	1,43	6,51	23,213	-16,703
SlopingPlate_NoFilter_0Degrees_ReScan	70	7,53	7,16	0,37	6,72	6,57	0,15	5,16	5,09	0,07	5,44	9,186	-3,746	6,15	10,286	-4,136
SlopingPlate_NoFilter_12Degrees_ReScan	70	9,19	8,27	0,92	7,08	7,05	0,03	4,88	5,03	-0,15	6,79	6,302	0,488	6,61	13,128	-6,518
SlopingPlate_NoFilter_0Degrees_ReScan	105	2,64	2,26	0,38	7,33	5,6	1,73	5,07	4,92	0,15	7,33	4,667	2,663	4,71	11,431	-6,721
SlopingPlate_NoFilter_12Degrees_ReScan	105	4,95	4,81	0,14	6,23	6,13	0,1	5,18	4,97	0,21	7,79	5,746	2,044	4,06	13,994	-9,934
SlopingPlate_NoFilter_0Degrees_ReScan	1	16,83	15,66	1,17	9,56	9,24	0,32	5,21	5,23	-0,02	7,37	7,328	0,042	6,36	8,622	-2,262
SlopingPlate_NoFilter_0Degrees_ReScan	27	13,58	13,31	0,27	8,44	8,15	0,29	5,06	4,78	0,28	7,45	7,375	0,075	6,24	8,477	-2,237
SlopingPlate_NoFilter_0Degrees_ReScan	55	9,94	9,2	0,74	7,34	7,25	0,09	5,16	5,57	-0,41	7,11	7,951	-0,841	5,58	26,601	-21,021
SlopingPlate_NoFilter_0Degrees_ReScan	80	6,02	5,71	0,31	6,74	6,25	0,49	5,48	5,4	0,08	7,33	19	-11,67	4,71	10,488	-5,778
SlopingPlate_NoFilter_0Degrees_ReScan	109	2,17	1,83	0,34	5,54	5,66	-0,12	4,89	4,61	0,28	7,33	5,333	1,997	6,16	2,684	3,476
SlopingPlate_NoFilter_12Degrees_ReScan	1	17,66	16,72	0,94	9,66	9,4	0,26	6,49	6,18	0,31	7,69	6,8	0,89	2,56	21,645	-19,085
SlopingPlate_NoFilter_12Degrees_ReScan	27	14,74	12,9	1,84	8,55	8,38	0,17	4,68	4,96	-0,28	8,4	6,493	1,907	6,38	10,002	-3,622
SlopingPlate_NoFilter_12Degrees_ReScan	55	11,04	10,04	1	8,09	7,68	0,41	5,16	5	0,16	7,22	6,826	0,394	6,51	8,509	-1,999
SlopingPlate_NoFilter_12Degrees_ReScan	80	7,89	7,32	0,57	7,12	6,87	0,25	4,88	5,13	-0,25	9,38	5,871	3,509	5,95	17,167	-11,217
SlopingPlate_NoFilter_12Degrees_ReScan	109	4,35	4,49	-0,14	6,08	6,12	-0,04	4,84	4,92	-0,08	9,53	5,8	3,73	6,03	10,077	-4,047
SlopingPlate_NoFilter_12Degrees_OnTheFly	112	2,13	2,02	0,11	5,473	5,54	-0,067	4,69	4,72	-0,03	12,5	3,282	9,218	8,5	8,318	0,182

Table 7.5 – Sloping plate with deactivated filters set of experimental data.

Analysis software. The fitted lines are a very good fit to all the values including the ones for a groove depth below 6mm. From here can be concluded that the use of the WinUser™ filters distorts the reading of shallow grooves due to its intrinsic behaviour. The filters use a number of data points (the filter size) to calculate the average and the median (in this case). In shallow grooves and for filters size 10 like the ones used in the previous experiments, the values of the groove walls are greatly influenced by the data points in the top surface and the groove bottom. Not many data points actually constitute the groove wall so the data points in the top surface and the groove bottom contribute more in the filter calculations.

Figure 7.77 shows the wall angles in the left and right side of the groove both with the filters ON and OFF. It is possible to see in this graph that there is a small variation to the target angles in the read value. The target angle was 9º degrees for the left wall and 5º degrees for the right one. In general there is quite good agreement for deeper grooves (above 6 mm). However, significant deviations occur below 6 mm. These deviations are considerably more significant with the filters ON than with the filters OFF. For the shallow part of the groove, no definite conclusions can be drawn, since there is also some uncertainty regarding the actual groove wall angles due to the preparation method.

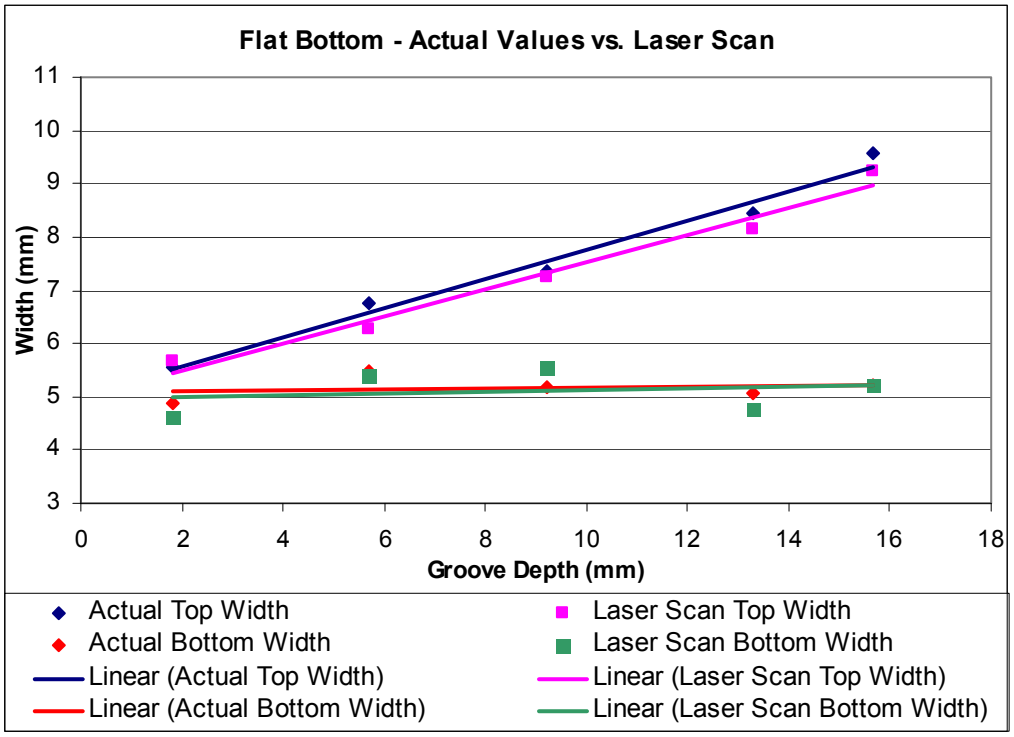

Figure 7.76 – Flat bottom data – measured values vs. software calculated values.

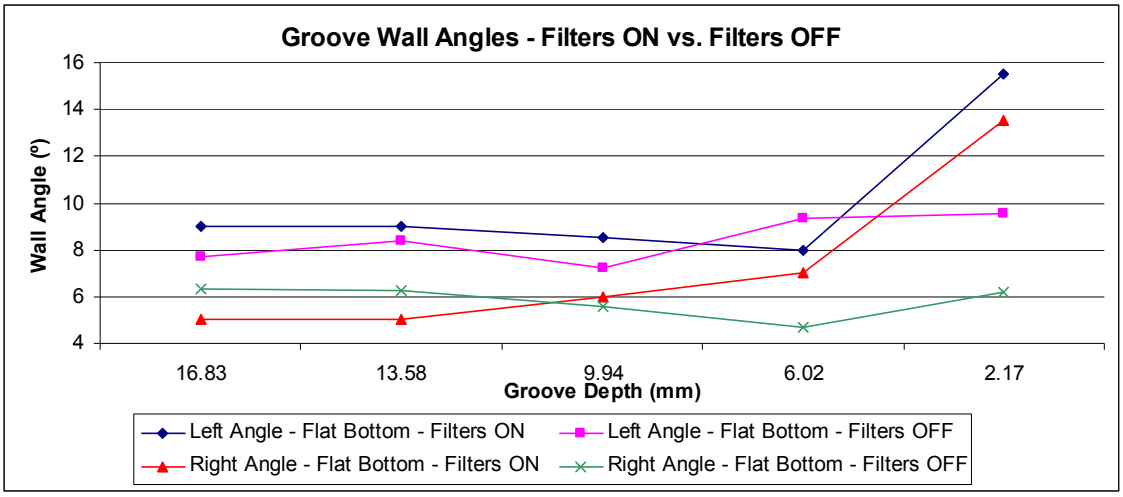

Figure 7.77 – Groove wall angle values – comparison between filters ON and OFF.

As a result of these sets of experiments is safe to conclude that the use of the WinUser™ filters introduces a significant amount of error when analysing shallow narrow grooves. For the studied grooves, a filter size ten is clearly excessive as distorts the groove shape. Ideally when scanning narrow grooves less deep than 6mm with the intention of analysing the groove bottom no filters should be used at all. The location and shape of the groove top corners does not appear to be altered in any way by the filters use. So, if the intention of the scan is, for example, seam tracking based on the location of the groove top corners, the use or not of the WinUser™ filters does not seem to be relevant.

From these experiments can be perceived the influence of the WinUser™ software filters, especially in narrow grooves less than 6mm deep. In the experiments where the filters were activated there was no clear distinction between the results with flat bottom or flat top.

7.3.6 Application of Real Time Assessment of Weld Quality

The objective in this phase of the work was to develop algorithms that could measure bead shapes and automatically determine whether a defective weld has been produced. The algorithms are intended to assess the weld bead shape and quality. It is also intended to evaluate whether the penetration from the next weld bead would fully fuse on the measured bead. The advantage of such information lies in the fact of knowing beforehand if the bead that is being scanned will generate or not a faulty bead when the next pass is performed. Information on the bead shape can help to develop weld procedures, perform parameter corrections in real time. It can also indicate areas that require grinding to remove or prevent defects.

An important factor in this study is the location of the laser sensor. The position of the sensor ahead or behind the welding torch determines the type of information that can be extracted from the data. In the performed study, the laser was positioned ahead of the welding torch. When the sensor is scanning in front of the torch, it can generate information to adjust the welding parameters in real time according to the groove shape, and to perform seam tracking and torch height adjustments based on the groove positioning. It can also indicate if it is advisable to lay a new weld bead on top of the existing one or not in order to minimise the likelihood of creating a defect in the next layer. On the other hand, if the sensor trails the torch by a short distance, it is possible to perform adjustments to welding parameters to modify bead shape. This would be performed with a short delay due to the distance between the measurement position and the welding torch. In terms of seam tracking if the laser trails the torch no accurate results can be achieved as the sensor would pass by a specific location after the weld was already on that location. Regardless on the sensor position in relation to the torch the acquired data can also provide offline information on bead shape and quality, indicate where grinding is advised, and may also be used for statistical, seam tracking and overall quality assessment.

This phase of the experiments used specimens produced by Liratzis [127]. He developed an experimental design to study the effect of welding parameters on weld bead shape. Liratzis studied the effect of travel speed, wire feed speed, arc length and wire position on weld quality. In those experiments a wide range of bead shapes were produced, including welds with convex and concave shapes, asymmetric welds, and undercut. These specimens provided an excellent series of shapes to be studied in this phase of the work.

The welds performed by Liratzis were all a first pass on a specimen base plate with groove dimensions described in Figure 7.78. In Figure 7.79 is possible to see a full test plate. In each test plate were performed four welds with four different configurations. The rig used to perform the Liratzis experiments is a different one from the one described earlier in this thesis. Figure 7.80 shows this rig being used weld a plate in the overhead position

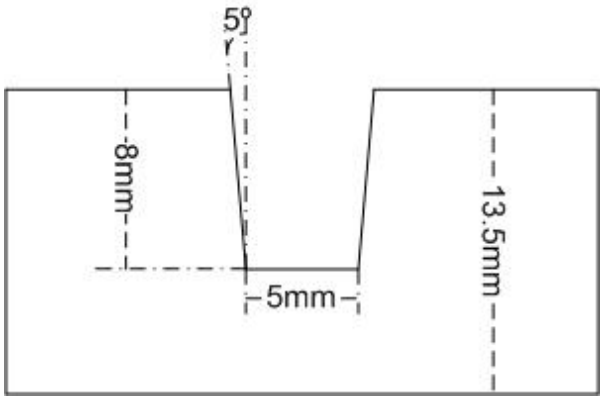

Figure 7.78 – Plate and groove geometry of Liratzis experiments.

Figure 7.79 – Photo of one of Liratzis plates.

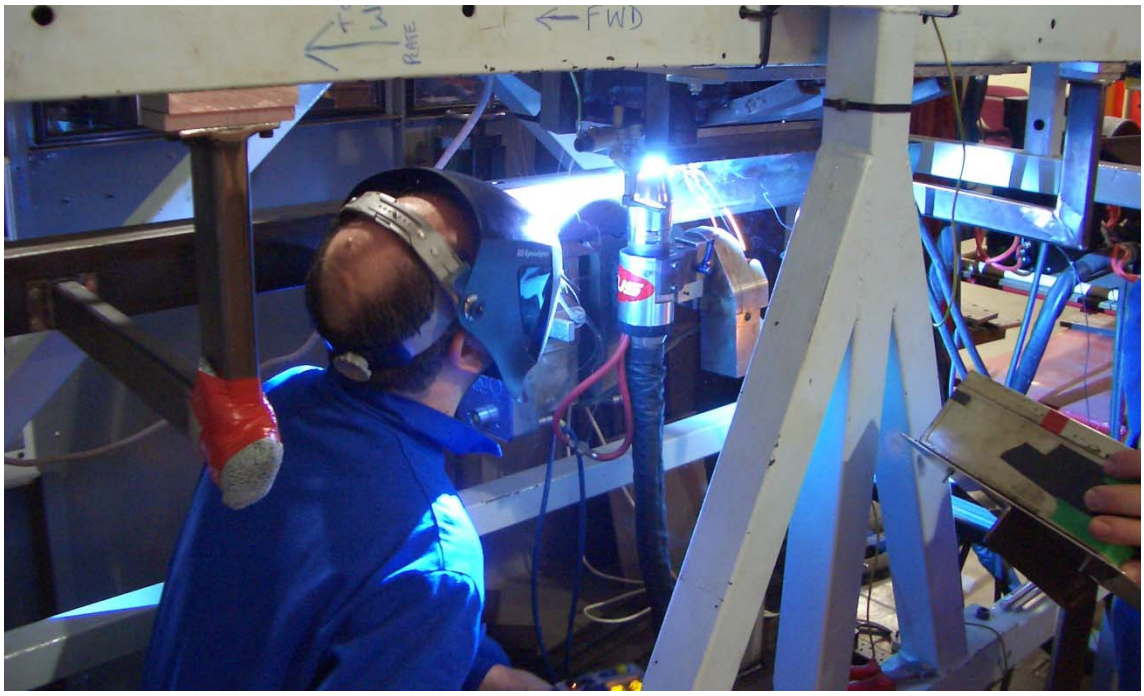

Figure 7.80 – Welding rig utilised by Liratzis to perform the experiments. System being prepared to weld in the Overhead position.

For the work described here, all the welds were scanned in the rig described in section 4.4.1 with the Servo Robot Mini-I60™ sensor. Those scans were then analysed and their description can be found below. All the following experiments share the same configuration of the WinUser™ software. This configuration can be seen in Appendix H3. Scans from all the experiments can be seen in Appendix I. In this section can be seen a selection of the experiments showing a diverse range of shapes in each position.

The following nomenclature applies: “run number” is the weld number (see for example the “Pre-scan File” field in SP7 screenshots) and “profile number” is the frame number in the laser vision sensor data (see the “Profile Counter” field in SP7 screenshots).

7.3.6.1 Flat Position

In the flat position the most common bead shapes obtain in these experiments were flat and slightly concave shapes. Flat bead profiles were obtained in the majority of the tested parameter configurations when welding in the flat position. Examples of flat weld bead shape can be seen in weld runs 5, 6, 7 (Figure 7.81), 9, 10, 11, 12, 17, 18, 19 (Figure 7.88), 20, 24, 25 and 28. Weld runs such as 3, 4, 8, 21, 22 (Figure 7.82) and 29 are borderline between concave and flat. On the other hand weld runs 1 (Figure 7.83), 2, 14, 15, 16, 23, 27 and 30 are concave shaped. The scans from the flat position can be seen in Appendix I1.

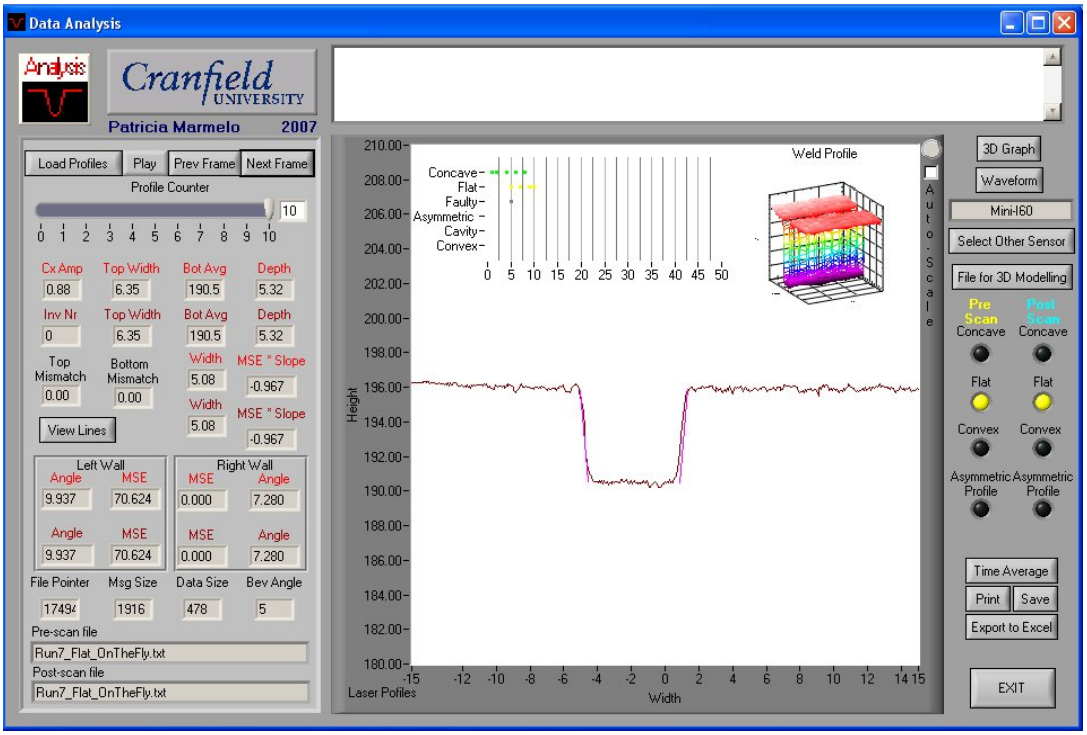

Figure 7.81 – Screenshot of profile 10 of “Run 7” in the Flat position.

In Figure 7.87 despite the scan appearing “flat” and acceptable SP7 is flagging the profile as “flat” and “faulty”, the reason for this is the height variation of the data points that form the groove bottom area. It was defined in the rules that a profile to be considered “flat” the data points needed to have a height variation of ±0.5mm from the straight line that is fitted to that section of the data. Such does not happen and so it is flagged as “faulty”.

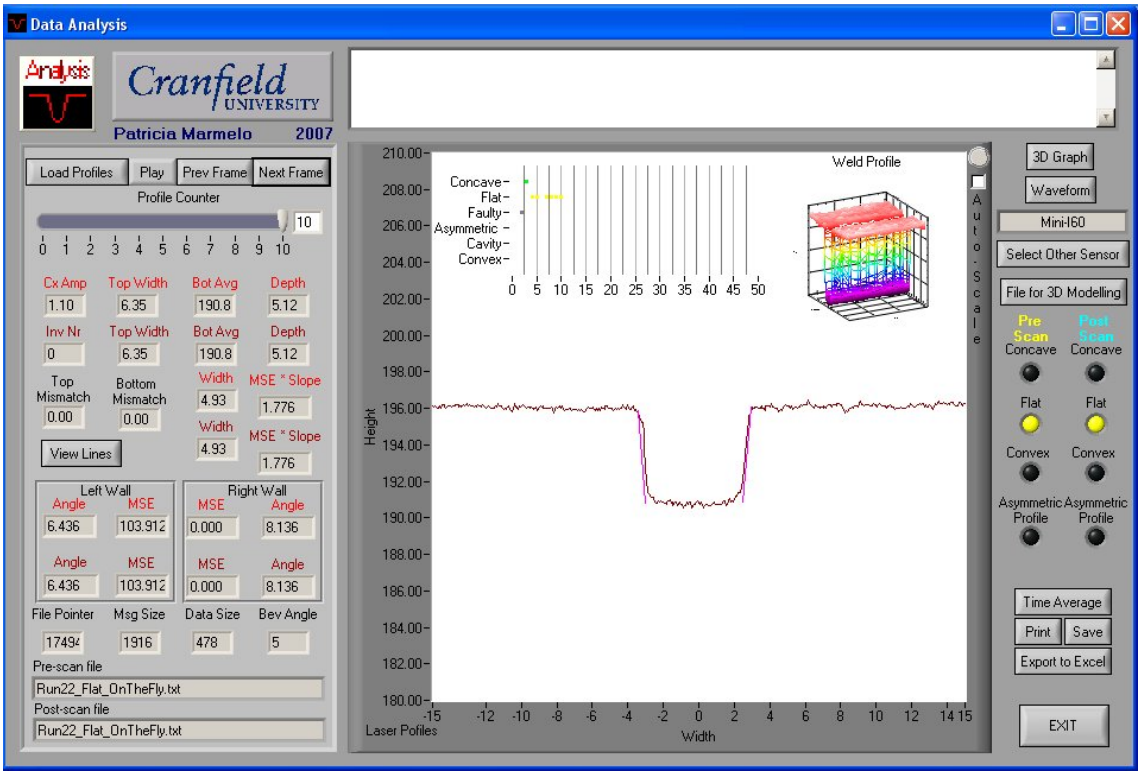

Figure 7.82 – Screenshot of profile 10 of "Run 22" in the Flat position.

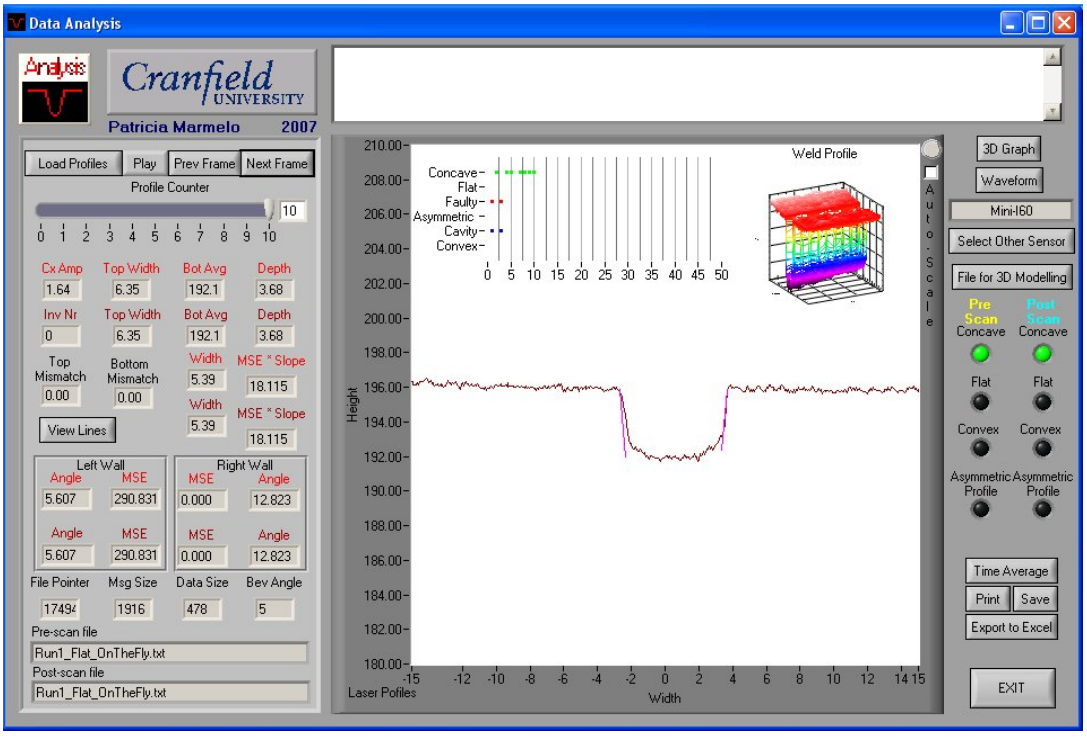

Figure 7.83 – Screenshot of profile 10 of "Run 1" in the Flat position.

A severe case of cavities occurred in weld run 13 its 3D profile can be seen in Figure 7.84. Looking at Figure 7.84, more exactly to the "Transversal Cut" graph is possible to see in red

the depth of the groove centre line and in green the depth of each profile lowest point. In the green plot is possible to see each of the cavities and for each of them their depth and length. Figure 7.85 is the screenshot of a profile showing one of those cavities. Not all the profiles show a cavity, some show an asymmetric bead (Figure 7.86) or even a flat shaped bead (Figure 7.87). If taken out of the context the profile in Figure 7.86 represents a good weld but that is not the case. Therefore, for a complete analysis of weld bead quality, it may be necessary to analyse on the basis of 3-D geometry, rather than just individual weld sections. 3D analysis is not a simple task so the use of the values of the groove centre point could be a good indicator of defects or lack thereof. But as it was noticed during the data analysis most of the times the centre line does not show any problem as they tend to be closer to the groove wall. With this in mind it was decided to plot the groove/scan lowest points. The groove lowest points proved to be a more accurate and reliable data set. This can give a good indication on the general weld quality as it can be seen on the green plot in Figure 7.84.

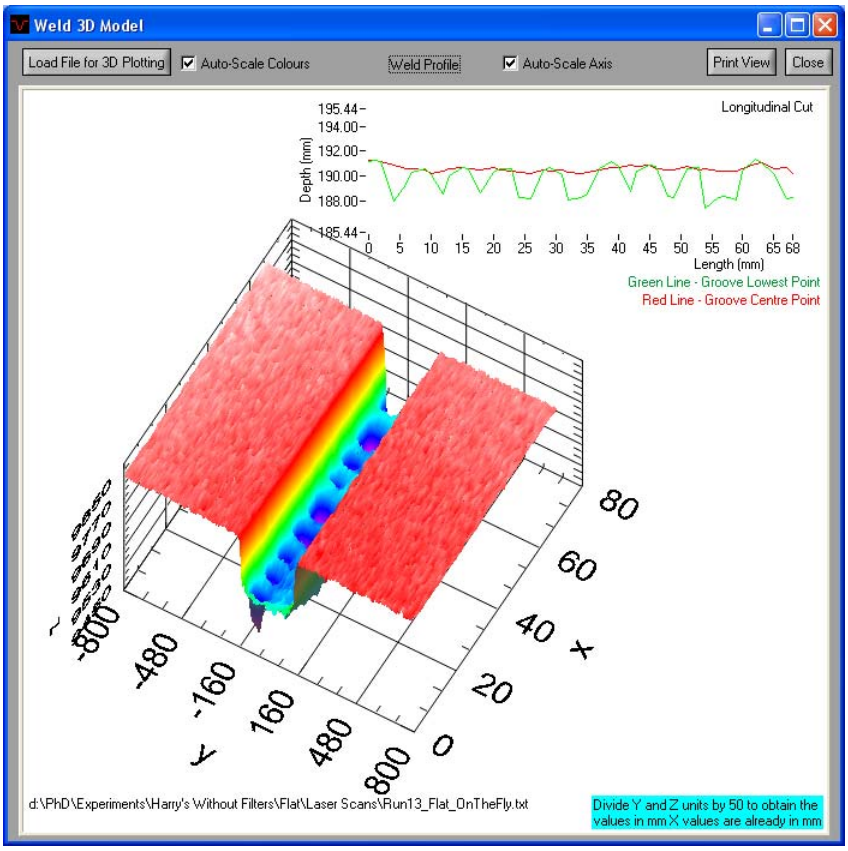

Figure 7.84 – Screenshot of "Run 13" in the Flat position 3D model.

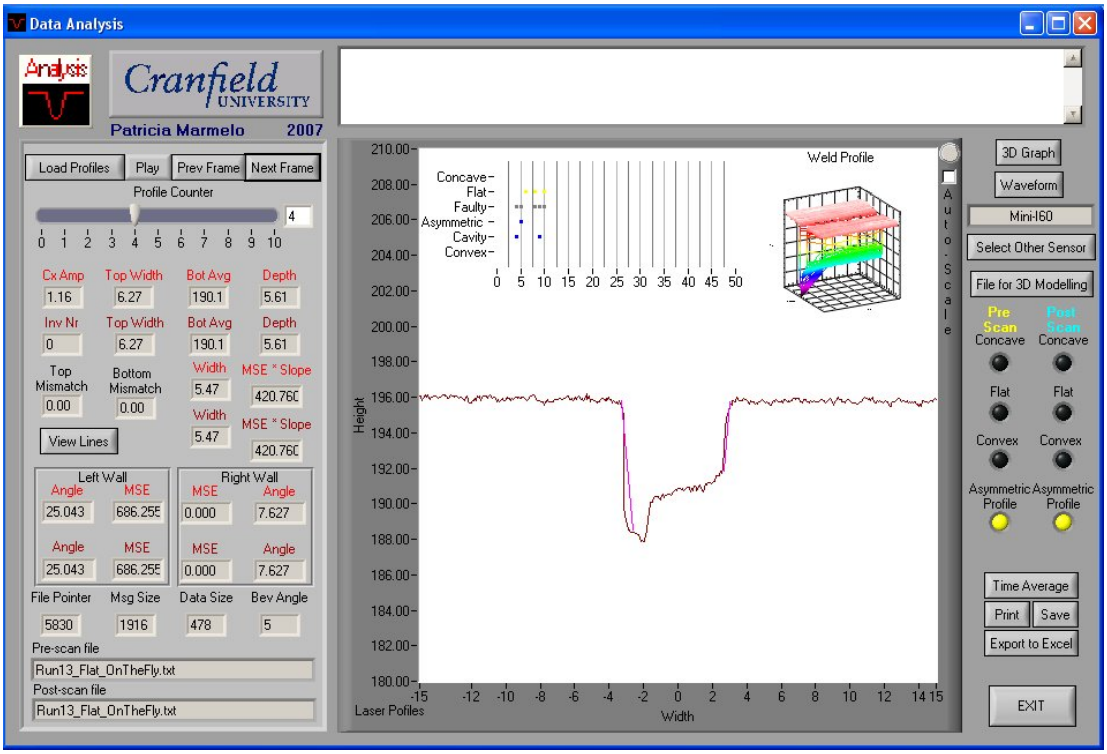

Figure 7.85 – Screenshot of profile 4 of "Run 13" in the Flat position. Showing a bead shape containing a cavity.

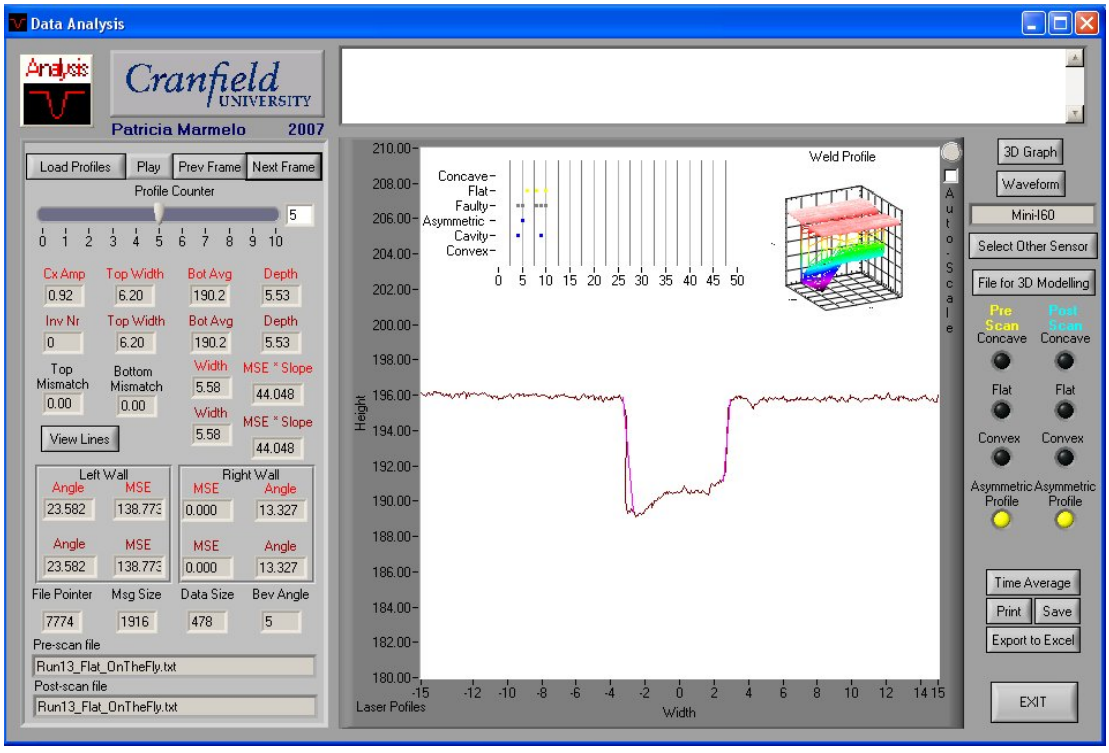

Figure 7.86 – Screenshot of profile 5 of "Run 13" in the Flat Position. Showing an asymmetric profile.

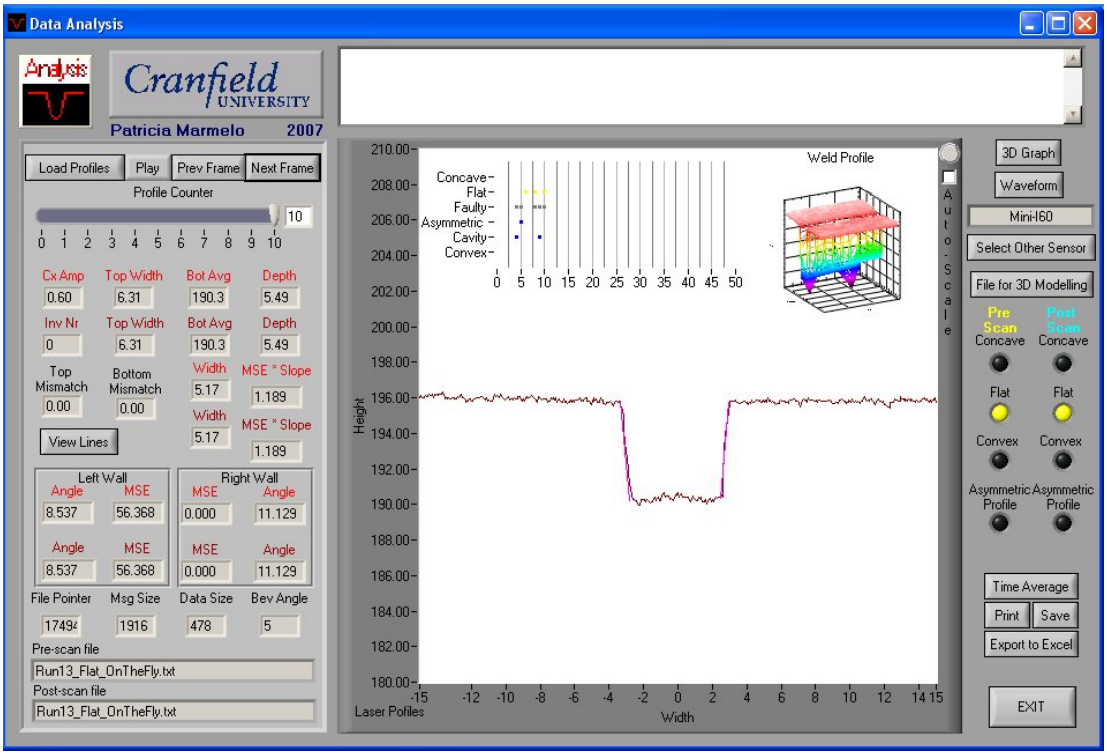

Figure 7.87 – Screenshot of profile 10 of "Run 13" in the Flat position. Showing a Flat bead shape.

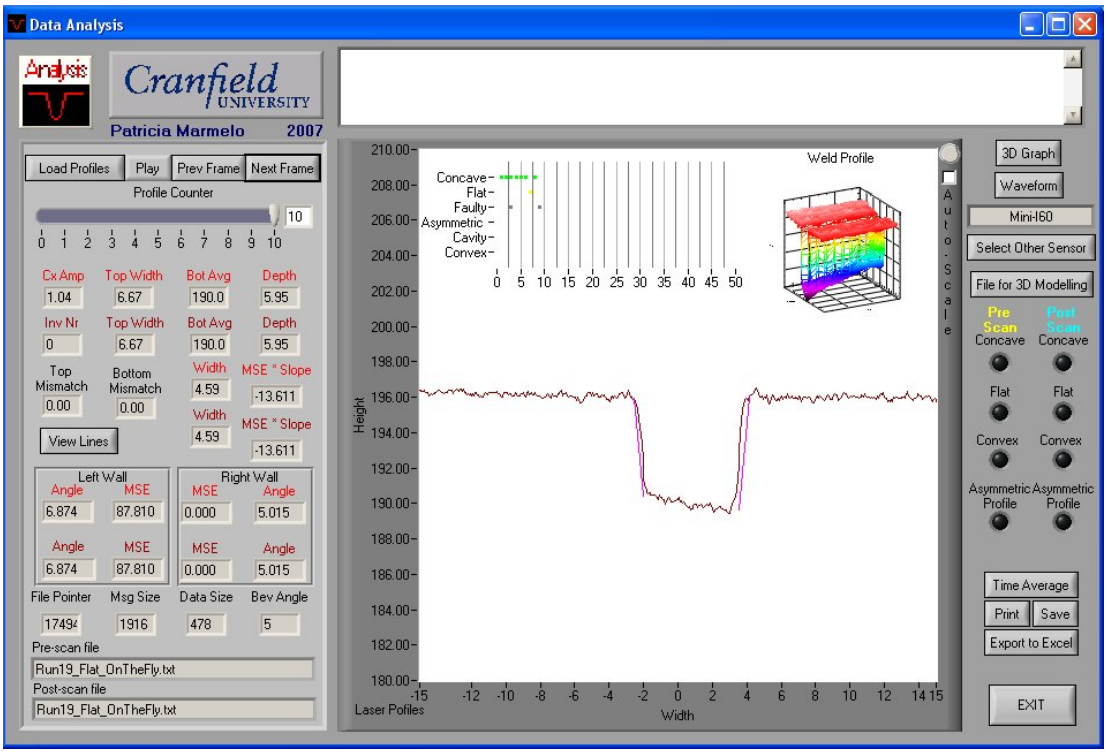

Figure 7.88 – Screenshot of profile 10 of "Run 19" in the Flat position.

Another bead shape to emphasize is the one seen in run 19 (Figure 7.88). This profile shows a flat bead shape, but one that is asymmetric. This bead shape occurred most likely due to a misalignment of the torch to the groove centre. In this case, it is not severe and can probably be corrected with the next weld pass. The next pass would require a more precise centring of the torch and perhaps a specific set of weld parameters, which would help to compensate the asymmetry in the bead or some oscillation dwelling on the right side of groove. The oscillation dwell increases the time the torch stays at the end of the oscillation, thus allowing more weld material to be deposited in the dwell location.

The screenshot of run 26 profile 10 (Figure 7.89) shows what seems to be a severe case of asymmetry in the bead or a mild case of cavity. This would imply the weld parameters set to perform this weld would not be the most appropriate to achieve an acceptable weld or that a defect would occurred on that location. Looking now at Figure 7.90, which shows profile 19 and gives an overall perspective of the 3D shape of the whole weld, and it is apparent that the asymmetry problem occurred at just one location in the weld.

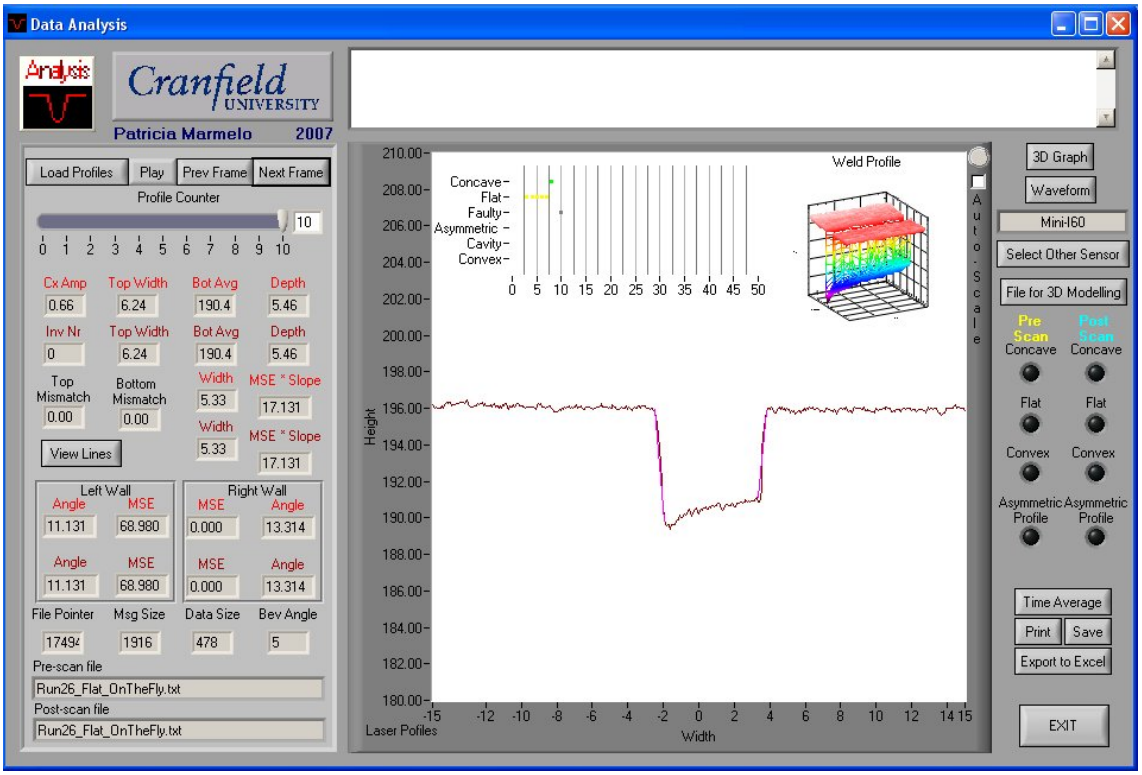

Figure 7.89 – Screenshot of profile 10 of "Run 26" in the Flat position showing an asymmetric profile.

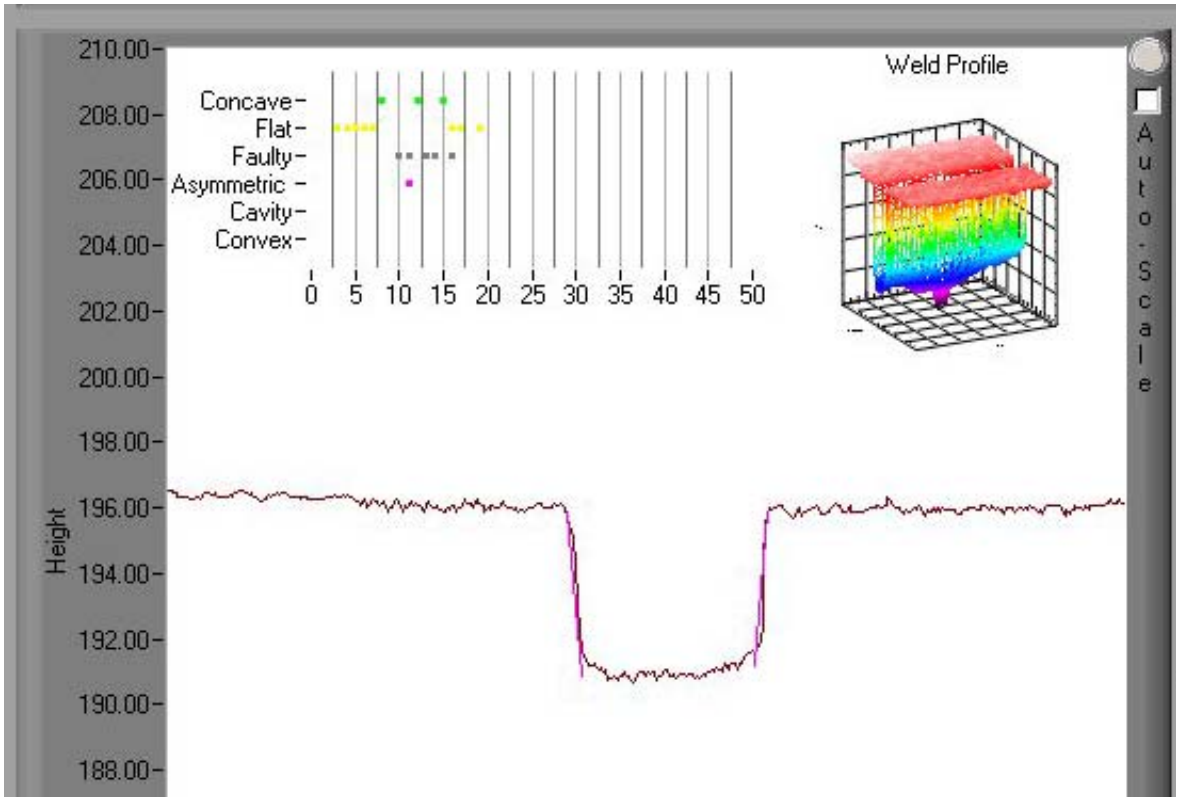

Figure 7.90 – Screenshot of profile 19 of "Run 26" in the Flat position showing a Flat bead shape.

7.3.6.2 Vertical-Down Position

On the vertical down position, the bead shapes obtained, using the tested set of parameters, were all concave. Weld runs 6, 7, 8, 10, 11, 12, 13, 14, 15, 16, 17, 18, 19, 24, 25, 26 and 32 resulted in a concave shape. Weld runs 1, 2, 3, 4, 5, 9, 20, 21, 22, 23, 27, 28, 29, 30 and 31 resulted very concave welds. The scans from the vertical-down position can be seen in Appendix I2.

Run 6 (Figure 7.91) and 17 (Figure 7.93) both show concave profiles. Run 6 has a greater concavity than run 17 but there should be no problem in putting another layer on top of the current one in either case, according to the welding technician.

Run 15 (Figure 7.92) has an unusual concave shape but it is not excessively concave. When looking solely to the acquired weld profile, no evident fault can be discerned. When analysing the macro of run 15 (Figure 7.94) a 0.25mm wide centreline crack is discernible. When overlaying the macro with the software screenshot (Figure 7.95) is possible to see that at the crack location there is an irregularity in the profile. It could not be ascertained if the irregularity in the profile represented the actual crack in the weld or if it was noise from the data. This is due to the crack small width and any algorithm based on the small irregularities in the profile would most of the time yield incorrect results.

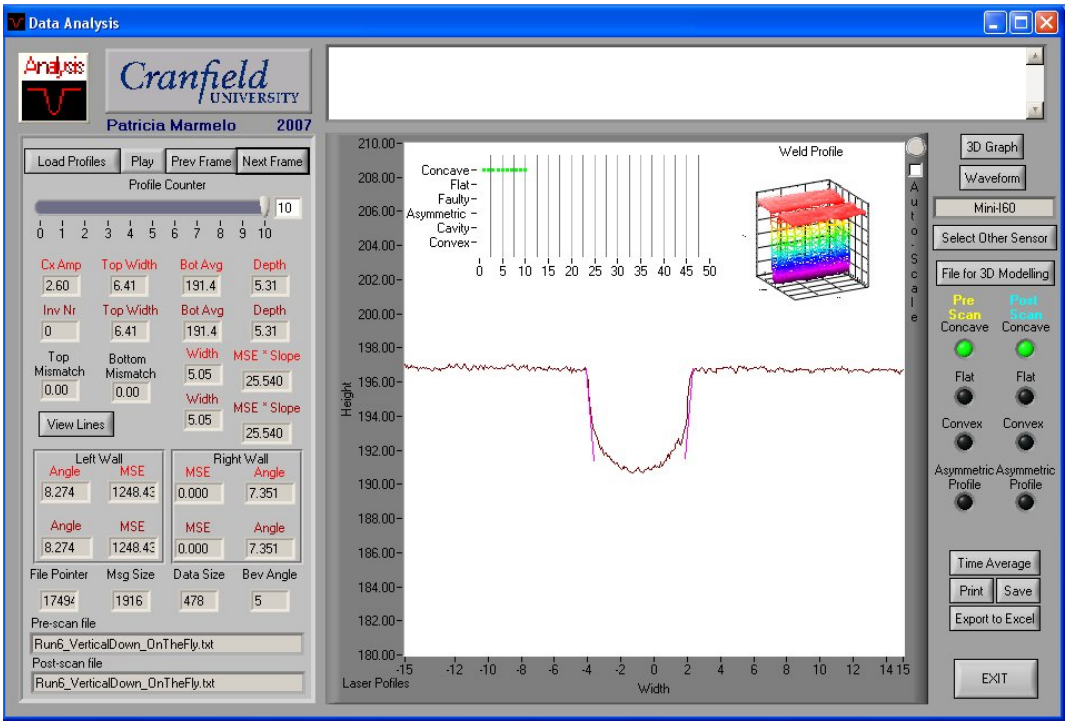

Figure 7.91 – Screenshot of profile 10 of "Run 6" in the Vertical Down position.

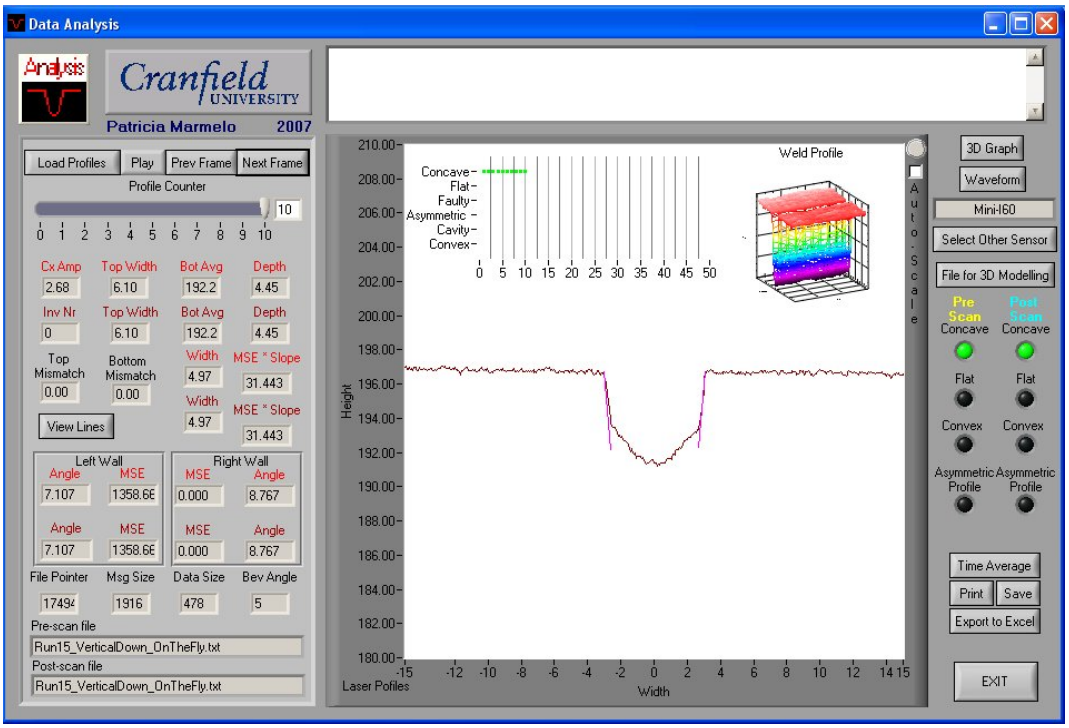

Figure 7.92 – Screenshot of profile 10 of "Run 15" in the Vertical Down position.

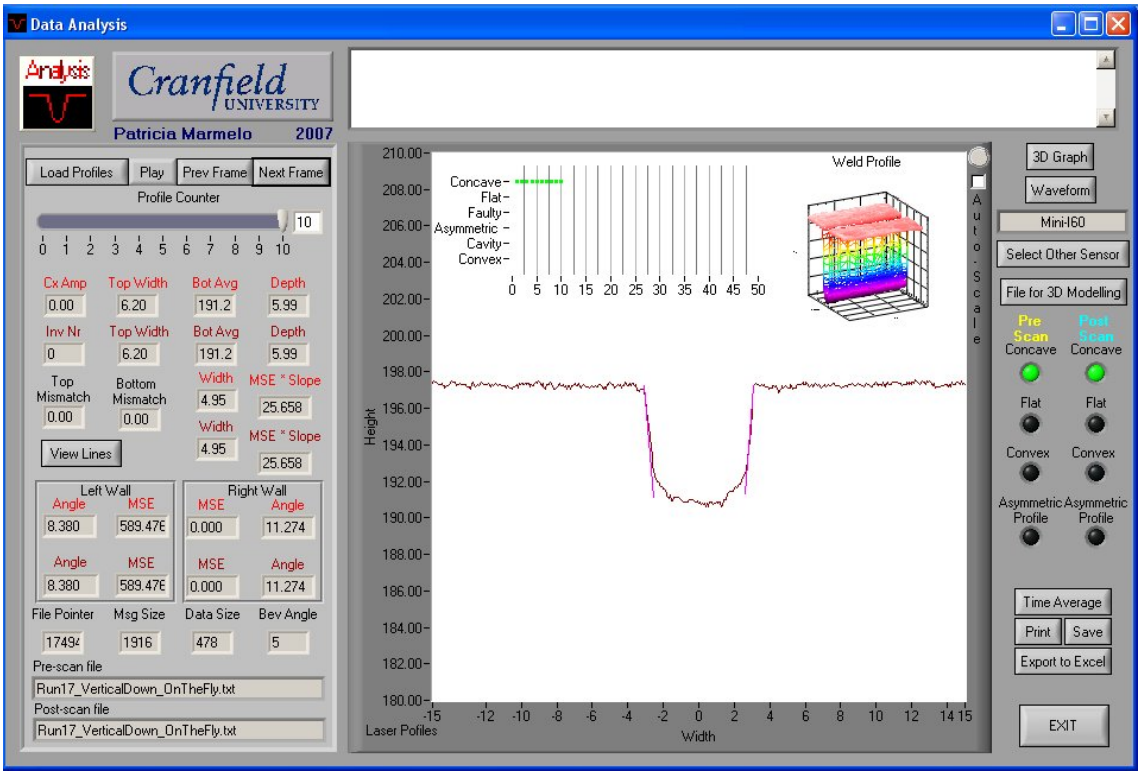

Figure 7.93 – Screenshot of profile 10 of "Run 17" in the Vertical Down position.

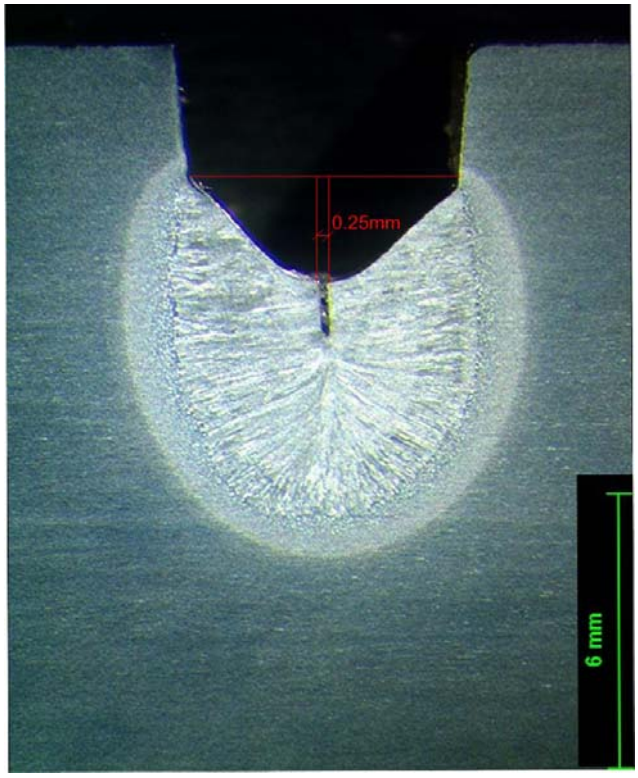

Figure 7.94 – Macro of weld "Run 15" in the Vertical Down position.

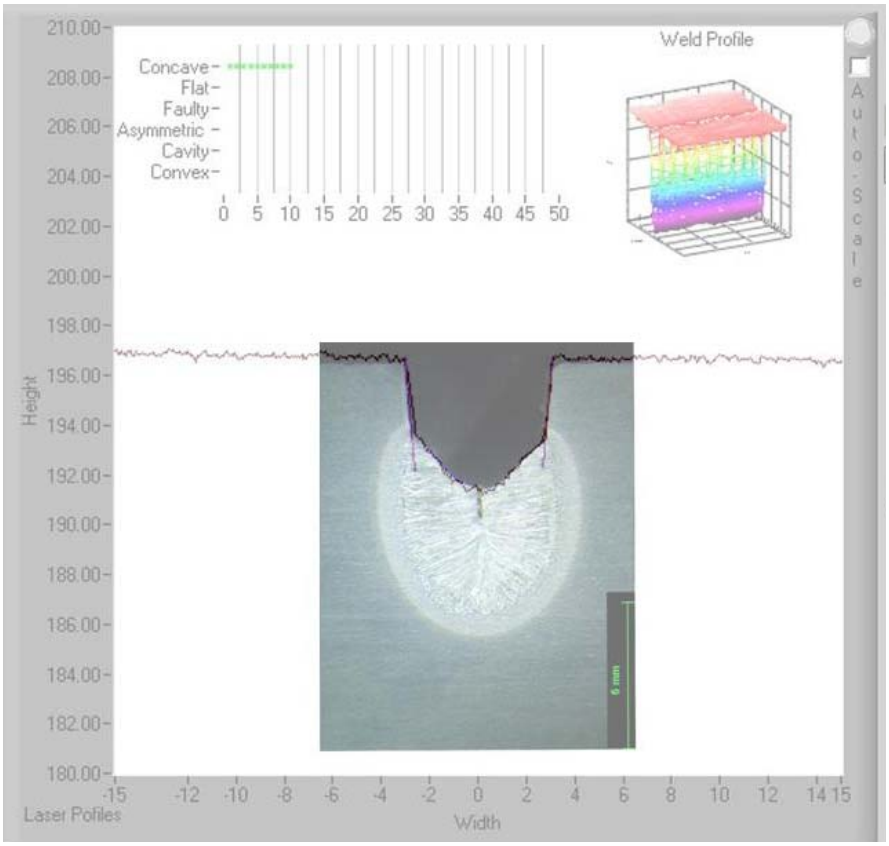

Figure 7.95 – Overlay of macro and screenshot of Weld "Run 15" profile 10 in the Vertical Down position.

7.3.6.3 Overhead Position

The most common bead shape in the overhead position is a convex or flat shape. Weld runs 1, 3, 5, 7 (Figure 7.96), 9, 10 (Figure 7.97), 16, 20, 23 and 30 have an acceptable convex shape. Weld run 2 has a boundary shape between acceptable and excessive convexity. Runs 4, 6, 8, 12, 14, 15, 17, 18 (Figure 7.101), 22, 24, 25, 26, 27 and 29 can be considered flat or boundary between flat and convex bead shapes. Runs 11 (Figure 7.98), 13, 21 and 28 have a convex profile with cavity. Run 19 has a slightly concave shape. The scans from the overhead position can be seen in Appendix I3.

Run 7 (Figure 7.96) shows a convex bead shape. The software did not flag this weld as convex since it does not have sufficient convexity to meet the definition used in the algorithms (see section 7.4.3).

Despite the fact that run 10 (Figure 7.97) has an acceptable convex nearly flat shape, it has quite sharp corners, which may increase the probability of lack-of-fusion defects in the next bead. In SP7 it is flagged as a flat bead shape but a faulty one because of the toe angles.

Runs 11 (1) (Figure 7.98), 13, 21 and 28 were produced with weld parameters that in the overhead position produce beads with cavities. A 3D model of run 11 (1) can be seen in Figure 7.99. If compared with the 3D model of run 13 in the flat position (Figure 7.84) it is clear that despite the fact that both runs present cavities the one in the flat position is intermittent, composed of several small cavities, the one in the overhead position is almost continuous. At first, this fact was attributed to the misalignment of the oscillation centre point, so the weld was repeated after realigning the torch. A 3D model of this new weld (run 11 (2)) can be seen in Figure 7.100. In this new weld, the cavity is no longer continuous but is still different from the one on the flat position. This leads to believe that the cause of the cavity is not a misalignment of the torch. It is most likely caused by instabilities in weld metal deposition with the welding parameters used.

Run 18 (Figure 7.101) has a flat shape with an asymmetric configuration. This asymmetry is not severe, and is most likely caused by a misalignment of the torch in relation to the groove centre. Welding another layer on top of this one should cause no defect on the subsequent layer although the torch centring should be corrected to avoid an aggravation of the condition.

It became clear after analysing the scans from the overhead position that this is a complicated position to weld. The overhead position is most likely to generate convex bead shapes compared to the flat and vertical down positions.

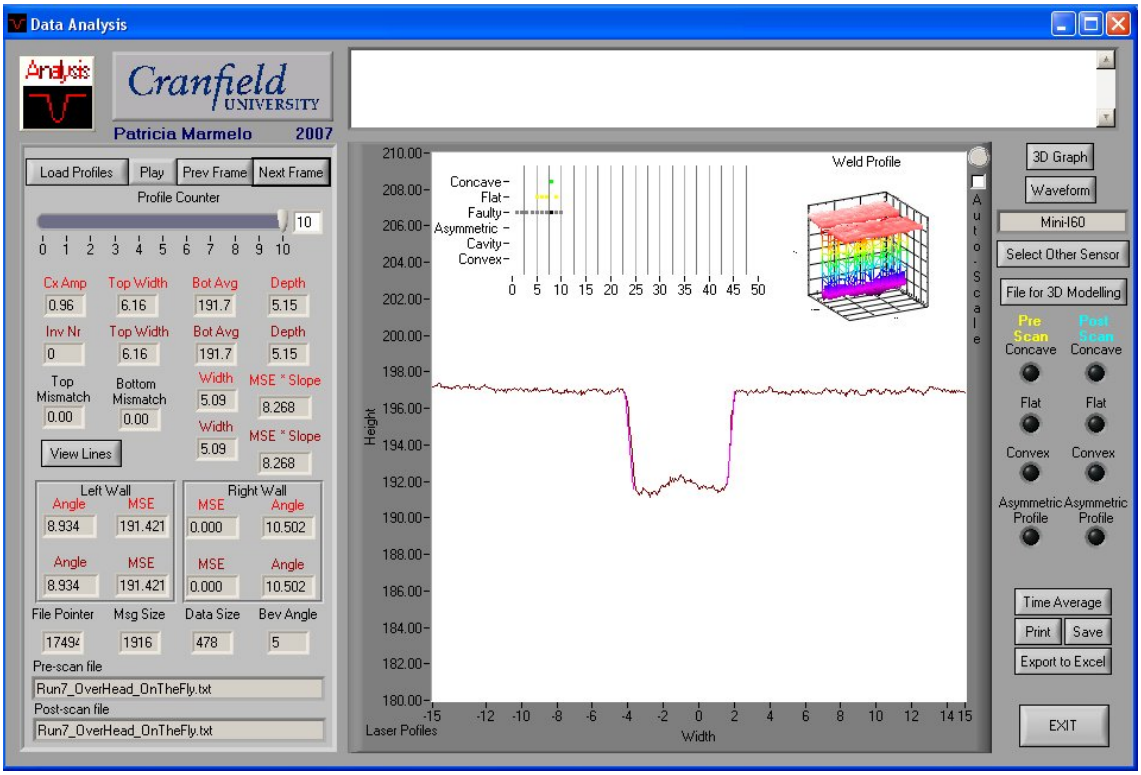

Figure 7.96 – Screenshot of profile 10 of "Run 7" in the Overhead position.

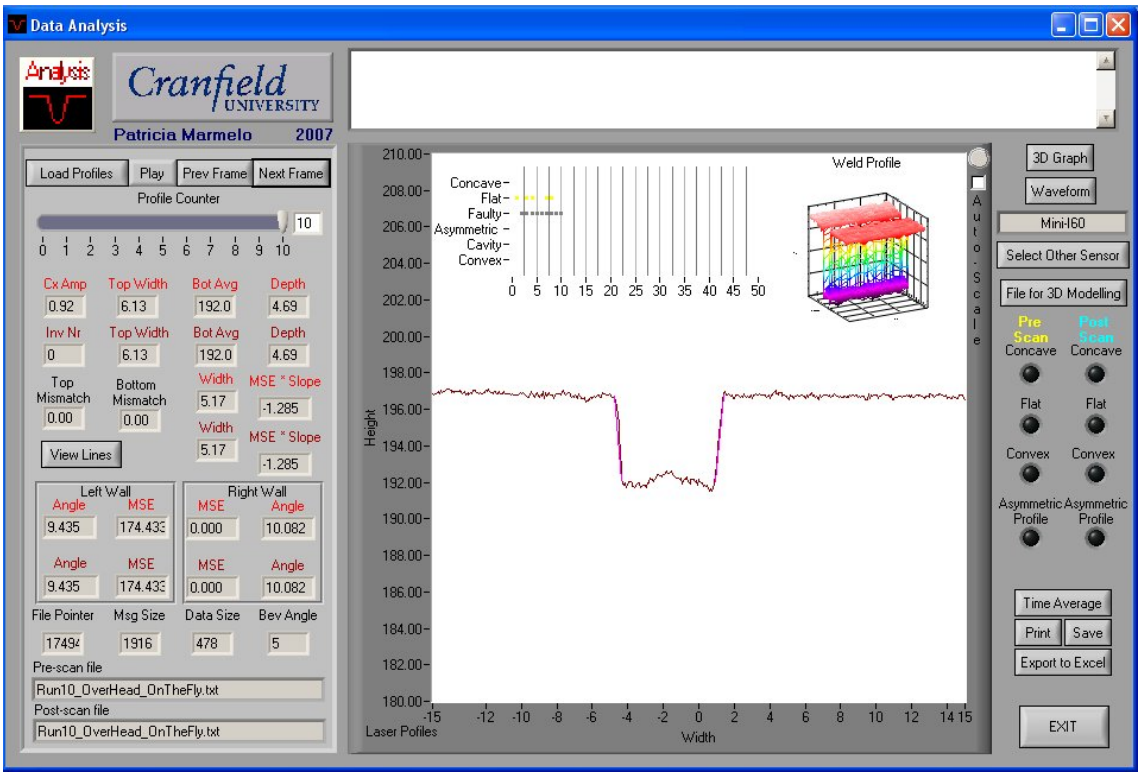

Figure 7.97 – Screenshot of profile 10 of "Run 10" in the Overhead position.

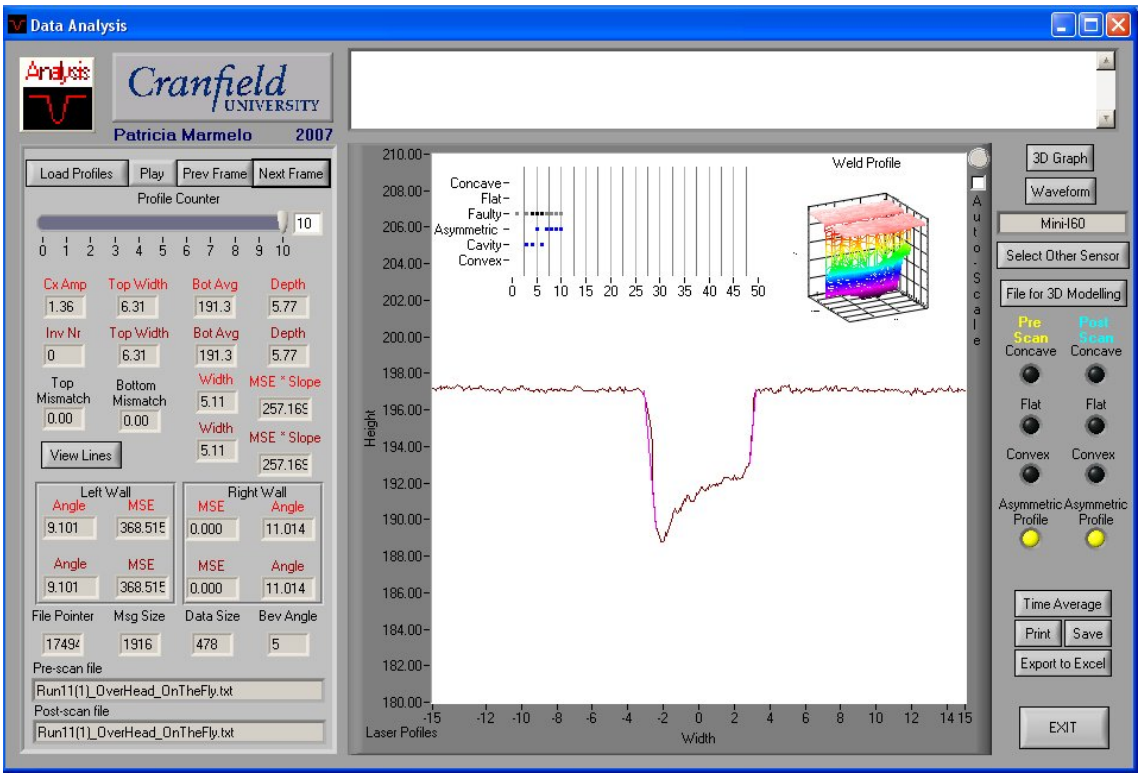

Figure 7.98 – Screenshot of profile 10 of "Run 11 (1)" in the Overhead position.

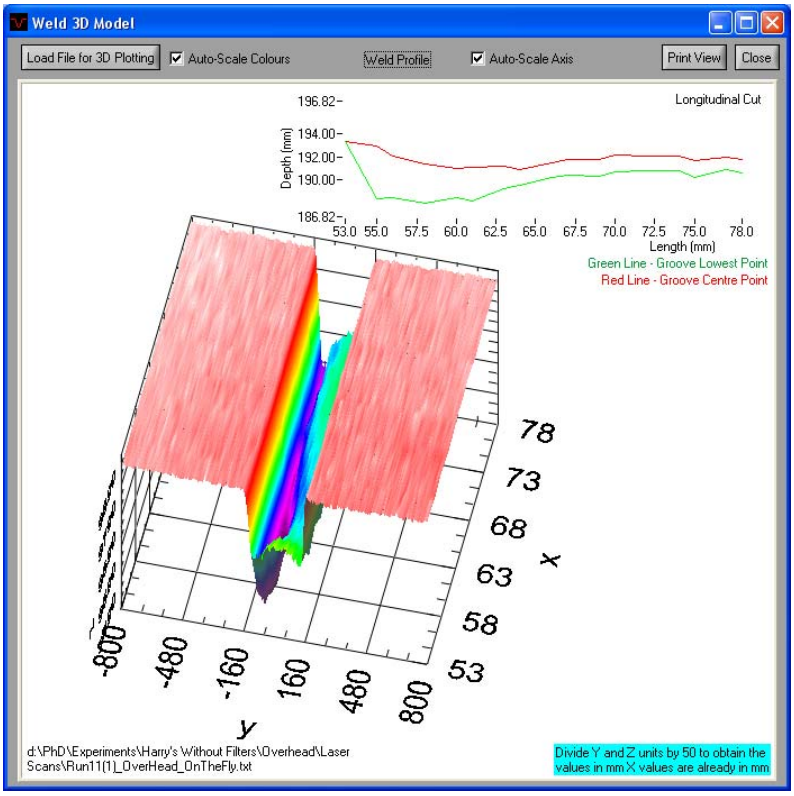

Figure 7.99 – Screenshot of "Run 11 (1)" in the Overhead position 3D model.

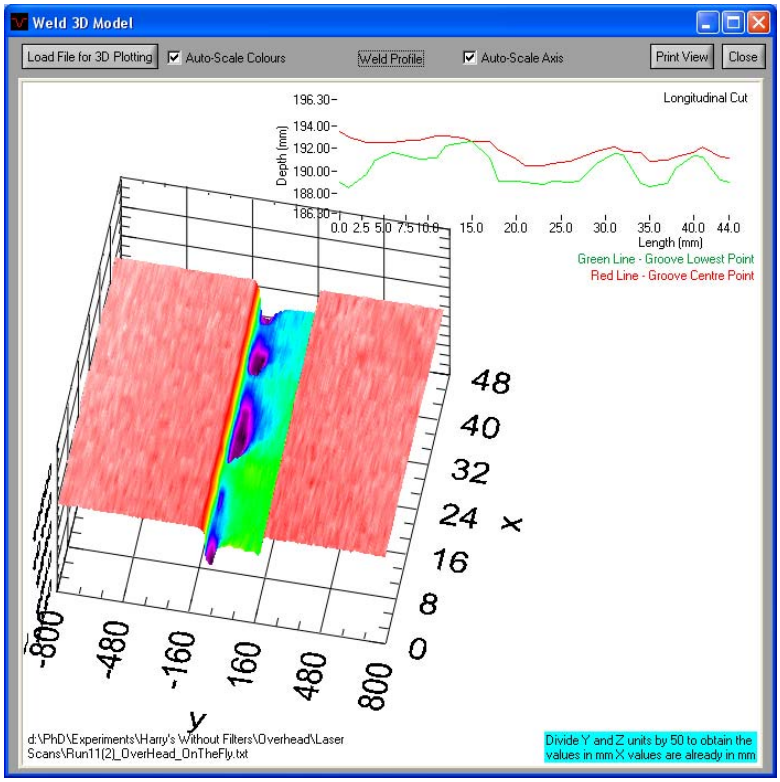

Figure 7.100 – Screenshot of "Run 11 (2)" in the Overhead position 3D model.

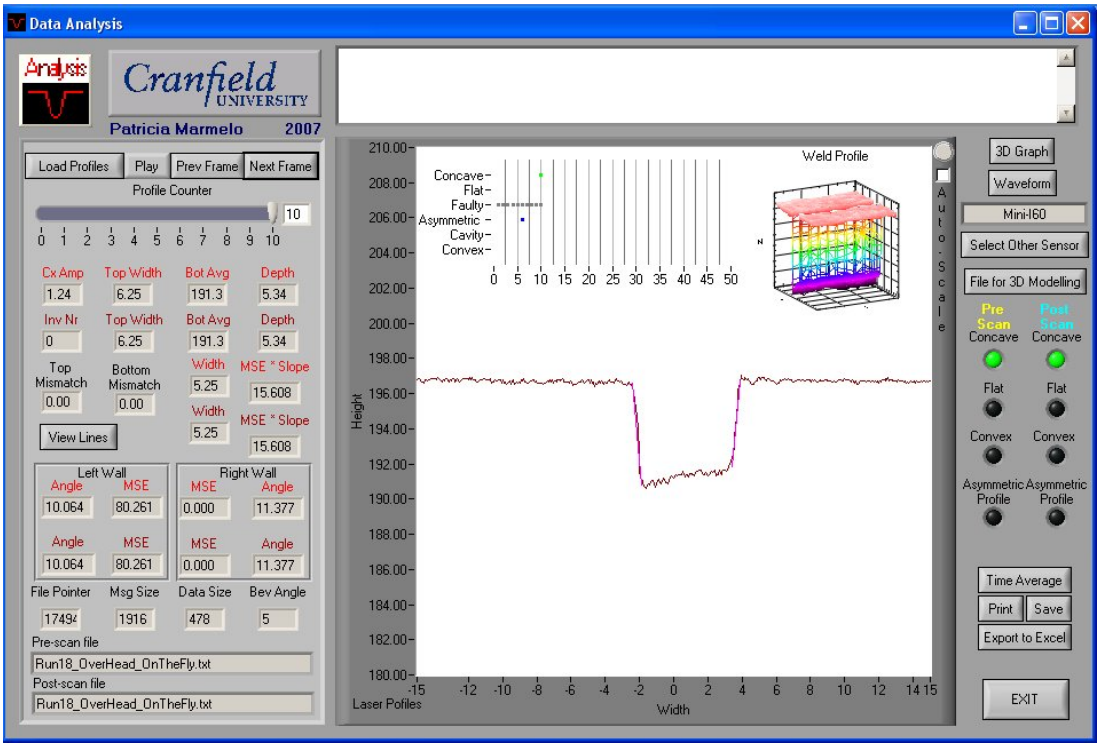

Figure 7.101 – Screenshot of profile 10 of "Run 18" in the Overhead position.

Run 20 (Figure 7.102) has a convex shape and although it is not excessive, caution should be taken when welding another layer on top of the current one. Dwell should be applied in the next pass to ensure proper fusion in the groove corners.

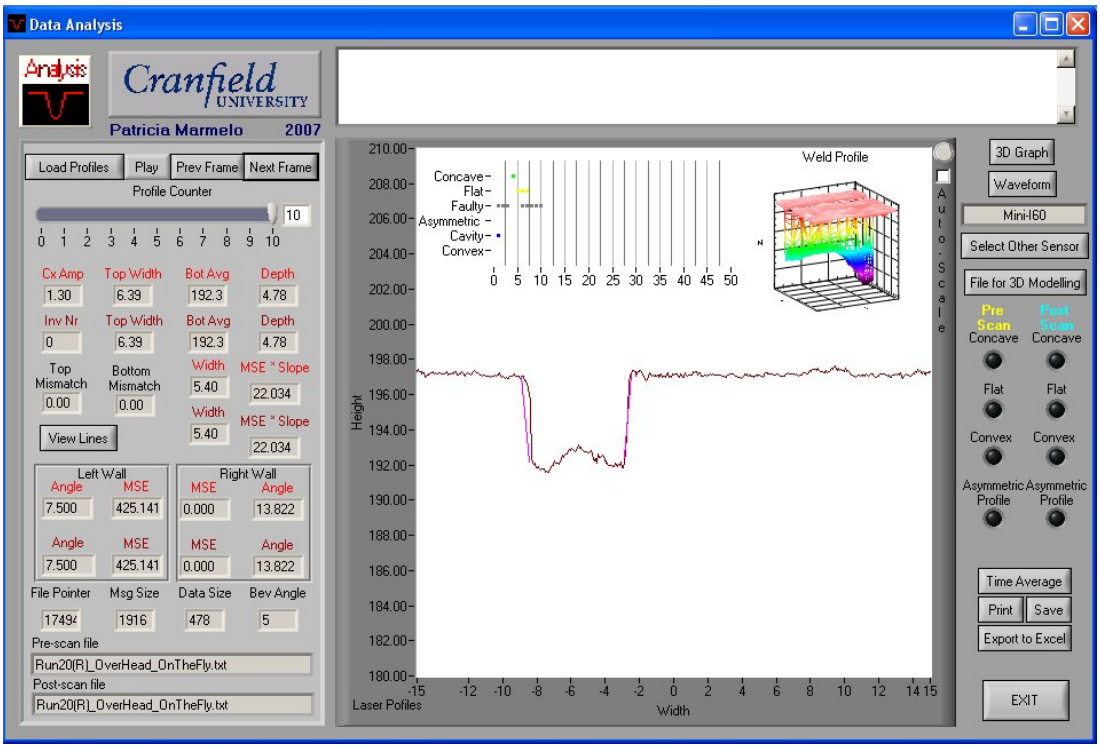

Figure 7.102 – Screenshot of profile 10 of "Run 20" in the Overhead position.

7.3.6.4 Intermediate Positions

Four intermediate angular positions at 30, 60, 120 and 150 degrees were also studied. The aim of these positions is to have a better understanding of the bead configurations variations when welding around a pipe in the 5G position.

7.3.6.4.1 30 Degrees

All bead shapes obtained when welding at the 30 degrees angular position have a concave shape. Runs 5 (Figure 7.104) and 9 are excessively concave and could cause cold lapping in the next bead. The remaining runs are strongly concave, although they should cause no problem for the next bead (example: run 4 – Figure 7.103). The scans from the 30 Degrees position can be seen in Appendix I4.1.

7.3.6.4.2 60 Degrees

In this position, all bead shapes are concave and none of them is excessively concave on the values of the set of parameters tested. Figure 7.105 shows run 10 and is a good example of the bead shapes obtained on this welding position. The scans from the 60 Degrees position can be seen in Appendix I4.2.

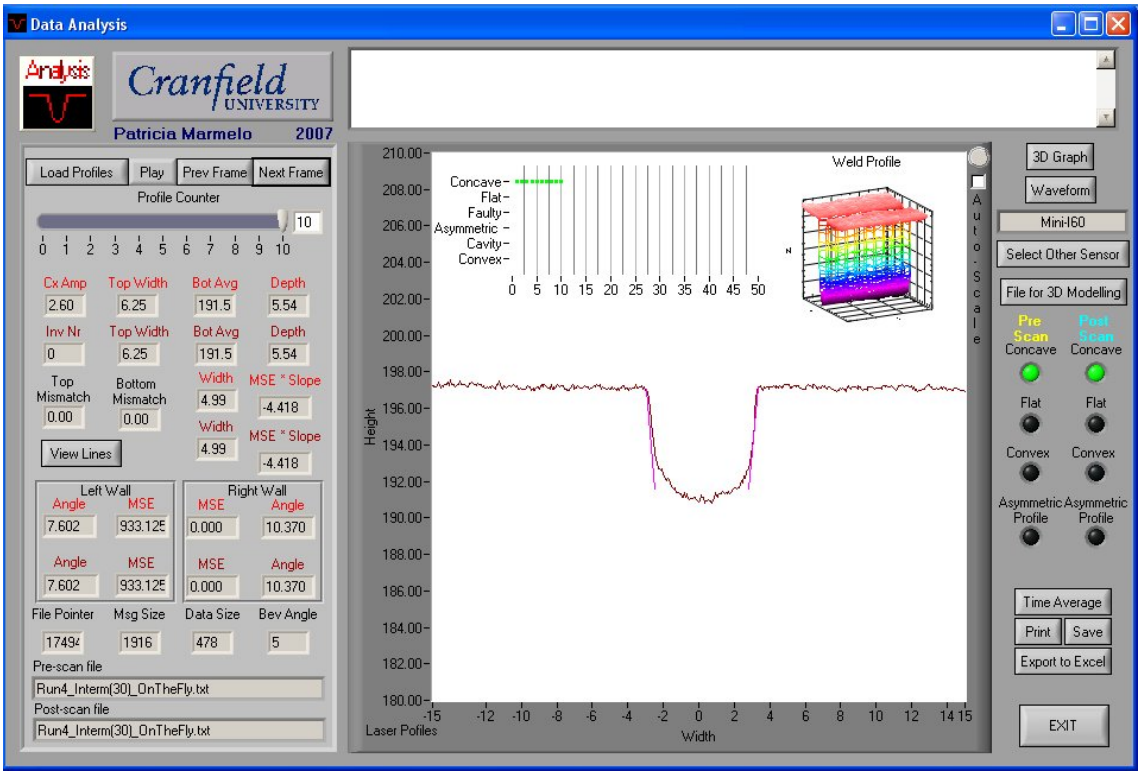

Figure 7.103 – Screenshot of profile 10 of "Run 4" positioned at 30 degrees.

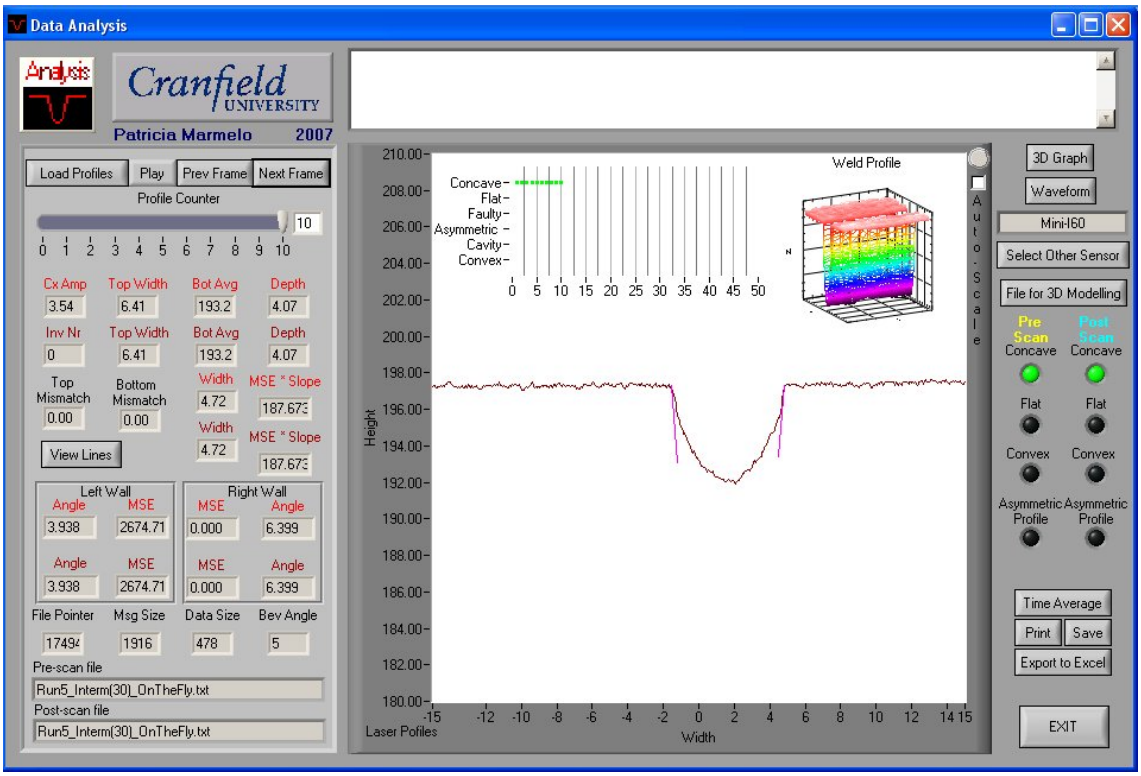

Figure 7.104 – Screenshot of profile 10 of "Run 5" positioned at 30 degrees.

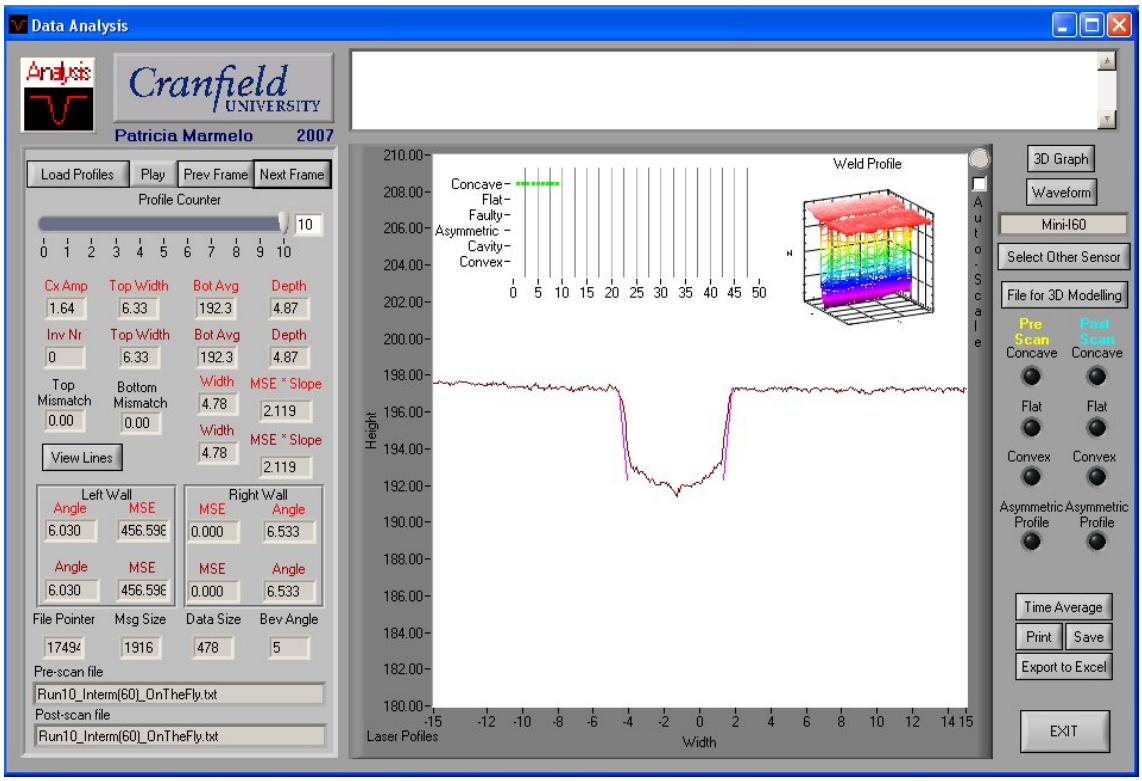

Figure 7.105 – Screenshot of profile 10 of "Run 10" positioned at 60 degrees.

7.3.6.4.3 120 Degrees

Again, in this position all bead shapes obtained are concave. Runs 20, 23 (Figure 7.107) and 27 are strongly concave and the other runs (example: run 19 – Figure 7.106) have acceptable concavity. The scans from the 120 Degrees position can be seen in Appendix I4.3.

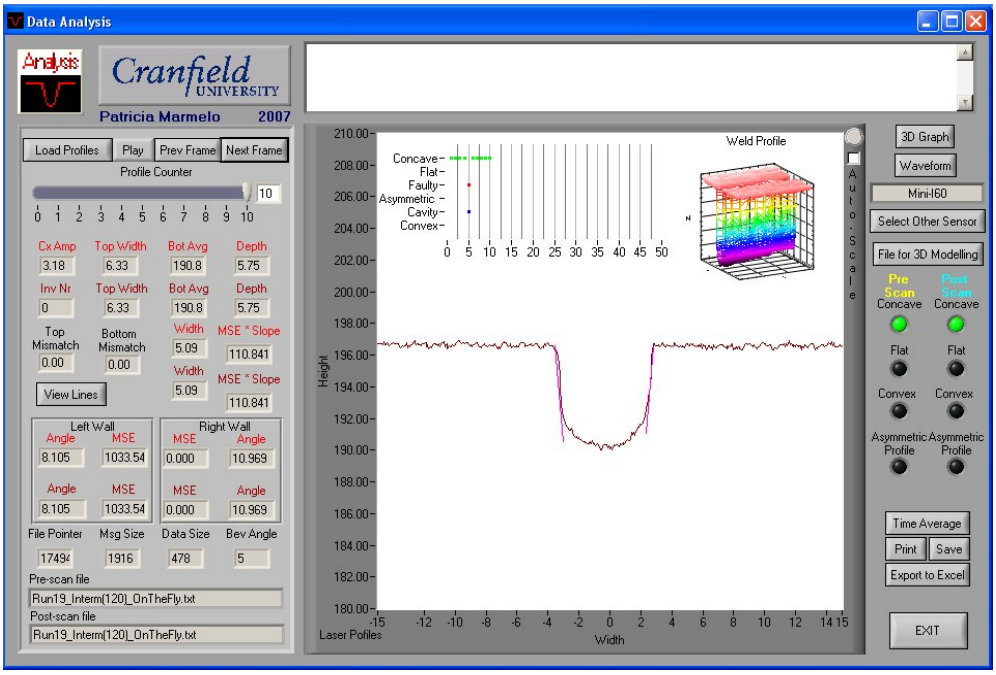

Figure 7.106 – Screenshot of profile 10 of "Run 19" positioned at 120 degrees.

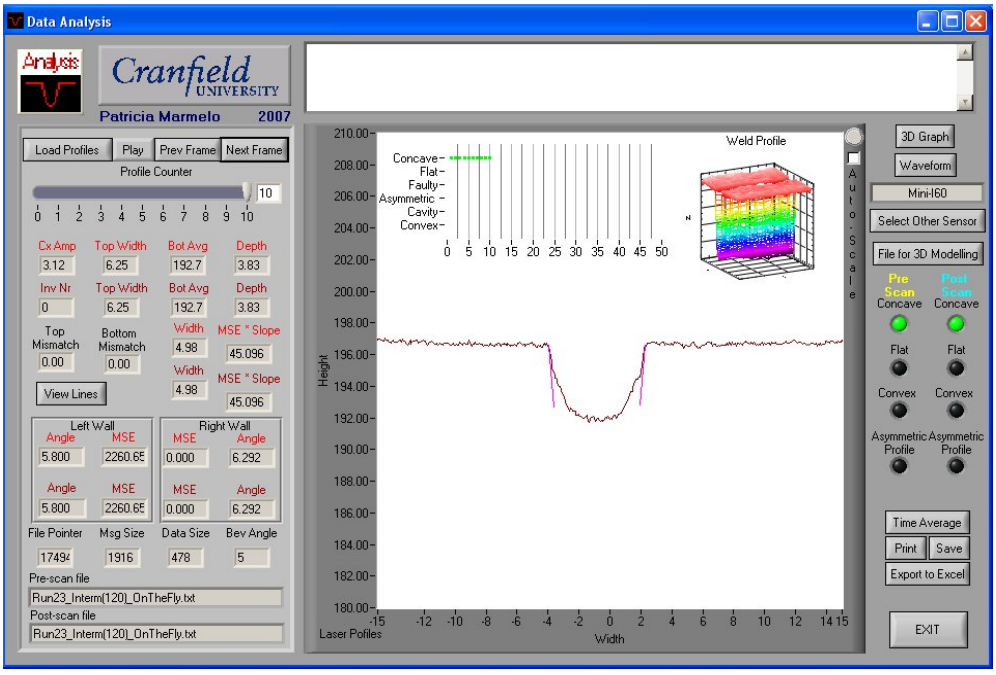

Figure 7.107 – Screenshot of profile 10 of "Run 23" positioned at 120 degrees.

7.3.6.4.4 150 Degrees

Welds at this position with the evaluated sets of parameters resulted in both concave and flat beads. Runs 28 (Figure 7.108), 31, 32, 33, 34, 35 and 36 are concave and runs 29 and 30 (Figure 7.109) are flat. The scans from the 150 Degrees position can be seen in Appendix I4.4.

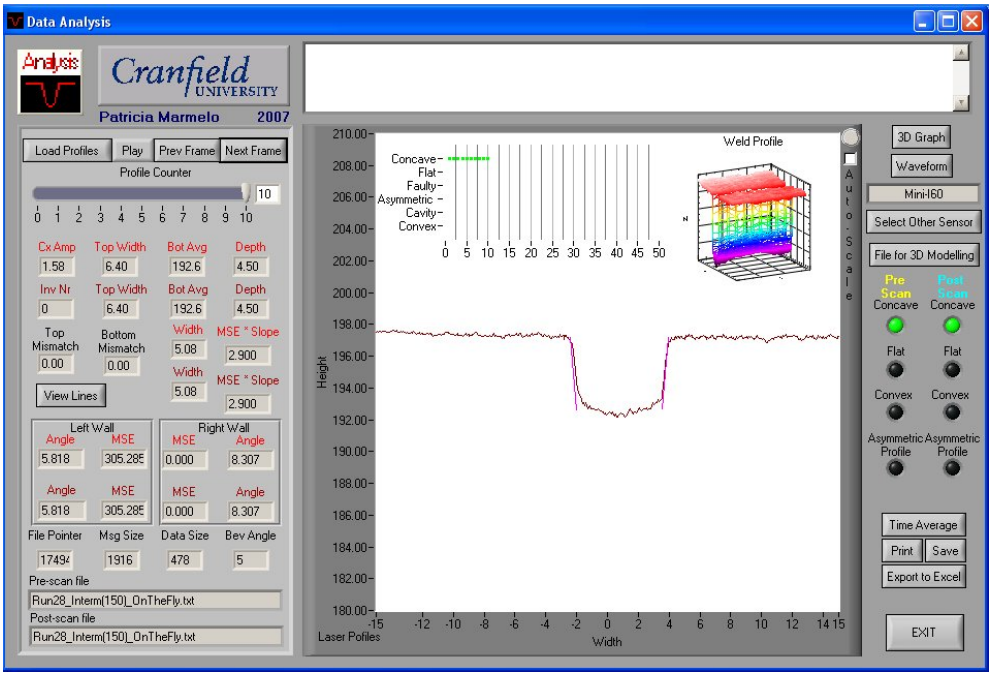

Figure 7.108 – Screenshot of profile 10 of "Run 28" positioned at 150 degrees.

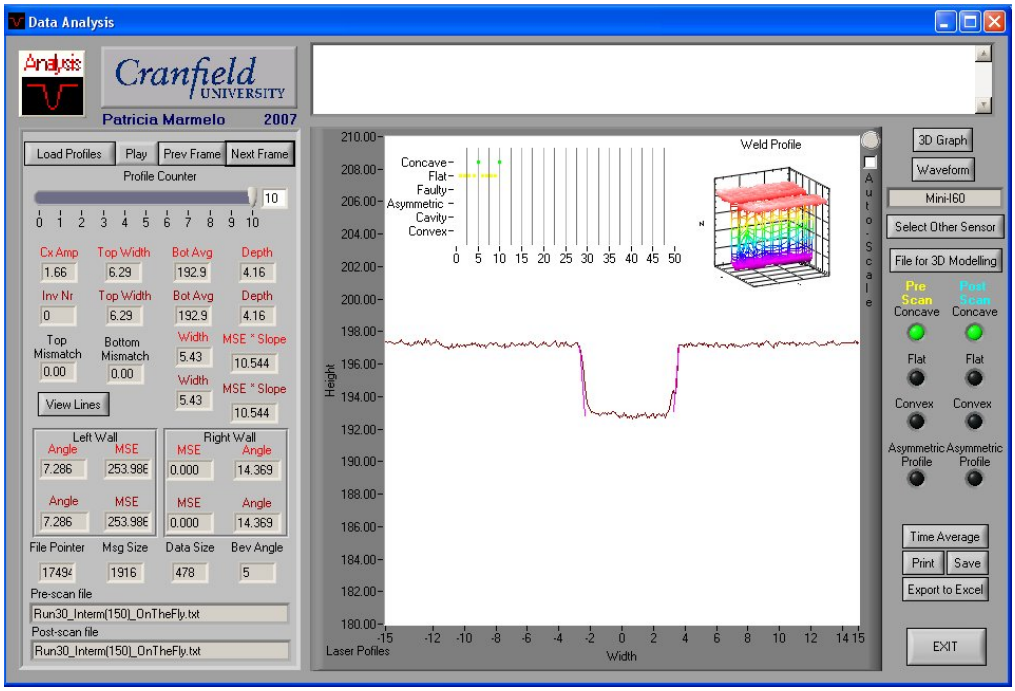

Figure 7.109 – Screenshot of profile 10 of "Run 30" positioned at 150 degrees.

7.4 Bead Shapes

From the real time assessment of weld quality experiments (section 7.3.6) a wide range of bead shape configurations was obtained. With the aim of developing new algorithms and improving the existing ones, the bead shapes were discussed with an experienced welding technician. From this discussion a better understanding of what is acceptable convex and concavity was obtained. This was translated into a set of rules to be integrated into the software. The shapes, their influence in the weld and the developed rules will be described below. The description will be made according to shape type.

7.4.1 Flat

A flat line is by definition a line with no curvature. When analysing weld bead shapes and attempting to determine if the bead is flat or not a tolerance must be given to the flatness. Also considering that no filters were used during the data acquisition and so it has a noise component. It is impractical to consider the possibility of obtaining a purely flat shape as the groove bottom. Hence a tolerance was added to the definition of flat. The welding technician considered that a tolerance of ±0.5mm would be the appropriate value to be added. See Figure 7.110 for the different definitions of flat bead profile introduced in the algorithms. In the developed algorithms “d” is the difference between the maximum and the minimum value in the data that define the groove bottom area.

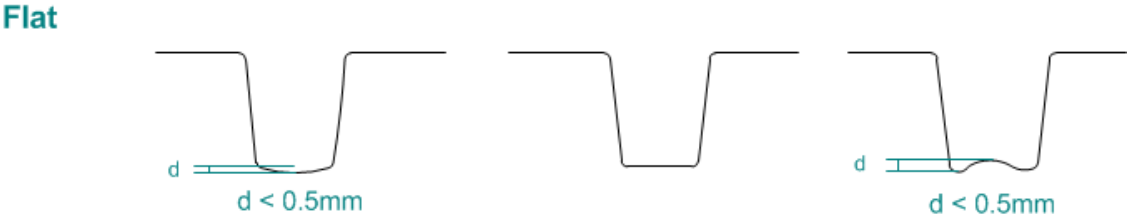

Figure 7.110 – Definition of flat bead profiles.

7.4.2 Concave

A concave line is one that has a curved shape. More precisely, it has the centre of the curvature as the lowest or as one of its lowest points. In terms of a concave weld bead shape, it is defined as a bead profile in which there is one inflection in the direction of growth of the data. Once again due to the noise in the profile data due to the lack of filtering more than one inflection can and do occur without invalidating the shape to be considered concave. This impeded the use of inflection count as a way to determine concavity/convexity. Due to the noise in the data and the ±0.5mm tolerance added to the definition of flat bead only beads which profiles have a “d” value greater than 0.5mm are considered concave. In the algorithms

“d” is the difference between the maximum and the minimum value in the data that define the groove bottom area.

Concave welds are defined as those where the concavity exceeds 0.5 mm, as shown in Figure 7.111. The dotted green lines indicate where the groove walls were originally located. On a weld, there is such a thing as unacceptable or excessive concavity. Bead shapes with excessive concavities are the ones that are likely to create defects on a subsequent run due to its shape, and are also more likely to exhibit centreline cracking.

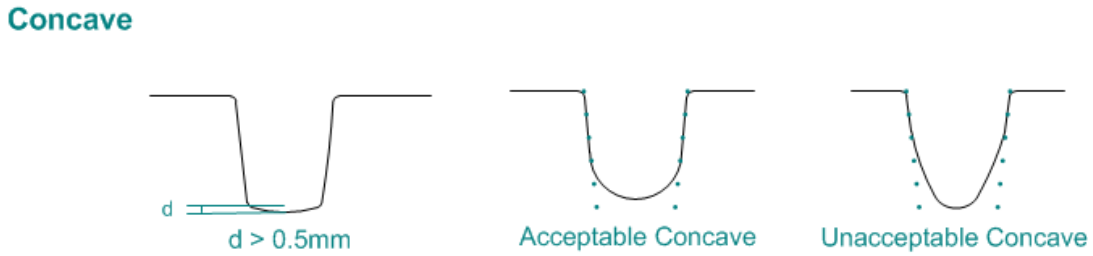

Figure 7.111 – Definition of concave bead profiles.

A factor, when determining if a weld is excessively concave or not, is the angle (β) between the original groove wall positioning and the bead concavity angle (Figure 7.112). This angle increases as the concavity increases. Another factor to consider when determining if the shape is acceptably concave is once again the “d” value. An excessively concave profile will have a “d” value greater than 1.5mm according to the welding technician. According to the same technician, the most likely defect to occur due to excessive concavity is cold lapping. This occurs because the heat from the welding arc does not reach deep enough to melt properly the previous layer and it does not fuse together with the new material.

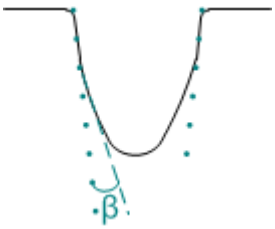

Figure 7.112 – Definition of β angle in concave bead profiles.

7.4.3 Convex

Convex welds are defined as those where the convexity exceeds 0.5 mm, as shown in Figure 7.113. Like concavity there can be acceptable and excessive convexity. Bead shapes with excessive convexities are likely to create defects on a subsequent run due to their shape.

Excessive convexity is linked not only to the height of the convexity (“d”) but also to the angle of the convexity (angles α and β in Figure 7.113). The higher the convexity angle the more it is likely that the profile has an unacceptable shape.

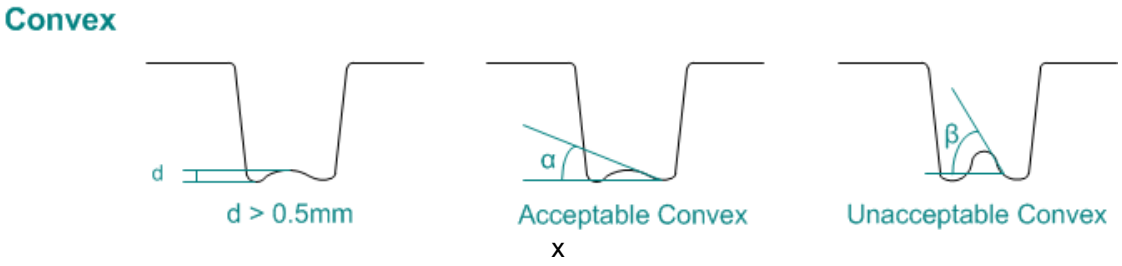

Figure 7.113 – Definition of convex bead profiles.

No conclusion was reached about which angles are acceptable and which are not when discussing the subject with the welding technician. The angles can be directly related to the width (“A”) and height (“B”) of the convex region of the profile. This is a more simple and practical way of analysing the shape. In Figure 7.114 can be seen two convex shapes: an acceptable profile on the left and an unacceptable on the right. What makes these shapes acceptable or not is the ratio between the “A” and “B” values. Discussing this with the welding technician the following conclusions were reached:

- A > 60% of Groove Bottom Width -> Good Profile
- 40% < A < 60% of Groove Bottom Width -> Acceptable Profile
- A < 40% of Groove Bottom Width-> Bad Profile

- B < 1.0mm -> Good Profile
- B = 1.0 to 1.5 with “wide” A -> Acceptable Profile
- Not Acceptable Otherwise

These conclusions were converted into rules and embedded in the control algorithms used to discern the weld bead shapes.

Figure 7.114 – Definition of A and B parameters in convex bead profiles.

For shapes like the ones described in Figure 7.115, the distinction between acceptable and unacceptable shapes is not only dependant on the value of “d” but it is also dependant on the

weld angular position. A summary of the conclusions concerning these types of profiles can be seen below.

- d < 1.0mm Good on the Flat Position
- d < 0.5mm Good on the Overhead Position
- d < 1.5mm Acceptable on the Flat Position
- d < 0.8mm Acceptable on the Overhead Position

Figure 7.115 – Examples of convex bead profiles.

From all the bead shapes the convex one is the most complex, both to determine and assess. It results from either the weld angular position or welding parameters such as oscillation width. Flat bead shapes are the most common in the flat position or surrounding areas. Concave shapes are the most common ones throughout the entire spectrum of angular positions. Despite the occurrence of excessive concavity for some welds, a concave shape is a very desirable shape as it is very easy to weld on top so it makes it a very attractive shape.

7.5 Welding Defects

Through the examination of the weld profiles acquired with the laser vision sensor and the correspondent weld macros, a range of weld defects were detected. Some are discernible in the laser profiles and others are not.

7.5.1 Asymmetric Profiles

An asymmetric bead profile is one which is tilted, whether it is concave, flat or convex. When considering a flat asymmetric profile (Figure 7.116) it is necessary to discern if the degree of asymmetry is acceptable or not. Again, the angular position of the weld location is relevant. When the weld is performed in the overhead position “d” should not exceed 1mm and the remaining positions a tolerance of 2mm is acceptable.

Similarly, when evaluating concave asymmetric profiles as the one described in Figure 7.117 the weld angular position is a factor but some more factors need to be taken in consideration. Again “d” value is an important factor and is dependent on the weld angular position. For the overhead position “d” should not be greater than 1mm according to the welding technician. In

addition, in the remaining positions it should not exceed 2mm. Another factor to have in consideration is the location of the asymmetric concavity in relation to the groove centre itself. The values “Xa”, “Xb” and “Xc” are respectively the “x” axis coordinate of the data points A, B and C in Figure 7.117.

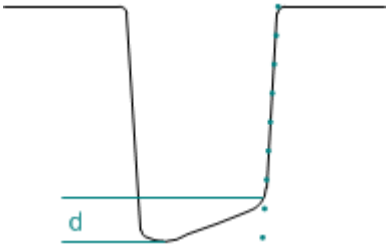

Figure 7.116 – Example of a flat asymmetric weld profile.

For the asymmetry to be acceptable in the overhead position, “Xb” has to be no further apart from the centreline 8% of groove bottom width (“Xa”-“Xc”) in either direction. In the other positions, the centre point deviation tolerance increases from 8% to 15%. Per angular position both rules need to be validated for the asymmetry to be acceptable.

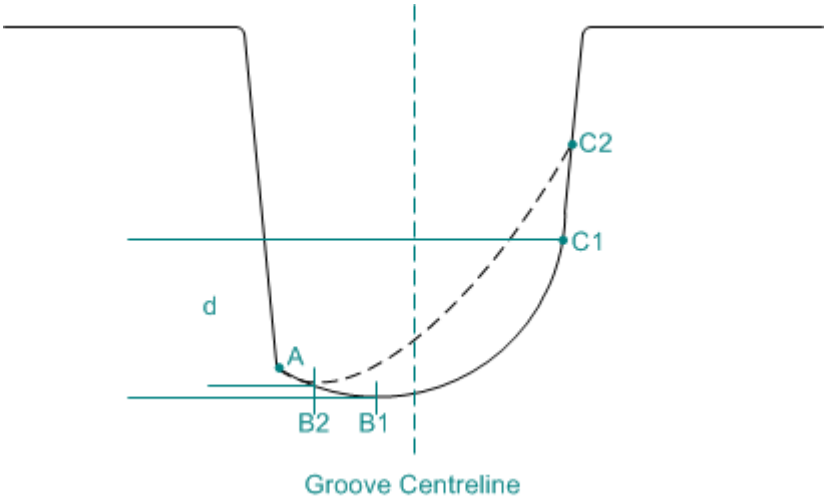

Figure 7.117 – Example of a concave asymmetric weld profile.

On the convex position two types of asymmetry can occur, they can be seen in Figure 7.118, and while no asymmetry is good in a weld, the second type (the one on the right side) is less desirable. The reason for this fact is that when the convexity rises above the height of the higher of the groove bottom ends (see Figure 7.7). On the opposite side of the groove bottom the weld arc will have more difficulty fusing the filler metal with the parent metal and so creating cold lapping. In the second case, the measure to have in consideration is “d2” as it is the one best representing that asymmetry. On the overhead position either “d” or “d2” need to be lower than 1mm and in the remaining angular positions lower than 2mm.

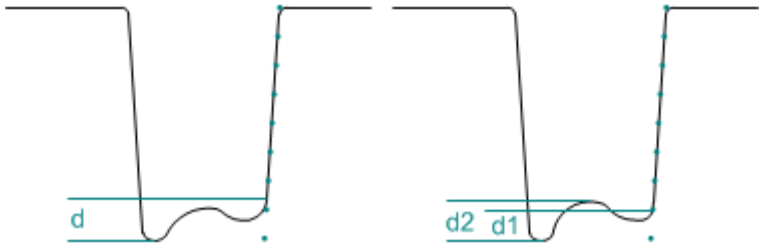

Figure 7.118 – Example of convex asymmetric weld profiles.

Asymmetric profiles are possible to detect with the laser vision sensor and the profile data is easily treatable to discern this kind of profiles and assess them. Information of the symmetry of a profile is convenient to have both for control and monitoring purposes. When detecting in real time an acceptable asymmetric profile prior to welding, on a specific location, it is possible to adjust weld parameters such as oscillation width, oscillation centre point or dwell to correct the fault. Both in real time and in post scanning operation, detecting an asymmetric bead is important to highlight the location as a possible source of defects and perform non-destructive testing in the highlighted area to establish the existence of defects or not. Once these algorithms are fully developed and field tested. It could be possible to skip doing NDT on the entire pipe circumference and do it only on the highlighted locations. This would save time and money.

7.5.2 Cavity

Cavities in the weld bead are also easily detectable with the laser vision sensor. To discern if the profile containing a cavity actually detected a cavity or if it is just erroneous scan data more than just one profile needs to be took in consideration. In real time, with pre-scan detection of a cavity, the system should adapt the weld parameters in order to correct the defect with the new layer if it is correctable. Otherwise, the welding process should be stopped so that the defect can be corrected in a different manner. On the other hand, if using the laser sensor in real time but trailing the weld torch, the system should adapt the welding parameters to stop the cavities to occur. Finally, if using the laser sensor as a post-weld scanning system, the detection of cavities should be used to assess their severity and decide on the corrective measures to take. In either of these situations, the detection of cavities should also be used to highlight areas for post weld inspection with other NDT methods to ensure weld quality.

Two cases of detected cavities can be found in welds “Run 13” in the flat position and “Run 11 (1)” in the overhead position. The respective 3D models can be seen on Figure 7.84 and Figure 7.99 and screenshots of profiles showing the cavity can be seen in Figure 7.85 and Figure 7.98 respectively.

7.5.3 Porosity and Inclusions

Porosity (internal) and inclusions are not possible to detect with the laser sensor as it is not possible to see them on the weld surface, with the exception of surface breaking porosity. This last defect did not occur in the range of weld tested so the sensor's performance under such conditions was not tested. A case of porosity was found in the macro of run 4 (Figure 7.119) on the vertical down position. It is obvious that a surface profile sensor cannot detect subsurface pores.

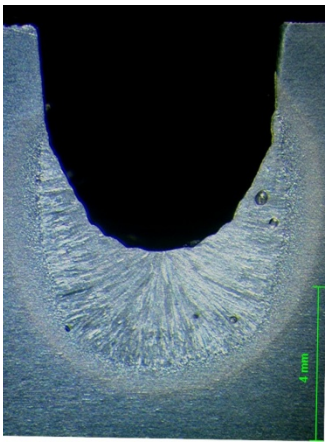

Figure 7.119 – Macro of weld "Run 4" in the Vertical Down position.

7.5.4 Undercut

Undercut was detected in run 20 of the overhead position. The macro of such weld can be seen in Figure 7.120 Red lines were added to the macro image to represent the location and shape of the original groove walls. When the screenshot of the weld profile acquired with the sensor is overlaid on the macro image, it is possible to see that the sensor is not able to detect the undercut as it is obscured by the top part of the groove wall. Figure 7.121 shows the overlay of the macro with the laser profile.

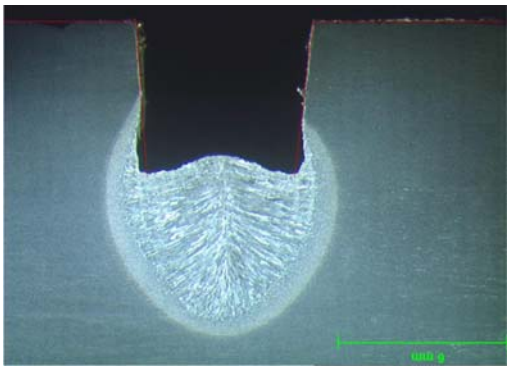

Figure 7.120 – Macro of weld "Run 20" in the Overhead position with the location and shape of the groove walls.

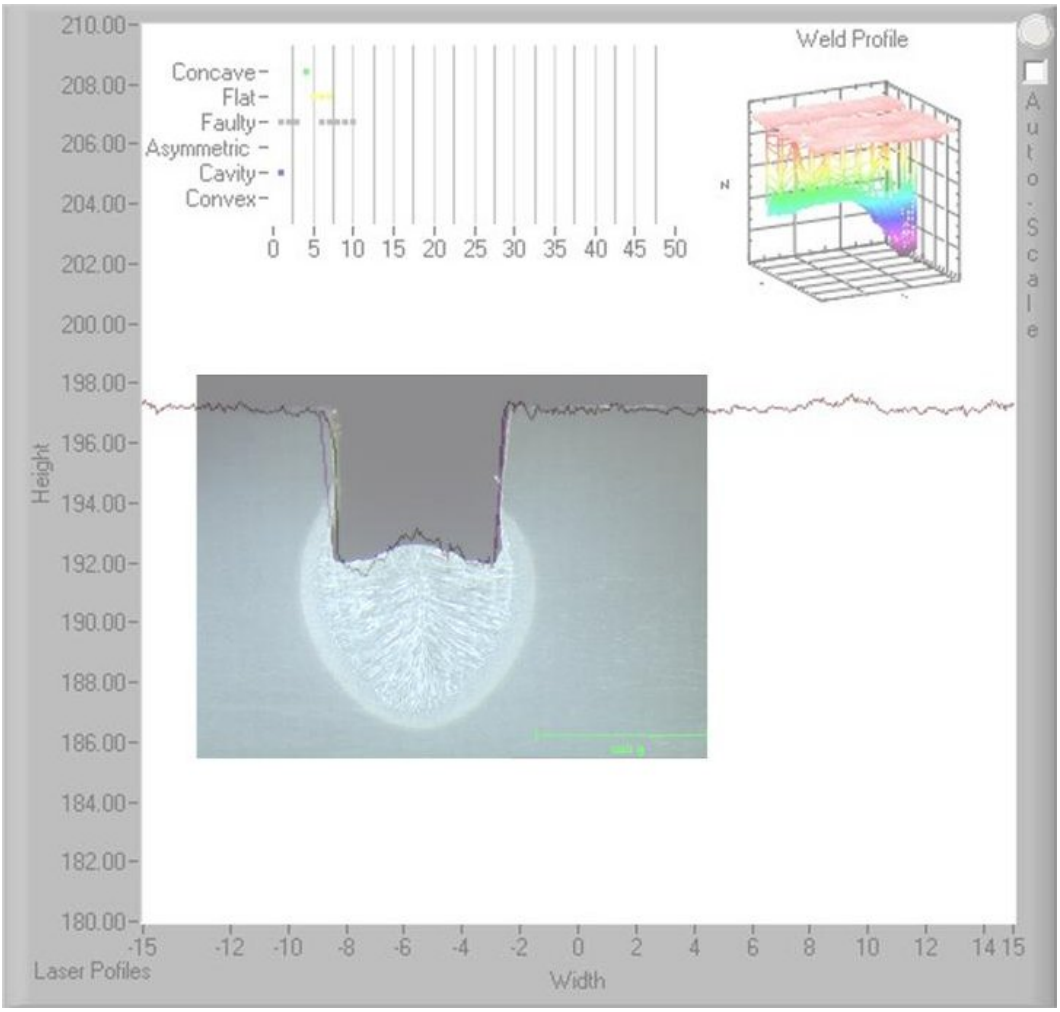

Figure 7.121 – Overlay of macro and screenshot of Weld "Run 20" profile 10 in the Overhead position.

7.5.5 Centreline Cracking

A case of centreline cracking occurred in run 15 of the vertical down position. The macro of this weld can be seen in Figure 7.94 and the profile acquired with the laser sensor can be seen Figure 7.92. The sensor is unable to detect the cases of centreline cracking which occurred in the tested sets of welds. This occurred due to the noise component that exists in the unfiltered data. Filtering the data might make it possible to discern features such as some centreline cracks not detectable under the present conditions. Filtering the data distorts it as it was presented earlier so it was decided to perform the scans without filtering the data. Depending on the aim of the application the use or not of the laser's control unit filters should be considered. Concerning the crack width, in the example given above, the crack size is 0.25mm, which is smaller than the 0.5mm horizontal resolution the sensor has. New sensors were developed since this work was performed and they may bring new light onto this matter

but for the work developed the laser horizontal resolution and filters are a limitation that prevents from developing an algorithm that could detect centreline cracks.

It was not possible to reliably detect any type of crack with the developed system as the resolution of the sensor that was used is 130µm and no software filters were applied. As no software filters were used, the profile has a considerable amount of noise in it. This noise, allied to the sensor's resolution makes it very hard to detect any cracks in the welds. As it can be seen for example in the macro of weld 16 in the vertical down position (Figure 7.122) a solidification crack occurred that could not be consistently detected by the system. This lack of consistency can be seen in Figure 7.123 and Figure 7.124.

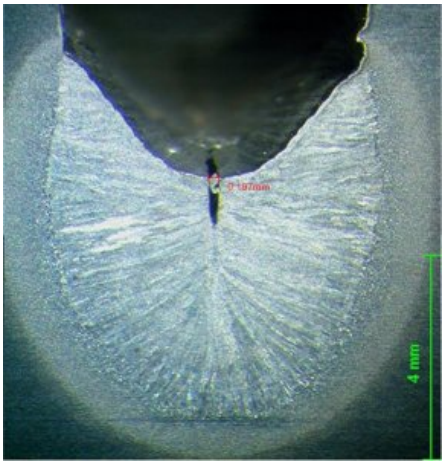

Figure 7.122 – Macrograph of Run 16 on the Vertical Down position with crack width measurement.

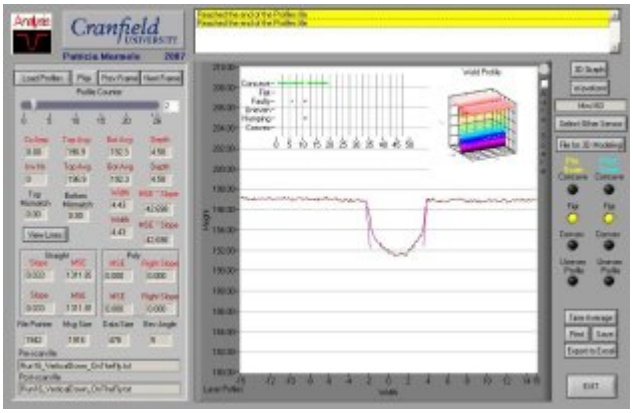

Figure 7.123 – Analysis software screenshot showing profile 2 of Run 16 in the Vertical Down position.

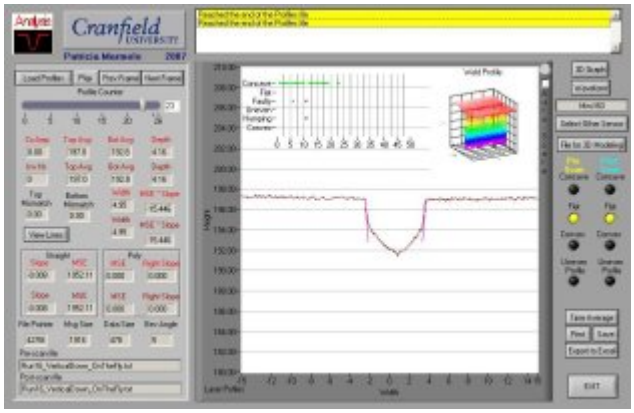

Figure 7.124 – Analysis software screenshot showing profile 23 of Run 16 in the Vertical Down position.

On other cases such as the run 16 on the flat position (Figure 7.125). In which the crack width is smaller. Nothing could be detected at all as it can be seen in Figure 7.126. The noise in the signal masked the existence of the crack making it impossible to detect it reliably. This can be overcome by the use of another sensor with higher resolution as it was demonstrated in the

paper by Reichert and Peterson [128]. The sensor used in their research has a resolution of 12µm (more than ten times higher than the one used in this research) which allowed them to effectively detect cracks in the spot welds they were analysing.

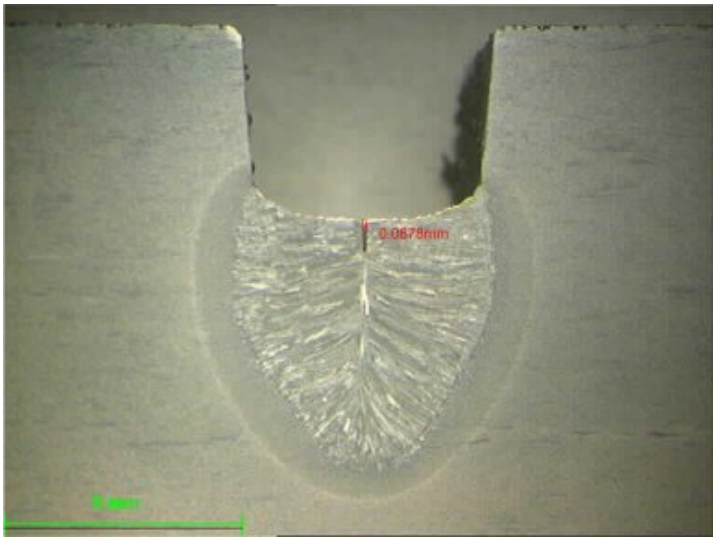

Figure 7.125 – Macrograph of Run 16 on the Flat position with crack width measurement.

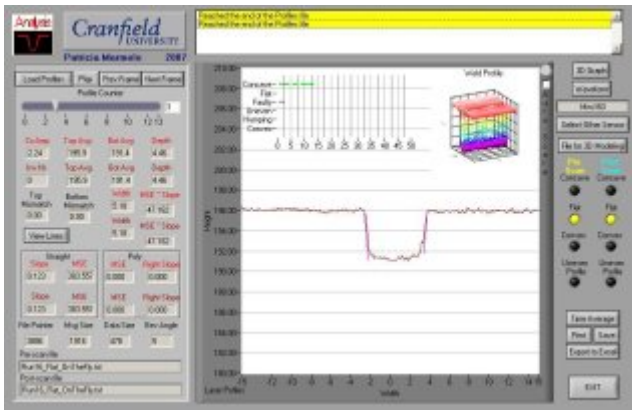

Figure 7.126 – Analysis software screenshot showing profile 3 of Run 16 in the Flat position.

7.6 Weld Ends

Another focus of the laser sensor application is the analysis of the weld ends shape. By weld end should be understood the final section of the weld, area in which the welding arc is suddenly extinguished. An example of a weld end can be seen in Figure 7.127 (photo) Figure 7.129 (3D model). The weld end shape is an indicator which helps understanding how the weld is being formed. Detecting the weld end shape is another application for the use of laser vision sensors. For this application, the sensing would have to take place post-welding or with the sensor trailing the torch.

Based on the previous experiments the data was analysed again, now with the intent of discerning the characteristics of the weld ends. Two different welds are represented below. When looking at their pictures (Figure 7.127 and Figure 7.128) the weld ends look similar. Their difference becomes clear when analysing their 3D models (Figure 7.129 and Figure 7.130). It is evident when looking at the 3D models itself but especially at their transversal cut that the welds ends have different geometries. No investigation was performed on what causes each of the different shapes obtained and neither on their influence on the next bead. During the final phase of this work it was noticed that usable data could be extracted from the profiles to evaluate the weld ends. As this was not an objective of the proposed work no algorithms were developed to analyse this specific part of the data. None the less it would be an interesting topic to research had there been time.

Figure 7.127 – Photo of the end part of "Run 6" on the Flat position.

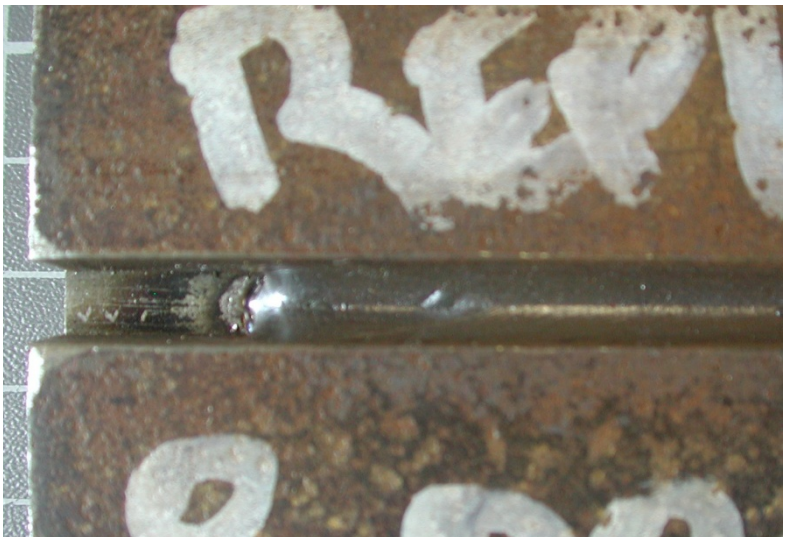

Figure 7.128 – Photo of the end part of "Run 21" on the Vertical Down position.

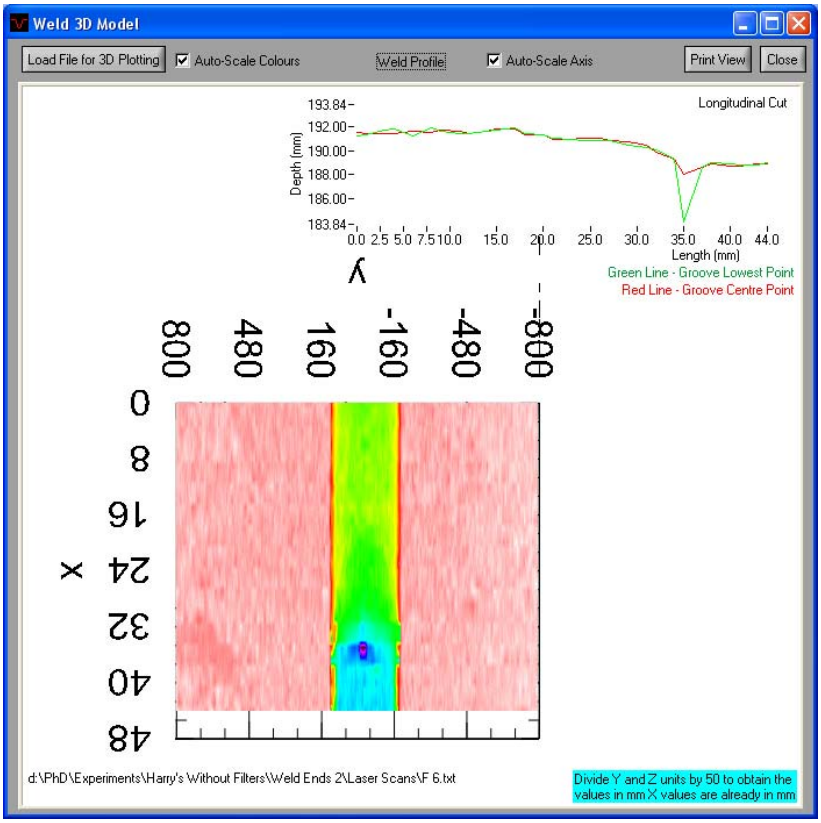

Figure 7.129 – End part of "Run 6" on the Flat position 3D model.

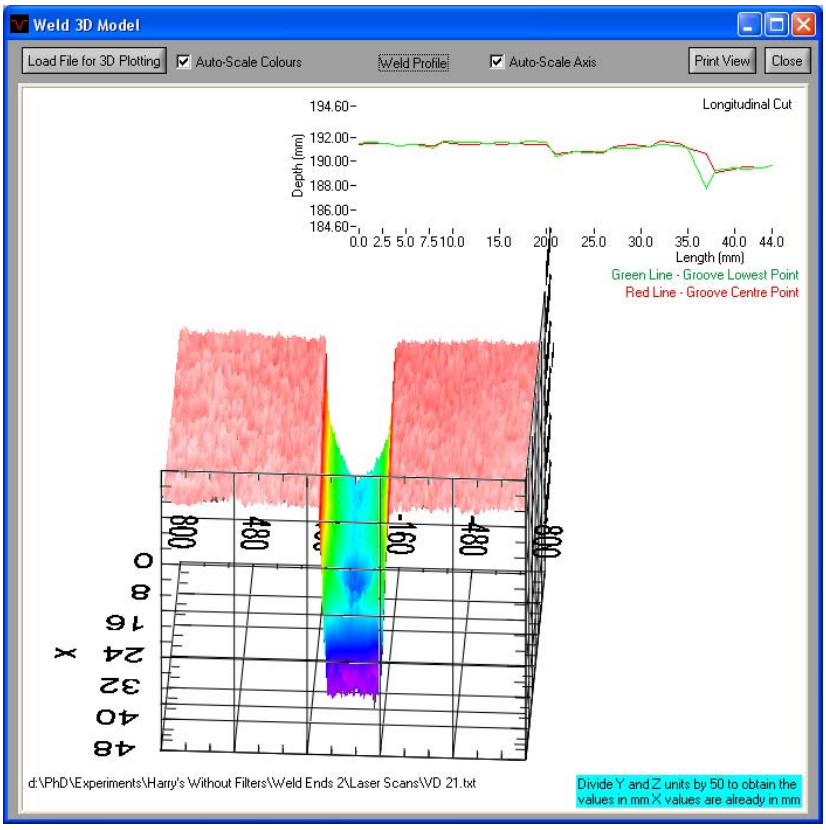

Figure 7.130 – End part of "Run 21" on the Vertical Down position 3D model.

7.7 EXAscan™ – 3D Laser Scanner Data

As part of the product demonstration at Cranfield University two sample plates were scanned using the EXAscan™ scanner. This hand scanner is from the Handyscan 3D™ line from Creaform™ company. This is a high definition handheld scanner which provides 3D data from the scanned object. A description of this equipment can be found in section 2.1.5.5. This scanner was used on a couple of specimens to test its usability for this application and to compare with the results obtained from the other sensors.

The scanned plates were the ones containing runs 28, 29, 30 and 31 from the flat position (sample 1) and 1, 2, 3, 4 (sample 2) in the vertical-down position. Both samples were covered with a white powder spray which is easily removed afterwards. Test samples 1 and 2 can be seen in Figure 7.131 and Figure 7.133 respectively.

The use of EXAscan™ to scan an object generates a text file (*.txt) and/or a stereolithography file (*.stl). The stereolithography files were imported into a freeware stereolithography file reader, the “MYRIAD 3DReader” to review the retrieved data. A screenshot of each of the scan results can be seen in Figure 7.132 and Figure 7.134.

From the obtained results it is possible to see that data is very accurate. Despite this, this is not a suitable solution for pipeline welding as the sensor is quite big and it would cause several setup constraints. Also the amount of data to be dealt with would be enormous when compared with the laser profile sensors. The processing power required to deal with the data as well as the algorithms to treat the data would be much larger. Another disadvantage of this sensor type is that it requires for the surface to be matte, so it would still have the same issue with reflectiveness as laser sensors do. In additions it also requires that some target dots are randomly placed in the surface to be scanned to serve as reference points.

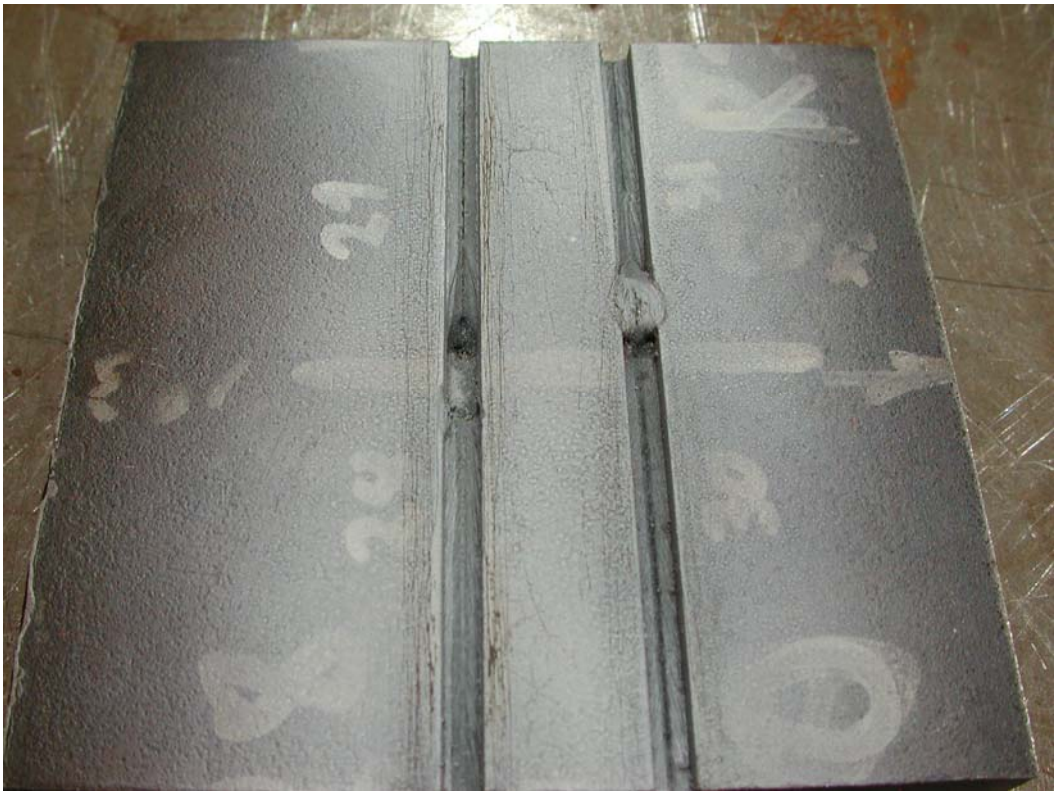

Figure 7.131 – Sample 1 of the 3D laser scanner experiments.

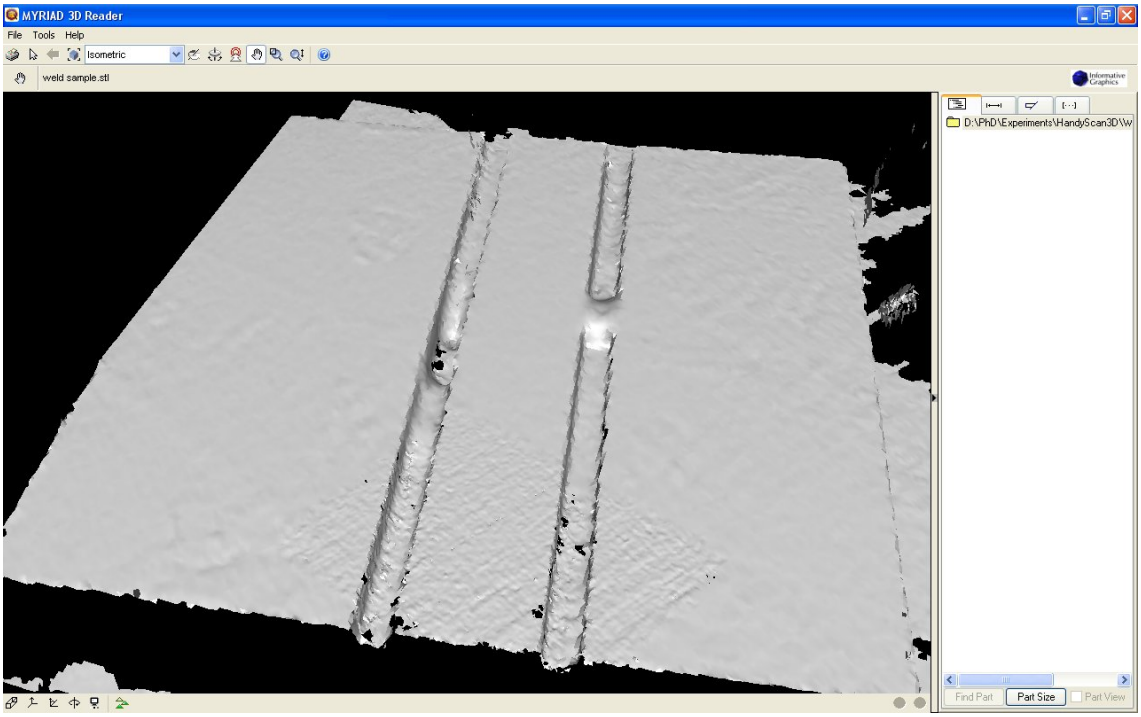

Figure 7.132 – Sample 1 of the 3D laser Scanner 3D model.

Figure 7.133 – Sample 2 of the 3D laser scanner experiments covered with a film spray.

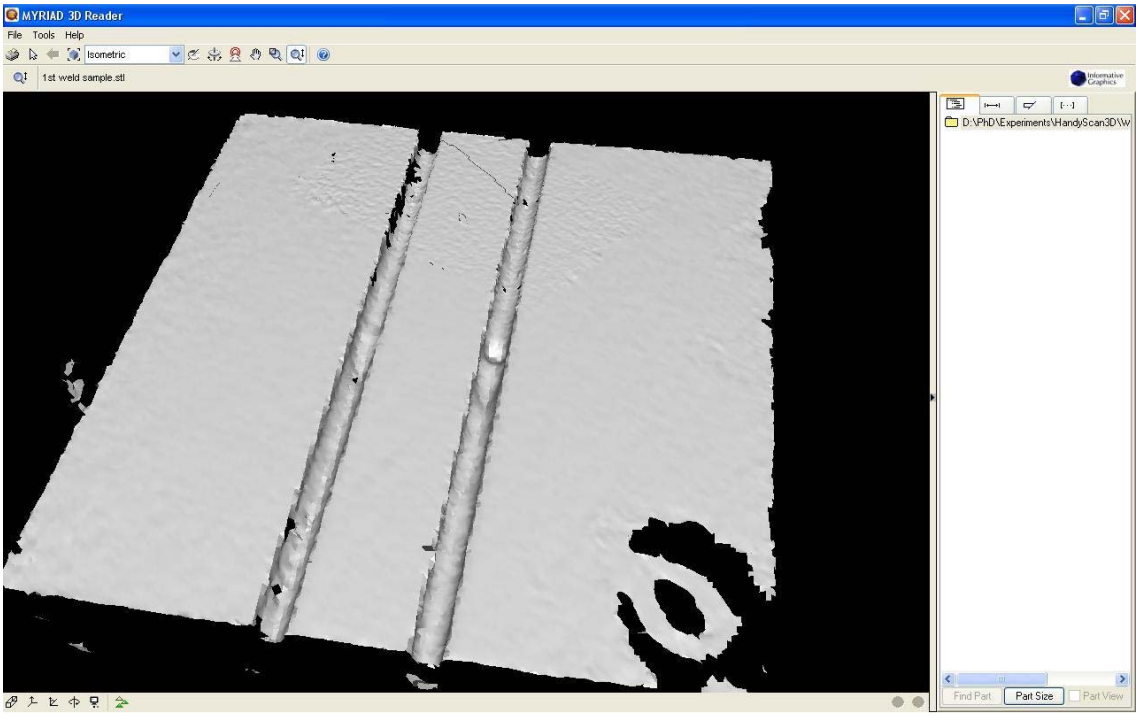

Figure 7.134 – Sample 2 of the 3D laser scanner 3D model.

7.8 Summary

It was found that the sensor output is not very sensitive to sensor rotation but it is sensitive to tilting of the sensor head. Experiments show the influence of surface reflectiveness on different surface conditions. From these experiments it was concluded that machined prepared narrow groove joints are the most problematic ones from the range of conditions tested. Throughout the experiments it was noticed that under certain conditions the groove shape was distorted. After some investigation it was concluded that this distortion was caused by the use of the sensor's control box own software filters. Further investigation on this topic revealed that the use of filters conditions the sensor performance, especially in shallow grooves and/or steep walls. In the narrow grooves studied, it became clear that the use of software filters has a great influence in the result especially in grooves less than 6mm deep. As the aim was to assess the performance in narrow grooves it was decided not to use the software filters. Once the sensor's general performance and limitations were tested a final phase of experiments was performed in order to access its performance when evaluating the weld bead shape and quality.

A software program was developed that is capable in real time to detect imperfections and defects in the bead shape. The rules applied to discern between a good shape, an imperfection and a defect were determined empirically and for a more precise output of the program a design of experiments needs to be performed to obtain the appropriate rules. Despite the rules values it was clear from the results that it is possible to detect bead shape quality in real time.

After examining these results it was concluded that the laser vision sensor is a good choice when groove features need to be obtained. It was shown by the results that is possible to detect weld groove shape, presence of asymmetric profiles or cavities. On the other hand when dealing with defects such as porosity, inclusions, undercut or centreline cracking the sensor either cannot detect such features because they are visible from the outside or it is inconclusive due to its extremely small size. The weld end of some of these last welds was examined and it is clear that the laser vision sensor can be applied to discern differences between them and the rest of the weld and so use the laser vision sensor to detect the previous weld end. A 3D laser scanner, from Creaform™, and two other laser profile sensors, from Meta Vision System™ and Oxford Sensor Technology™ were tested for performance and compared with the data extracted from the Servo Robot™ sensor.

8 Discussion

What is for the human unconsciously easy to detect, such as a straight line, a circle, the beginning and/or end of a line, can be complex to put into an algorithm in order to achieve the same outcome.

The different parts of any system introduce not only data but also noise in that data that will impair achieving the correct result. In order to minimise the impact of such noise, each source and their effects need to be understood. In order to do that, in this particular application the system was tested for sources of “noise”. This meant exploring the sensor’s capabilities and limitations. Once the challenging issues were detected an assessment to each of them was performed.

8.1 Influence of the Sensor Positioning

Experiments were performed on sensor positioning to determine sensitivity to sensor’s orientation in relation to the weld groove. The results show that the sensor is fairly insensitive to small misalignments. This would mean the sensor can be placed and roughly aligned manually, without the need to use any inclination sensor to assure perfect alignment.

As expected the sensor rotation in relation to the weld seam has little effect on sensor performance up to a rotation angle of 15º (see Figure 7.16 to Figure 7.23). Beyond 15º the fact that the cross section sampled in far from perpendicular to the weld axis is increasingly noticeable and as such it is far from being a reliable measurement.

As it can be seen from Figure 7.26 to Figure 7.34 tilting the sensor beyond 3º starts to affect results. There are two reasons for this: groove shadowing begins to occur; and also due to insufficient data points defining one of the top surfaces of the weld preparation. This last reason is clearly just a function of laser beam misplacement in the preparation surface and can be easily detected just by looking at the projected light and corrected by adjusting the sensor position so that the weld preparation is roughly centred in the projected light. Shadowing on the other hand is a real problem as it will affect measurement and will impair the correct detection of the bead shape and discontinuities on the bead edges. Kang et al [129] developed a system containing two laser diode modules and a CCD camera. They needed to view a width that was wider than the laser diode module would provide so they doubled the length of the illumination

by placing two laser diodes in series (Figure 8.1). Their approach would not overcome the shadowing problem as it is not caused by a narrow width of measurement but by a measurement angle. A solution opposite to theirs might, one laser diode module and two CCD cameras placed at a slight included angle from each other. Both cameras pointing to the centre of the laser light but looking from opposing view angles. The acquired images would have to be somehow stitched to form a single image that would then be analysed for feature extraction. Trucco et al [130] developed a system as described and tested its applicability in different surface conditions reporting good results. They said “the consistency tests described can improve dramatically range measurements in the presence of highly reflective surfaces and holes, and eliminate most of the wrong measurements arising from spurious reflections. This problem is usually circumvented in applications by coating reflective objects with matt paint, but this is obviously not always possible. Our solution can be of considerable interest for 3-D shape inspection applications”. A sketch describing their system can be seen in Figure 8.2.

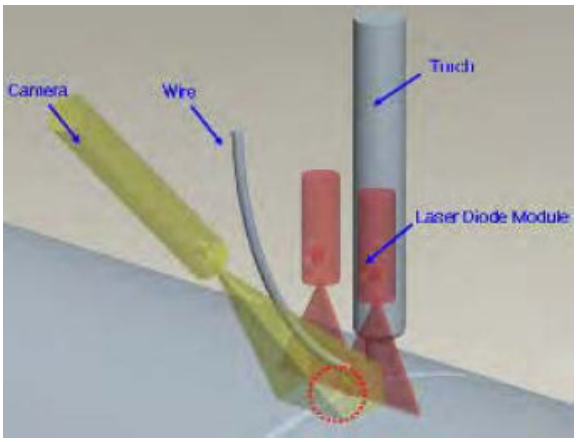

Figure 8.1 – Kang et al [129] layout of the laser diode module.

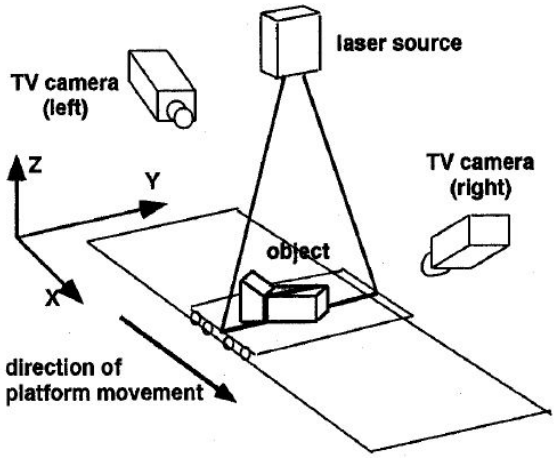

Figure 8.2 – Single laser with dual camera system developed by Trucco et al [130].

8.2 Light Reflection

As it was demonstrated in section 7.3.3 highly reflective surfaces create a problem with the type of sensor used for the experiments. Reflections are not an issue for the fill passes which are the core topic if this thesis. However, laser stripe sensors are required for the root pass in a fully automated welding system, so it was first necessary to understand why this type of surface was a problem. And only later attempts could be made to find ways to overcome it. For the following passes the groove walls are already covered with welding fumes and dust which make the surface non reflective. For the remaining passes, surface condition is no longer an issue and the acquired data is reliable.

Figure 8.3 shows the CCD images of both a highly reflective machined preparation and the same weld joint covered with graphite paint. To overcome this issue, and as the initial weld preparation shape is known, template matching can be performed to extract the general groove shape. Only seam tracking is required at this point so no great detail is needed regarding the groove bottom. Suga et al [131] developed a system for robotic visual inspection using structured light and they used a shadowing plate in order to decrease the arc light influence on the laser sensor. Moon et al [132] developed a system for heavy industry welding applications capable of welding from root to cap pass. Their system overcome the reflections problems by using an image processing algorithm which they did not describe but claimed it made the system immune to reflection problems.

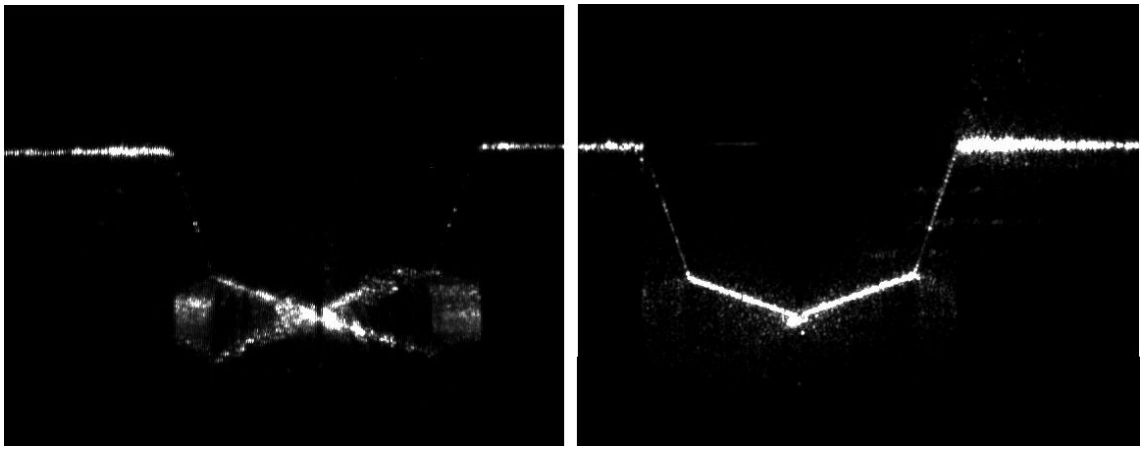

Figure 8.3 – CCD Image from the Meta Vision Systems (MVS) sensor. Scanning of Plate 2 with a shiny preparation (on the left) and with graphite coated surface (on the right).

It is known that paint (weldable primer) has been used in the past to avoid reflections [133]. However, paint of this type can cause welding issues such as porosity [134]. The techniques assessed in this work were white paint, graphite paint and wet blasting. All were successful in

avoiding reflections, and all gave similar images. White paint was only used to prove that good and accurate images could be achieved with the commercial system but it was never considered as a field technique. Graphite paint was considered but it may cause welding issues (increase in carbon content), but this was not assessed. Wet blasting appears to be a viable technique, with only issues of extra time and cost.

8.3 Influence of Filters

The series of experiments described in section 7.3.4 on the use of filters was primarily performed to optimise the system for best performance. The filters in question are provided as parameters for the Servo Robot™ laser control box. The initial results from the laser system seemed distorted and inaccurate, so the filters were tested for its influence on the acquired profile. Without the use of filters the noise level in the image is too high, and with occasional outlier data points. However, filters can also distort the images, producing erroneous results and remove detail of the actual surface profile. In this work the surface profile detail is essential to capture the actual bead shape. Different parameter settings were tested and the contribution of the individual types of filters was assessed to determine which filters should be used and what should be their settings. The conclusion of this work was to determine the best compromise between reducing noise and generating accurate bead profiles.

The experiments described in section 7.3.5 further strengthen the conclusions obtained with the filters experiments (section 7.3.4). In there it is possible to see the measurement distortions introduced by the incorrect use of filters parameters especially on shallow grooves as it can be seen in Figure 7.77.

Similar issues were reported by Kim et al [135] regarding the averaging window size and they concluded a window size (filter parameter) N=3 would be the optimum for the seam tracking application they were developing. This value is in line with the results obtained although for the bead shape assessment it was found that the filters should be off and the continuity parameter should be activated to avoid the outlier data points.

Xu et al [136] also studied the impact of the average and medial filters as a way to reduce data noise when extracting the profile data. They also found that a window size of 3 was the most appropriate.

8.4 Bead Shape

Section 7.3.6 and Appendix I provide detailed measurements on a series of trial welds showing a wide variety in bead shape and quality, including convexity, concavity, asymmetry, and cavity profiles among other. In general there is excellent agreement between actual and measured bead profile. See Figure 7.95 for an overlay of a macro image and a SP7 screenshot.

There were two situations where measured bead shape deviated from the actual shape. They were, welds with undercut and narrow centre line cracking. The profiles could not show the undercut region (Figure 7.121) due to shadowing caused by the narrow groove itself.

Undercut on wide angle or butt joints can be detected as it has been shown on previous research. Reichert [100] reported the development of a portable inspection system for fillet welding in the ship building industry capable of measure undercut. Kobayashi et al [137] developed a fully automatic welding system capable to perform 5G TIG welding with a defect detecting assessment. According to them, their system was able to detect undercut, overlap and surface porosity among other discontinuities with a laser sensor. Drews et al [138] also developed work in which they manage to detect undercut with a laser stripe sensor but only on fillet and butt welding joints. From the performed literature review other papers were found that confirmed the possibility of detecting undercut on wide angle weld preparations [56, 63, 101, 139-142], but no paper was found reporting the possibility of undercut detection on narrow “V” grooves. The main cause for the undercut not to be detectable on narrow grooves is a combination of groove geometry and sensor viewing point. As the groove walls are almost vertical (5º angle) and the sensor is aligned perpendicularly with the groove bottom the undercut will be hidden from the sensor’s viewing angle by the groove walls themselves.

Centreline cracking was also not detected consistently; see Figure 7.123 and Figure 7.124. The wider cracks observed were 0.2mm wide (Figure 7.122) and although some response was seen from the crack (Figure 7.124) it cannot easily be distinguished from noise or other surface irregularities. It is considered that centreline cracks near the top of the bead are often relmelted in the next pass (Yapp [143]). So when the post-weld inspection is performed, by ultrasound or radiography methods, the cracks will no longer exist.

8.5 3D Visualization

Three dimensional weld models can be visualized using the scanned profile data file combined with the profile acquisition location file. These profiles are quite accurate and the closer together they are acquired the more detailed the 3D model will be. In Figure 8.4 is possible to see a 3D visualization of a weld performed in the flat position with torch to groove centre misalignment that resulted in the formation of a series of cavities on one side of the weld profile. It is also possible to see the screenshot the longitudinal cut graph showing the groove centre depth and the deepest point of each profile. For the profiles that did not contain any cavity the deepest point actually match the depth of the groove centre. For the other ones it is very noticeable the discrepancy in those values.

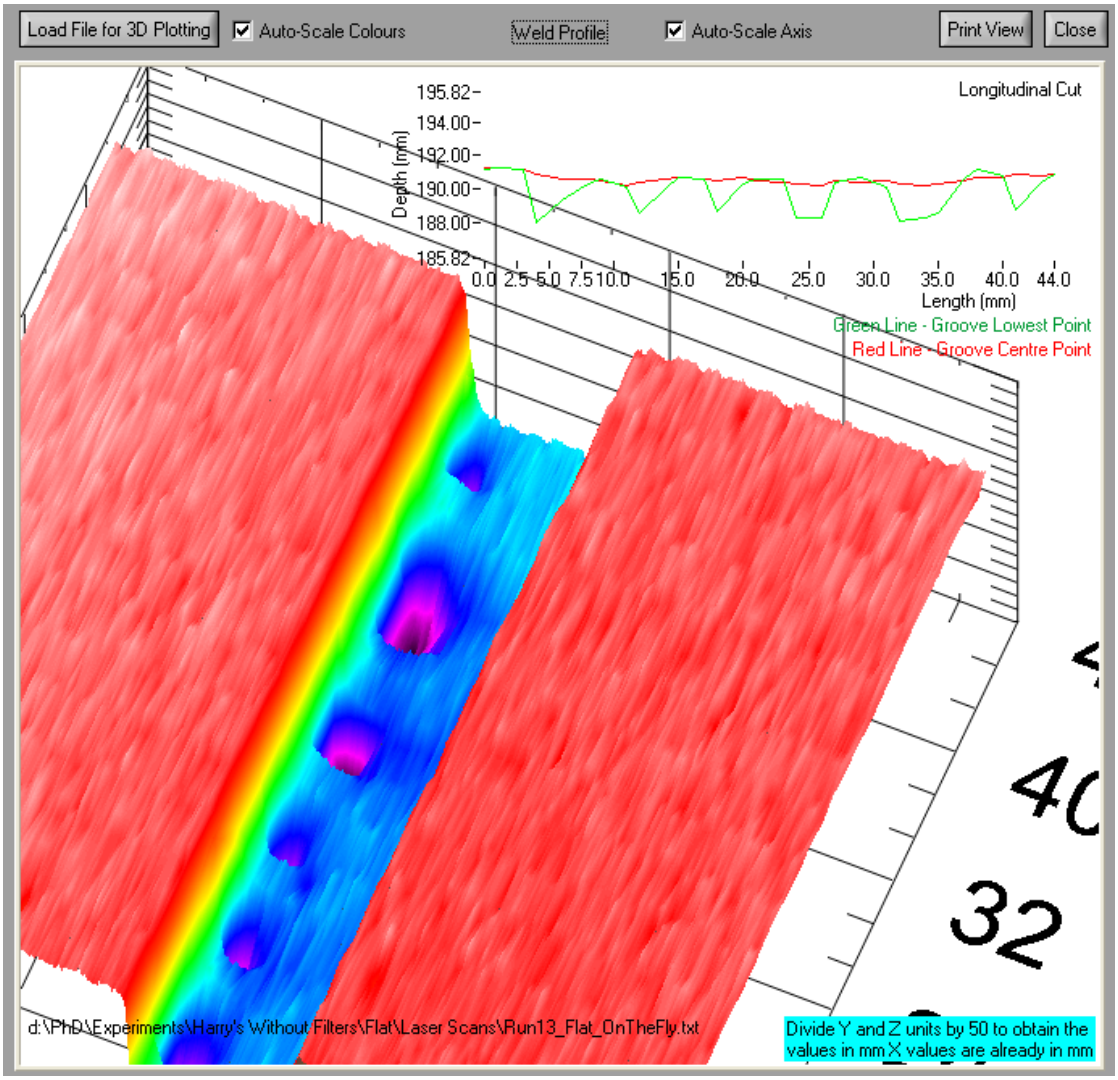

Figure 8.4 – Screenshot of the 3D model of "Run 13" in the Flat position.

When scanning over the end part of the welds it became clear that it was possible with this system to determine the location of the weld end position. This information can be very useful in a fully automatic pipeline welding system as it could be used to determine the start or end point for the next bead, being it on top of the weld end or at a certain distance from it. Figure 8.5 clearly shows the location and shape of weld run 6 performed on the flat position.

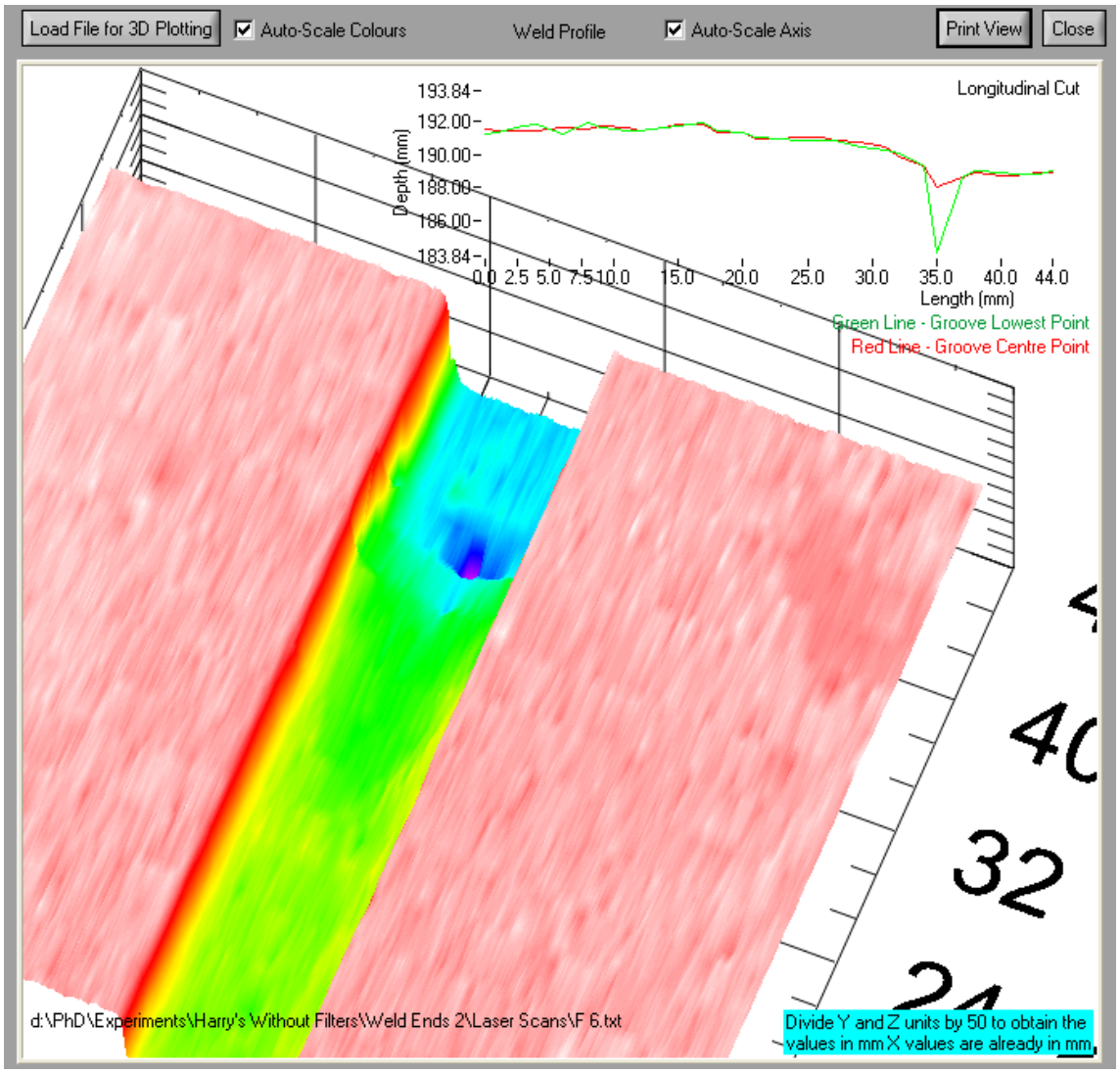

Figure 8.5 – Screenshot of the weld end 3D model of "Run 6" in the Flat position.

8.6 Automatic Determination of Weld Shape Acceptability

A key requirement of fully automatic welding is the production of a fully fused bead when welding on top of the previous bead. For example, very convex beads would produce lack of fusion defects on both side, very asymmetric ones would create lack of fusion on one side.

To scientifically evaluate and determine at what level of convexity, concavity, or asymmetry defects were produced when welding over, a series of weld experiments would be required. However, time and resources were not available in this work to perform the necessary experiments to derive rules for acceptable bead shape. An alternate method of generating the rules was to obtain the opinion of an experience welder. Although this is somewhat subjective; it serves to illustrate the purpose of the system and its performance. Very little published work was found on bead shape quality measurements. The ones that were found were not incorporated on automatic bead assessment systems. Reichert [100] used the developed system for weld inspection, Kobayashi et al [137] developed a 5G welding system and Shibata et al [139] developed the sensor application for groove geometry and defect detection. Although system or application being reported to work as quality inspection systems neither of them reported the rules or values used for the distinction between a discontinuity and a defect. Otsuki et al [144] were the only authors to have specified the rules applied in their system, see Figure 8.6. No direct comparison can be made regarding the values used in this work and the one developed by them as again this work was developed for narrow groove weld joints and theirs for wide “V” grooves. “Distance from bead edge to bead top” on Otsuki et al work is the same as “groove asymmetry” in the present work and “Gap of groove depth” was referred here as “Cavity”.

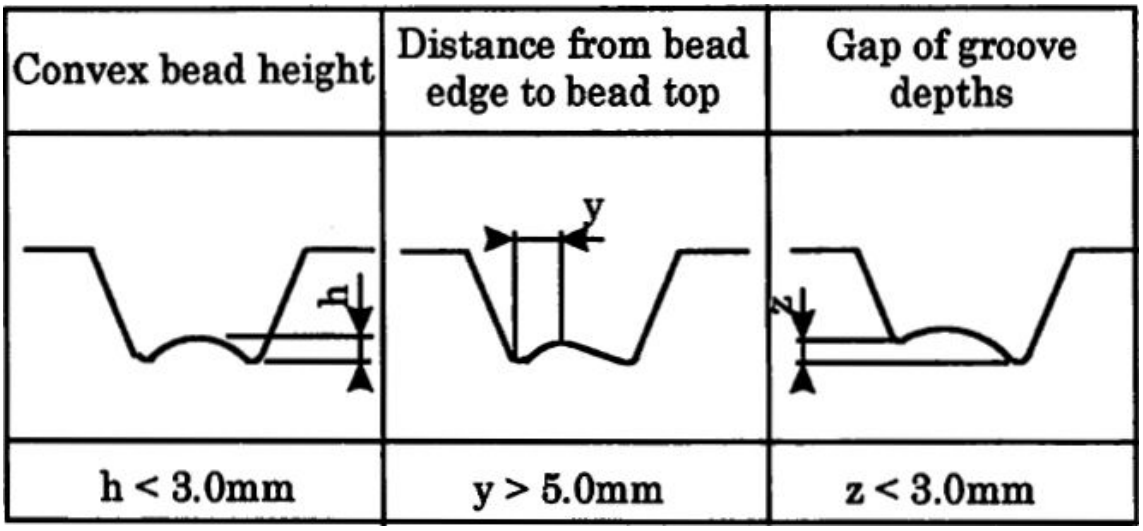

Figure 8.6 – Otsuki et al [144] bead assessment rules.

In order to evaluate weld bead quality scientifically welds would have to be made which would produce different degrees of convexity, concavity, asymmetry and other discontinuities. As a first stage of investigation the influence/effect of parameters such as weave width, contact tip to workpiece distance, travel speed, wire feed speed and centre of oscillation, in all positions, would be evaluated for the different processes. A design of experiment similar to the one

developed by Liratzis in his work [127] should be done to generate the optimum welding conditions, and conditions which result in convex/asymmetric beads. Using a design of experiment software and accounting for the variation of 4 parameters, only 32 welds would need to be made.

On a second stage of investigation a range of different convex and asymmetric beads need to be selected. These would then be used on the third stage of the study. On the selected welds a next weld would be performed on top to determine which levels of convexity and asymmetry would be acceptable to weld on top.

8.7 Application of a Bead Quality Assessment System

There are several areas of pipe welding where the bead quality assessment system can be applied on:

- Fully automatic pipe welding systems, to flag problems or their likelihood, and if required record quality data. Fully automatic pipe welding is the next major step in the pipe welding industry, and it could have a major impact. It would now allow the control of weave width, cross seam position, contact tip to workpiece distance, either by thru-arc or by laser stripe systems. Of course then the welder would no longer be supervising the weld quality by direct observation and adjusting the parameters based on the weld bead shape. This task could then be performed by the system developed during this work. The bead quality assessment system provides accurate measurement of bead quality, enabling the process to be stopped, or alternatively record or mark the areas for post rectification if needed The developed system, as it can be seen in SP7 screenshots, has the possibility to flag the profiles that fall out of the acceptability rules and mark them as faulty;
- Welder controlled mechanized welding to indicate problems or required rectification locations. The bead quality assessment system is then being used for fully automatic to flag issues. This is probably the first step (to implementation) before fully automating the pipeline welding process;
- Feedback control of weld parameters to control bead shape, with the sensor placed behind the torch. This is only possible if a model has been developed, relating bead shape to weld input parameters;
- During procedure development, to immediately indicate bead quality. This would help with rapidly evaluating quality during process development.

8.8 Implementation

This new technology can be implemented to achieve fully automatic pipe welding system which is the next major step for the pipeline industry after mechanization. This will have a major impact

in the industry allowing for faster welding systems with lower time and financial costs and with better quality. Integration would allow flagging problems or their likelihood during weld without having to wait form post-weld inspection systems and in many cases implicate major repair works. Quality data could also be recorded for further use.

Mechanized systems mostly controlled by welders would also benefit from imbedding this technology as it would allow flagging problems and locations where repairs may be required.

It allows feedback control based on bead shape and quality. It can also be used as a tool for procedure development saving time and further and more expensive testing. Integration on industrial systems would not require much more than installing an off the shelf laser stripe system, which some companies already use, and the developed algorithms implementation.

Some of the major pipeline installation companies are now beginning to use laser stripe systems for seam tracking. CRC-Evans for example have introduced laser stripe sensors on both their internal and external pipe welding equipment [8]. The fact that their system is even on the front cover of World Pipelines magazine [145] (Figure 8.7) shows how important this technology is in the pipeline industry. It is hence a relatively small step to use this existing technology to perform bead quality assessment. Effectively it would just require implementing the control algorithms described in this thesis.

Figure 8.7 – Front cover of World Pipelines volume 10 issue 6.

9 Conclusions

A new system has been developed to automatically assess the quality of intermediate weld profiles in a multipass narrow groove weld, and to determine whether the bead shape is suitable for the next pass to be welded on top, without forming a defect.

- A system was developed to control the welding parameters and welding torch motion on a pipe welding system (SP5);
- An experimental rig and the corresponding software package (SP6) was developed to assess the laser stripe system performance;
- A profile data analysis software (SP7) was developed to accurately and detailed measure and analyse bead shape;
- A comprehensive evaluation of the laser stripe sensor has been performed. The limits on sensor positioning have been assessed. It was shown that various surface preparation methods could be used to eliminate the effect of reflections on a weld preparation with machined surfaces;
- Algorithms have been developed to process laser profile data, and to evaluate deviations from an acceptable bead profile. The results show the good agreement between the bead shape quality assessment analysis and the measured values;
- Empirical rules were used to determine what bead shape is acceptable for welding over without creating any defects on a subsequent pass;
- A software package (SP7) was produced with a friendly user interface which displays bead quality in real time.

10 Further Work Recommendations

As next steps in the further development of this work, is recommended that:

- Experiments are performed to scientifically obtain the rules that should be used in the automatic determination of weld shape acceptability algorithms;
- Procedures should be developed to be able to weld automatically minor cases of bead asymmetry and cavities avoiding repair work;
- A new algorithms should be created, and applied to an automatic system, to overcome the reflection problems when scanning the root pass;
- A database is created for the automatic selection of weld parameters based on the angular position of the welding head around the pipe;
- Integration of Liratzis [127] findings into the software so good welds are performed all around the pipe;
- As image processing is quite resource consuming in terms of computation, integration of thru arc seam tracking systems, as the one developed by Lopes [28], in the control system could be attempted to improve overall system performance;
- The dual tandem option for SP5 – Pipe Girth Software is developed;
- Later on the software and communications are transferred to an embedded computer;
- Control algorithms integration into a commercial system for true industry application.

REFERENCES

1. AWS, A.W.S., *Standard welding terms and definitions: including terms for brazing, soldering, thermal spraying and thermal cutting*. 1994, American Welding Society. p. 119 pages.

2. Servo-Robot, *VISUS - Image Processing Software Module*. 1999, Servo-Robot Inc.: Canada. p. 52.

3. American Welding Society, *Specification For Welding Procedure and Performance Qualification*. 1998, AWS. p. 221.

4. API-AGA Joint Committee on Oil and Gas Pipeline Field Welding Practices, *Welding of Pipelines and Related Facilities*. 1999, American Petroleum Institute. p. 86.

5. Yapp, D., *High productivity Pipe Girth Welding: Developments in Mechanized Arc Welding of Pipelines.* Pipelines International, 2011: p. 44-46.

6. Teale, B., *The Long and Welding Road to Pipelines.* Pipelines International, 2011: p. 54-55.

7. Yapp, D. and S.A. Blackman, *Recent Developments in High Productivity Pipeline Welding.* Journal of the Brazilian Society of Mechanical Sciences and Engineering, 2004. **XXVI**(1): p. 89-97.

8. Rajagopalan, S., *New Generation of Welding Systems... The Vision System.* World Pipelines, 2010. **10**(6): p. 19-24.

9. CRC Evans, *Control Systems (Equipment brochure).* Pipelines International, 2006.

10. Serimax. *Saturmax Datasheet*. 2011.

11. Hirsch, R.L., R. Bezdek, and R. Wendling, *Peaking of World Oil Production: Impacts, Mitigation, & Risk Management*. 2005. p. 91.

12. Energy Information Administration, U.S.D.o.E., *Annual Energy Outlook 2005 with Projections to 2025*. 2005, U. S. Department of Energy - Office of Integrated Analysis and Forecasting: Washington, USA p. 248 pages.

13. Satoru, S., *Sensing Technology for the Welding Process.* Welding International, 2006. **20**(3): p. 183-196.

14. Brat, I. *Where Have All the Welders Gone, As Manufacturing and Repair Boom?* The Wall Street Journal Online [Web Page] 2006 [cited 2006 18-10-06]; Available from: http://online.wsj.com/article/SB115560497311335781.html.

15. Sugitani, Y., et al., *1.8 Pipeline*, in *Recent Technology of Arc Welding in Vessel and Pipe - Welding Guide Book IV*. 2000, Technical Comission on Welding Processes - Japan Welding Society. p. I63 - I74.

16. de Keijzer, A. and R.J. de Groot, *Laser-based arc welding sensor monitors weld preparation.* Sensor Review, 1984: p. 8-10.

17. *Sensor*. [Webpage] 2005 [cited 2005 07-10-2005]; Available from: http://www.answers.com/topic/sensor

18. Pan, J., et al., *Crawl-type Robot Tackles Difficult Jobs.* Welding Journal, 2005. **84**(1): p. 50-54.

19. Bastos, T.F., et al. *Weld Seams Detection and Recognition for Robotic Arc-Welding Through Ultrasonic Sensores*. in *IEEE International Symposium on Industrial Electronics, 1994*. 1994. Santiago, Chile IEEE.

20. Pan, J., *Arc Welding Control*, ed. C. Press. 2003, Cambridge, UK: Woodhead Publishing Limited. 603.

21. Holder, S.J., S.B. Jones, and J. Weston, *Mechanical Approaches to Seam Tracking for Arc Welding*. 1981, TWI - The Welding Institute: Abington Hall, Abington, Cambridge. CBl 6AL. p. 23.

22. Ushio, M. and W. Mao, *Sensors for arc welding: advantages and limitations.* Transactions of JWRI, 1994. **23**(2): p. 135-141.

23. Berge, J.M., *Automating the Welding Process: Successful Implementation of Automated Welding Systems*. 1st ed. 1993, New York, NY, USA: Industrial Press. 208.

24. Richardson, R.W., *Robotic weld joint tracking systems - theory and implementation methods.* Welding Journal, 1986. **65**(11): p. 43-51.

25. Eichhorn, F. *Aspects of the Mechanization, Automation and the Utilisation of Robots in Welding*. in *Automation and Robotisation in Welding and Allied Processes, IIW International Conference*. 1985. Strasbourg, France: Pergamon Press (for IIW).

26. Lopes, G., et al. *"Through the arc" sensing in pulsed GMAW for pipe welding applications.* in *Computer Technology in Welding and Manufacturing. Proceedings, 14th International Conference*. 2004. Sheffield, UK: Cambridge, CB1 6Al, UK; TWI Ltd.

27. Corlett, B.J., J. Lucas, and J.S. Smith, *Sensors for narrow-gap welding.* Science, Measurement and Technology, IEE Proceedings, 1991. **138**(4): p. 213 - 222

28. Lopes, A.G., *Arc-Based Sensing in Narrow Groove Pipe Welding*, in *Welding Engineering Research Centre*. 2007, Cranfield University, UK: Cranfield. p. 385.

29. Tapp, J. and D. Yapp. *Techniques and instruments for monitoring arc welding processes*. in *Computer Technology in Welding and Manufacturing. Proceedings, 14th International Conference*. 2004. Sheffield, UK: Cambridge, CB1 6Al, UK; TWI Ltd.

30. Livingston, D.J., *Improving resistance weld quality with monitoring.* Fabricator, 1995. **25**(9): p. 52-54.

31. Yu, J.-Y. and S.-J. Na, *A study on vision sensors for seam tracking of height-varying weldment. Part 1: Mathematical model* Mechatronics, 1997. **7**(7): p. 599-612

32. Yu, J.-Y. and S.-J. Na, *A study on vision sensors for seam tracking of height-varying weldment. Part 2: Applications* Mechatronics, 1998. **8**(1): p. 21-36

33. Zuech, N., *Understanding and Applying Machine Vision* 1999: Marcel Dekker. 403.

34. Neipold, R. and F. Brummer, *PASS - A Visual Sensor for Seam Tracking and On-line Process Parameter Control in Arc Welding Applications*, in *Robotic Welding*. 1987, IFS Publications. p. 129-140.

35. Linden, G.L., G.; Nilsson, L, *A Control System Using Optical Sensing for Metal-inert Gas Arc Welding*, in *Developments in Mechanised, Automated and Robotic Welding: International Conference*, W. Institute, Editor. 1980: London, UK. p. 17-1 - 17-6.

36. Drews, P. and F.J. King, *Automatic Seam Tracking by an Opical Method*, in *Symposium on Advanced Welding Technology*. 1975, Japan Welding Society: Osaka.

37. Nayak, N.R. and A. Ray, *Intelligent Seam Tracking for Robotic Welding*. 1993, London, SW19 7JZ, UK: Springer-Verlag London Ltd. 225.

38. Keyence Corporation. *Keyence Development History* [Webpage] [cited 2005 21-04-05]; Available from: http://world.keyence.com/corporate/proddev.html.

39. Dancer, J., *Laser Scanning Helps Shrink Digital Projector.* Photonics Spectra, 2005. **39**(3): p. 31-32.

40. Stutz, G., *Laser Scanners Extend Machine-Vision Capability.* Laser Focus World, 1999. **35**(7).

41. Nakata, S., et al., *Determination on Geometrical Arrangement of Optical Equipment and Photographic Parameters for Construction of Visual Sensing System.* Quarterly Journal of the Japan Welding Society, 1989. **7**(3): p. 358-362.

42. Lee, C.W. and S.J. Na, *A study on the influence of reflected arc light on vision sensors for welding automation* Welding Journal, 1996. **75**(12): p. 379-387.

43. Pritschow, G., G. Mueller, and H. Horber. *Fast and robust image processing for laser stripe-sensors in arc welding automation*. in *ISIE 2002 - IEEE International Symposium on Industrial Electronics*. 2002: IEEE.

44. Oxford Sensor Technology, *Company Brochure*, O.S. Technology, Editor. 2006: Oxford, UK.

45. Xu, P., et al., *A visual seam tracking system for robotic arc welding.* International Journal of Advanced Manufacturing Technology, 2008. **37**(1-2): p. 70-75.

46. Beattie, R.J., S.K. Cheng, and P.S. Logue, *The use of vision sensors in multipass welding applications.* Welding Journal, 1988. **67**(11): p. 28-33.

47. Blais, F., *Review of 20 Years of Range Sensor Development.* Journal of Electronic Imaging, 2004. **13**(1): p. 231–240.

48. Buzinski, M., A. Levine, and W.H. Stevenson. *Performance Characteristics of Range Sensors Utilizing Optical Triangulation*. in *Aerospace and Electronics Conference, 1992. NAECON 1992., Proceedings of the IEEE 1992 National*. 1992. Dayton, OH, USA: IEEE.

49. Clark, J., E. Trucco, and H.F. Cheung. *Improving laser triangulation sensors using polarization*. in *Proceedings. Fifth International Conference on Computer Vision (Cat. No.95CB35744)*. 1995: IEEE Comput. Soc. Press, Los Alamitos, CA, USA.

50. Claus, P.K. and M. Michael, *Testing bench for laser triangulation sensors.* Sensor Review, 1998. **18**(3): p. 183-187.

51. Curless, B. and M. Levoy. *Better optical triangulation through spacetime analysis*. in *Fifth International Conference on Computer Vision*. 1995. Cambridge, MA, USA: IEEE.

52. Dorsch, R.G., G. Hausler, and J.M. Herrmann, *Laser triangulation: fundamental uncertainty in distance measurement.* Applied Optics, 1994. **33**(7): p. 1306.

53. Dumberger, M., *The Evolution Of Laser Triangulation.* Product Design & Development, 2002. **57**(10): p. 18.

54. Dumberger, M. (2002) *Taking the Pain out of Laser Triangulation*. Sensors Magazine Online, 4 pages.

55. Dumberger, M. *CCD Technology - The "Cure" for the Common Triangulation Laser*. 2003 [cited 2003 17-02-1003]; Available from: http://www.globalspec.com/MicroEpsilon/ref/CCD3.htm.

56. Li, Y., et al., *On-line Visual Measurement and Inspection of Weld Bead Using Structured Light* in *IMTC 2008 - Instrumentation and Measurement Technology Conference Proceedings*. 2008: Victoria, BC. p. 2038 - 2043

57. Lombardo, V., et al., *A time-of-scan laser triangulation technique for distance measurements.* Optics and Lasers in Engineering, 2003. **39**(2): p. 247-254

58. Meta Vision Systems. *Laser Sensors - Principle of Operation*. [Web Page] 2006 [cited 2006 September 2006]; Available from: http://www.meta-mvs.com/lasersensors.html.

59. Pastorius, W., *Triangulation Sensors - An Overview.* InTech, 2001: p. 6.

60. Pierce, D.S., T.S. Ng, and B.R. Morrison. *A Novel Laser Triangulation Technique for High Precision Distance Measurement*. in *Conference Record of the 1992 IEEE - Industry Applications Society Annual Meeting*. 1992. Houston, TX, USA.

61. Snow, M. (2002) *Laser Triangulation Sensors in the Tire Industry*. Sensors Magazine Online, 5 pages.

62. White, P., *Video-Camera or Laser-Triangulation?* Design Engineering, 2002: p. 10-11.

63. Xu, M., M. Zhao, and Y. Zou, *On-line visual inspection system for backside weld of tailored blanks laser welding* in *ICACC, 2010 - 2nd International Conference on Advanced Computer Control*. 2010: Shenyang. p. 525 - 529

64. Zou, Y., et al., *Development of laser stripe sensor for automatic seam tracking in robotic tailored blank welding*, in *WCICA 2008 - 7th World Congress onIntelligent Control and Automation*. 2008. p. 3062 - 3066.

65. Gilles, K. *Vision Systems for Welding - Find it. Track it. Inspect it.* [Web page] 2006 [cited 2008 August 2008]; Available from: http://weldingmag.com/processes/news/wdf_21446/.

66. Li, Y., et al. *Measurement and Defect Detection of the Weld Bead Based on Online Vision Inspection*. in *IEEE Transactions on Instrumentation and Measurement*. 2010.

67. Petersson, G. and L.-E. Lindholm, *Position Sensitive Light Detectors with High Linearity.* IEEE Journal of Solid-State Circuits, 1978. **13**(3): p. 392- 399.

68. Lucas, B. and J.S. Smith, *Keeping an Electronic Eye on Automated Arc Welding.* Welding and Metal Fabrication, 2000. **68**(4): p. 6, 9, 10, 13.

69. , H.D. *EXAscan > Description > Handyscan 3D*. 2007 [cited 2007 20-09-2007]; Available from: http://www.handyscan3d.com/en/description/exascan.php.

70. , H.D. *In action > Handyscan 3D*. 2007 [cited 2007 20-09-2007]; Available from: http://www.handyscan3d.com/en/in-action/index.php.

71. Agapiou, G., et al. *Development of a laser-based seam tracking system for real-time industrial robot welding applications*. in *Ninth International School on Quantum Electronics: Lasers Physics and Applications*. 1996. Varna, Bulgaria.

72. Bae, K.Y. and S.-J. Na, *A study of vision-based measurement of weld joint shape incorporating the neural network.* Proceedings of the Institution of Mechanical Engineers, Part B: Journal of Engineering Manufacture, 1994. **208**(B1 / 1994): p. 61 - 69.

73. Beattie, R.J., *Applications of Laser Seam Tracking in Welding Thick Wall Vessels.* 2004.

74. Beattie, R.J., S. Kelly, and J. Zhao, *Laser Vision Guidance for Automated Welding and NDT of Tubes and Pipes.*

75. Boillot, J., G. Begin, and B. Beranek. *Advanced Laser Vision Sensor for Adaptive Welding*. in *Vision 86*. 1986. Detroit: Dearborn, MI 48121, USA; Society of Manufacturing Engineers (SME), Machine Vision Association.

76. Boillot, J.P., A. Galibois, and K. Uota. *Present situation and future trends in vision-guided welding robots*. in *Metal Welding and Applications (Le soudage des metaux et ses applications) and Thermomechanical Processing of Alloys (Le traitement*

thermomecanique des alliages), Proceedings, 38th Annual Conference of Metallurgists of CIM. 1999. Quebec City, Quebec, Canada: Montreal, Quebec, H3Z 3B8, Canada; Canadian Institute of Mining, Metallurgy and Petroleum.

77. Wilson, M., *Laser seam tracking for robotic welding.* The Fabricator, 1998. **28**(6): p. 42-45.

78. Wilson, M. *Developments in laser vision weld tracking systems*. in *Advances in Welding and Cutting Technology, International Welding Conference (IWC-2001)*. 2001. New Delhi, India: Calcutta, 700017, India; Indian Institute of Welding.

79. Wilson, M., *The role of seam tracking in robotic welding and bonding.* Industrial Robot, 2002. **29**(2): p. 132-137.

80. Doumanidis, C.C. and Y.-M. Kwak, *Geometry Modeling and Control by Infrared and Laser Sensing in Thermal Manufacturing with Material Deposition.* Journal of Manufacturing Science and Engineering, 2001. **123**(1): p. 45-52.

81. Miller, M., et al., *Development of automated real-time data acquisition system for robotic weld quality monitoring.* MECHATRONICS, 2002. **12**(9-10): p. 1259-1269.

82. Rehfeldt, D., M.D. Rehfeldt, and G. Ryeznikov, *Process Monitoring and Quality Assurance for GMAW*, in *17th International Conference Computer Technology in Welding and Manufactoring*. 2008: Cranfield University, Cranfield, UK.

83. Simpson, S.W. and P.W. Hughes, *Industrial Application of Welding Signatures for Real Time Quality Assurance and Process Improvment*, in *12th International TWI Computer Technology in Welding & Manufacturing Conference*. 2002: Sydney.

84. Jones, B.A., *Statistical Process Control as Applied to Gas Metal Arc Welding in a Production Environment*. 1995, The Ohio State University.

85. Nikiforova, T.V. and N.G. Fedotov, *Methods of Stochastic Geometry in Recognition of Weld Defects.* Pattern Recognition and ImageAnalysis, 2006. **16**(1): p. 12-14.

86. Williams, R.H. and A. Kent, *Encyclopedia of Computer Science and Technology*. 1993: Marcel Dekker. 408.

87. Wells, A.M., *Through-the-arc Sensing and Control Methods in Robotic Arc Welding*. 1988, Vanderbilt University: Nashville, TN, USA. p. 202.

88. Cary, H.B., *Arc Welding Automation*. 1995, New York, NY, USA: Marcel Dekker, Inc. 527.

89. Widgery, D.J., *Mechanised Welding of Pipelines.* Svetsaren - The ESAB Welding and Cutting Journal, 2005. **60**(1): p. 23-26.

90. Alfaro, S.C.A., *Sensors for Quality Control in Welding*, in *Arc Welding*, W. Sudnik, Editor. 2011, InTech. p. 81-106.

91. Ancona, A., et al., *A Sensing Torch for On-line Monitoring of the Gas Tungsten Arc Welding Process of Steel Pipes.* Measurement Science and Technology, 2004. **15**(12): p. 7.

92. Barborak, D. and C.C. Conrardy, *Monitoring of Weld Quality During Thin-Sheet GMA Welding*. 1998, Edison Welding Institute. p. 4.

93. Rehfeldt, D., T. Polte, and C.S. Wu, *Welding Quality Determination by Using Fuzzy Logic or Neural Networks*. 2000.

94. Quinn, T.P., et al., *Arc sensing for defects on constant-voltage gas metal arc welding.* Welding Journal, 1999: p. 322-328.

95. Verhaeghe, G. and G.B. Melton, *An Investigation of the Use of Transient Arc Data to Detect Process Deviations.* 2000: p. 39.

96. Koelsch, J.R., *Check Welds in Process.* Quality, 2001. **40**(8): p. 42-47.

97. Cook, G.E., et al., *Automated visual inspection and interpretation system for weld quality evaluation* in *Thirtieth IAS Annual Meeting, IAS '95., Conference Record of the 1995 IEEE Industry Applications Conference*. 1995: Orlando, FL, USA. p. 1809 - 1816.

98. Schreiber, D., et al., *Online Visual Quality Inspection for Weld Seams.* International Journal of Advanced Manufacturing Technology, 2009(42): p. 497–504.

99. Kumar, G.S., U. Natarajan, and S.S. Ananthan, *Vision Inspection System for the Identification and Classification of Defects in MIG Welding Joints.* International Journal of Advanced Manufacturing Technology, 2012. **61**(9-12): p. 923–933.

100. Reichert, C.T., *Pre- and Post-weld Inspection Using Laser Vision*, in *Proc. SPIE 3396, Nondestructive Evaluation of Materials and Composites II*. 1998: San Antonio, TX, USA. p. 244 - 254.

101. White, R.A., J.S. Smith, and J. Lucas, *Vision-based gauge for online weld profile metrology.* Science, Measurement and Technology, IEE Proceedings, 1994. **141**(6): p. 521 - 526.

102. Lincoln Electric, *Power Wave F355i - Operator's Manual*. 2002, Lincoln Electric: Cleveland, Ohio, USA.

103. Lincoln Electric, *Lincoln Electric - Digital Comunications*, Lincoln Electric: Cleveland, Ohio, USA. p. 12.

104. Lincoln Electric, *PowerWave F355i (IM755-A)*, Lincoln Electric, Editor. 2005, Lincoln Electric.

105. Lincoln Electric, *Wave Disigner - Software for Waveform Control Technology*, L. Electric, Editor, Lincoln Electric.

106. Doyle, T., *Lincoln Electric - Communication DLL Package*, P. Marmelo, Editor. 2003, Tom Doyle: Cranfield.

107. Lincoln Electric. *System Interface - Equipment | Lincoln Electric*. [Webpage] [cited 2006 September 2006]; Available from: http://www.mylincolnelectric.com/Catalog/equipmentdatasheet.asp?p=23031.

108. Lincoln Electric, *Lincoln Electric - Power Feed 10R*, Lincoln Electric: Cleveland, Ohio, USA. p. 6.

109. Lincoln Electric, *Power Feed 10 Robotic - Operator's Manual*. 2002, Lincoln Electric: Cleveland, Ohio, USA.

110. Lincoln Electric. *Power Feed 10R - Wire Feeders - Equipment | Lincoln Electric*. [Webpage] [cited 2006 September 2006]; Available from: http://www.lincolnelectric.com/assets/servicenavigator-public/lincoln3/im772.pdf.

111. Galil Motion Control Inc. *Galil Motion Control: Products: DMC-2100 & DMC-2200*. [Webpage] 2002 [cited 2006 20-09-06]; Available from: http://www.galilmc.com/products/dmc-22x0.php.

112. Galil Motion Control Inc. *Galil Motion Control: Products: IMC-1900*. [Webpage] 2002 [cited 2006 20-09-06]; Available from: http://www.galilmc.com/support/appnotes/optima/note1425.pdf.

113. Advanced Motion Controls. *12A8 Amplifier*. [Webpage] [cited 2006 20/09/06]; Available from: http://www.a-m-c.com/download/datasheet/12a8.pdf.

114. Sensorex, *Low Cost Inclinometer SX 42400 Series*, Sensorex, Editor, Sensorex.

115. Serimax, *Saturnax 5 - Manual, chapter 8*. 2003, Serimax: Cranfield, UK. p. 64.

116. Lincoln Electric, *Pulsed Spray Metal Transfer*. 2004, Lincoln Electric. p. 8.

117. Moon, H.-S., S.-H. Ko, and J.-C. Kim, *Automatic seam tracking in pipeline welding with narrow groove*. The International Journal of Advanced Manufacturing Technology, 2009. **41**(3): p. 234-241.

118. Servo-Robot, *MINI-I/60/90 - 3-D Laser Vision Camera Installation And Operation Manual*. 2001, Servo-Robot Inc.: Canada. p. 14.

119. Servo-Robot, *Mini-I - Miniature Joint Tracker*. 2001, Servo-Robot Inc.: Canada. p. 2.

120. Servo-Robot, *EzTrack - Vision & Motion Controllers for Seam Tracking*. 1999, Servo-Robot Inc.: Canada. p. 40.

121. Servo-Robot, *WinUser - User's Manual*. 2001, Servo-Robot Inc.: Canada. p. 31.

122. Meta Vision Systems, *Laser Pilot MTF - Product Brochure*, Meta Vision Systems: Oxford. p. 2.

123. Oxford Sensor Technology, *Oxford Sensor Technology - Circular Scaning Sensor*, O.S. Technology, Editor. 2006: Oxford, UK.

124. Yokogawa Electric Corporation, *DL Series Digital Oscilloscopes*. 2006, Yokogawa Electric Corporation. p. 4.

125. Svetkoff, D.J. and D.B.T. Kilgus, *Method and System for Suppressing Unwanted Reflections in an Optical System*. 2000, General Scanning, Inc.: USA. p. 19.

126. Agapakis, J.E., *Approaches for Recognition and Interpretation of Workpiece Surface Features Using Structured Lighting.* The International Journal of Robotics Research, 1990. **9**(5): p. 3-16.

127. Liratzis, T., *Tandem Gas Metal Arc Pipeline Welding*, in *SCHOOL OF APPLIED SCIENCES*. 2007, Cranfield University, UK: Cranfield, UK. p. 373.

128. Reichert, C. and W. Peterson, *Inspecting RSW Electrodes and Welds with Laser-Based Imaging.* Welding Journal, 2007. **86**(2): p. 38-46.

129. Kang, M.-G., et al., *Laser Vision System for Automatic Seam Tracking of Stainless Steel Pipe Welding Machine.*, in *ICCAS 2007 - International Conference on Control, Automation and Systems*. 2007: Seul. p. 1046–1051.

130. Trucco, E., et al., *Calibration, data consistency and acquisition with laser stripers model.* International Journal of Computer Integrated Manufactu, 1998. **11**(4): p. 293 - 310.

131. Suga, Y., et al., *A Robust Visual Sensing System Using Light Section Method for Detecting Weld Line Positionin Robot Welding*, in *Proceedings of the Information Integration Workshop*. 1995, IIW: Stockholm, Sweden. p. 99-106.

132. Moon, H.-S., Y.B. Kim, and R.J. Beattie, *Multi Sensor Data Fusion for Improving Performance and Reliability of Fully Automatic Welding System.* The International Journal of Advanced Manufacturing Technology, 2006. **28**(3-4): p. 286-293.

133. Yapp, D., *Use of Weldable Primer to avoid Reflections (Personal communication)*, P. Marmelo, Editor. 2004: Cranfield, UK.

134. Blomquist, P.A., *Simultaneous Triger-edge Pre-weld Cleaning* in *Ship Production Symposium*. 1996, Society of Naval Architects and Marine Engineers: San Diego, California, USA.

135. Kim, C.-H., et al., *Intelligent vision sensor for the robotic laser welding*, in *INDIN 2008. 6th IEEE International Conference on Industrial Informatics*. 2008: Daejeon. p. 406 - 411

136. Xu, M., et al., *Research on Fast Method for Centerline Extraction of Laser Stripe for Vision Inspection System* in *Modelling, Simulation, and Identification*, H. Ma and S. Narayanan, Editors. 2009: Beijing, China. p. 738 - 742.

137. Kobayashi, M., et al., *Full Automatic Welding System for TIG All Position*, in *Welding Guide Book III - Automation Technology of Arc Welding*. 1996, Japan Welding Society. p. II-207 - II-212.

138. Drews, P., U. Strunz, and K. Willms, *Quality Control and Post-Welding Inspection with an Optical Sensor System*. 1993, IIW IIS - Metallurgy Prossesses Automation Standardisation: Glasgow. p. 257 - 269.

139. Shibata, N., et al., *A Visual Sensor for an Automatic Welding System*. 2000, Technical Comission on Welding Processes - Japan Welding Society. p. II-79 - II-83.

140. Zhang, L., et al., *A New Surface Inspection Method of TWBS Based on Active Laser-Triangulation* in *WCICA 2008 - 7th World Congress on Intelligent Control and Automation* 2008: Chongqing. p. 1174 - 1179.

141. Orozco, N.J., et al., *Real-time Control of Laser-hybrid Welding Using Weld Quality Attributes*, in *23rd International Congress on Applications of Lasers & Electro-Optics 2004*. 2004.

142. Eriksson, I., *Methods for Automatic Inspection of Weld Geometry*, in *Engineering Science*. 2008, University West: Trollhattan, Sweden. p. 59.

143. Yapp, D., *Weldability of Beads with Centreline Cracks on Narrow Groove Joints (Personal communication)*, P. Marmelo, Editor. 2012: Southampton, UK.

144. Otsuki, M., et al., *Application of All Position Automatic GMAW System for High Quality Heavy Wall Vessel*, in *Recent Technology of Arc Welding in Vessel and Pipe*. 2000, Japan Welding Society - Technicaal Commission on Welding Processes. p. II-163 - II-167.

145. CRC Evans, World Pipelines, 2010. **10**(6): p. Front Cover.

Appendix A SP1 – *Single* Software User Manual

Single Power Supply Control Software

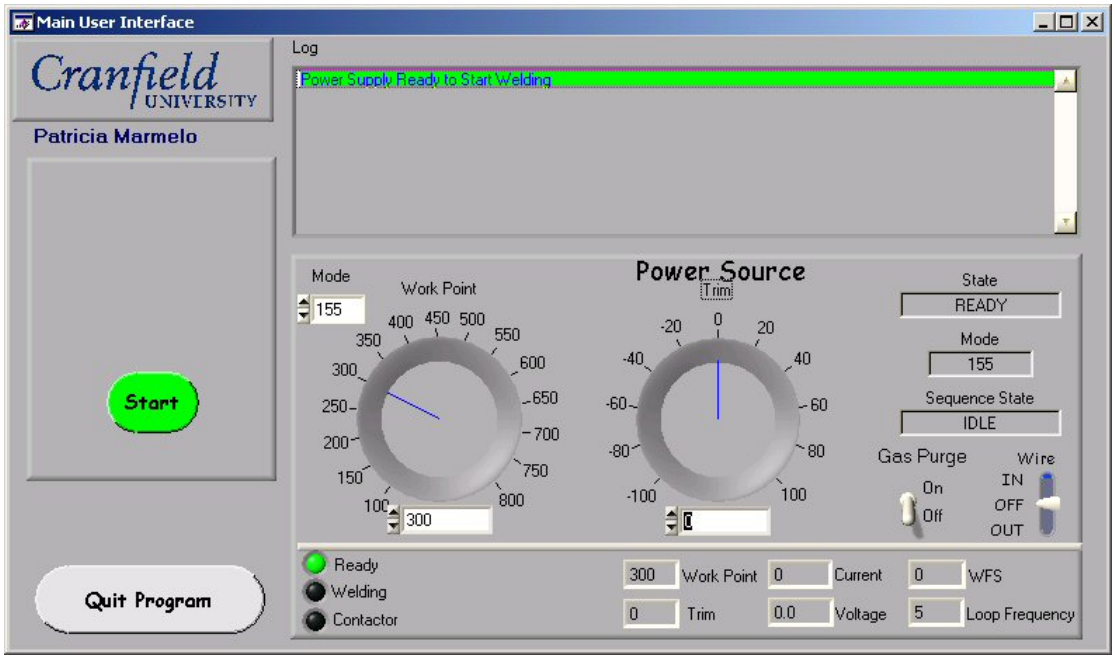

Index

1 Introduction

The Single Power Supply Control Software was developed to control one Lincoln Electric – Power Wave F355i power supply (PS). This program is to be used when a single torch (one wire only) is in use.

The Lincoln Electric – Power Wave F355i power supply has no standard user interface and the communications are made through an Ethernet port. Each Power Supply (PS) has a fixed IP (Internet Protocol) address which comes set from factory. All the communications have to be addressed to the machine's IP address.

2 Installation

To install the Single Power Supply Control Software double click on the installation setup icon and follow the on screen instructions.

3 Before Running the Program

Before running the program make sure you have made all the required connections and the necessary files are in the program directory. The files required are: "Single PowerWave.ini" and a "Mode *XXX*.scm" per PS per mode *XXX* define in the ".ini" file. Where *XXX* stands for the mode number. A default file of each it is placed in the program directory when the software is installed. A description of each of these files follows.

3.1 Single PowerWave.ini *File*

This file contains the communications, weld and general system configurations necessary for the program functioning. This file is divided into *sections*, each of them started by "[Section Name]". Inside the section is a list of *tags* followed by its *value*, one per line (ex. tag=value).

No sections or tags should be removed as the program will not run without them. Others should not be added as the software will not recognise them and will ignore them. The section order can be changed and the order of the tags INSIDE the section can be changed as well. They should not be moved to another section, this will result in the program being unable to run

properly due to lack information. The program is not case sensitive and so it does not matter if the contents of the .ini file are capital letters or not.

The Sections available in this file are *GENERAL CONFIGURATION*, *POWER SUPPLY* and *MODE LIST*. An explanation of each of them follows.

3.1.1 The GENERAL CONFIGURATION *section*

This must contain the following tags:

- **Log File** – The Log File equals to the file name of the file containing the program/weld event logging. This file should have a LOG extension;
- **Enable Event Logging** – This tag will either equal “TRUE” or “FALSE” depending if a log file is requested;
- **Loop Delay** – Time added to loop time to ensure the process has time to be completed. Time in milliseconds;
- **Welding Watchdog Timeout** – Time which is waited until a PS system hang is assumed. Time in seconds;
- **Thread Watchdog Timeout** – Time which is waited until a software thread hang is assumed. Time in seconds;
- **Wire Jog Speed** – The Wire Feed Speed (WFS) while jogging the wire in and out. Value in inches per minute;

Example:

```
[GENERAL CONFIGURATION]
LOG FILE=Single PowerWave.log
ENABLE EVENT LOGGING=TRUE
LOOP DELAY=200
WELDING WATCHDOG TIMEOUT=1.0
THREAD WATCHDOG TIMEOUT=1.0
WIREJOG SPEED=100 THREAD WATCHDOG TIMEOUT=1.0
WIREJOG SPEED=100
ENABLE PHASE GENERATOR=TRUE
```

3.1.2 The POWER SUPPLY section

It must contain the following tags:

- **Communication Channel** – Type and number of the communication port, typically EN1 for Ethernet communication;

- **EN1 ADDRESS** – The IP address and UDP protocol port number. Standard port number 4321;

Example:

[POWER SUPPLY]

COMMUNICATION CHANNEL=EN1

EN1 ADDRESS=192.168.1.2 -UDP 4321

3.1.3 Mode Count Section

It must contain the following tags:

- **Mode Count** – Indicates the number of modes in the PS that need to be loaded into the machine and will be active;
- **Mode XXX** – Mode number existent in the PS to be loaded, where "XXX" represents the mode index. Should exist as many tags like this as the *Mode Count* value.

Example:

[MODE LIST]

MODE COUNT=2

MODE 1=155

MODE 2=156

A complete example file can be found in Appendix A.

3.2 Mode XXX.scm File

The SCM file contains for the each PS state the expected attribute state or value.

List of the PS states:

- Idle;
- Setup;
- Pre Purge;
- Strike;
- Start;
- Up Slope;
- Weld 1;
- Weld 2;
- Down Slope;
- Crater;
- Burn Back;

- Post Purge;
- Re-Strike;
- Fault.

List of attributes:

- State Timer – True/False;
- State – True/False;
- State Timer Preset – time in milliseconds;
- Output Command – value;
- Work Point – in inches per minute;
- Arc Length Trim – trim value from -1 to 1;
- Miscellaneous Trim 1 – value;
- Miscellaneous Trim 2 – value;
- Miscellaneous Trim 3 – value;
- Miscellaneous Trim 4 – value;
- Motor Commando for Welding – value;
- Set Welding Wire Feed Speed – set value of WFS in inches per minute;
- Gas Command – True/False.

A complete example file can be found in Appendix B.

4 Running the Program

The program can be called either from the program directory (where it was installed) or from the list of programs in the “Start Menu”.

The program when started will startup the communications with the Power Supply (PS) and will get them to ready state. While in ready state changes to the *Work Point*, *Trim* and *Mode* can be performed. The *Work Point* (WP) is the Wire Feed Speed (WFS) in inches per minute. By setting the WFS all the other welding parameters are set according to the predefined synergic curve. To better understand the concept of trim and its operation the manufacturer manuals should be consulted Lincoln Electric, *Pulsed Spray Metal Transfer*., (2004), Lincoln Electric. In this application a representation of the range displayed in terms of percentage, [-100%; 100%] The *Mode* is a set of rules to be applied in the PS for the different stages of the welding process. It can be configured in the “Mode XXX.scm” file. These rules concern among other

things the pre and post purge duration and the ability to jog the wire or purge the gas. This file configuration is documented in section 3.2 of this manual.

In ready state is possible to purge the gas and jog the wire in or out to prepare for the next weld. It is also possible to change the mode that is going to be used in each of the PSs independently. Two other operations are possible: start welding and quit the program. To start welding the *Start* button needs to be pressed and the weld sequence will then be started. While welding, gas purge and wire jog functions are disabled as they cannot be performed during welding. When the *Quit Program* button is pressed the PS is shutdown. This implies that the communications are disconnected and the user interface terminated.

This software has two ways of setting the values in the numerical input objects (controls). The most intuitive is by sliding the knob objects with the use of the mouse. The other is by double clicking in the control and on-screen numerical keyboard pops-out. This allows for a more precise value entry in case the user is having problems updating the value with the mouse movement.

5 User Interface Objects

The objects on the screen are divided in two groups, *General Purpose* and *Welding*. The *General Purpose* objects are either input or output objects providing control over the user interface (UI) and reporting the weld and UI status. The *Welding* group is divided in two parts: *Controls* and *Indicators*. The *Controls* are objects which allow changing weld parameters and perform weld related tasks, while *Indicators* are objects that return the PS status and weld conditions. A brief description of the UI objects and its functionalities follows next.

5.1 General Purpose

- *(1) Start* – Turns the PS contactor ON to start the weld sequence;
- *(2) Stop* – Turns the PS contactor OFF to stop the weld sequence. This object in the image is faded as it only appears when object *1* disappears as it is pressed and the PSs are started;
- *(3) Log* – The log list box lists in a timeline of events occurred since the program started. The message background colour indicates the message severity:
    - *White* – Normal;
    - *Green* – Status (ex. PS ON);

- *Yellow* – Interventions: user intervention is required to correct an unexpected situation;
- *Red* – High: a very serious situation occurred and the PS contactor will be turned OFF;

- *(4) Quit Program* – Shuts down the PS, closes the communications to the PS and finishes the user interface.

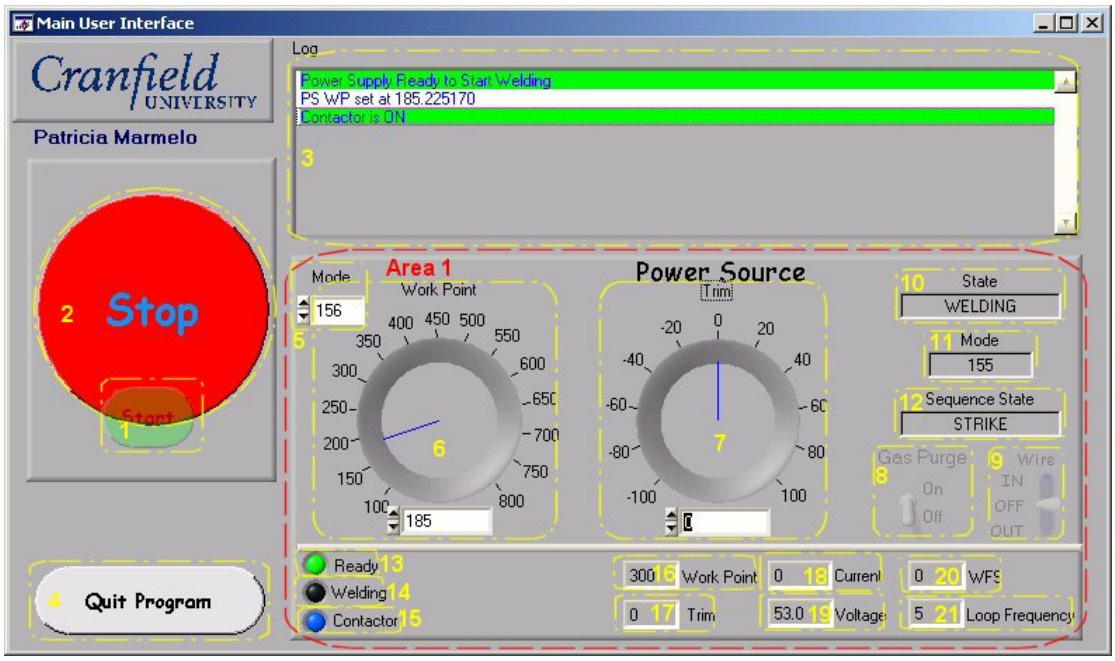

Figure A.5.1 – Program Screenshot with Numbered Objects.

5.2 Power Supply (area 1)

5.2.1 Controls

- *(5) Mode* – Allow selecting the weld mode between the available ones. It is only possible to change the mode while the PS is in *Ready* state, meaning contactor OFF;
- *(6) Work Point* – Sets the PS work point (Wire Feed Speed) selecting in the synergic curve the welding parameters according to the WFS;
- *(7) Trim* – Sets the trim value between ±100%;
- *(8) Gas Purge* – Binary switch that allows purging the gas. It needs to be turned ON for the gas to flow and OFF for it to stop. This object will only work while the PS is in *Ready* state;
- *(9) Wire* – Jogs the wire IN or OUT depending on the direction selected. This is a tri-state switch and it needs to be OFF for the wire to be halted.

5.2.2 Indicators

- *(10) State* – Indicates the PS state;
- *(11) Mode* – Indicates the mode that is active inside the PS;
- *(12) Sequence State* – Indicates the Weld state, the same states as defined in the "Mode XX.scm" file;
- *(13) Ready* – If the LED is ON (green) indicates the PS is in *Ready* mode. If it is OFF (grey) means it is in any other state. For information on the other states look at the *State* object;
- *(14) Welding* – If the LED is ON (green) indicates weld state is *Weld 1* or *Weld 2* mode. When OFF is in any of the other states, see *Sequence State* for more information;
- *(15) Contactor* – If the LED is ON (blue) indicates the PS contactor is on;
- *(16) Work Point* – While welding indicates the instantaneous work point;
- *(17) Trim* – While welding indicates the instantaneous trim;
- *(18) Current* – While welding indicates the average welding current;
- *(19) Voltage* – While welding indicates the average welding voltage;
- *(20) WFS* – While welding indicates the instantaneous wire feed speed;
- *(21) Loop Frequency* – While welding indicates the instantaneous loop frequency.

5.3 Keyboard

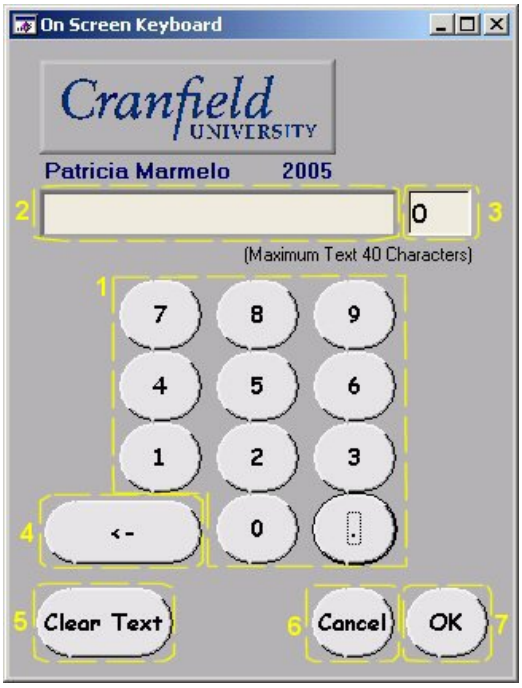

Figure A.5.2 – Keyboard Screenshot with Numbered Objects.

- *(1) Numerical Keypad* – Ten objects representing the numbers zero to nine and on representing the dot. This allows the entry of numbers with decimal precision;
- *(2) Text* – Indicator showing the number inserted;
- *(3) Character Count* – Indicates the number of characters inserted. Up to a maximum of 40;
- *(4) Backspace* – Deletes the last inserted character;
- *(5) Clear Text* – Deletes all the inserted characters;
- *(6) Cancel* – Closes the screen without transferring the inserted value into the object which called the keyboard;
- *(7)* OK – Closes the screen transferring the inserted value into the object which called the keyboard;

Appendix 1 – “Single PowerWave.ini” File Example

[GENERAL CONFIGURATION]
LOG FILE=Single PowerWave.log
ENABLE EVENT LOGGING=TRUE
LOOP DELAY=200
WELDING WATCHDOG TIMEOUT=1.0
THREAD WATCHDOG TIMEOUT=1.0
WIREJOG SPEED=100

[POWER SUPPLY]
COMMUNICATION CHANNEL=EN1
EN1 ADDRESS=192.168.1.2 -UDP 4321

[MODE LIST]
MODE COUNT=2
MODE 1=155
MODE 2=156

Appendix 2 – “Mode XXX.scm” File Example

;ATTR. NAME\STATE	IDLE	SETUP	PRE PURGE	STRIKE	START	UP SLOPE	WELD 1	WELD 2	DOWN SLOPE	CRATER	BURN BACK	POST PURGE	RE STRIKE	FAULT
;														
;														
STATE_TIMER_ENABLE	#	#	TRUE	TRUE	TRUE	TRUE	FALSE	FALSE	TRUE	TRUE	TRUE	TRUE	TRUE	#
STATE_ENABLE	#	#	TRUE	TRUE	TRUE	TRUE	TRUE	FALSE	TRUE	TRUE	TRUE	TRUE	TRUE	#
STATE_TIMER_PRESET	#	#	500	15000	100	50	#	#	50	30	20	2500	1000	#
OUTPUT_COMMAND	#	#	#	#	#	#	#	#	#	#	#	#	#	#
WORKPOINT	#	#	#	200	#	300	300	#	200	250	250	#	450	#
ARC_LENGTH_TRIM	#	#	#	0	#	#	0	#	#	#	0	#	0	#
MISCELLANEOUS_TRIM_1	#	#	#	0	#	#	0	#	#	#	0	#	0	#
MISCELLANEOUS_TRIM_2	#	#	#	#	#	#	#	#	#	#	#	#	#	#
MISCELLANEOUS_TRIM_3	#	#	#	#	#	#	#	#	#	#	#	#	#	#
MISCELLANEOUS_TRIM_4	#	#	#	#	#	#	#	#	#	#	#	#	#	#
MOTOR_COMMAND_FOR_WELDING	#	#	#	#	#	#	#	#	#	#	#	#	#	#
SET_WELDING_WIRE_FEED_SPEED	#	#	#	100	#	#	#	#	#	#	#	#	250	#
GAS_COMMAND	#	#	TRUE	TRUE	TRUE	TRUE	TRUE	TRUE	TRUE	TRUE	TRUE	TRUE	TRUE	#

Appendix B SP2 – *Duo* Software User Manual

Duo Power Supply Control Software

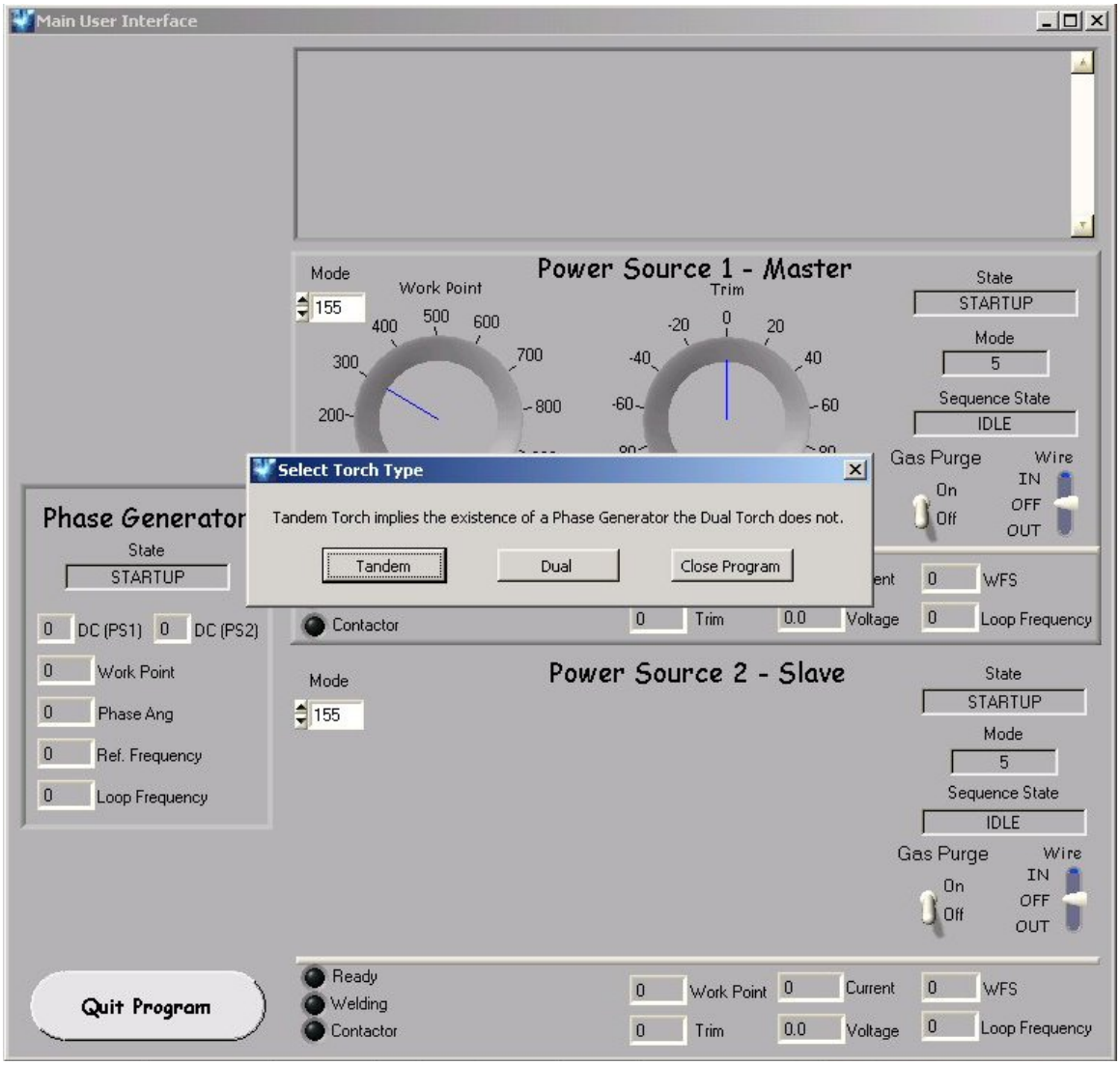

Index

Introduction

The Duo Power Supply Control Software was developed to control two Lincoln Electric – Power Wave F355i power supplies (PSs). This program was developed to control a set of two PSs in a dual or tandem torch (two wires) configuration. In case a Tandem torch is used a *Phase Generator* (PG) is required to synchronise the two PSs.

The Lincoln Electric – Power Wave F355i power supply has no standard user interface and the communications are made through an Ethernet port. Each of these Power Supplies (PSs) has a fixed IP (Internet Protocol) address which comes set from factory. All the communications have to be addressed to the machine's IP address, with the phase generator having an IP address of its own.

1 Installation

To install the Duo Power Supply Control Software double click on the installation setup icon and follow the on screen instructions.

2 Before Running the Program

Before running the program make sure you have made all the required connections and the necessary files are in the program directory. The files required are: "Dual PowerWave.ini" or "Sync PowerWave.ini" depending on the torch type. A "Mode *XXX*.scm" per PS per mode defined in the ".ini" file used. Where *XXX* stands for the mode number. A default file of each it is placed in the program directory when the software is installed. A description of each of these files follows.

2.1 Sync PowerWave.ini *File*

This file is the required one to control a set of two PSs in the tandem mode. The tandem mode does not indicate that the PSs have to be synchronized, but it indicates the presence in the system of the PG and the capability of synchronizing the waveforms if such is intended.

This file is divided into *sections*, each of them started by “[Section Name]”. Inside the section is a list of *tags* fallowed by its *value*, one per line (ex. tag=value).

No sections or tags should be removed as the program will not run without them. Other should not be added as well as the software will not recognise them and will ignore them. The section order can be changed and the order of the tags INSIDE the section be changed as well. They should not be moved to another section, this will result in the program being unable to run properly due to lack information. The program is not case sensitive and so it does not matter if the contents of the .ini file are capital letters or not.

The Sections available in this file are *GENERAL CONFIGURATION*, *POWER SUPPLY 1*, *POWER SUPPLY 2* and *PHASE GENERATOR*. An explanation of each of them follows.

2.1.1 The GENERAL CONFIGURATION *section*

This must contain the following tags:

- **Log File** – The Log File equals to the file name of the file containing the program/weld event logging. This file should have a LOG extension;
- **Torch Count** – Number of PSs (wires) in use;
- **Enable Event Logging** – This tag will either equal “TRUE” or “FALSE” depending if a log file is requested;
- **Loop Delay** – Time added to loop time to ensure the process has time to be completed. Time in milliseconds;
- **Welding Watchdog Timeout** – Time which is waited until a PS system hang is assumed. Time in seconds;
- **Thread Watchdog Timeout** – Time which is waited until a software thread hang is assumed. Time in seconds;
- **Wire Jog Speed** – The Wire Feed Speed (WFS) while jogging the wire in and out. Value in inches per minute;
- **Enable Phase Generator** – This tag must be “TRUE” in order for the system expect the existence of PG equipment and for its features to be enabled.

Example:

[GENERAL CONFIGURATION]
LOG FILE=SYNC PowerWave
TORCH COUNT=2
ENABLE EVENT LOGGING=TRUE
LOOP DELAY=92
WELDING WATCHDOG TIMEOUT=1.0

THREAD WATCHDOG TIMEOUT=1.0
WIREJOG SPEED=100
ENABLE PHASE GENERATOR=TRUE

2.1.2 The POWER SUPPLY 1 section

It must contain the following tags:

- **Communication Channel** – Type and number of the communication port, typically EN1 for Ethernet communication;
- **EN1 ADDRESS** – The IP address and UDP protocol port number. Standard port number 4321;
- **Mode Count** – Indicates the number of modes in the PS that need to be loaded into the machine and will be active;
- **Mode XXX** – Mode number existent in the PS to be loaded, where "XXX" represents the mode index. Should exist as many tags like this as the *Mode Count* value.

Example:
[POWER SUPPLY 1]
COMMUNICATION CHANNEL=EN1
EN1 ADDRESS=192.168.1.1 -UDP 4321
MODE COUNT=
MODE=155

2.1.3 The POWER SUPPLY 2 section

It must contain the following tags:

- **Communication Channel** – Type and number of the communication port, typically EN1 for Ethernet communication;
- **EN1 ADDRESS** – The IP address and UDP protocol port number. Standard port number 4321;
- **Mode Count** – Indicates the number of modes in the PS that need to be loaded into the machine and will be active;
- **Mode XXX** – Mode number existent in the PS to be loaded, where "XXX" represents the mode index. Should exist as many tags like this as the *Mode Count* value.
- **Default Mode** – Default mode parameters to be active at startup in case there is more than one mode to be active in the PS.

Example:
[POWER SUPPLY 2]
COMMUNICATION CHANNEL=EN1

EN1 ADDRESS=192.168.1.2 -UDP 4321
MODE COUNT=2
MODE 1=155
MODE 2=156
DEFAULT MODE=155

2.1.4 The PHASE GENERATOR section

It must contain the following tags:

- **Communication Channel** – Type and number of the communication port, typically EN1 for Ethernet communication;
- **EN1 ADDRESS** – The IP address and UDP protocol port number. Standard port number 4321.

Example:
[PHASE GENERATOR]
COMMUNICATION CHANNEL=EN1
EN1 ADDRESS=192.168.1.3 -UDP 4321

A complete example file can be found in Appendix A.

2.2 Dual PowerWave.ini *File*

This file is the required one to control a set of two PSs in the dual mode. The dual mode indicates that the PSs will not be synchronized at any time. This indicates the system does not need a PG equipment to be connected to the system.

This file is divided into *sections*, being each of them started by "[Section Name]". Inside the section is a list of *tags* fallowed by its *value*, one per line (ex. tag=value).

No sections or tags should be removed as the program will not run without them. Other should not be added as well as the software will not recognise them and will ignore them. The section order and the order of the tags INSIDE the section can be changed. They should not be moved to another section, this will result in the program being unable to run properly due to lack information and. The program is not case sensitive and so it does not matter if the contents of the .ini file are capital letters or not.

The Sections available in this file are *GENERAL CONFIGURATION*, *POWER SUPPLY 1* and *POWER SUPPLY 2*. An explanation of each of them follows.

2.2.1 The GENERAL CONFIGURATION section

It must contain the following tags:

- **Log File** – The Log File equals to the file name of the file containing the program/weld event logging. This file should have a LOG extension;
- **Torch Count** – Number of PSs (wires) in use;
- **Enable Event Logging** – This tag will either equal “TRUE” or “FALSE” depending if a log file is requested;
- **Loop Delay** – Time added to loop time to ensure the process has time to be completed. Time in milliseconds;
- **Welding Watchdog Timeout** – Time which is waited until a PS system hang is assumed. Time in seconds;
- **Thread Watchdog Timeout** – Time which is waited until a software thread hang is assumed. Time in seconds;
- **Wire Jog Speed** – The Wire Feed Speed (WFS) while jogging the wire in and out. Value in inches per minute;
- **Enable Phase Generator** – This tag must “FALSE” so a PG equipment is not expected by the system.

Example:

[GENERAL CONFIGURATION]
LOG FILE=SYNC PowerWave
TORCH COUNT=2
ENABLE EVENT LOGGING=TRUE
LOOP DELAY=92
WELDING WATCHDOG TIMEOUT=1.0
THREAD WATCHDOG TIMEOUT=1.0
WIREJOG SPEED=100
ENABLE PHASE GENERATOR=FALSE

2.2.2 The POWER SUPPLY 1 section

It must contain the following tags:

- **Communication Channel** – Type and number of the communication port, typically EN1 for Ethernet communication;
- **EN1 ADDRESS** – The IP address and UDP protocol port number. Standard port number 4321;

- **Mode Count** – Indicates the number of modes in the PS that need to be loaded into the machine and will be active;
- **Mode XXX** – Mode number existent in the PS to be loaded, where “XXX” represents the mode index. Should exist as many tags like this as the *Mode Count* value.

Example:

[POWER SUPPLY 1]

COMMUNICATION CHANNEL=EN1

EN1 ADDRESS=192.168.1.1 -UDP 4321

MODE COUNT=1

MODE=155

2.2.3 The POWER SUPPLY 2 section

It must contain the following tags:

- **Communication Channel** – Type and number of the communication port, typically EN1 for Ethernet communication;
- **EN1 ADDRESS** – The IP address and UDP protocol port number. Standard port number 4321;
- **Mode Count** – Indicates the number of modes in the PS that need to be loaded into the machine and will be active;
- **Mode XXX** – Mode number existent in the PS to be loaded, where “XXX” represents the mode index. Should exist as many tags like this as the *Mode Count* value.
- **Default Mode** – Default mode parameters to be active at startup in case there is more than one mode to be active in the PS.

Example:

[POWER SUPPLY 2]

COMMUNICATION CHANNEL=EN1

EN1 ADDRESS=192.168.1.2 -UDP 4321

MODE COUNT=2

MODE 1=155

MODE 2=156

DEFAULT MODE=155

A complete example file can be found in Appendix B.

2.3 Mode XXX.scm File

The SCM file contains for the each PS state the expected attribute state or value.

List of the PS states:

- Idle;
- Setup;
- Pre Purge;
- Strike;
- Start;
- Up Slope;
- Weld 1;
- Weld 2;
- Down Slope;
- Crater;
- Burn Back;
- Post Purge;
- Re-Strike;
- Fault.

List of attributes:

- State Timer – True/False;
- State – True/False;
- State Timer Preset – time in milliseconds;
- Output Command – value;
- Work Point – in inches per minute;
- Arc Length Trim – trim value from -1 to 1;
- Miscellaneous Trim 1 – value;
- Miscellaneous Trim 2 – value;
- Miscellaneous Trim 3 – value;
- Miscellaneous Trim 4 – value;
- Motor Commando for Welding – value;
- Set Welding Wire Feed Speed – set value of WFS in inches per minute;
- Gas Command – True/False.

A complete example file can be found in Appendix B.

3 Running the Program

The program can be called either from the program directory (where it was installed) or from the list of programs in the “Start Menu”.

The program when started will startup the communications with the Power Supplies (PSs) and will get them to ready state. While in ready state changes to the *Work Point*, *Trim* and *Mode* can be performed. The *Work Point* (WP) is the Wire Feed Speed (WFS) in inches per minute. By setting the WFS all the other welding parameters are set according to the predefined synergic curve. To better understand the concept of trim and its operation the manufacturer manuals should be consulted (Lincoln Electric, *Pulsed Spray Metal Transfer*. 2004, Lincoln Electric). In this application a representation of it is displayed in terms of percentage, [-100%; 100%] The *Mode* is a set of rules to be applied in the PS for the different stages of the welding process. Those rules can be configured in the appropriate mode file. These rules concern among other things the pre and post purge duration and the ability to jog the wire or purge the gas. This file’s configuration was previously documented in section Appendix 3 – “Mode XXX.scm” File Example from this manual.

In ready state is possible to purge the gas and jog the wire in or out to prepare for the next weld. It is also possible to change the mode that is going to be used in each of the PSs independently. Two other operations are possible: start welding and quit the program. To start welding the Start button needs to be pressed and the weld sequence will then be started. While welding, gas purge and wire jog functions are disabled as such is not possible to perform during welding. When the Quit Program button is pressed the PS is shutdown. This implies that the communications are disconnected and the user interface terminated.

This software has two ways of setting the values in the numerical input objects (controls). One that the most intuitive is by sliding the knob objects with the use of the mouse. The other is by double clicking in the control an on-screen numerical keyboard pops-out. This allows for a more precise value entrance in case the user is having problems updating the value with the mouse movement.

4 User Interface Objects

The objects on the screen are divided in three groups, *General Purpose*, *Welding Control* and *Welding Status*. The *General Purpose* objects are either input or output objects providing control over the user interface (UI) and reporting the weld and UI status. *Welding Control* objects allow changing weld parameters and perform weld related tasks. On the other hand *Welding Status* objects return the status of PS and weld conditions. A brief description of the UI objects and its functionalities follows next. The welding controls and status objects are divided into three different areas, *Power Supply 1*, *Power Supply 2* and *Phase Generator*. The *Power Supply 1* and *Power Supply 2* areas contain the same objects and they are associated to the respective PS.

4.1 General Purpose

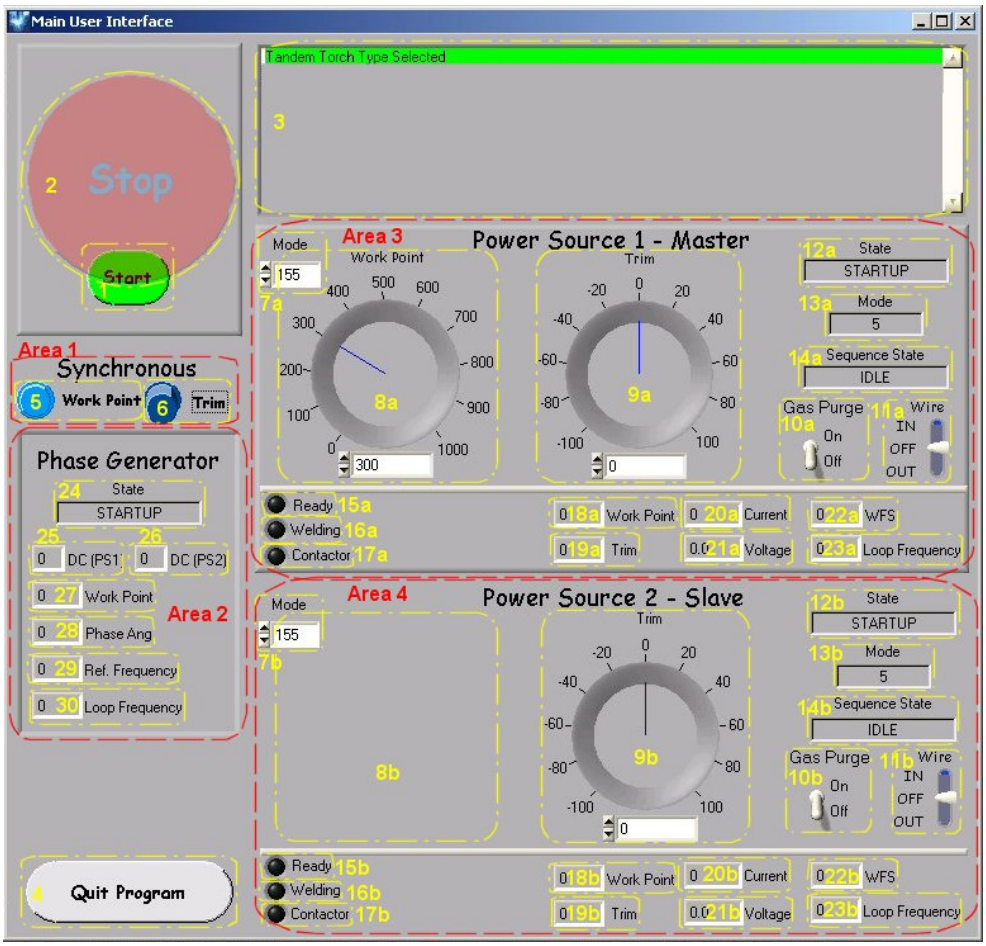

Figure B.4.1 – Program Screenshot with Numbered Objects.

- *(1) Start* – Turns the PS contactor ON to start the weld sequence;
- *(2) Stop* – Turns the PS contactor OFF to stop the weld sequence. This object in the image is faded as it only appears when object *1* disappears as it is pressed and the PSs are started;
- *(3) Log* – The log list box lists in a timeline of events occurred since the program started. The message background colour indicates the message severity:
    - *White* – Normal;
    - *Green* – Status (ex. PS ON);
    - *Yellow* – Interventions: user intervention is required to correct an unexpected situation;
    - *Red* – High: a very serious situation occurred and the PS contactor will be turned OFF;
- *(4) Quit Program* – Shuts down the PS, closes the communications to the PS and finishes the user interface.

4.2 Welding Control *(area 1)*

- *(5) Synchronous Work Point* – Determines if the WP in both PSs is synchronised or not. If the button is pressed (light blue colour) the WPs will be synchronised and the value in both PSs will be the one selected in PS 1. If not pressed (dark blue colour) the PSs will have independent WP values. The synchronism can be changed either with the PSs idle or welding;
- *(6) Synchronous Trim* – It determines if the Trim in the PSs is synchronised or not. Working in the same way as the *Synchronous Work Point* button.

4.2.1 Power Supply 1 (area 3) and Power Supply 2 (area 4)

- *(7a; 7b) Mode* – Allow selecting the weld mode between the available ones. It is only possible to change the mode while the PS is in *Ready* state, meaning contactor OFF;
- *(8a, 8b) Work Point* – Sets the PS work point (Wire Feed Speed) selecting in the synergic curve the welding parameters according to the WFS;
- *(9a, 9b) Trim* – Sets the trim value between ±100%;
- *(10a, 10b) Gas Purge* – Binary switch that allows purging the gas. It needs to be turned ON for the gas to flow and OFF for it to stop. This object will only work while the PS is in *Ready* state;
- *(11a, 11b) Wire* – Jogs the wire IN or OUT depending on the direction selected. This is a tri-state switch and it needs to be OFF for the wire to be halted.

4.2.2 Phase Generator (area 2)

The Phase Generator has no welding controls.

4.3 Welding Status

4.3.1 Power Supply 1 (area 3) and Power Supply 2 (area4)

- *(12a, 12b) State* – Indicates the PS state;
- *(13a, 13b) Mode* – Indicates the mode that is active inside the PS;
- *(14a, 14b) Sequence State* – Indicates the Weld state, the same states as defined in the "Mode XX.scm" file;
- *(15a, 15b) Ready* – If the LED is ON (green) indicates the PS is in *Ready* mode. If it is OFF (grey) means it is in any other state, welding, startup, an error, …, look at the *State* object for more information;
- *(16a, 16b) Welding* – If the LED is ON (green) indicates weld state is *Weld 1* or *Weld 2* mode. When OFF is in any of the other states, see *Sequence State* for more information;
- *(17a, 17b) Contactor* – If the LED is ON (blue) indicates the PS contactor is on;
- *(18a, 18b) Work Point* – While welding indicates the instantaneous work point;
- *(19a, 19b) Trim* – While welding indicates the instantaneous trim;
- *(20a, 20b) Current* – While welding indicates the average welding current;
- *(21a, 21b) Voltage* – While welding indicates the average welding voltage;
- *(22a, 22b) WFS* – While welding indicates the instantaneous wire feed speed;
- *(23a, 23b) Loop Frequency* – While welding indicates the instantaneous loop frequency.

4.3.2 Phase Generator (area 2)

- *(24) State* – Indicates the PS state;
- *(25) DC (PS1)* – While welding indicates the average welding voltage in PS 1;
- *(26) DC (PS2)* – While welding indicates the average welding voltage in PS 2;
- *(27) Work Point* – Indicates the PG work point during welding;
- *(28) Phase Angle* – Indicates the mismatch angle between the pulses of both PSs;
- *(29) Reference Frequency* – The average pulse frequency;
- *(30) Loop Frequency* – Indicates the loop frequency.

4.4 Keyboard

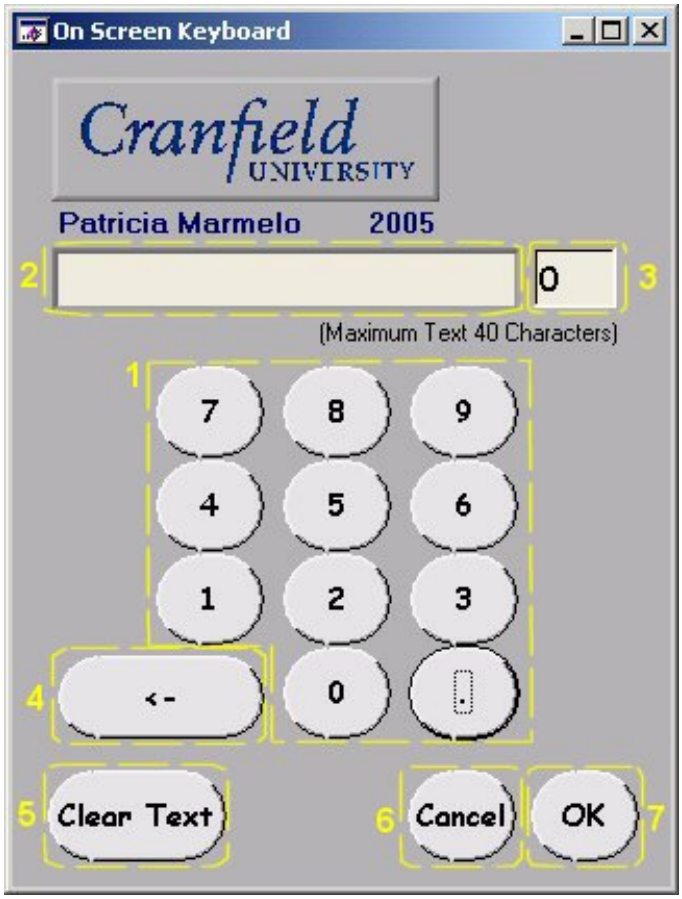

Figure B.4.2 – Keyboard Screenshot with Numbered Objects.

- *(1) Numerical Keypad* – Ten objects representing the numbers zero to nine and on representing the dot. This allows the entry of numbers with decimal precision;
- *(2) Text* – Indicator showing the number inserted;
- *(3) Character Count* – Indicates the number of characters inserted. Up to a maximum of 40;
- *(4) Backspace* – Deletes the last inserted character;
- *(5) Clear Text* – Deletes all the inserted characters;
- *(6) Cancel* – Closes the screen without transferring the inserted value into the object which called the keyboard;
- *(7)* OK – Closes the screen transferring the inserted value into the object which called the keyboard;

Appendix 1 – “Sync PowerWave.ini” File Example

[GENERAL CONFIGURATION]
LOG FILE=SYNC PowerWave
TORCH COUNT=2
ENABLE EVENT LOGGING=TRUE
LOOP DELAY=92
WELDING WATCHDOG TIMEOUT=1.0
THREAD WATCHDOG TIMEOUT=1.0
WIREJOG SPEED=100
ENABLE PHASE GENERATOR=TRUE

[POWER SUPPLY 1]
COMMUNICATION CHANNEL=EN1
EN1 ADDRESS=192.168.1.1 -UDP 4321
MODE COUNT=2
MODE 1=155
MODE 2=156

[POWER SUPPLY 2]
COMMUNICATION CHANNEL=EN1
EN1 ADDRESS=192.168.1.2 -UDP 4321
MODE COUNT=2
MODE 1=155
MODE 2=156
DEFAULT MODE=155

[PHASE GENERATOR]
COMMUNICATION CHANNEL=EN1
EN1 ADDRESS=192.168.1.3 -UDP 4321

Appendix 2 – “Dual PowerWave.ini” File Example

[GENERAL CONFIGURATION]
LOG FILE=SYNC PowerWave
TORCH COUNT=2
ENABLE EVENT LOGGING=TRUE
LOOP DELAY=92
WELDING WATCHDOG TIMEOUT=1.0
THREAD WATCHDOG TIMEOUT=1.0
WIREJOG SPEED=100
ENABLE PHASE GENERATOR=FALSE

[POWER SUPPLY 1]
COMMUNICATION CHANNEL=EN1
EN1 ADDRESS=192.168.1.1 -UDP 4321
MODE COUNT=2
MODE 1=155
MODE 2=156

[POWER SUPPLY 2]
COMMUNICATION CHANNEL=EN1
EN1 ADDRESS=192.168.1.2 -UDP 4321
MODE COUNT=2
MODE 1=155
MODE 2=156
DEFAULT MODE=156

Appendix 3 – “Mode XXX.scm” File Example

;ATTR. NAME\STATE ; ;	IDLE	SETUP	PRE PURGE	STRIKE	START	UP SLOPE	WELD 1	WELD 2	DOWN SLOPE	CRATER	BURN BACK	POST PURGE	RE STRIKE	FAULT
STATE_TIMER_ENABLE	#	#	TRUE	TRUE	TRUE	TRUE	FALSE	FALSE	TRUE	TRUE	TRUE	TRUE	TRUE	#
STATE_ENABLE	#	#	TRUE	TRUE	TRUE	TRUE	TRUE	FALSE	TRUE	TRUE	TRUE	TRUE	TRUE	#
STATE_TIMER_PRESET	#	#	500	15000	100	50	#	#	50	30	20	2500	1000	#
OUTPUT_COMMAND	#	#	#	#	#	#	#	#	#	#	#	#	#	#
WORKPOINT	#	#	#	200	#	300	300	#	200	250	250	#	450	#
ARC_LENGTH_TRIM	#	#	#	0	#	#	0	#	#	#	0	#	0	#
MISCELLANEOUS_TRIM_1	#	#	#	0	#	#	0	#	#	#	0	#	0	#
MISCELLANEOUS_TRIM_2	#	#	#	#	#	#	#	#	#	#	#	#	#	#
MISCELLANEOUS_TRIM_3	#	#	#	#	#	#	#	#	#	#	#	#	#	#
MISCELLANEOUS_TRIM_4	#	#	#	#	#	#	#	#	#	#	#	#	#	#
MOTOR_COMMAND_FOR_WELDING	#	#	#	#	#	#	#	#	#	#	#	#	#	#
SET_WELDING_WIRE_FEED_SPEED	#	#	#	100	#	#	#	#	#	#	#	#	250	#
GAS_COMMAND	#	#	TRUE	TRUE	TRUE	TRUE	TRUE	TRUE	TRUE	TRUE	TRUE	TRUE	TRUE	#

Appendix C SP3 – *Motion* Software

1 Main Window

1.1 Indicators (blue)

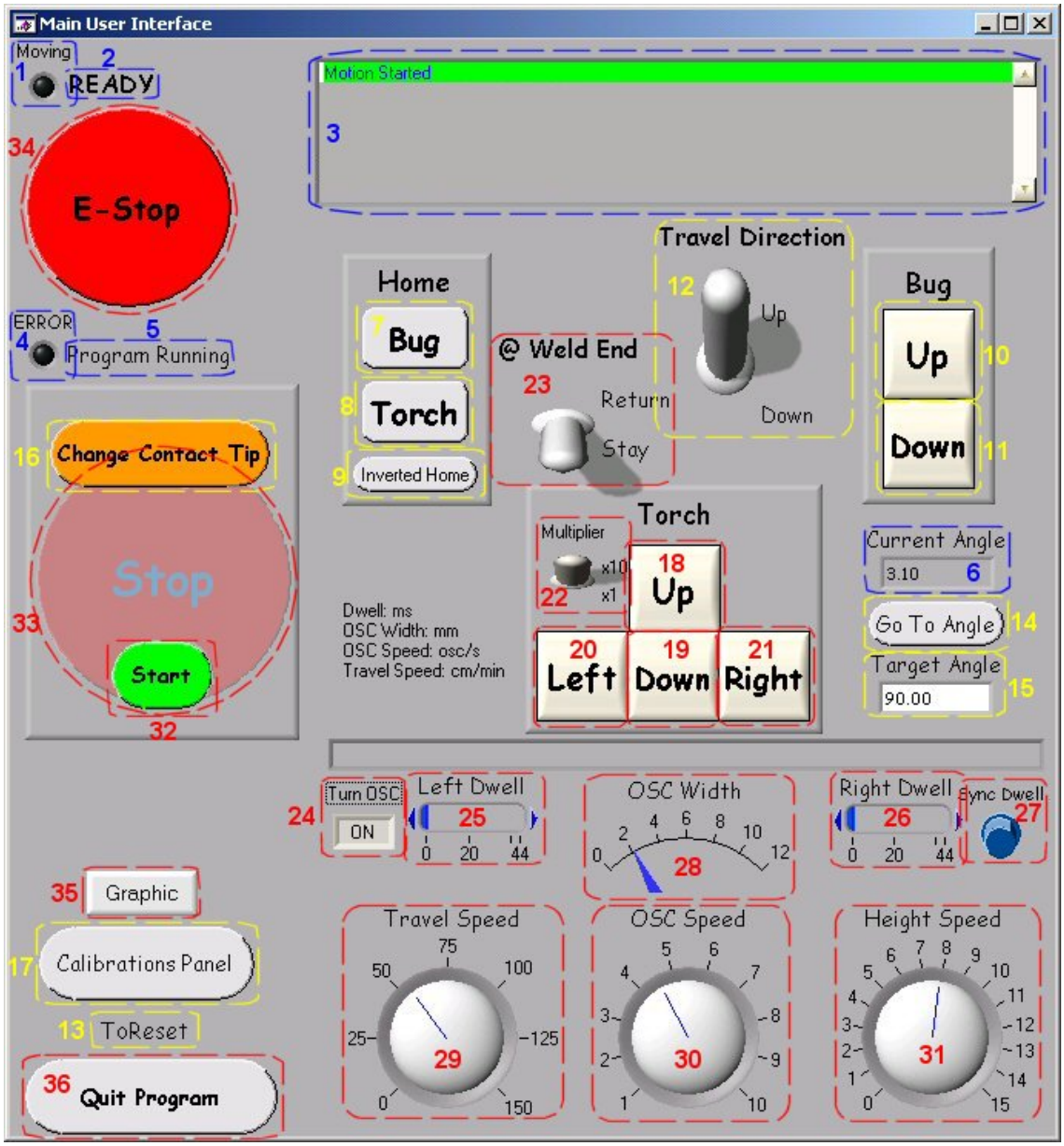

Figure C.1.1 – Motion Program Screenshot with Numbered Objects.

- *(1) Moving* – If the LED is ON (red) indicates the welding carrier is performing some form of motion;

- *(2) Motion State* – Indicates if the welding carrier is either in the *startup*, *initializing*, *ready*, *running*, *shutdown*, *error*, *com error*, *alarm error*, *system error* or *reset*;
- *(3) Log* – The log list box lists a timeline of events occurred since the program started. The message background colour indicates the message severity:
    - *White* – Normal;
    - *Green* – Status (ex. PS ON);
    - *Yellow* – Interventions: user intervention is required to correct an unexpected situation;
    - *Red* – High: a very serious situation occurred and the PS contactor will be turned OFF;
- *(4) Error* – If the LED is ON (red) indicates that an error occurred and the motion controller needs to be reset;
- *(5) Program State* – Indicates the state the program is in. The state is either *motion startup timeout*, *program running*, *waiting for input* and *trace*;
- *(6) Current Angle* – Indicates the instantaneous welding carrier angular position around the pipe.

1.2 Controls

1.2.1 Objects that can only be used only while the system is not welding (yellow)

- *(7) Home Bug* – Sends the welding head to a position on the top of the pipe where the torch is aligned with vertical line that passes through the centre of the pipe. This is controlled based on the welding carrier angular position;
- *(8) Home Torch* – Move the welding head to the torch home position plus an increment. This increment is the angular off set between the torch and the laser head. The laser head will be pointing the laser beam at the position where the torch will start welding. The aim of this is to start scanning the area of the groove between the sensor and the torch before welding starts, so all the weld length is scanned before the weld is performed;
- *(9) Inverted Home* – Sends the bug to the opposite position to the *Home Bug*. The torch will be again aligned with the vertical line passing on the centre of the pipe but this time the welding head will be under the pipe;
- *(10) Bug Up, (11) Bug Down* – Moves the welding head up and down respectively around the pipe*;*
- *(12) Travel Direction* – Toggles the conventional travel direction between upward and downward;

- *(13) Reset* – Is a button which allows resetting the motion system in case of an error or system freeze;
- *(14) Go To Angle* – Sends the welding carrier to move to an angular position;
- *(15) Target Angle* – Angle value to be reached when the *Go To Angle* button is pressed;
- *(16) Change Contact Tip* – When this button is pressed a message window pops-out which has on screen instructions on the procedure to change the contact tip.
- *(17) Calibrations Window* – Calls the *Calibration* window which allows for weld carrier and torch calibrations to be performed;

The functions based on the welding carrier's angular position are based in the values read from the inclinometer located inside the welding head. The inclinometer operation will be described in greater detail in section 5.1.3.1.

1.2.2 Objects that can be used during welding or not welding (red)

- *(18, 19) Torch Up, Torch Down* – Moves the torch vertically to alter the torch stand-off;
- *(20, 21) Torch Left, Torch Right* – Moves the torch horizontally to change the centre point of the oscillation;
- *(22) Multiplier* – Determines if the jog movements are in steps of 1 or 10mm each;
- *(23) @ Weld End* – Selects if the bug stays down or returns to home position when it finishes performing the weld or a dry run. By *dry run* should be understood a weld simulation, the system performs exactly as during normal mode with the exception that the welding arc is not struck;
- *(24) Turn Oscillation* – Turns the torch oscillation ON and OFF;
- *(25, 26) Dwell Left, Dwell Right* – Is a sliding bar which allows control of the dwell (delay time) in each of the sidewalls;
- *(27) Sync Dwell* – Determines if the left and right dwells are synchronous (light blue and flat) or not (dark blue and outward);
- *(28) OCS Width* – Allows changing the amplitude of oscillation as well as to display the current value while it is being changed by the software and not the user;
- *(29) Travel Speed* – Controls and indicates the welding head travel speed around the pipe;
- *(30) OSC Speed* – Regulates the torch speed of oscillation. Again functions as a control and an indicator;
- *(31) Height Speed* – Adjusts the speed at which the torch moves up and down for torch height adjustments*;*
- *(32) Start* – This button is enabled after startup and until it is pressed. Once pressed it become disabled and invisible until the *(33) Stop* button is pressed;

- *(33) Stop* – This button is visible and active after startup is finished and the *(32) Start* button is pressed. It remains visible until being pressed;
- *(34) E-Stop* – This button is an emergency stop button to be pressed when a problem occurs and the entire system goes to a halt immediately. Once pressed it will arm the alarm until it is pressed again (bi-stable button);
- *(35) Graphic* – A window containing a graphic with the welding carrier's trajectory pops-out;
- *(36) Quit Program* – Stops the motion controller and its communications and finishes the user interface. Just before exiting the user interface, the user is asked if he wishes to return the bug to the home position before shutting down. See below Figure C.1.2.

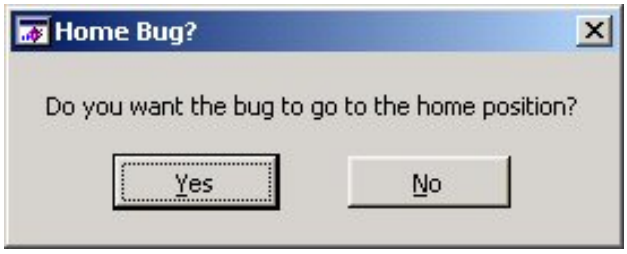

Figure C.1.2 – Program Screenshot Showing the Question About Returning the Weld Carrier to the Home Position Before Exiting the User Interface.

1.3 Calibrations Window

It is possible to calibrate the welding head (AKA "Bug") inclinometer and the torch centre point in this software. To calibrate the inclinometer object *(1) "Calibrate Active Bug"* (Figure C.1.3) is pressed. The program will generate a series of motions and will require the user to perform some actions. Details of the process and required actions are given through-out the calibration process. Similarly the torch calibration can be assessed by pressing an on-screen button. This time the button is object *(2) "Calibrate Torch"* (Figure C.1.3). Although the process is different, on screen information and requests are presented to the user during the calibration process.

The inclinometer calibrations aims to determine the key positions around the pipe that the inclinometer needs to accurately calculate the weld head angular position around the pipe. This position is independent from the pipe diameter. The torch centre point calibration is needed to determine the angular displacement between the weld head and the torch. This is required so the weld is started, modified and ended where is intended. Once all required calibrations were performed and this window is no longer required and the button *(3) "Close"* (Figure C.1.3) can be pressed. This will hide the calibrations window from the screen.

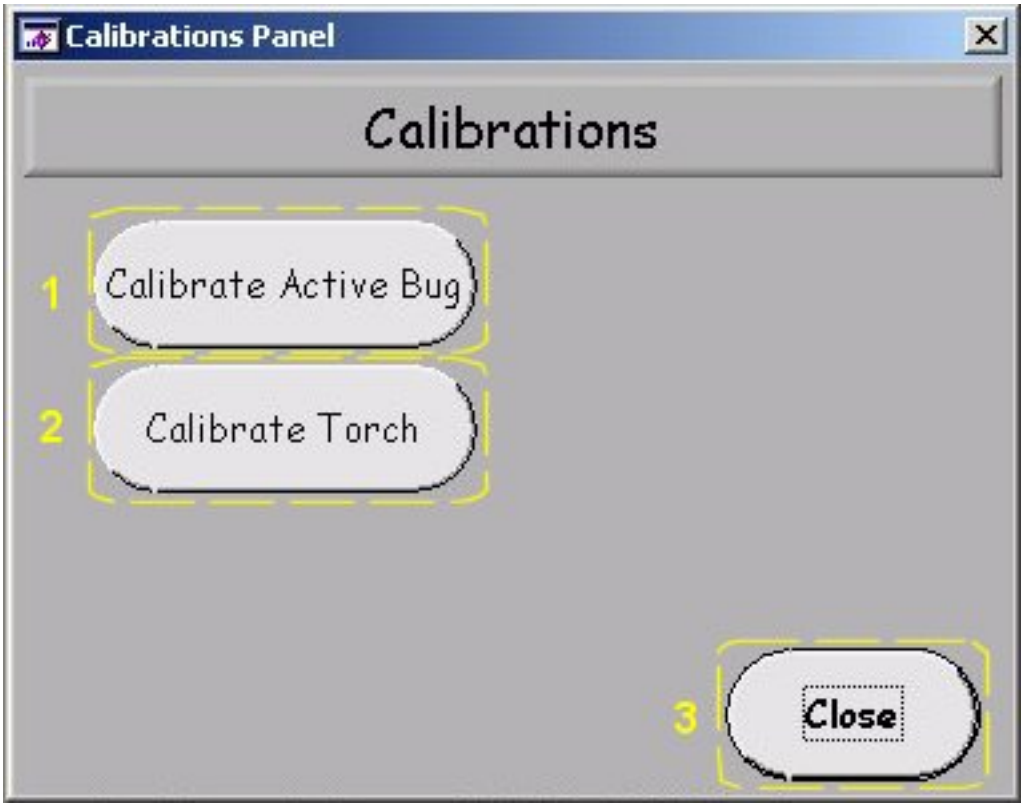

Figure C.1.3 – Calibration Window Screenshot with Numbered Objects.

1.4 Graphics Window

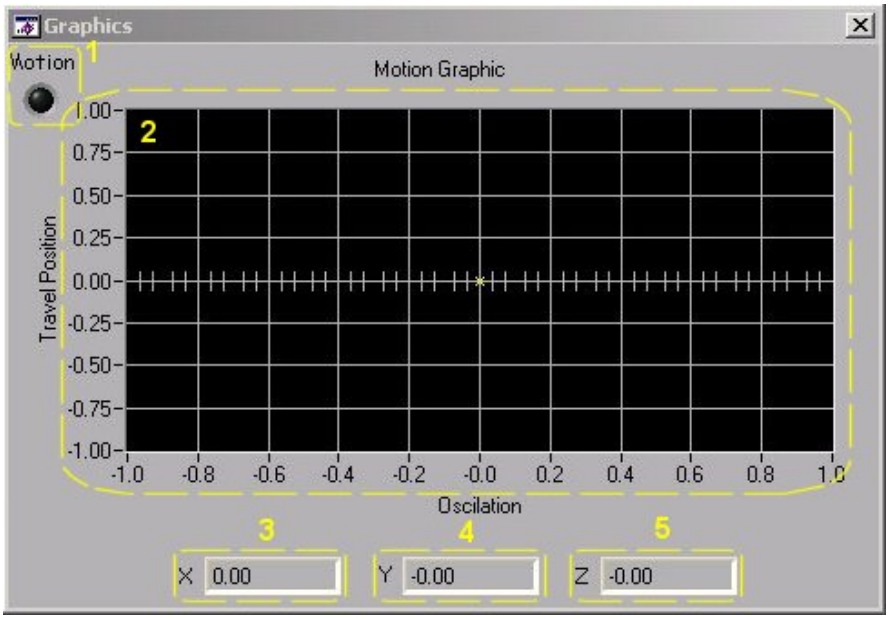

Figure C.1.4 – Graphics Window Screenshot with Numbered Objects.

The main object in the *Graphics Window* is the graph in the centre, Figure C.1.4, the *(2) Motion Graphic*. The *(1) Motion* (Figure C.1.4) LED indicates if the welding carrier is in motion (red) or not. The three objects in the bottom of the window *(3) X, (4) Y* and *(5) Z* (Figure C.1.4) indicate the Cartesian coordinates of the torch along the run that is being or was just performed.

1.5 Keyboard Window

This software has two ways of setting the controls (values in the alphanumerical input objects). One, and the most intuitive, is by sliding the knob objects with the use of the mouse. The other is by double clicking in the control to generate an on-screen alphanumerical keyboard. This allows for a more precise value entrance. The virtual keyboard was designed with the general configuration of a "QWERTY" keyboard in order to be as user friendly as possible. The virtual keyboard can be seen in Figure C.1.5 and a description can be found bellow.

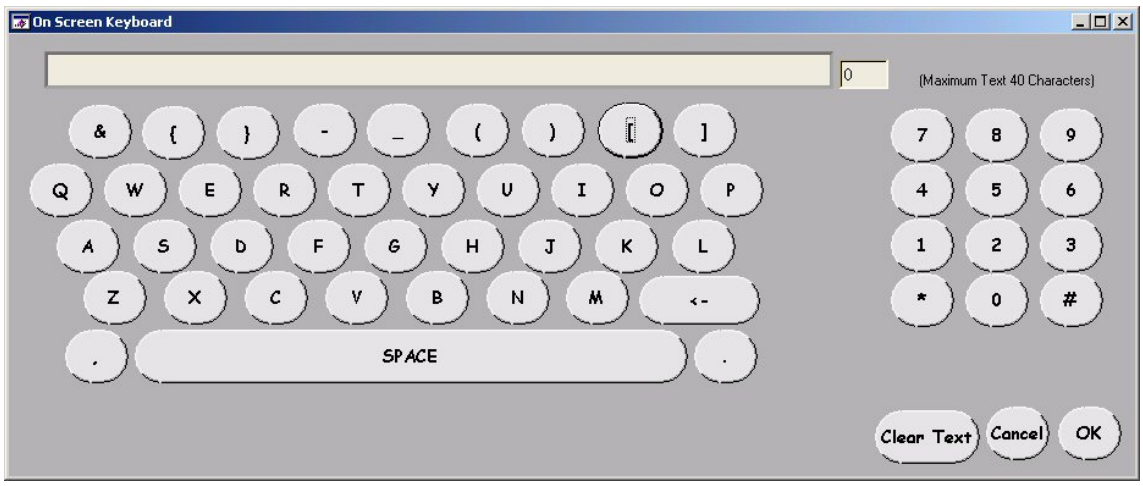

Figure C.1.5 – Alphanumerical Keyboard Screenshot with Numbered Objects.

Appendix D SP4 – *Laser Profile* Software

The *Laser Profile* software (SP4) is a simple program developed to acquire and playback the laser vision sensor data. Prior to start grabbing the data the user decides if the data should be saved for later use. The saved scan sequences can be played back for post-weld visual inspection. Data acquired with SP4 can be loaded for analysis in SP7. This program was developed in order to be possible to acquire data from the laser sensor and to be able to play it back independently from the motion and welding equipment. This program also allows other people, who may not be familiar with the use of this type of system, to acquire data and visualise it without difficulty.

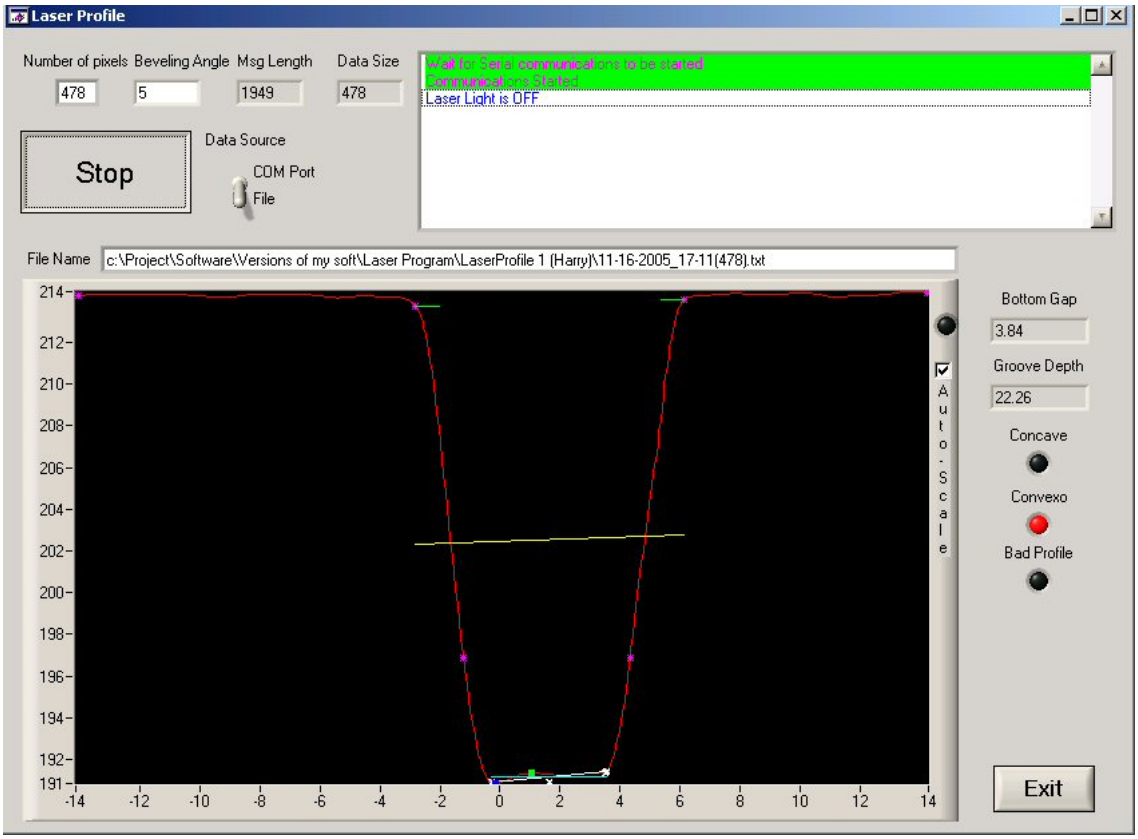

Figure D.0.1 – *Laser Profile* Screenshot Playing Back Saved Data.

This program is composed of one single window (Figure D.0.1) and it was kept as simple and intuitive as possible so it can be easily as possible by other people. A description of the objects and their function follows.

- *(1) Number of pixels* – This is an input object where the user sets the number of pixels to be acquired per scan in case the data source is the laser vision sensor or the number of pixels present in each profile case the data source is a saved file;
- *(2) Bevelling Angle* – This is an input object in which the user sets the groove sidewalls bevelling angle, for both data sources. The bevelling angle is used for data analysis;

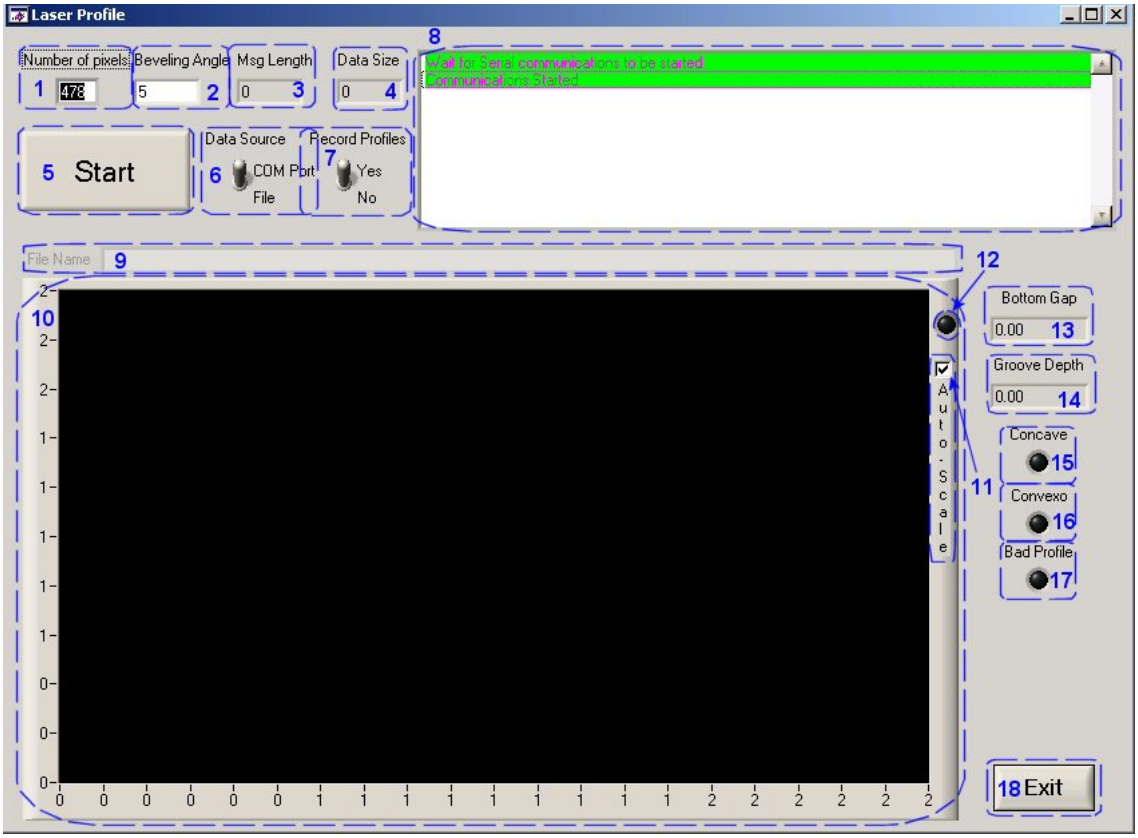

Figure D.0.2 – *Laser Profile* Screenshot with Numbered Objects.

- *(3) Msg Length* – This object is an indicator that shows the total length (number of bytes) of the data received from the sensor;
- *(4) Data Size* – This objects is similar to the previous one but this one indicates the number of bytes in the message that actually contains the profile data;
- *(5) Start* – This is a bi-stable button that both starts and stops the data acquisition or playback depending on the data source. In case the data source is the laser vision sensor, profile data is requested from the sensor control box. On the other hand, if the selected data source is a data file, once the button is pressed to start the sequence, a standard file selection window pops-up for the user to select which file to be loaded. After the file is loaded the profiles are played exactly as if they originated in the sensor itself;
- *(6) Data Source* – This two state switch allows selecting the source of the data, either the sensor or a stored data file;
- *(7) Record Profiles* – This switch is only visible if the data source is the sensor (a.k.a. the COM port) and determines if the acquired data is saved into a data file or not;
- *(8) Log* – The log list box lists in a timeline of events which have occurred since the program started. The message background colour indicates the message severity:
    - *White* – Normal;

    - *Green* – Status (ex. “Communications Started”);
    - *Yellow* – Interventions: user intervention is required to correct an unexpected situation;
    - *Red* – High: a very serious situation occurred and the sensor light will be turned OFF;
- *(9) File Name* – This object is only active if the data source is a data file and it indicates the name of the file that is being used;
- *(10) Profile* – This is a graph that shows the joint profile;
- *(11) Auto-Scale* – This check box determines if the scales in the *(10) Profile* graph are automatic or not;
- *(12) Processing* – This LED indicates if the program is acquiring and processing the profile data (red colour) or not (grey colour);
- *(13) Bottom Gap* – This object indicates the width of the groove bottom of the profile shown in the *(10) Profile* graph;
- *(14) Groove Depth* – This object indicates the groove depth of the profile shown in the *(10) Profile* graph;
- *(15) Concave* – If the LED is ON (green) indicates the groove bottom has a concave shape;
- *(16) Convex*– If the LED is ON (red) indicates the groove bottom has a convex shape
- *(17) Bad Profile* – If the LED is ON (yellow) indicates the groove bottom shows an unexpected shape. By unexpected can be understood asymmetric profiles, and other recognisable defects;
- *(18) Exit* – Closes the user interface terminating the program;

Appendix E SP6 – *Rig* Software

(Single & Dual/Tandem)

The version for the single torch is going to be described first and it will be followed by the differences in the dual/tandem version.

1 Single

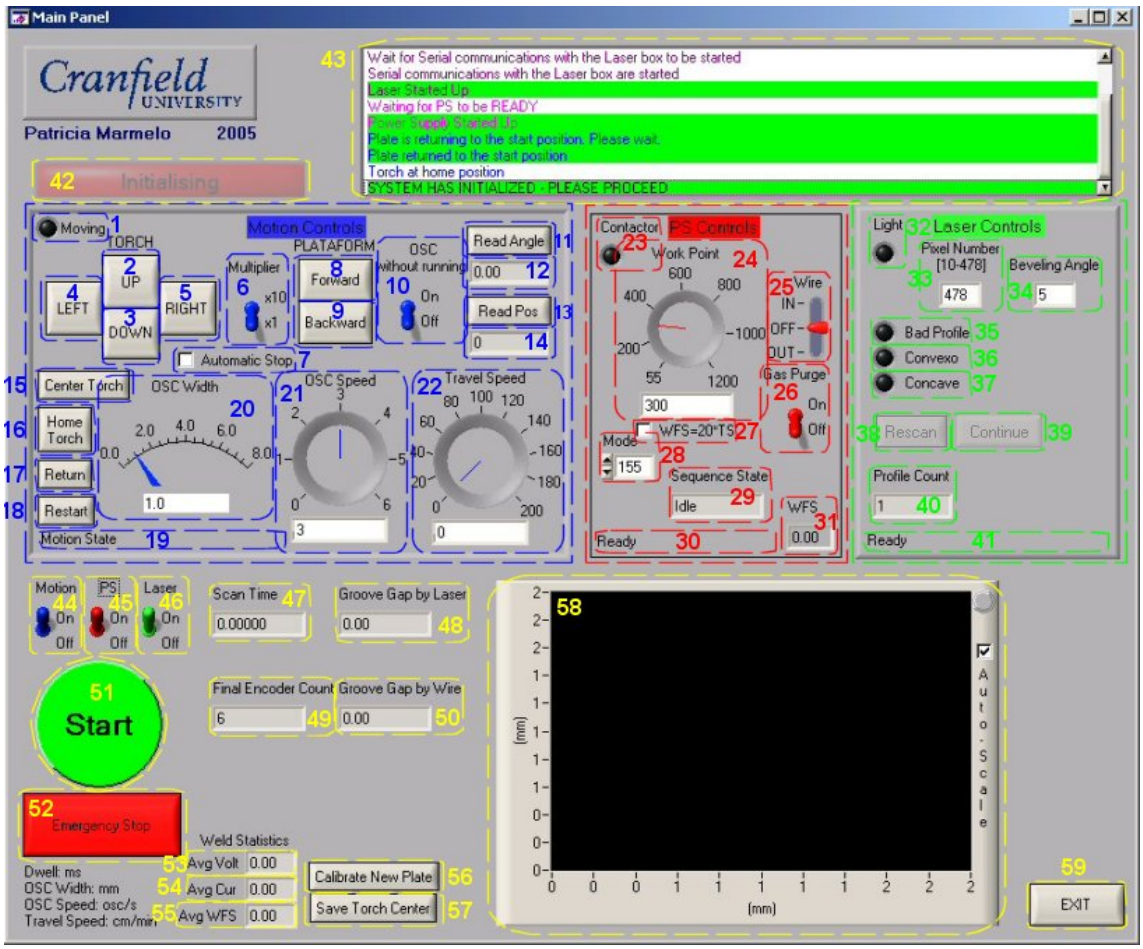

Figure E.1.1.1 – Rig Single Software Screenshot with Numbered Objects.

This software is divided into four different areas, motion (associated with the colour blue), power supply (red), laser sensor (green) and the general items (yellow). The items in the first three areas are visible and active depending on the status of the three coloured switches under the motion area. If any of those switches are OFF the corresponding equipment will not execute any task when the start button is pressed.

1.1 Motion Objects (blue area)

- *(1) Moving* – If the LED is ON (red) indicates the welding head is performing some form of motion;
- *(2, 3) Torch Up, Torch Down* – Moves the torch vertically to alter the torch stand-off. The amount moved is influenced by the *Multiplier* value. It will move either 1 or 10mm;
- *(4, 5) Torch Left, Torch Right* – Moves the torch horizontally to change the centre point of the oscillation. The amount moved is influenced by the *Multiplier* value. It will move either 1 or 10mm;
- *(6) Multiplier* – Determines if the jog movements are in steps of 1 or 10mm each;
- *(7) Automatic Stop* – If ticked it means that the travel motion will be limited from the home position to a predefined position;
- *(8) Forward, (9) Backward* – Moves the specimen bed forward and backward respectively. The amount moved is influenced by the *(6) Multiplier* value. It will move either 1 or 10mm*;*
- *(10) OSC Without Running* – This binary switch allows oscillating the torch without running any of the other motion, PS or laser functions. This allows testing of the oscillation prior to welding;
- *(11) Read Angle* – Once this object is pressed the welding head and specimen bed angular position is read and the value is placed in *(12) Angle*;
- *(12) Angle* – Indicates the welding carrier and specimen's bed angular position after *Read Angle* is pressed. Value in degrees;
- *(13) Read Position* – Once this object is pressed the position of the specimen's bed in relation to the homing position is read and the value is placed in *(14) Position*;
- *(14) Position* – Indicates the specimen's bed position in relation to the homing position. Value in encoder counts;
- *(15) Centre Torch* – Moves the torch in/out so that it reaches a previously configured torch centre point. This configuration is made by pressing *Save Torch Centre*;
- *(16) Home Torch* – Moves the torch in so it gets as close to the weld carrier's main body as possible. Make sure the torch is clear from the groove before homing the torch;
- *(17) Return* – Returns the specimen's bed to its homing position;
- *(18) Restart* – Resets the motion controller to clear any error that may have occurred;
- *(19) Motion State* – Indicates if the welding carrier is either in the *startup*, *initializing*, *ready*, *running*, *shutdown*, *error*, *com error*, *alarm error*, *system error* or *reset;*
- *(20) OCS Width* – Allows changing the amplitude of oscillation as well as to display the current value while it is being changed by the software and not the user;
- *(21) OSC Speed* – Regulates the torch speed of oscillation. Functions as a control and an indicator;

- *(22) Travel Speed* – Controls and indicates the welding head travel speed around the pipe.

1.2 Power Supply Objects (red area)

- *(23) Contactor* – If the LED is ON (blue) indicates the PS contactor is on;
- *(24) Work Point* – Sets the PS work point (Wire Feed Speed) selecting in the synergic curve the welding parameters according to the WFS;
- *(25) Wire* – Jogs the wire IN or OUT depending on the direction selected. This is a tri-state switch and it needs to be OFF for the wire to be halted;
- *(26) Gas Purge* – Binary switch that allows purging the gas. It needs to be turned ON for the gas to flow and OFF for it to stop. This object will only work while the PS is in Ready state;

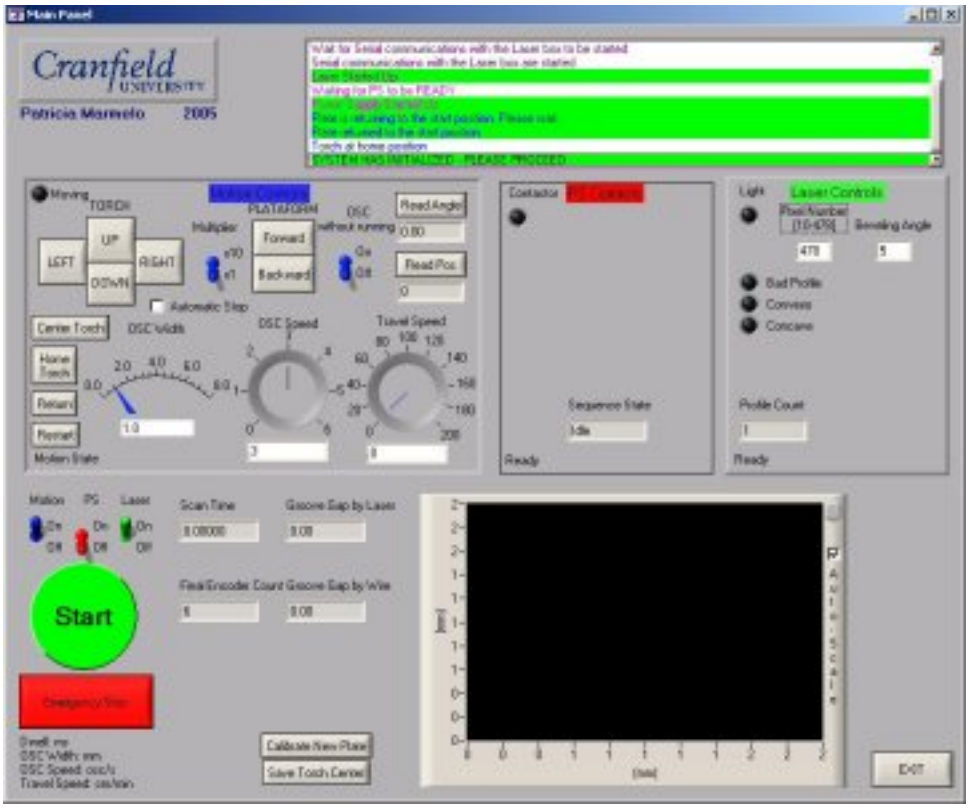

Figure E.1.1.2 – Rig Single Software Screenshot, PS Switch OFF.

- *(27) WFS-TS Ratio* – If ticked the ratio between the WFS and the Travel Speed (TS) will be kept constant. The main value is the TS, the WFS will be calculated in relation to the set TS;
- *(28) Mode* – Allow selecting the weld mode between the available ones. It is only possible to change the mode while the PS is in Ready state, meaning contactor OFF;

- *(29) Sequence State* – Indicates the Weld state, the same states as defined in the "Mode XXX.scm" file;
- *(30) State* – Indicates the PS state;
- *(31) WFS* – While welding indicates the instantaneous wire feed speed.

1.3 Laser Sensor Objects (green area)

- *(32) Light* – If the LED is ON (green) indicates the laser light is ON;
- *(33) Pixel Number* – Number of pixels to be acquired per profile. Number between 10 and 478, with 478 being the maximum of possible points to be acquired by the sensor and 10 being the minimum two digit number;
- *(34) Bevelling Angle* – Angle at which the groove walls were bevelled;
- *(35) Bad Profile* – If the LED is ON (yellow) indicates groove shape is inappropriate;
- *(36) Convexo* – If the LED is ON (red) indicates the groove bottom has a concave shape;
- *(37) Concave* – If the LED is ON (green) indicates the groove bottom has a concave shape;
- *(38) Rescan* – This object appears after a run is performed. Pressing button causes the specimen's bed to return to the home position. Afterwards a scan will be performed at the same position it was performed during the previous run;
- *(39) Continue* – Once the laser sensor reaches the first rescan the motion is halted and the system will wait for the user to press this object to perform the remaining scans;
- *(40) Profile Count* – Indicates the number of profiles acquired in the current run;
- *(41) State* – Indicates the Laser sensor state;

1.4 General Purpose Objects (yellow)

- *(42) Initialise* – When ON (red) indicates the system is initialising. Once the initialisation is completed the object disappears;
- *(43) Log* – The log list box lists in a timeline of events occurred since the program started. The message background colour indicates the message severity:
    - *White* – Normal;
    - *Green* – Status (ex. PS ON);
    - *Yellow* – Interventions: user intervention is required to correct an unexpected situation;
    - *Red* – High: a very serious situation occurred and the PS contactor will be turned OFF;
- *(44) Motion* – Binary switch that determines if the Motion sub-system is going to run or not once *Start* button is pressed. Once *Start* is pressed the switch is disabled and is enabled again when *Stop* is pressed;

- *(45) PS* – Binary switch that determines if the PS sub-system is going to run or not once *Start* button is pressed. Once *Start* is pressed the switch is disabled and is enabled again when *Stop* is pressed;
- *(46) Laser* – Binary switch that determines if the Laser sub-system is going to run or not once *Start* button is pressed. Once *Start* is pressed the switch is disabled and is enabled again when *Stop* is pressed;
- *(47) Scan Time* – Indicates the time required to process the data acquired in the last scan;
- *(48) Groove Gap by Laser* – Indicates the groove gap measured by the laser sensor at the groove bottom;
- *(49) Final Encoder Count* – Indicates the final encoder count of the last movement;
- *(50) Groove Gap by Wire* – Indicates a manual measurement of groove gap and groove centre by positioning the wire at each end of gap of the groove bottom;
- *(51) Start/Stop* – This is a bi-stable button whose default value (OFF - green) is *Start.* When pressed it starts the motion, PS and laser sub-systems, and changes to (ON - red) *Stop,* waiting for the user to press it and stop the referred sub-systems;
- *(52) Emergency Stop* – This button is an emergency stop button to be pressed when a problem occurs and the entire system halts immediately;
- *(53) Avg Volt* – Indicates the average voltage from the welding arc measured through the PS;
- *(54) Avg Cur* – Indicates the average current from the welding arc measured through the PS;
- *(55) Avg WFS* – Indicates the average WFS measured through the PS;
- *(56) Calibrate New Plate* – Once pressed, this button set in motion the plate calibration procedure. It will guide the user through-out the process of calibrating a new plate. This button should be pressed when a new plate is inserted to verify its alignment;
- *(57) Save Torch Centre* – Pressing this button sets the current torch position as at the groove centre in terms of oscillation;
- *(58) Graph* – In this graph is shown the acquired profile is shown while the weld is being performed/scanned or rescanned. After a scan or rescan task is performed the graph will continue to show the last result;
- *(59) Exit* – Stops the motion controller, PS and laser and their respective communications and closes the user interface.

2 Dual/Tandem

The dual/tandem version of this program is capable of handling two PSs. The principle and mode of operation is the same as the single version. The differences, both in terms of operation and design reflect the use of a second PS. These differences can be seen in Figure E.1.1.1 and Figure E.2.2.1.

2.1 Motion Objects (blue area)

The objects in the blue area are the same and perform the same tasks as in the single version of the software. For their description see section 1.1

2.2 Power Supply Objects (red area)

In this area is where the most changes lie. With the need to deal with two PSs the amount of required objects more than doubled. In order to accommodate the required objects and still maintaining the user interface dimension the same the PS and laser areas were re-arranged. An extra window (PSs Controls) was created and can be called when extra settings need to be changed. The changes to the main window can be seen in Figure E.2.2.1 and the PSs Controls window can be seen in Figure E.2.2. A description of the PS objects in main window follow next and the ones contained in the PSs Controls window will be described afterwards.

2.2.1 Main Window Objects

- *(23a, 23b) Contactor* – If the LED is ON (blue) indicates the PS contactor is ON;
- *(25a, 25b) Wire* – Jogs the wire IN or OUT depending on the direction selected. This is a tri-state switch and it needs to be OFF for the wire to be halted;
- *(26a, 26b) Gas Purge* – Binary switch that allows purging the gas. It needs to be turned ON for the gas to flow and OFF for it to stop. This object will only work while the PS is in Ready state;
- *(30a, 30b) State* – Indicates the PS state;
- *(31a, 31b) WFS* – While welding indicates the instantaneous wire feed speed;
- *(53a, 53b) Avg Volt* – Indicates the average voltage from the welding arc measured through the PS;
- *(54a, 54b) Avg Cur* – Indicates the average current from the welding arc measured through the PS;
- *(55a, 55b) Avg WFS* – Indicates the average WFS measured through the PS;

- *(62) Synchronous Work Point* – Determines if the WP in both PSs is synchronised or not. If the button is pressed (light blue colour) the WPs will be synchronised and the value in both PSs will be the one selected in PS 1. If not pressed (dark blue colour) the PSs will have independent WP values. The synchronism can be changed either with the PSs idle or welding;

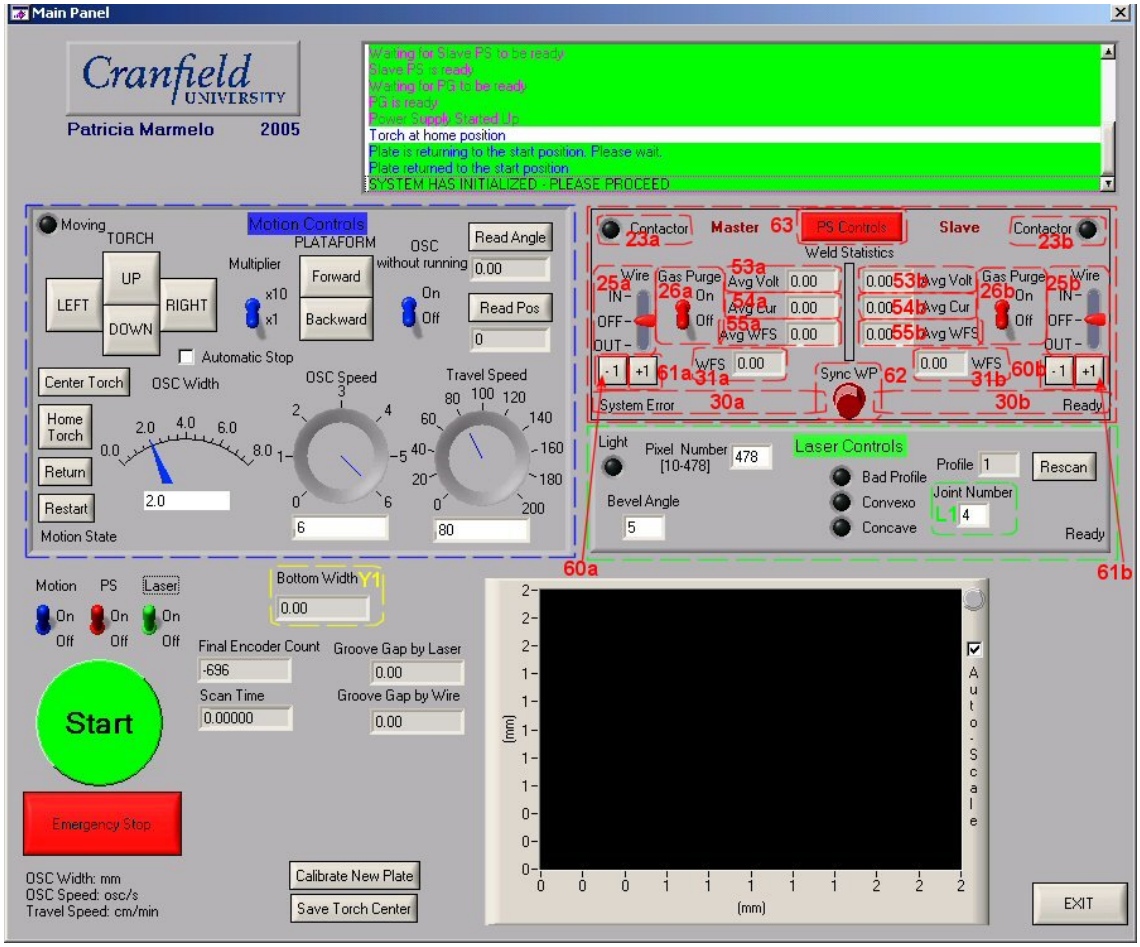

Figure E.2.2.1 – Rig Dual/Tandem Software Screenshot with Numbered Objects.

- *(63) PS Controls* – This is bi-stable button, once pressed (dark red colour) the secondary window containing the other PS controls becomes visible. At this point is possible to alter the welding settings. To hide again the window this button should be pressed, it will go OFF (red colour).

The jumps in the numeration occur to maintain the numbering on the single software. The missing numbers can be found in the secondary window. All the “a” represent the master PS and the “b” represent the Slave PS.

2.2.1.1 PSs Controls Window Objects

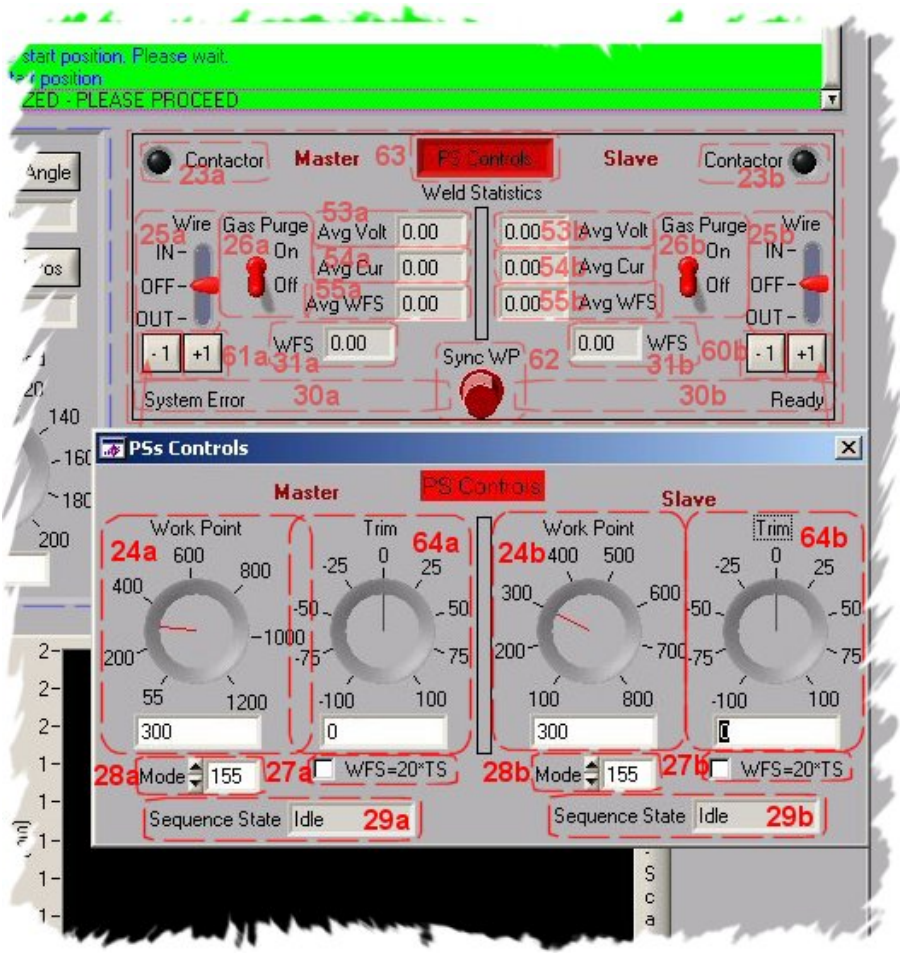

Figure E.2.2 – Detail of Rig Dual/Tandem Software Screenshot with Numbered Objects Showing the PSs Controls Window.

- *(24a, 24b)* *Work Point* – Sets the PS work point (Wire Feed Speed) selecting the welding parameters on the synergic curve according to the WFS;
- *(27a, 27b)* *WFS-TS Ratio* – If ticked the ratio between the WFS and the Travel Speed (TS) will be kept constant. The main value is the TS, the WFS will be calculated in relation to the set TS;
- *(28a, 28b)* *Mode* – Allow selecting the weld mode from the available modes. It is only possible to change the mode while the PS is in Ready state, meaning contactor OFF;
- *(29a, 29b)* *Sequence State* – Indicates the Weld state, the same states as defined in the "Mode XXX.scm" file;
- *(64a, 64b)* *Trim* – Sets the trim value between ±100%.(Trim adjusts arc length)

2.3 Laser Sensor Objects (green area)

In this area together with the previously described objects there is an extra object, *(L1)* *Joint Number*. In *Joint Number* the pre-configured joint can be selected. Prior to scanning, the joint type and its configurations need to be set in the *WinUser*™ software. Each configured joint automatically is associated with a number. This number is attributed sequentially and each set of configurations can be applied by selecting the appropriate joint number. The description of the remaining objects can be found in 1.3.

2.4 General Objects (yellow)

There are some alterations to these objects. The indicators showing the Average Voltage *(53)*, Current *(54)* and WFS *(55)* in the single version of the program are not present in the dual/tandem version. These objects are in this version of the software part of the PSs area and their description can be found in 2.2.1. An extra indicator can be found, the *(Y1)* *Bottom Width*. This object indicates the groove bottom width based on the laser scan reading. The description of the remaining objects can be found in 1.4.

Appendix F SP7 – *Analysis* Software

The software developed to analyse the data acquired from the laser vision sensor in depth was SP7, named *Analysis*. Unlike the previous software developed, the SP7 was not designed to control any equipment. It was developed with the intent of evaluating the data acquired by the digital oscilloscope and either SP4, SP5 or SP6. The data generated by the SP5 and SP6 includes both the laser vision sensor data and the welding voltage, current and WFS retrieved from the PS.

SP7 was developed over an extensive period of time and was progressively modified as new algorithms were created to provide specific information on weld shape and quality. Only the final version of the software is described here.

This software has five windows: *Sensor Selection*, *Data Analysis*, *Feature Selection*, *Weld 3D Model* and *Waveforms*. Each of these windows and the purpose they serve is described below.

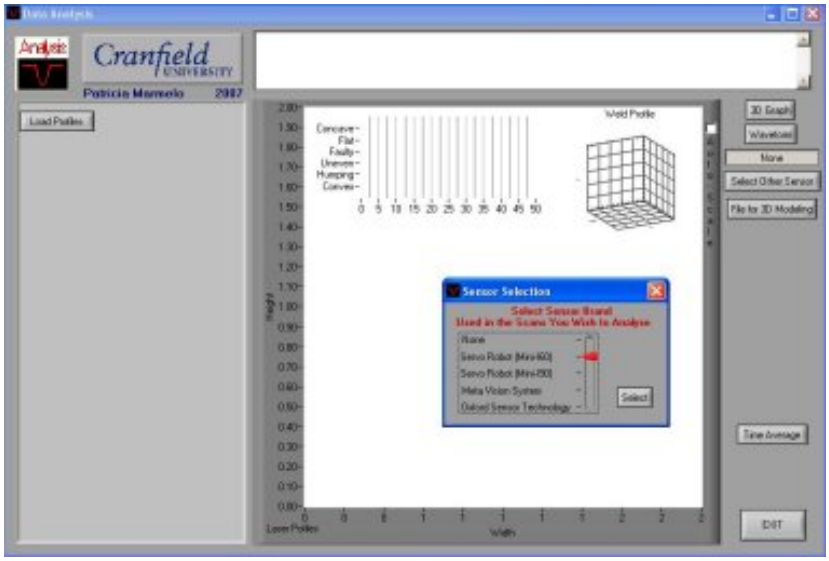

Figure F.0.1 – Screenshot of the *Analysis* Software Immediately after Start-up.

1 Sensor Selection Window

This window pops-up at start-up to allow for the selection of the sensor used in the scans that are to be evaluated. Depending on the sensor used some of the program features may/may not be available and some settings differ from sensor to sensor which needs to be taken in consideration. Object *(1) Sensor Model* (Figure F.1.1) allows for the use of four different sensors or none. The selection of the option “None” implies that no laser vision sensor data is going to be examined. When this option is selected it is still possible to use some of the program options,

including data files from the digital oscilloscope and the *Rig* software. The Mini-I60 was used to perform the majority of the work and the other sensors were used for comparison. Object *(2) Select* makes the *Sensor Selection* window disappear and sets the sensor type to the one selected in the *Sensor Model* object. The sensor type can be altered at any time during the execution of the program by pressing *(11) Sensor* in the *Data Analysis* window.

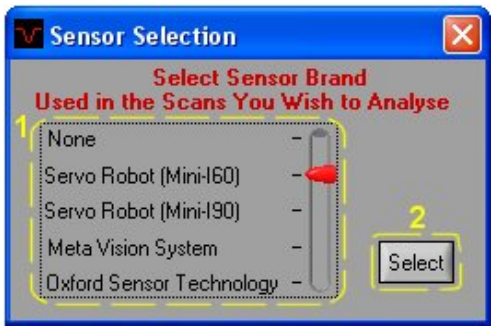

Figure F.1.1 – *Sensor Selection* Window Screenshot with Numbered Objects.

2 Data Analysis Window

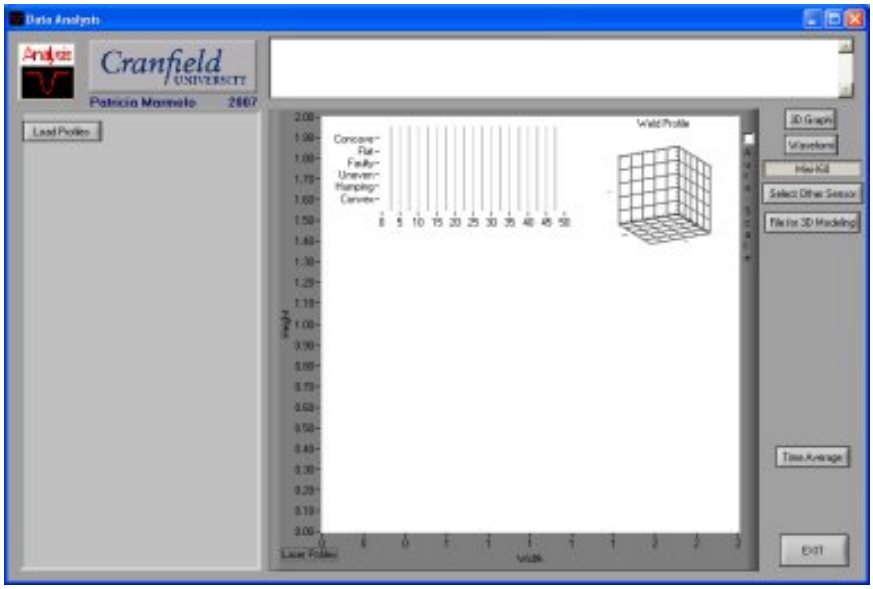

Figure F.2.1 – *Data Analysis* Window Screenshot before a Laser Scan File is Selected.

Once the sensor type is chosen the *Sensor Selection* window disappears leaving only the *Data Analysis* (main) window visible. Until the *Load Profiles* button is pressed the window remains as can be seen in Figure F.2.1. At this stage the number of possible actions is limited to six tasks,

including: selection of the laser data files to be loaded; opening a widow to examine the 3D profile of a weld; opening another window to analysis the files containing the electrical characteristics of a weld; opening a window to select a different sensor type; generating a file for a 3D modelling external program; time averaging a laser data file (if the sensor selected is from Servo Robot); or quit the program.

On Figure F.2.2 is possible to see all the objects present in the *Data Analysis* window once a set of files is loaded and their analysis can begin. A brief description of the user interface and its functionalities follows next.

- *(0) Logo* – Area where the University logo, developer's name and version date is shown;
- *(3) Log* – The log list box lists in a timeline of events which have occurred since the program started. The message background colour indicates the message severity:
    - *White* – Normal;
    - *Green* – Status (ex. PS ON);
    - *Yellow* – Interventions: user intervention is required to correct an unexpected situation;
    - *Red* – High: a very serious situation occurred and the PS contactor will be turned OFF;
- *(4) Load Profiles* – Once this button is pressed a series of windows pop-up. First laser data files containing the pre-scan and post-scan data must be selected. Next it is necessary to input the number of points per profile and the groove bevelling angle;
- *(5) Laser Profiles* – A 2D graph showing the profiles being analysed. The pre-scan profile can be seen in the red colour and the post-scan profile in the dark red colour. In case both files loaded are the same only one profile will be seen, it will be the post-scan one;
- *(6) Weld Quality Trace* – A graph showing the result of the concavity and quality analysis of the profiles. It only shows the results relative to the pre-scan profile;
- *(7) Weld Profile* – A 3D graph showing the weld profile from the first profile to the last that has been analysed. Every time the *(18) Next Frame* button is pressed or while the *(16) Play* button is ON the graph is updated;
- *(8) Auto-Scale* – If ticked indicates the scales in *(5) Laser Profiles* graph are automatic otherwise they are determined by the sensor type;
- *(9) 3D Graph* – Pressing this button shows the *3D Weld Model* window*;*
- *(10) Waveform* – Pressing this button shows the *Waveforms* window;
- *(11) Sensor* – Indicates the sensor type that was selected in the *Sensor Selection* window;

- *(12) Select Other Sensor* – Pressing this button show the *Sensor Selection* window so a different sensor can be selected;
- *(13) File for 3D Modelling* – Once this button is pressed a window pops-up, requesting the data file. The data (all the profiles) is exported into a .csv file on a particular format to be input into an external program in order to generate a 3D model of the weld;
- *(14) Time Average* – Pressing this button sets the *Data Analysis* window into a mode in which the profiles are processed in groups of three. This is better explained in 3;
- *(15) Exit* – Closes the user interface;
- *(16) Play* – This is a bi-stable button, when OFF it has the label “Play” and when ON it has the label “Stop” Pressing this button when it is on the OFF state activates a timer and when ON it stops the timer. Every time the timer is up another weld profile is read and analysed. Simulates *(18) Next Frame* being pressed continuously on a regular bases;

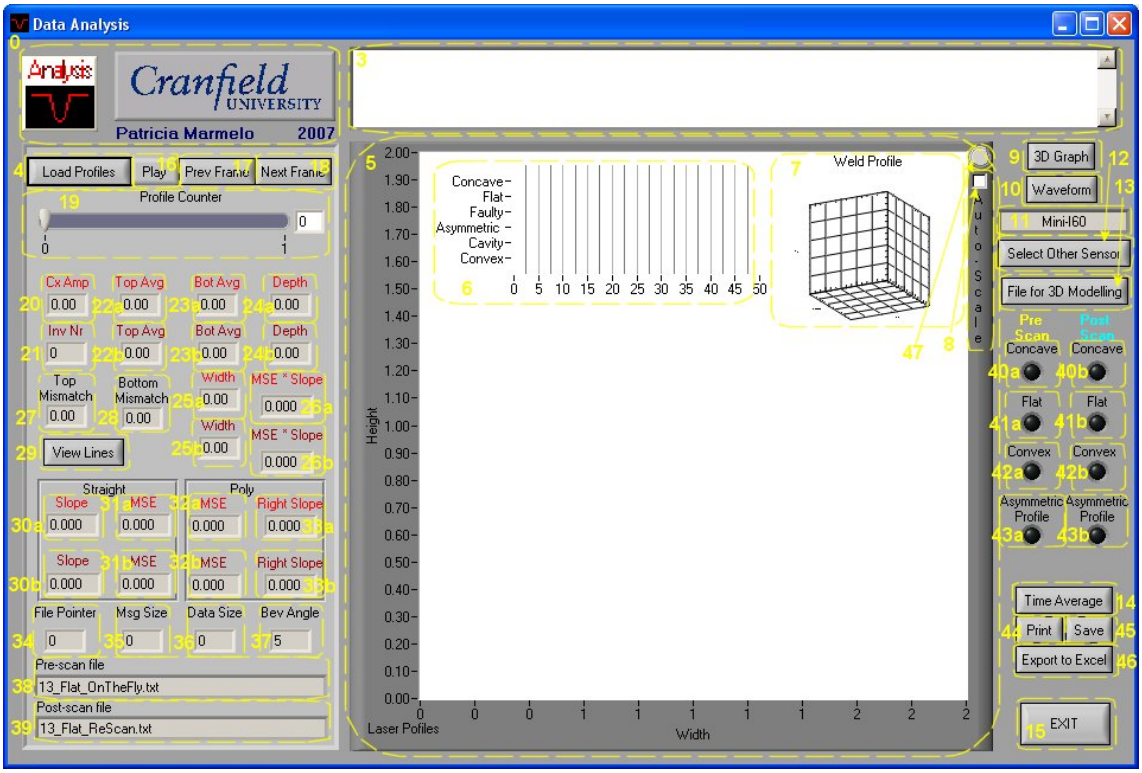

Figure F.2.2 – *Data Analysis* Window Screenshot with Numbered Objects.

- *(17) Prev Frame* – Pressing this button decrements the profile counter and reads a block of data containing the previous profile. This data is then analysed and shown in the screen. Once the *(19) Profile Counter* reaches one it cannot decrement anymore and even if this object is pressed again profile one will be processed again;

- *(18) Next Frame* – Pressing this button increments the profile counter and reads a block of data containing the next profile. This data is then analysed and shown in the screen. When this object is pressed and the *(19) Profile Counter* is already showing the last profile (the end of the data file was reached) the *(19) Profile Counter* will be set to one the profiles are shown again. The same occurs when the *(16) Play* object is still ON and the end of the data file is reached;
- *(19) Profile Counter* – This is numerical slide which both indicates the number of the profile being shown and allows selecting another one*;*
- *(20) Cx Amp* – Indicates the convexity amplitude, meaning the convexity depth on the pre-scan profile;
- *(21) Inv Nr* – Indicated the number of inversions of direction in the shape of the groove bottom, in the post-scan profile;

The red colour is the value of the pre-scan profile and the dark red the one for the post-scan profile from objects

- *(22a, 22b) Top Avg* – Indicates the average height of the specimen top surface.
- *(23a, 23b) Bot Avg* – Indicates the average height of the specimen bottom surface;
- *(24a, 24b) Depth* – Indicates the groove depth of the specimen, based on the top and bottom groove corners;
- *(25a, 25b) Width* – Indicates the groove width at the bottom corners, meaning the groove bottom width;
- *(26a, 26b) MSE * Slope* – Shows the multiplication value of the MSE (mean square error) with the slope (inclination) of the polynomial line fitted to the groove bottom. It is used as an indication of the quality of the fitted line, and was used to develop the algorithms to determine the weld quality and shape;
- *(27) Top Mismatch* – Indicates the mismatch in the height of the specimen top surfaces;
- *(28) Bottom Mismatch* – Indicates the mismatch in the height of the specimen top surfaces;
- *(29) View Lines* – Once this button is pressed *Feature Selection* window pops-up. This window contains a series of tick boxes representing different data that can be shown in the *Data Analysis* window or not;
- *(30a, 30b) Slope (Straight)* – Indicates the slope (inclination) of the straight line fitted to the groove bottom. It is used as an indication of the quality of the fitted line, used to develop the algorithms to determine the weld quality and shape. The red colour is the value of the pre-scan profile and the dark red the one for the post-scan profile;
- *(31a, 31b) MSE (Straight)* – Indicates the MSE (mean square error) of the straight line fitted to the groove bottom. It is used as an indication of the quality of the fitted line, was used to develop the algorithms to determine the weld quality and shape. The red colour is the value of the pre-scan profile and the dark red the one for the post-scan profile;

- *(32a, 32b)* *MSE (Poly)* – Indicates the MSE (mean square error) of the polynomial line fitted to the groove bottom. It is used as an indication of the quality of the fitted line, used to develop the algorithms to determine the weld quality and shape. The red colour is the value of the pre-scan profile and the dark red the one for the post-scan profile;
- *(33a, 33b)* *Right Slope (Poly)* – Indicates the slope (inclination) of the polynomial line fitted to the groove bottom. It is used as an indication of the quality of the fitted line, used to develop the algorithms to determine the weld quality and shape. The red colour is the value of the pre-scan profile and the dark red the one for the post-scan profile;
- *(34)* *File Pointer* – Indicates the file pointer to the end of the profile data set;
- *(35)* *Msg Size* – Indicates the message block size in the profile data set;
- *(36)* *Data Size* – Indicates the data block size in the profile data set;
- *(37)* *Bev Angle* – Indicates the groove wall bevel angle;
- *(38)* *Pre-Scan File* – Indicates the pre-scan file being used;
- *(39)* *Post-Scan File* – Indicates the post-scan file being used;
- *(40a, 40b)* *Concave* – If the LED is ON (green) indicates the groove bottom has a concave shape The “a” object is the value of the pre-scan profile and the “b” the one for the post-scan profile;
- *(41a, 41b)* *Flat* – If the LED is ON (yellow) indicates the groove bottom has a flat shape The “a” object is the value of the pre-scan profile and the “b” the one for the post-scan profile;
- *(42a, 42b)* *Convex* – If the LED is ON (red) indicates the groove bottom has a convex shape The “a” object is the value of the pre-scan profile and the “b” the one for the post-scan profile;
- *(43a, 43b)* *Asymmetric Profile* – If the LED is ON (yellow) indicates the groove bottom has a asymmetric shape The “a” object is the value of the pre-scan profile and the “b” the one for the post-scan profile;
- *(44)* *Print* – Once this button is pressed a window pops-up asking if the user wants to print the entire *Data Analysis* window or just *(5)* *Laser Profiles* graph (see Figure F.2.3). The cancel option is also present. The printing options window follows to conclude the process;
- *(45)* *Save* – Pressing this button causes the entire *Data Analysis* window to be saved into a “.jpeg” file in the hard drive. The image is saved in the same directory the pre-scan file is located. The file’s name will be composed of the pre-scan file name plus a time stamp. In case a file already exists with the same name the user is prompted decide if the file should be replaced or a new one should be saved (with an incremental name);
- *(46)* *Export to Excel* – Pressing this button causes the data from the profile being analysed to be exported to an excel file;

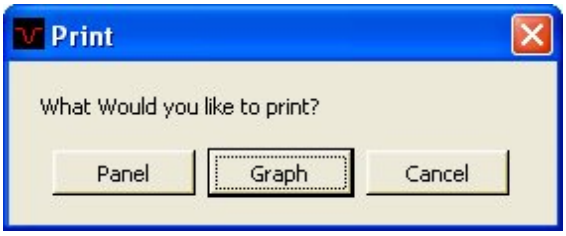

Figure F.2.3 – 2D Graph Print Selection Window.

- *(47) Processing* – This LED indicates if the program is processing data or is waiting for a user input or action. Grey colour indicates the program is idle and red colour indicates it is processing;

3 Time Average Mode

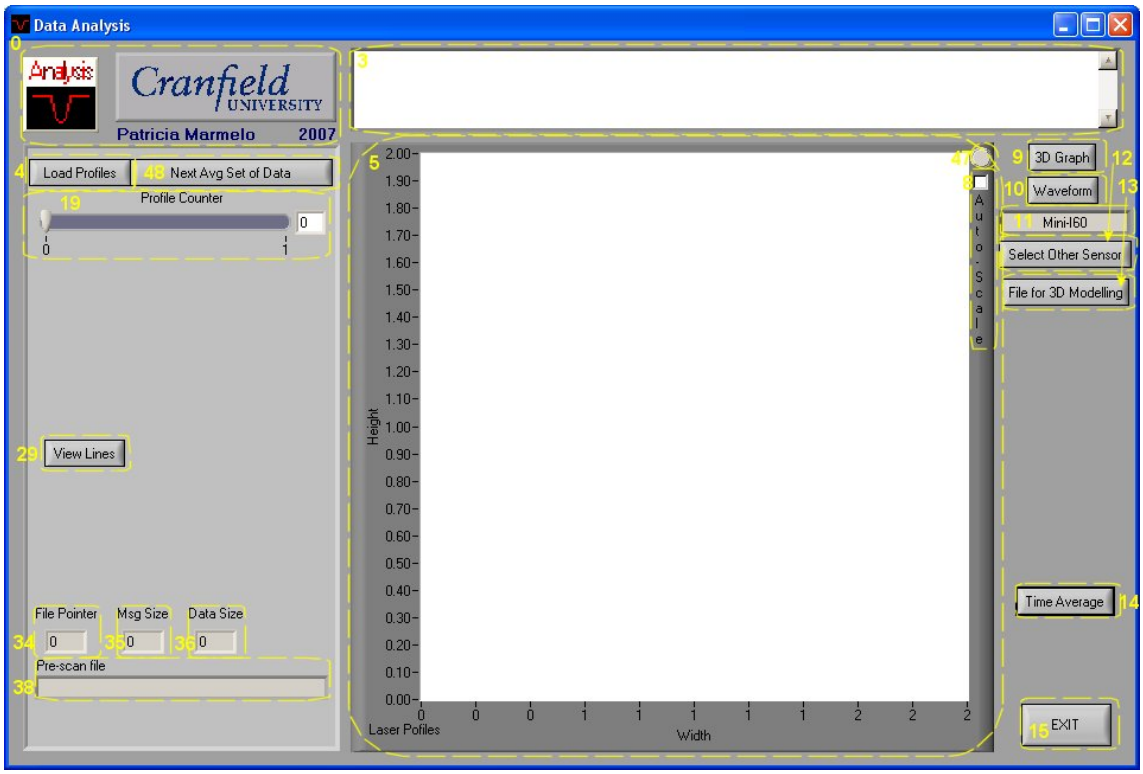

Figure F.3.1 – *Data Analysis* Window on Tome Average Mode Screenshot with Numbered Objects.

When the *Time Average* button is pressed the *Data Analysis* window changes, showing a reduced number of objects. The objects in this mode can be seen in Figure F.3.1. Apart from object *(48) Next Avg Set of Data* that does not appear in the in the previous window modes the

other objects present in the window are: *(0) Logo; (3) Log; (4) Load Profiles; (5) Laser Profiles; (8) Auto-Scale; (9) 3D Graph; (10) Waveform; (11) Sensor; (12) Select Other Sensor; (13) File for 3D Modelling; (14) Time Average; (15) Exit; (19) Profile Counter; (29) View Lines; (34) File Pointer; (35) Msg Size; (36) Data Size; (38) Pre-Scan File* and *(47) Processing*. Object *(48) Next Avg* has a similar function to *(18) Next Frame* object. It plots the next profile but in this case the next profile is not an actual profile from the laser sensor but the average value of each of the points in three consecutive laser scans. When the button is pressed for the first time the routine loads the first three profiles from the data file, makes the average of each of the data points and stores it in a temporary variable. In this variable that is then processed as a normal profile from the laser sensor. After the first three profiles being loaded, the next time the button is pressed only one new profile is acquired from the laser data file and used to calculate the new average. This new average contains only three profiles which mean that the one with the lowest profile index is discarded and replaced by the new one.

4 Feature Selection Window

In this panel the extra features that can be seen in the *(5) Laser Profiles* graph can be selected. The features are shown in both profiles and as was mentioned in relation to the *(5) Laser Profiles* graph the pre and post-scan data is shown in the same colour but in different shades. The light colour shade is associated with the pre-scan profile and the dark shade is associated with the post-scan profile. That can be seen in Figure F.4.2 and Figure F.4.3. The description of the object in the *Feature Selection* window (Figure F.4.1) can be found below.

- *(49) Breakpoints* – Determines if the calculated breakpoints are shown in the *(5) Laser Profiles* graph or not. If the box if ticked the breakpoints are shown if not this feature will be hidden;
- *(50) Groove Walls* – Determines if the calculated groove walls are shown in the *(5) Laser Profiles* graph or not. If the box is ticked the groove walls are shown if not this feature will be hidden. The groove walls are calculated based on fitted lines applied to the data segments that constitute both top surfaces and both sidewalls;
- *(51, 52, 53) Toe Angle 1, 2, 3* – Determines if the calculated toe angles are shown in the *(5) Laser Profiles* graph or not. If the box if ticked each of the toe angles are shown if not these features will be hidden. The different toe angles are calculated based on different approaches to the profile data;
- *(54) Poly Long Bottom 1* – Determines if the calculated bottom shape is shown in the *(5) Laser Profiles* graph or not. If the box is ticked, the bottom shape is shown if not this feature will be hidden. The bottom shape is calculated based on the fitting of a

polynomial line to the groove bottom data; The algorithm that calculates the groove bottom based on the polynomial line approach can be seen in section 8.1.3.12;

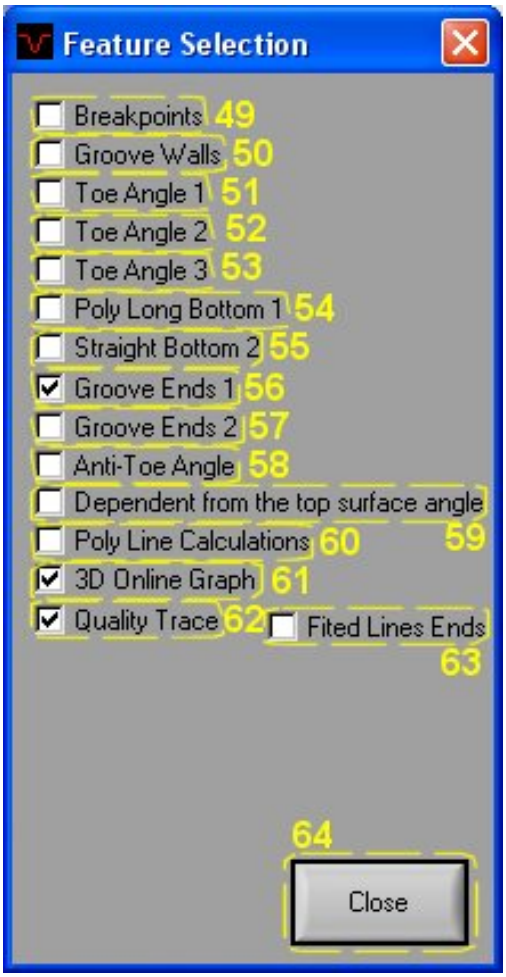

Figure F.4.1 – *Feature Selection* Screenshot with Numbered Objects.

- *(55) Straight Bottom 2* – Determines if the calculated bottom shape shown in the *(5) Laser Profiles* graph or not. If the box if ticked the bottom shape is shown if not this feature will be hidden, The bottom shape is calculated based on the fitting of a straight line to the groove bottom data;
- *(56, 57) Groove Ends 1, 2* – Determines if the calculated groove ends are shown in the *(5) Laser Profiles* graph or not. If the box if ticked the groove ends are shown if not this feature will be hidden. *Groove Ends 1* and *2* are calculated based on two different approaches in order to determine which approach generates more accurate results in each situation;
- *(58) Anti-Toe Angle* – Determines if the calculated "anti-toe" angles are shown in the *(5) Laser Profiles* graph or not. If the box if ticked the anti-toe angle are shown if not this feature will be hidden. By "anti-toe" should be understood not the opposite of the toe

angle but a toe angle value calculated based on a fitted line only to the first and last millimetre of the groove bottom. This value often returns a toe angle different to the toe angle calculated using all the data. Only the right side feature will be shown;

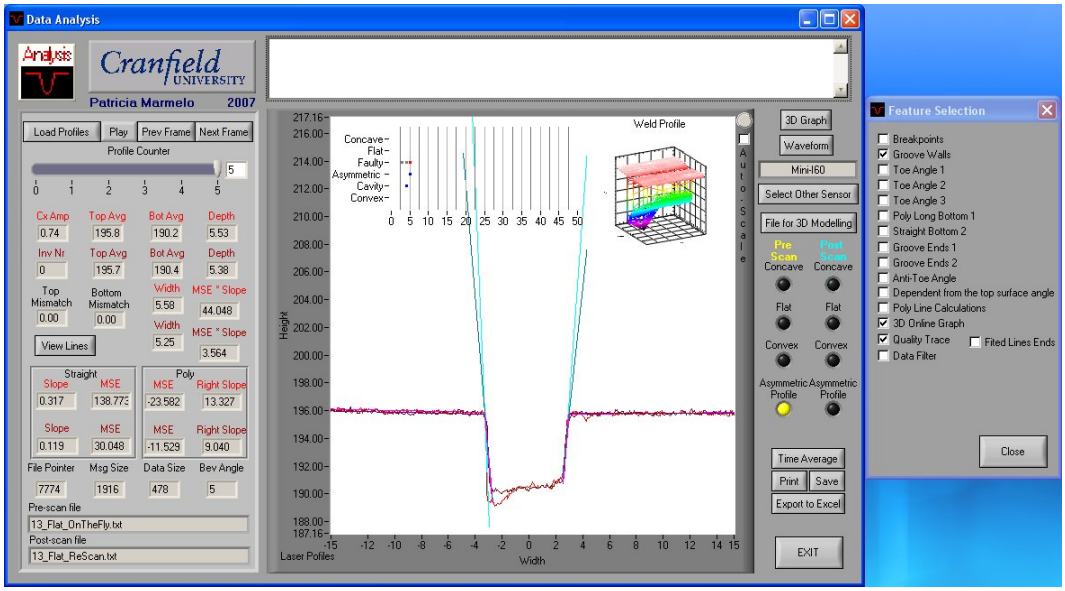

Figure F.4.2 – Data Analysis and Feature Selection Windows Screenshot Showing the Measured Groove Walls.

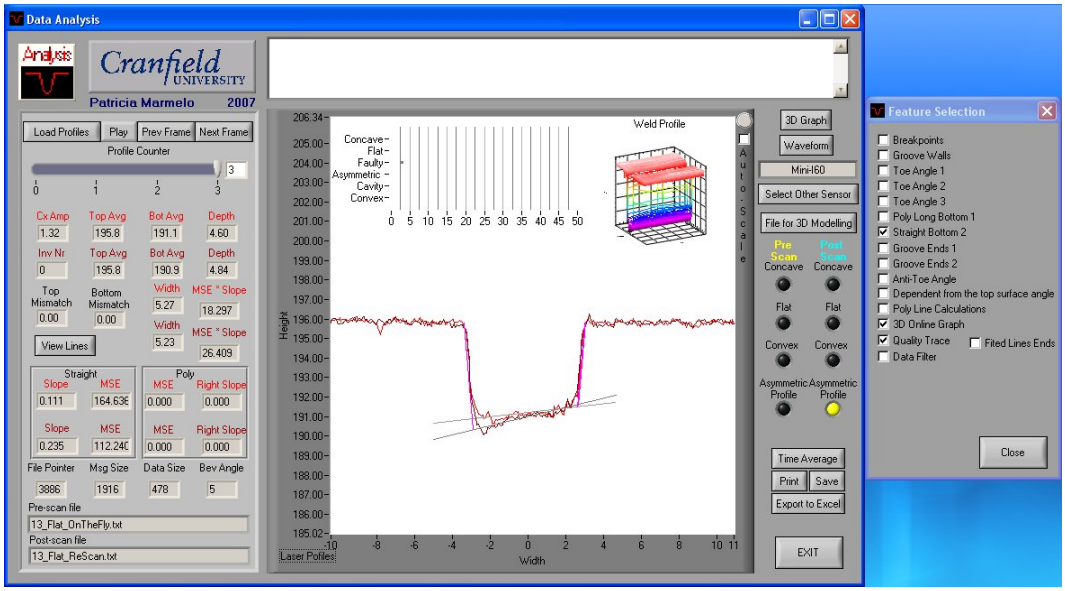

Figure F.4.3 – Data Analysis and Feature Selection Windows Screenshot Showing the Straight Groove Bottom.

- *(59) Dependent From the Top Surface Angle* – Determines if the expected groove walls based on the bevelling angle should be calculated having in consideration the inclination of the top surface walls or not. If the box if ticked the expected groove walls will have in consideration the top surface inclination if not the walls will be calculated merely based on the input bevelling angle. These lines act as a reference on where the groove walls are expected be by the software based on the bevelling angle;
- *(60) Poly Line Calculations* – Determines if the calculations should be made using a polynomial approach. If the calculations are made and the other appropriate features are selected they will be shown in the *(5) Laser Profiles* graph or not. If the box if ticked the features are calculated otherwise they are not;
- *(61) 3D Online Graph* – Determines if the 3D graph is visible on top of the *(5) Laser Profiles* graph or not. If the box if ticked the 3D graph is visible if not this feature will be hidden. The *3D Online Graph* shows a 3D representation of all the profiles analysed up to the one indicated in the *(19) Profile Counter* object;
- *(62) Quality Trace* – Determines if the quality trace graph is visible on top of the *(5) Laser Profiles* graph or not. If the box if ticked the quality trace graph is visible if not this feature will be hidden. The quality trace shows a summary of some of the conclusions extracted from each of the profiles analysed;

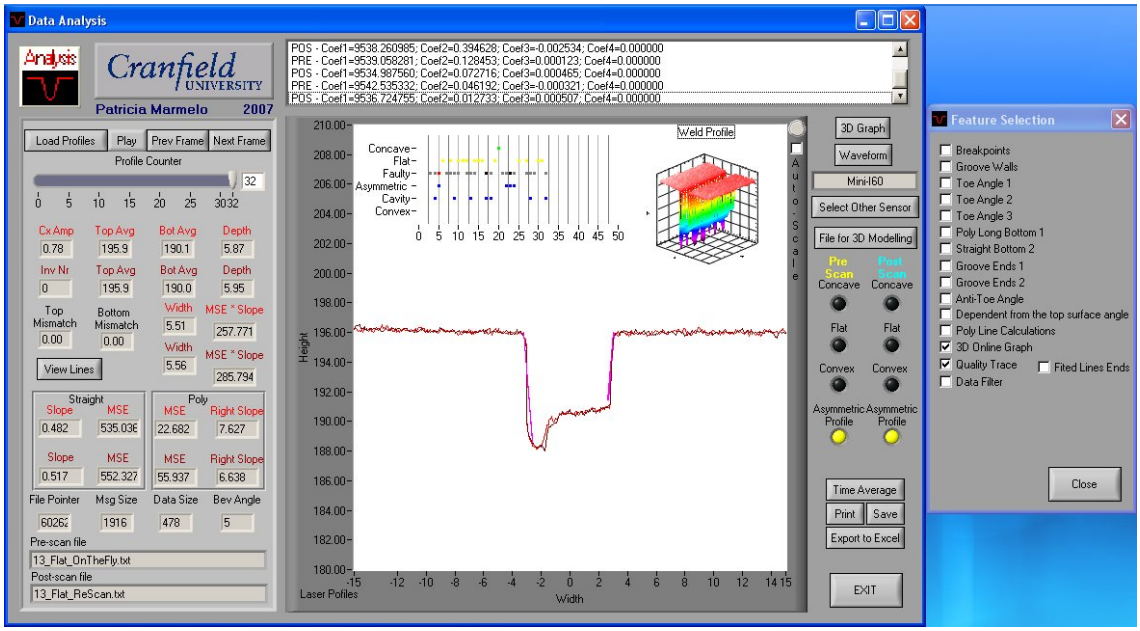

Figure F.4.4 – Data Analysis and Feature Selection Windows Screenshot with Visible Data.

- *(63) Fitted Line Ends* – Determines if the terminus of the fitted walls are shown in the *(5) Laser Profiles* graph or not. If the box if ticked the line ends are shown if not this feature

will be hidden. This applies to the top surface, groove walls and groove bottom fitted lines;

- *(64) Close* – Hides the *Feature Selection* window;

5 Weld 3D Model Window

Pressing *(9) 3D Graph* button shows the *Weld 3D Model* window. This window can be seen in Figure F.5.1 and the description of the objects in it can be found below. The aim of this window is to be able to load a laser scan from Servo Robot file and see the entire weld in 3D. It is also possible to see a transversal cut of such weld. The transversal cut is performed in two locations: the groove centre and the points where the groove has its lowest data points. See Figure F.5.4 and Figure F.5.5.

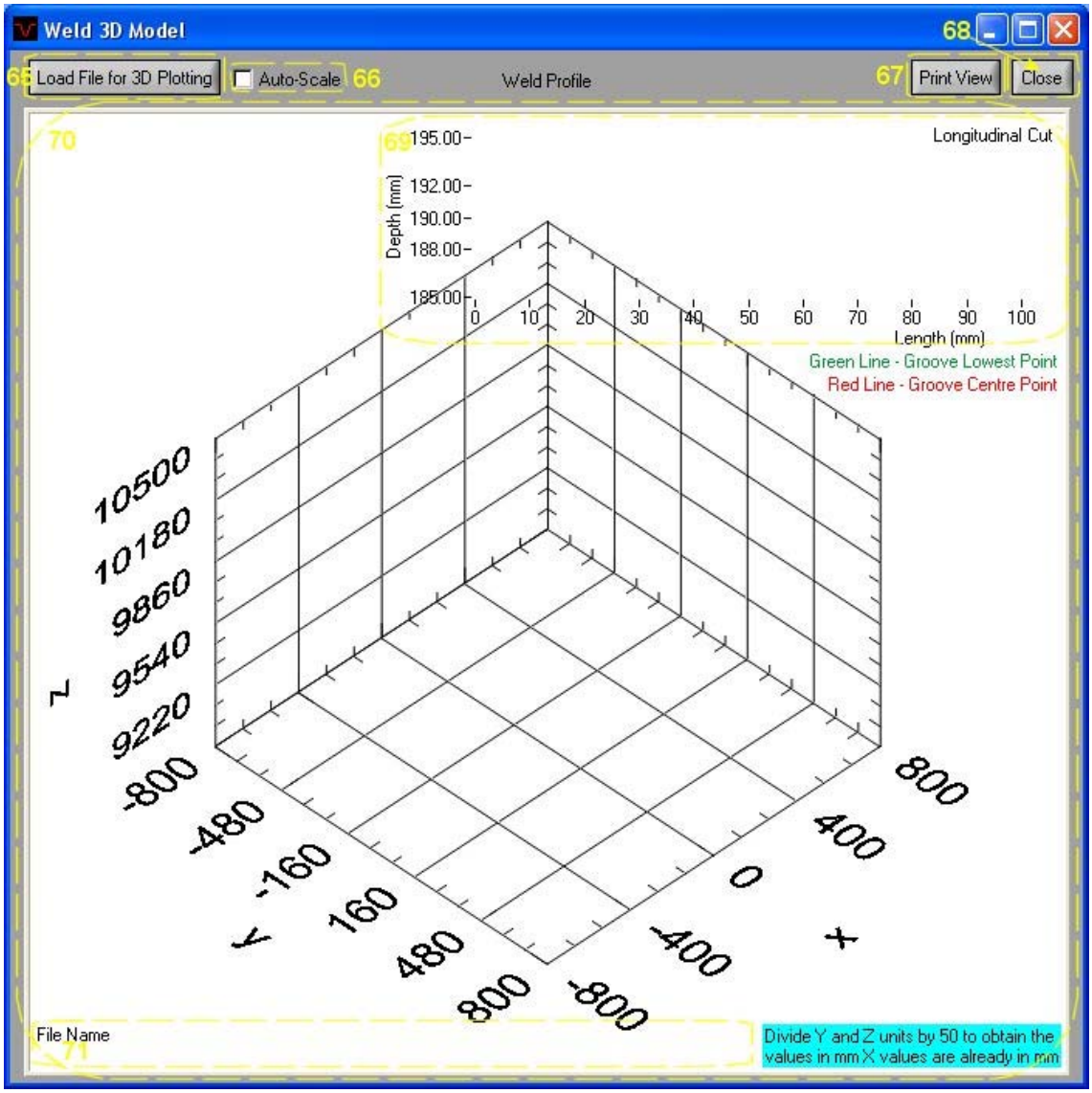

Figure F.5.1 – *Weld 3D Model* Screenshot with Numbered Objects.

- *(65) Load File for 3D Plotting* – Once this button is pressed two windows pop-up. The first requests the user to select a laser data file containing the scan data to be analysed, the other requests the scan positions file. The scan positions file contains the exact location, in terms of the *X* axis, of each of the performed scans;
- *(66) Auto-Scale* – Determines if the colour map in the *(70) Weld Profile* graph is automatic or not. If the box if ticked the colour map is automatic if not the colour map was set to fixed values. The fixed value colour map was selected in order to be possible to see the weld profile in a consistent manner specially when analysing the weld end shapes. This colour map was selected so the weld ends could be seen in greater detail;
- *(67) Print View* – Pressing his button causes a selection window to pop-up (see Figure F.5.2). In this new window is possible to select between saving and printing the contents of the *Weld 3D Model* window or to cancel the action. In case the user decides

to “save” the image the file will be saved with the profile data file name and a time stamp. It will be saved in the same directory as the profile data file is stored. A sample of the saved file can be seen in Figure F.5.3. In case the user decides to “print” the file a printing properties window appears. If “Cancel” is chosen no action will be taken and the selection window disappears;

- *(68) Close* – Hides the *Weld 3D Model* window;
- *(69) Transversal Cut* – This graph displays the weld specimen transversal cut performed in the groove centre (red colour) and a cut in the groove lowest points (green colour). This graph gives an indication of the height variation along the weld. This object is overlaid on top of *(70) Weld Profile* object;
- *(70) Weld Profile* – In this 3D graph, after the *(65) Load File for 3D Plotting* button is pressed and a profile data file is loaded, shows the 3D model of the scanned weld. This objects has pan (pressing “Shift+Ctrl”), zoom (pressing “Alt”) and rotation (pressing “Ctrl”) options activated;
- *(71) File Name* – This object shows the loaded profile data file name and path. This object is overlaid on top of *(70) Weld Profile* object;

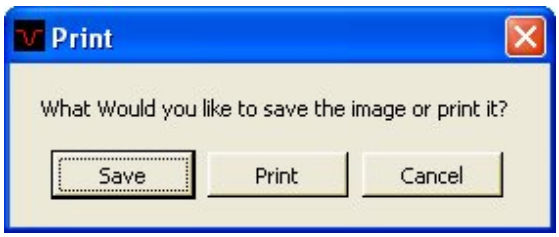

Figure F.5.2 – 3D Graph Print Selection Window.

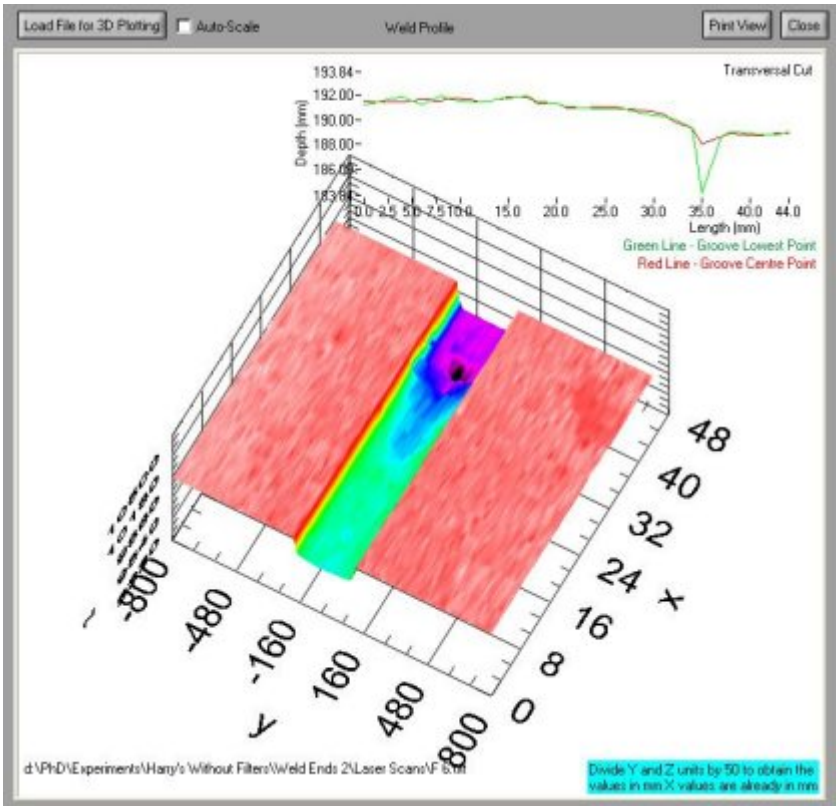

Figure F.5.3 – Sample Image of the Saved *Weld 3D Model* Window

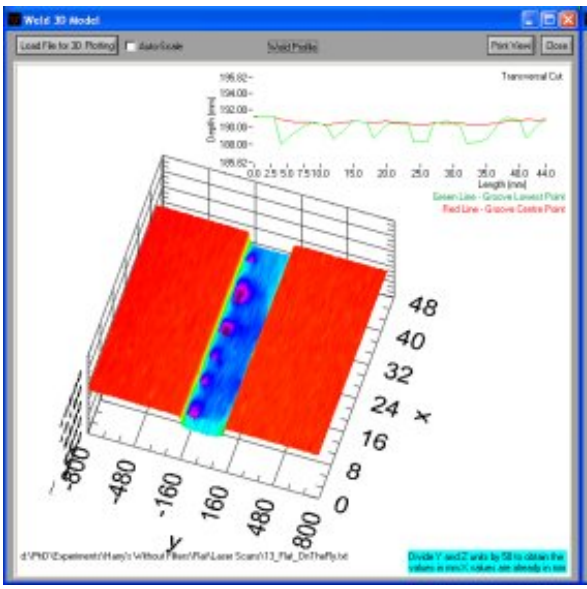

Figure F.5.4 – *Weld 3D Model* Window Screenshot Showing a Weld Mid Section.

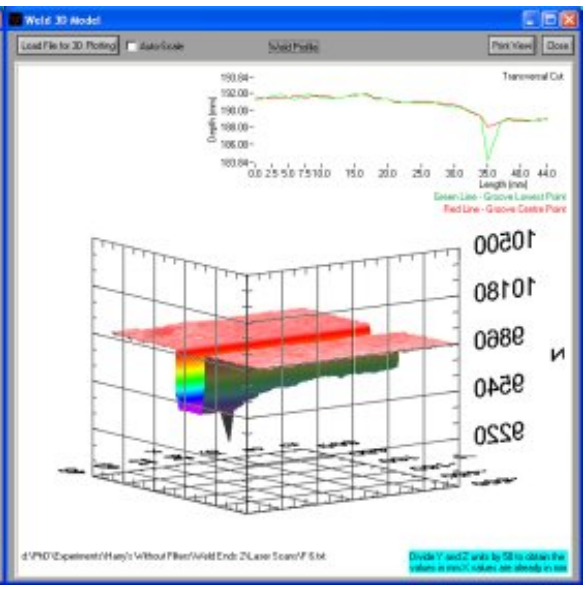

Figure F.5.5 – *Weld 3D Model* Window Screenshot Showing a Weld End Section.

6 Waveforms Window

The creation of this window and its contents arose from the need to assess and compare the files containing the electrical characteristics of each weld. The files containing the electrical characteristics are of two different sources. One is the digital oscilloscope described in section 8.1.1.3 and the other is the power supply described in section 5.1.1.2.1. The files from both sources need to be loaded in order for the program to analyse the data. The digital oscilloscope was set to acquire the arc current and voltage at a sampling rate of 10 MHz. The data acquired from the power supply was read every 0.3 seconds. As the sampling rates are different and so that both sets of data could be analysed together, and assuming they both represent the same weld time. Every time a pair of files is loaded they are both read to verify how many data points there is in each of them in order to determine the ratio between them. The ratio represents the number of data points from the oscilloscope data correspond to one data point in the data extracted from the PSs. This ratio will then be used to relate both set of data. This window is called from the main window (*(10) Waveform*) it has the aspect that can be seen in Figure F.6.1.

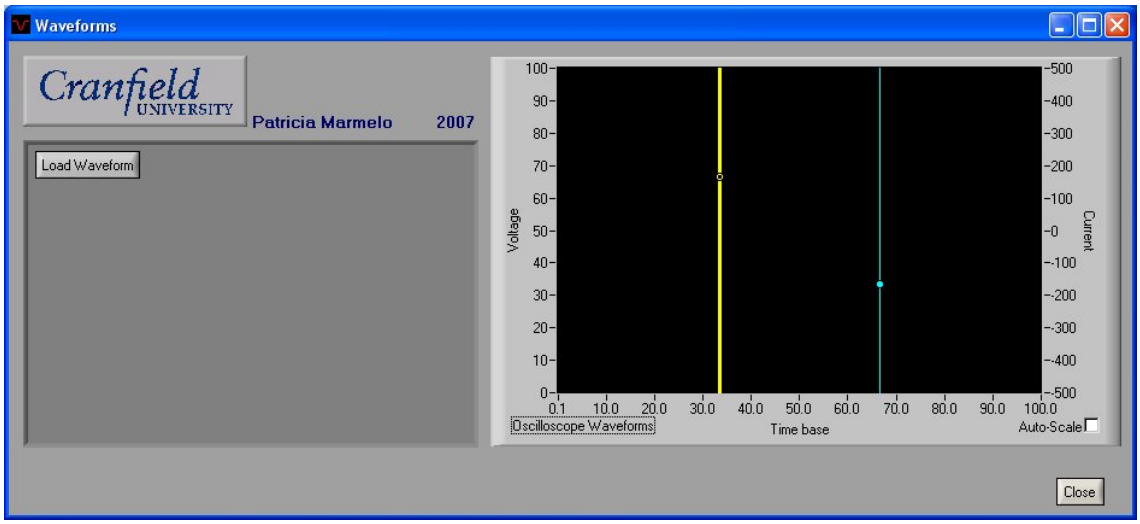

Figure F.6.1 – *Waveforms* Window before the Waveform files are Loaded.

At first the window only has two options available: *(72) Load Waveform* and *(106) Close*. If *(72) Load Waveform* button is pressed two file selection windows will pop-up sequentially. First the oscilloscope date file is requested (Figure F.6.2) and then the PS file (Figure F.6.3). Once the files are selected they are then loaded and the initial five thousand data points from the oscilloscope data file are loaded as well as the correspondent data points in the PS file. Due to program memory restrictions and program fluidity it was decided to only load the first five thousand data points of the oscilloscope file. Once the files are loaded the remaining objects appear in the window as it can be seen in Figure F.6.4. A description of the existing objects can be found below.

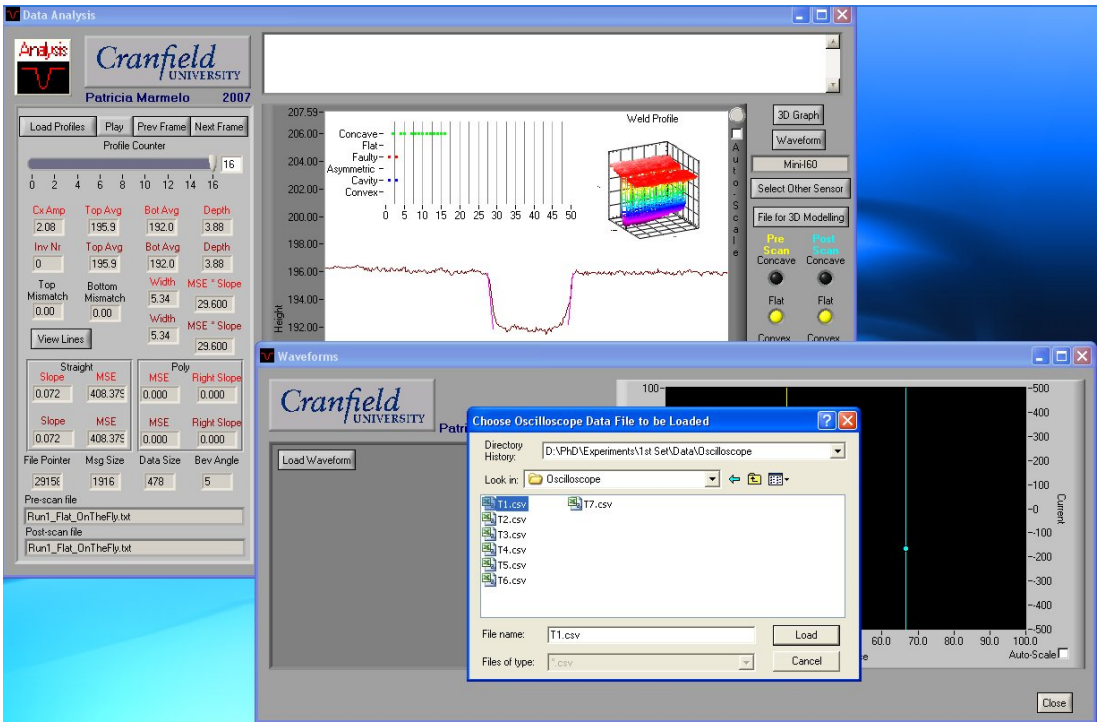

Figure F.6.2 – Program Screenshot with Request for the Oscilloscope Data File.

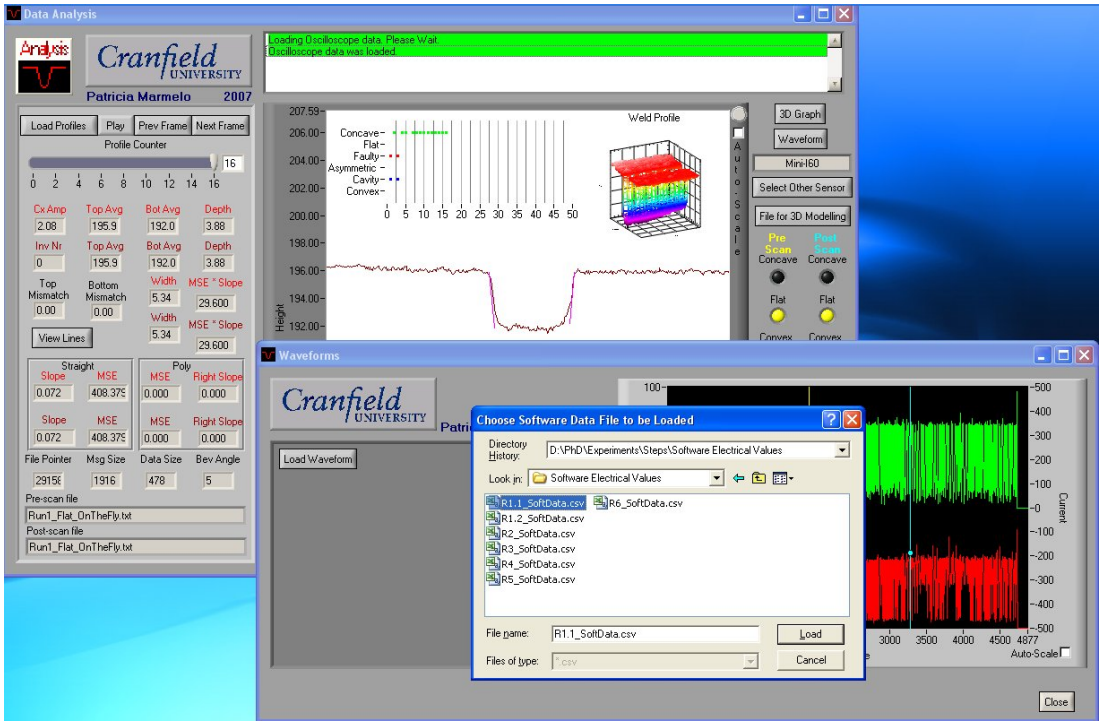

Figure F.6.3 – Program Screenshot with Request for the Power Supply Data File.

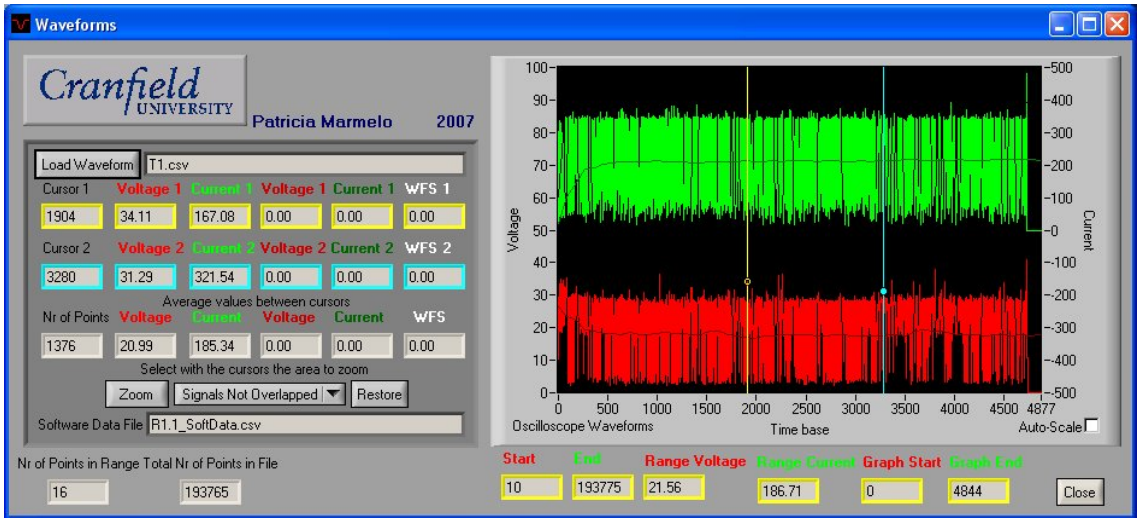

Figure F.6.4 – *Waveforms* Window After Waveform Files are Loaded.

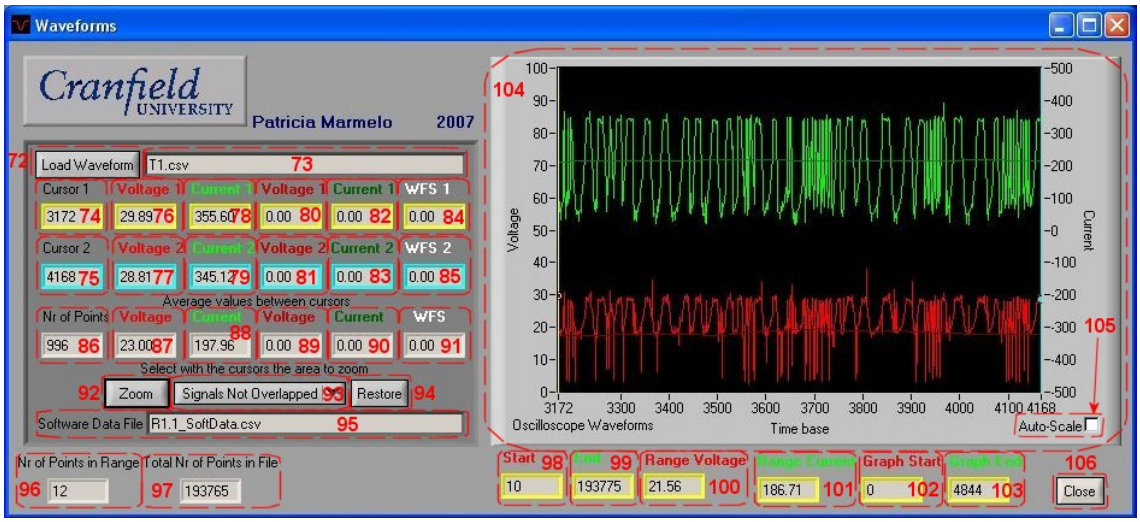

Figure F.6.5 – *Waveforms* Window Screenshot with Numbered Objects.

- *(72) Load Waveform* – Once this button is pressed two windows pop-up. The first requests the user to select the data file containing the data acquired with the digital oscilloscope, the other requests the file with the electrical data extracted from the power supplies;
- *(73) File Name* – This object shows the loaded oscilloscope data file name. This file is the first to be loaded when *(72) Load Waveform* object is pressed;
- *(74) Cursor 1* – This object indicates the number of the data point from the oscilloscope file that is located under the cursor 1 (yellow);
- *(75) Cursor 2* – This object indicates the number of the data point from the oscilloscope file that is located under the cursor 2 (blue);

- *(76) Voltage 1* – This object indicates the arc voltage of the data point located under the cursor 1 (yellow), data from the oscilloscope data file;
- *(77) Voltage 2* – This object indicates the arc voltage of the data point from the oscilloscope file that is located under the cursor 2 (blue);
- *(78) Current 1* – This object indicates the arc current of the data point acquired with the oscilloscope that is located under the cursor 1 (yellow);
- *(79) Current 2* – This object indicates the arc current of the data point acquired with the oscilloscope that is located under the cursor 2 (blue);
- *(80) Voltage 1* – This object indicates the arc voltage of the data point acquired with the power supply that is located under the cursor 1 (yellow);
- *(81) Voltage 2* – This object indicates the arc voltage of the data point acquired with the power supply that is located under the cursor 2 (blue);
- *(82) Current 1* – This object indicates the arc current of the data point acquired with the power supply that is located under the cursor 1 (yellow);
- *(83) Current 2* – This object indicates the arc current of the data point acquired with the power supply that is located under the cursor 2 (blue);
- *(84) WFS 1* – This object indicates the WFS of the data point acquired with the power supply that is located under the cursor 1 (yellow);
- *(85) WFS 2* – This object indicates the WFS of the data point acquired with the power supply that is located under the cursor 2 (blue);
- *(86) Nr of Points* – Indicates the difference between cursor 1 and 2 in terms of data points from the oscilloscope file;
- *(87) Voltage* – This object indicates the average value of the arc voltage between cursor 1 and 2. Using the values extracted from the oscilloscope;
- *(88) Current* – This object indicates the average value of the arc current between cursor 1 and 2. Using the values extracted from the oscilloscope;
- *(89) Voltage* – This object indicates the average value of the arc voltage between cursor 1 and 2. Using the values extracted from the power supply;
- *(90) Current* – This object indicates the average value of the arc current between cursor 1 and 2. Using the values extracted from the power supply;
- *(91) WFS* – This object indicates the average value of the WFS between cursor 1 and 2. Using the values extracted from the power supply;
- *(92) Zoom* – Pressing this button causes the data shown in *(104) Graph* to be zoomed in to show only the data between the two cursors;
- *(93) Overlapping Mode* – This object is a drop down menu which permits to select between two options: *Signals Not Overlapped* and *Signals Overlapped*. By default the values should not overlap. This selection will only take effect when a new set of files is selected or *(92) Zoom* are pressed causing the *(104) Graph* to update;

- *(94) Restore* – Pressing this button causes all the data to be shown again in the *(104) Graph*;
- *(95) Software Data File* – This object shows the loaded software data file name containing the electrical characteristics extracted from the power supplies. This file is the second to be loaded when *(72) Load Waveform* object is pressed;
- *(96) Nr of Points in Range* – Indicates the number of data points from the power supply extracted data are visible in *(104) Graph*;
- *(97) Total Nr of Points in File* – Indicates the total number of points in the oscilloscope data file;
- *(98) Start* – Indicates which is the first data point to have an arc current higher that 5A;
- *(99) End* – Indicates the value number for the last entry in the oscilloscope data file;
- *(100) Range Voltage* – Indicates the average voltage including all the data points in the oscilloscope file;
- *(101) Range Current* – Indicates the average current including all the data points in the oscilloscope file;
- *(102) Graph Start* – Indicates which is the first data point to be displayed in *(104) Graph*;
- *(103) Graph End* – Indicates which is the last data point to be displayed in *(104) Graph*;
- *(104) Graph* – A graph showing the plot of the voltage and current extracted from both the oscilloscope data file and the power supply. The voltage plots can be seen in the red colour and the currents in the green colour. The light shade of each colour is the plot from the oscilloscope data file and the dark one from the power supply data;
- *(105) Auto-Scale* – If ticked indicates the scales in *(104) Graph* are automatic, otherwise the graph will have a pre-determined fixed value;
- *(106) Close* – Hides the *Waveforms* window;

Appendix G *Analysis Software Screenshots*

G1 Sloping Plate – Activated Filters – Flat Bottom

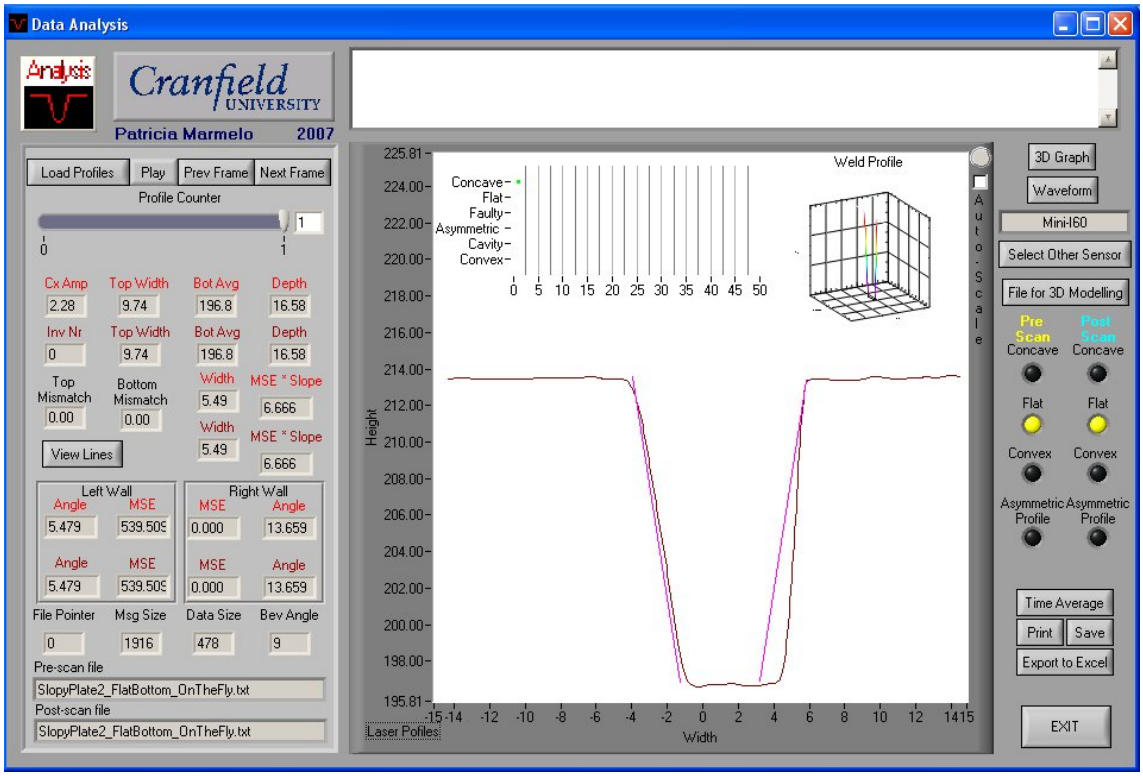

Figure G.1.0.1 – Screenshot of Profile 1 of Sloping Plate with a Flat Bottom.

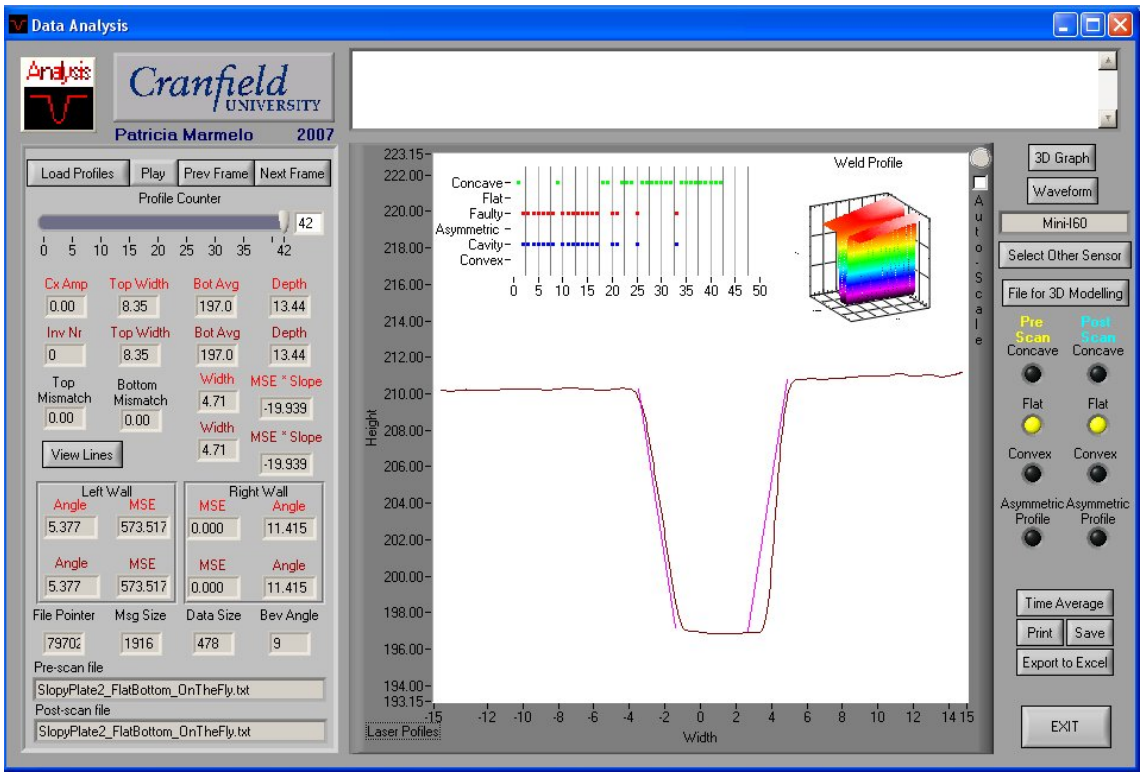

Figure G.1.0.2 – Screenshot of Profile 42 of Sloping Plate with a Flat Bottom.

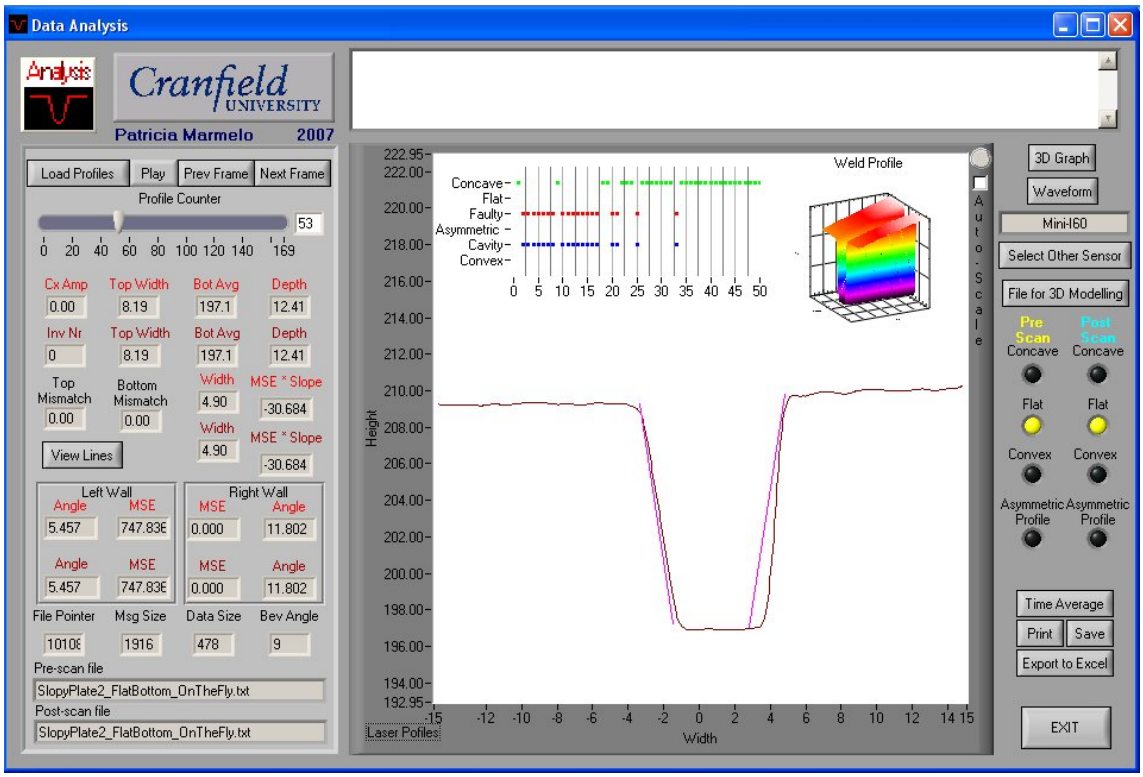

Figure G.1.0.3 – Screenshot of Profile 53 of Sloping Plate with a Flat Bottom.

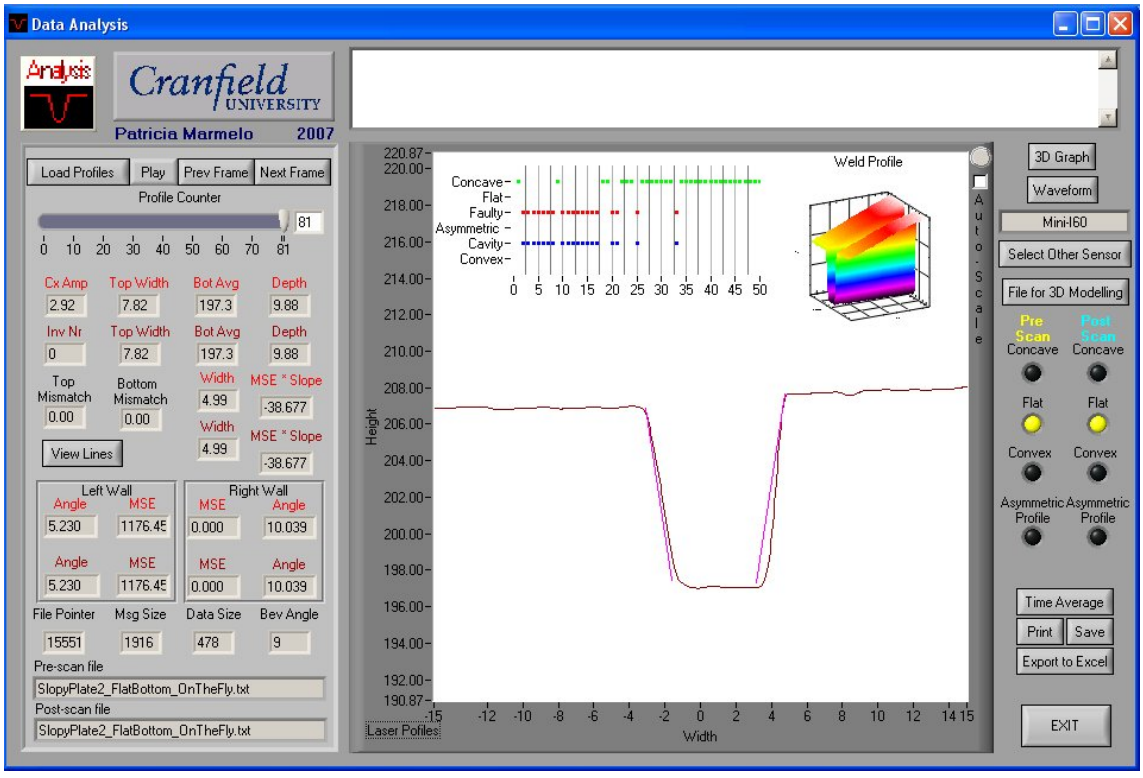

Figure G.1.0.4 – Screenshot of Profile 81 of Sloping Plate with a Flat Bottom.

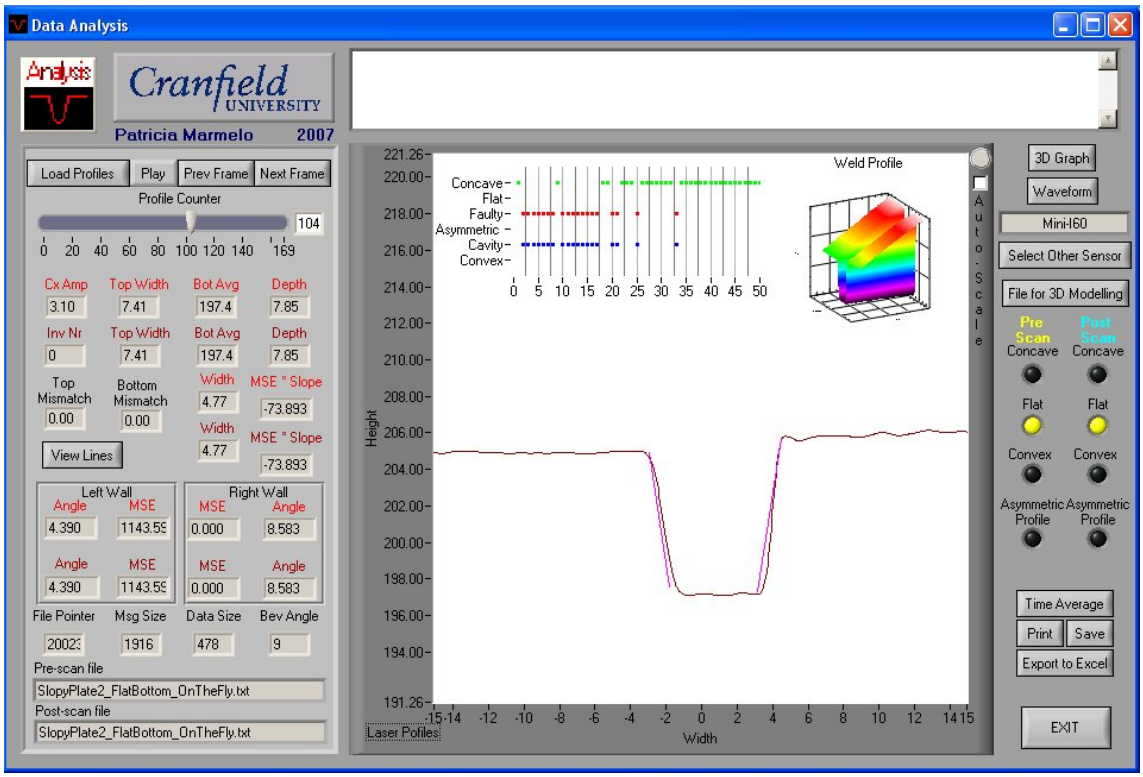

Figure G.1.0.5 – Screenshot of Profile 104 of Sloping Plate with a Flat Bottom.

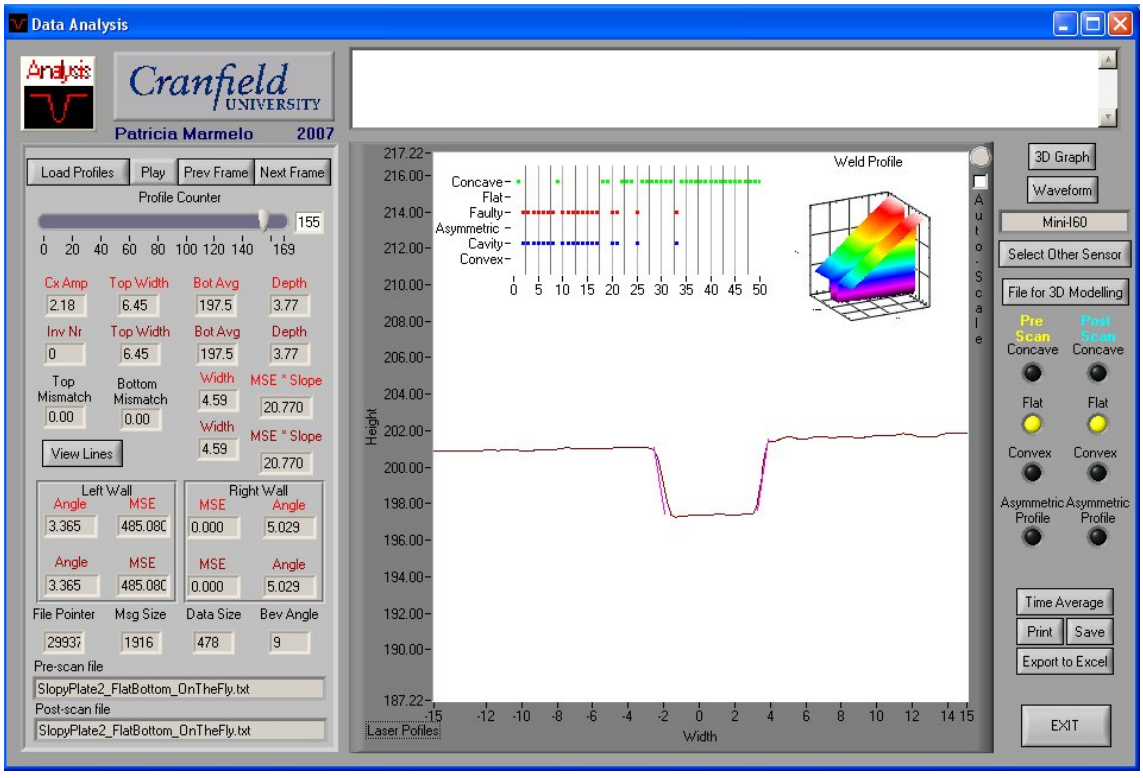

Figure G.1.0.6 – Screenshot of Profile 155 of Sloping Plate with a Flat Bottom.

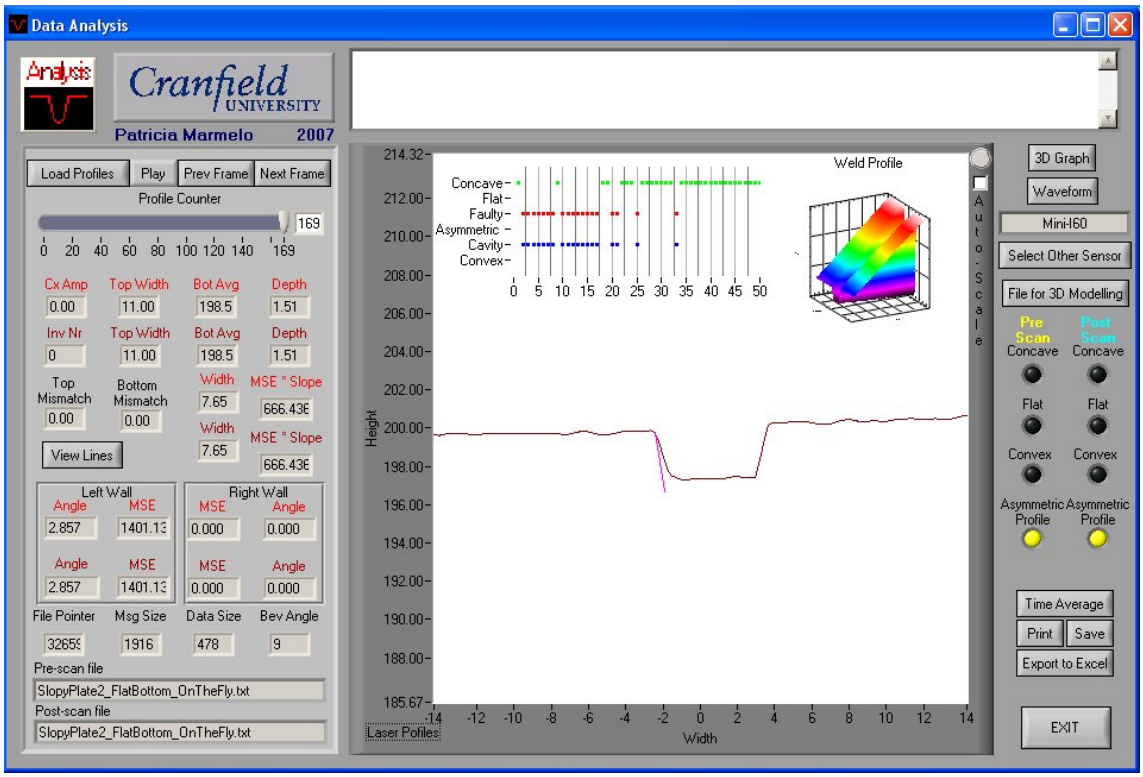

Figure G.1.0.7 – Screenshot of Profile 169 of Sloping Plate with a Flat Bottom.

G2 Sloping Plate – Activated Filters – Flat Top

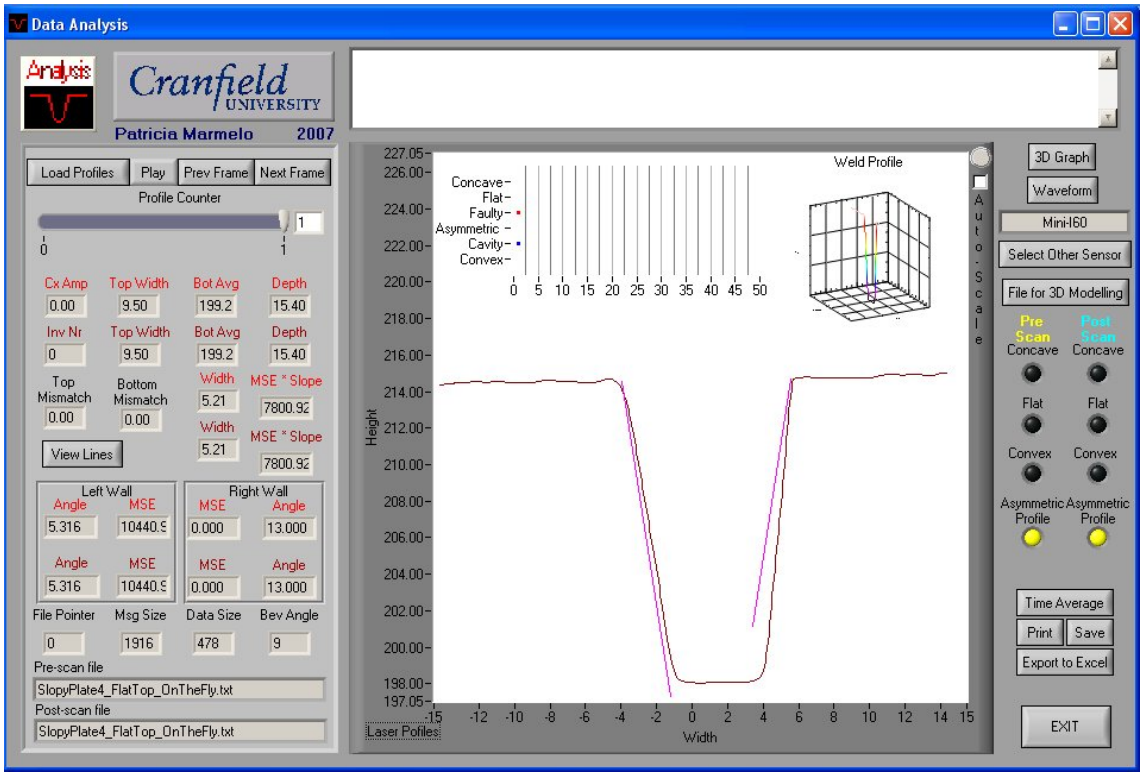

Figure G.2.0.8 – Screenshot of Profile 1 of Sloping Plate with a Flat Top.

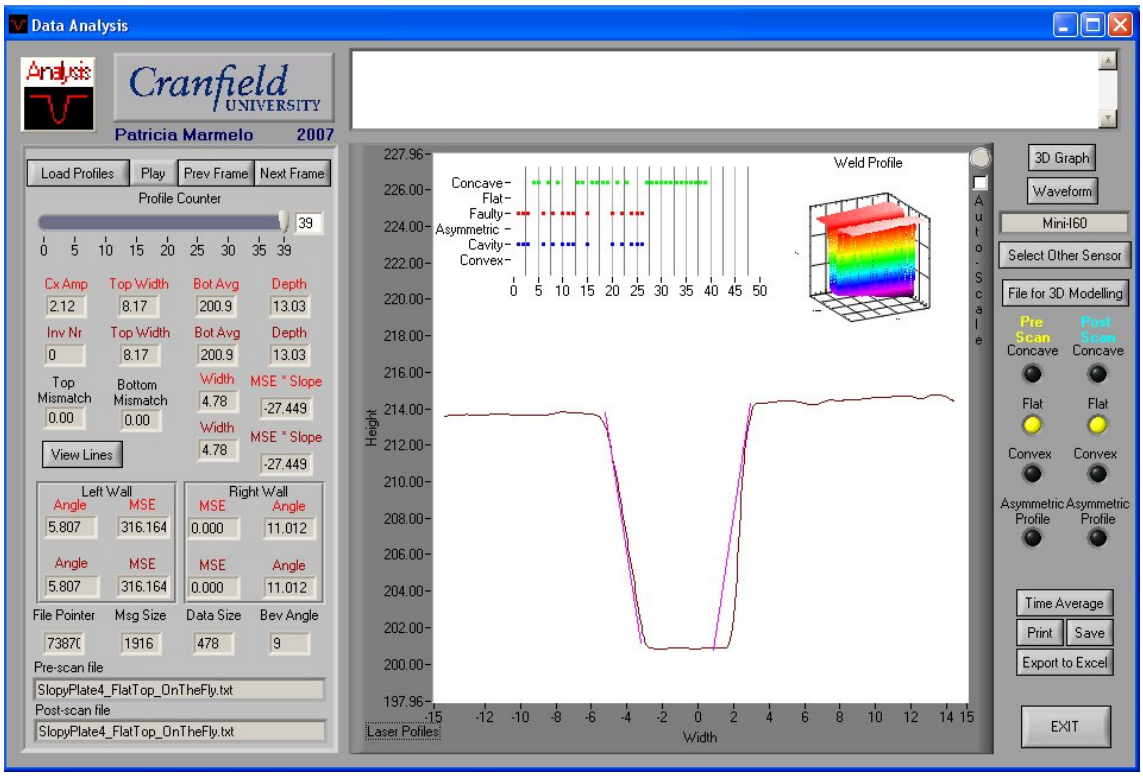

Figure G.2.0.9 – Screenshot of Profile 39 of Sloping Plate with a Flat Top.

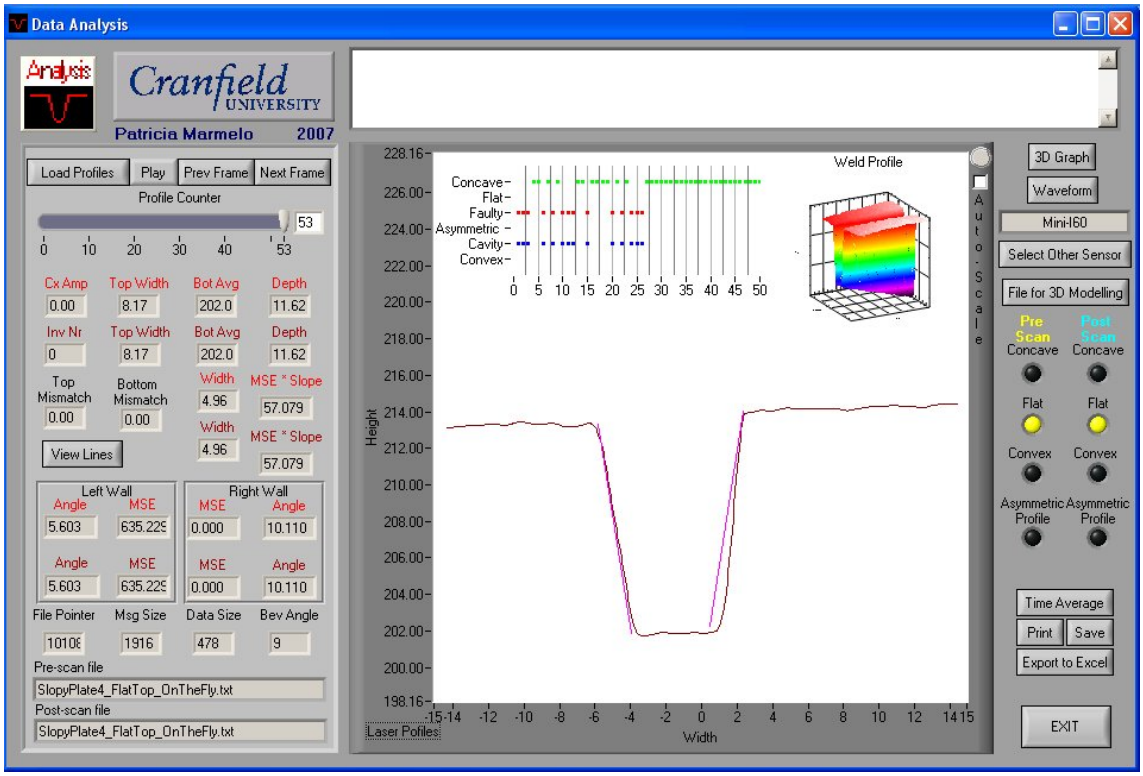

Figure G.2.0.10 – Screenshot of Profile 53 of Sloping Plate with a Flat Top.

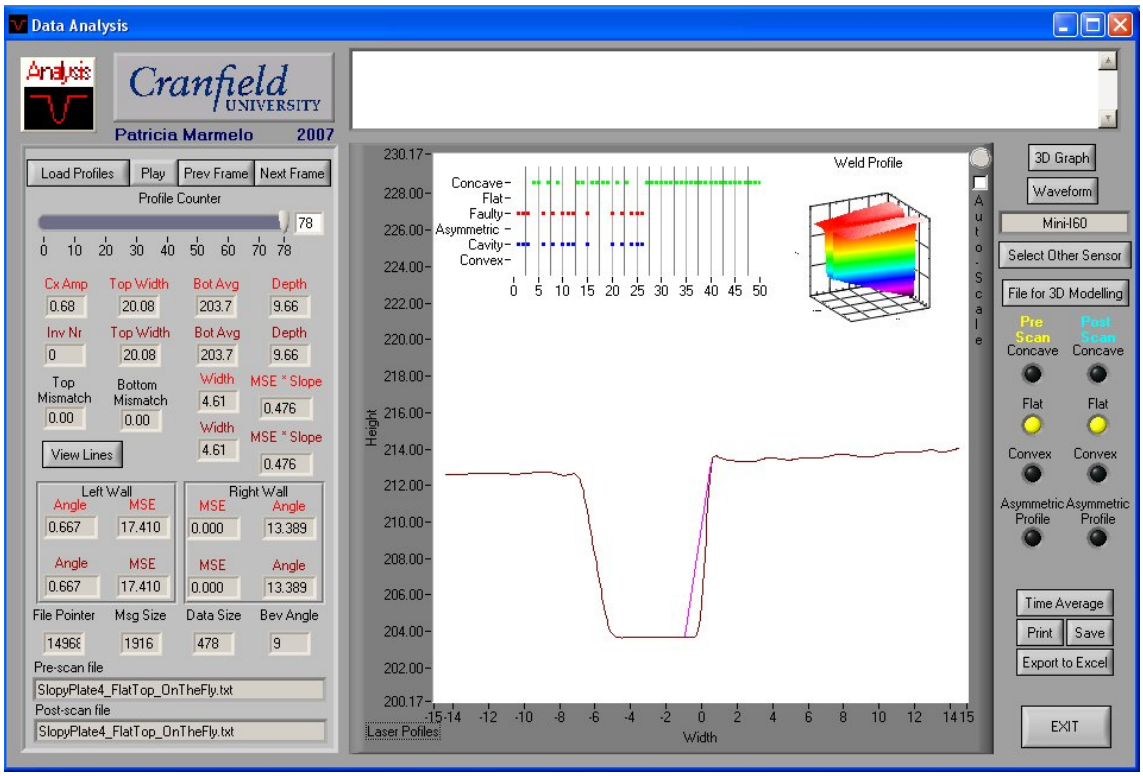

Figure G.2.0.11 – Screenshot of Profile 78 of Sloping Plate with a Flat Top.

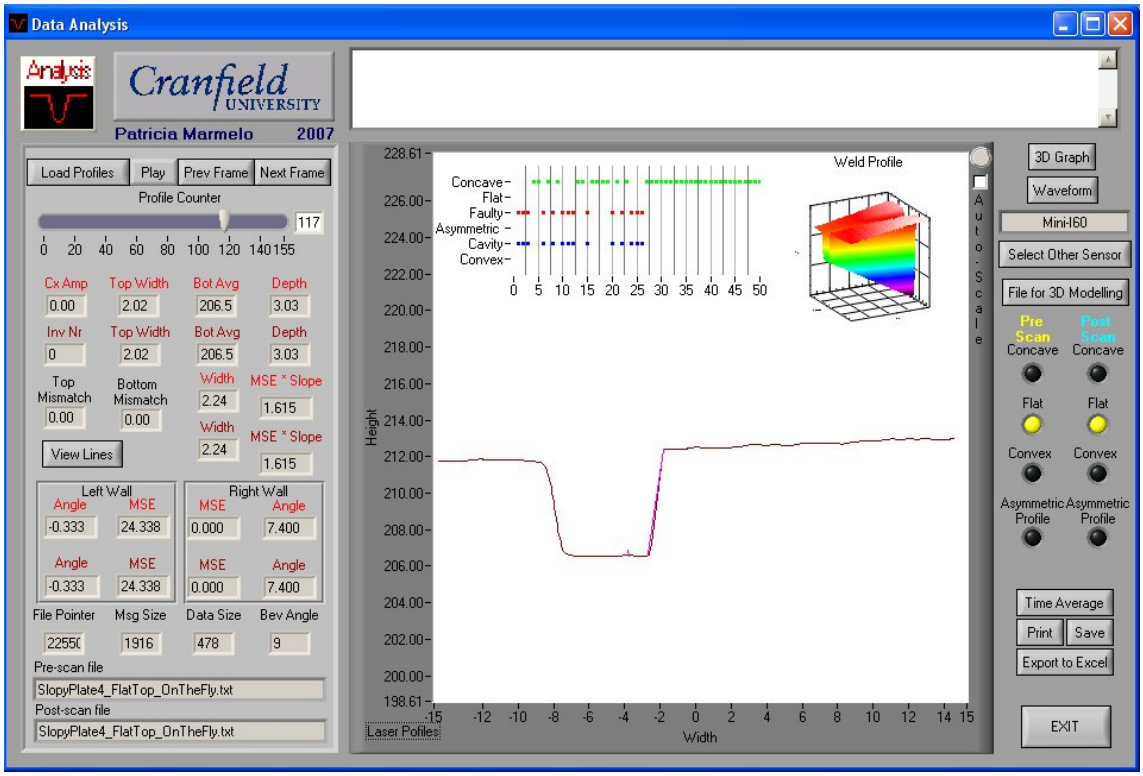

Figure G.2.0.12 – Screenshot of Profile 117 of Sloping Plate with a Flat Top.

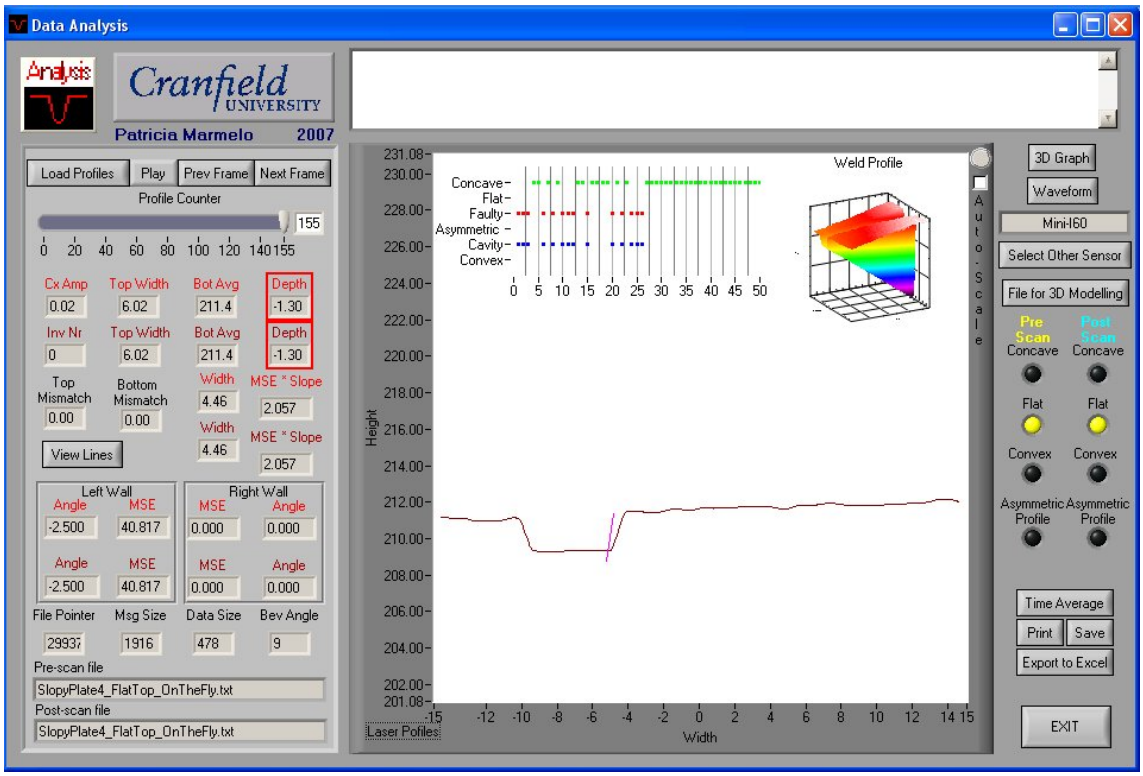

Figure G.2.0.13 – Screenshot of Profile 155 of Sloping Plate with a Flat Top.

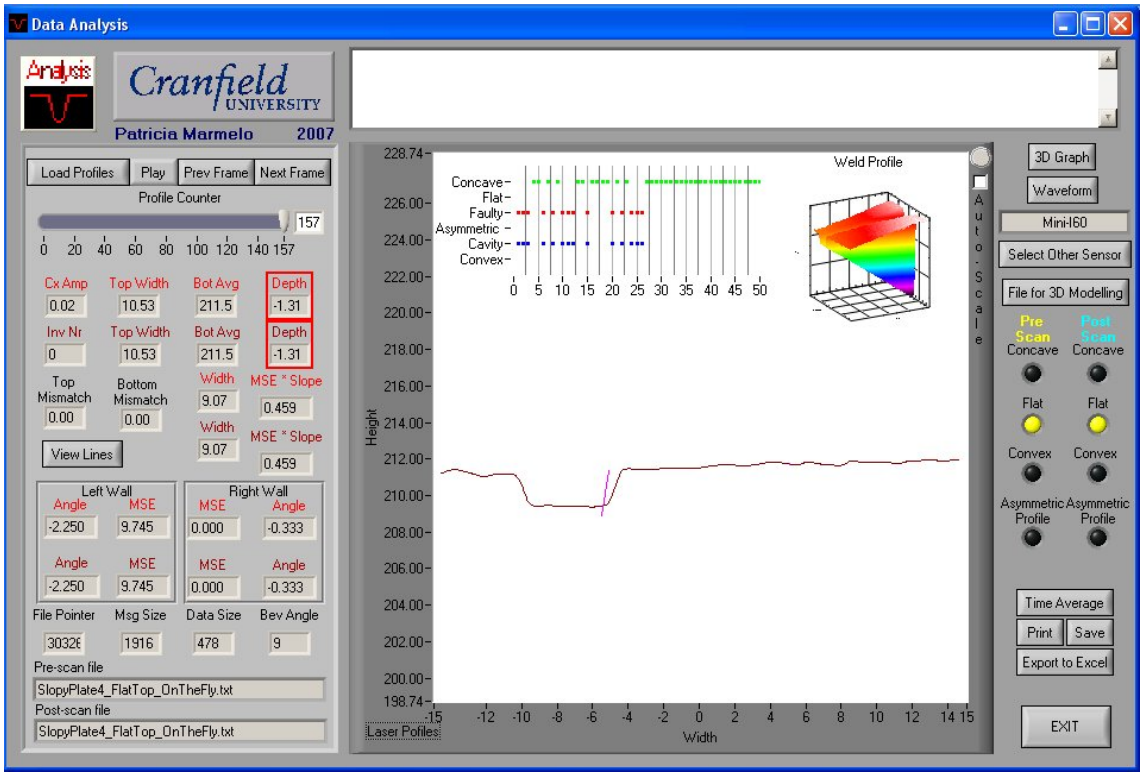

Figure G.2.0.14 – Screenshot of Profile 157 of Sloping Plate with a Flat Top.

G3 Sloping Plate – Deactivated Filters

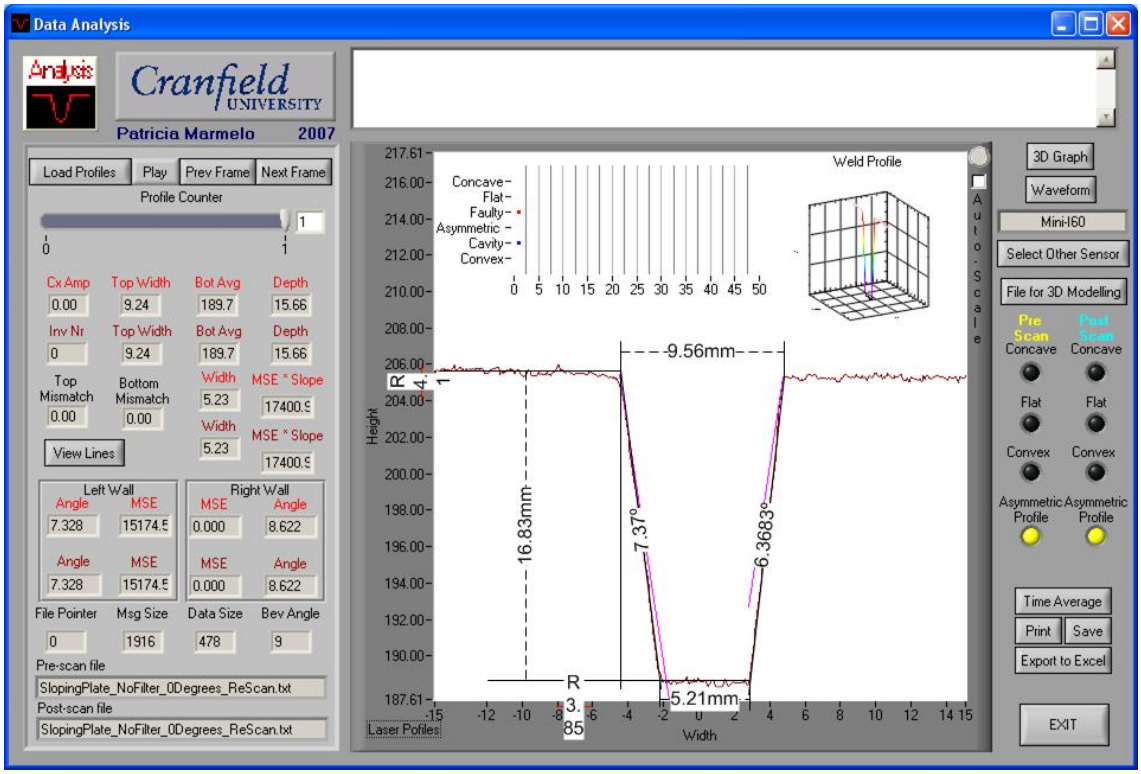

Figure G.3.0.15 – Screenshot of Profile 1 of Sloping Plate with 0 Degrees Inclination.

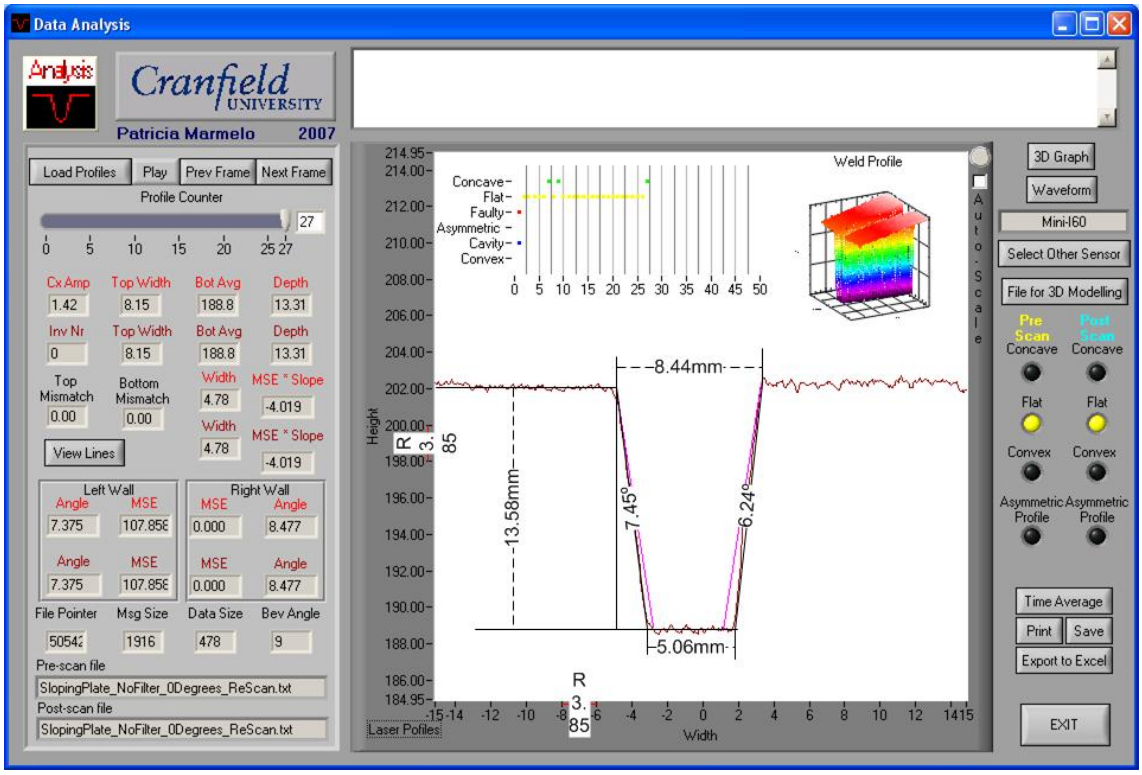

Figure G.3.0.16 – Screenshot of Profile 27 of Sloping Plate with 0 Degrees Inclination.

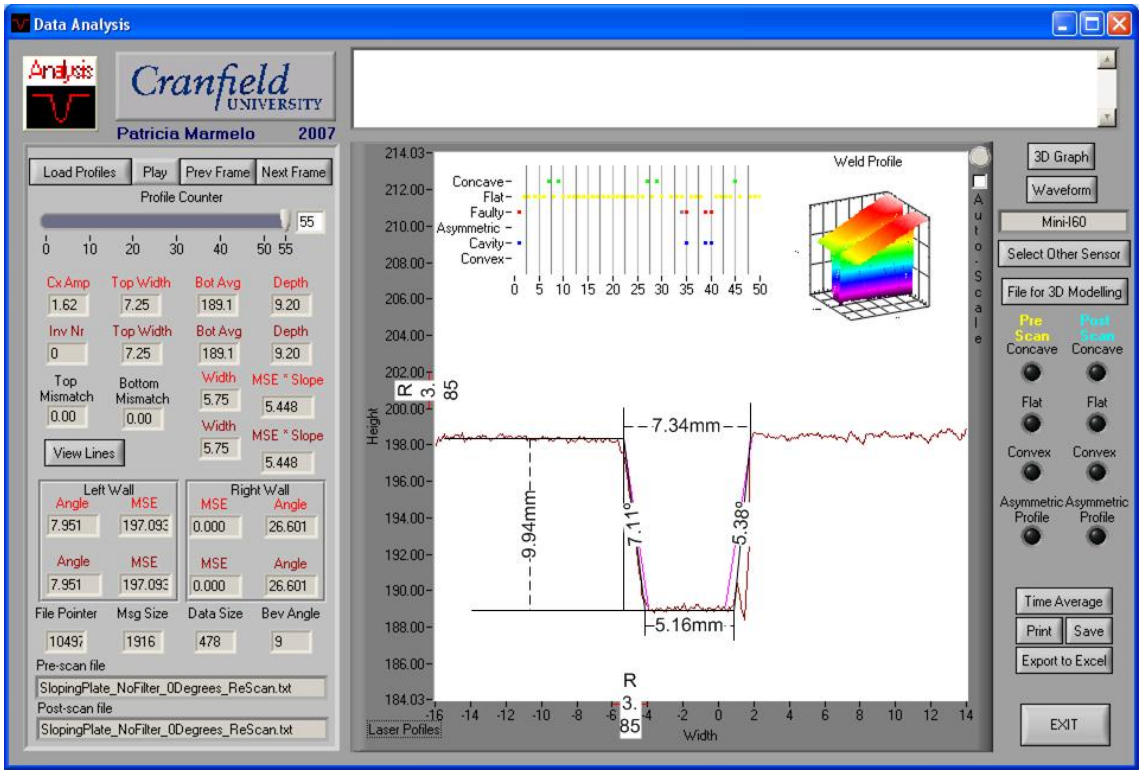

Figure G.3.0.17 – Screenshot of Profile 55 of Sloping Plate with 0 Degrees Inclination.

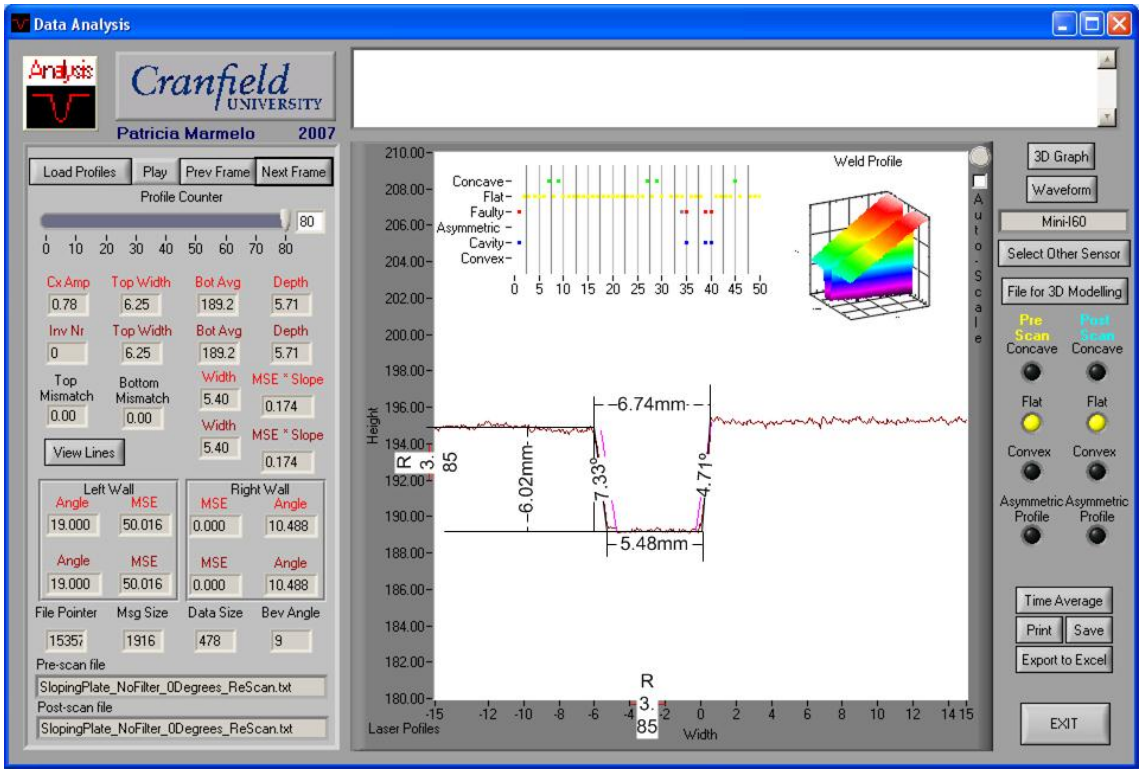

Figure G.3.0.18 – Screenshot of Profile 80 of Sloping Plate with 0 Degrees Inclination.

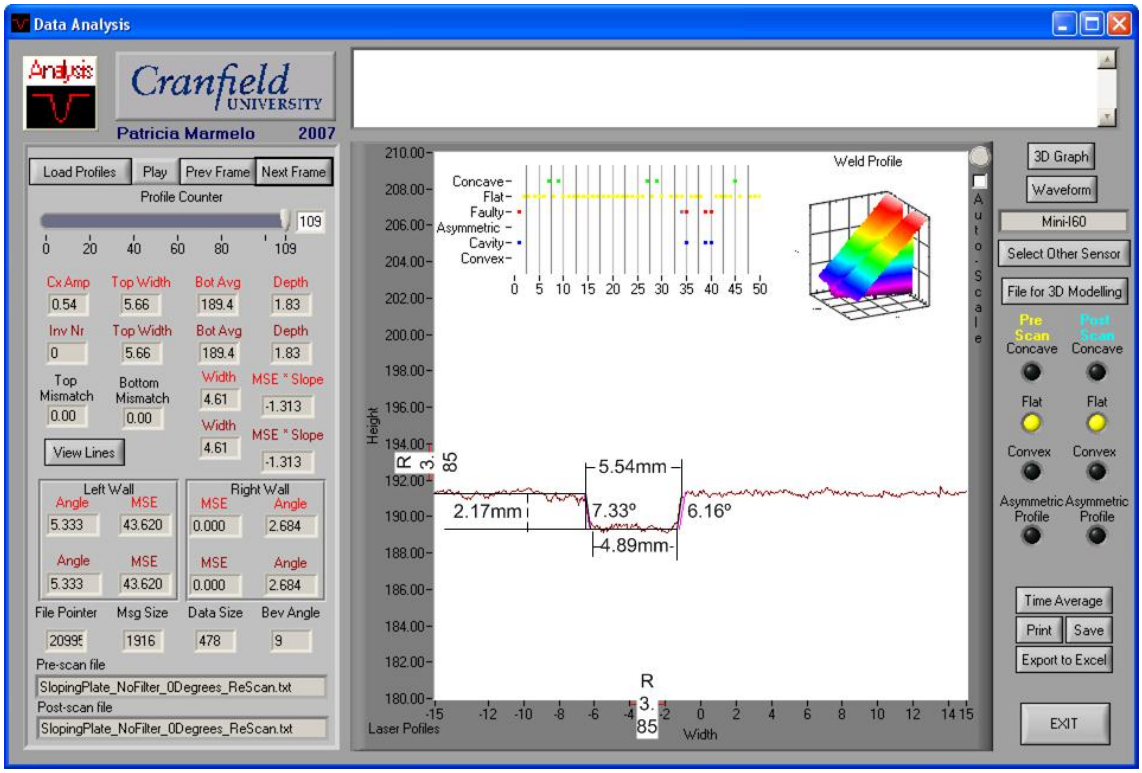

Figure G.3.0.19 – Screenshot of Profile 109 of Sloping Plate with 0 Degrees Inclination.

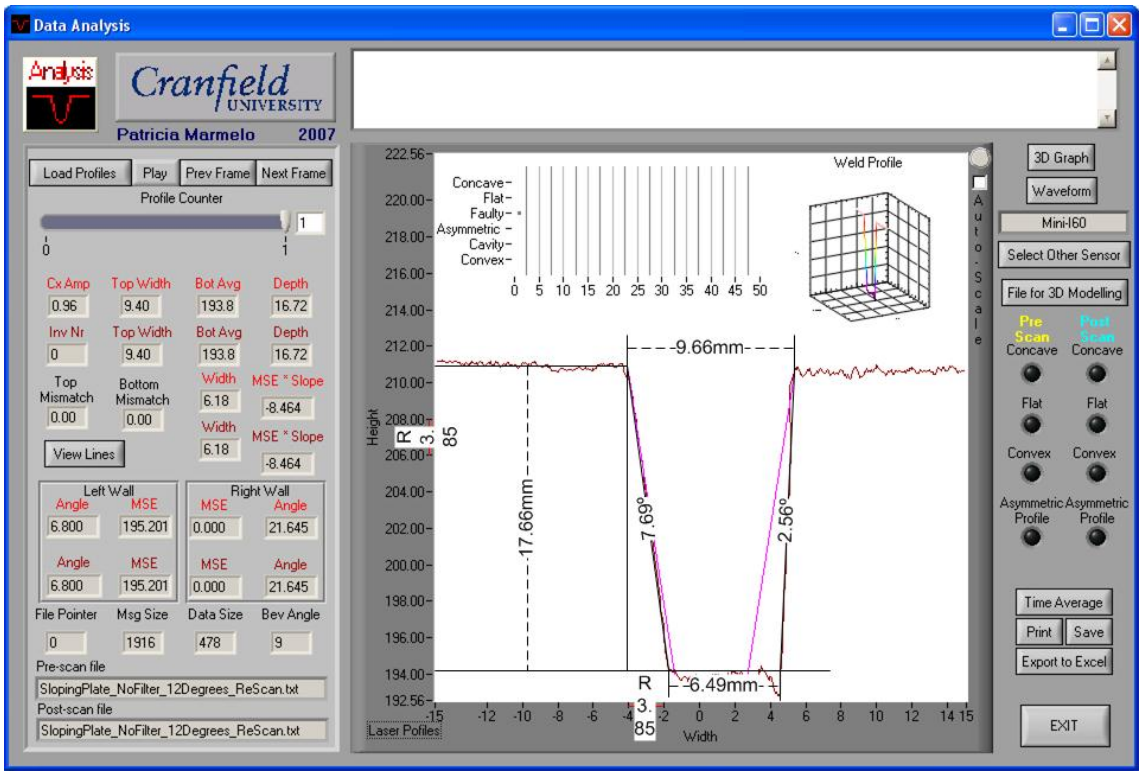

Figure G.3.0.20 – Screenshot of Profile 1 of Sloping Plate with 12 Degrees Inclination.

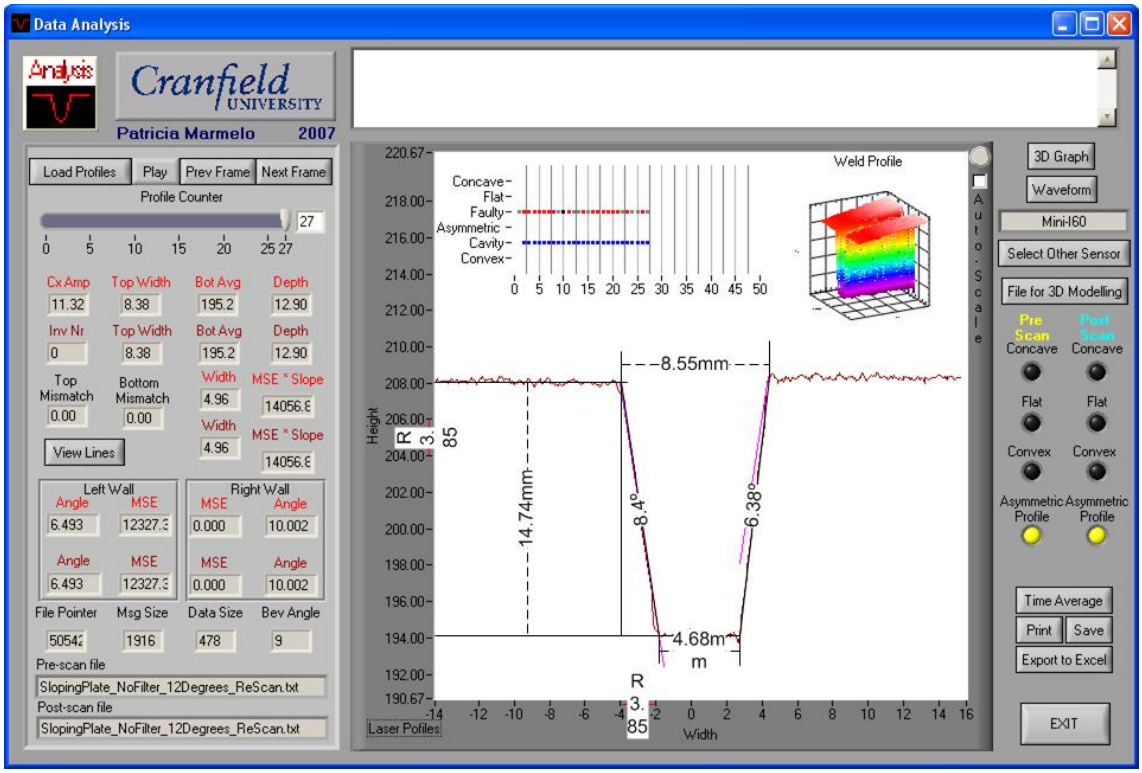

Figure G.3.0.21 – Screenshot of Profile 27 of Sloping Plate with 12 Degrees Inclination.

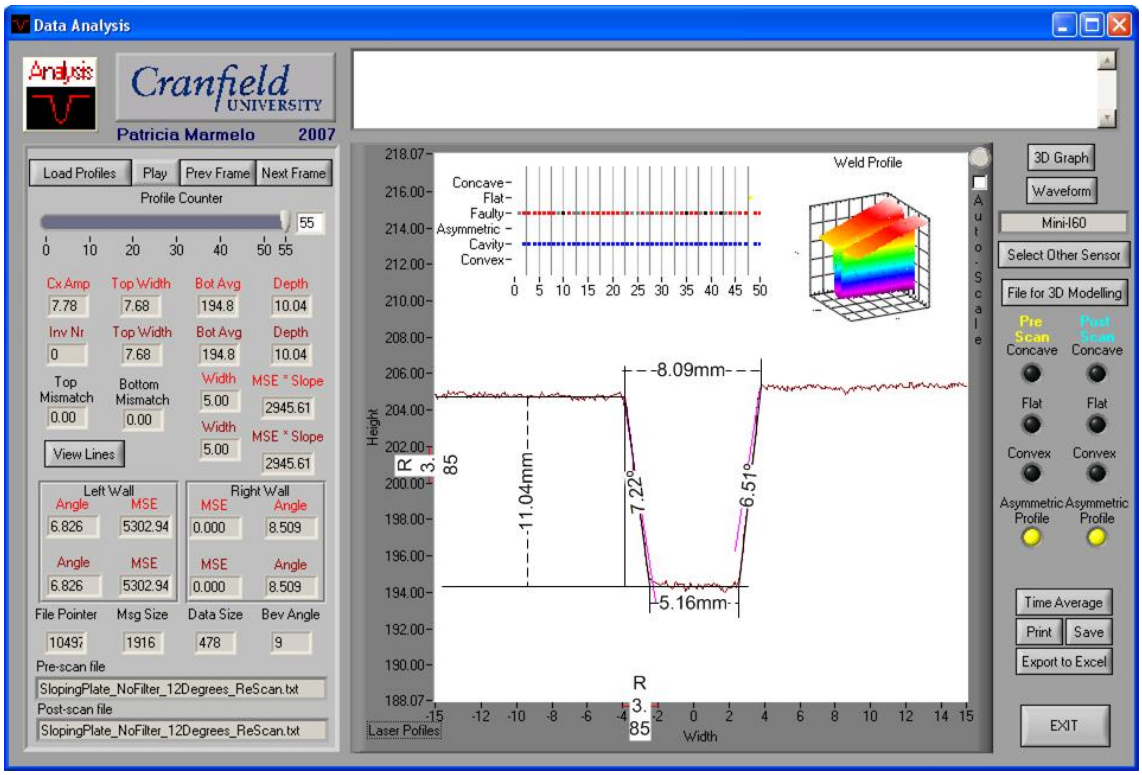

Figure G.3.0.22 – Screenshot of Profile 55 of Sloping Plate with 12 Degrees Inclination.

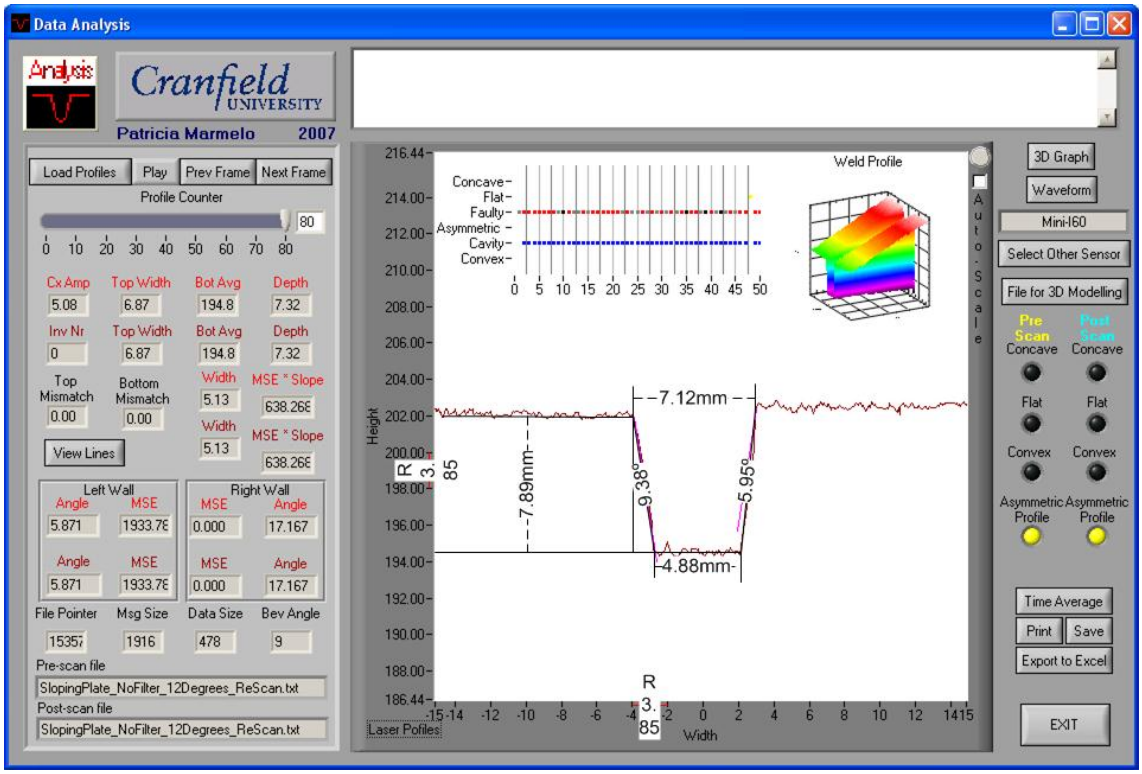

Figure G.3.0.23 – Screenshot of Profile 80 of Sloping Plate with 12 Degrees Inclination.

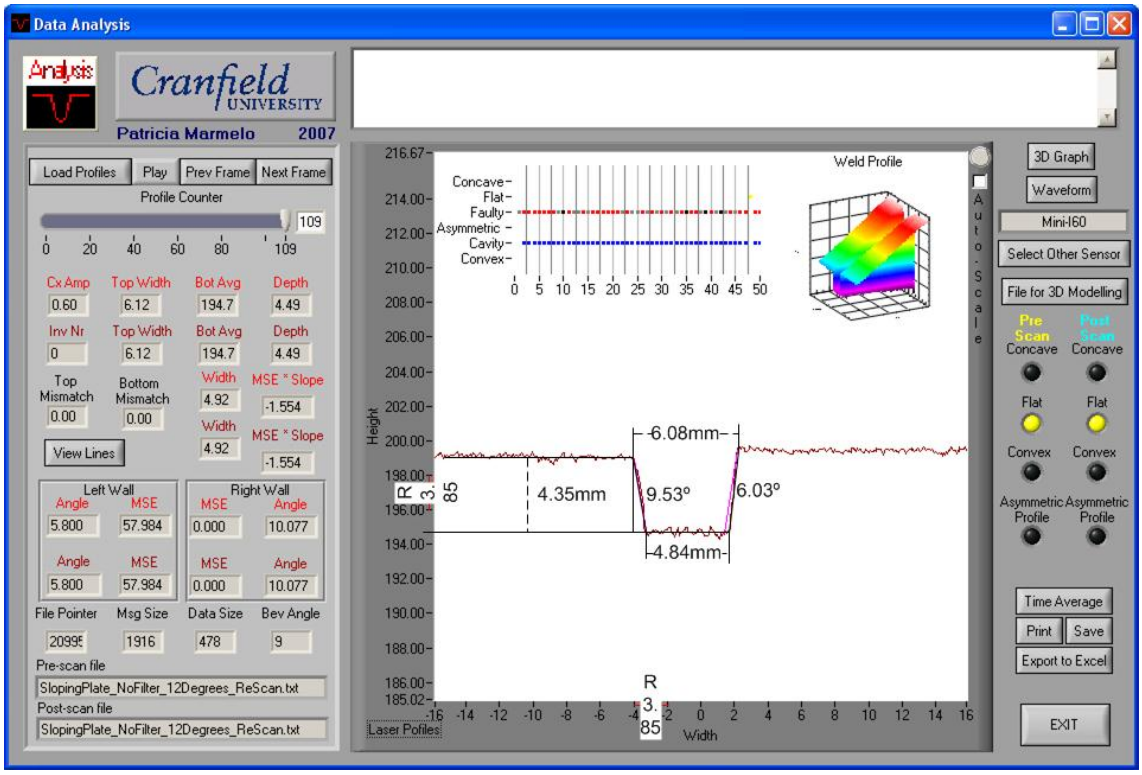

Figure G.3.0.24 – Screenshot of Profile 109 of Sloping Plate with 12 Degrees Inclination.

Appendix H *WinUser Settings*

H1 Sloping Plate – Filters ON

Settings Library				
	Joint Library			
		Current Joint	**4 – CU_GEN**	
Visus				
	Configuration			
		Left Boundary Size	**10%**	
		Right Boundary Size	**10%**	
		Tracking Point Method	**0**	
		Gap Validation	**YES**	
		Minimum Gap	**0mm**	
		Maximum Gap	**15mm**	
		Mismatch Validation	**YES**	
		Minimum Mismatch	**-10mm**	
		Maximum Mismatch	**10mm**	
	Filters			
		Filters	**Median & Average**	
		Filter Size	**10**	
		Continuity	**ON**	
		Anti-Reflection	**Disabled**	
	Generic Groove			
		Gap Definition	**Bottom**	
		Plate Thickness	**21mm**	
		Bottom Shape	**General**	
		Plate Shape		
			Left	**General**
			Right	**General**
		Bevel Shape		
			Left	**General**
			Right	**General**

		Layer		
			Definition	**From Bottom**
			Left Level	**4mm**
			Right Level	**4mm**
		Joint Normal		
			Method	**From Left Plate**
			Angle	**5 Degrees**
Camera				
	Camera Settings			
		Power Control		**Automatic**
			Automatic Set Point	**128**
		Video Settings		
			Video Gain	**Low**
			Dynamic Gain	**MEDIUM**
			Exposure Time	**42**
		Field of View		
			Number of Pixels per Profile	**512**
Configuration				
	User Port Settings			
		Serial Port		
			Baud Rate	**38400**

H2 Sloping Plate – Filters OFF

Settings Library				
	Joint Library			
		Current Joint	**4 – CU_GEN**	
Visus				
	Configuration			
		Left Boundary Size	**10%**	
		Right Boundary Size	**10%**	
		Tracking Point Method	**0**	
		Gap Validation	**YES**	
		Minimum Gap	**0mm**	
		Maximum Gap	**15mm**	
		Mismatch Validation	**YES**	
		Minimum Mismatch	**-10mm**	
		Maximum Mismatch	**10mm**	
	Filters			
		Filters	**OFF**	
		Continuity	**ON**	
		Anti-Reflection	**Disabled**	
	Generic Groove			
		Gap Definition	**Bottom**	
		Plate Thickness	**21mm**	
		Bottom Shape	**General**	
		Plate Shape		
			Left	**General**
			Right	**General**
		Bevel Shape		
			Left	**General**
			Right	**General**
		Layer		

			Definition	**From Bottom**
			Left Level	**4mm**
			Right Level	**4mm**
		Joint Normal		
			Method	**From Left Plate**
			Angle	**5 Degrees**
Camera				
	Camera Settings			
		Power Control		**Automatic**
			Automatic Set Point	**128**
		Video Settings		
			Video Gain	**Low**
			Dynamic Gain	**MEDIUM**
			Exposure Time	**42**
		Field of View		
			Number of Pixels per Profile	**512**
Configuration				
	User Port Settings			
		Serial Port		
			Baud Rate	**38400**

H3 Real Time Assessment of Weld Quality

Settings Library				
	Joint Library			
		Current Joint	**4 – CU_GEN**	
Visus				
	Configuration			
		Left Boundary Size	**10%**	
		Right Boundary Size	**10%**	
		Tracking Point Method	**0**	
		Gap Validation	**YES**	
		Minimum Gap	**0mm**	
		Maximum Gap	**15mm**	
		Mismatch Validation	**YES**	
		Minimum Mismatch	**-10mm**	
		Maximum Mismatch	**10mm**	
	Filters			
		Filters	**OFF**	
		Continuity	**ON**	
		Anti-Reflection	**Disabled**	
	Generic Groove			
		Gap Definition	**Bottom**	
		Plate Thickness	**8mm**	
		Bottom Shape	**General**	
		Plate Shape		
			Left	**General**
			Right	**General**
		Bevel Shape		
			Left	**General**
			Right	**General**
		Layer		

			Definition	**From Bottom**
			Left Level	**4mm**
			Right Level	**4mm**
		Joint Normal		
			Method	**From Left Plate**
			Angle	**30 Degrees**
Camera				
	Camera Settings			
		Power Control		**Automatic**
			Automatic Set Point	**128**
		Video Settings		
			Video Gain	**Low**
			Dynamic Gain	**MEDIUM**
			Exposure Time	**42**
		Field of View		
			Number of Pixels per Profile	**512**
Configuration				
	User Port Settings			
		Serial Port		
			Baud Rate	**38400**

Appendix I *Real Time Assessment of Weld Quality Scans*

I1 Flat Position

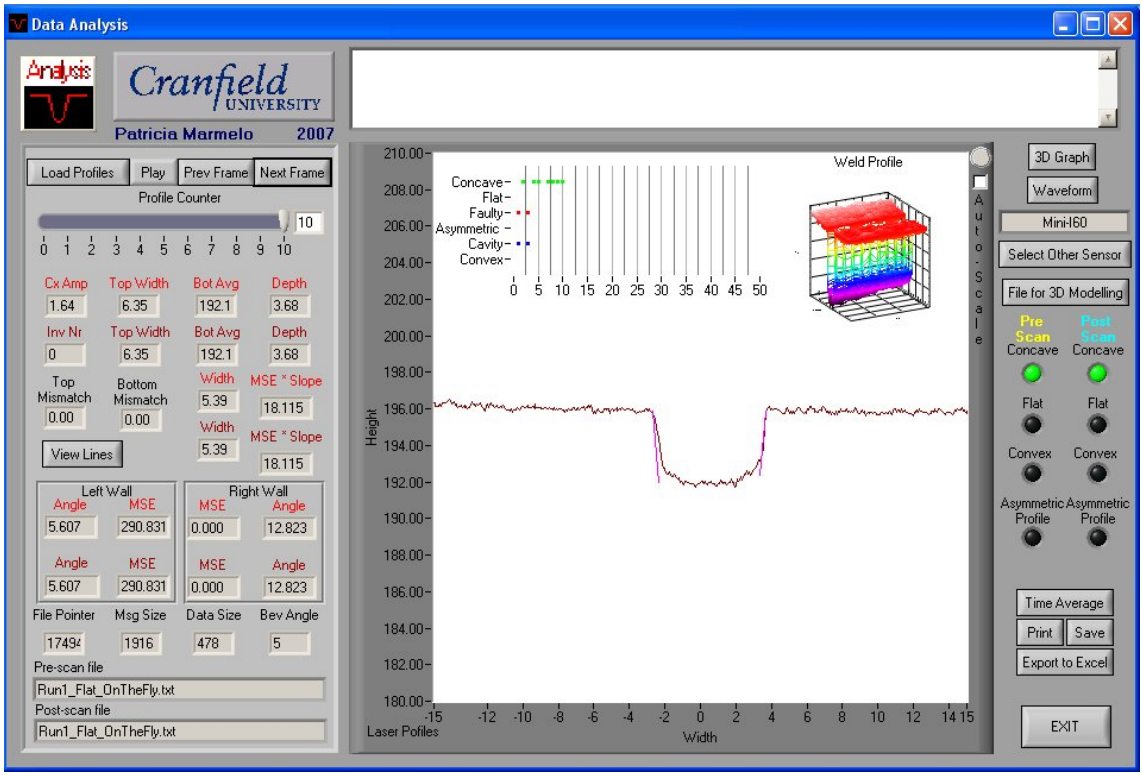

Figure I.1.0.1 – Screenshot of Profile 10 of "Run 1" in the Flat Position.

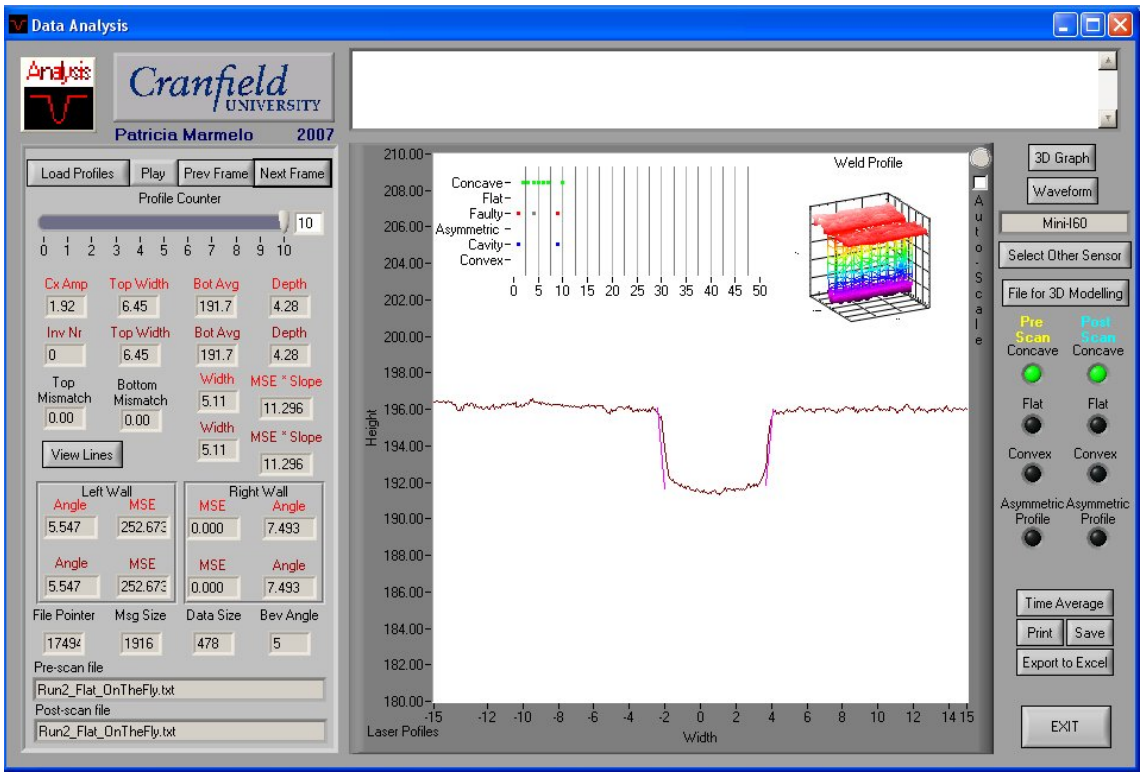

Figure I.1.0.2 – Screenshot of Profile 10 of "Run 2" in the Flat Position.

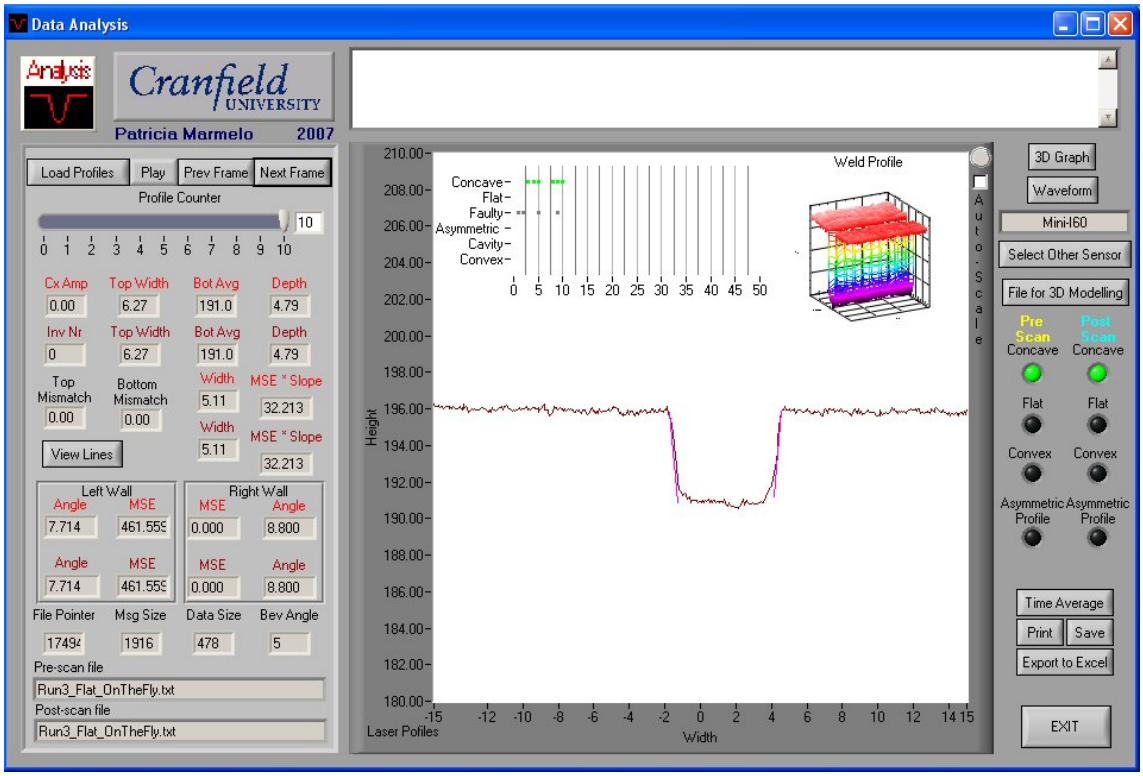

Figure I.1.0.3 – Screenshot of Profile 10 of "Run 3" in the Flat Position.

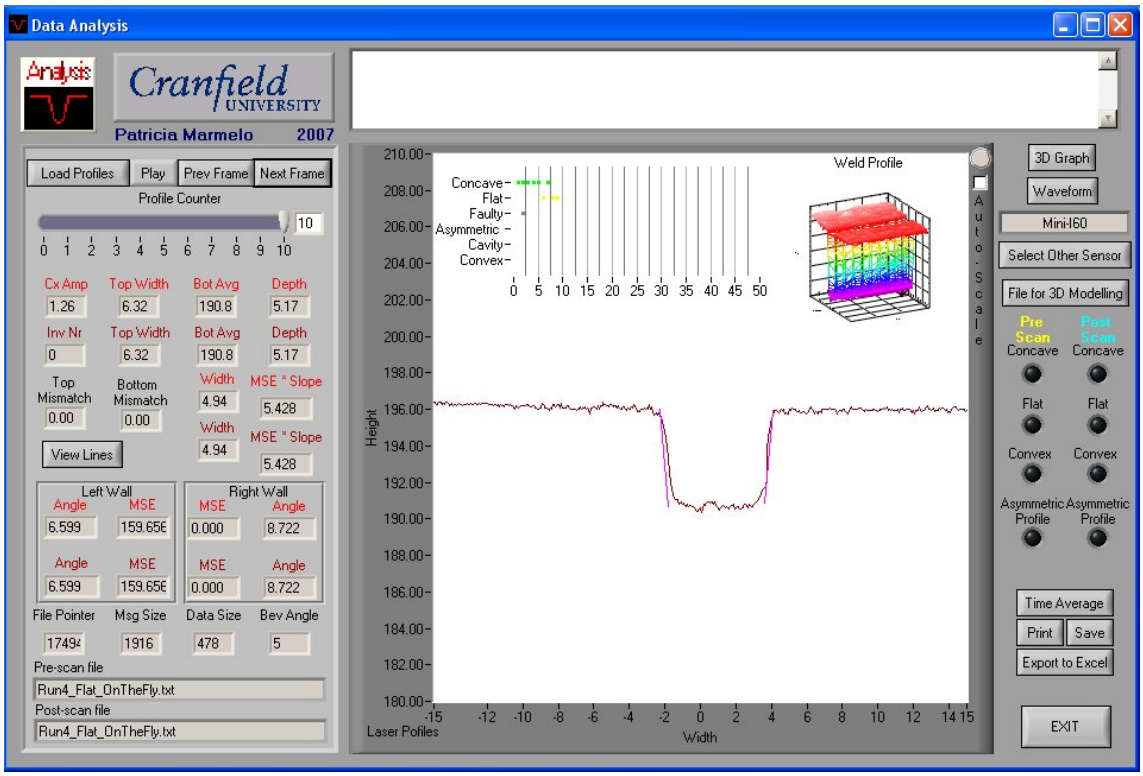

Figure I.1.0.4 – Screenshot of Profile 10 of "Run 4" in the Flat Position.

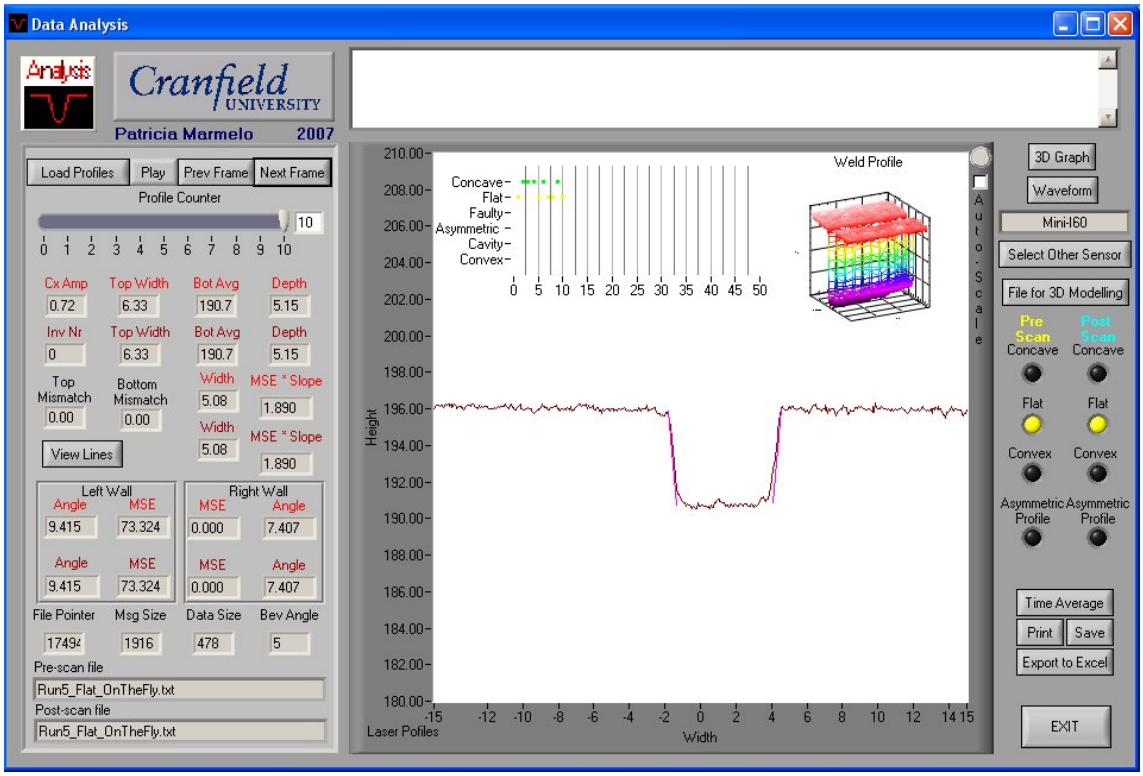

Figure I.1.0.5 – Screenshot of Profile 10 of "Run 5" in the Flat Position.

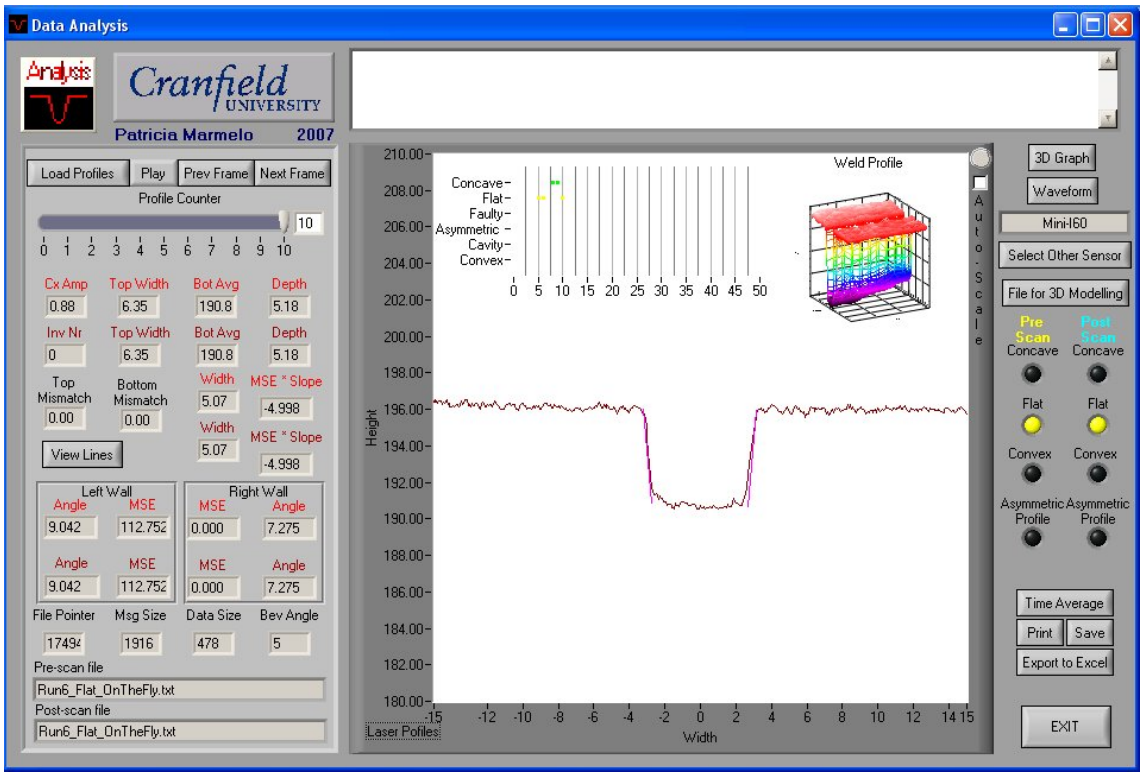

Figure I.1.0.6 – Screenshot of Profile 10 of "Run 6" in the Flat Position.

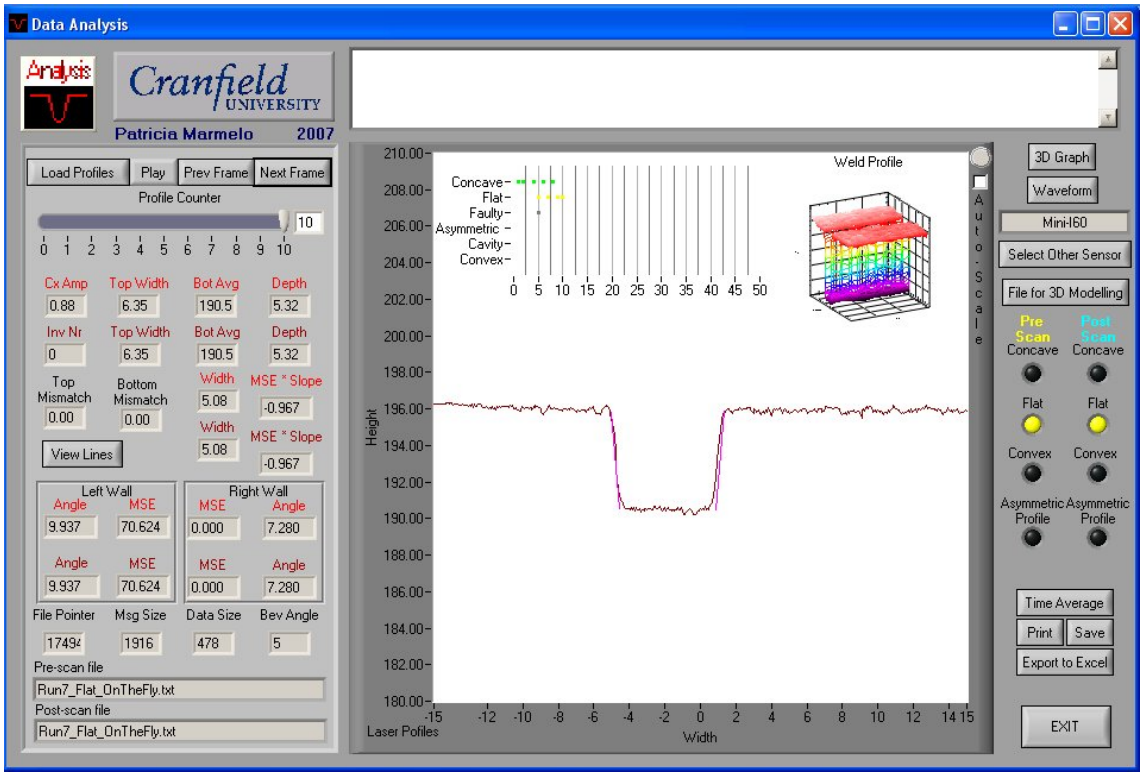

Figure I.1.0.7 – Screenshot of Profile 10 of "Run 7" in the Flat Position.

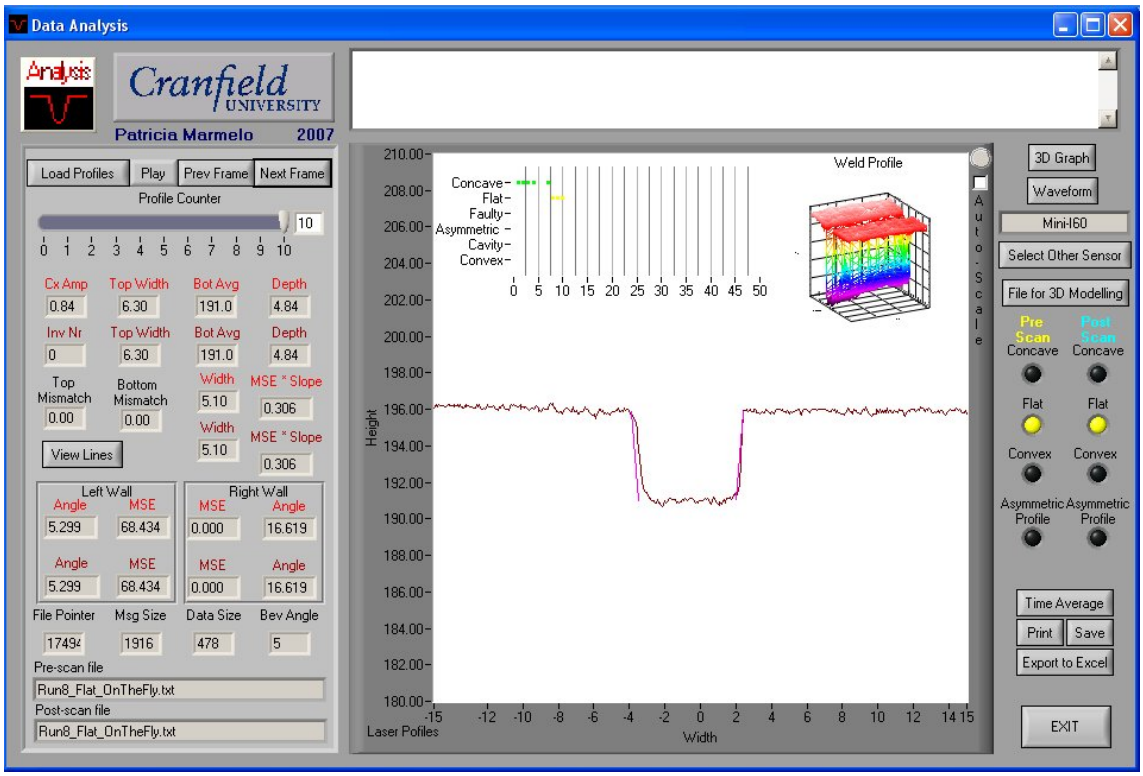

Figure I.1.0.8 – Screenshot of Profile 10 of "Run 8" in the Flat Position.

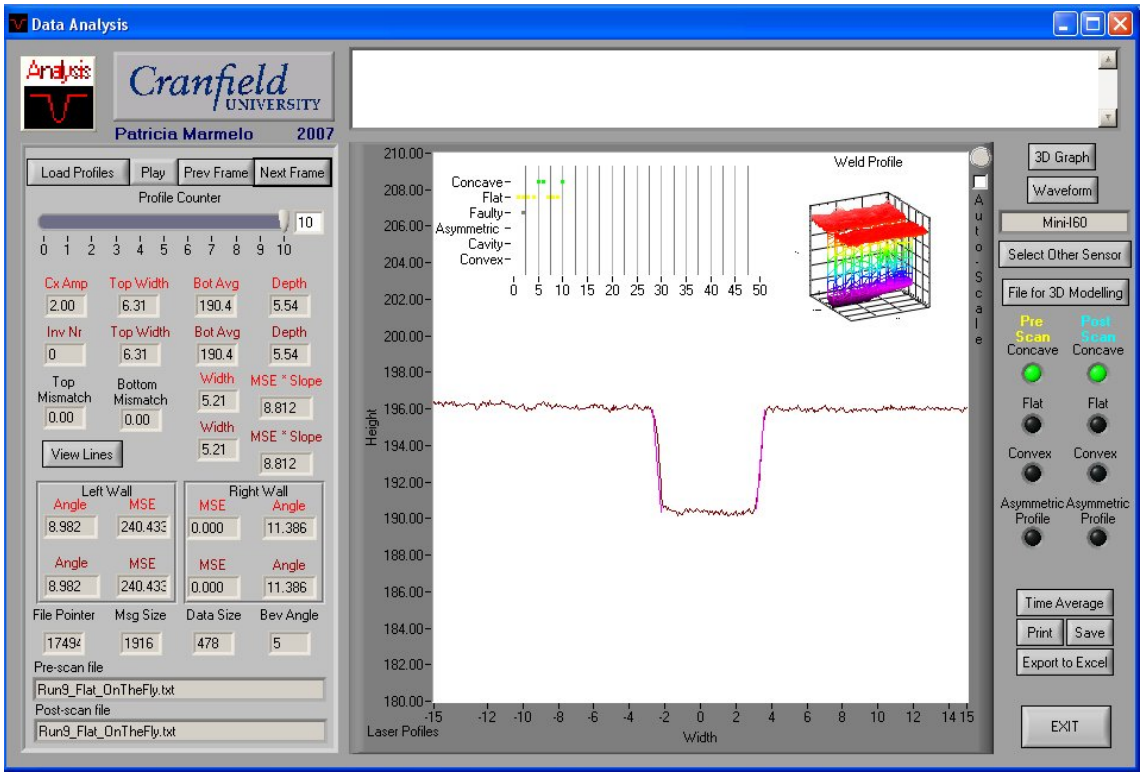

Figure I.1.0.9 – Screenshot of Profile 10 of "Run 9" in the Flat Position.

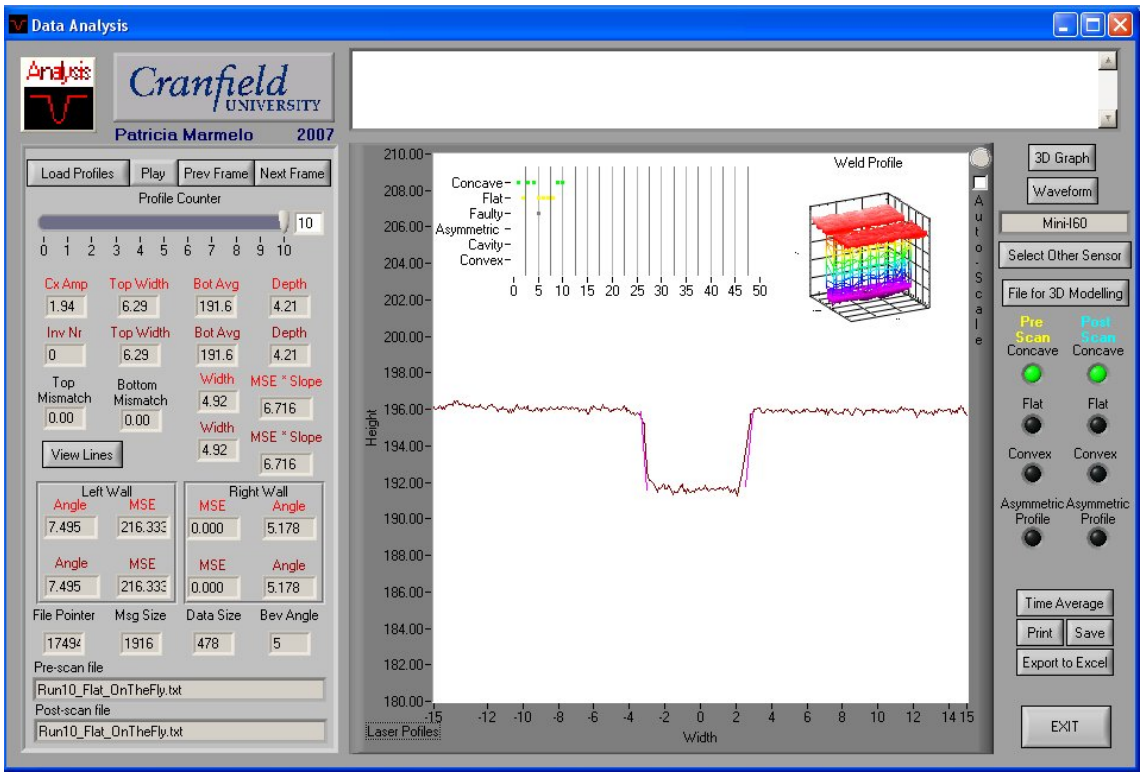

Figure I.1.0.10 – Screenshot of Profile 10 of "Run 10" in the Flat Position.

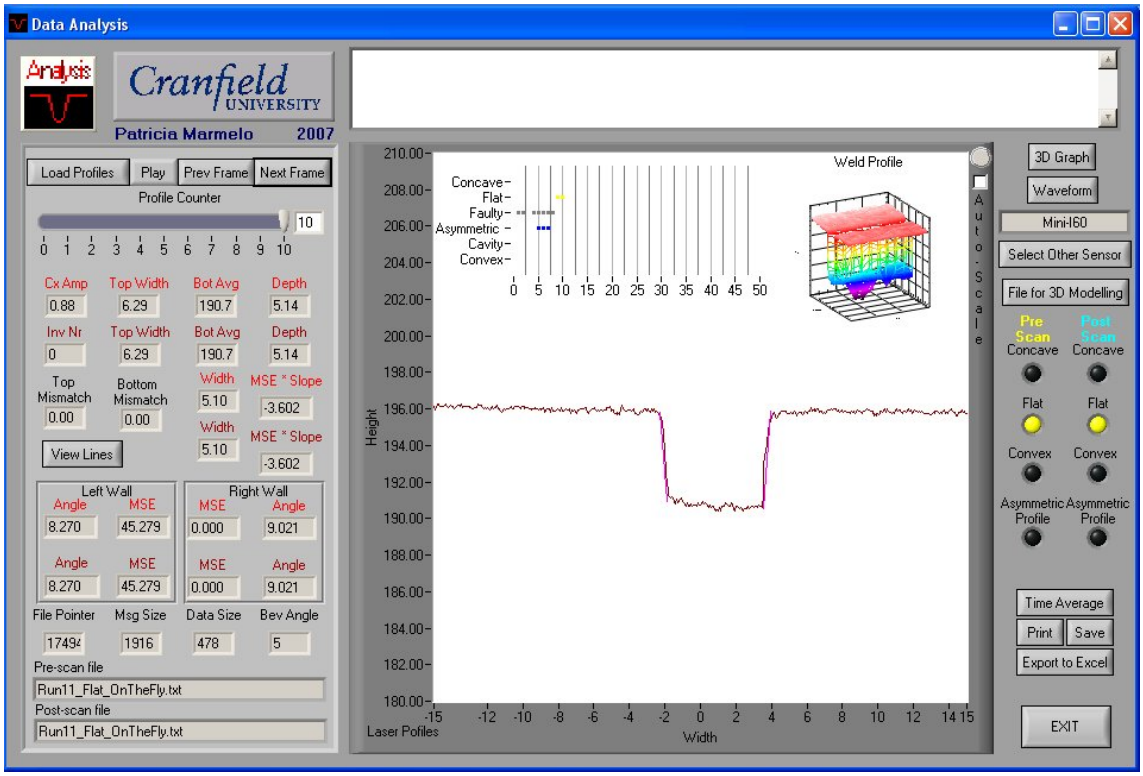

Figure I.1.0.11 – Screenshot of Profile 10 of "Run 11" in the Flat Position.

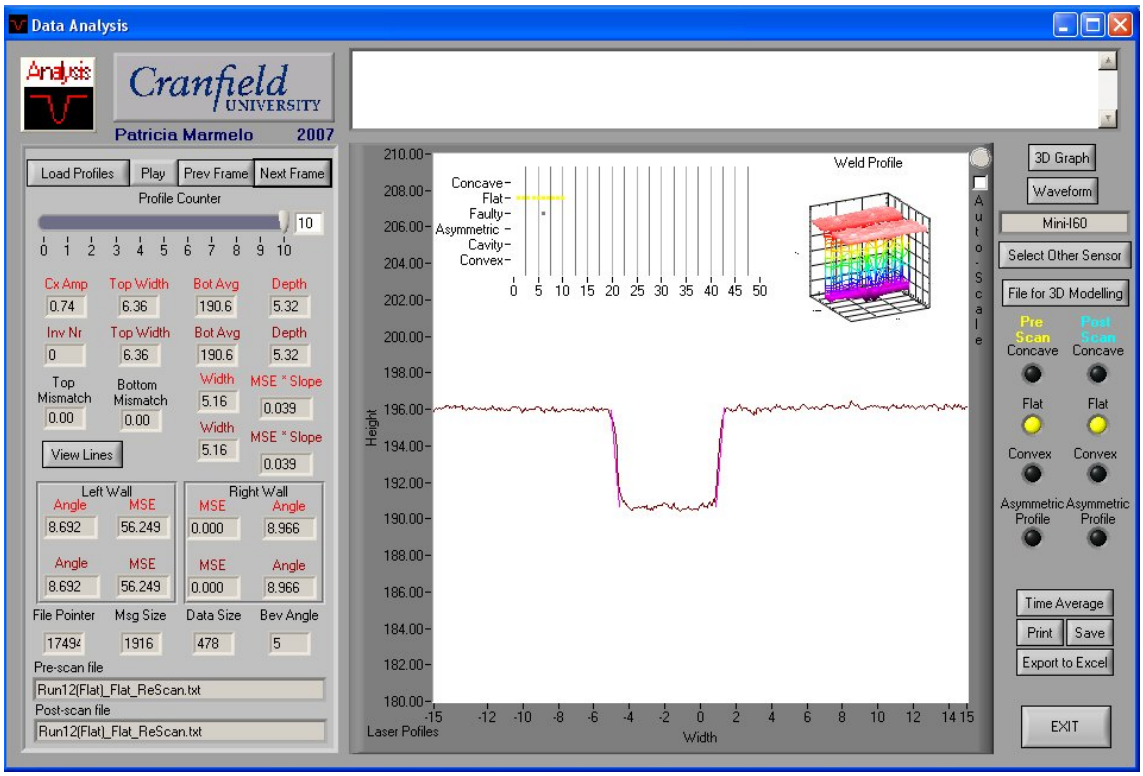

Figure I.1.0.12 – Screenshot of Profile 10 of "Run 12" in the Flat Position.

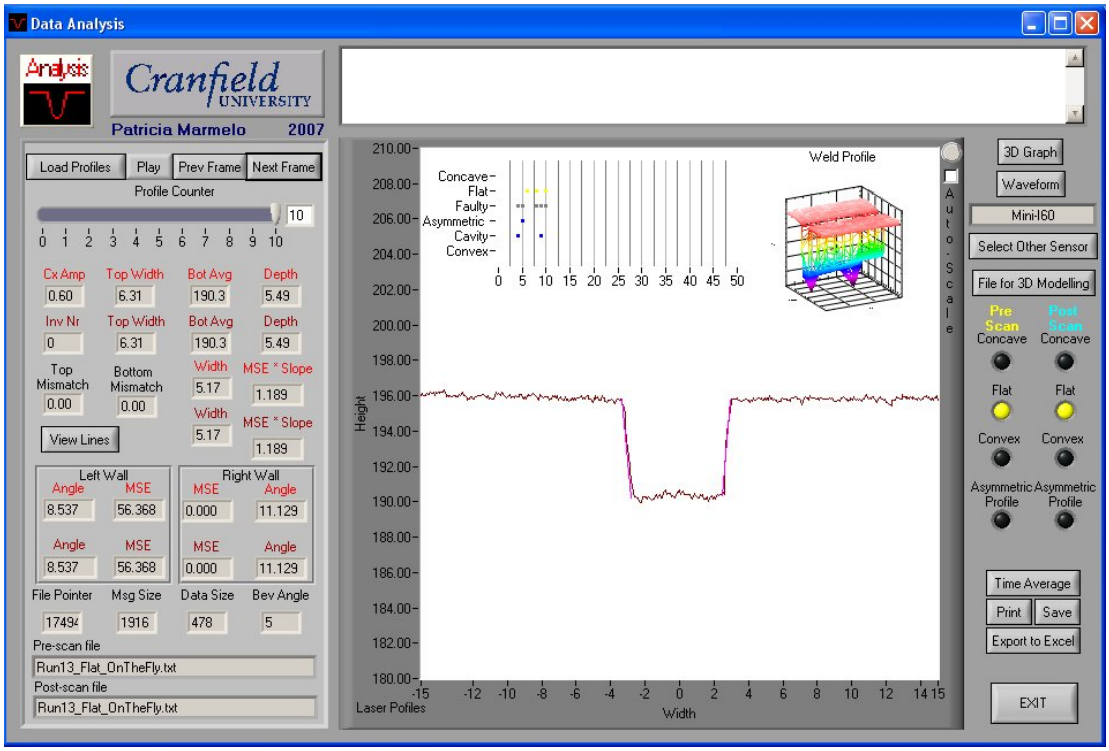

Figure I.1.0.13 – Screenshot of Profile 10 of "Run 13" in the Flat Position, Showing a Flat Bead Shape.

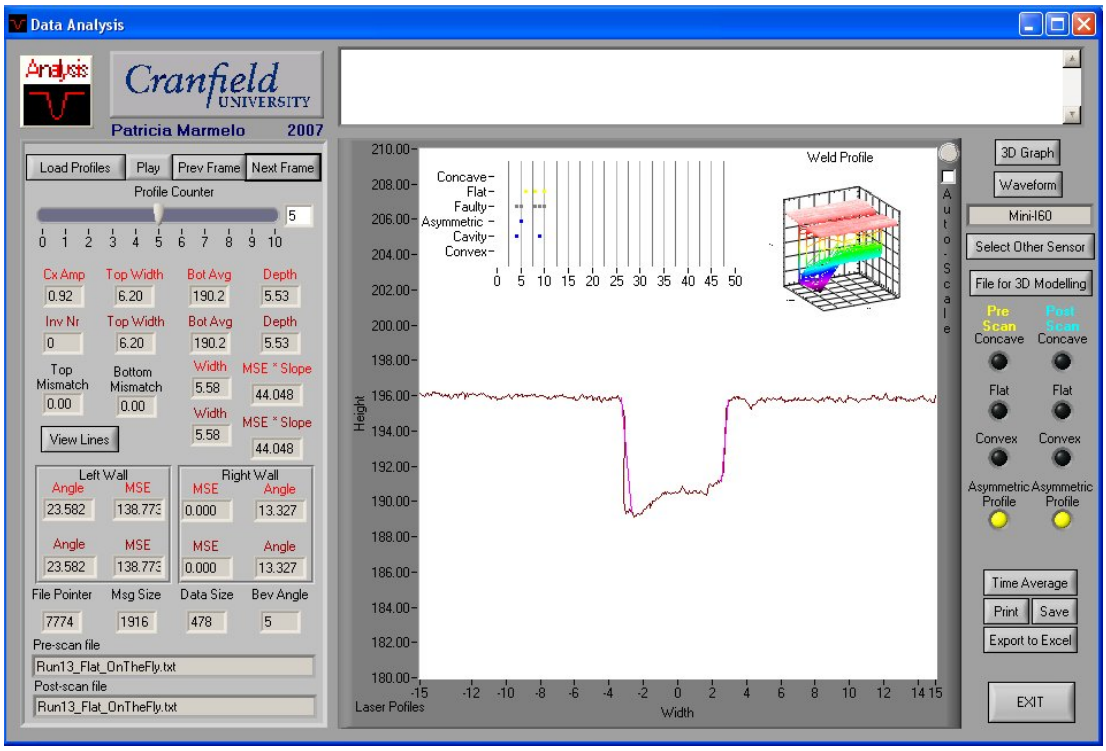

Figure I.1.0.14 – Screenshot of Profile 5 of "Run 13" in the Flat Position, Showing an Asymmetric Profile.

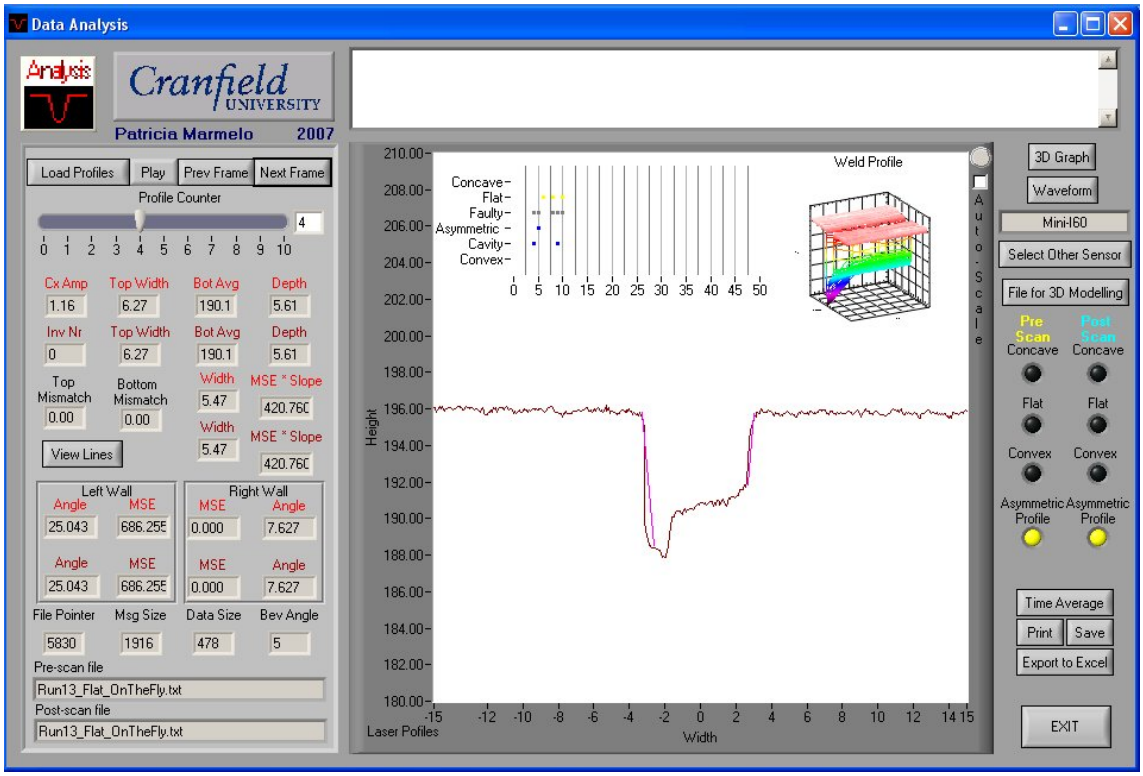

Figure I.1.0.15 – Screenshot of Profile 4 of "Run 13" in the Flat Position, Showing a Bead Shape Containing a Cavity.

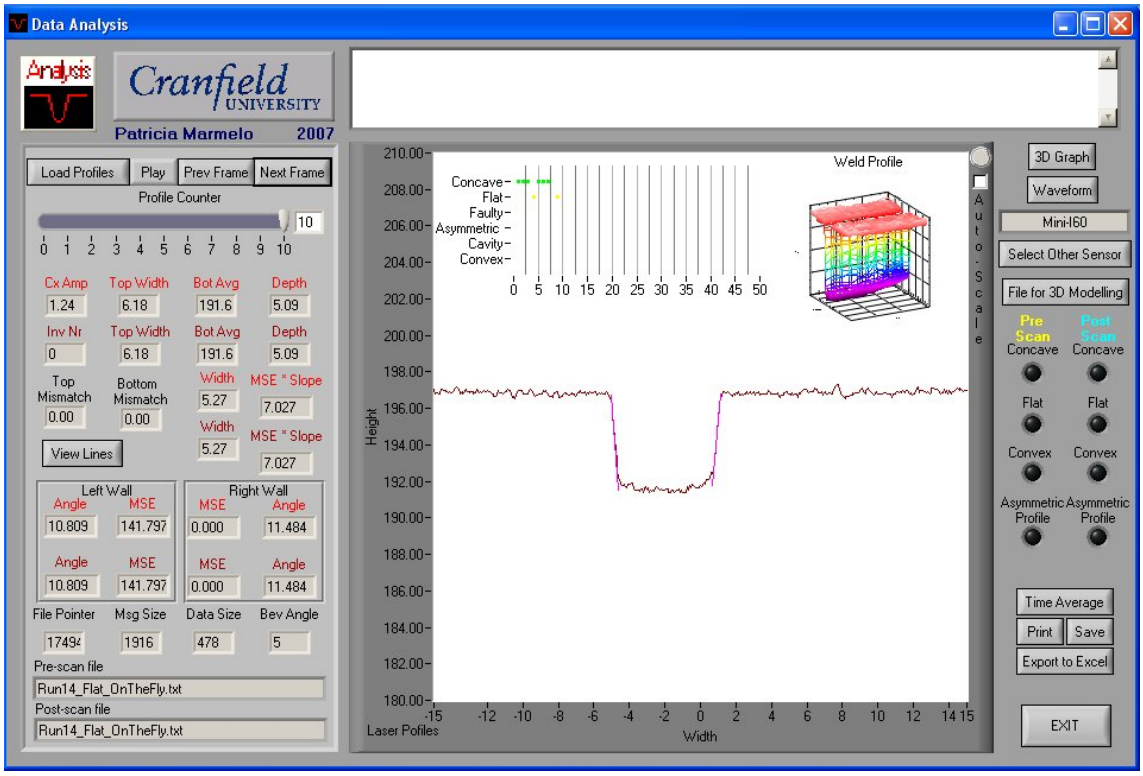

Figure I.1.0.16 – Screenshot of Profile 10 of "Run 14" in the Flat Position.

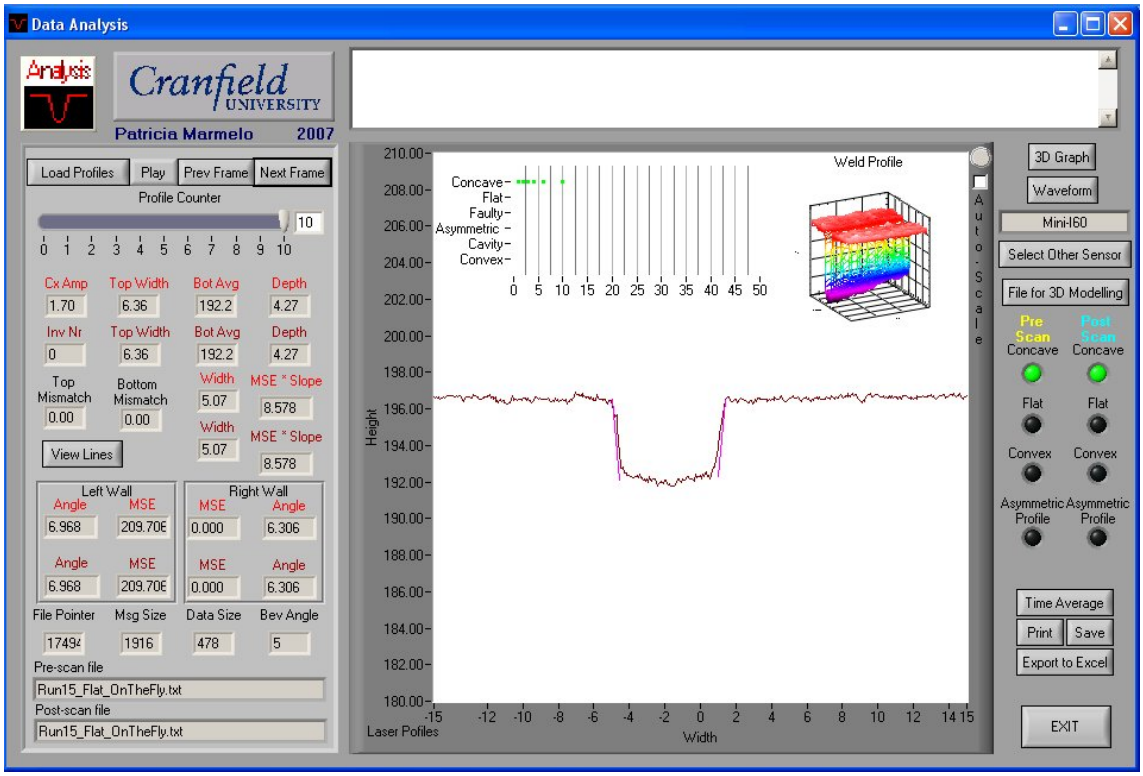

Figure I.1.0.17 – Screenshot of Profile 10 of "Run 15" in the Flat Position.

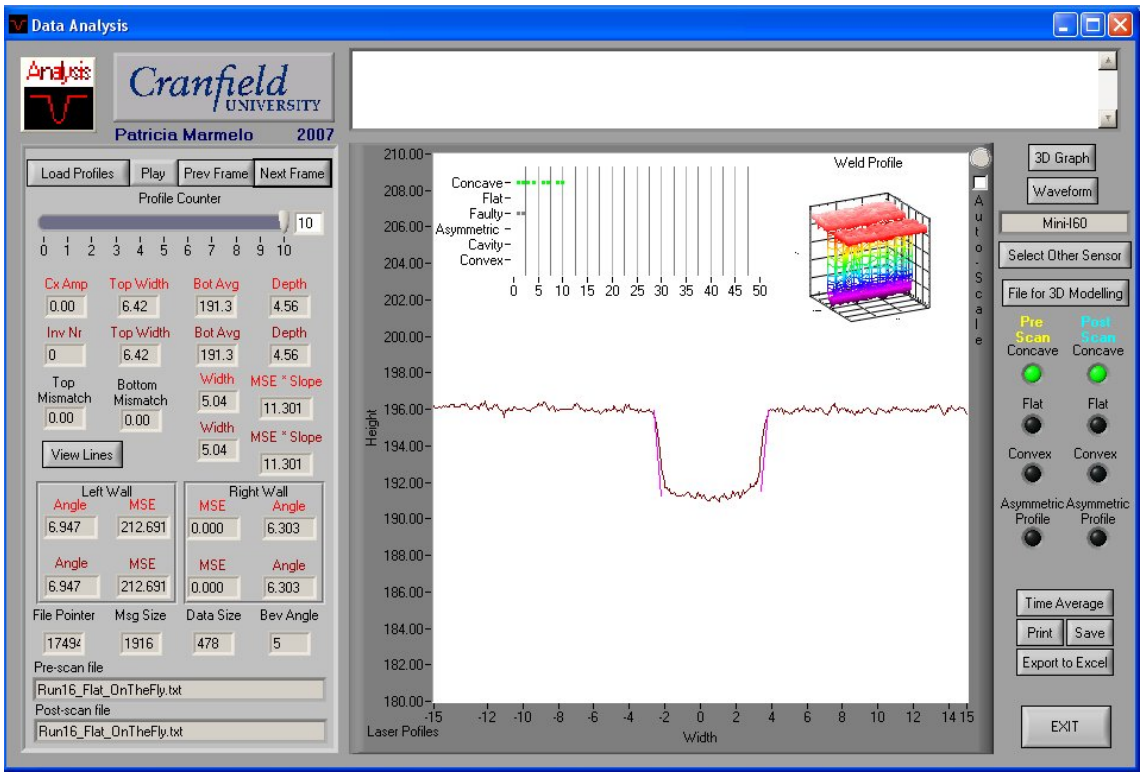

Figure I.1.0.18 – Screenshot of Profile 10 of "Run 16" in the Flat Position.

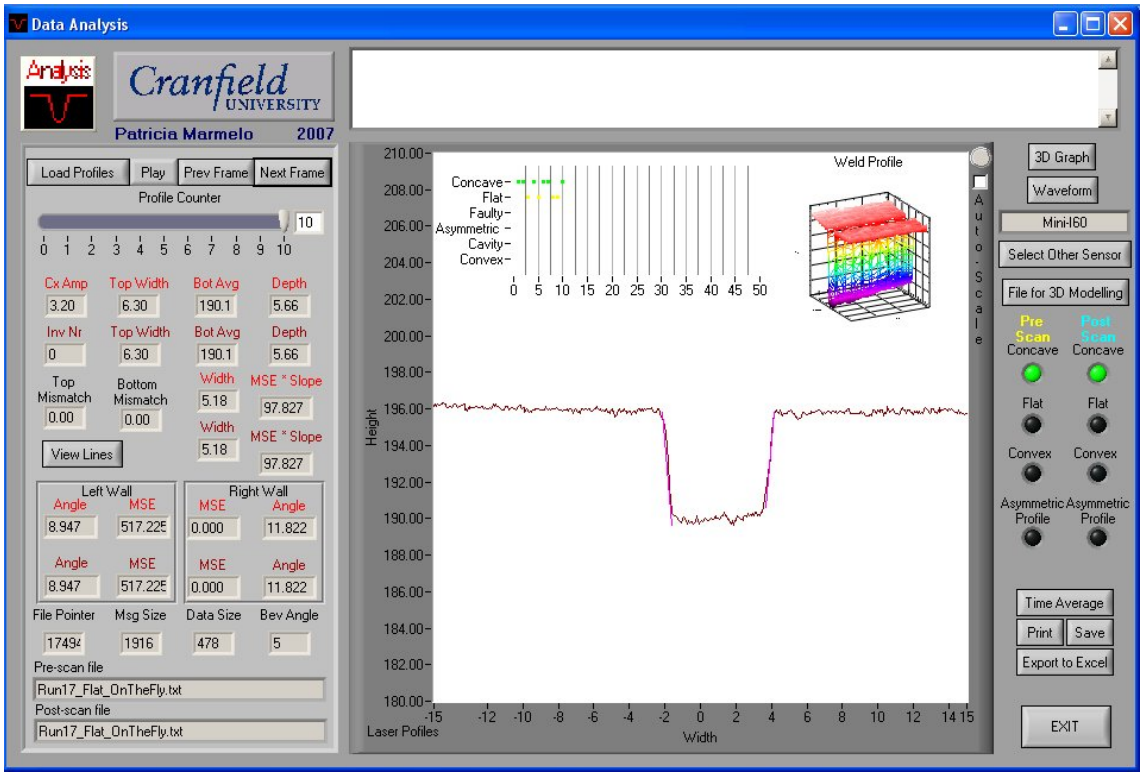

Figure I.1.0.19 – Screenshot of Profile 10 of "Run 17" in the Flat Position.

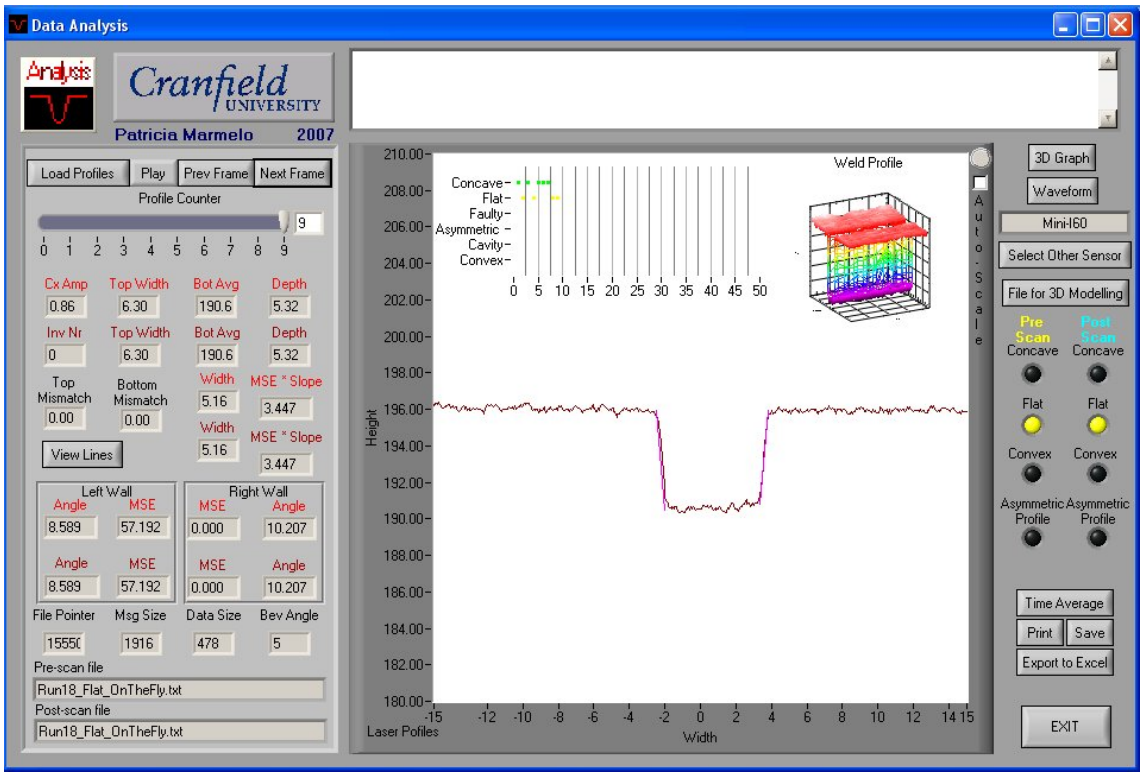

Figure I.1.0.20 – Screenshot of Profile 10 of "Run 18" in the Flat Position.

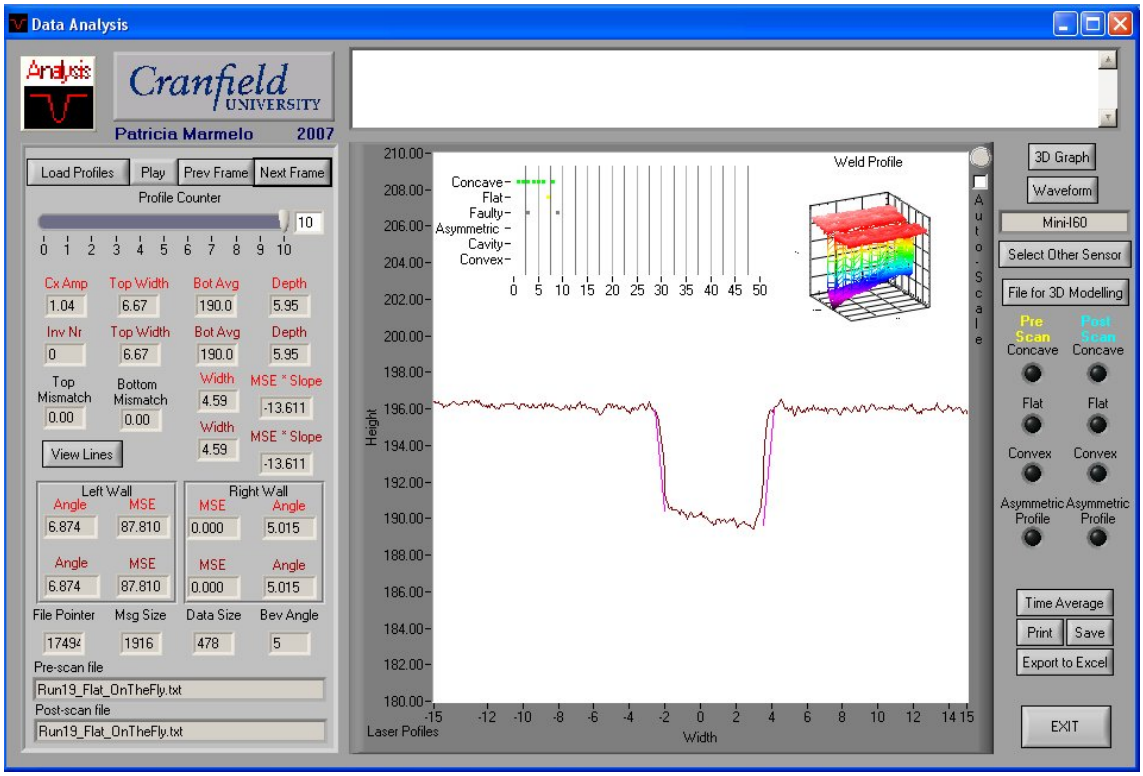

Figure I.1.0.21 – Screenshot of Profile 10 of "Run 19" in the Flat Position.

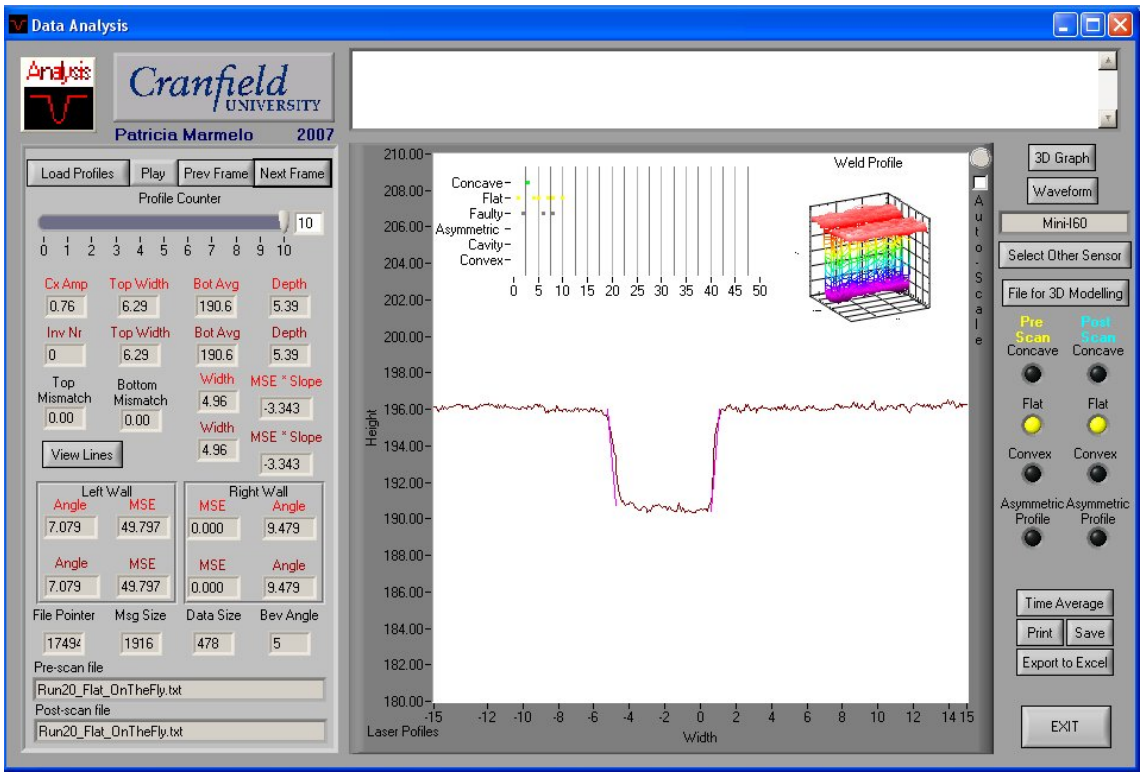

Figure I.1.0.22 – Screenshot of Profile 10 of "Run 20" in the Flat Position.

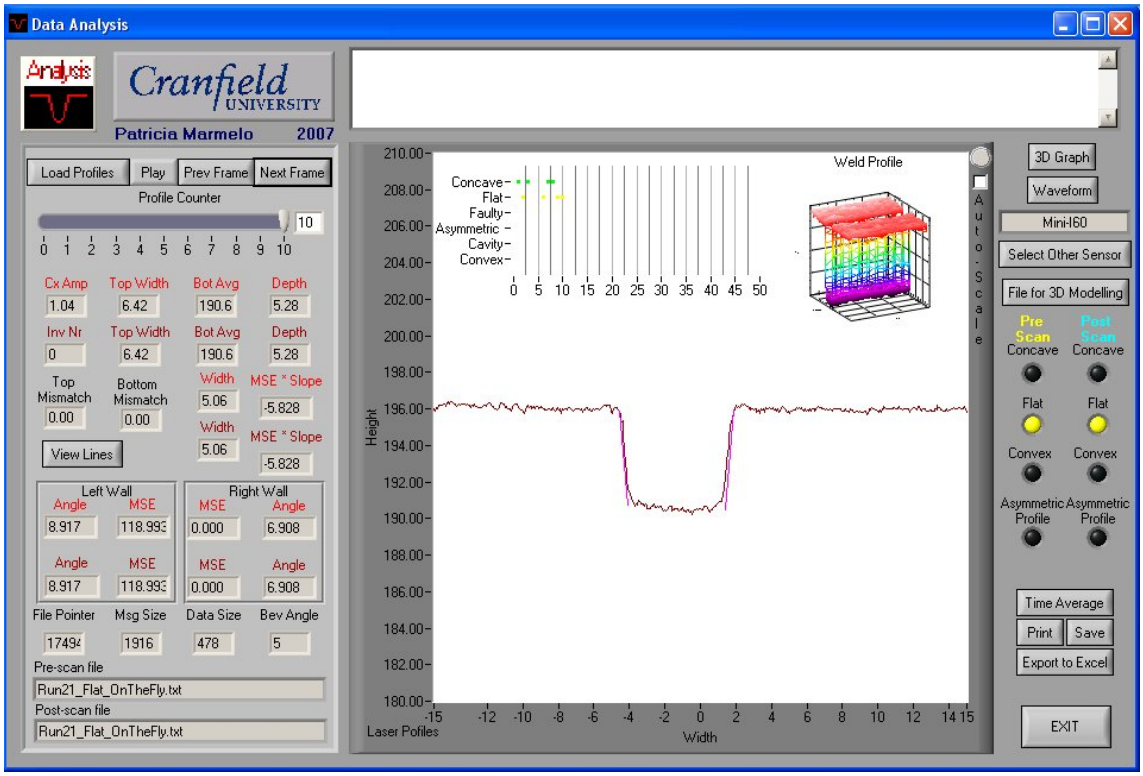

Figure I.1.0.23 – Screenshot of Profile 10 of "Run 21" in the Flat Position.

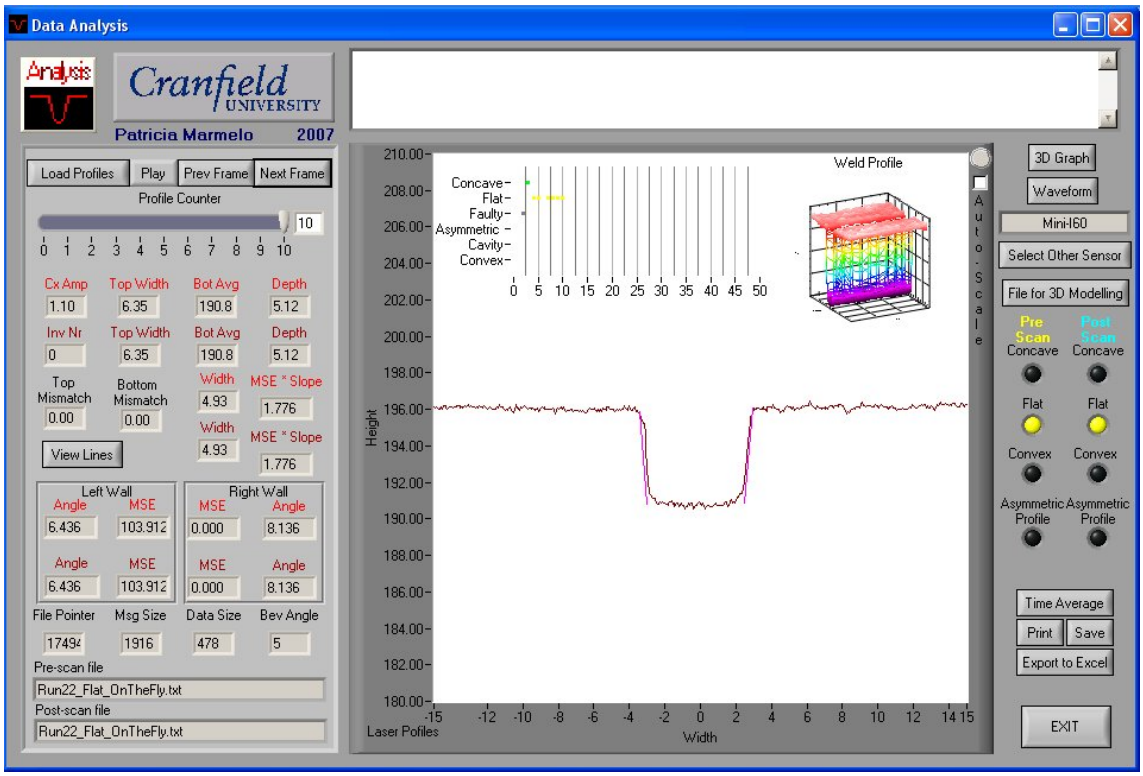

Figure I.1.0.24 – Screenshot of Profile 10 of "Run 22" in the Flat Position.

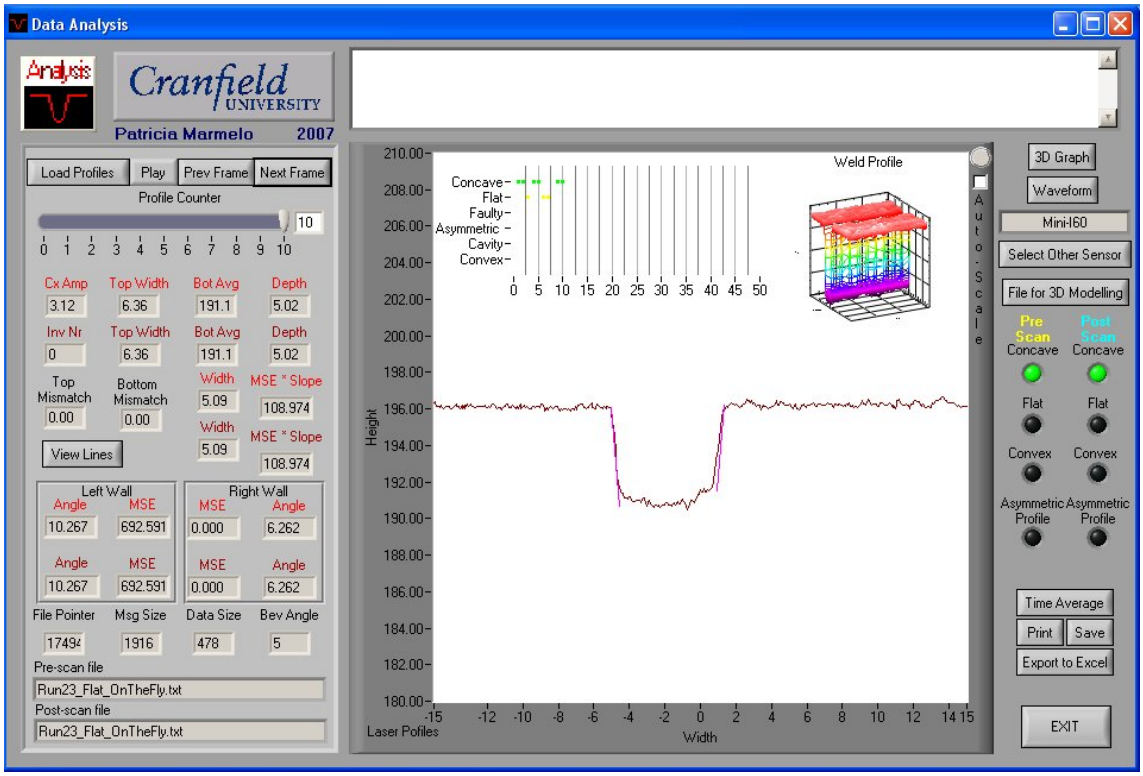

Figure I.1.0.25 – Screenshot of Profile 10 of "Run 23" in the Flat Position.

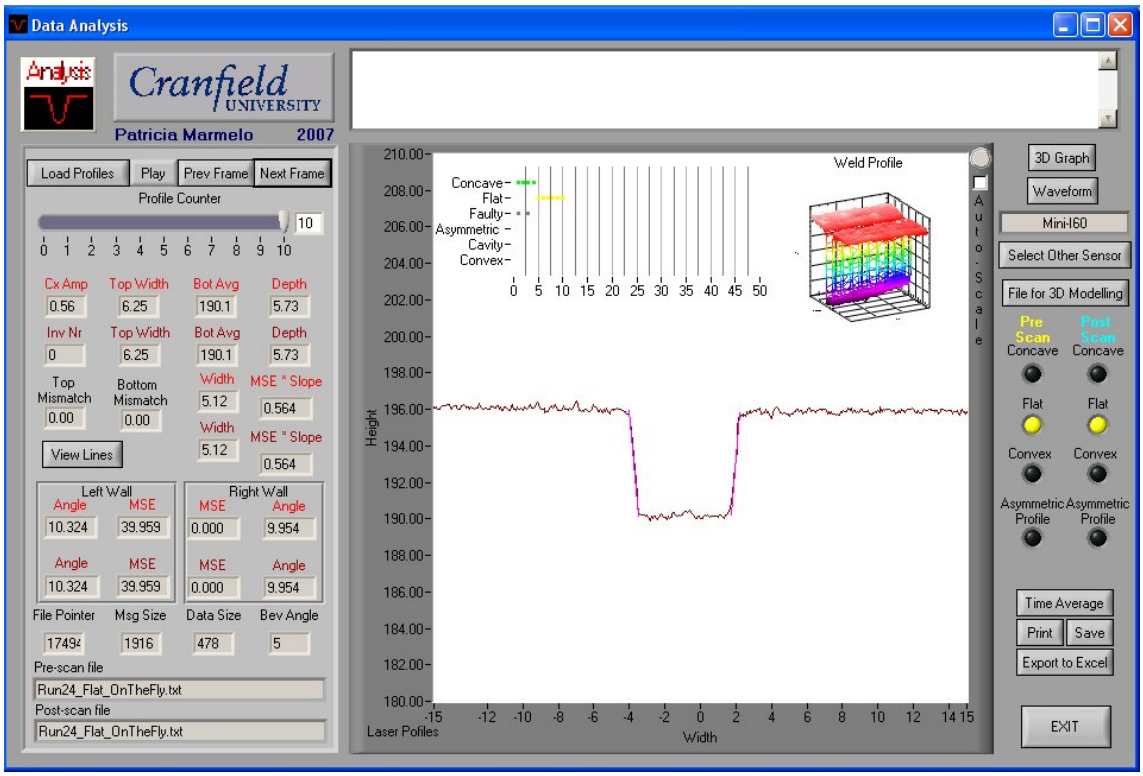

Figure I.1.0.26 – Screenshot of Profile 10 of "Run 24" in the Flat Position.

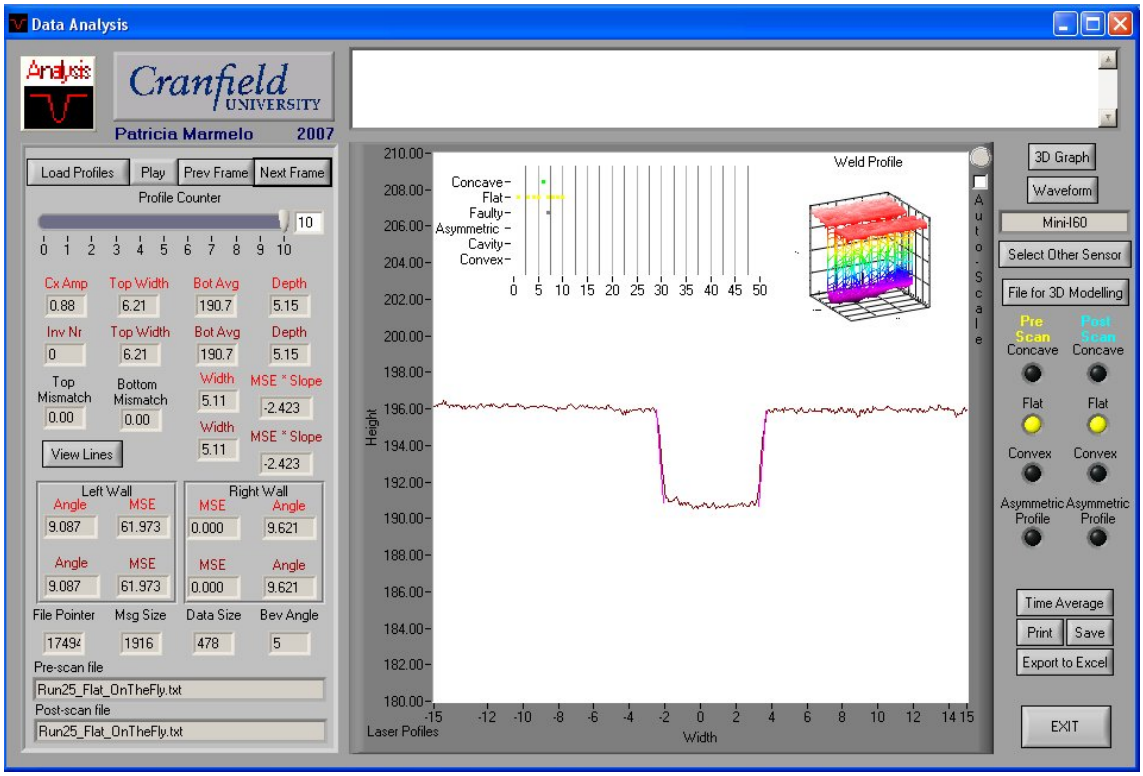

Figure I.1.0.27 – Screenshot of Profile 10 of "Run 25" in the Flat Position.

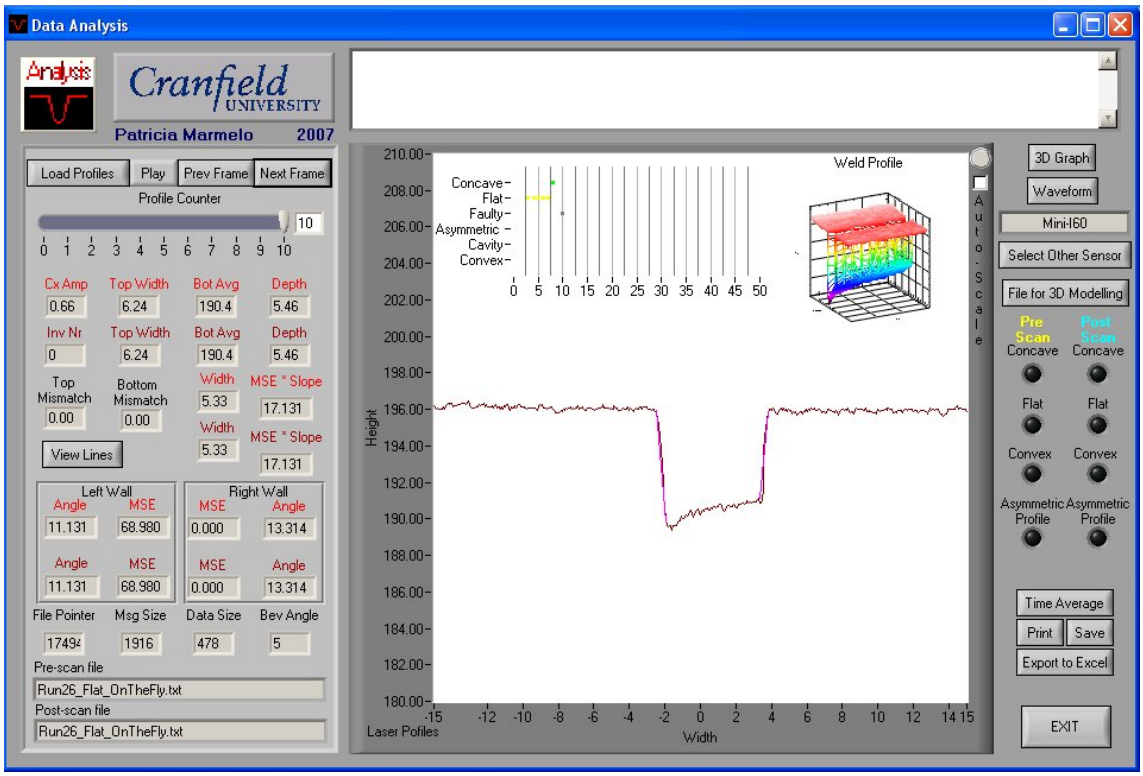

Figure I.1.0.28 – Screenshot of Profile 10 of "Run 26" in the Flat Position, Showing an Asymmetric Profile.

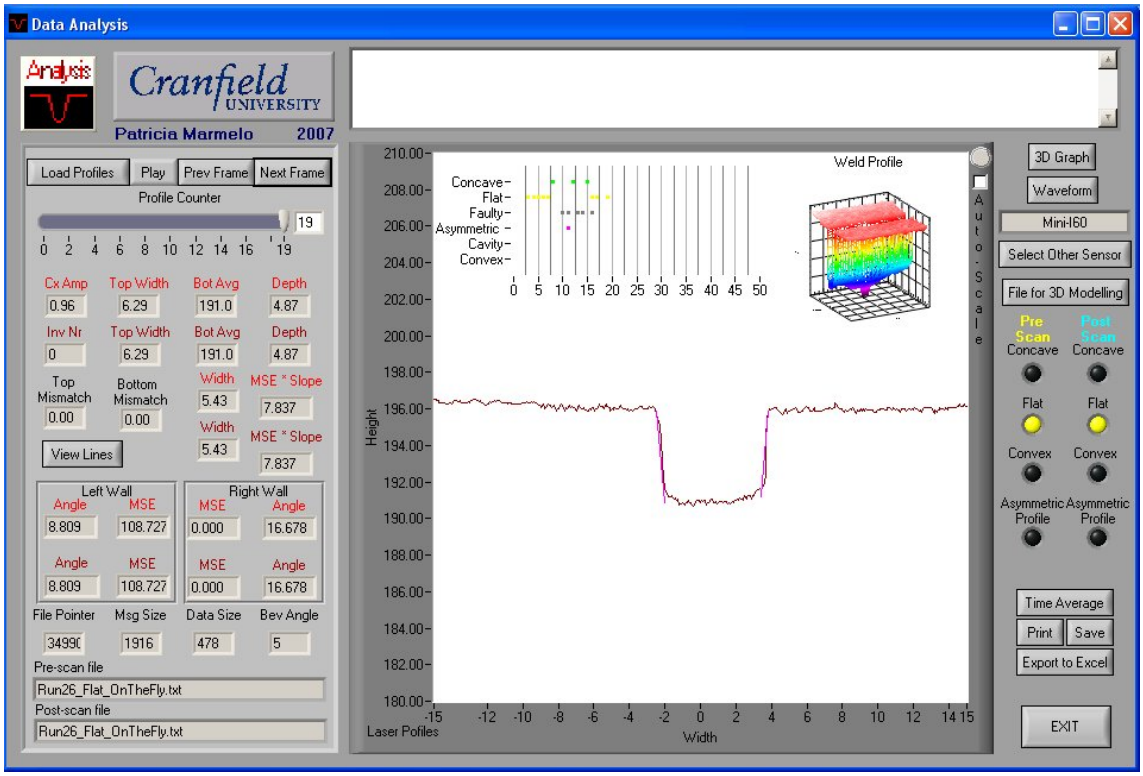

Figure I.1.0.29 – Screenshot of Profile 19 of "Run 26" in the Flat Position, Showing a Flat Bead Shape.

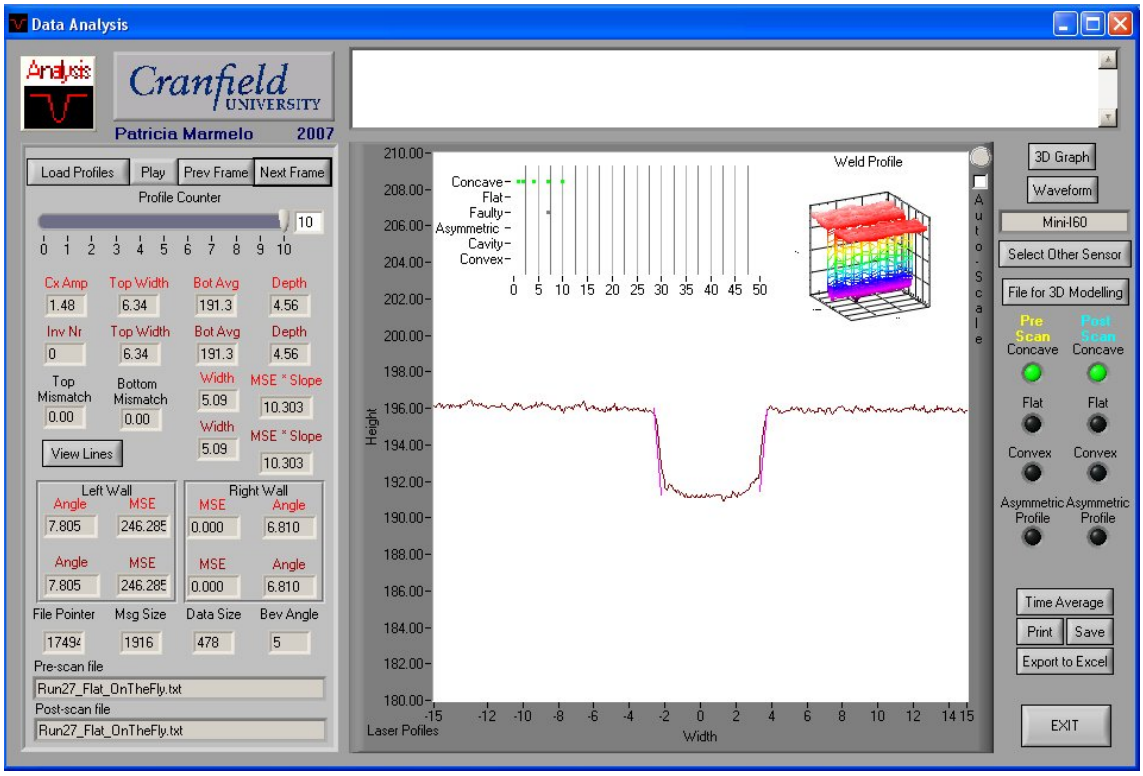

Figure I.1.0.30 – Screenshot of Profile 10 of "Run 27" in the Flat Position.

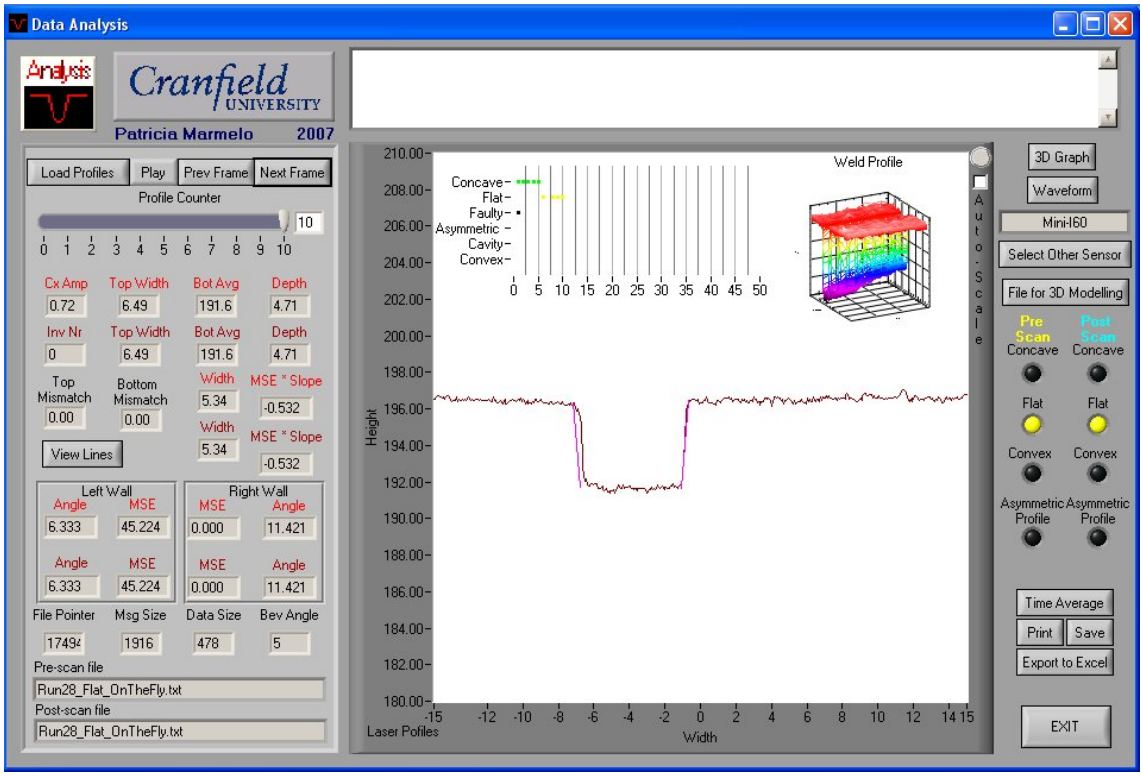

Figure I.1.0.31 – Screenshot of Profile 10 of "Run 28" in the Flat Position.

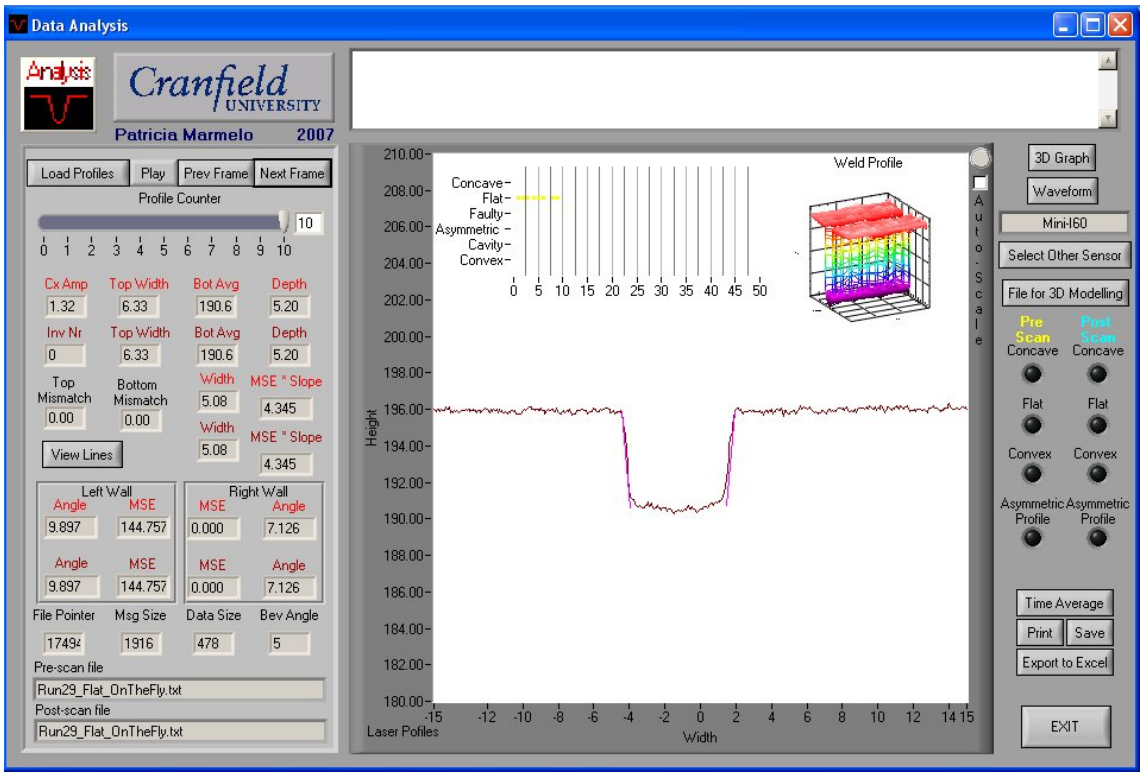

Figure I.1.0.32 – Screenshot of Profile 10 of "Run 29" in the Flat Position.

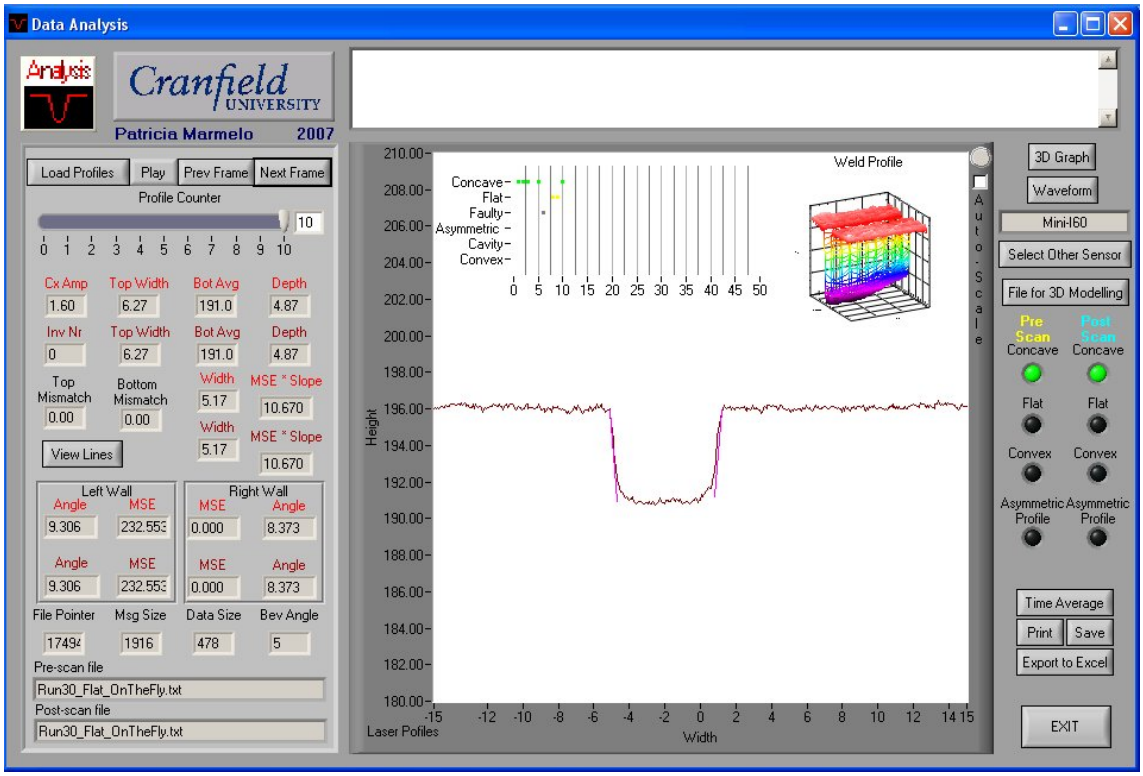

Figure I.1.0.33 – Screenshot of Profile 10 of "Run 30" in the Flat Position.

I2 Vertical-Down (Down Hand) Position

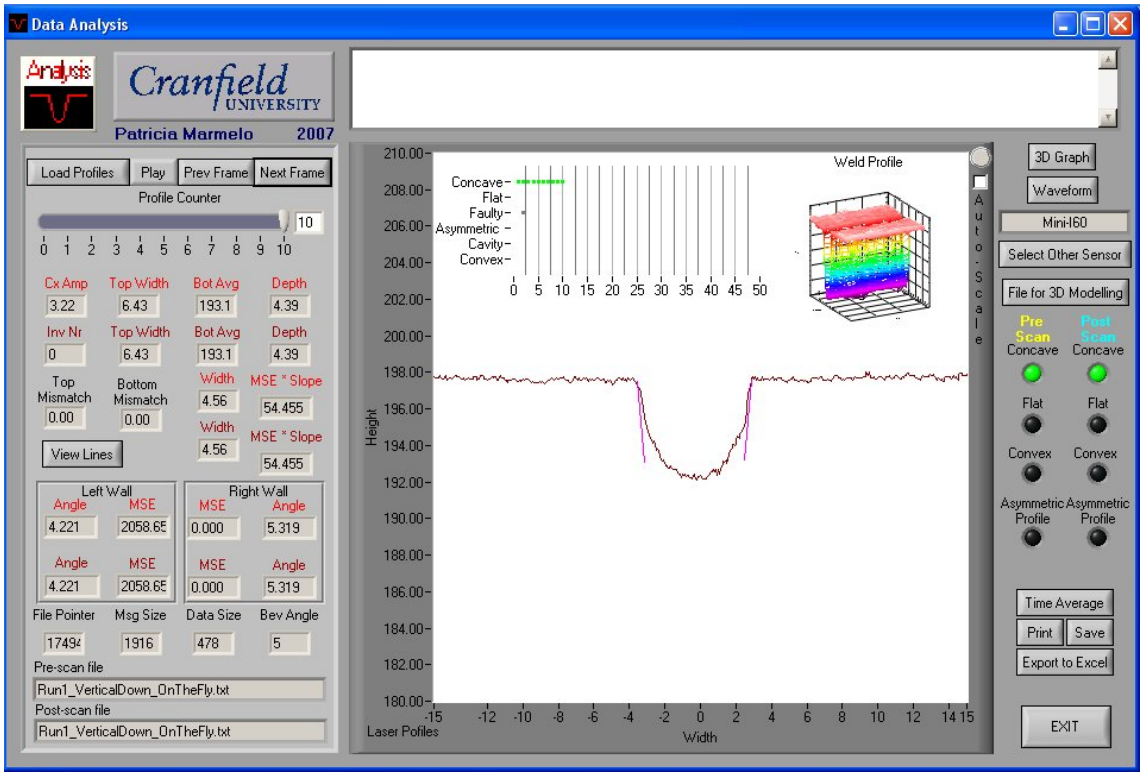

Figure I.2.0.34 – Screenshot of Profile 10 of "Run 1" in the Vertical (Down Hand) Position.

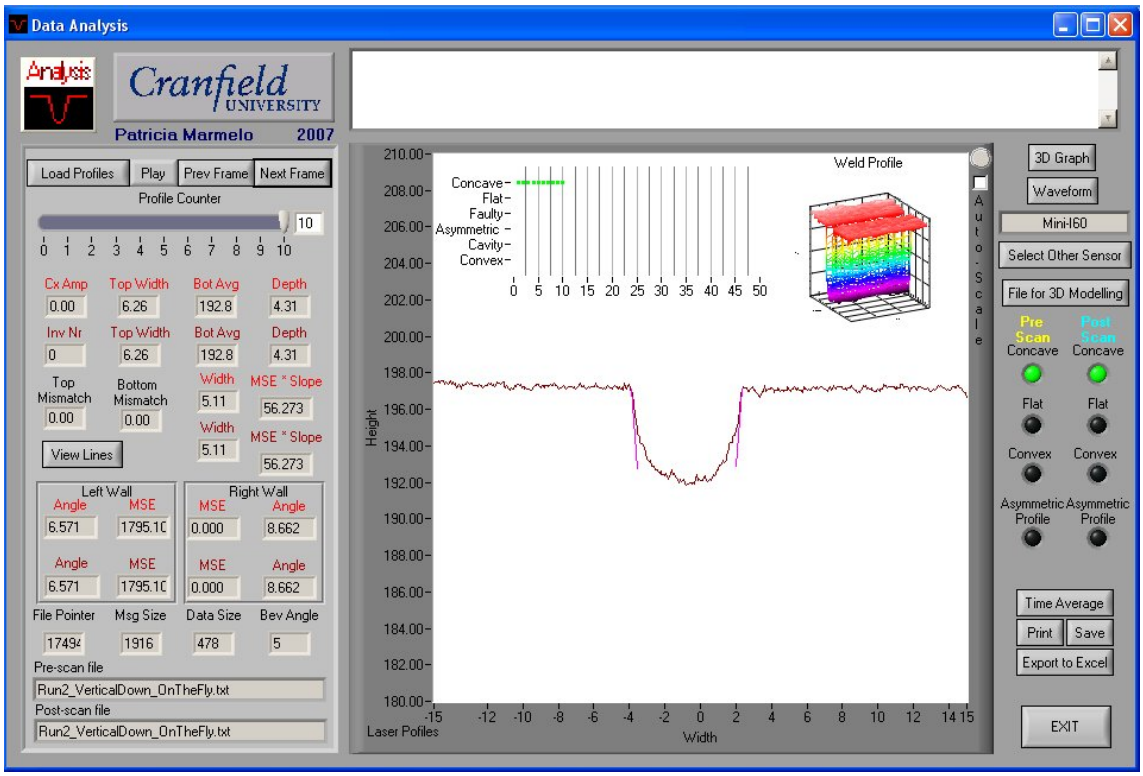

Figure I.2.0.35 – Screenshot of Profile 10 of "Run 2" in the Vertical (Down Hand) Position.

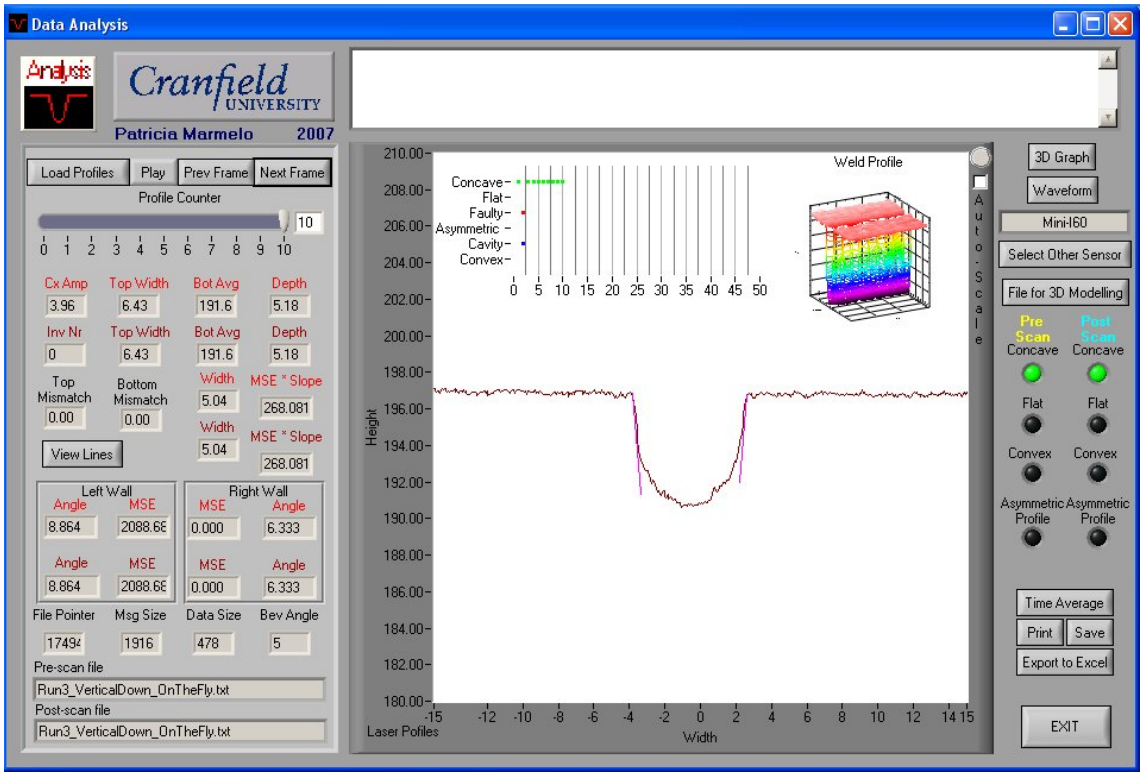

Figure I.2.0.36 – Screenshot of Profile 10 of "Run 3" in the Vertical (Down Hand) Position.

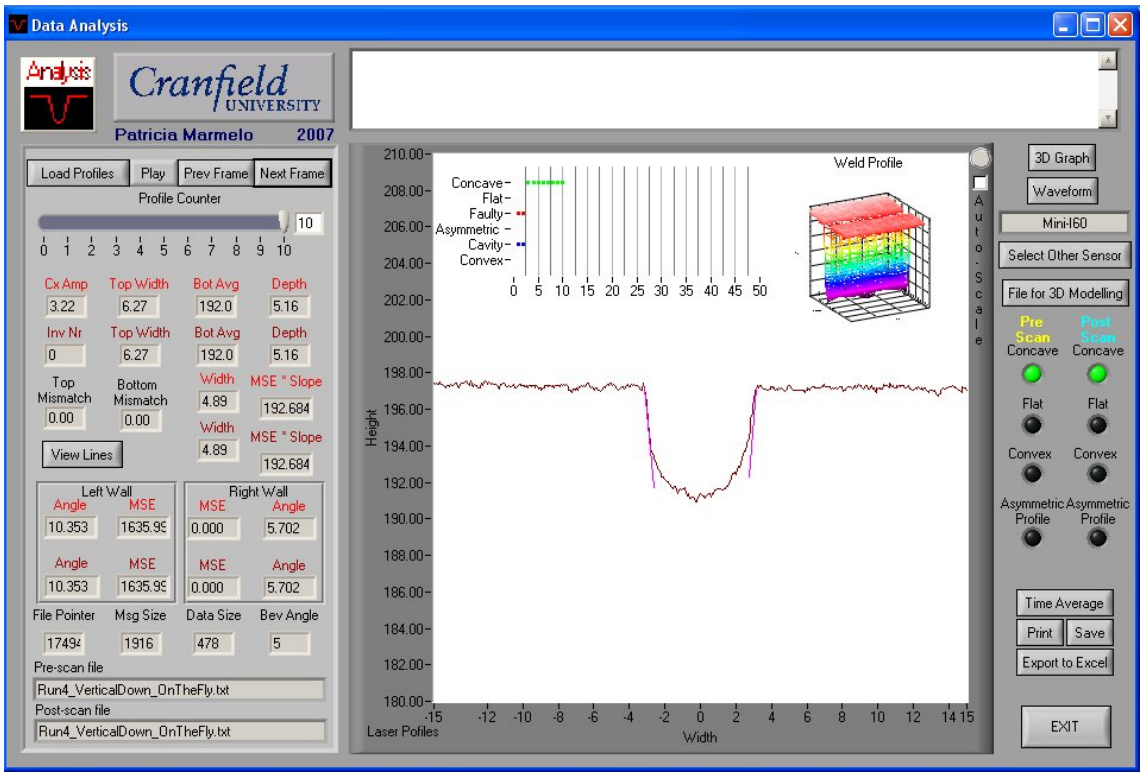

Figure I.2.0.37 – Screenshot of Profile 10 of "Run 4" in the Vertical (Down Hand) Position.

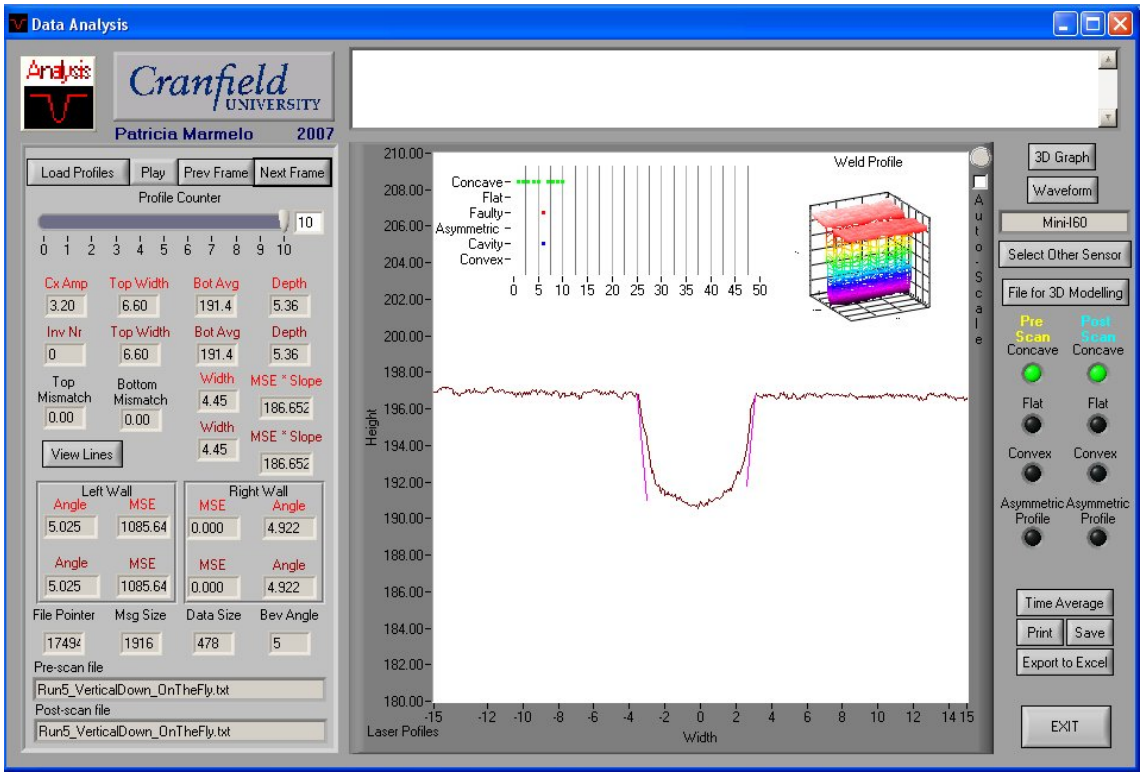

Figure I.2.0.38 – Screenshot of Profile 10 of "Run 5" in the Vertical (Down Hand) Position.

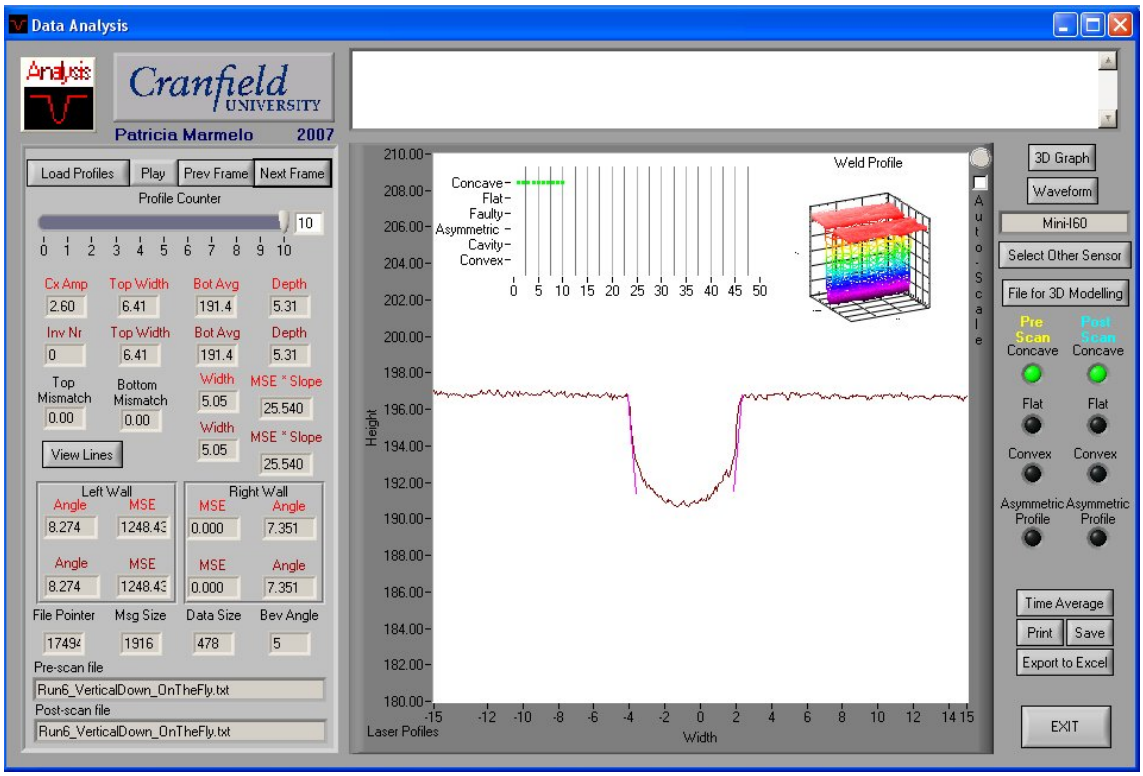

Figure I.2.0.39 – Screenshot of Profile 10 of "Run 6" in the Vertical (Down Hand) Position.

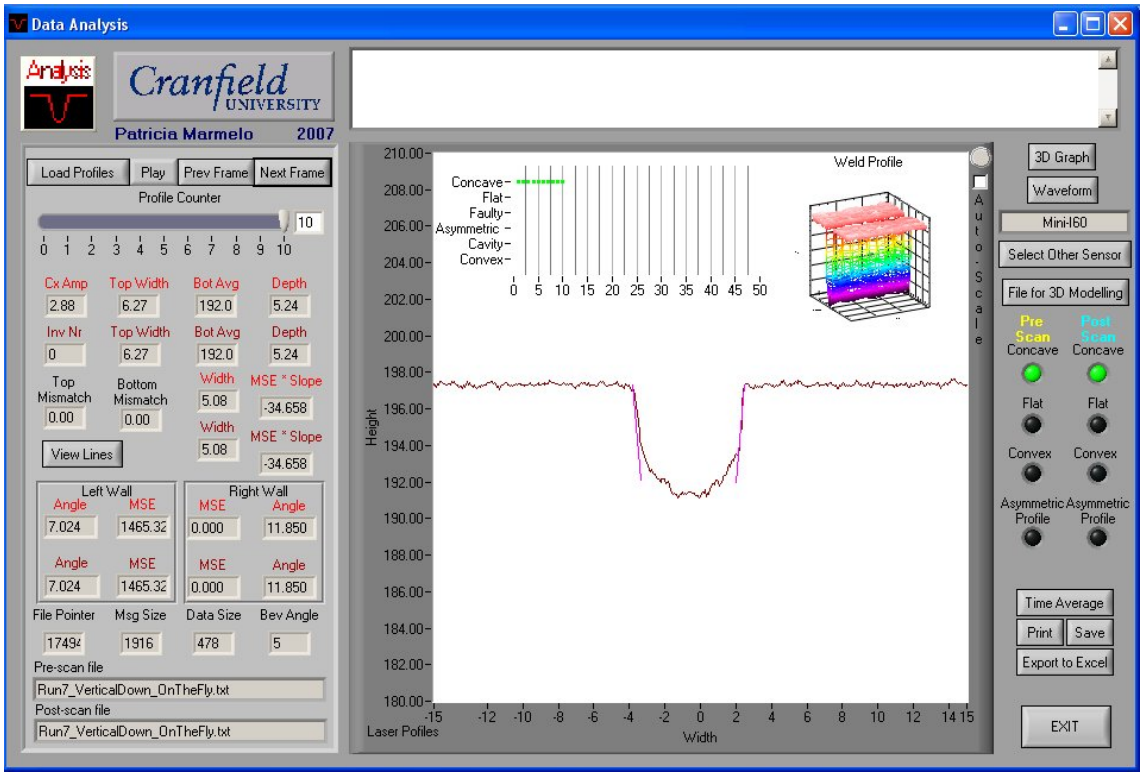

Figure I.2.0.40 – Screenshot of Profile 10 of "Run 7" in the Vertical (Down Hand) Position.

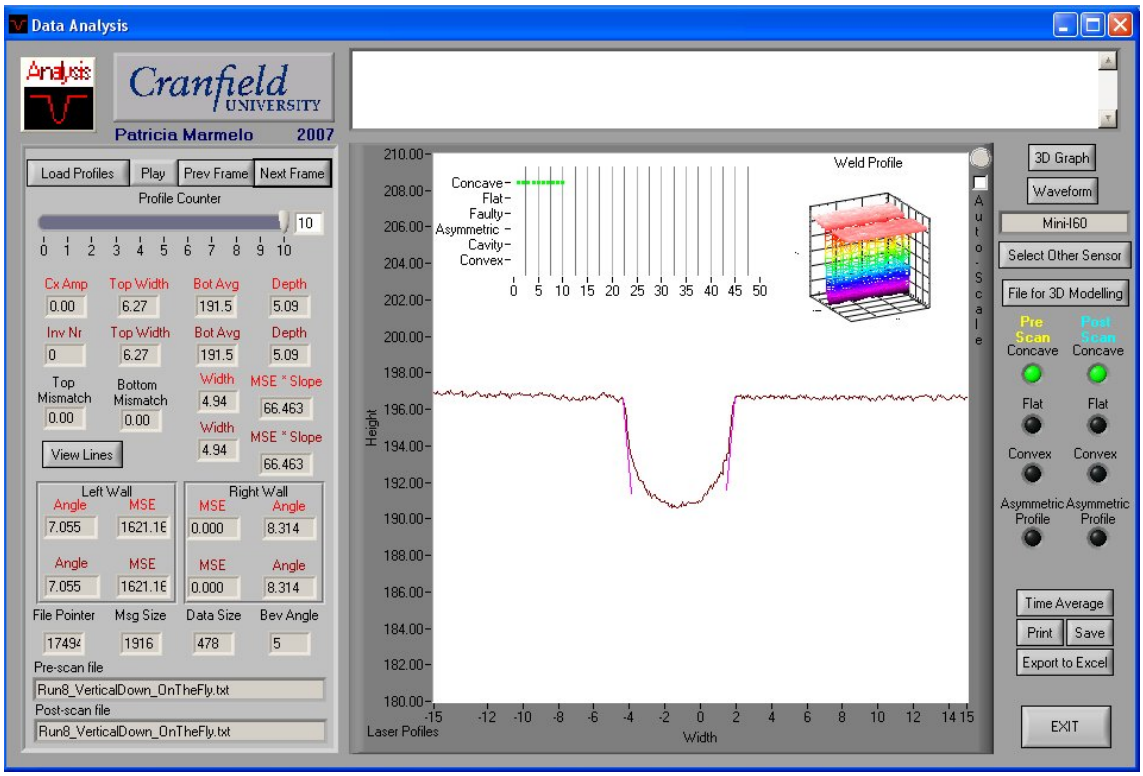

Figure I.2.0.41 – Screenshot of Profile 10 of "Run 8" in the Vertical (Down Hand) Position.

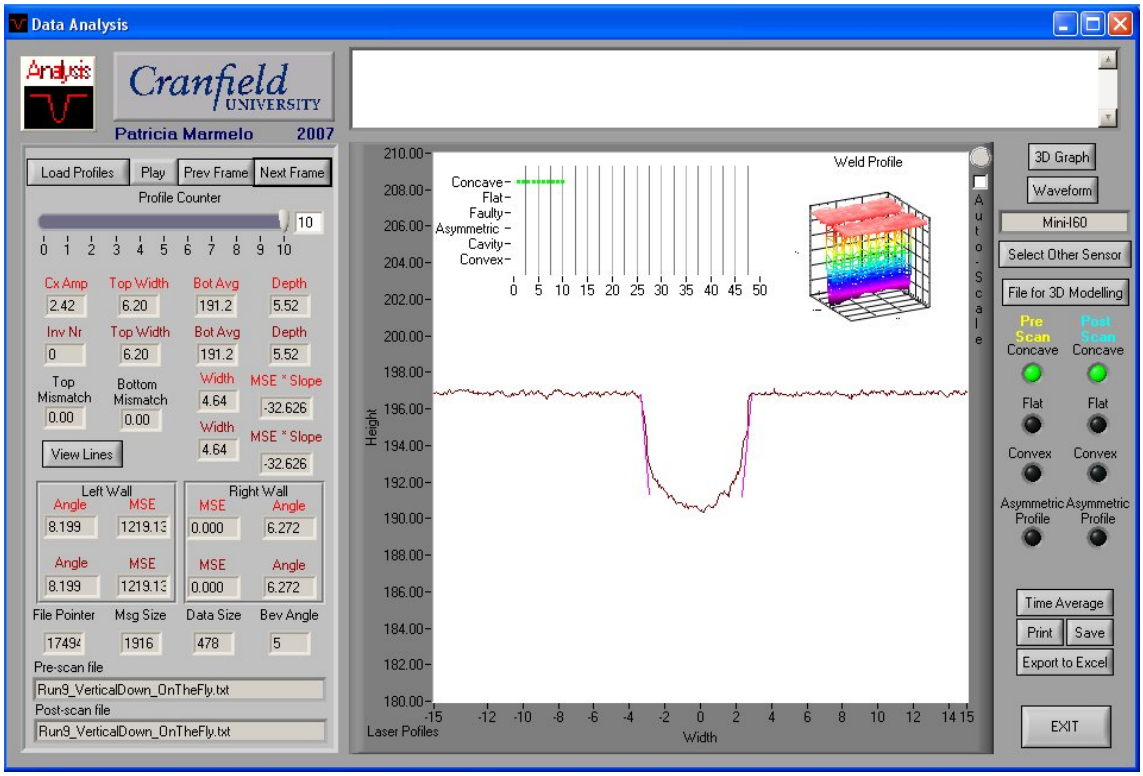

Figure I.2.0.42 – Screenshot of Profile 10 of "Run 9" in the Vertical (Down Hand) Position.

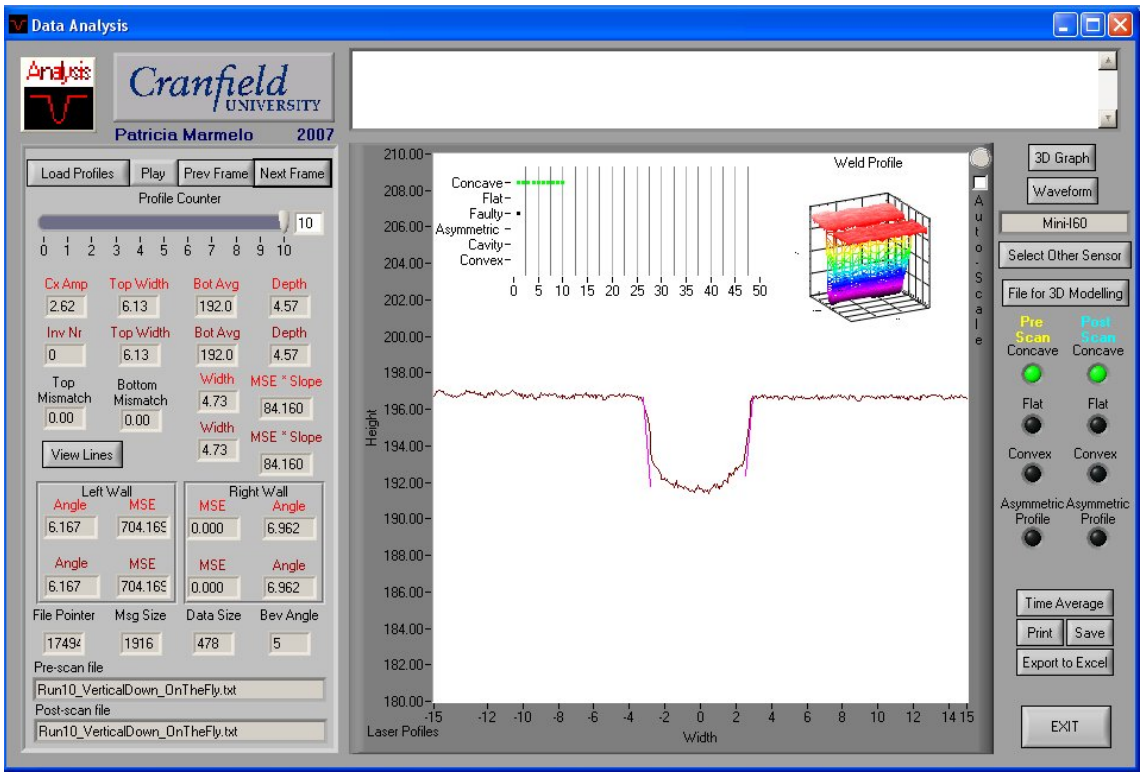

Figure I.2.0.43 – Screenshot of Profile 10 of "Run 10" in the Vertical (Down Hand) Position.

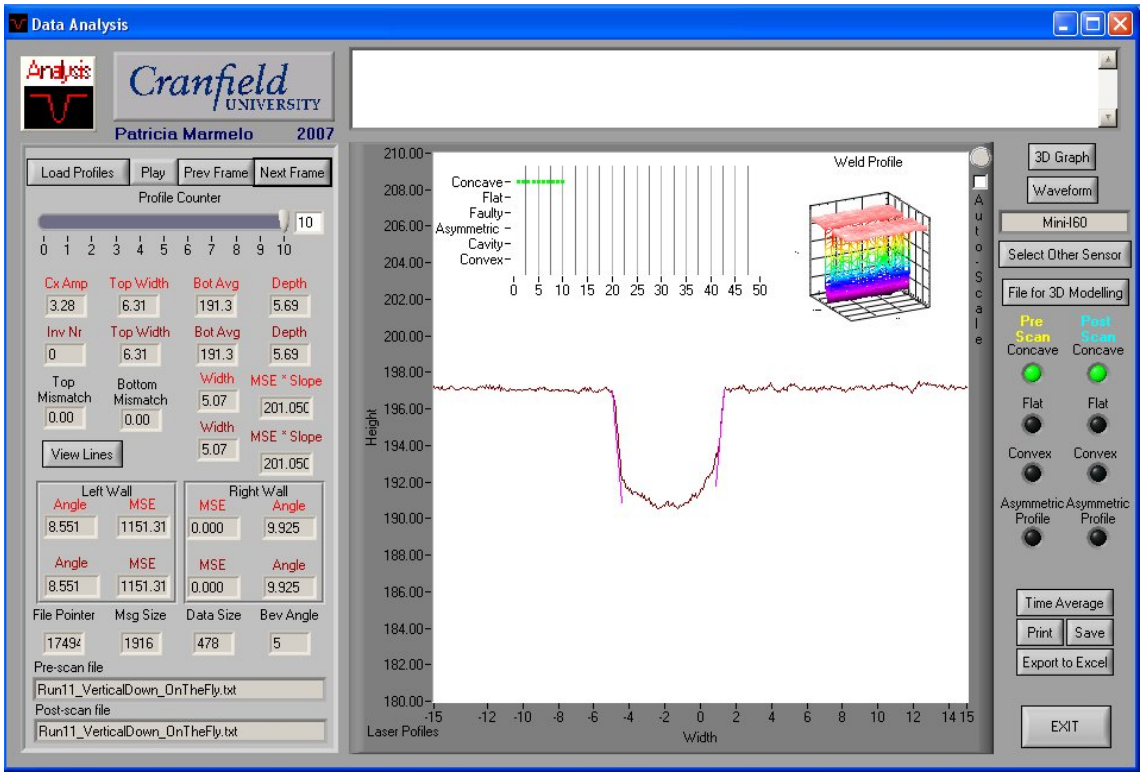

Figure I.2.0.44 – Screenshot of Profile 10 of "Run 11" in the Vertical (Down Hand) Position.

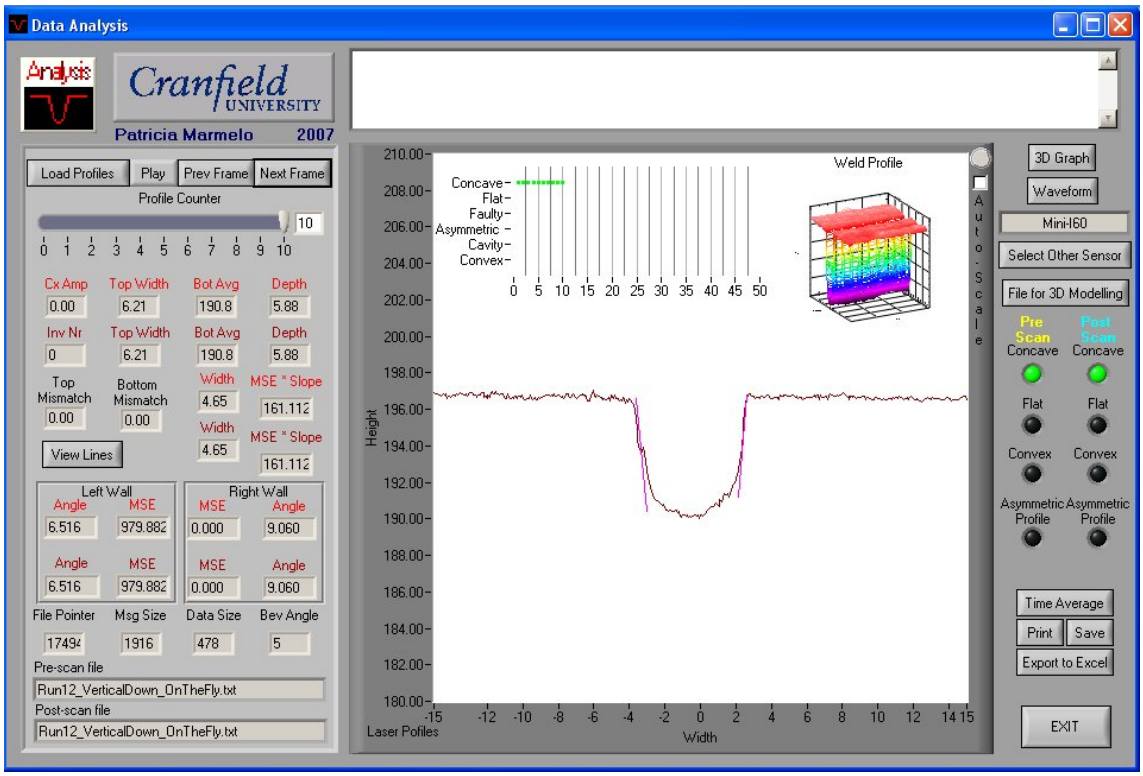

Figure I.2.0.45 – Screenshot of Profile 10 of "Run 12" in the Vertical (Down Hand) Position.

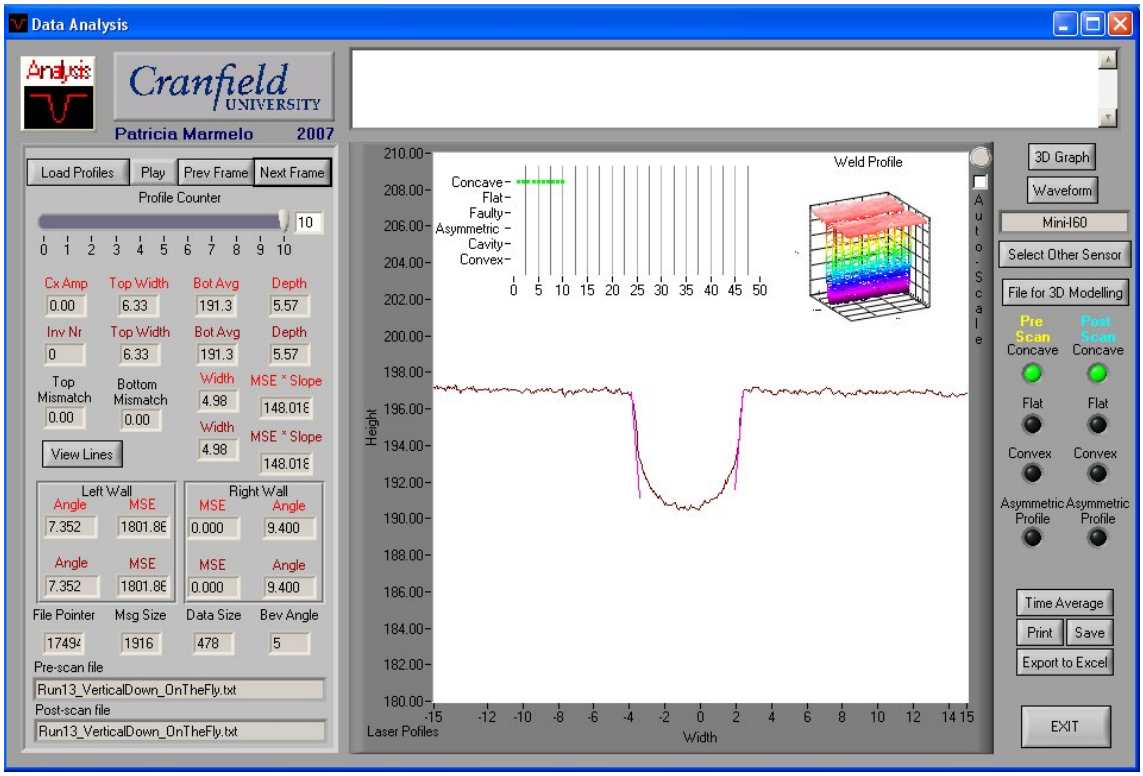

Figure I.2.0.46 – Screenshot of Profile 10 of "Run 13" in the Vertical (Down Hand) Position.

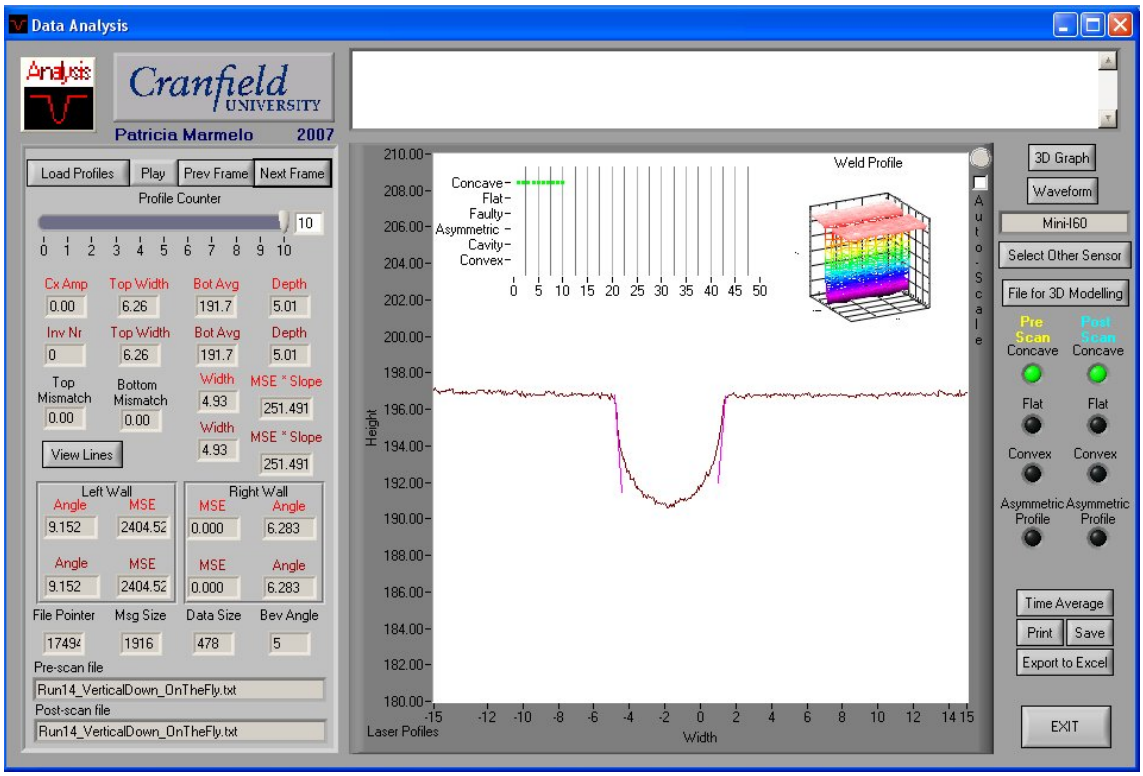

Figure I.2.0.47 – Screenshot of Profile 10 of "Run 14" in the Vertical (Down Hand) Position.

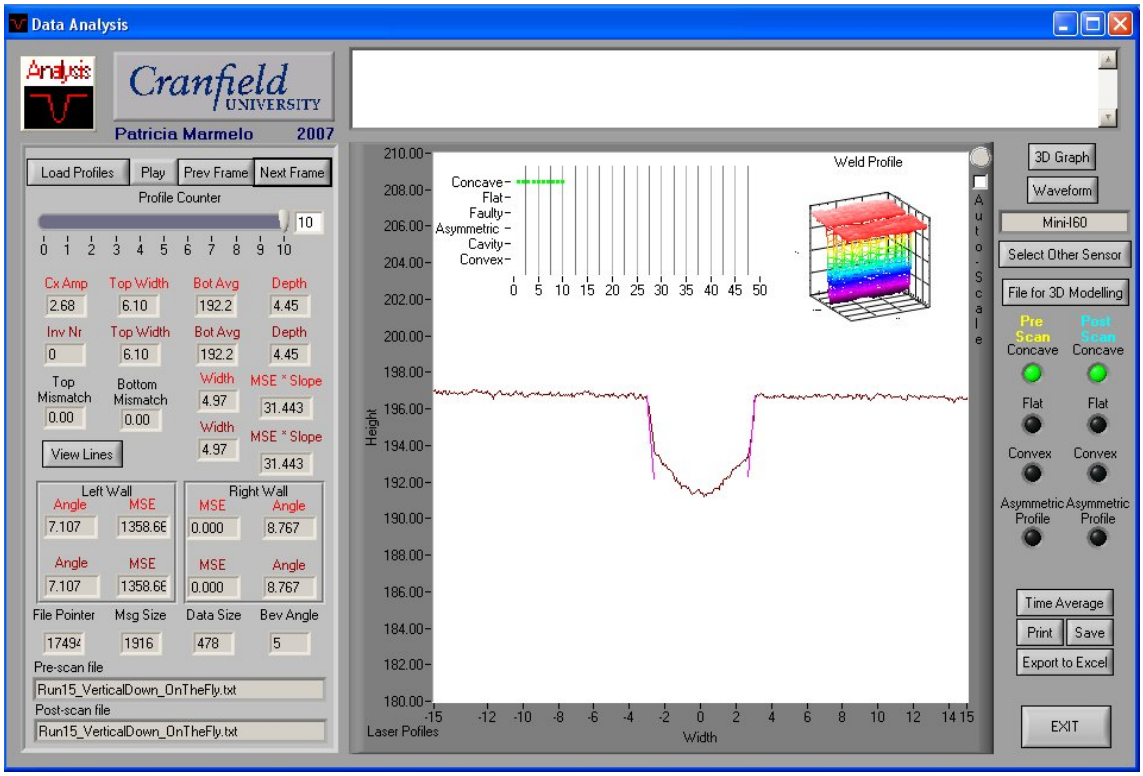

Figure I.2.0.48 – Screenshot of Profile 10 of "Run 15" in the Vertical (Down Hand) Position.

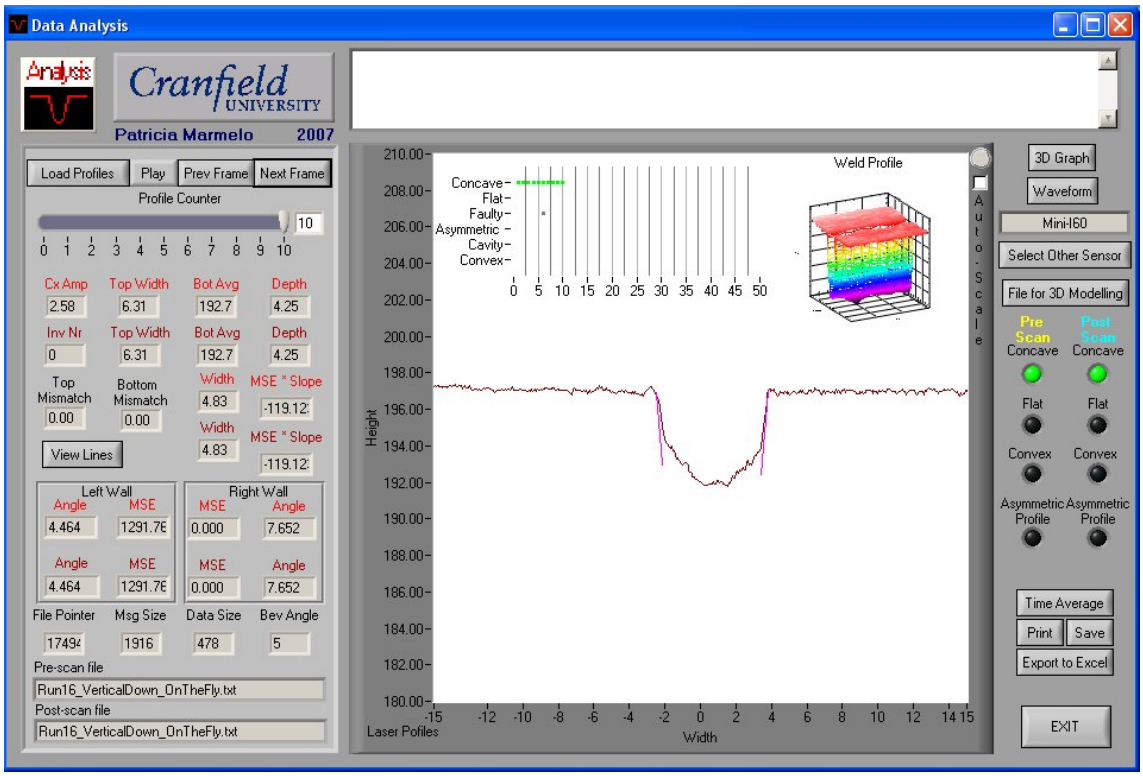

Figure I.2.0.49 – Screenshot of Profile 10 of "Run 16" in the Vertical (Down Hand) Position.

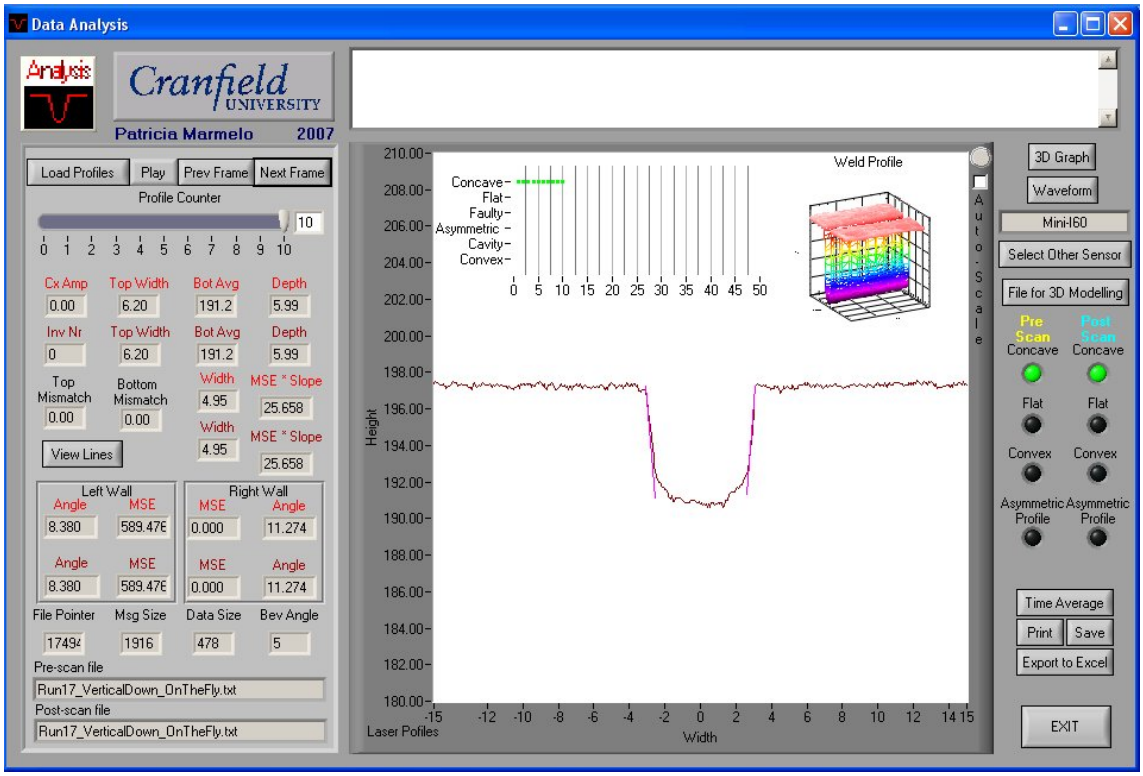

Figure I.2.0.50 – Screenshot of Profile 10 of "Run 17" in the Vertical (Down Hand) Position.

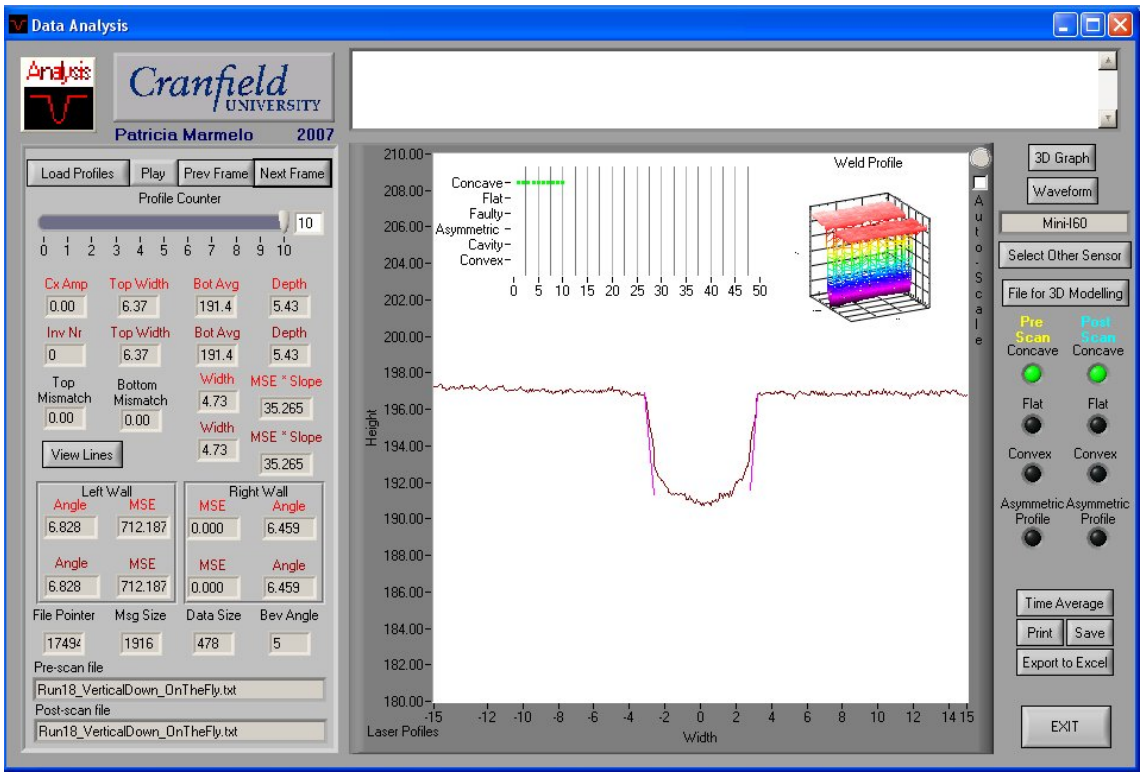

Figure I.2.0.51 – Screenshot of Profile 10 of "Run 18" in the Vertical (Down Hand) Position.

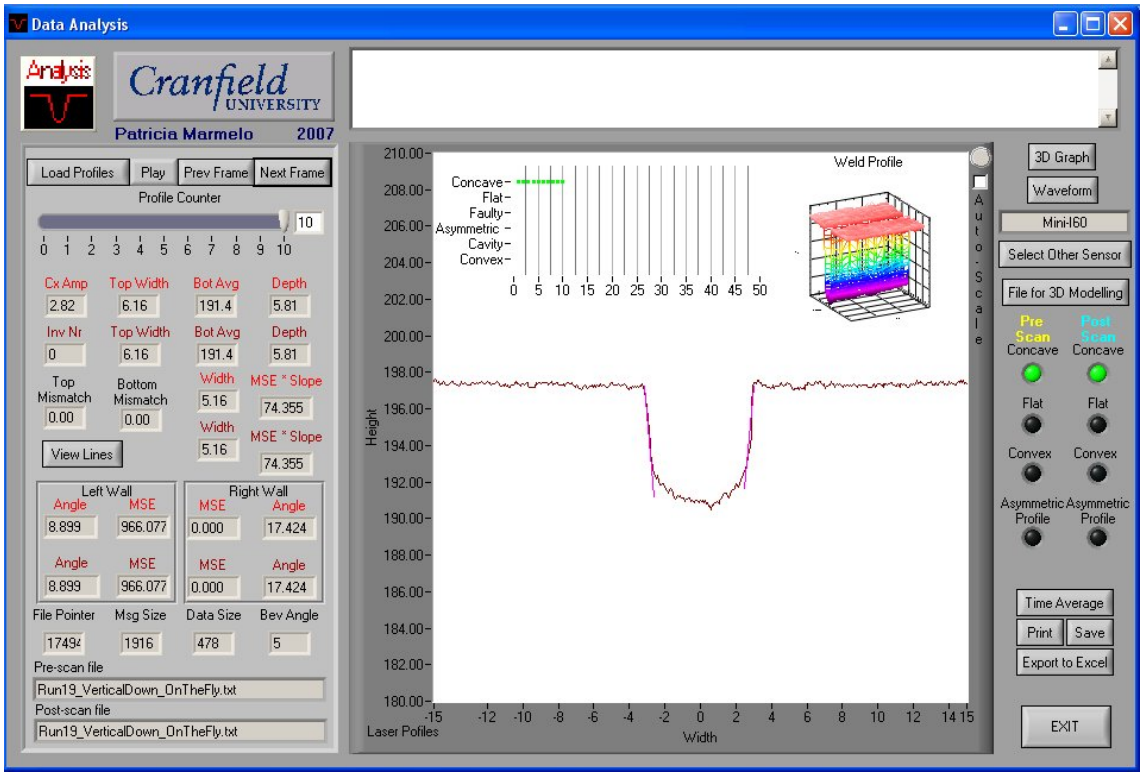

Figure I.2.0.52 – Screenshot of Profile 10 of "Run 19" in the Vertical (Down Hand) Position.

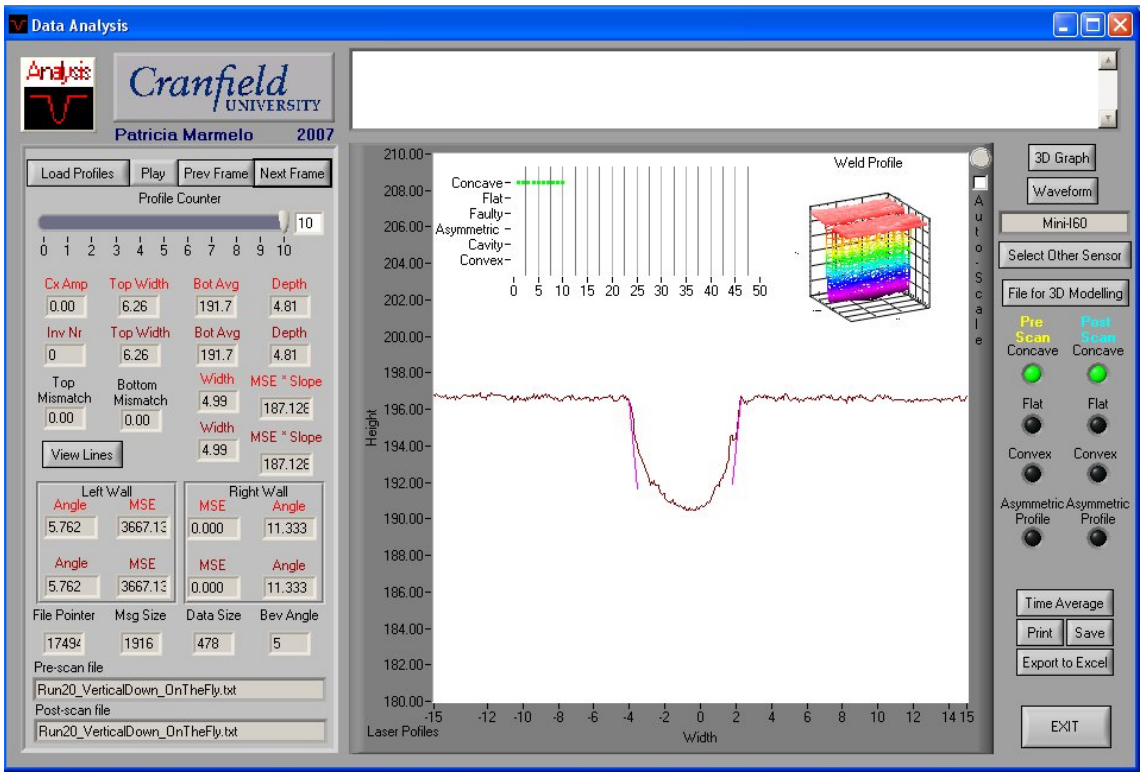

Figure I.2.0.53 – Screenshot of Profile 10 of "Run 20" in the Vertical (Down Hand) Position.

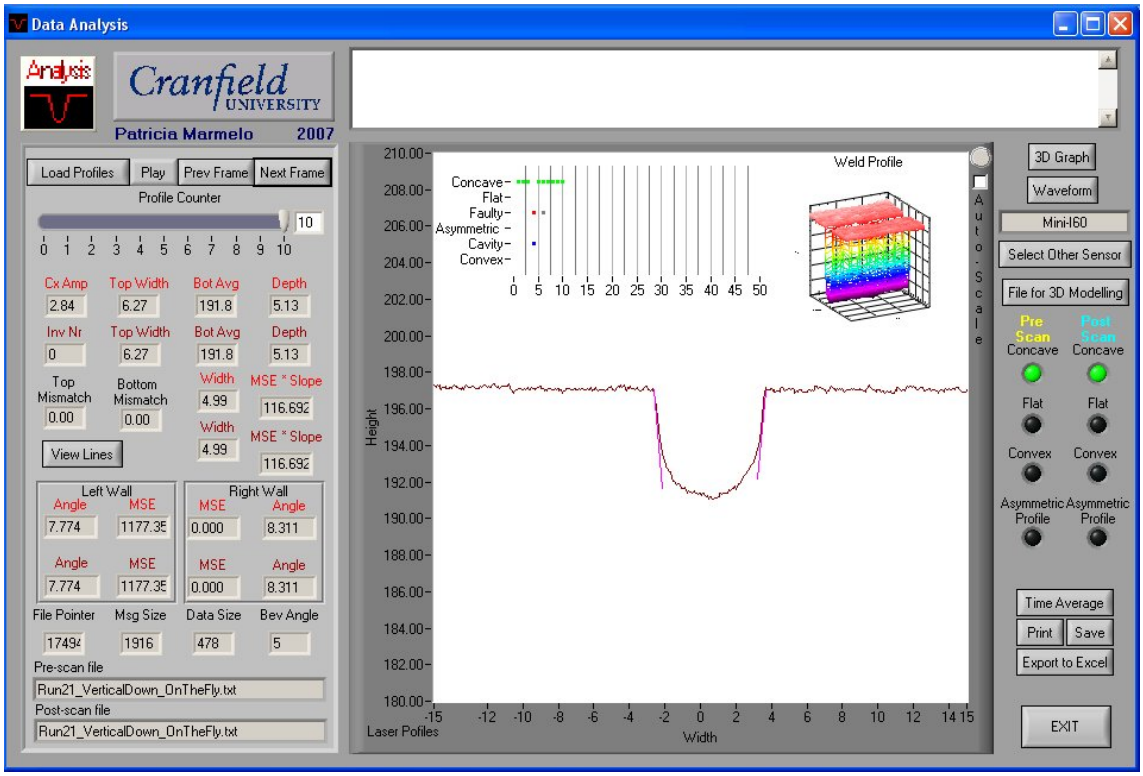

Figure I.2.0.54 – Screenshot of Profile 10 of "Run 21" in the Vertical (Down Hand) Position.

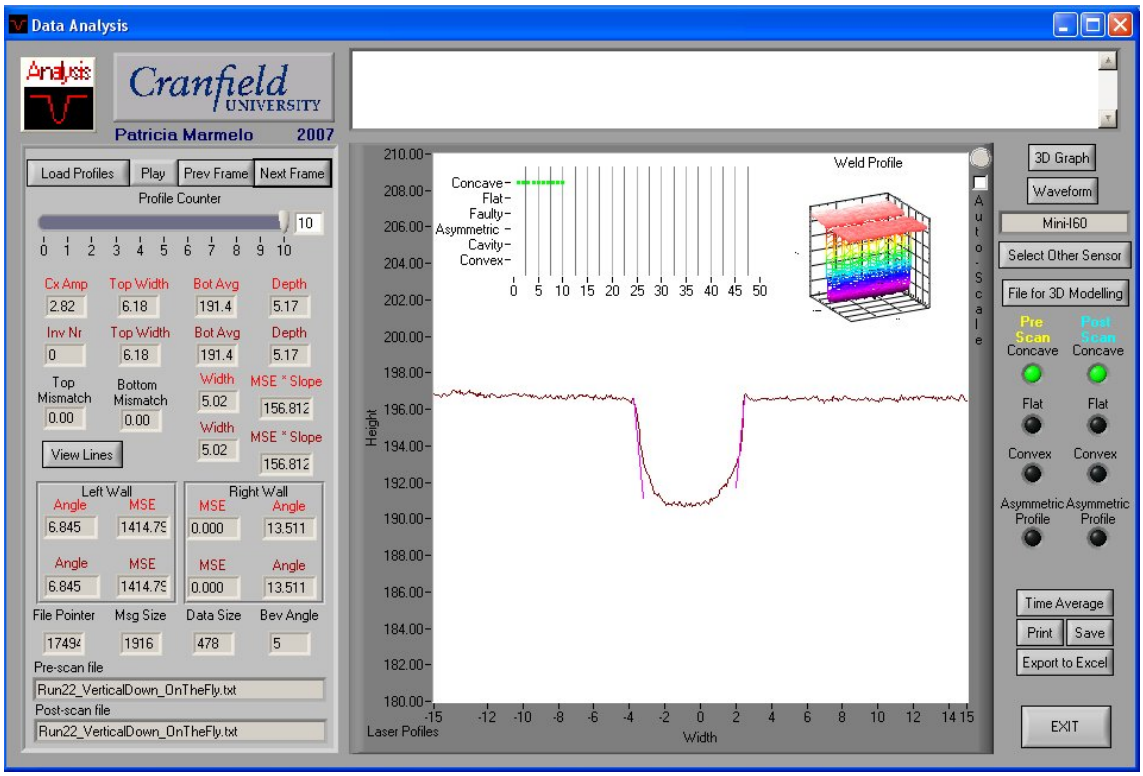

Figure I.2.0.55 – Screenshot of Profile 10 of "Run 22" in the Vertical (Down Hand) Position.

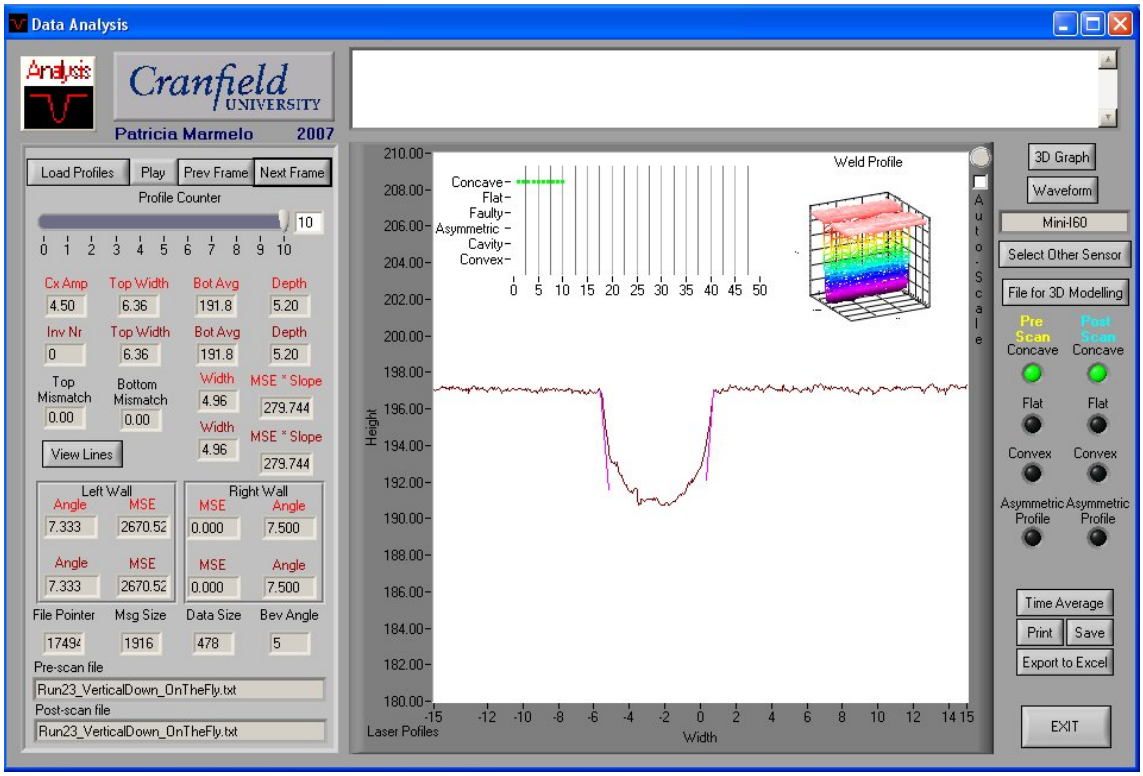

Figure I.2.0.56 – Screenshot of Profile 10 of "Run 23" in the Vertical (Down Hand) Position.

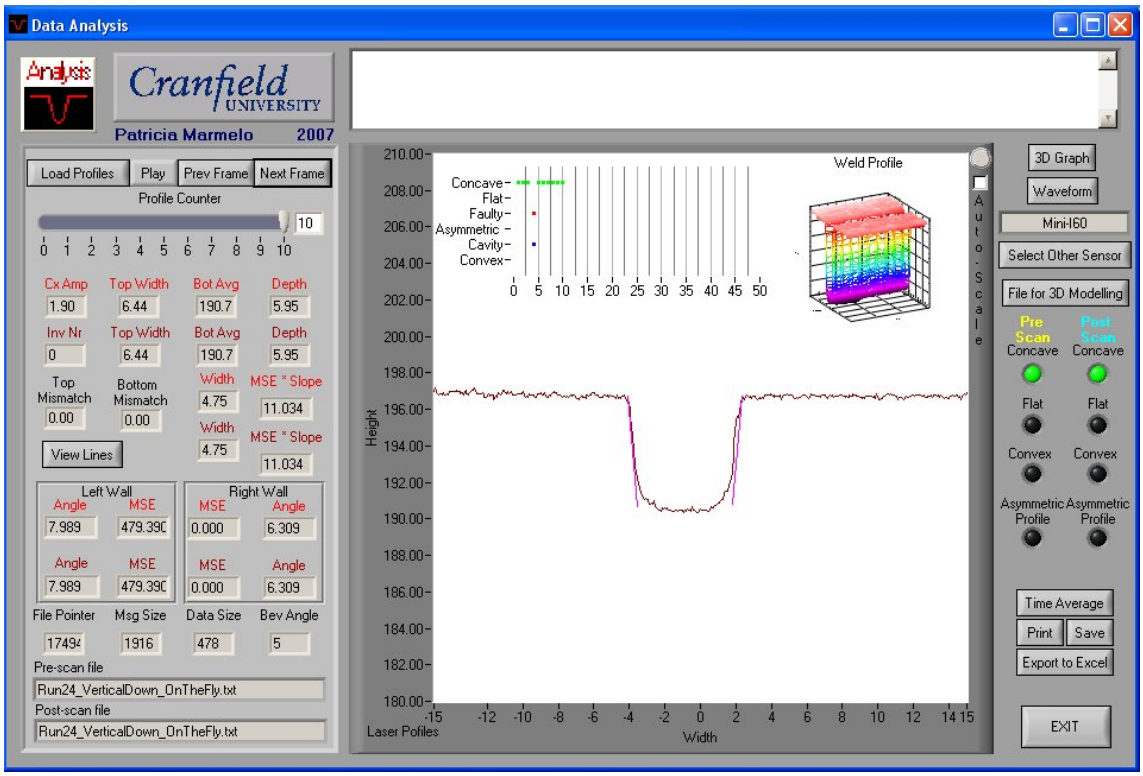

Figure I.2.0.57 – Screenshot of Profile 10 of "Run 24" in the Vertical (Down Hand) Position.

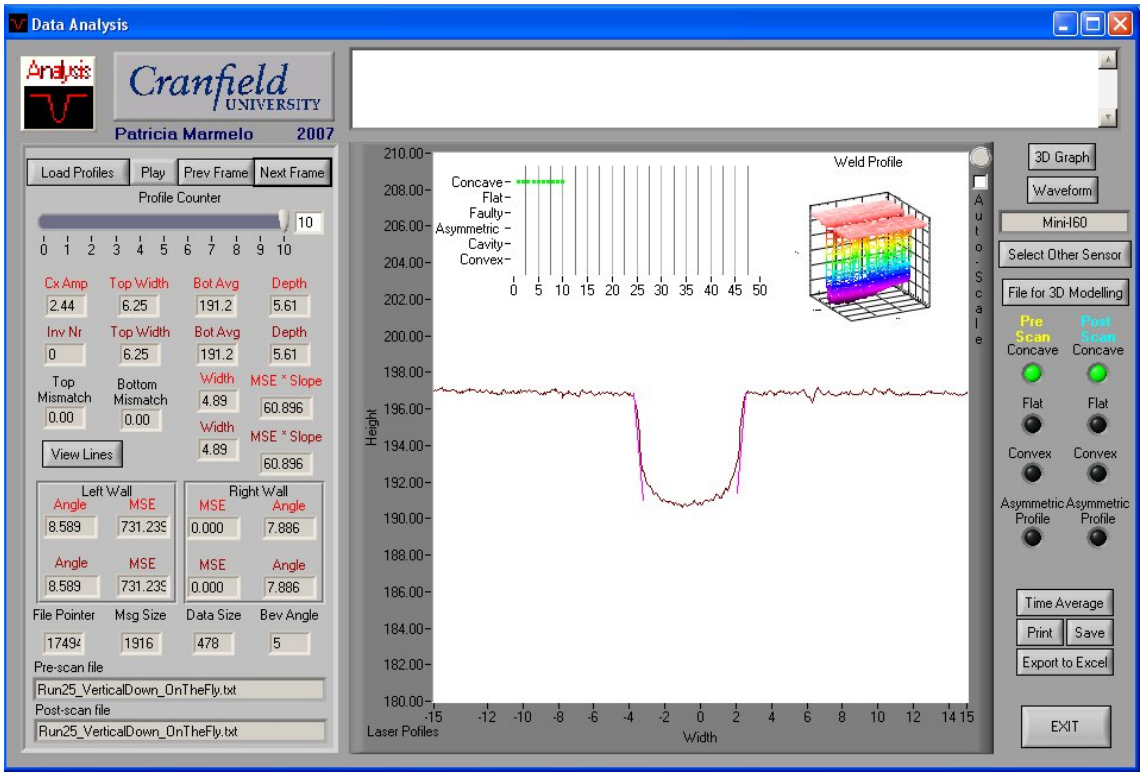

Figure I.2.0.58 – Screenshot of Profile 10 of "Run 25" in the Vertical (Down Hand) Position.

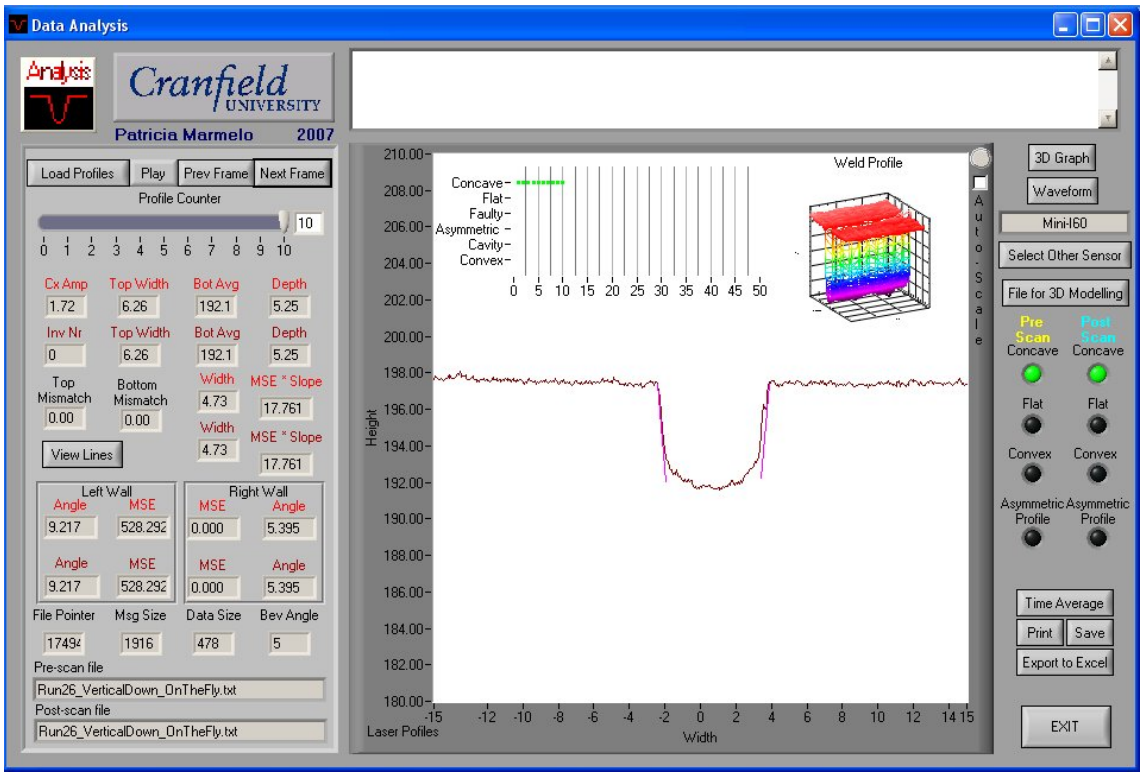

Figure I.2.0.59 – Screenshot of Profile 10 of "Run 26" in the Vertical (Down Hand) Position.

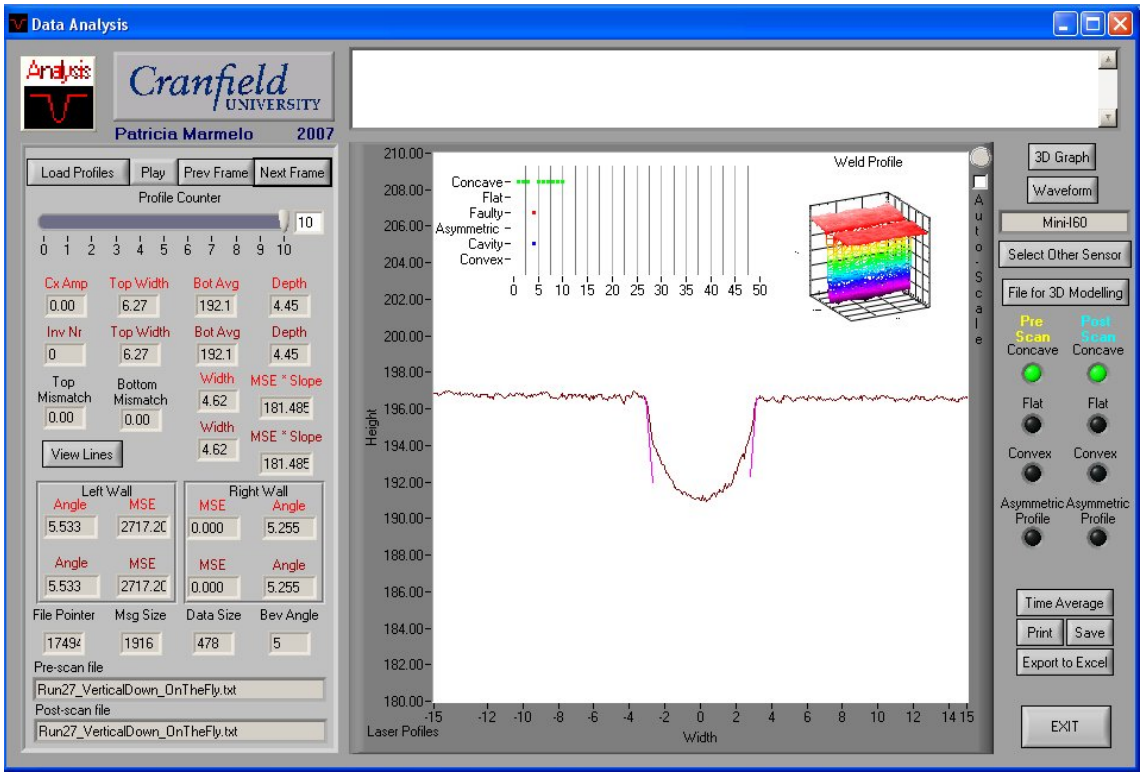

Figure I.2.0.60 – Screenshot of Profile 10 of "Run 27" in the Vertical (Down Hand) Position.

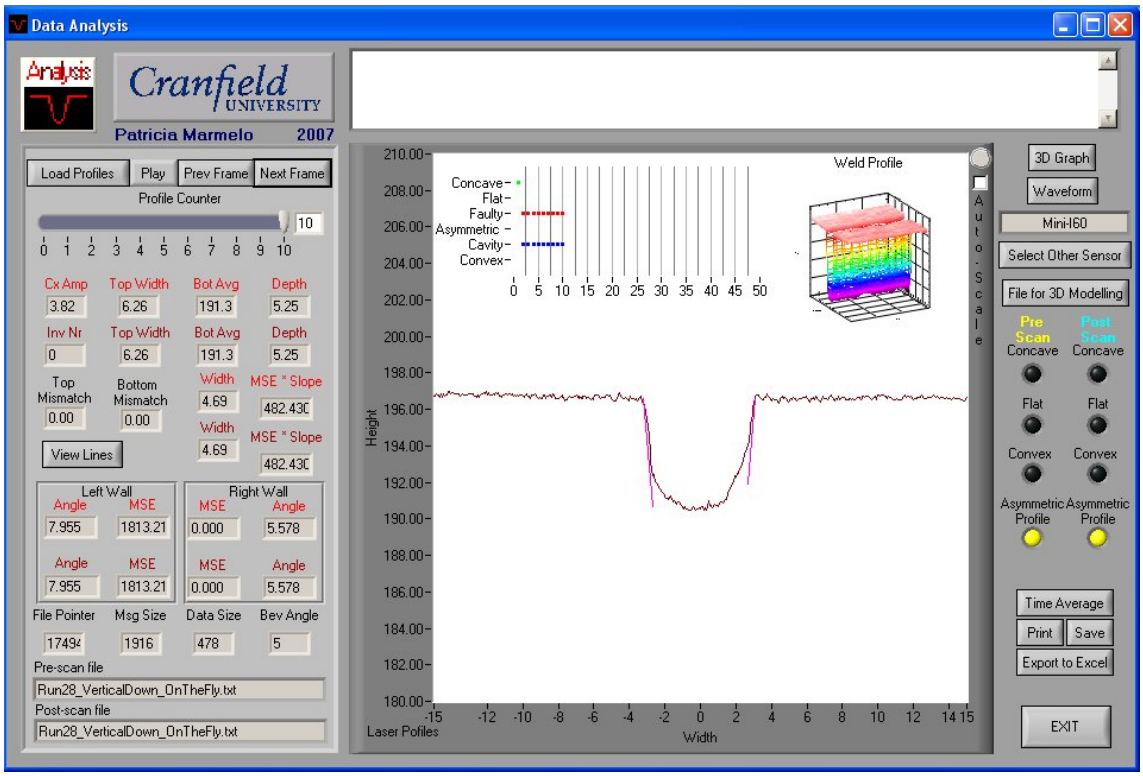

Figure I.2.0.61 – Screenshot of Profile 10 of "Run 28" in the Vertical (Down Hand) Position.

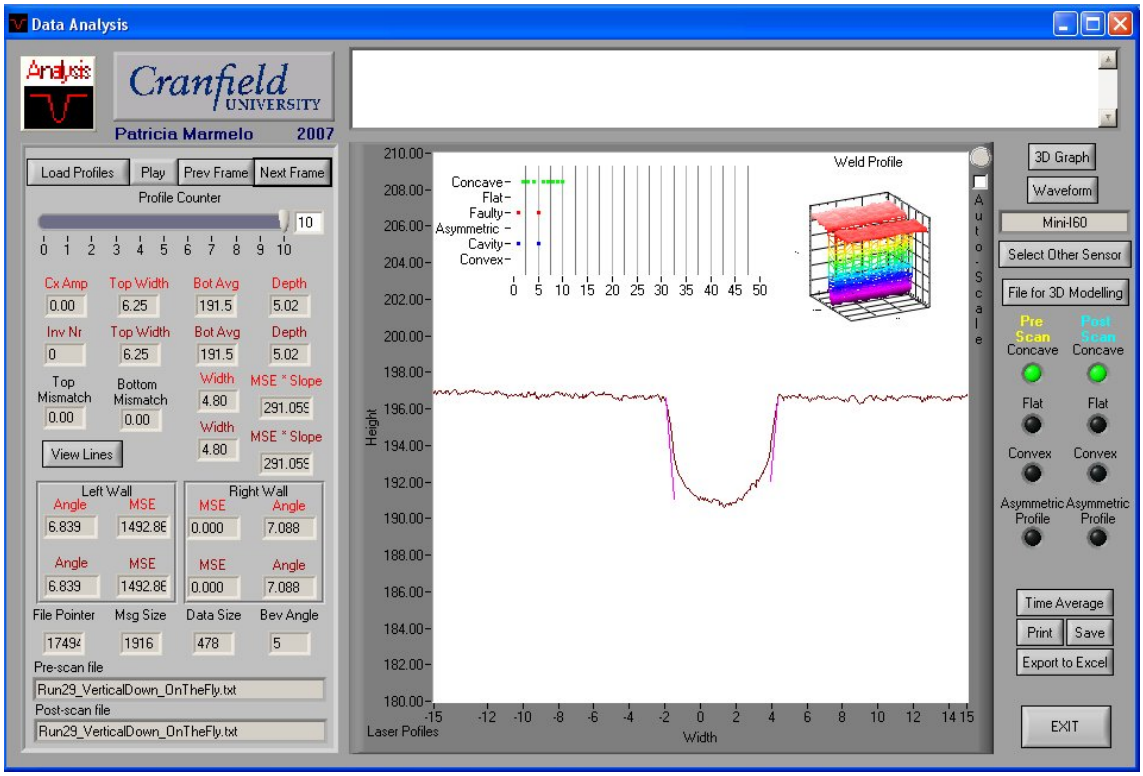

Figure I.2.0.62 – Screenshot of Profile 10 of "Run 29" in the Vertical (Down Hand) Position.

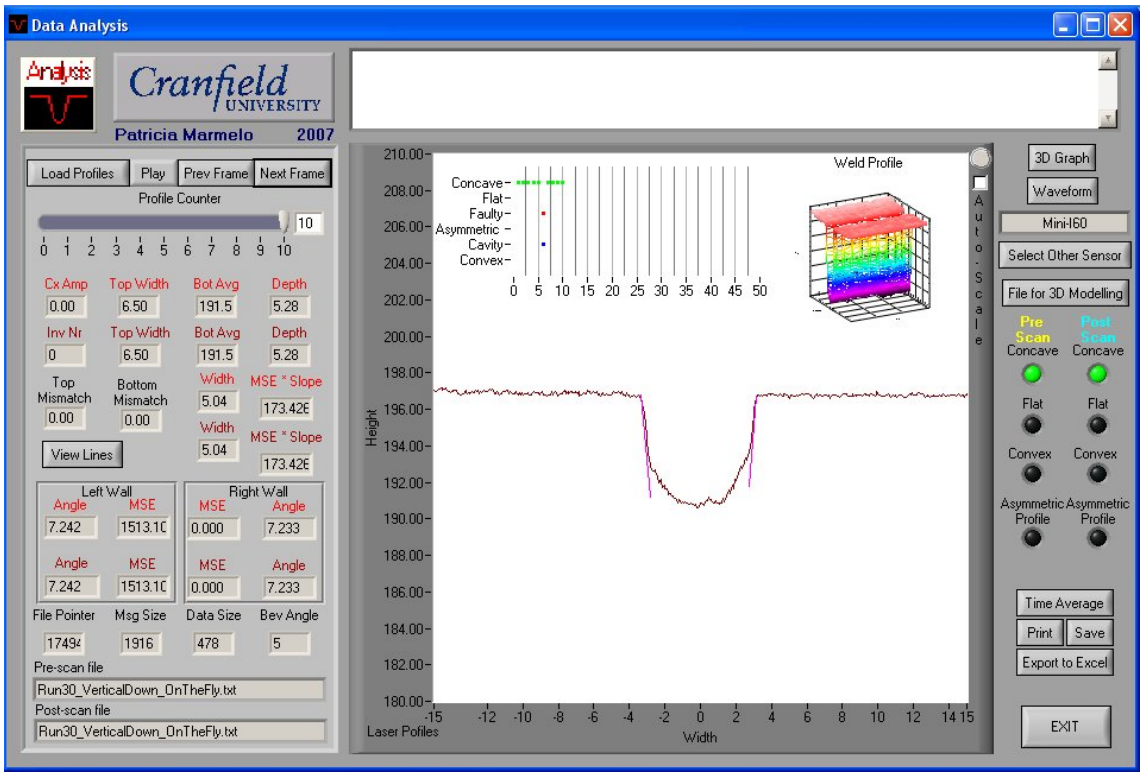

Figure I.2.0.63 – Screenshot of Profile 10 of "Run 30" in the Vertical (Down Hand) Position.

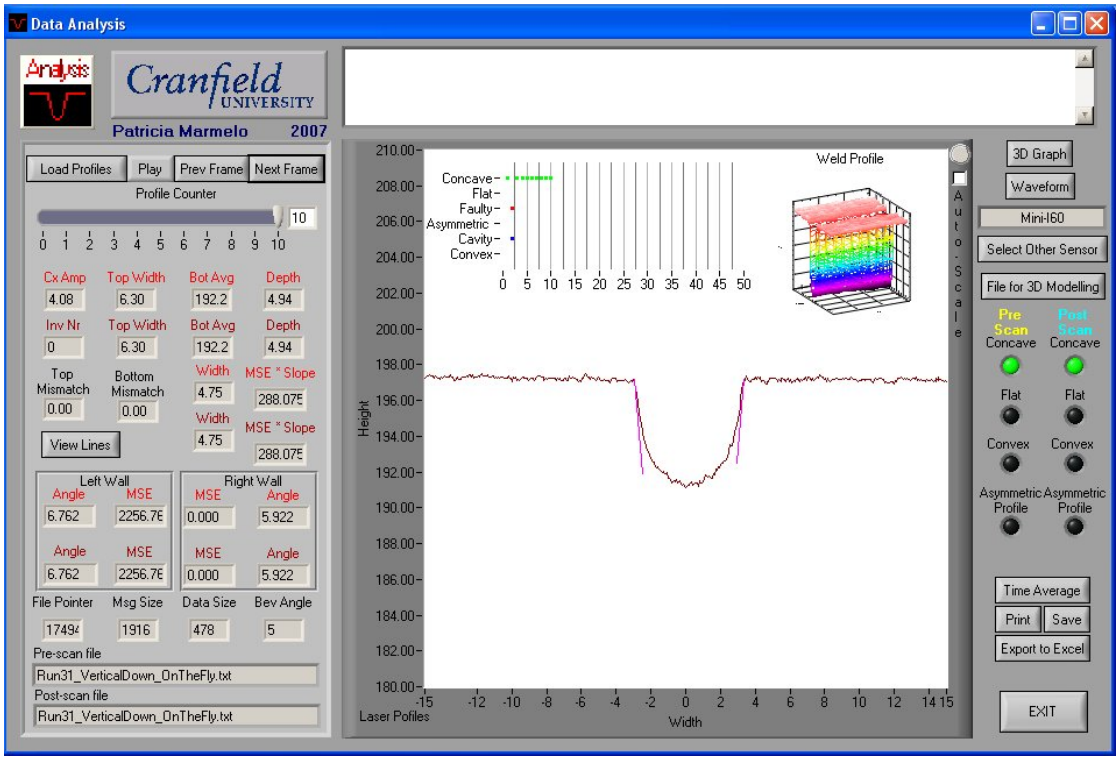

Figure I.2.0.64 – Screenshot of Profile 10 of "Run 31" in the Vertical (Down Hand) Position.

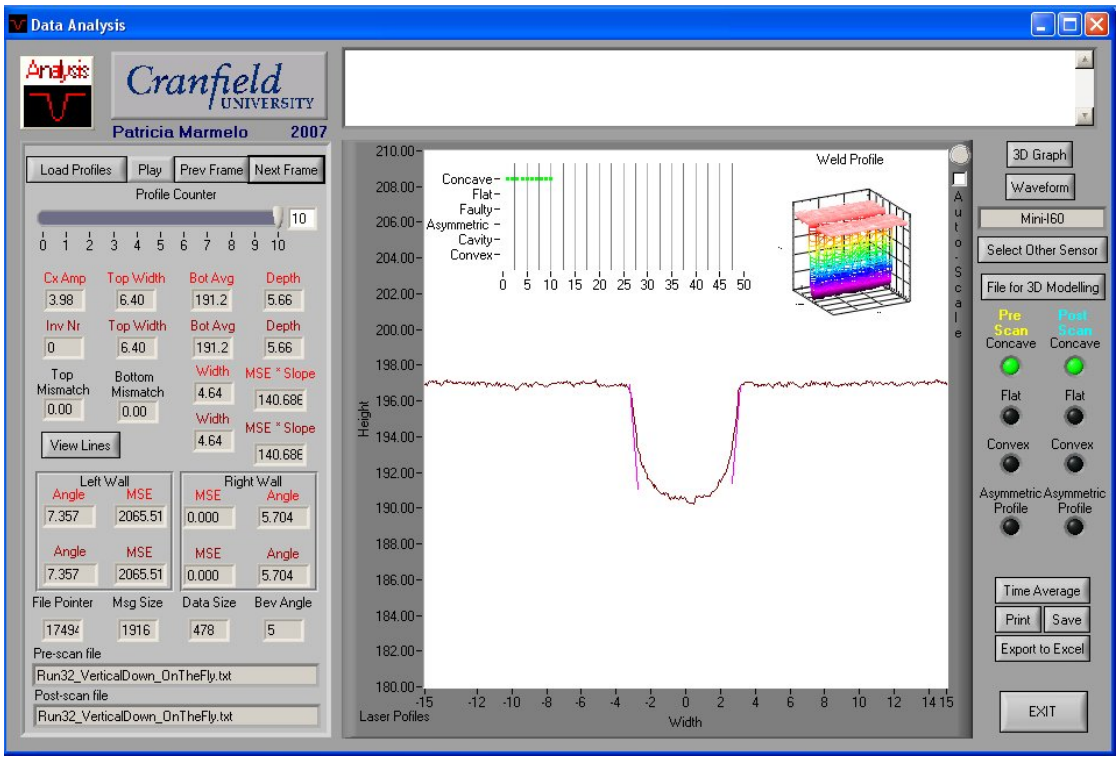

Figure I.2.0.65 – Screenshot of Profile 10 of "Run 32" in the Vertical (Down Hand) Position.

I3 Overhead Position

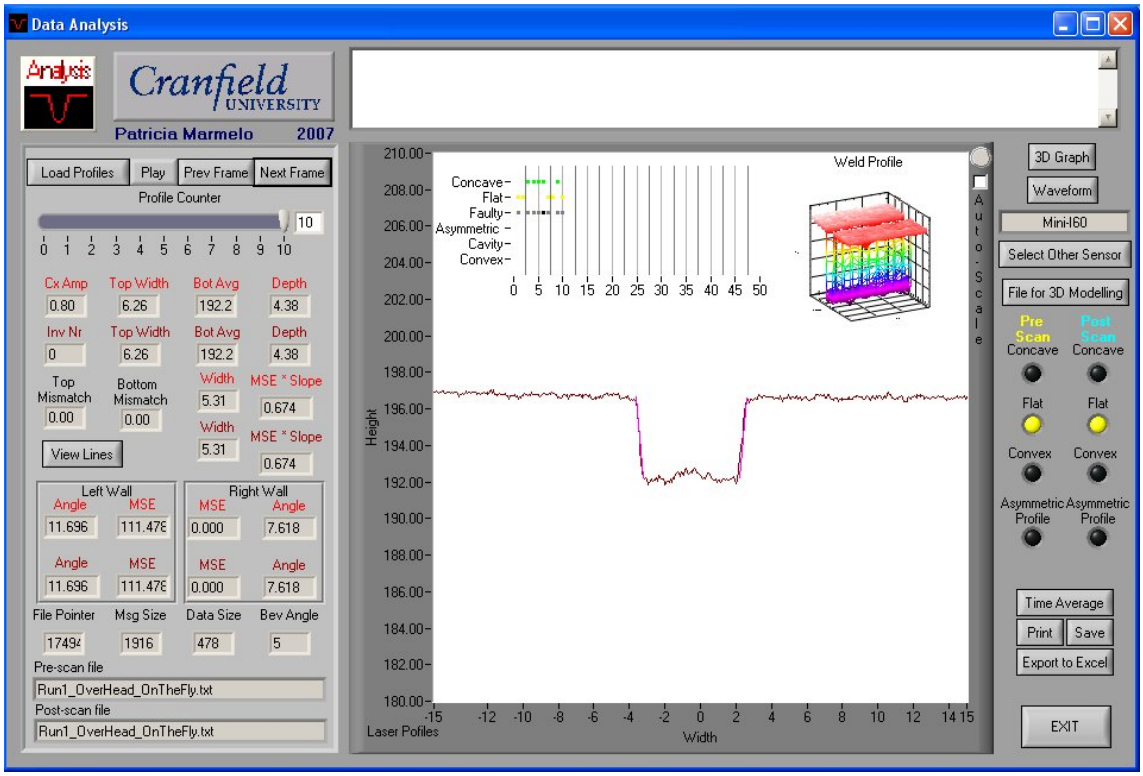

Figure I.3.0.66 – Screenshot of Profile 10 of "Run 1" in the Overhead Position.

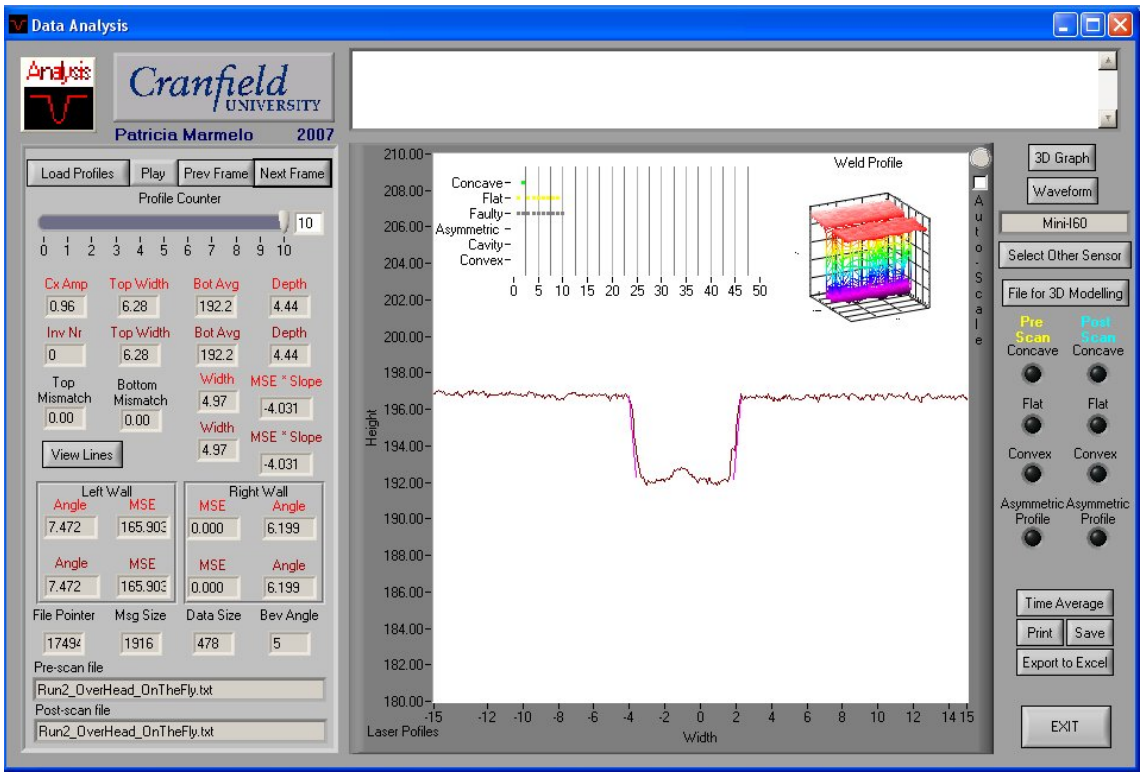

Figure I.3.0.67 – Screenshot of Profile 10 of "Run 2" in the Overhead Position.

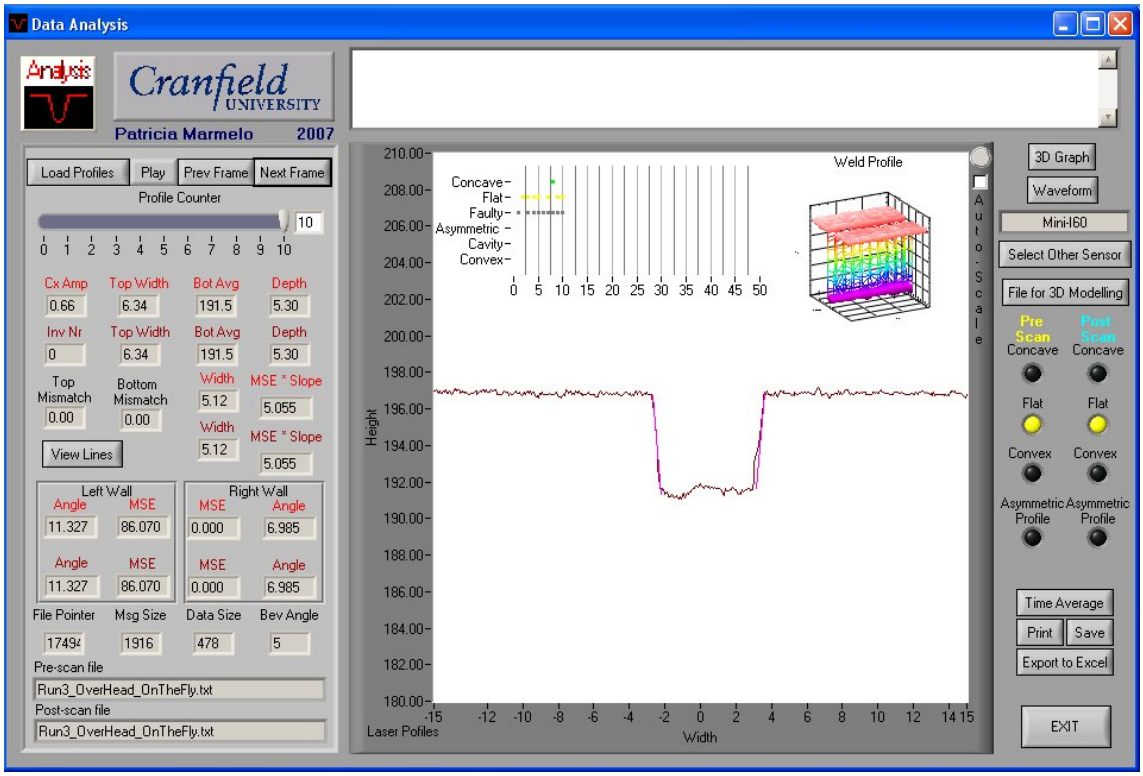

Figure I.3.0.68 – Screenshot of Profile 10 of "Run 3" in the Overhead Position.

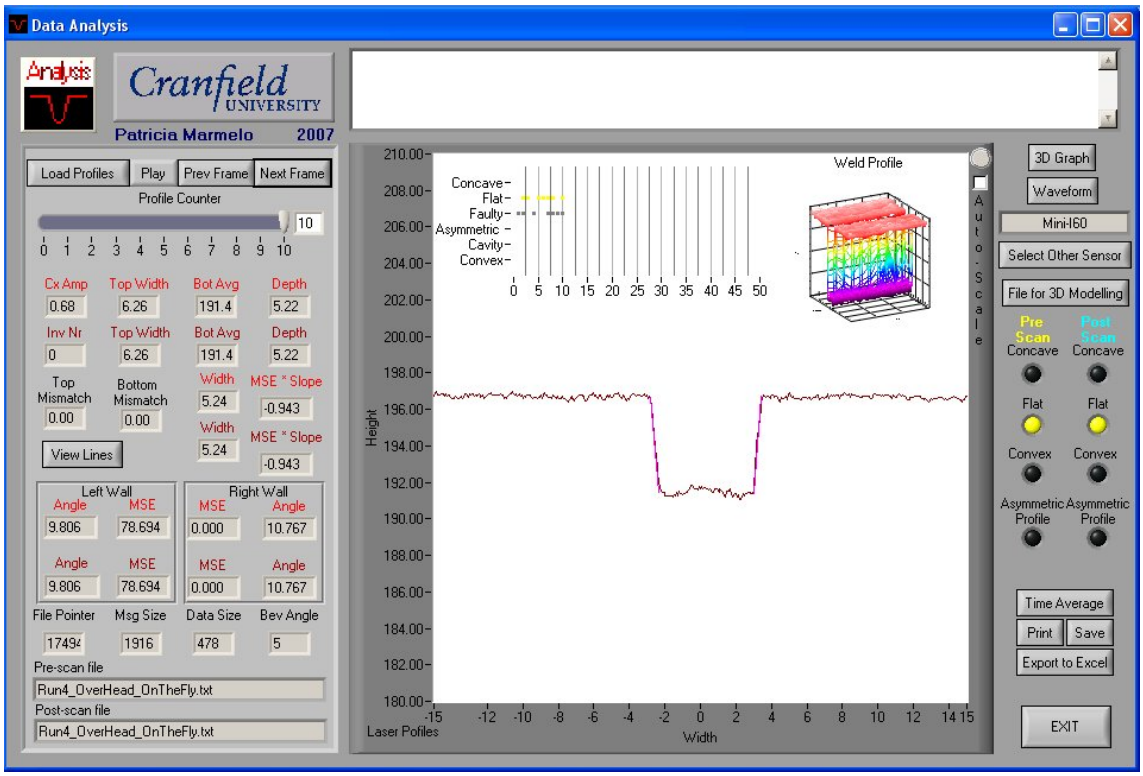

Figure I.3.0.69 – Screenshot of Profile 10 of "Run 4" in the Overhead Position.

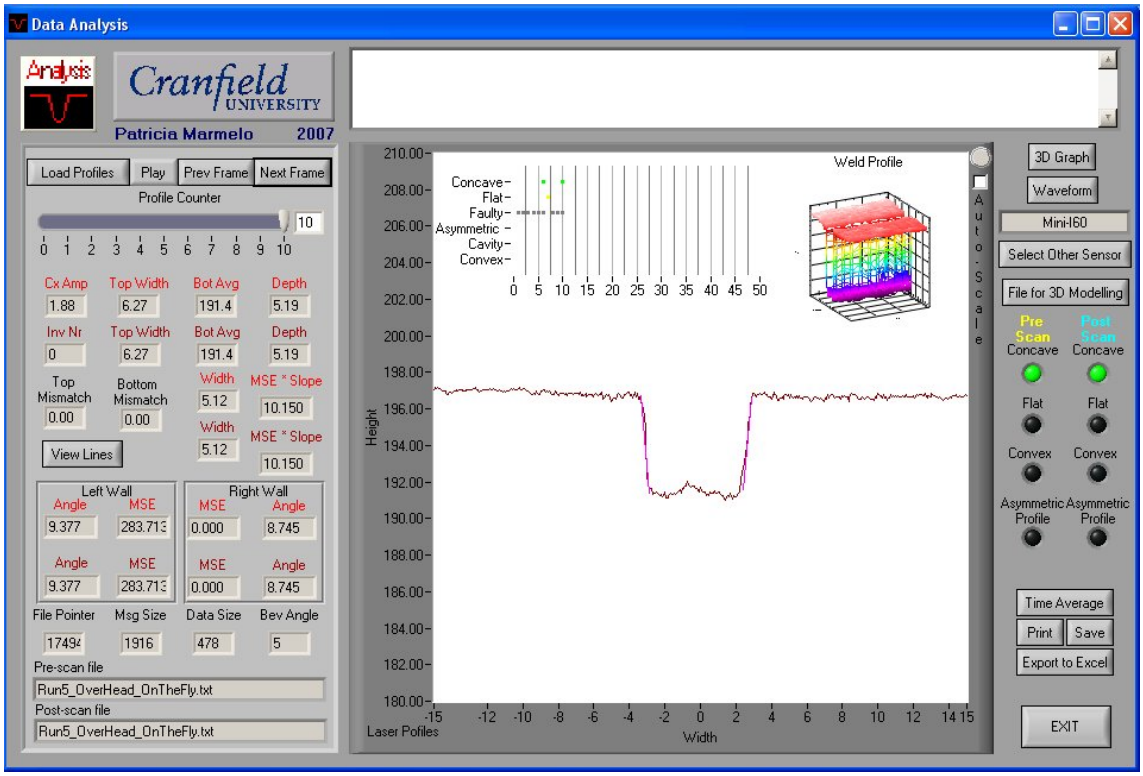

Figure I.3.0.70 – Screenshot of Profile 10 of "Run 5" in the Overhead Position.

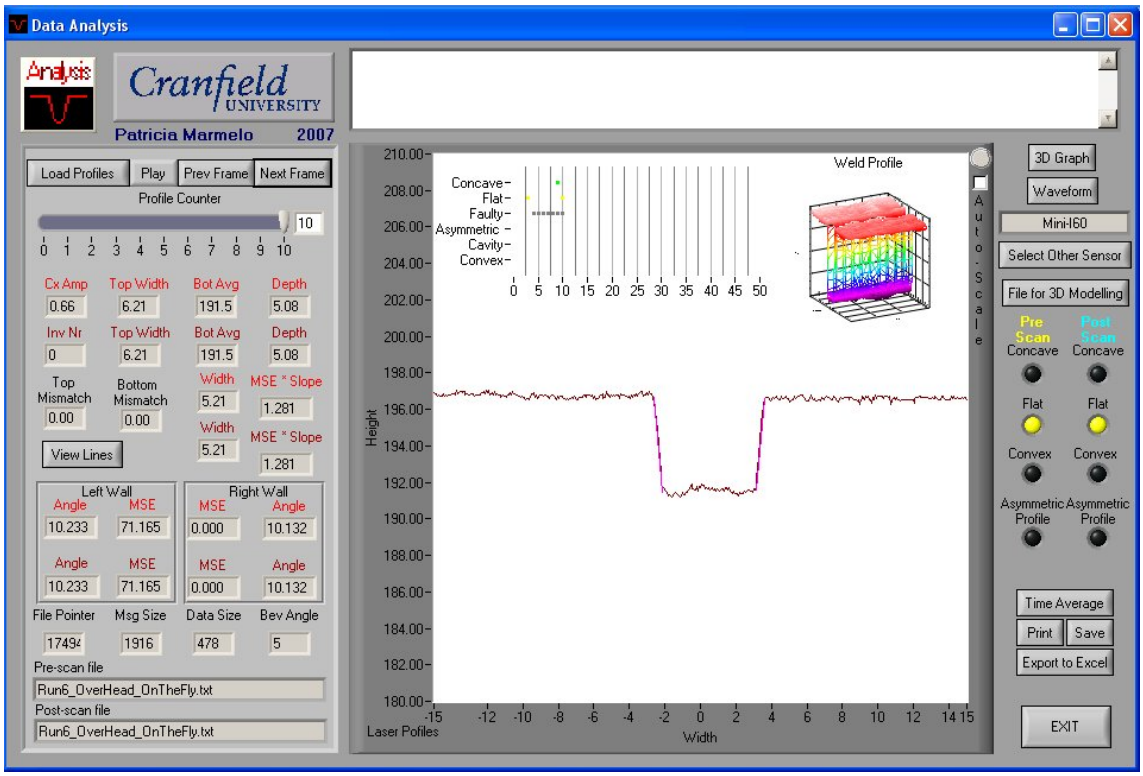

Figure I.3.0.71 – Screenshot of Profile 10 of "Run 6" in the Overhead Position.

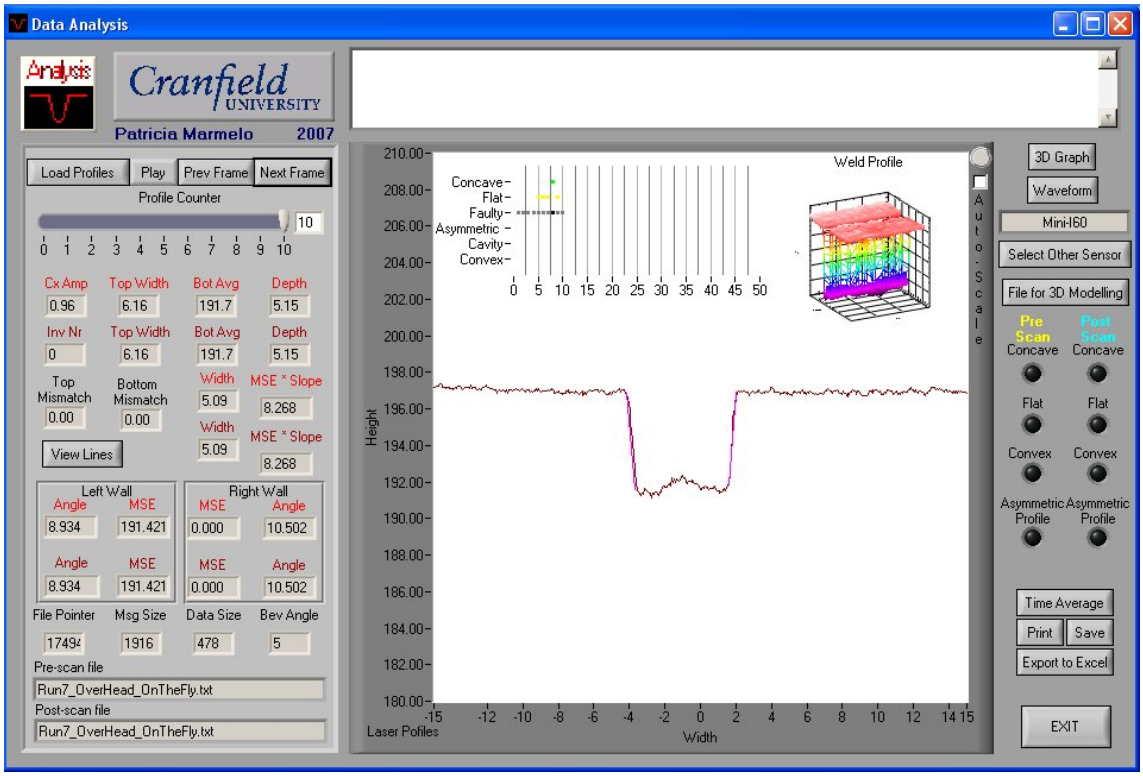

Figure I.3.0.72 – Screenshot of Profile 10 of "Run 7" in the Overhead Position.

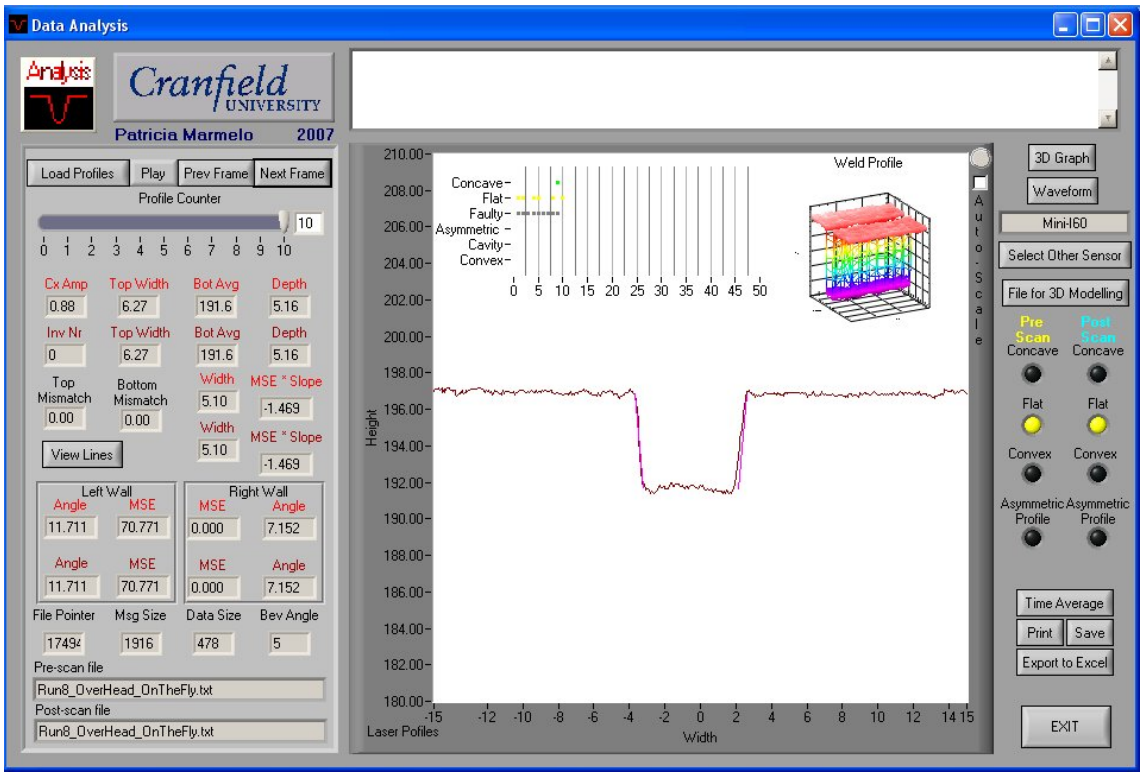

Figure I.3.0.73 – Screenshot of Profile 10 of "Run 8" in the Overhead Position.

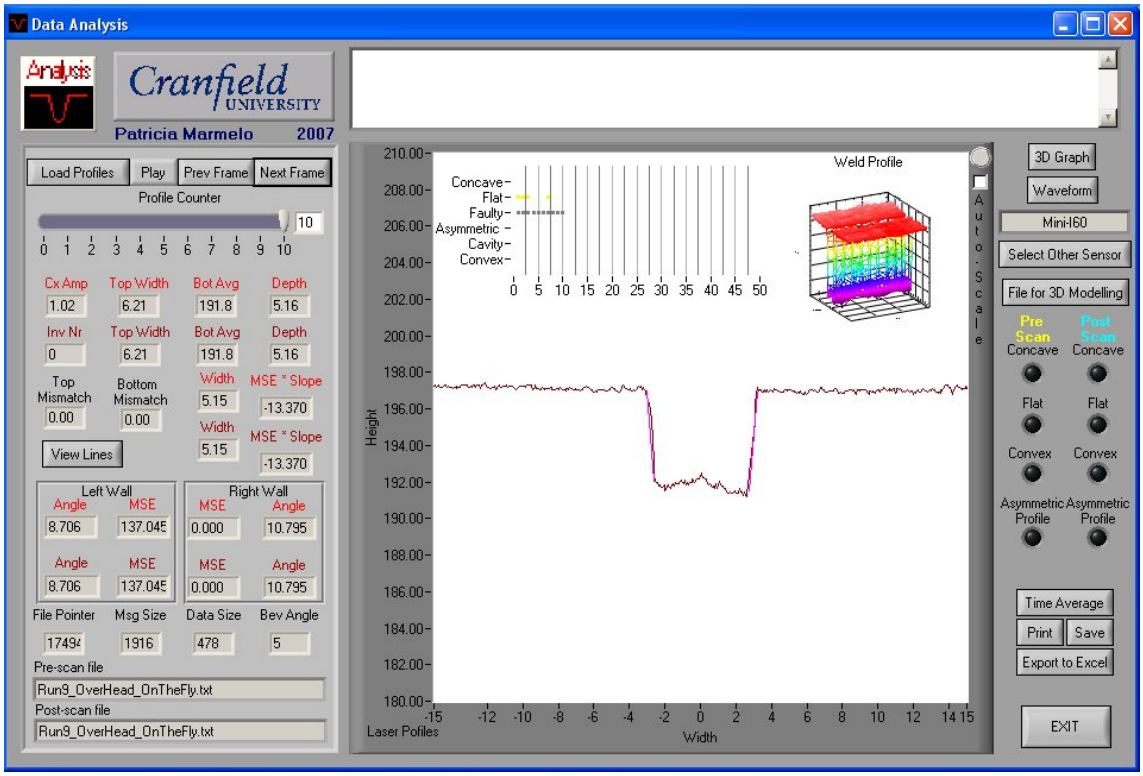

Figure I.3.0.74 – Screenshot of Profile 10 of "Run 9" in the Overhead Position.

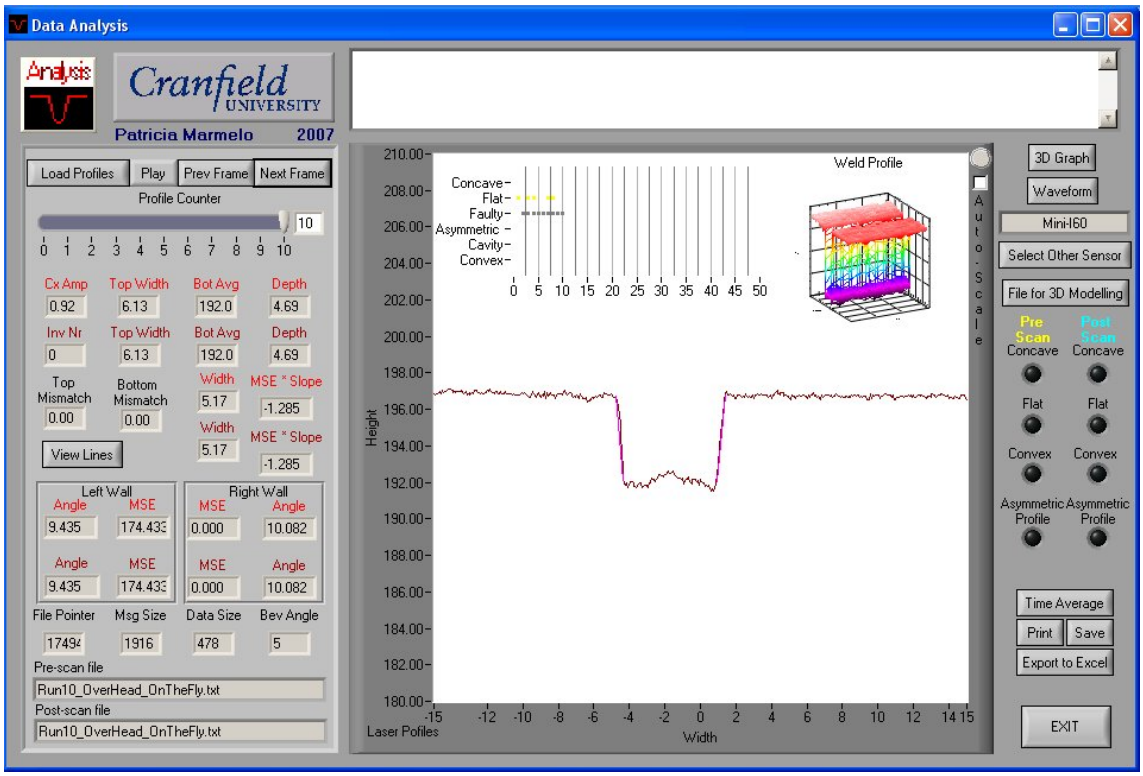

Figure I.3.0.75 – Screenshot of Profile 10 of "Run 10" in the Overhead Position.

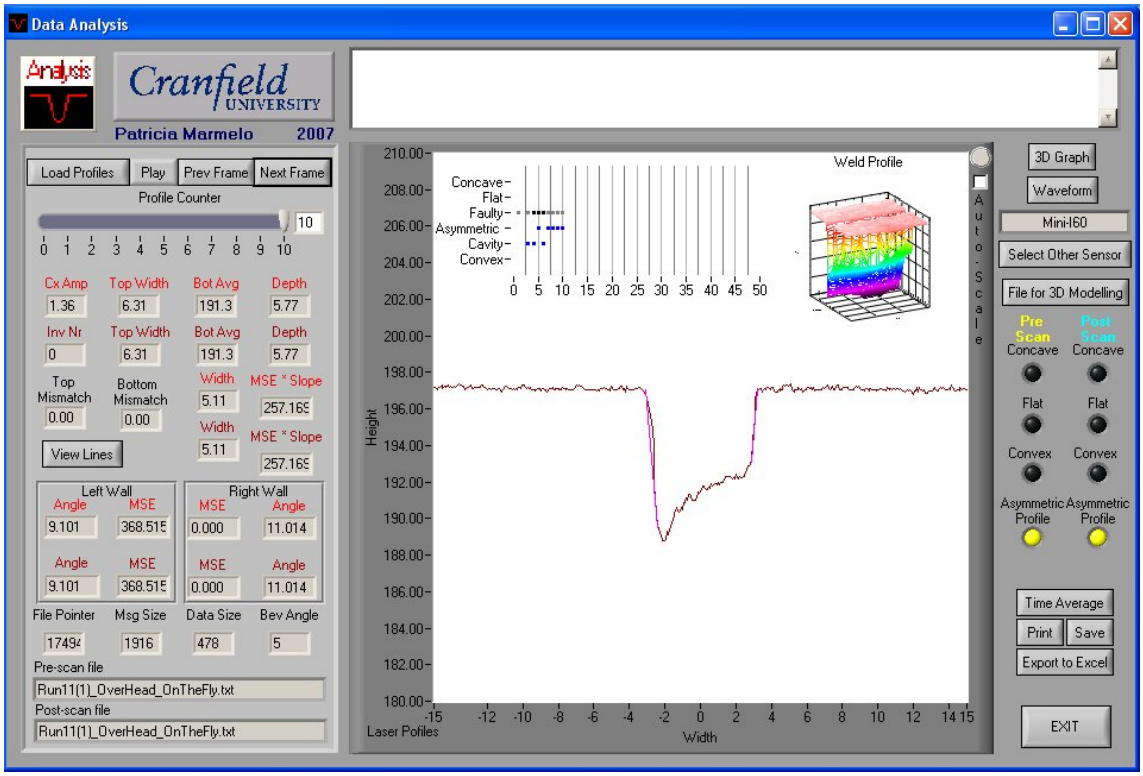

Figure I.3.0.76 – Screenshot of Profile 10 of "Run 11" in the Overhead Position.

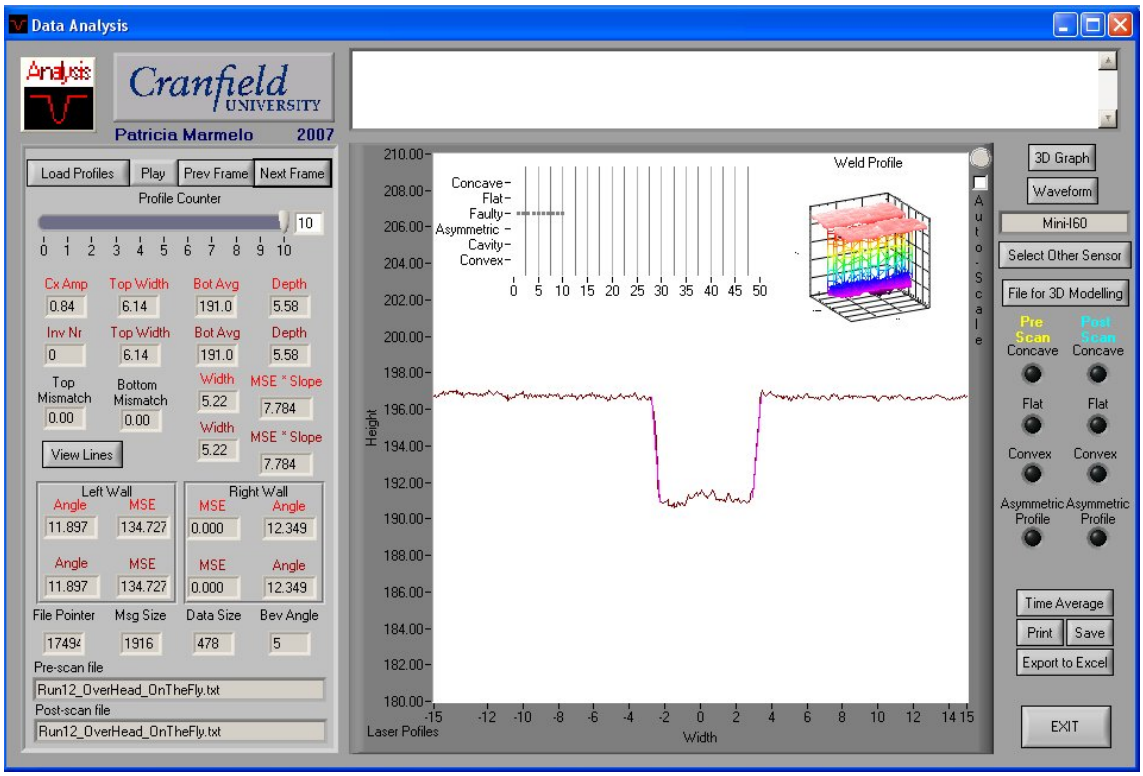

Figure I.3.0.77 – Screenshot of Profile 10 of "Run 12" in the Overhead Position.

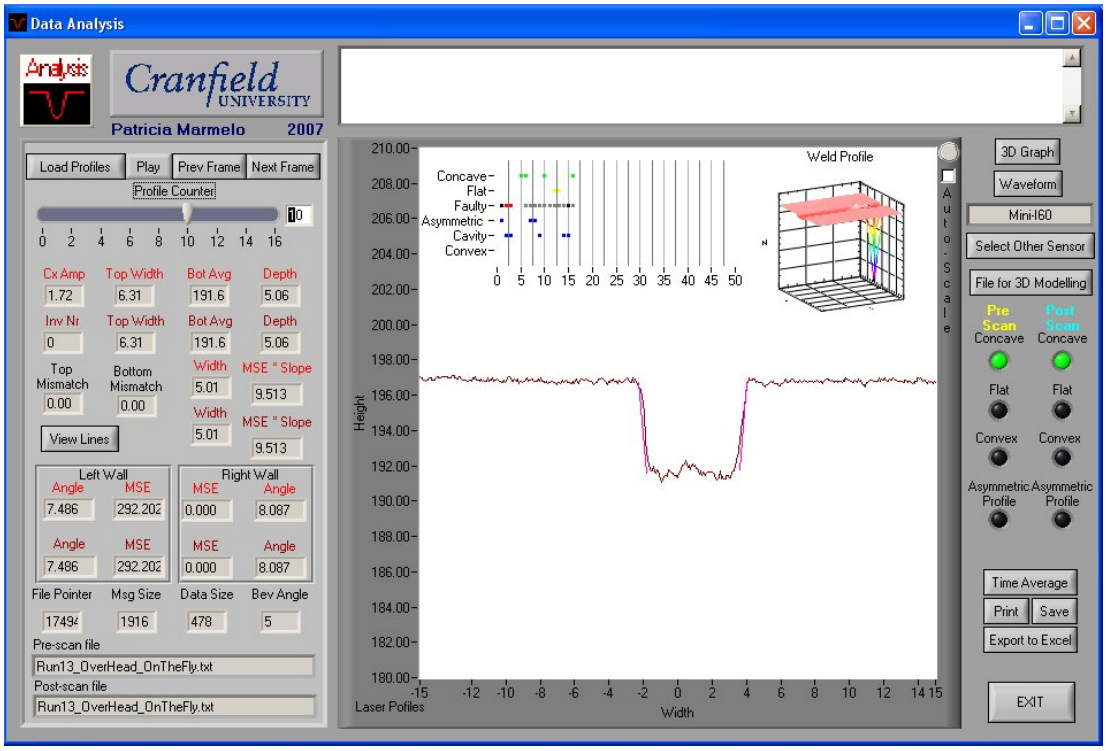

Figure I.3.0.78 – Screenshot of Profile 10 of "Run 13" in the Overhead Position, Showing a Flat Bead Shape.

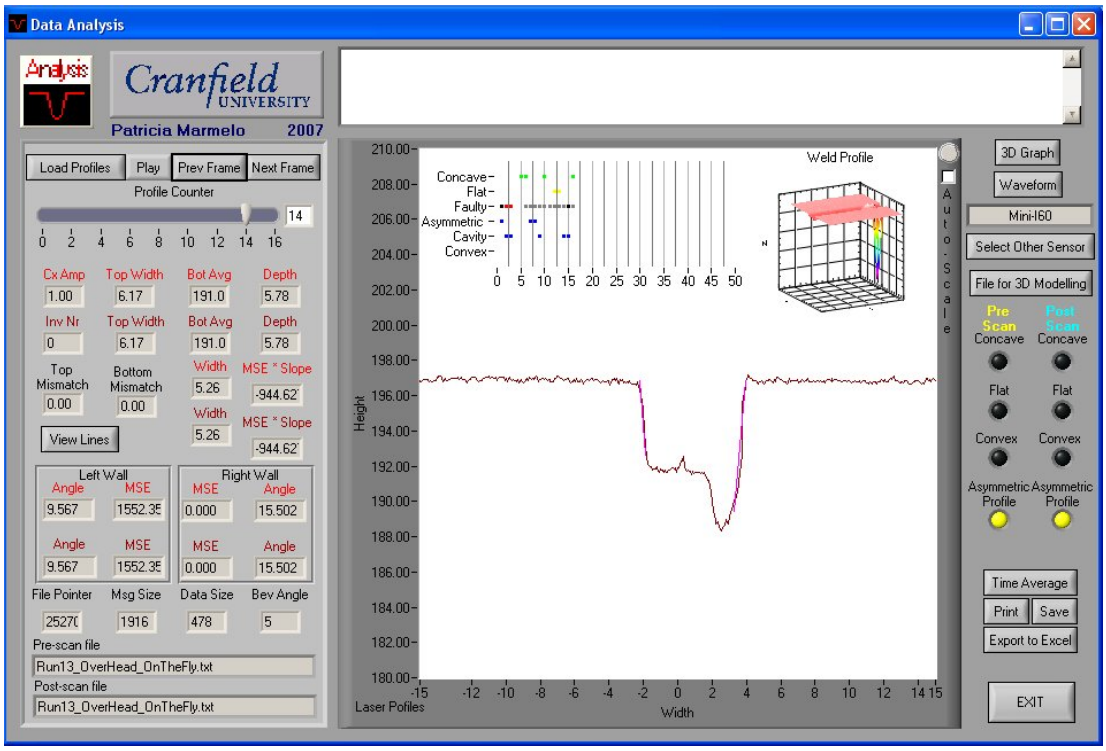

Figure I.3.0.79 – Screenshot of Profile 14 of "Run 13" in the Overhead Position, Showing a Profile with a Cavity.

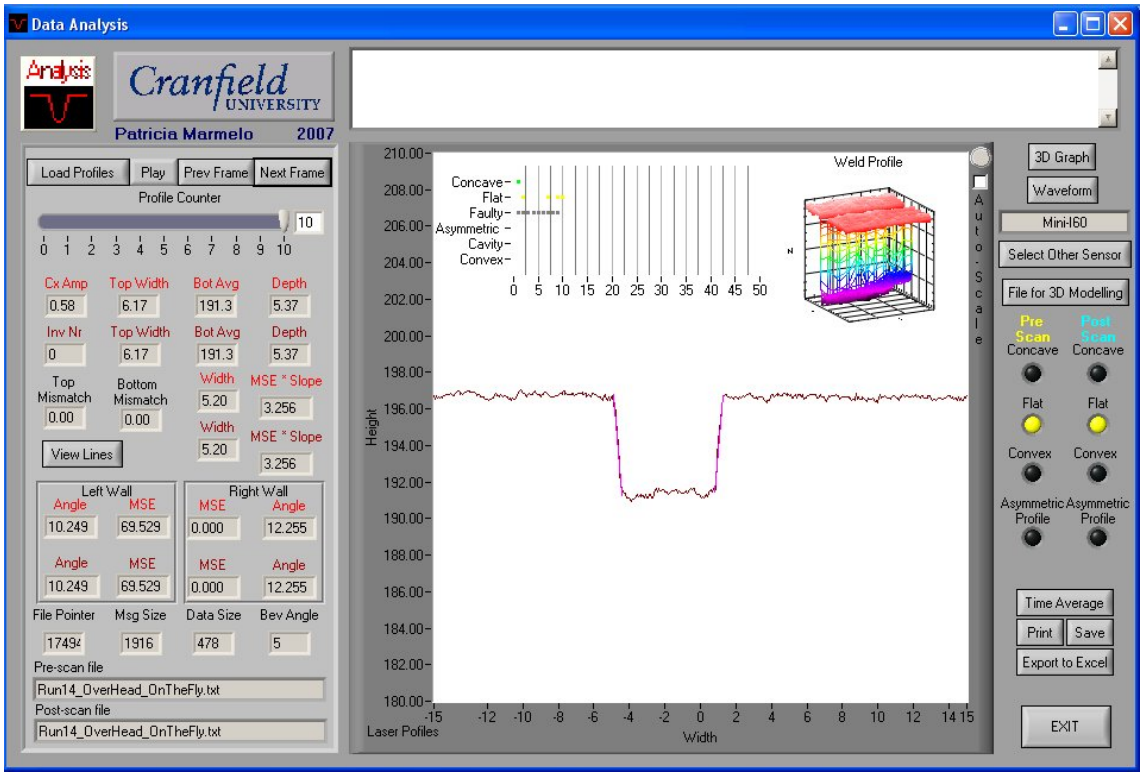

Figure I.3.0.80 – Screenshot of Profile 10 of "Run 14" in the Overhead Position.

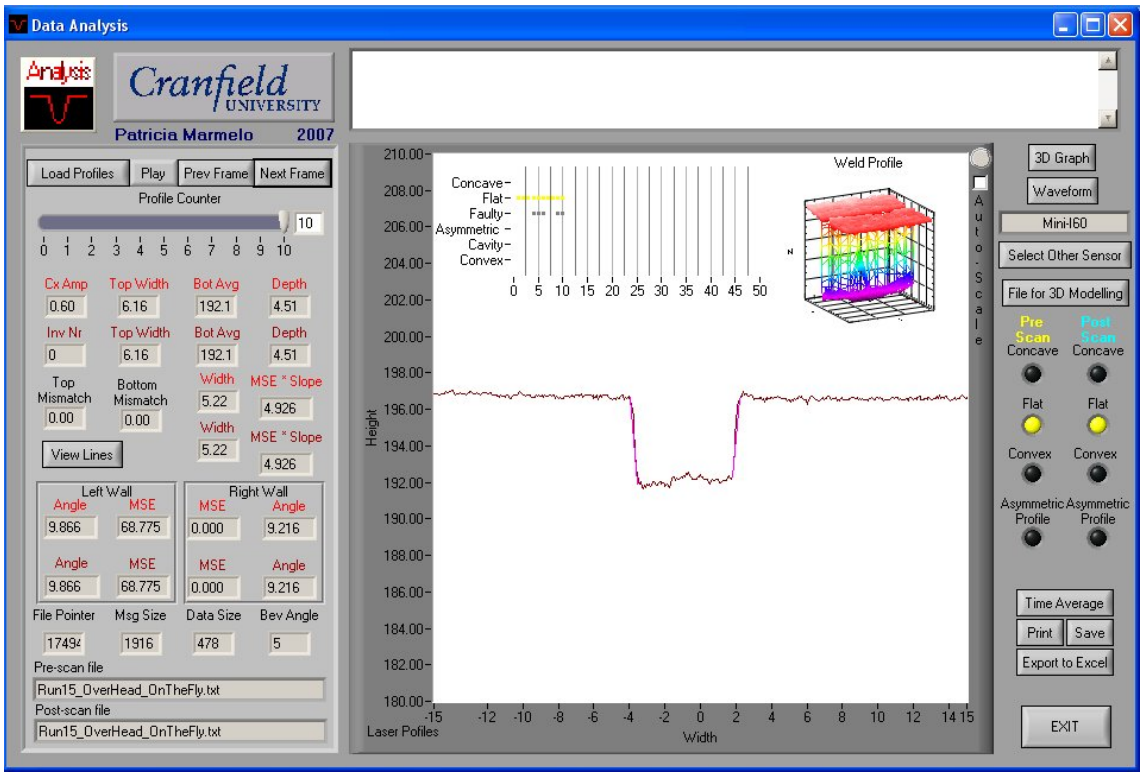

Figure I.3.0.81 – Screenshot of Profile 10 of "Run 15" in the Overhead Position.

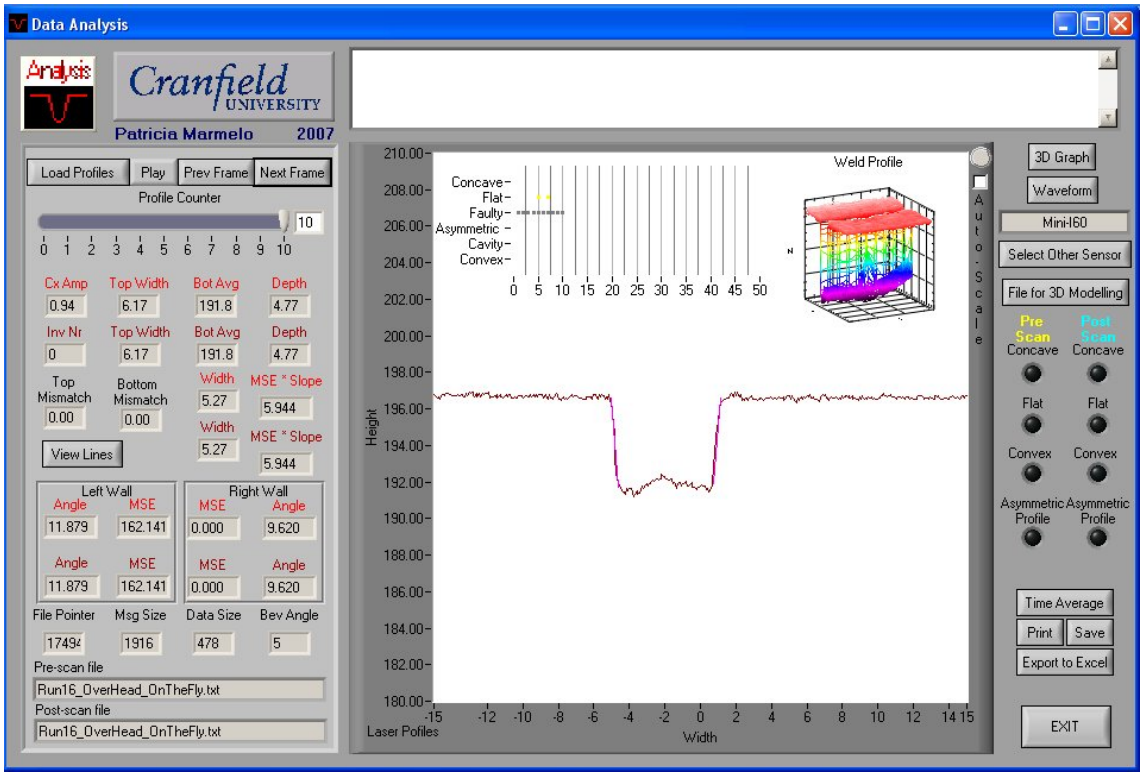

Figure I.3.0.82 – Screenshot of Profile 10 of "Run 16" in the Overhead Position.

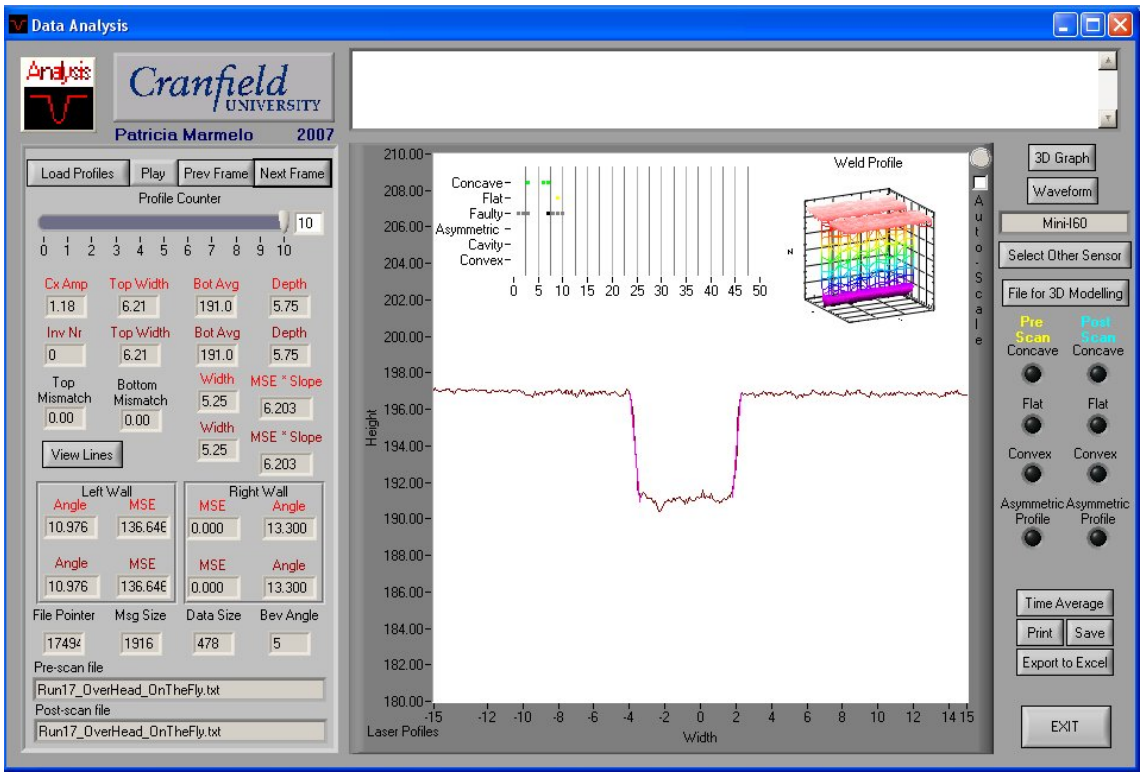

Figure I.3.0.83 – Screenshot of Profile 10 of "Run 17" in the Overhead Position.

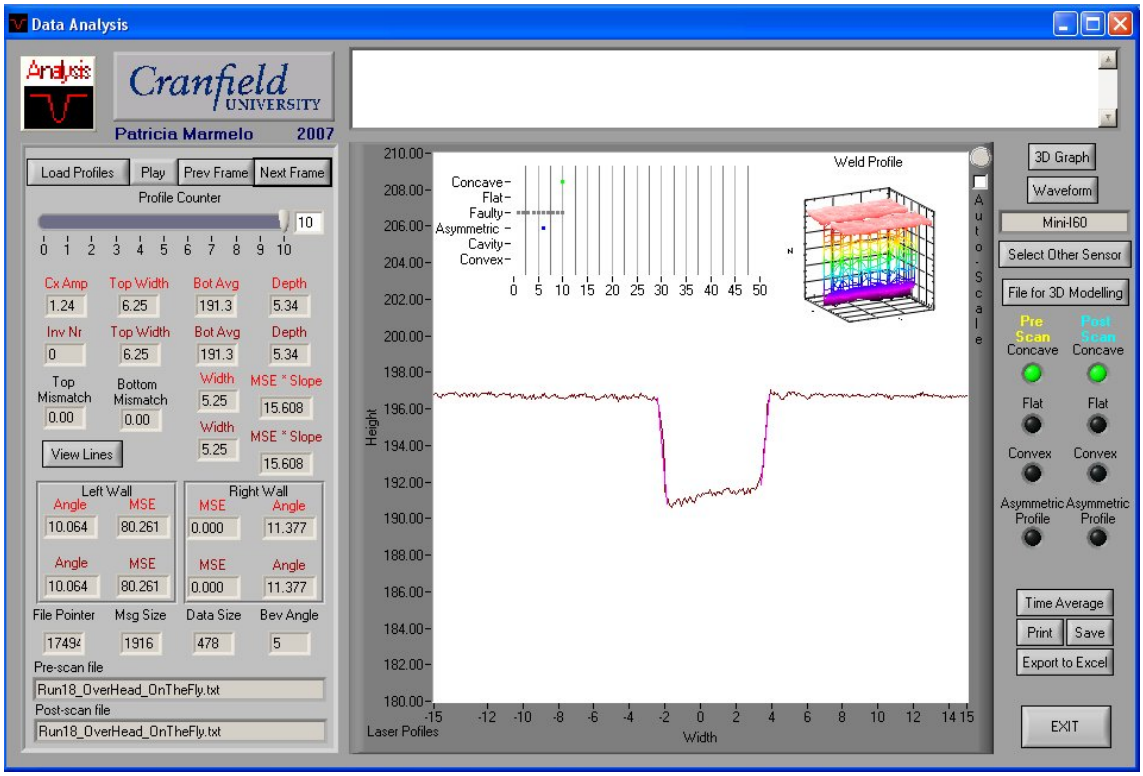

Figure I.3.0.84 – Screenshot of Profile 10 of "Run 18" in the Overhead Position.

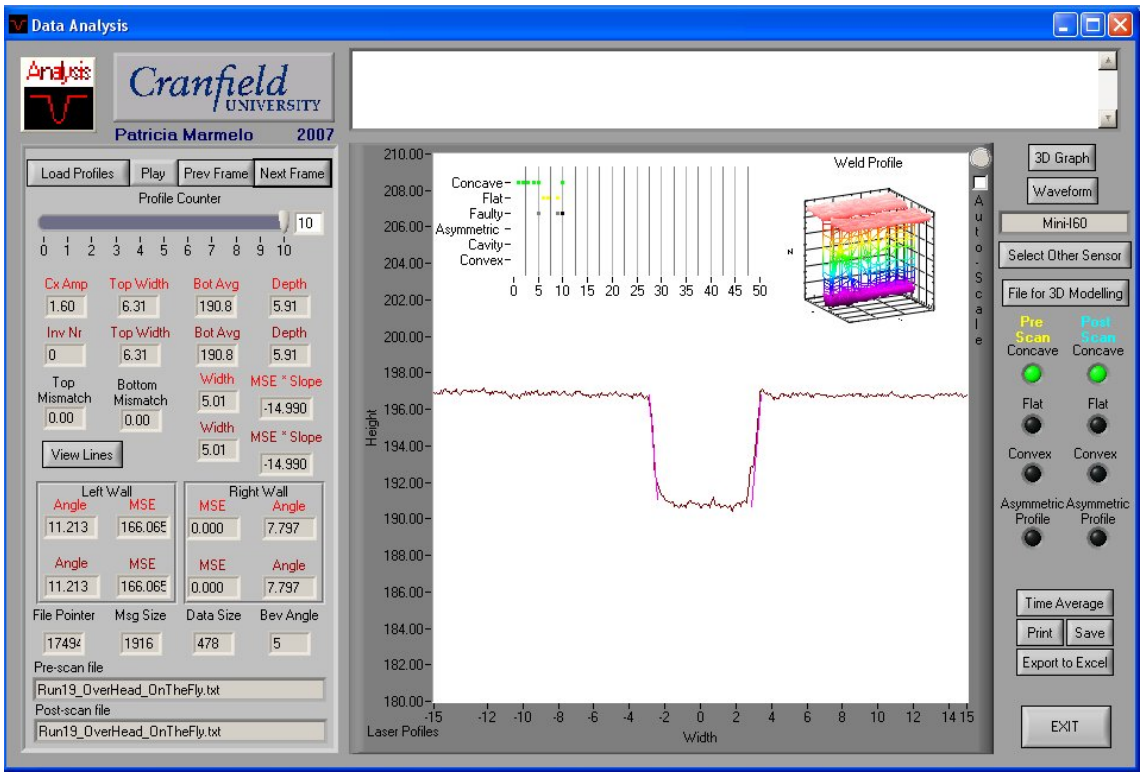

Figure I.3.0.85 – Screenshot of Profile 10 of "Run 19" in the Overhead Position.

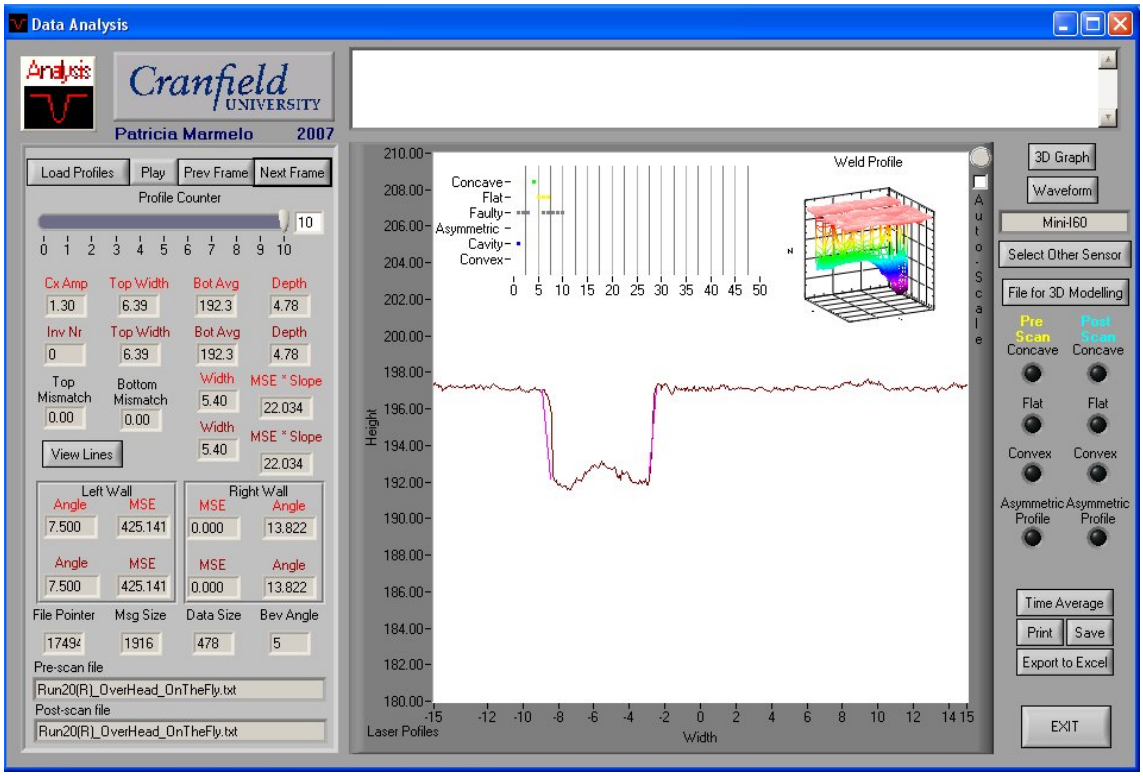

Figure I.3.0.86 – Screenshot of Profile 10 of "Run 20" in the Overhead Position.

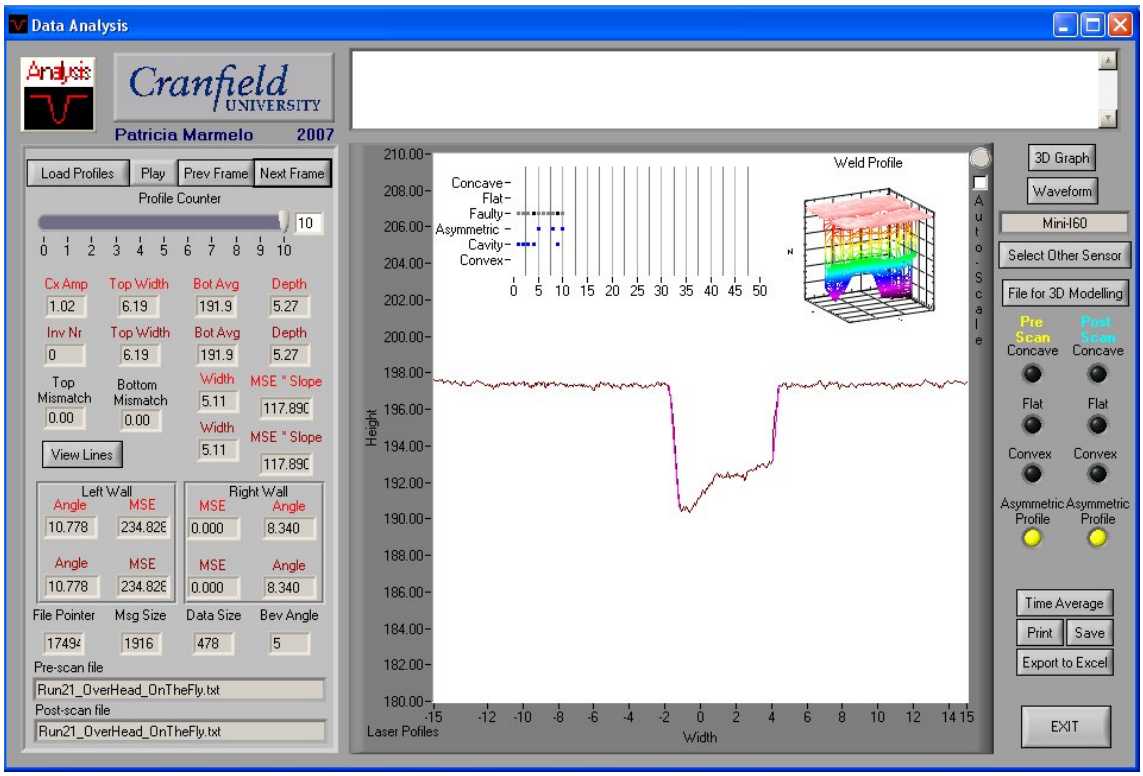

Figure I.3.0.87 – Screenshot of Profile 10 of "Run 21" in the Overhead Position.

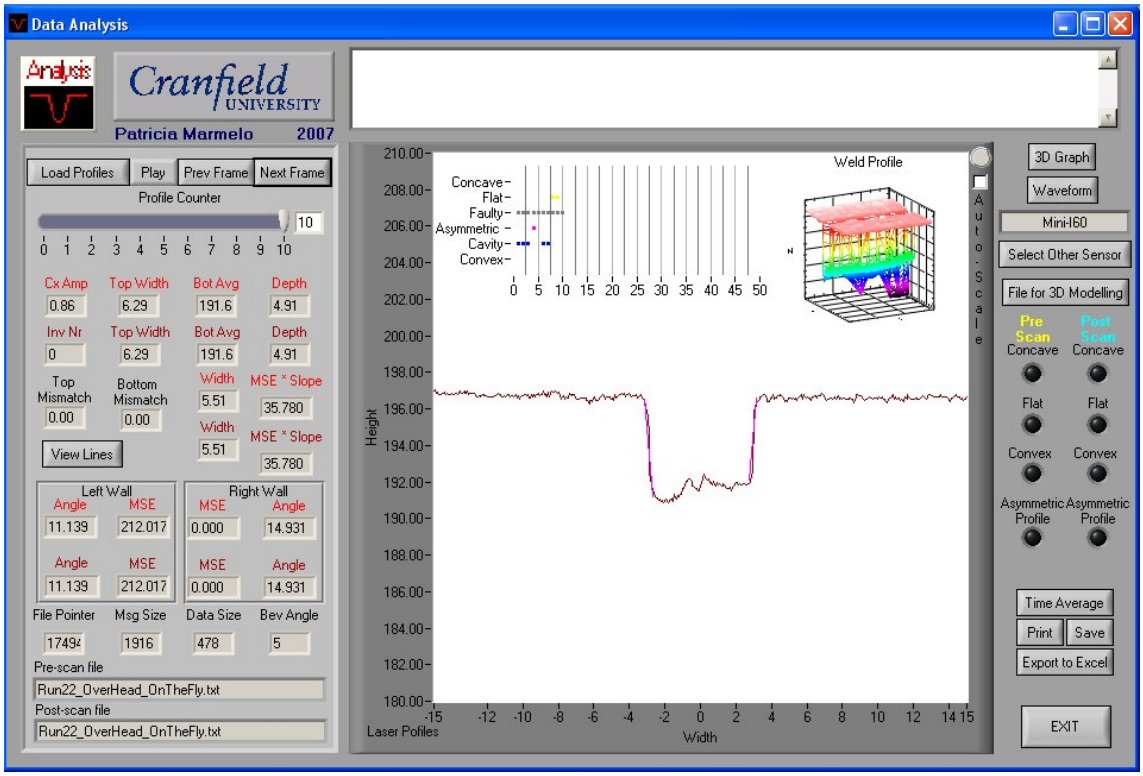

Figure I.3.0.88 – Screenshot of Profile 10 of "Run 22" in the Overhead Position.

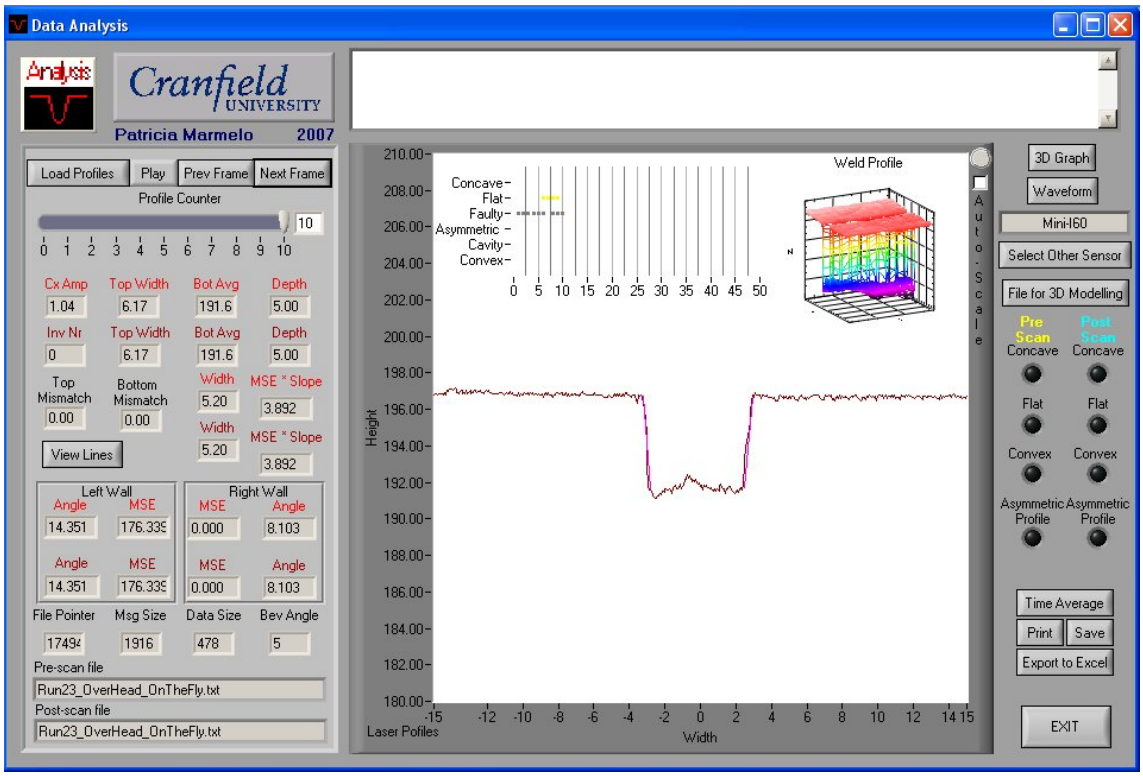

Figure I.3.0.89 – Screenshot of Profile 10 of "Run 23" in the Overhead Position.

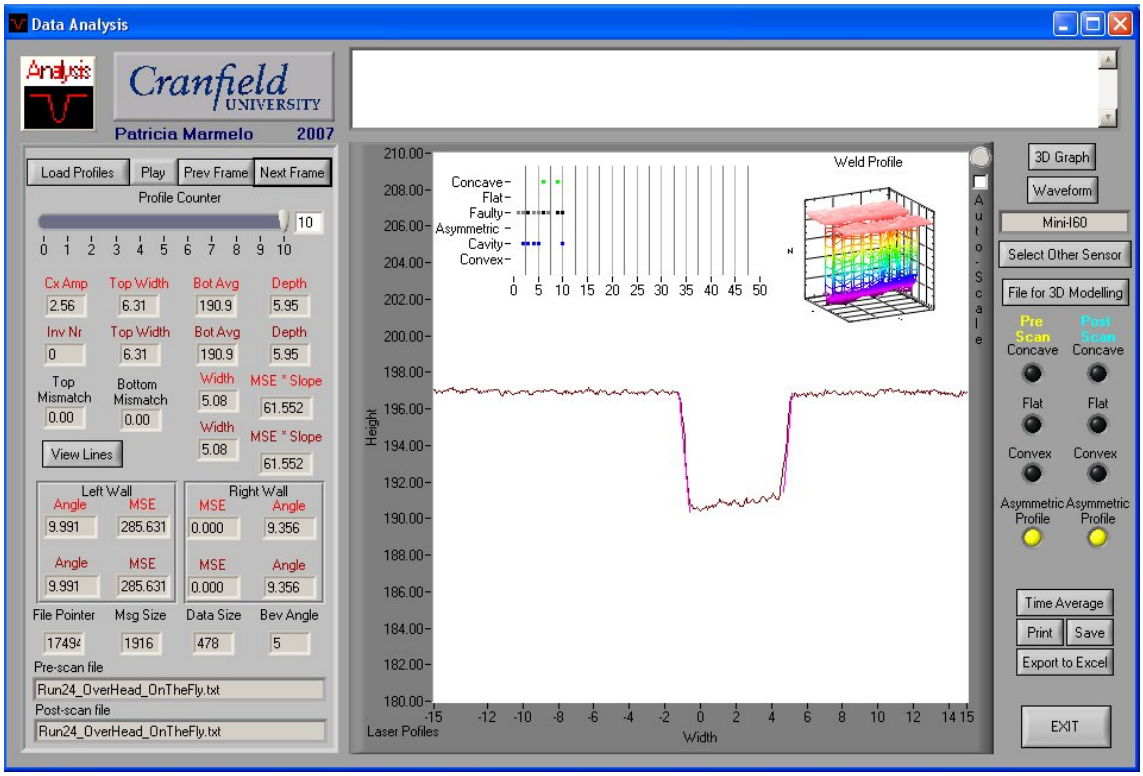

Figure I.3.0.90 – Screenshot of Profile 10 of "Run 24" in the Overhead Position.

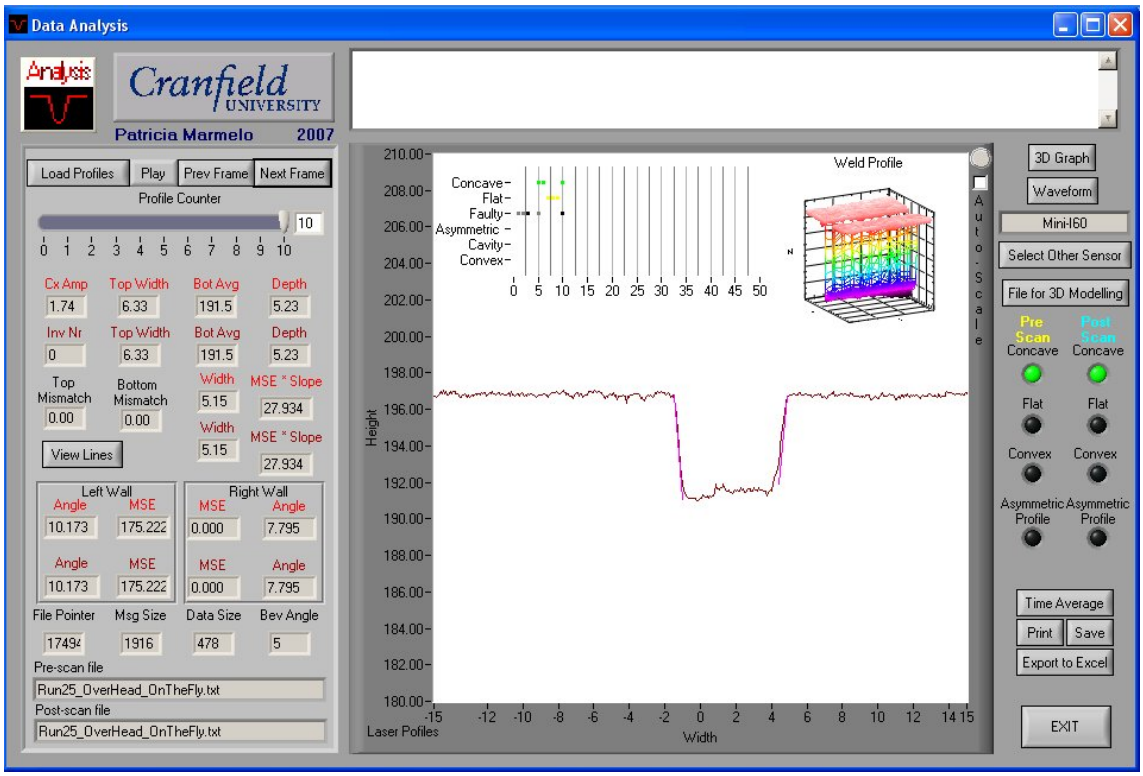

Figure I.3.0.91 – Screenshot of Profile 10 of "Run 25" in the Overhead Position.

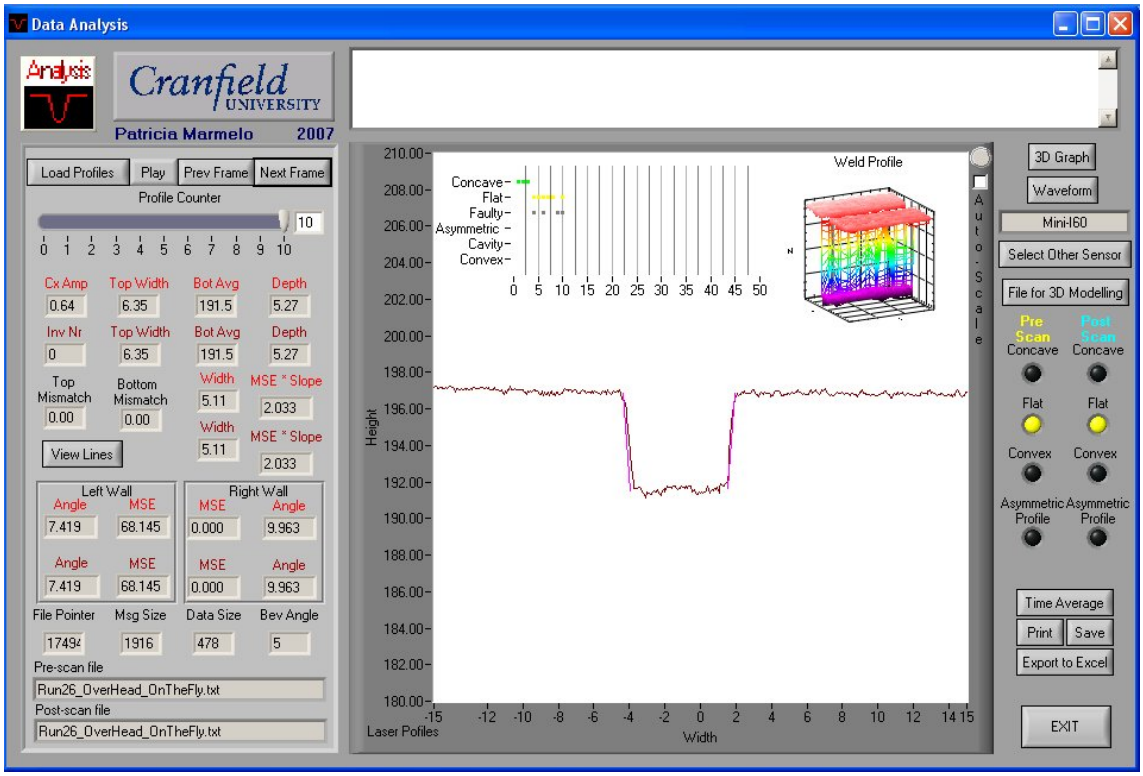

Figure I.3.0.92 – Screenshot of Profile 10 of "Run 26" in the Overhead Position.

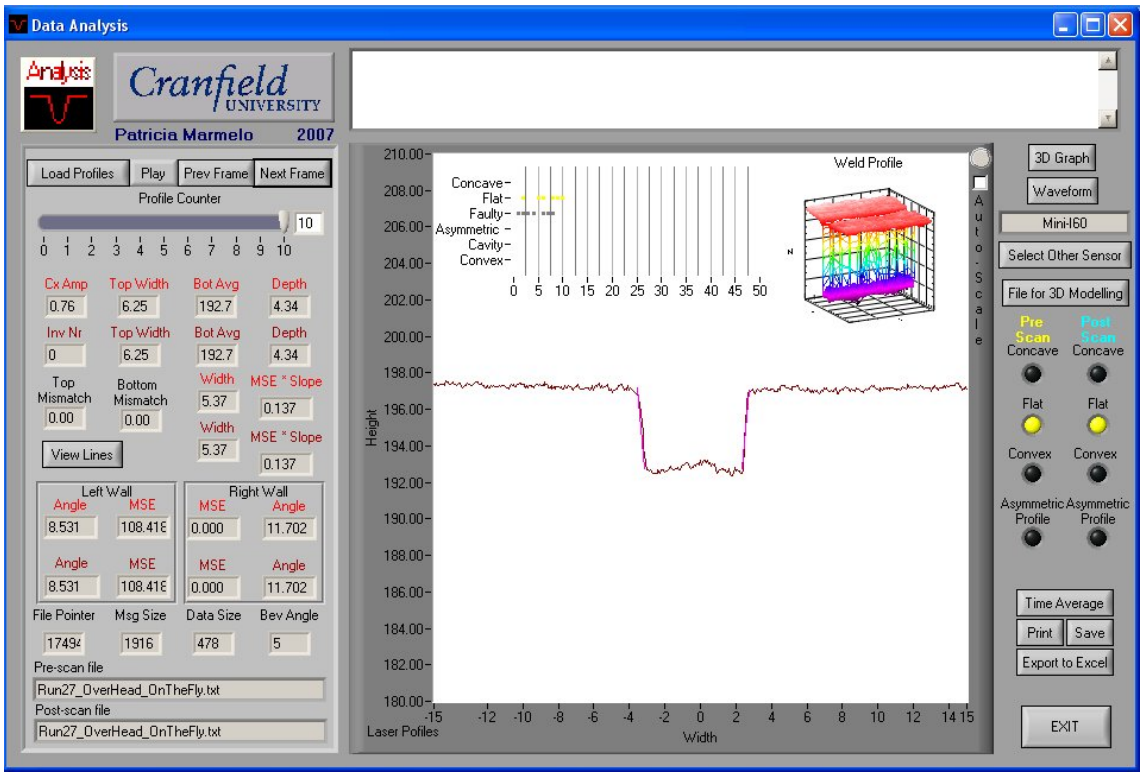

Figure I.3.0.93 – Screenshot of Profile 10 of "Run 27" in the Overhead Position.

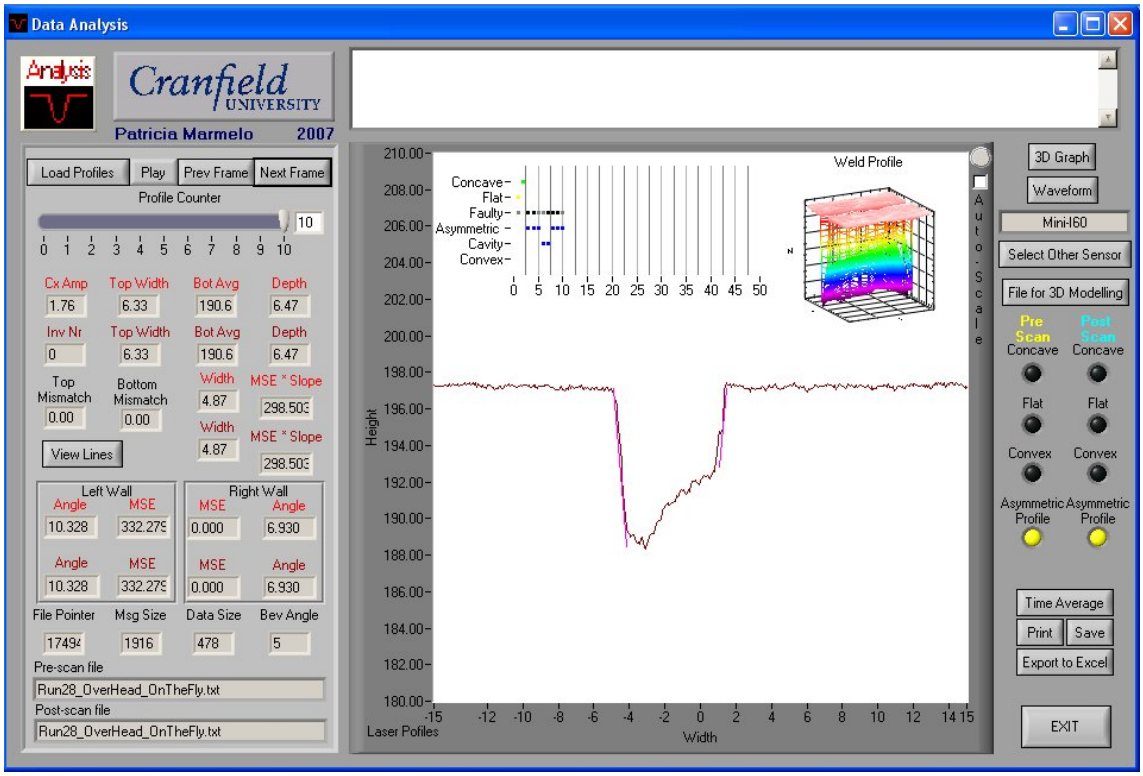

Figure I.3.0.94 – Screenshot of Profile 10 of "Run 28" in the Overhead Position.

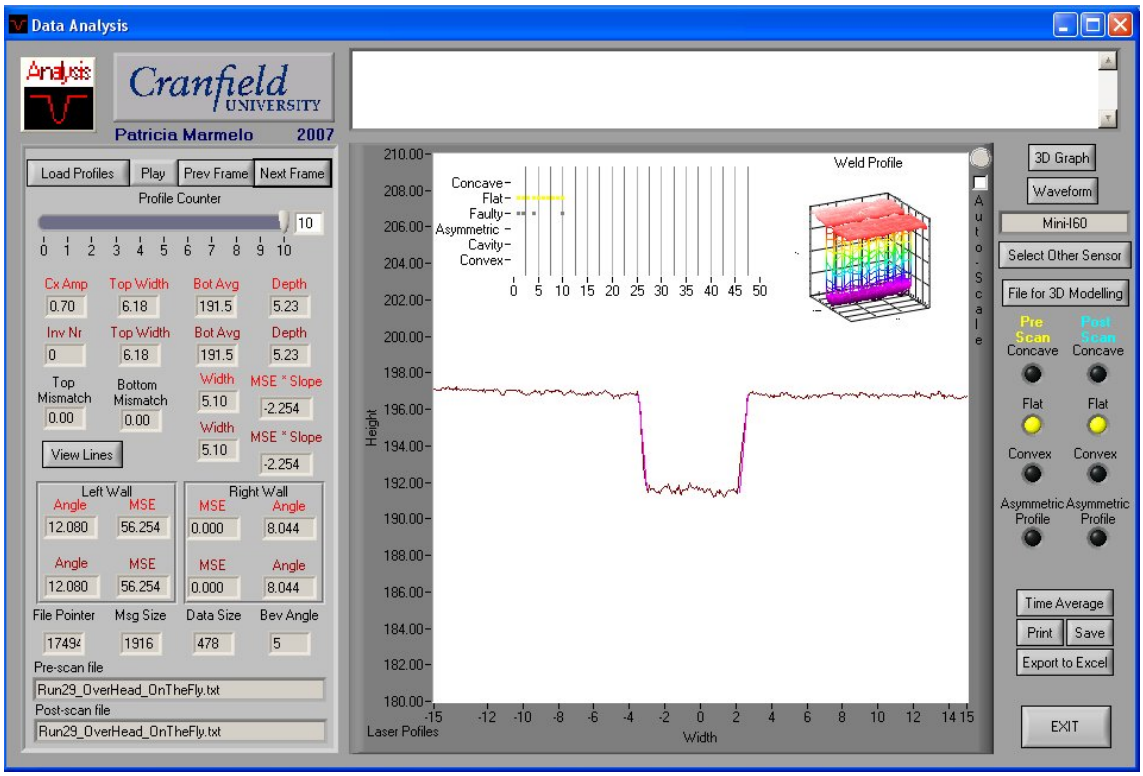

Figure I.3.0.95 – Screenshot of Profile 10 of "Run 29" in the Overhead Position.

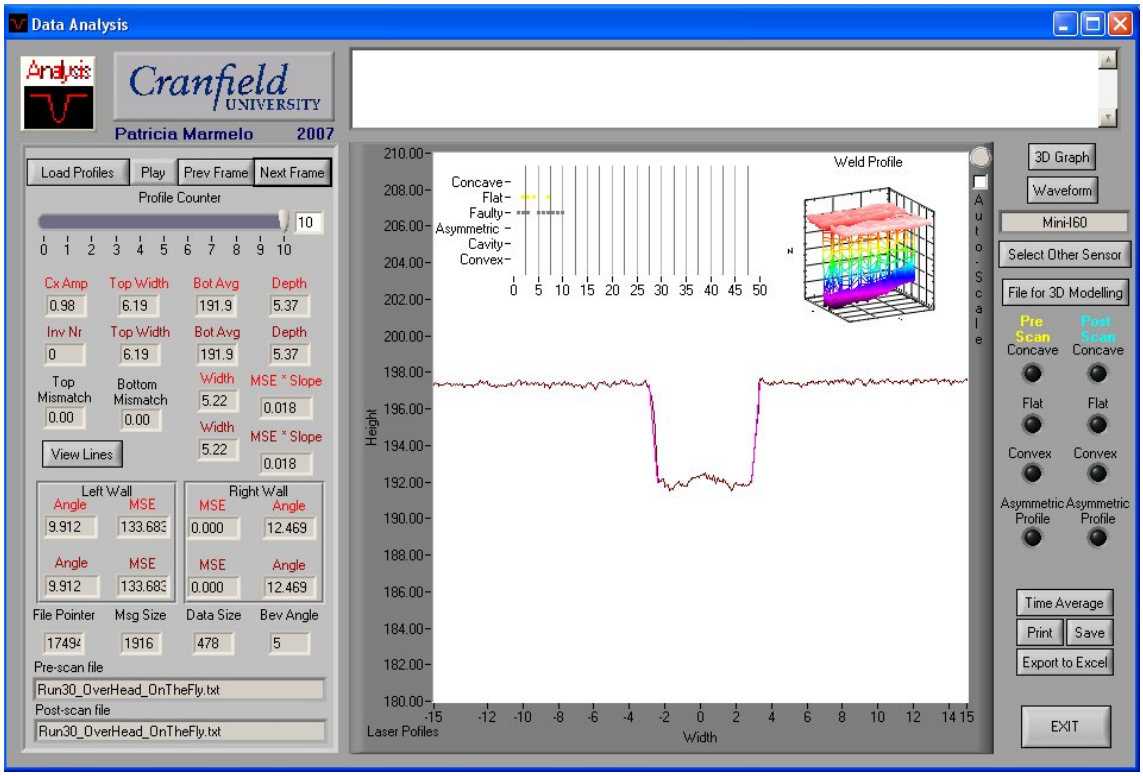

Figure I.3.0.96 – Screenshot of Profile 10 of "Run 30" in the Overhead Position.

I4 Intermediate Positions

I4.1 30 Degrees

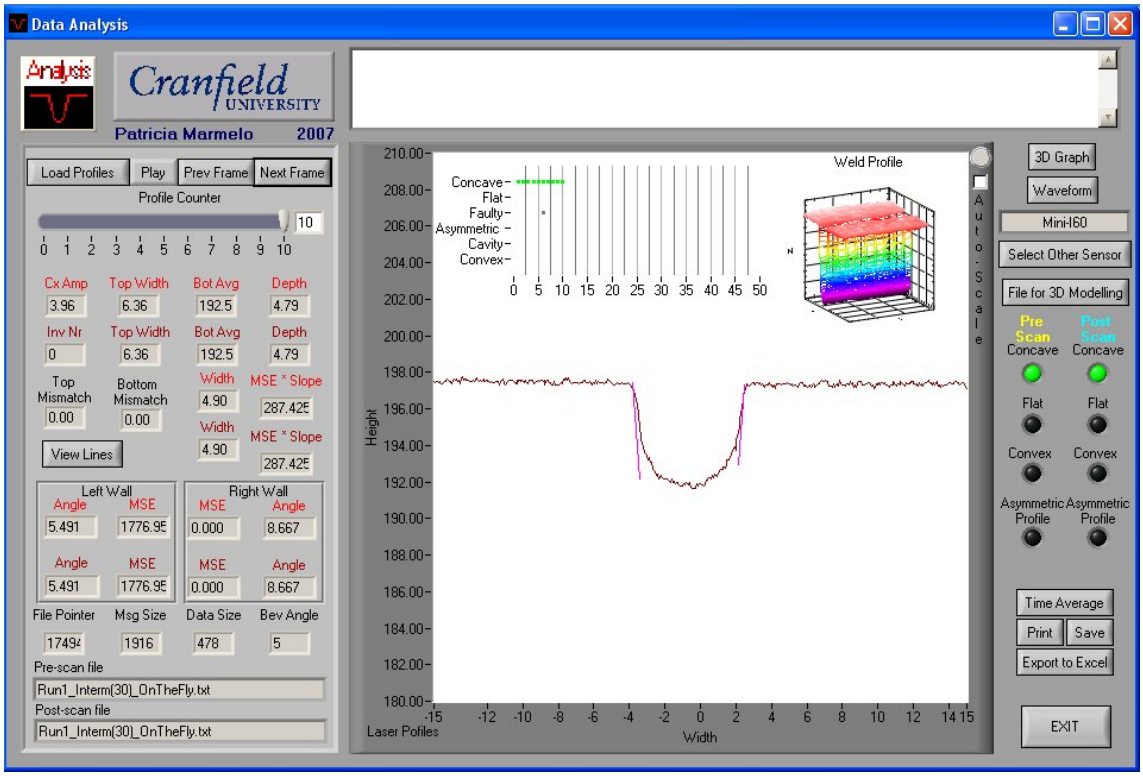

Figure I.4.1.0.97 – Screenshot of Profile 10 of "Run 1" Positioned at 30 Degrees.

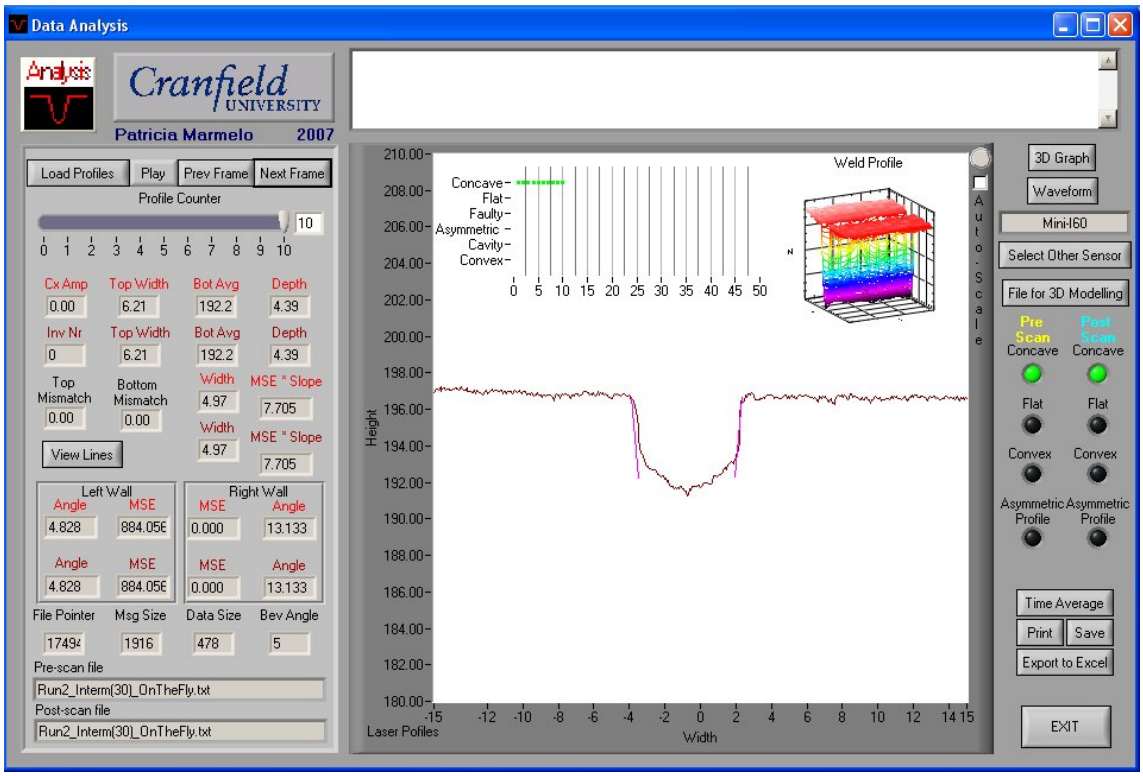

Figure I.4.1.0.98 – Screenshot of Profile 10 of "Run 2" Positioned at 30 Degrees.

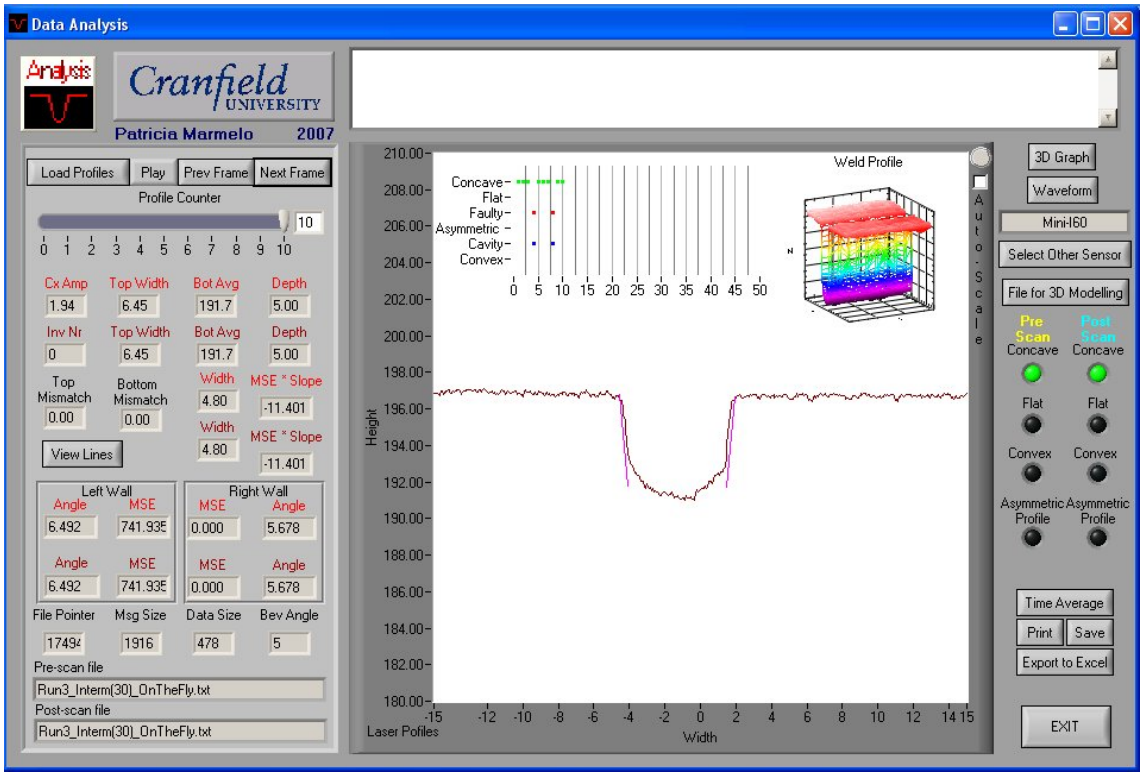

Figure I.4.1.0.99 – Screenshot of Profile 10 of "Run 3" Positioned at 30 Degrees.

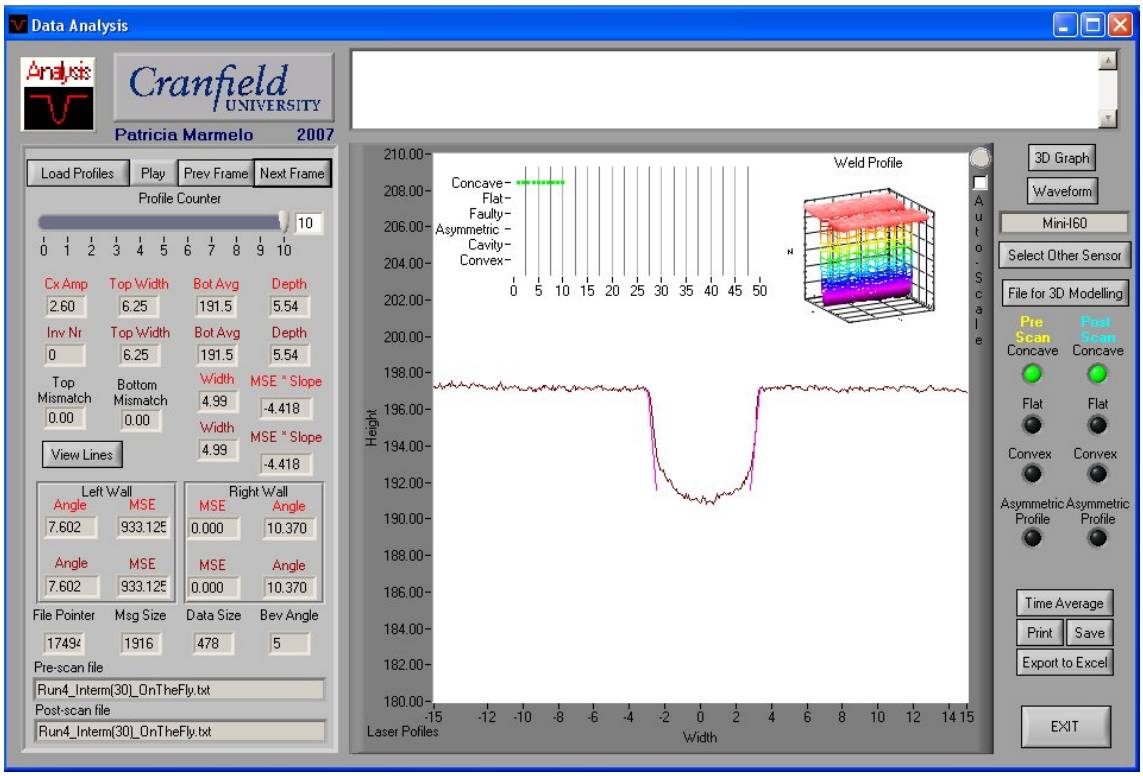

Figure I.4.1.0.100 – Screenshot of Profile 10 of "Run 4" Positioned at 30 Degrees.

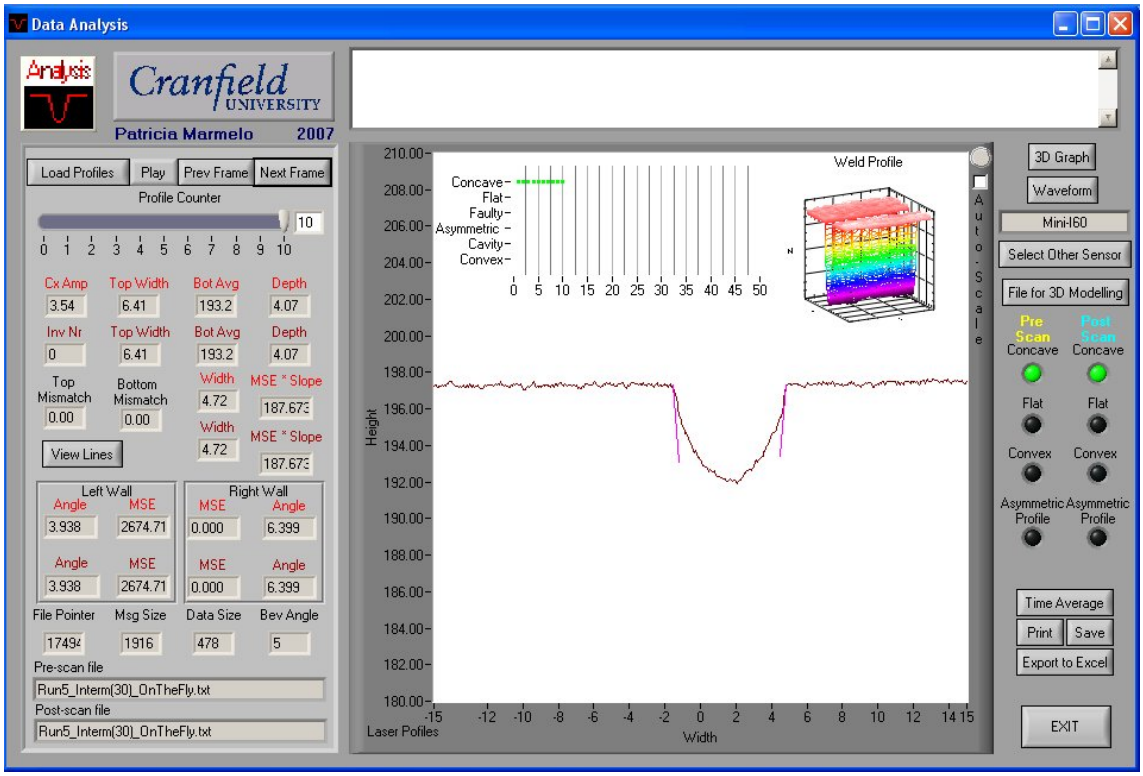

Figure I.4.1.0.101 – Screenshot of Profile 10 of "Run 5" Positioned at 30 Degrees.

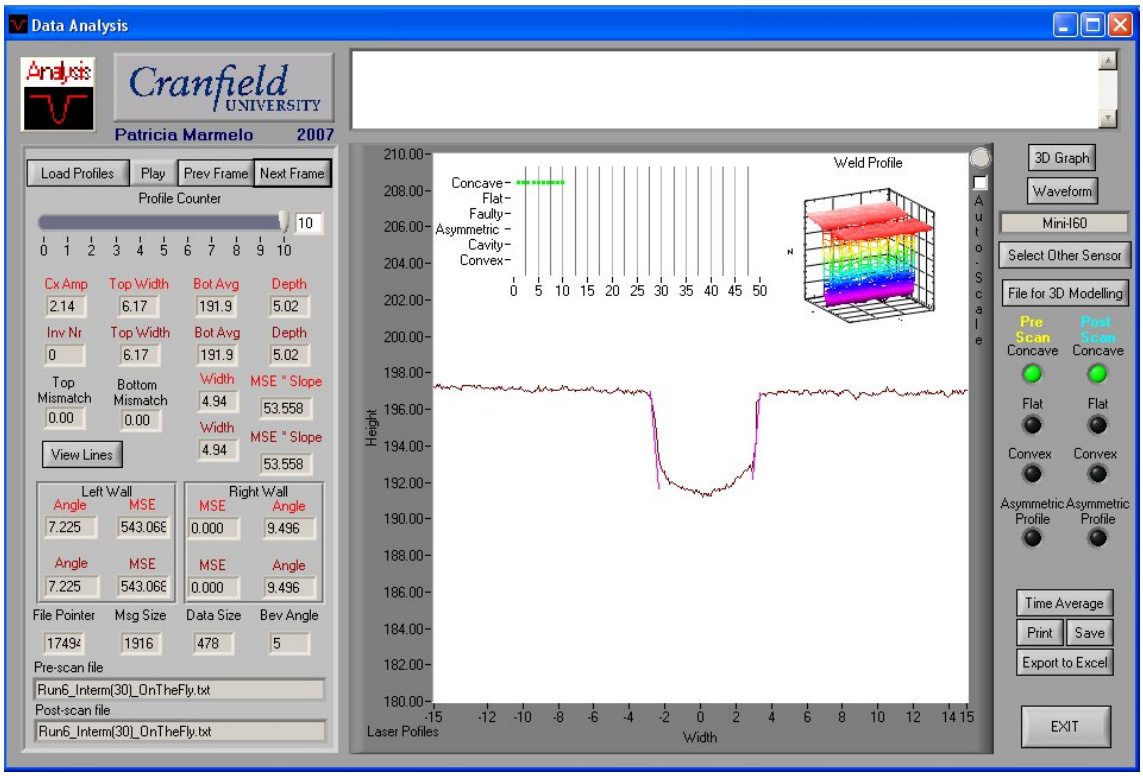

Figure I.4.1.0.102 – Screenshot of Profile 10 of "Run 6" Positioned at 30 Degrees.

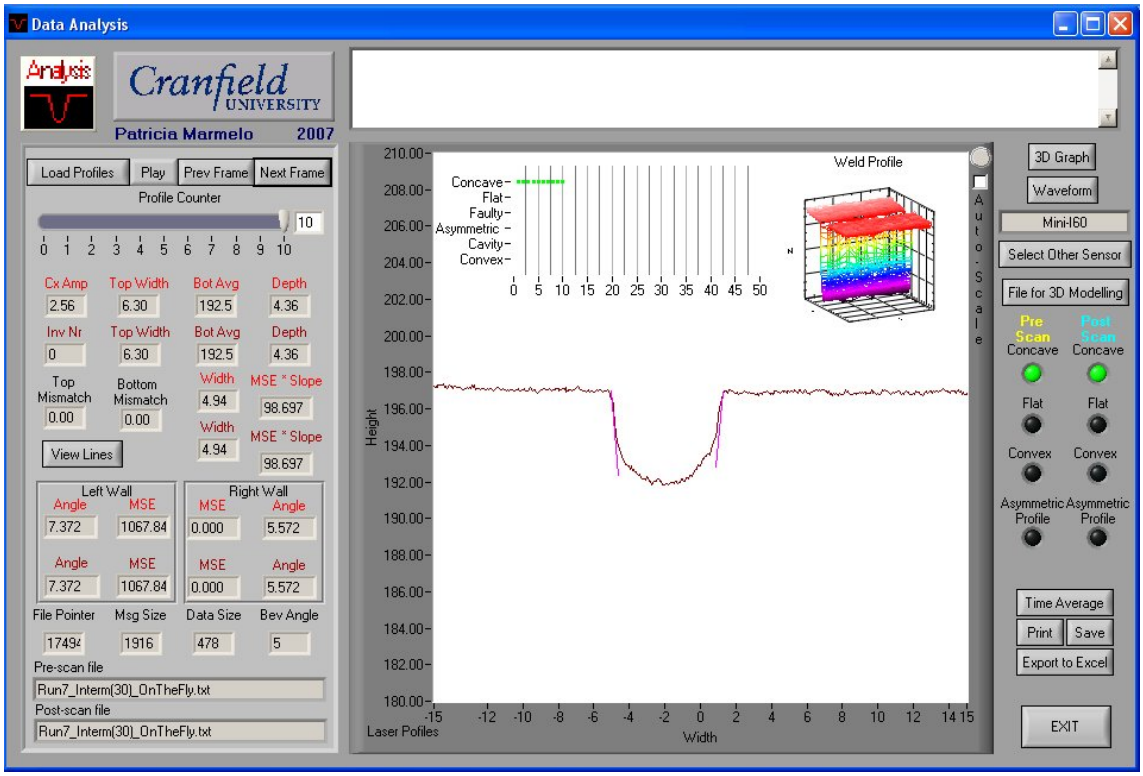

Figure I.4.1.0.103 – Screenshot of Profile 10 of "Run 7" Positioned at 30 Degrees.

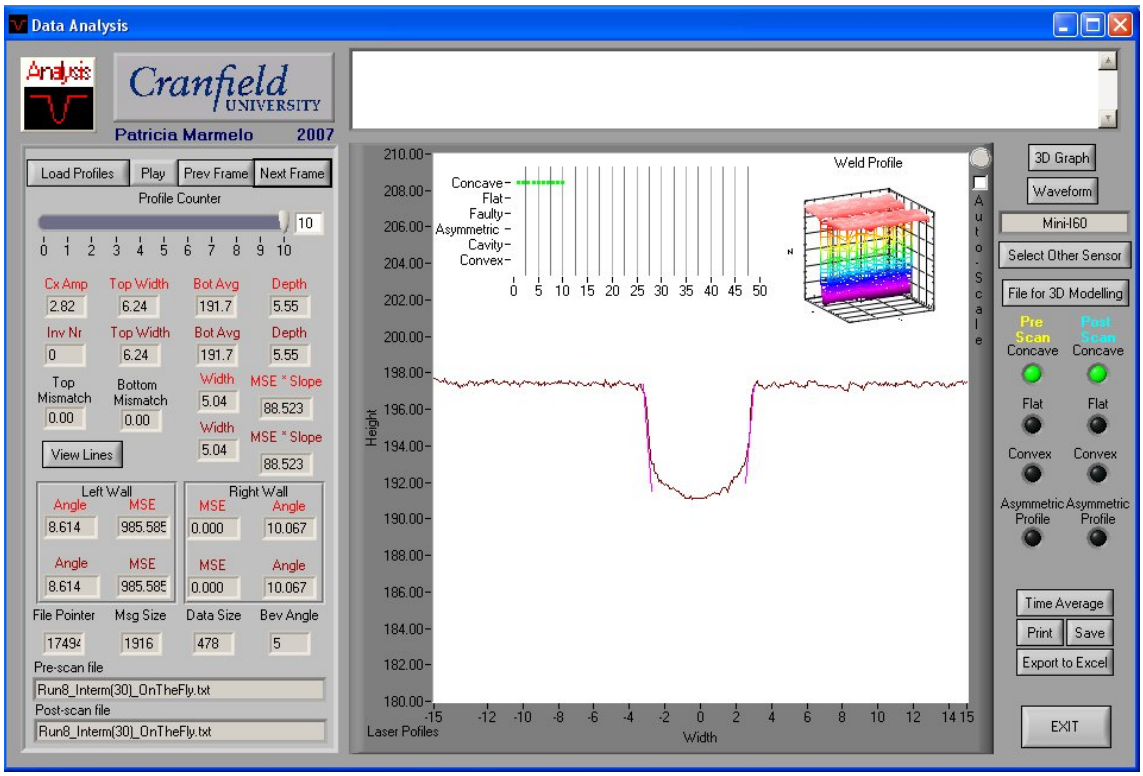

Figure I.4.1.0.104 – Screenshot of Profile 10 of "Run 8" Positioned at 30 Degrees.

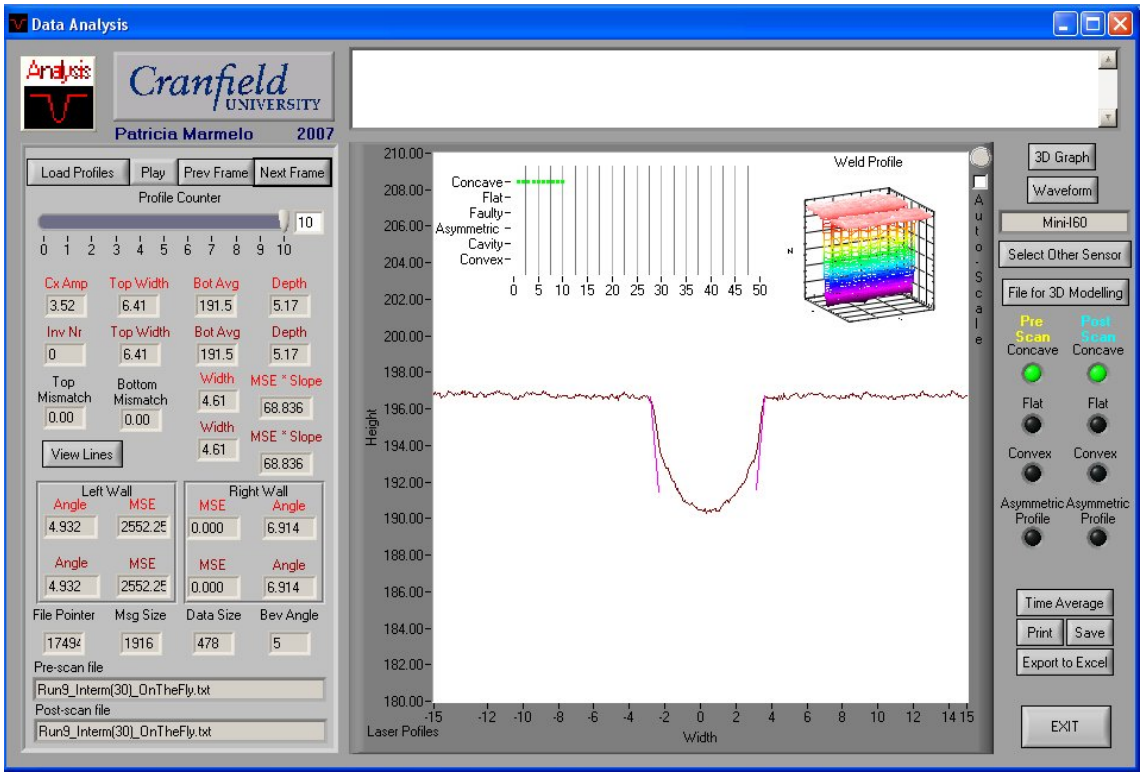

Figure I.4.1.0.105 – Screenshot of Profile 10 of "Run 9" Positioned at 30 Degrees.

I4.2 60 Degrees

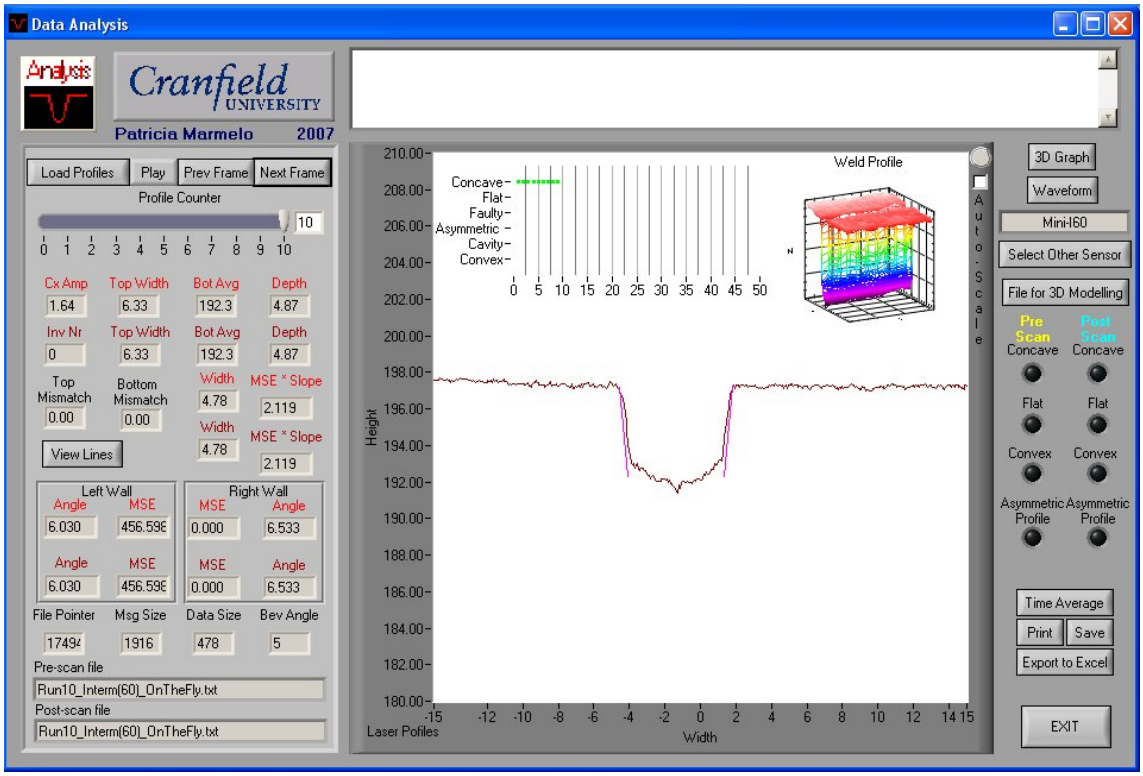

Figure I.4.2.0.106 – Screenshot of Profile 10 of "Run 10" Positioned at 60 Degrees.

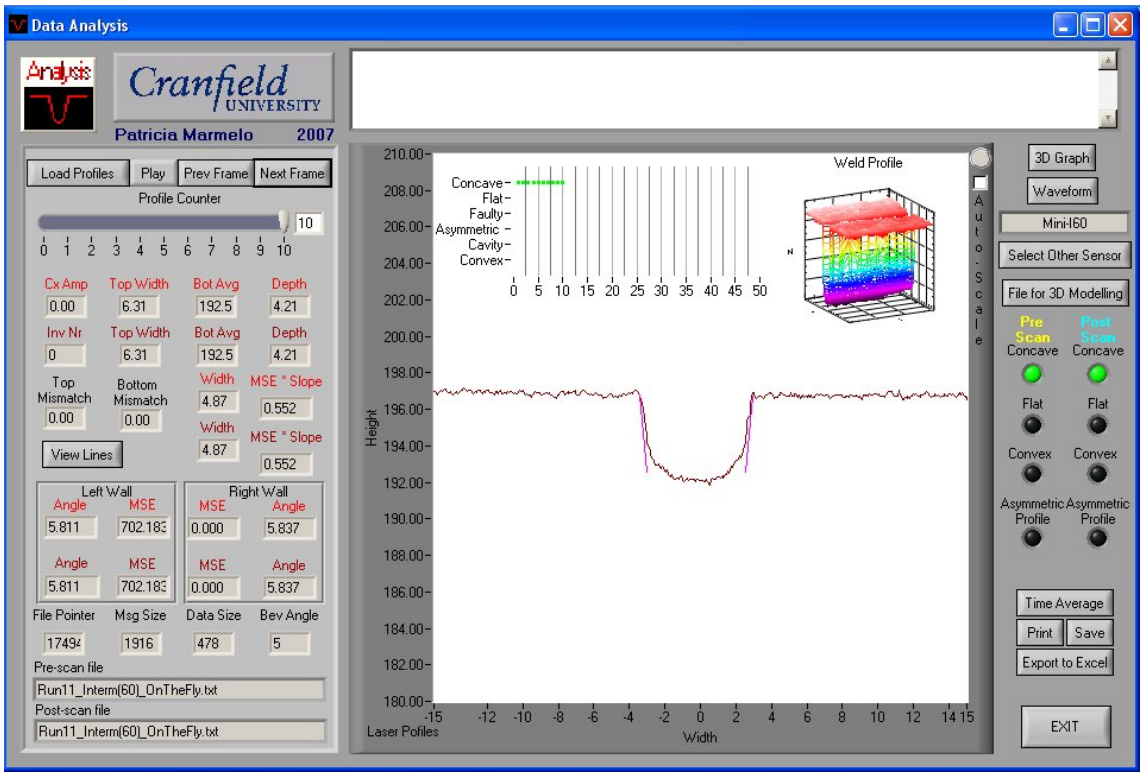

Figure I.4.2.0.107 – Screenshot of Profile 10 of "Run 11" Positioned at 60 Degrees.

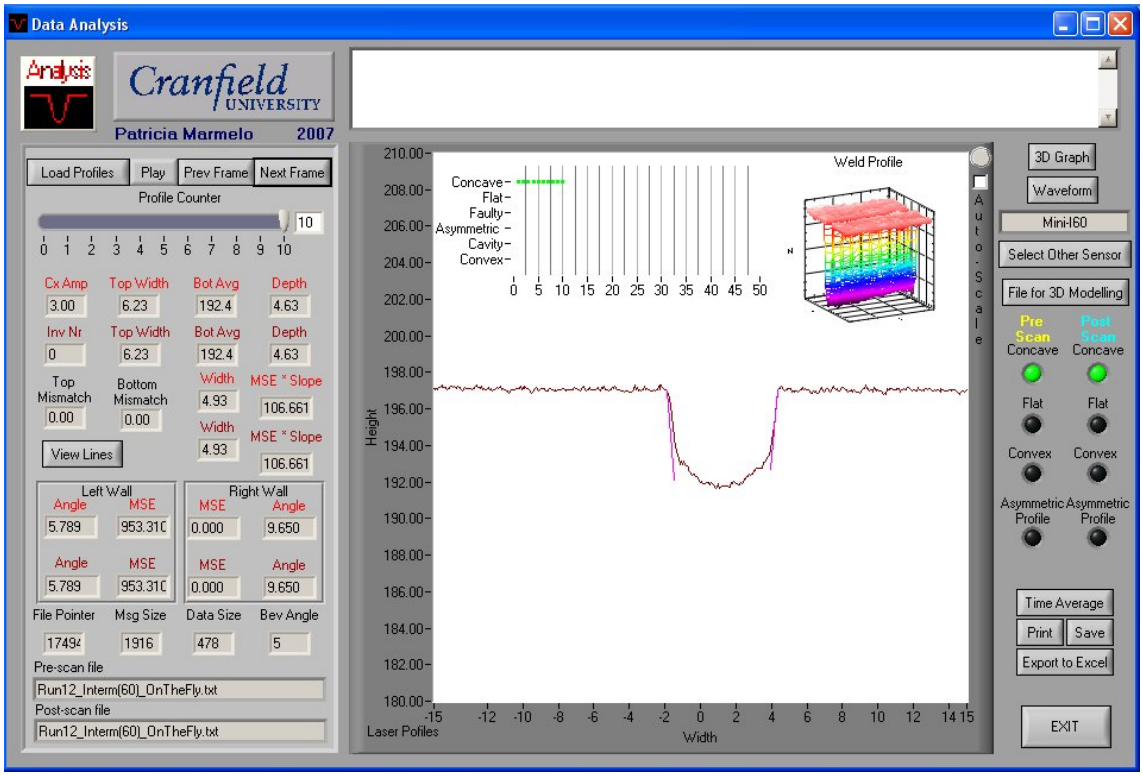

Figure I.4.2.0.108 – Screenshot of Profile 10 of "Run 12" Positioned at 60 Degrees.

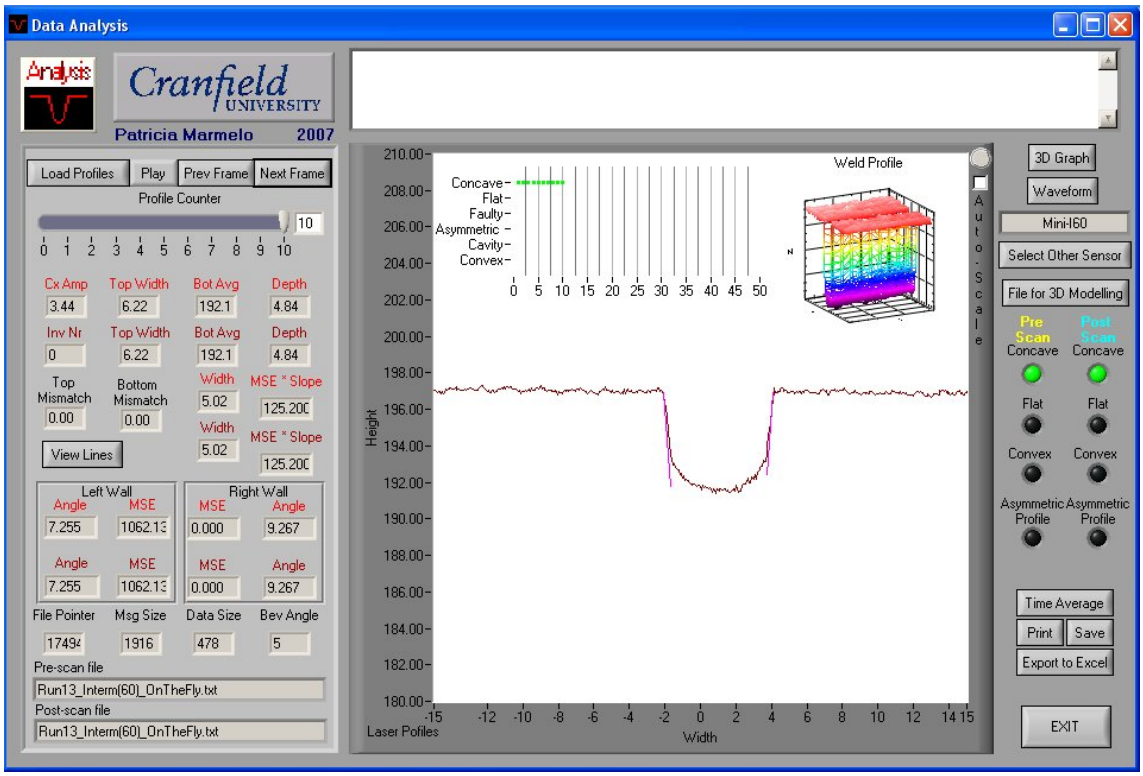

Figure I.4.2.0.109 – Screenshot of Profile 10 of "Run 13" Positioned at 60 Degrees.

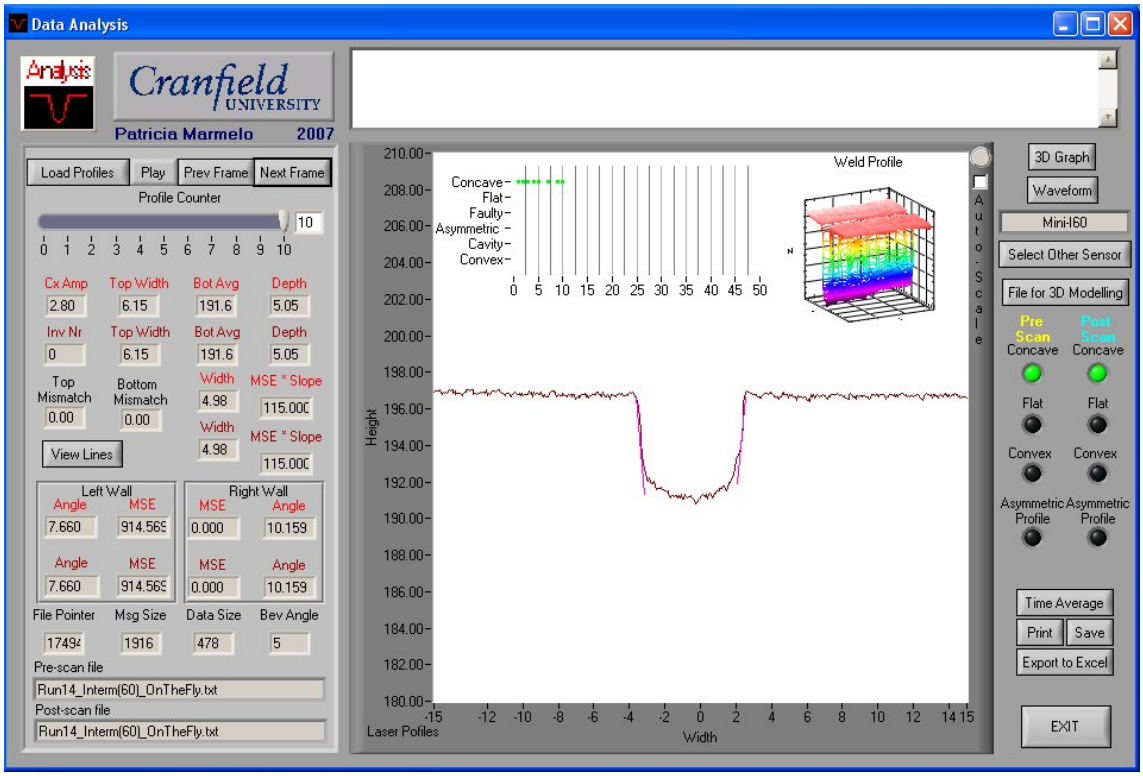

Figure I.4.2.0.110 – Screenshot of Profile 10 of "Run 14" Positioned at 60 Degrees.

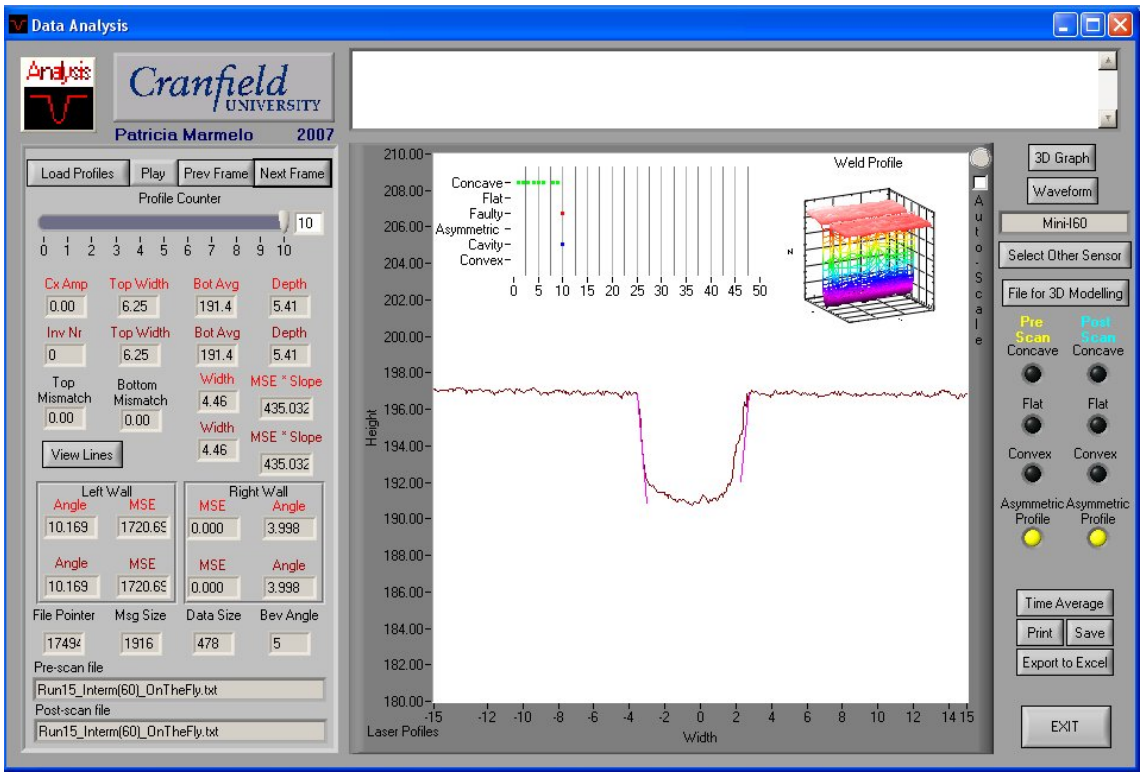

Figure I.4.2.0.111 – Screenshot of Profile 10 of "Run 15" Positioned at 60 Degrees.

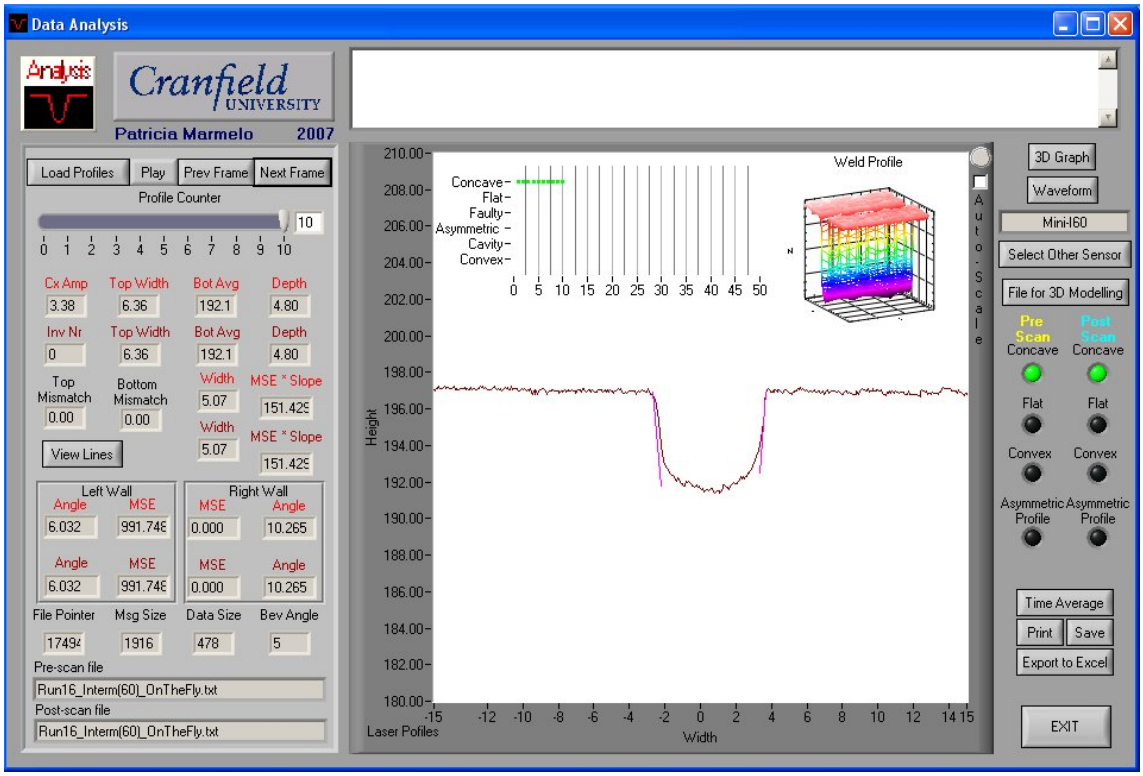

Figure I.4.2.0.112 – Screenshot of Profile 10 of "Run 16" Positioned at 60 Degrees.

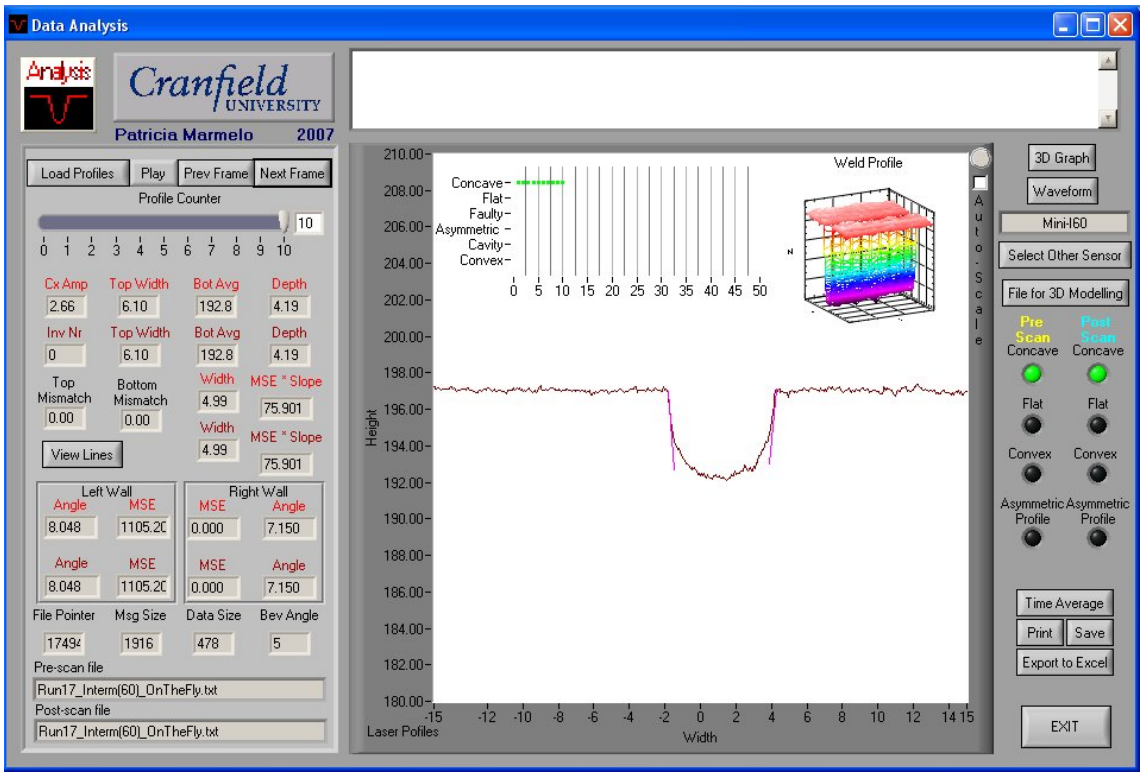

Figure I.4.2.0.113 – Screenshot of Profile 10 of "Run 17" Positioned at 60 Degrees.

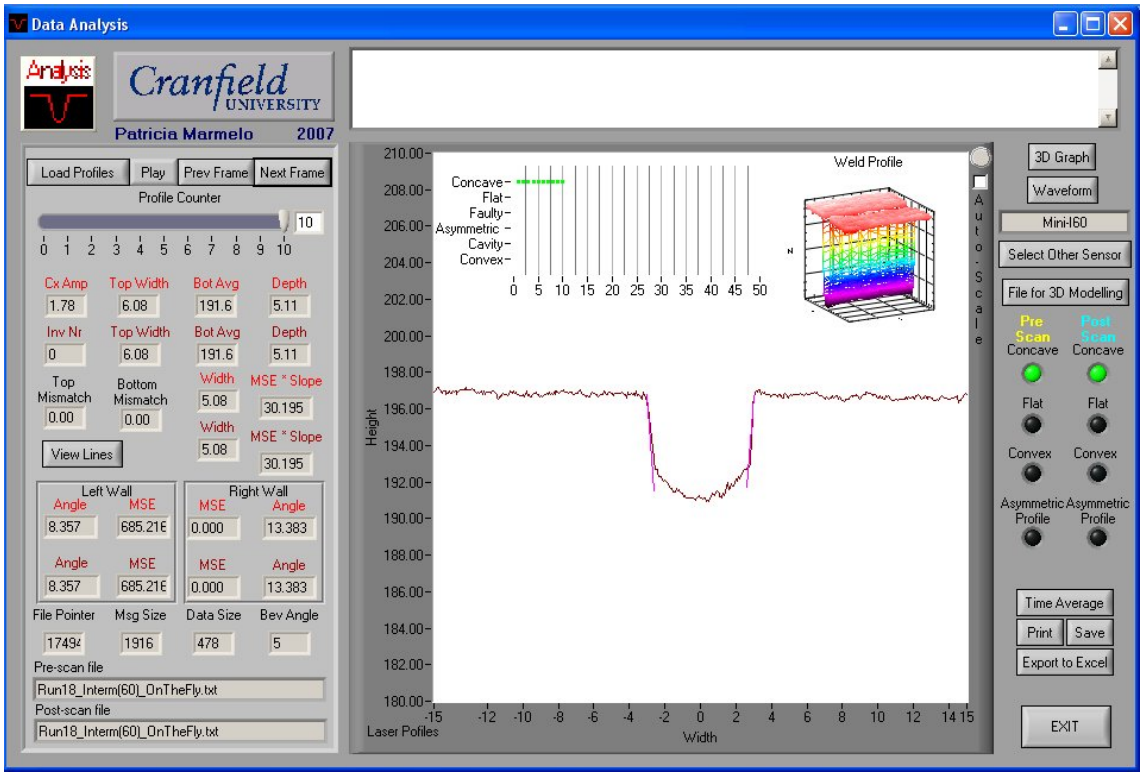

Figure I.4.2.0.114 – Screenshot of Profile 10 of "Run 18" Positioned at 60 Degrees.

I4.3 120 Degrees

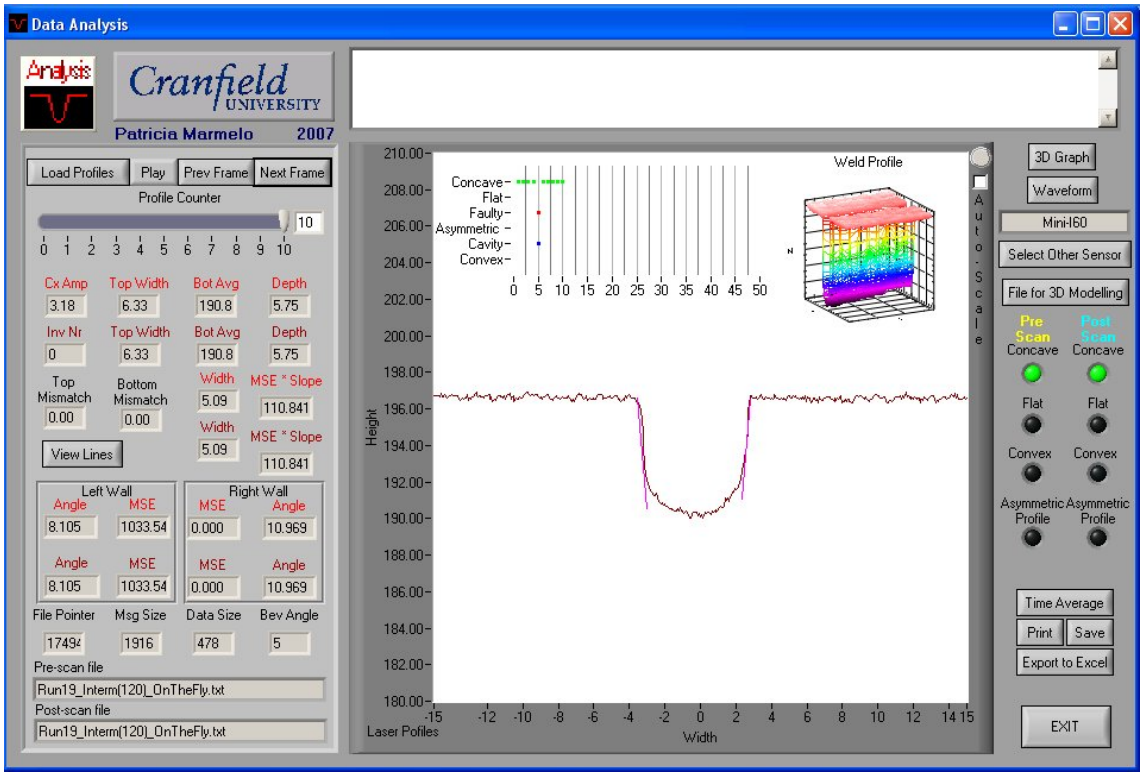

Figure I.4.3.0.115 – Screenshot of Profile 10 of "Run 19" Positioned at 120 Degrees.

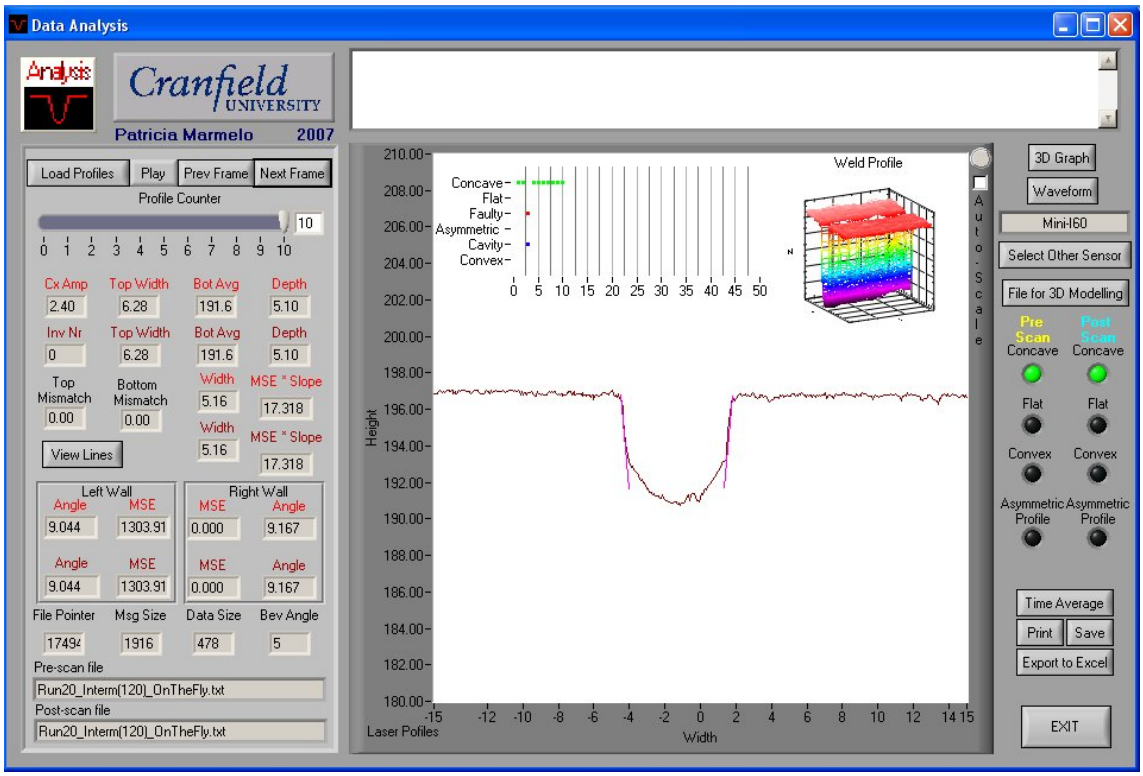

Figure I.4.3.0.116 – Screenshot of Profile 10 of "Run 20" Positioned at 120 Degrees.

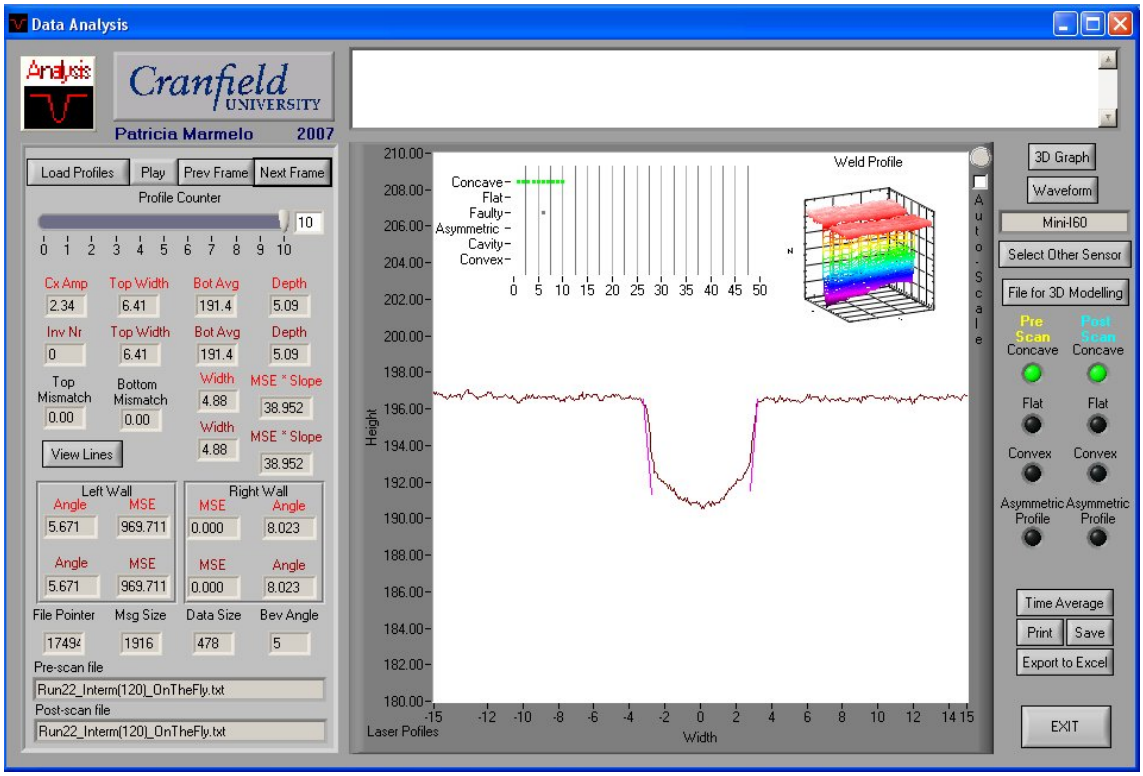

Figure I.4.3.0.117 – Screenshot of Profile 10 of "Run 21" Positioned at 120 Degrees.

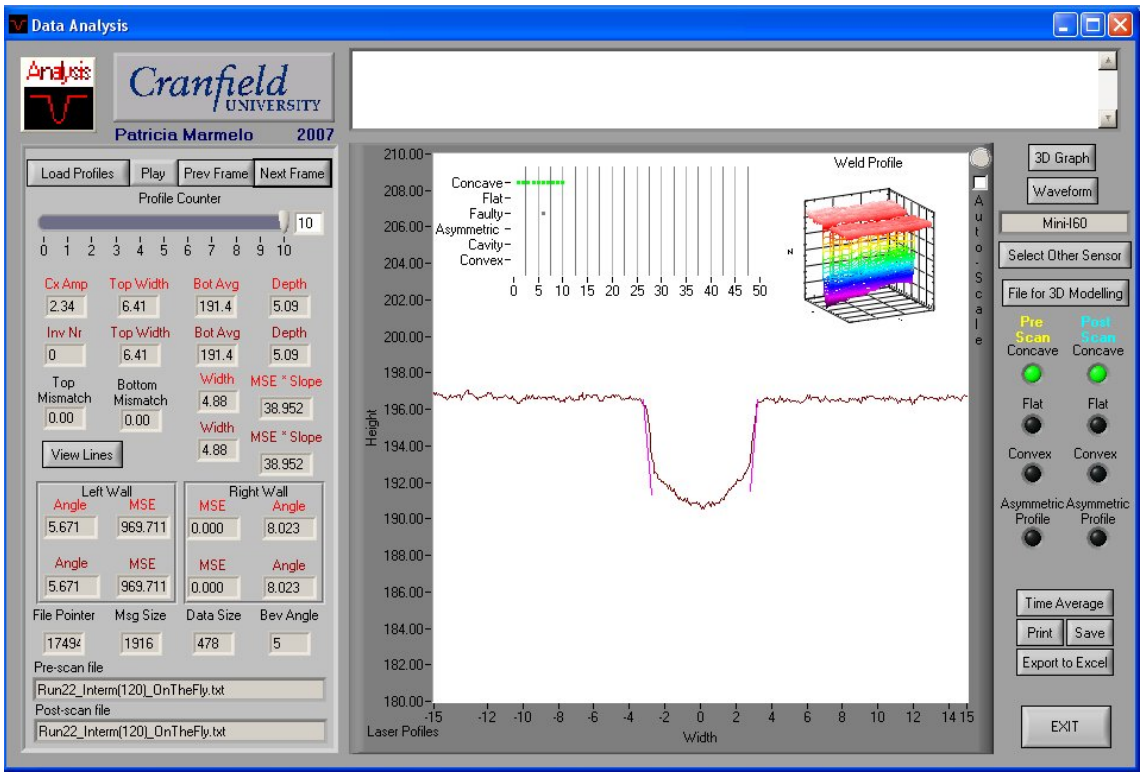

Figure I.4.3.0.118 – Screenshot of Profile 10 of "Run 22" Positioned at 120 Degrees.

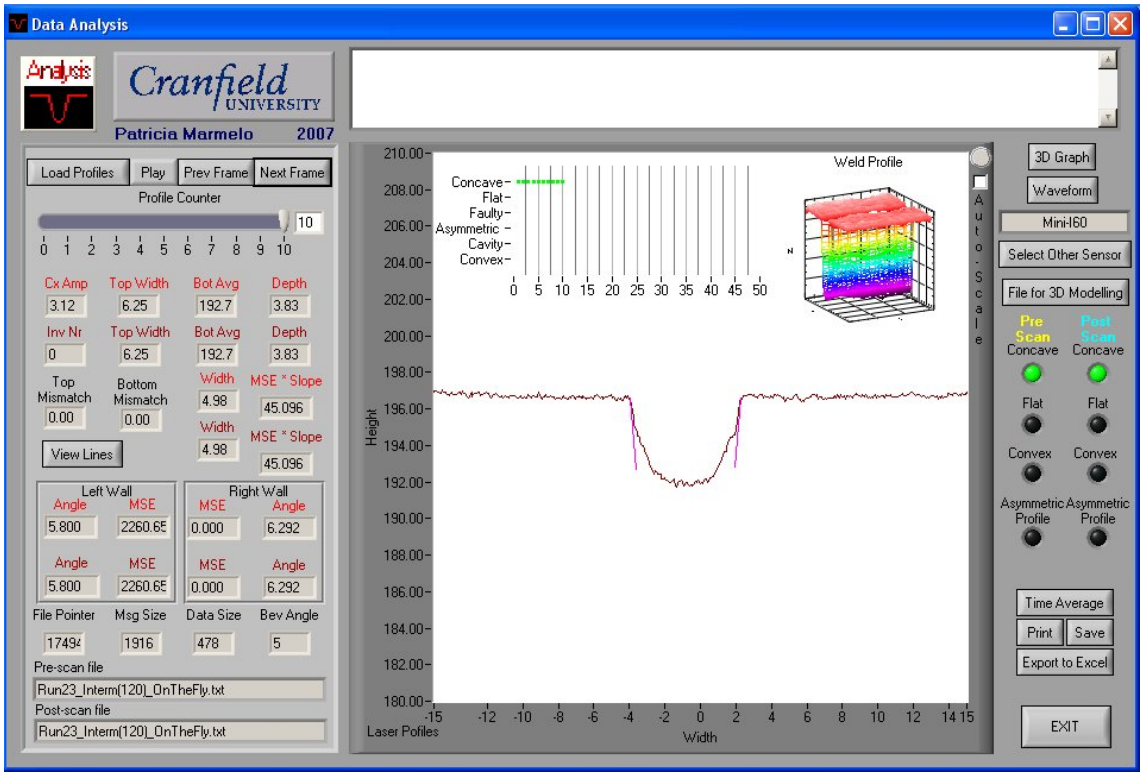

Figure I.4.3.0.119 – Screenshot of Profile 10 of "Run 23" Positioned at 120 Degrees.

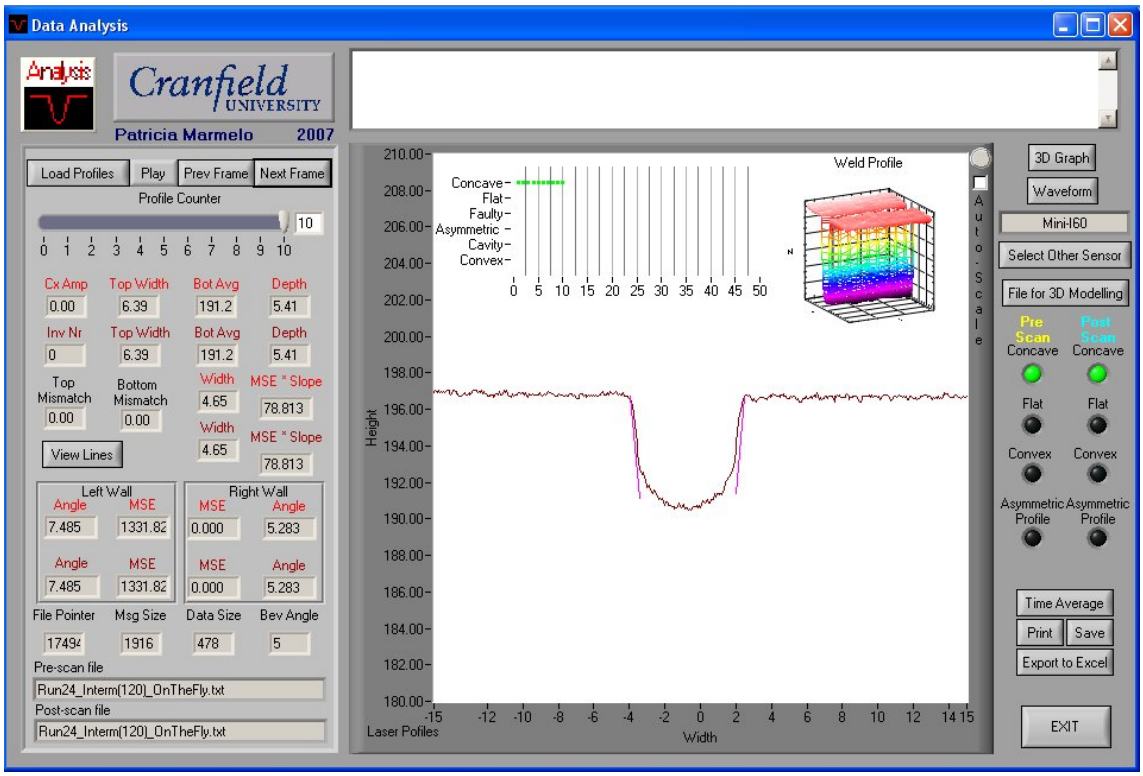

Figure I.4.3.0.120 – Screenshot of Profile 10 of "Run 24" Positioned at 120 Degrees.

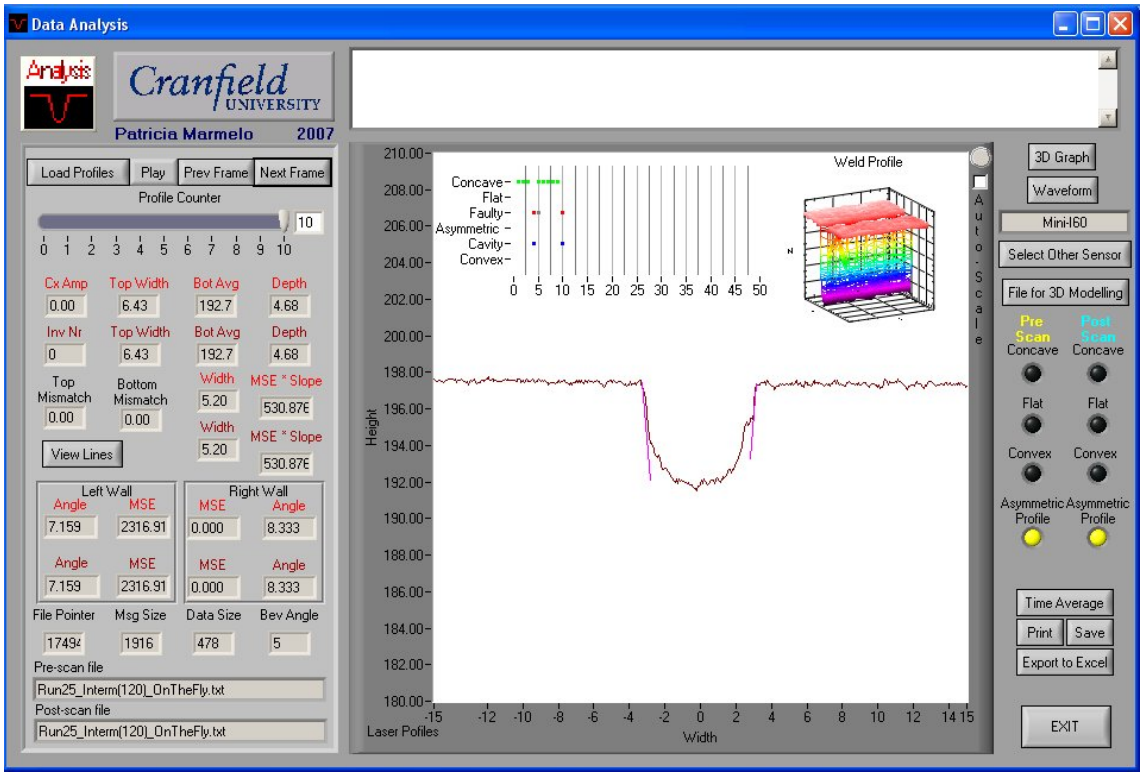

Figure I.4.3.0.121 – Screenshot of Profile 10 of "Run 25" Positioned at 120 Degrees.

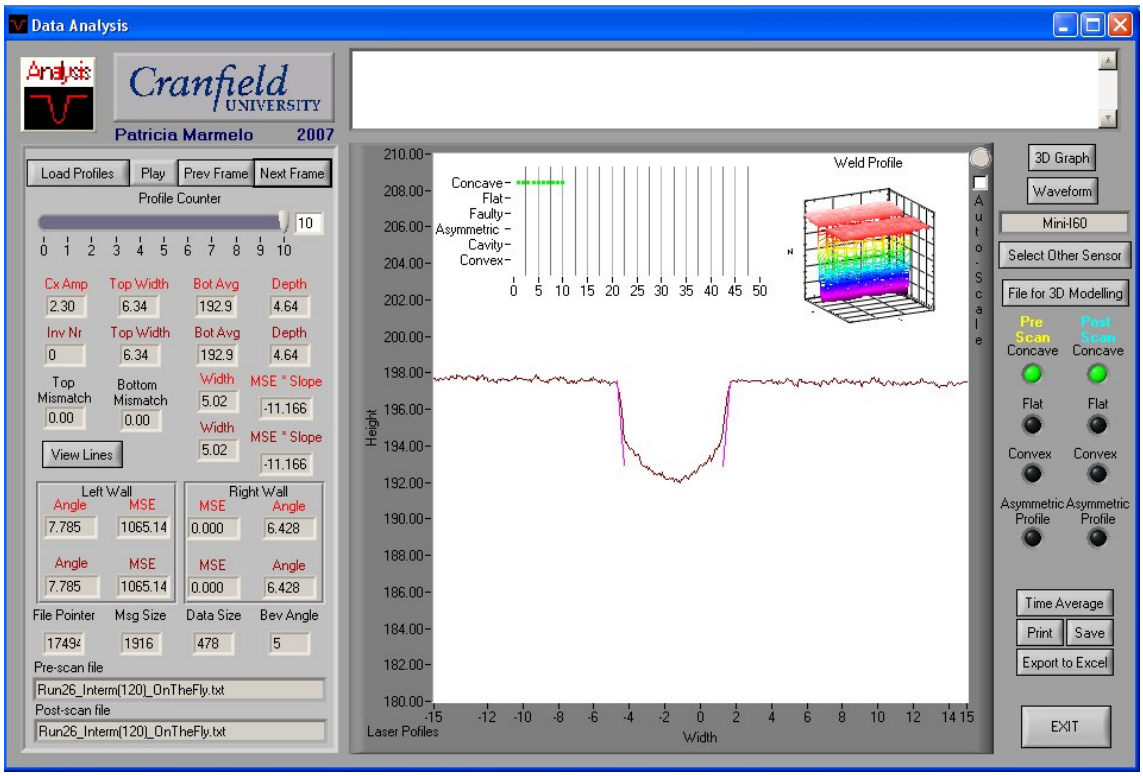

Figure I.4.3.0.122 – Screenshot of Profile 10 of "Run 26" Positioned at 120 Degrees.

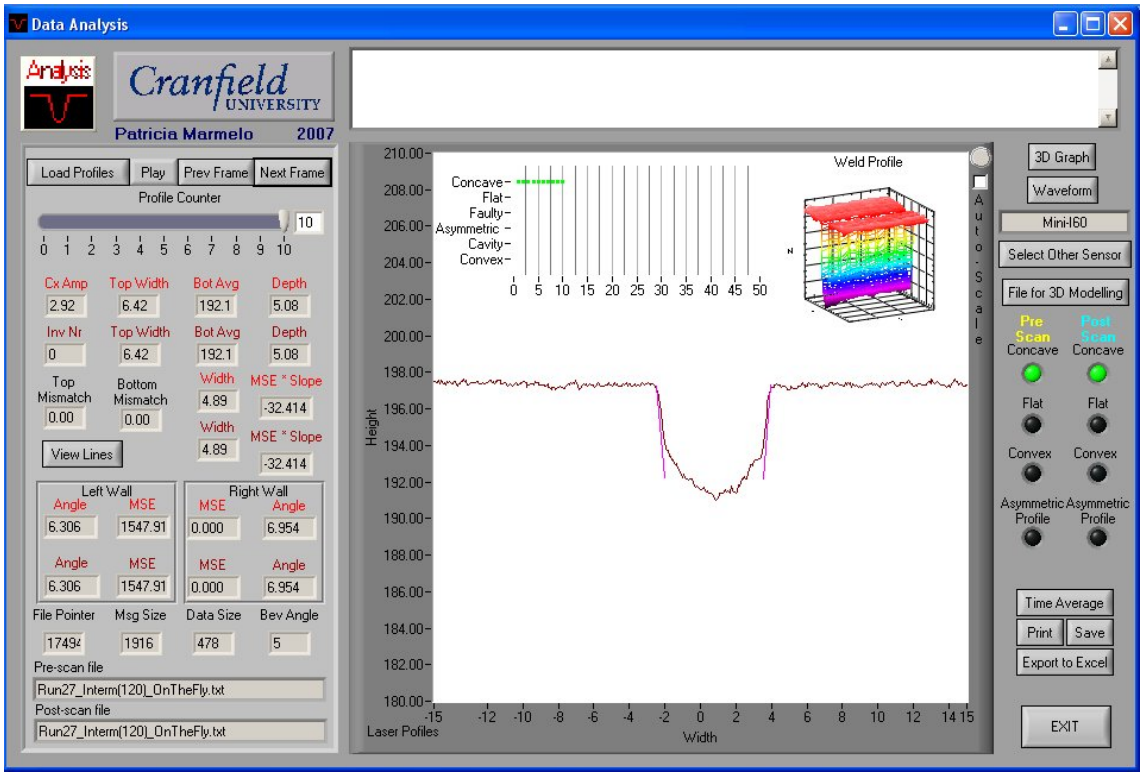

Figure I.4.3.0.123 – Screenshot of Profile 10 of "Run 27" Positioned at 120 Degrees.

I4.4 150 Degrees

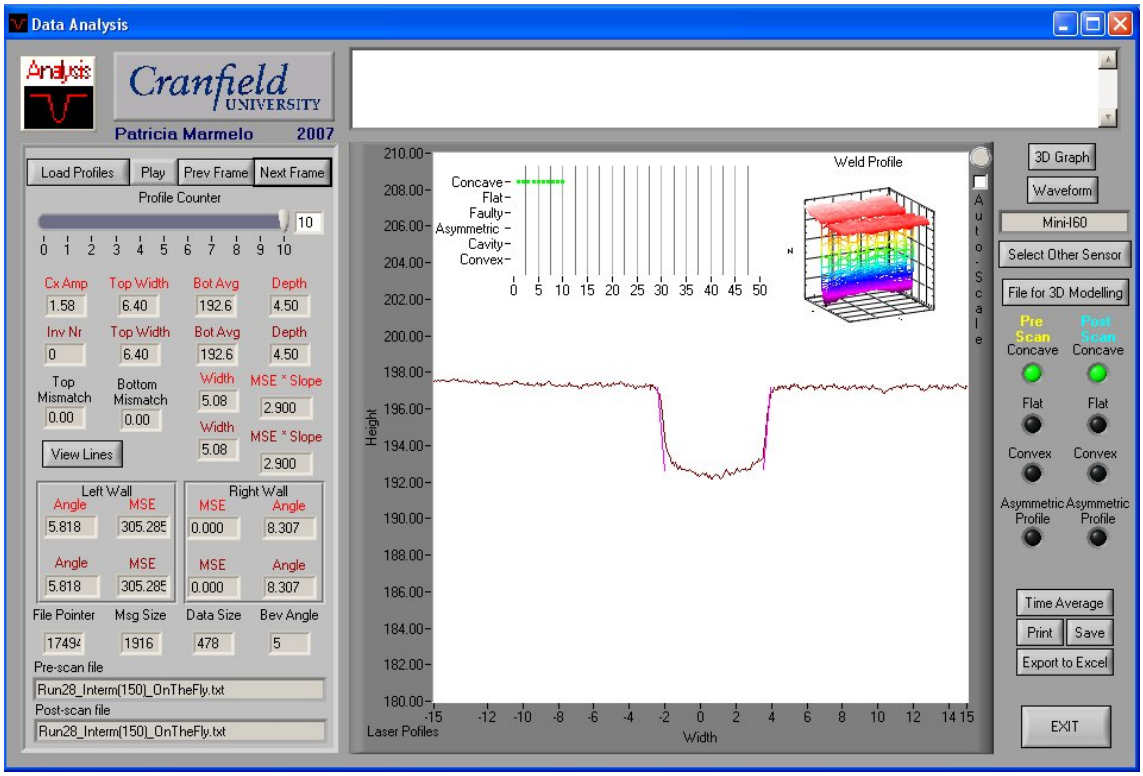

Figure I.4.4.0.124 – Screenshot of Profile 10 of "Run 28" Positioned at 150 Degrees.

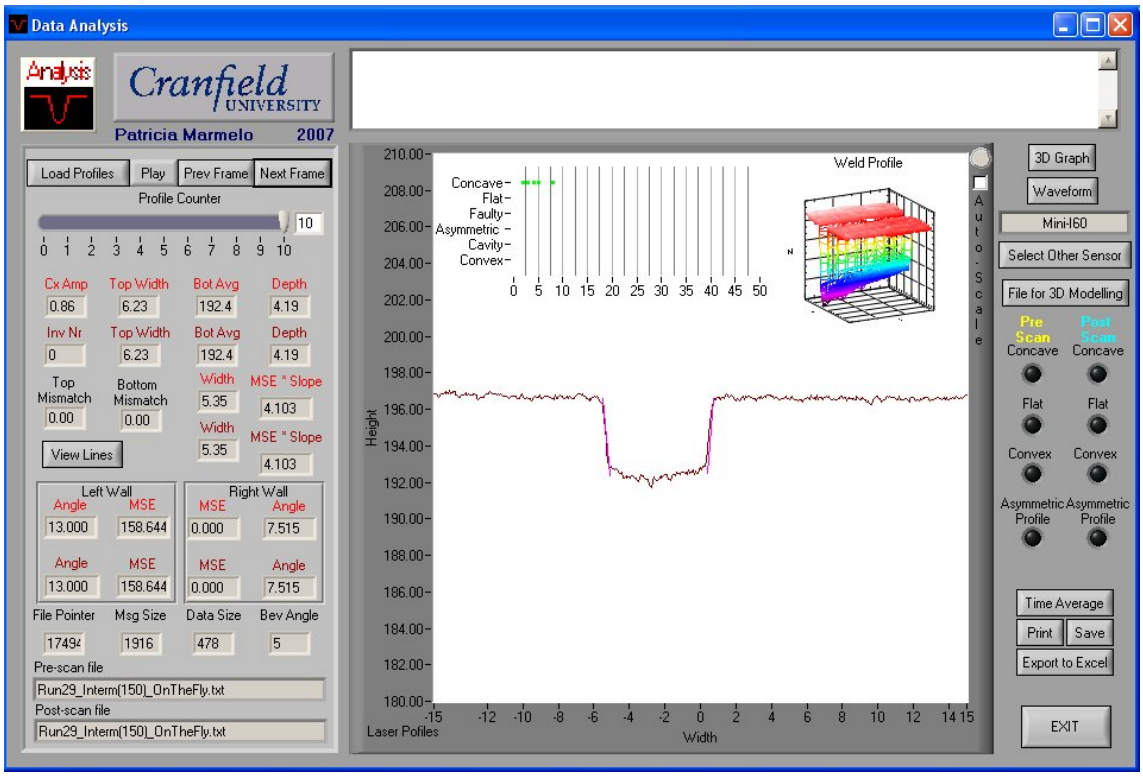

Figure I.4.4.0.125 – Screenshot of Profile 10 of "Run 29" Positioned at 150 Degrees.

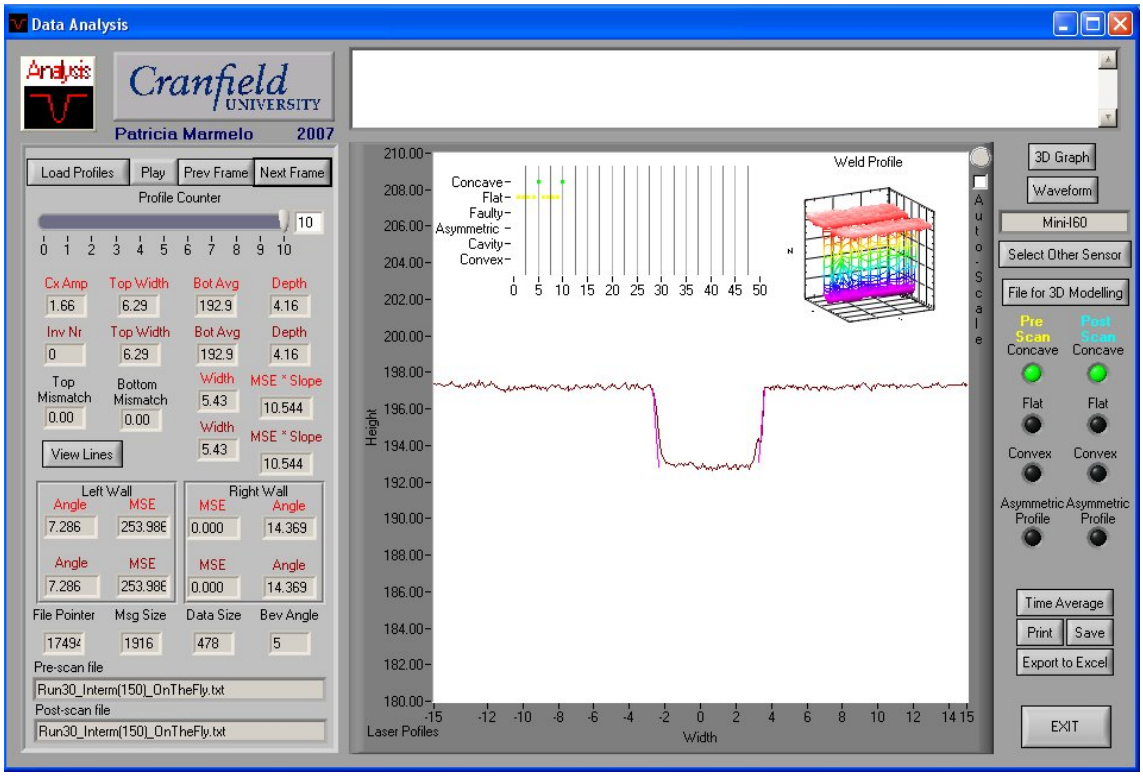

Figure I.4.4.0.126 – Screenshot of Profile 10 of "Run 30" Positioned at 150 Degrees.

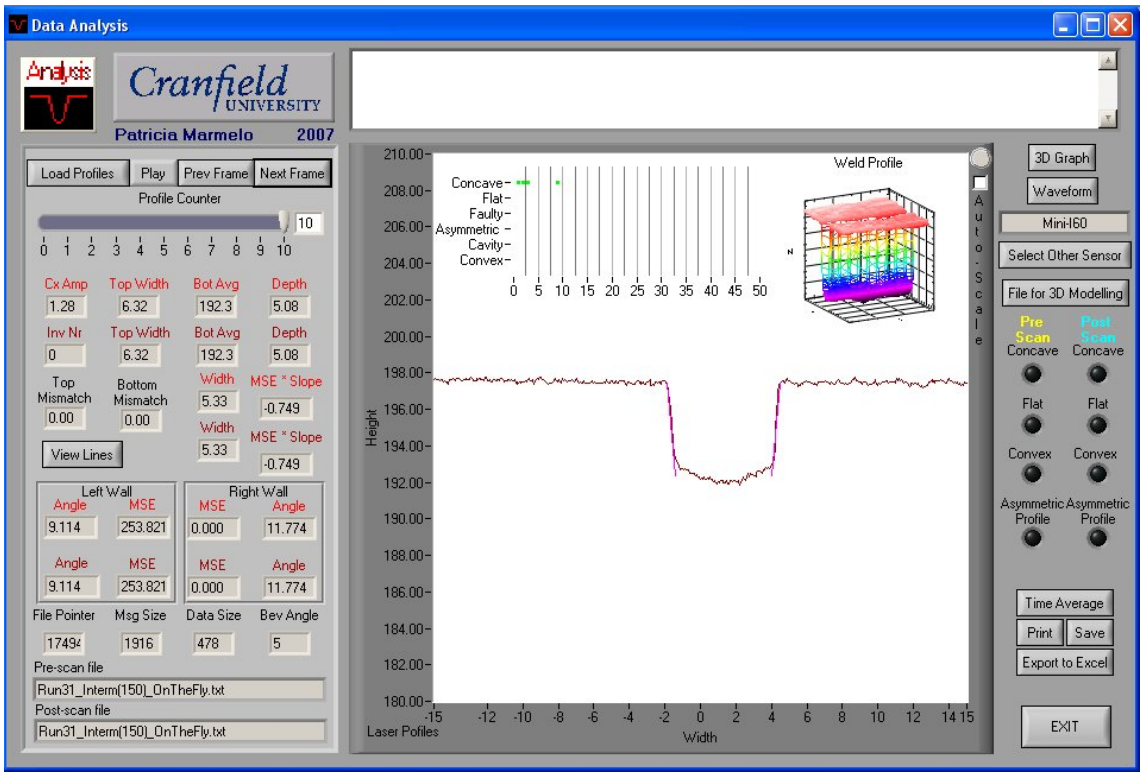

Figure I.4.4.0.127 – Screenshot of Profile 10 of "Run 31" Positioned at 150 Degrees.

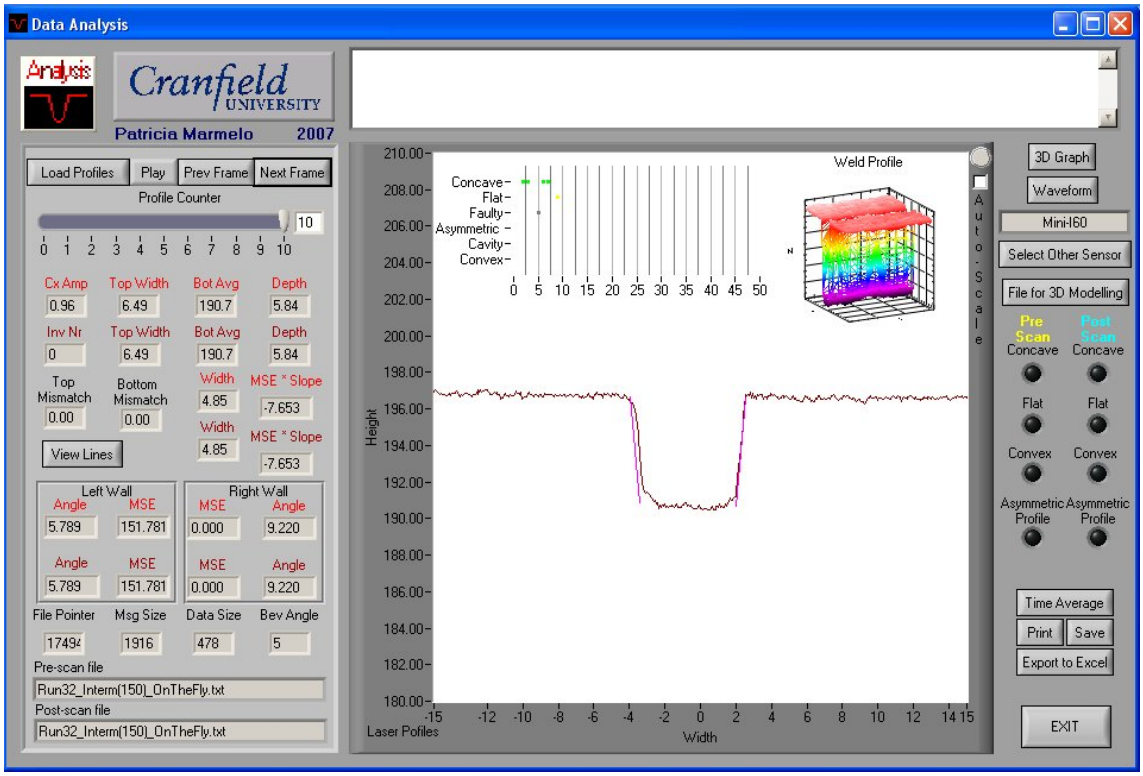

Figure I.4.4.0.128 – Screenshot of Profile 10 of "Run 32" Positioned at 150 Degrees.

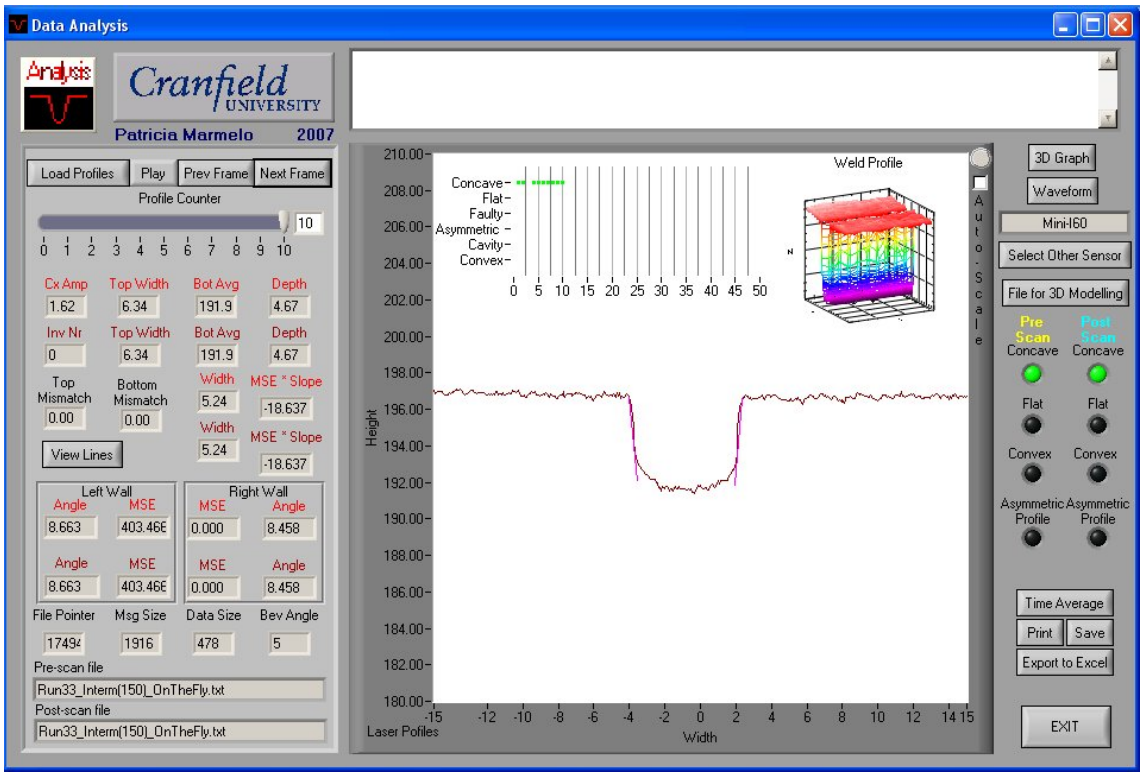

Figure I.4.4.0.129 – Screenshot of Profile 10 of "Run 33" Positioned at 150 Degrees.

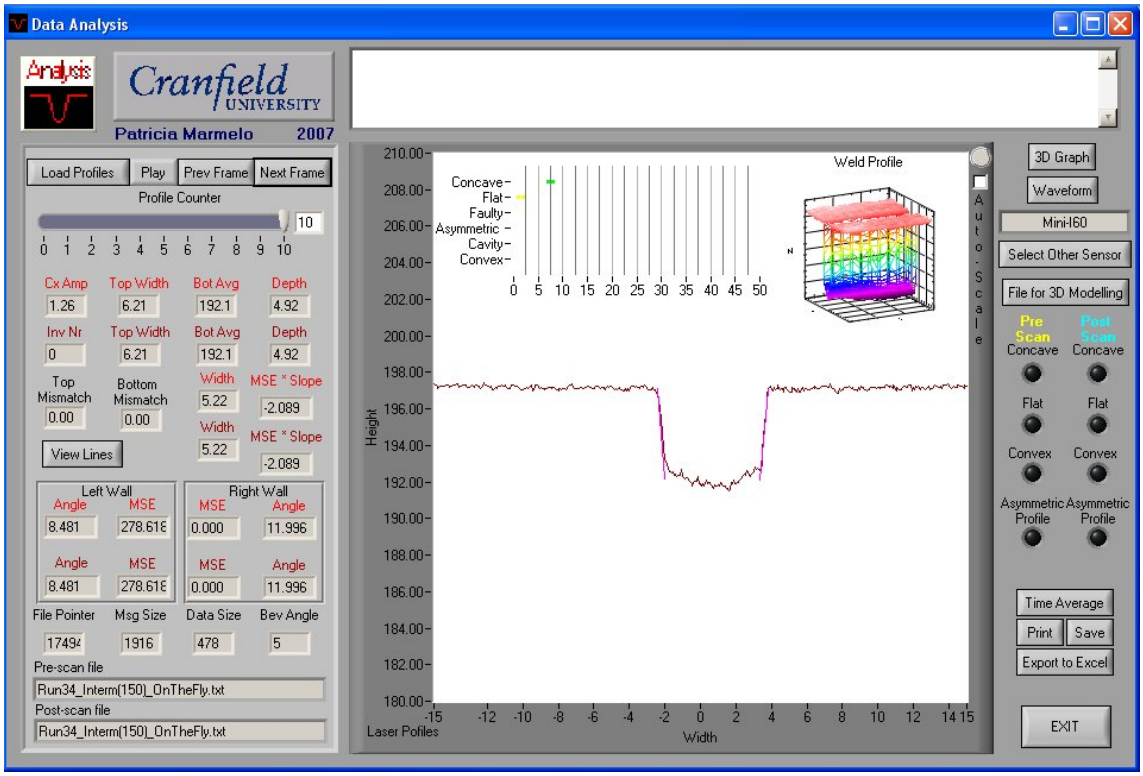

Figure I.4.4.0.130 – Screenshot of Profile 10 of "Run 34" Positioned at 150 Degrees.

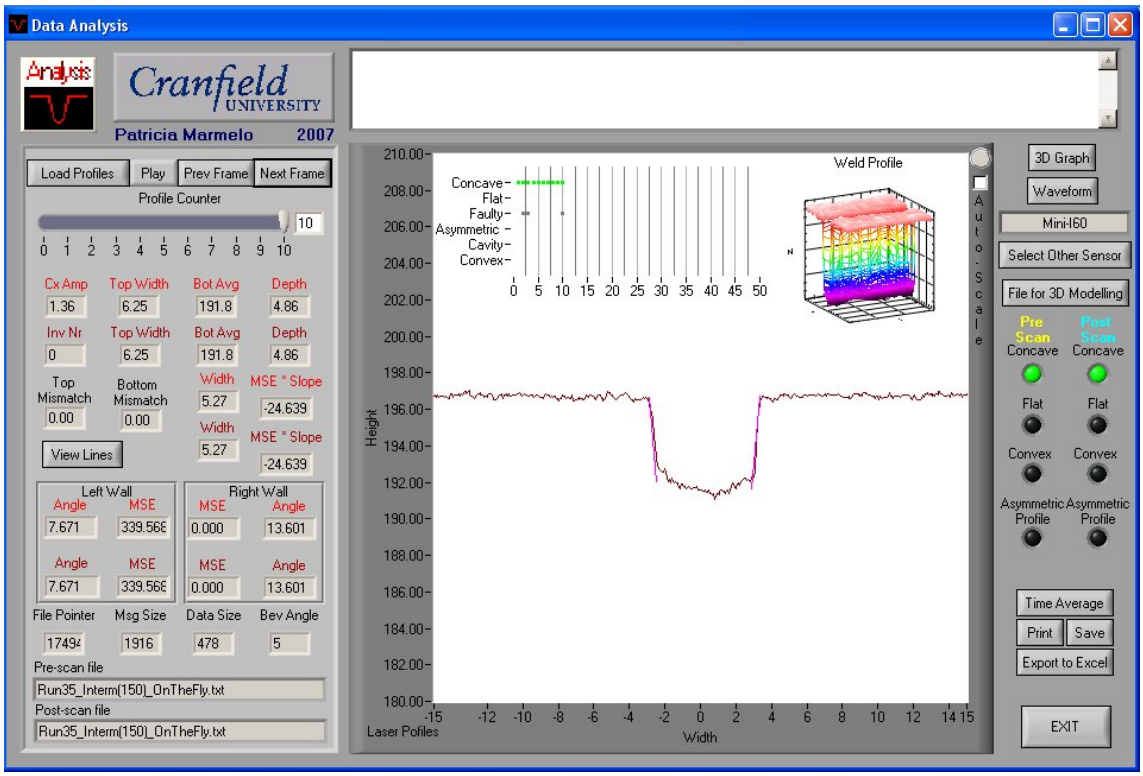

Figure I.4.4.0.131 – Screenshot of Profile 10 of "Run 35" Positioned at 150 Degrees.

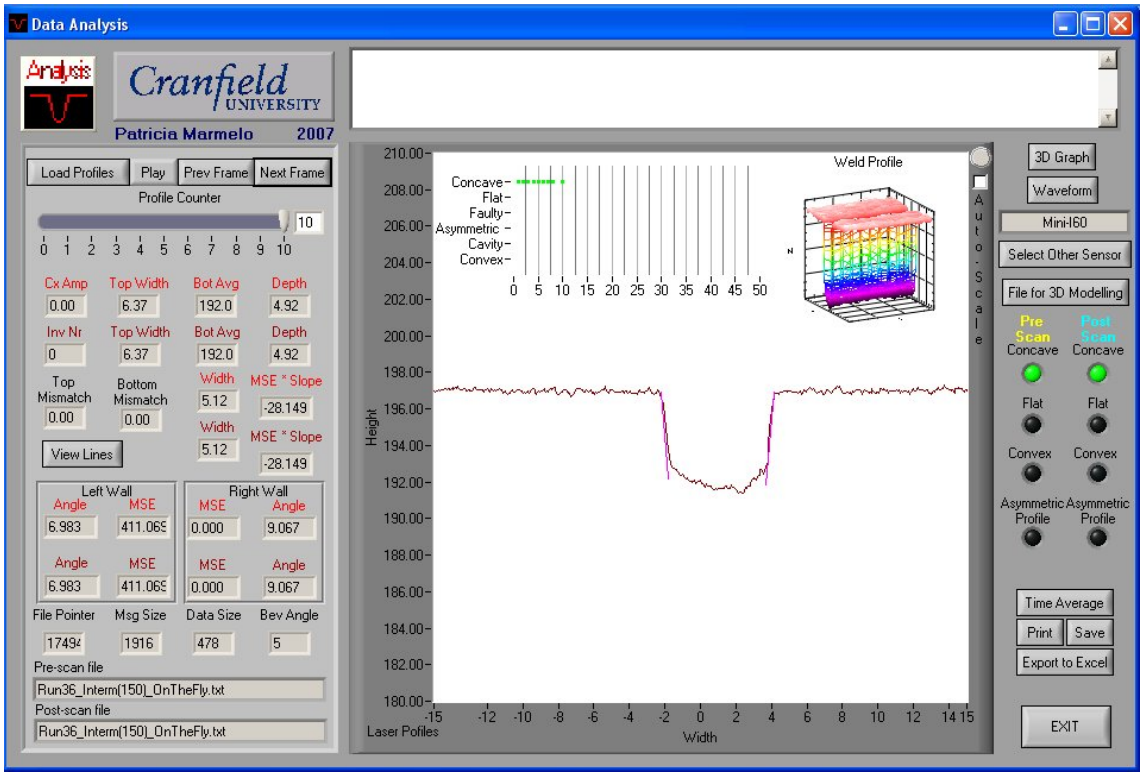

Figure I.4.4.0.132 – Screenshot of Profile 10 of "Run 36" Positioned at 150 Degrees.

Appendix J *Analysis Algorithms*

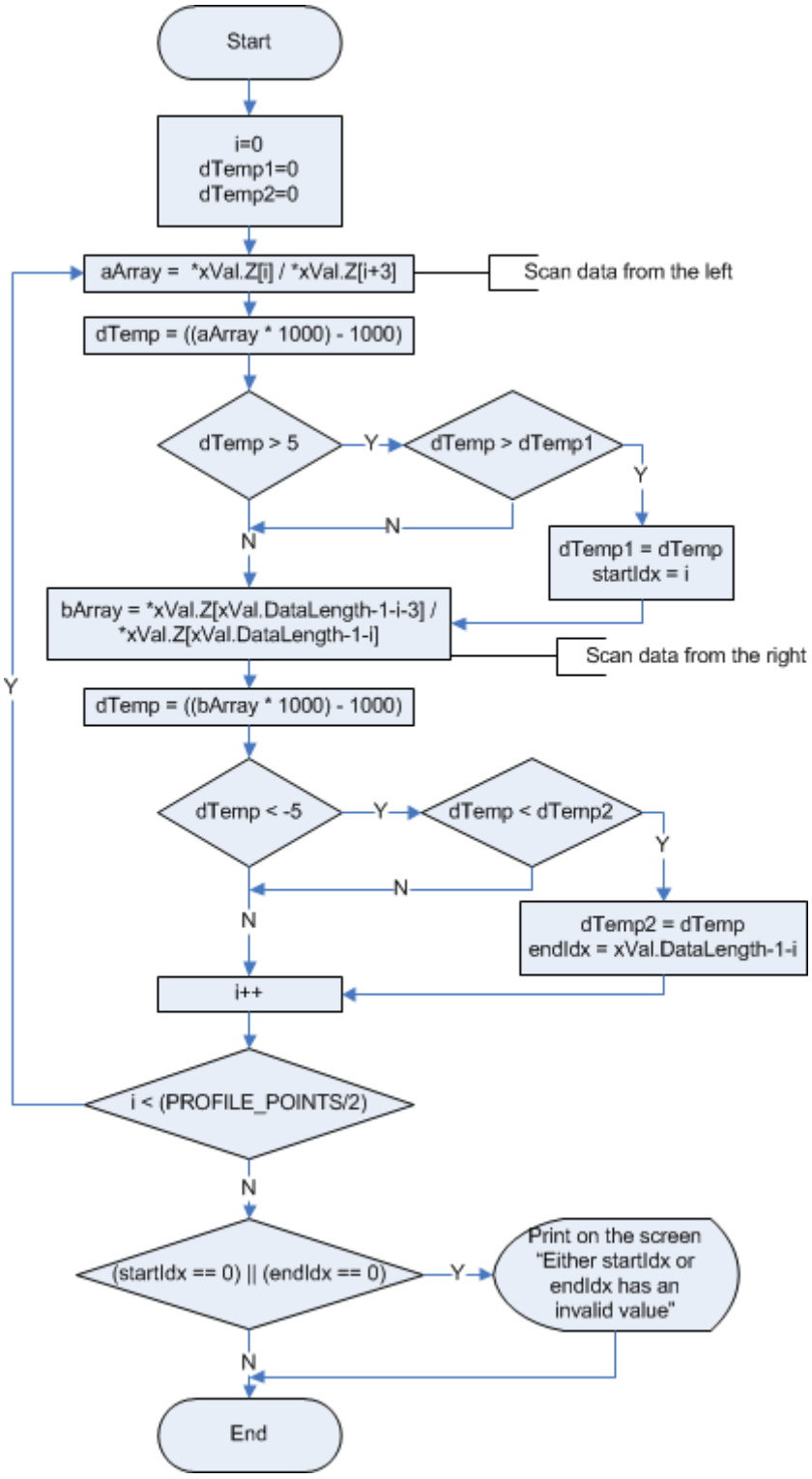

Figure J.0.1 – Initial Groove Bottom Detection Flowchart.

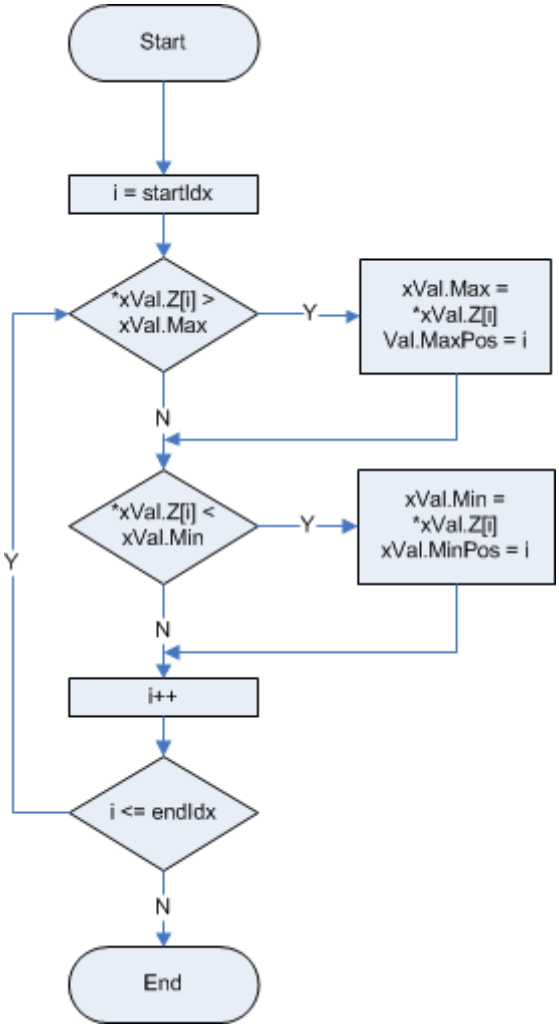

Figure J.0.2 – Groove Bottom Maximum and Minimum Points Detection Flowchart.

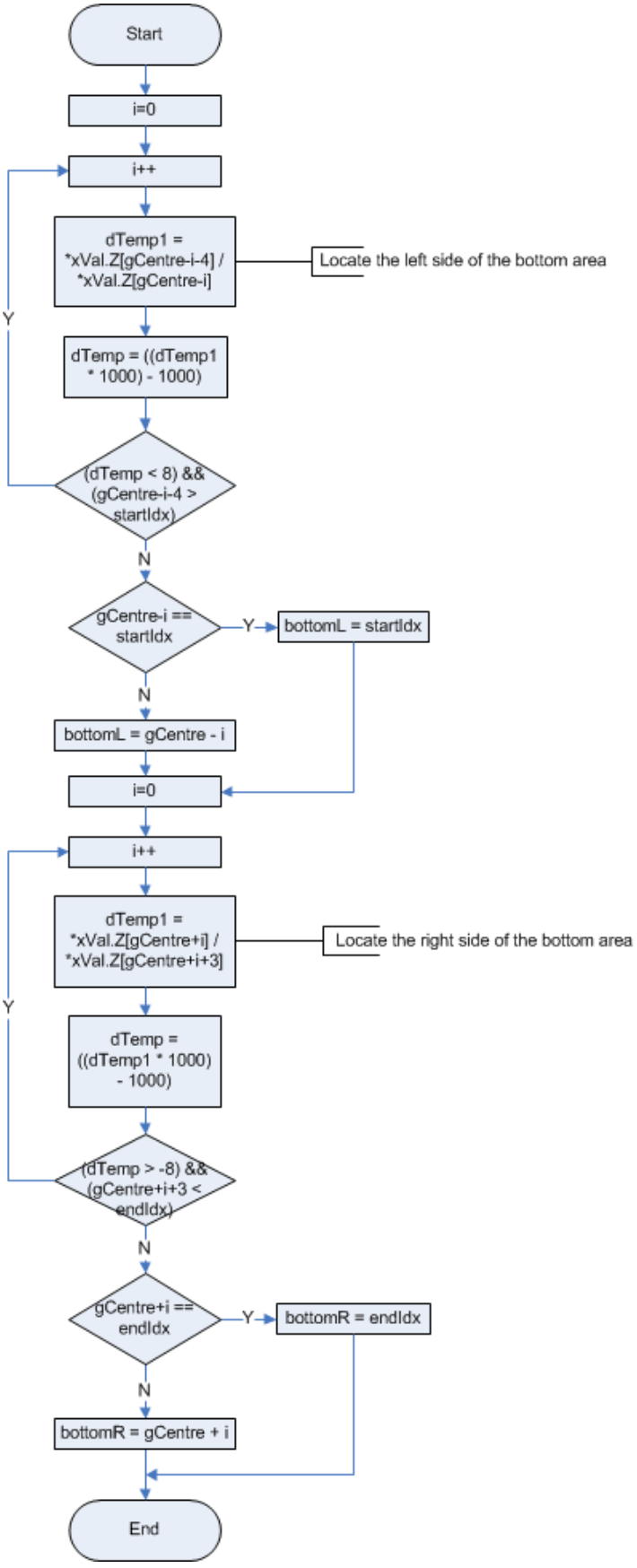

Figure J.0.3 – Groove Bottom Detection Third Step Flowchart.

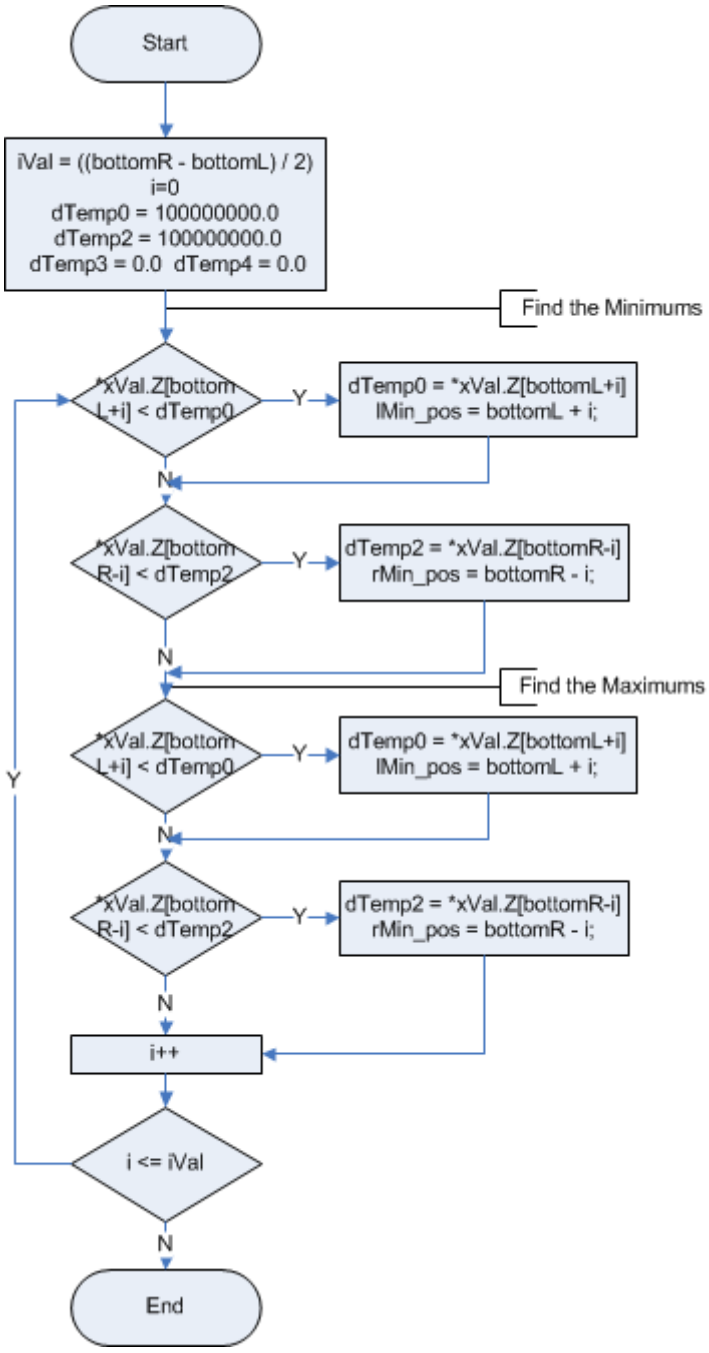

Figure J.0.4 – Find the Minimum and Maximum Points of the Groove Bottom Flowchart.

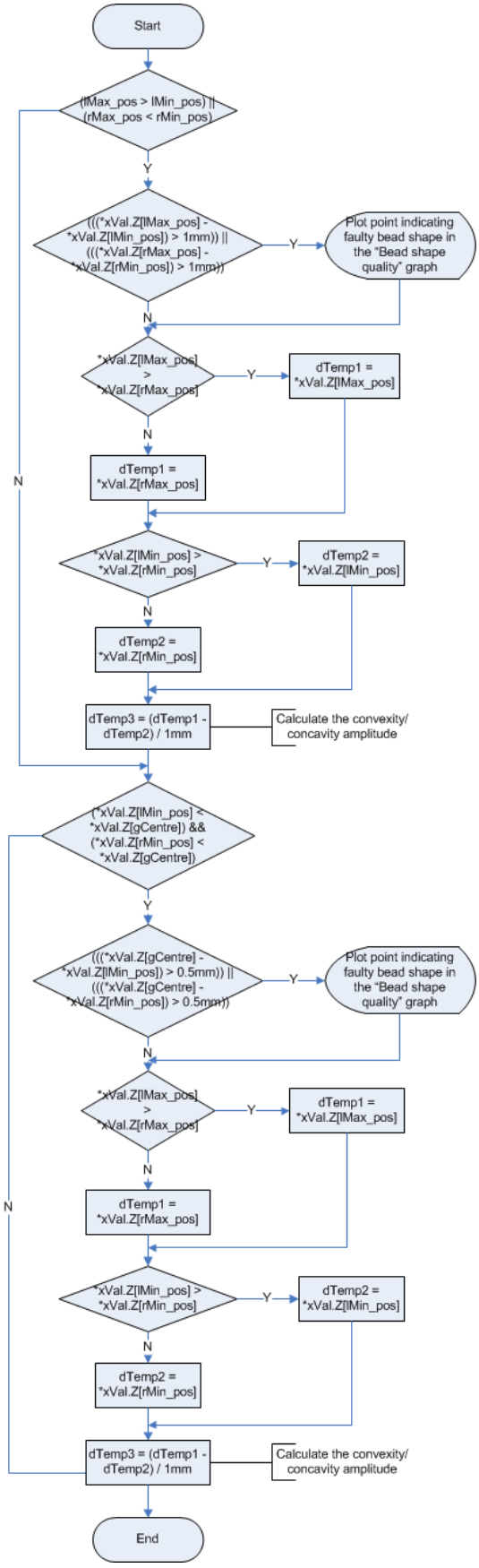

Figure J.0.5 – Bead Shape Assessment (part 1) Flowchart.

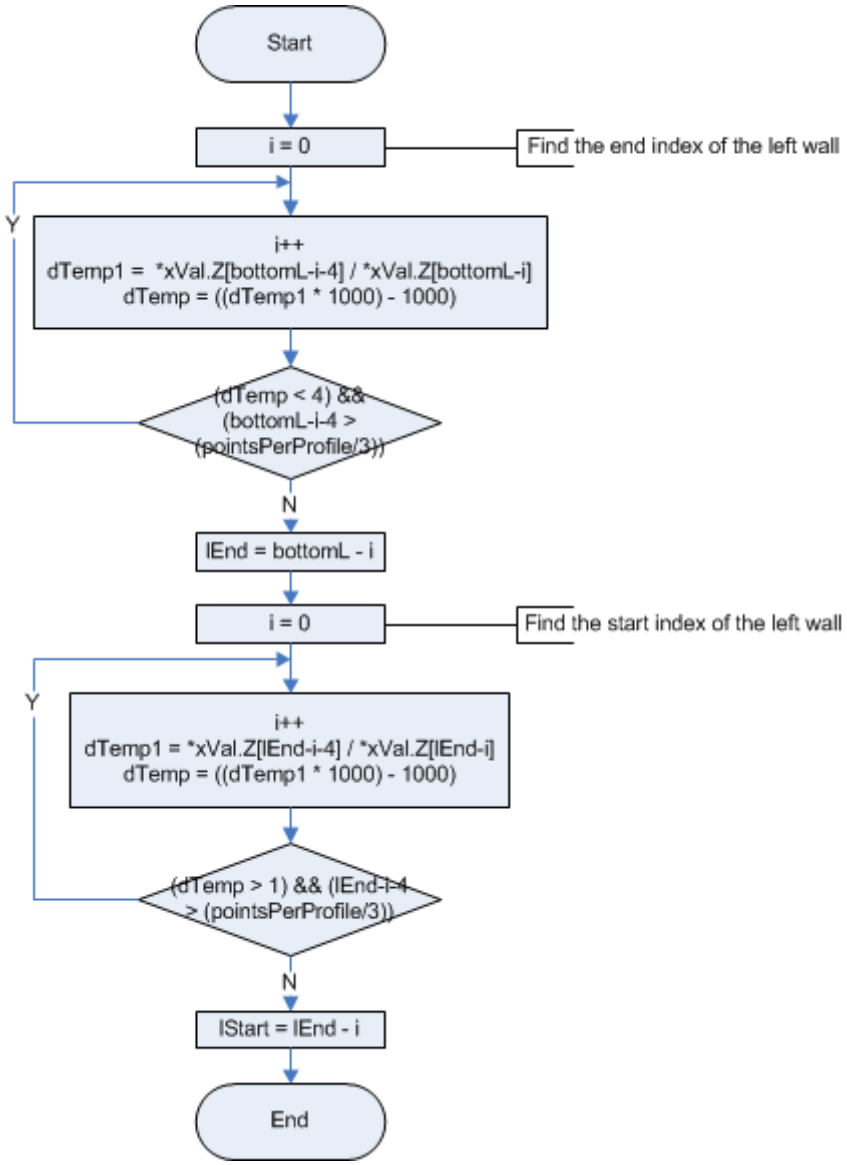

Figure J.0.6 – Left Wall Detection Flowchart.

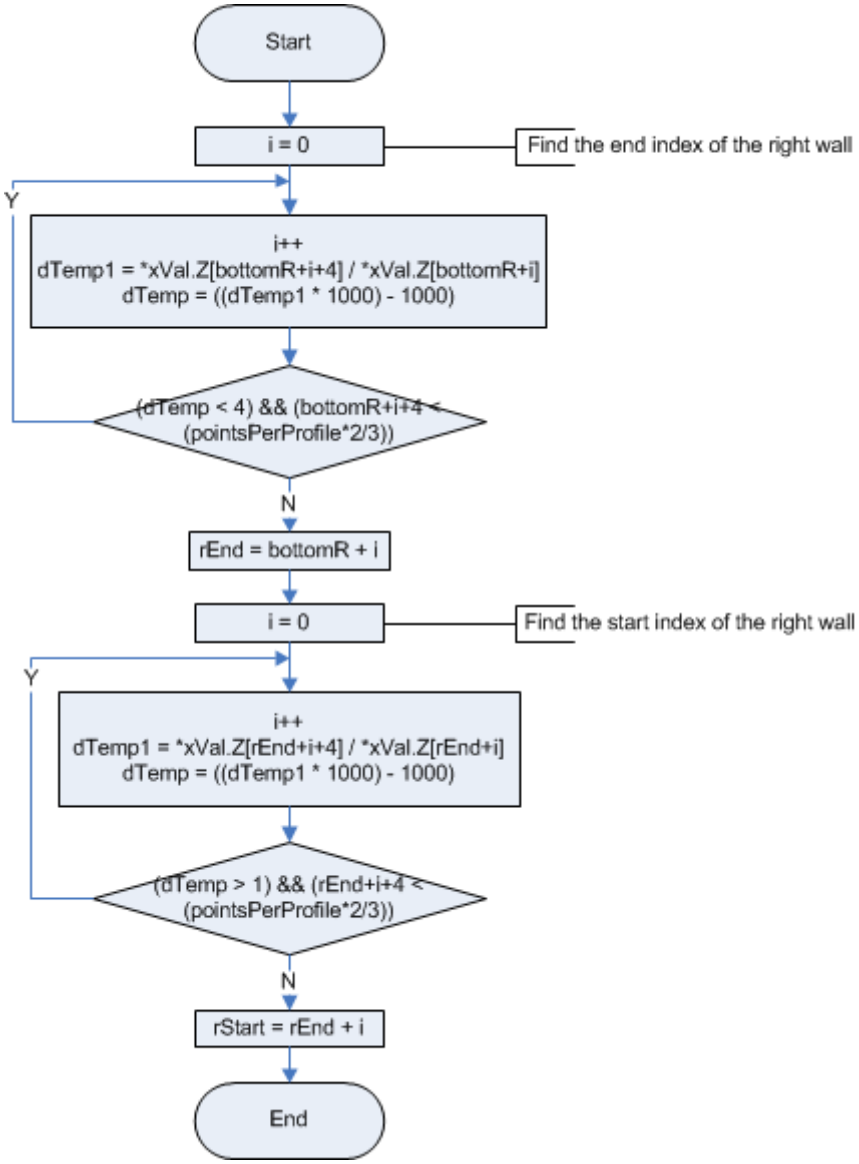

Figure J.0.7 – Right Wall Detection Flowchart.

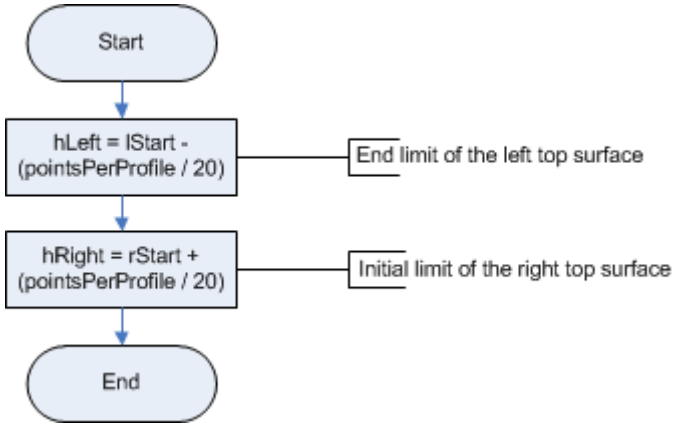

Figure J.0.8 – Top Surfaces Limits Detection Flowchart.

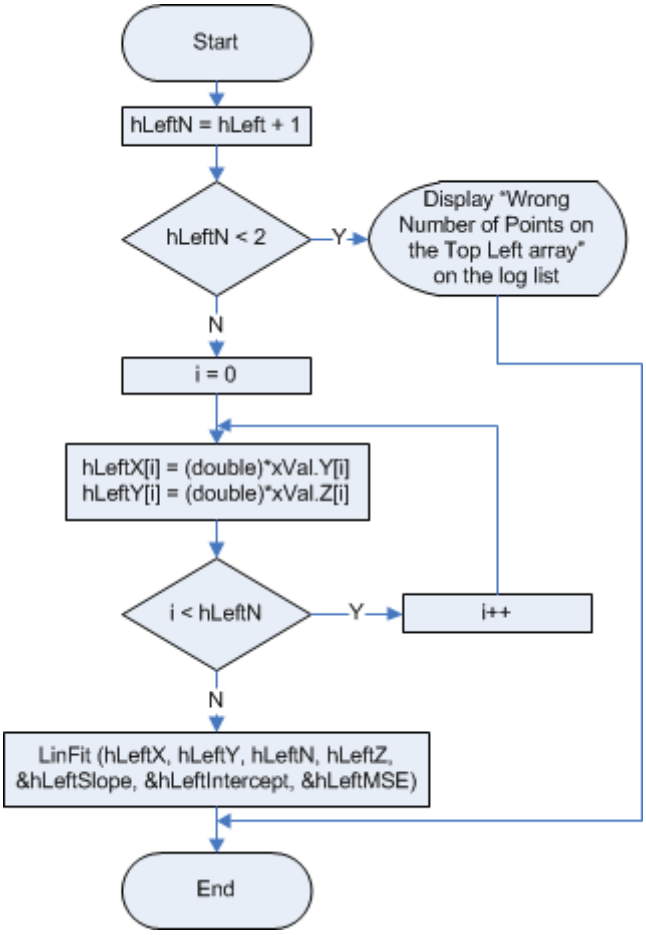

Figure J.0.9 – Fit Left Top Surface Flowchart.

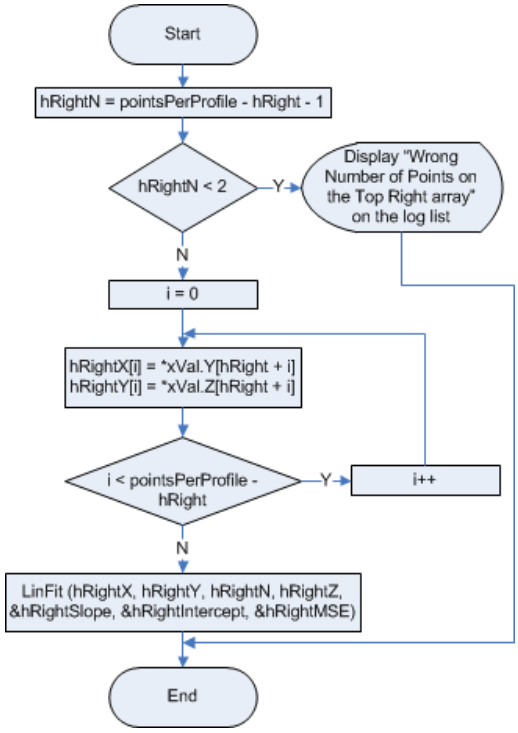

Figure J.0.10 – Fit Right Top Surface Flowchart.

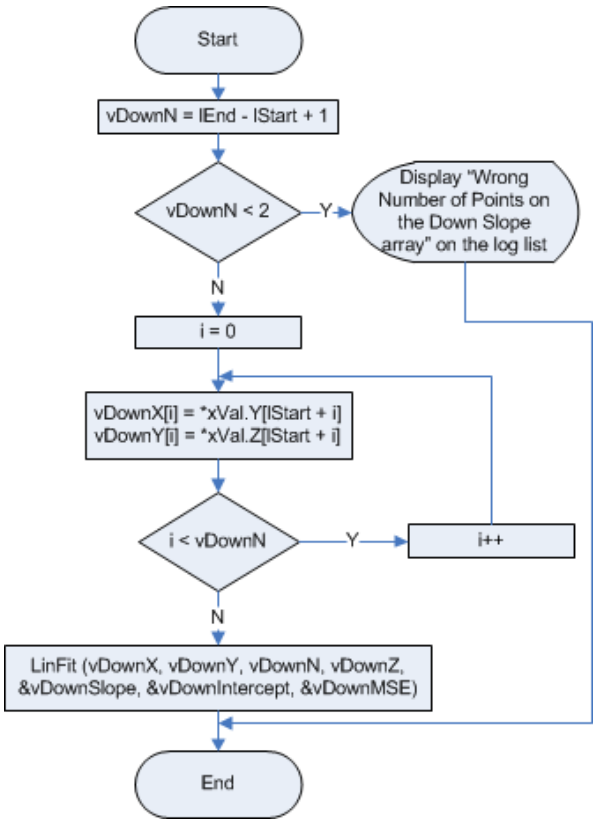

Figure J.0.11 – Fit Left groove Wall Flowchart.

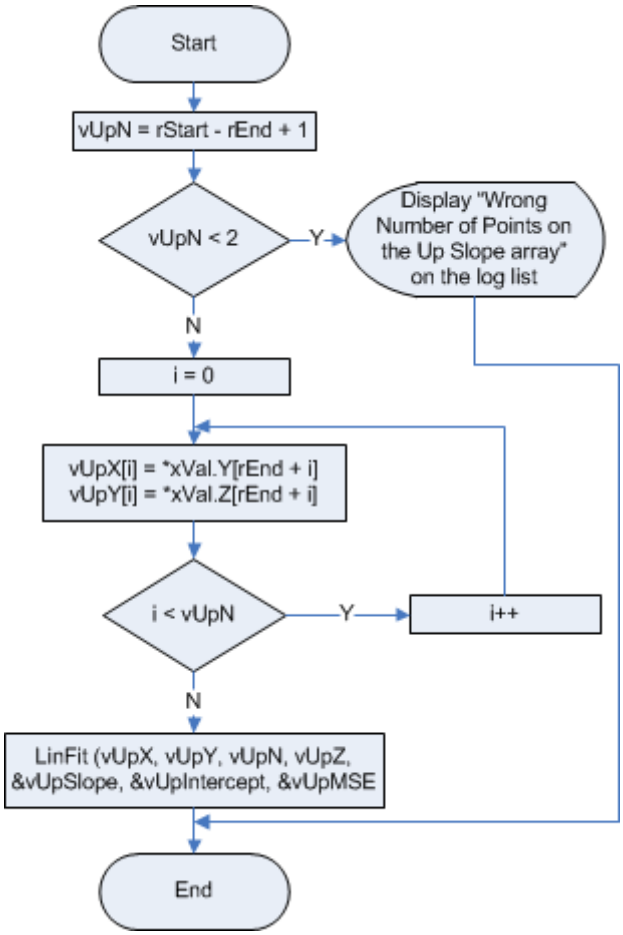

Figure J.0.12 – Fit Right groove Wall Flowchart.

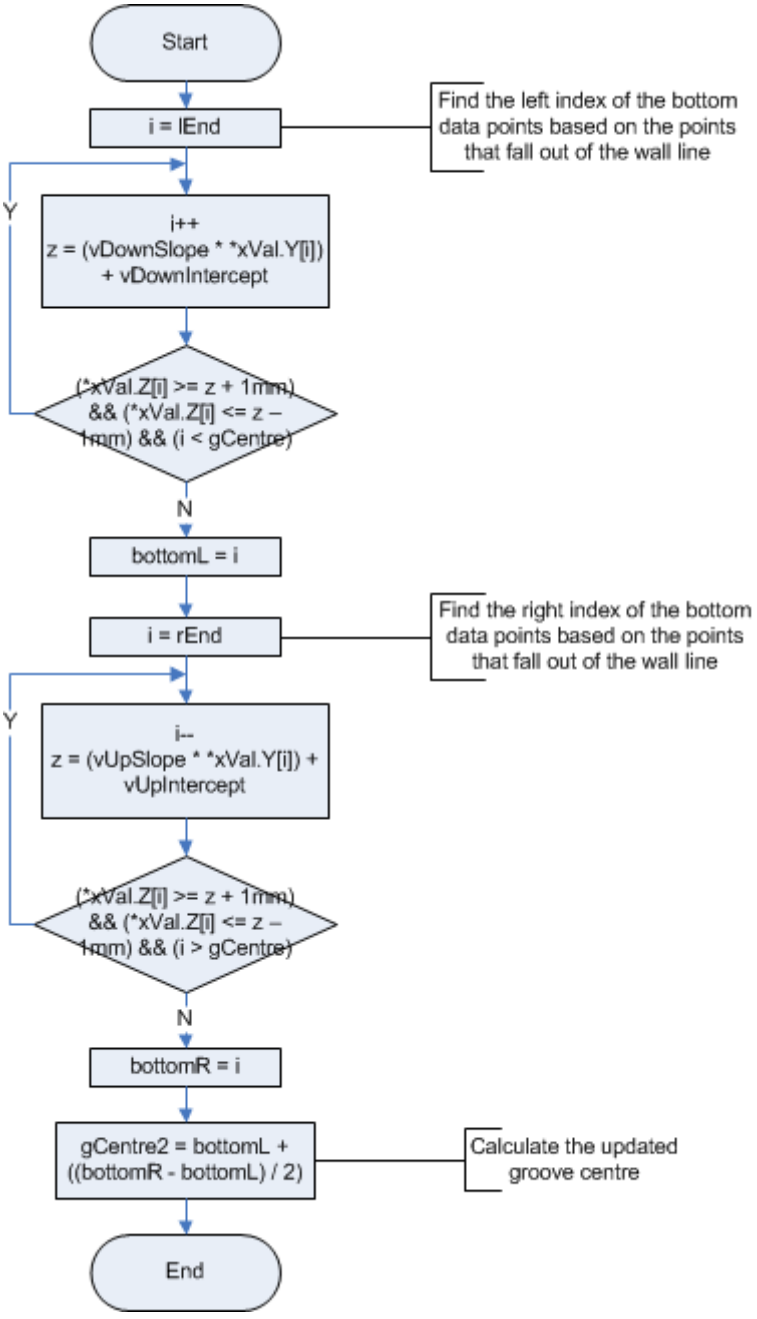

Figure J.0.13 – Groove Bottom Detection (third) Flowchart.

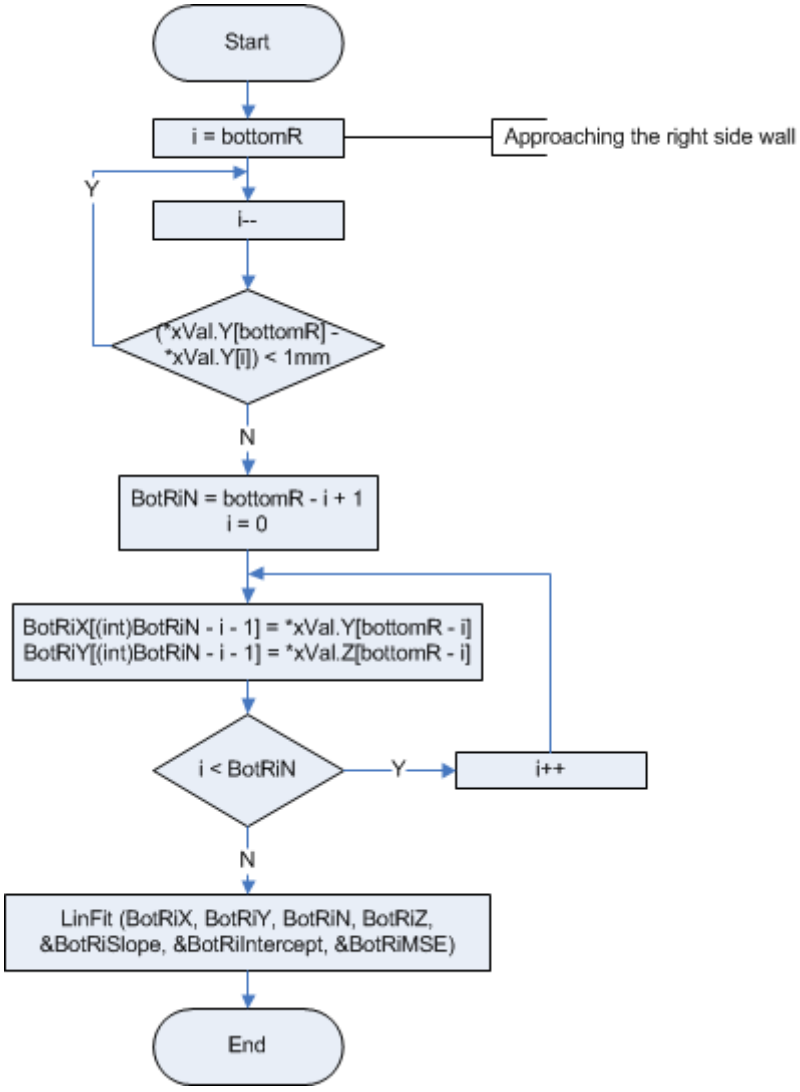

Figure J.0.14 – Toe Angle 2 Flowchart.

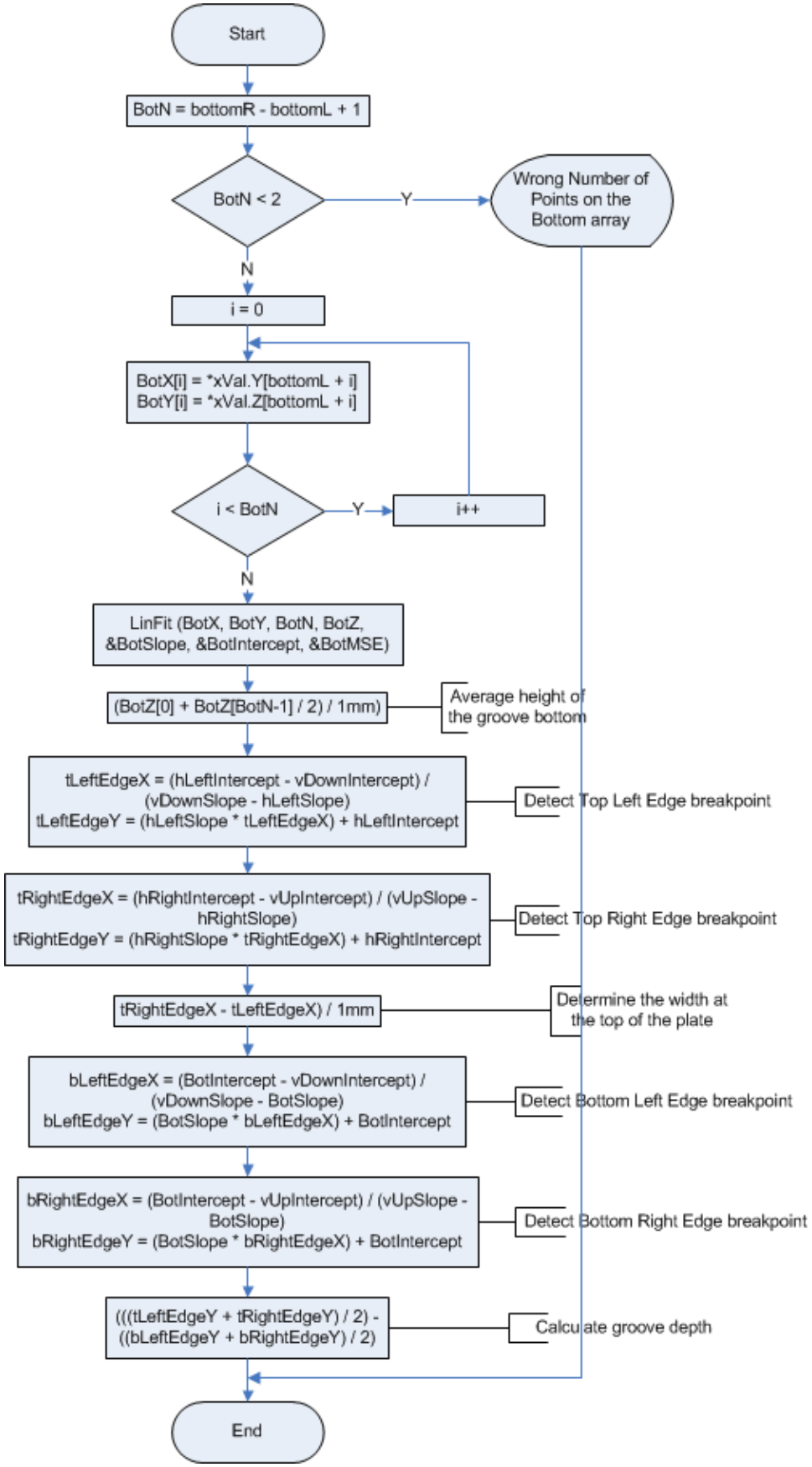

Figure J.0.15 – Fit a Straight Line to the Bottom Data Points Flowchart.

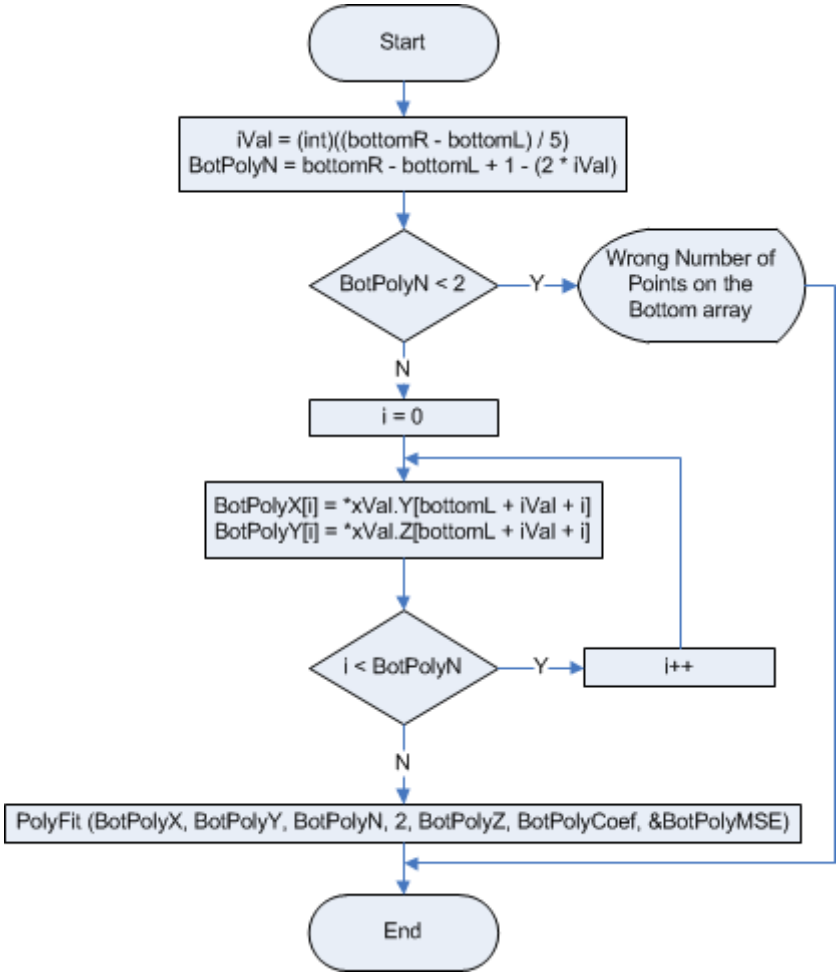

Figure J.0.16 – Fit a Polynomial Line to the Bottom Data Points Flowchart.

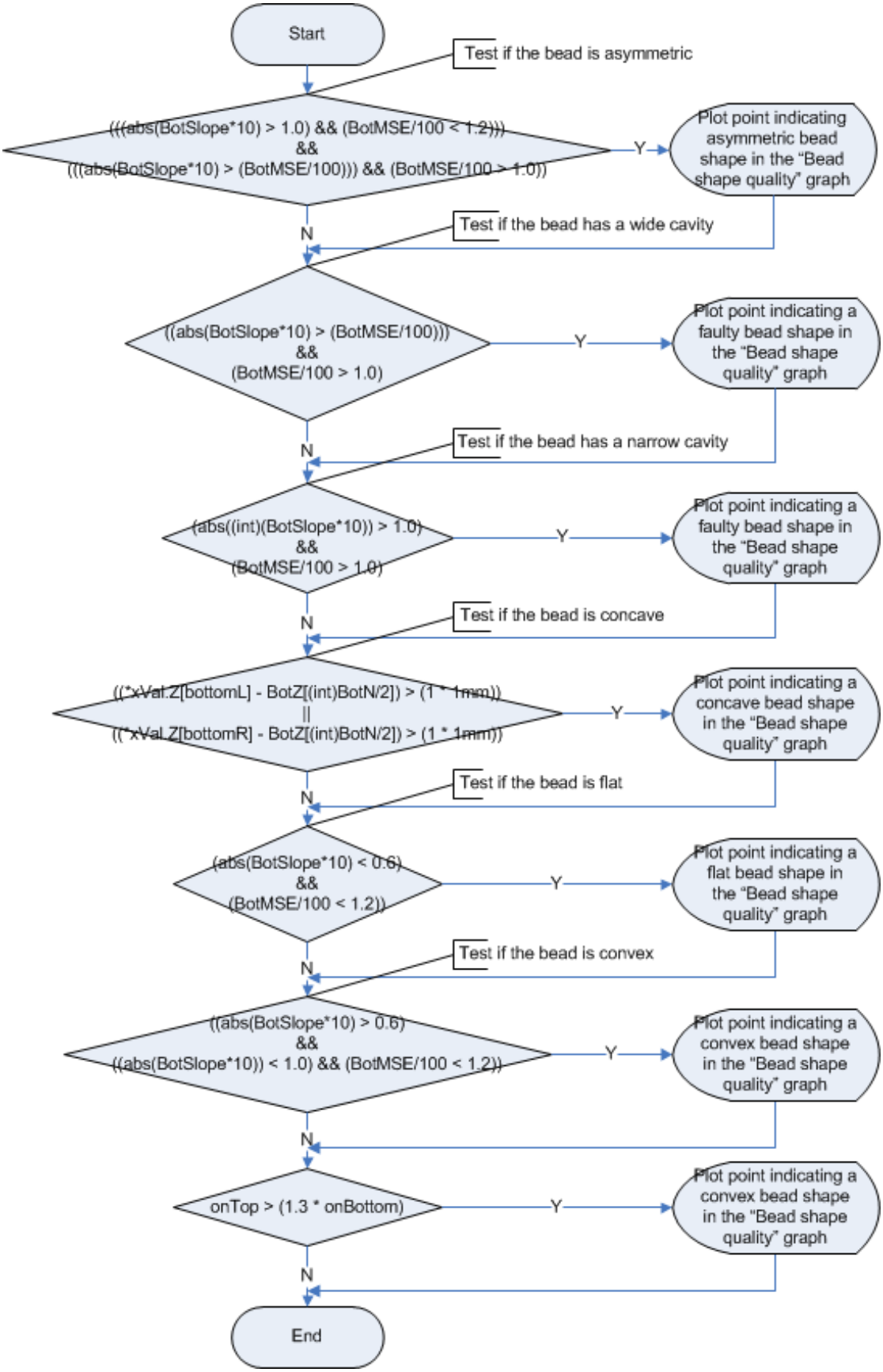

Figure J.0.17 – Bead Shape Assessment (part 2) Flowchart.